# INVESTIGATION FOR THE IDENTIFICATION OF EFFICIENT DEEP EUTECTIC SOLVENTS MEDIA FOR THE SYNTHESIS OF SOME METAL-BASED NANOPARTICLES



Thesis submitted to
BHARATHIDASAN UNIVERSITY, Tiruchirappalli
In partial fulfilment of the requirements
for the Degree of
DOCTOR OF PHILOSOPHY
IN
CHEMISTRY

By

R. BALAJI, M.Sc., M.Phil., B.Ed., (Ref. No.: 10974 / Ph.D.K2 / Chemistry / Part-Time (3-5) / November- 2018)

**Under the Guidance Of** 

**Dr. D. ILANGESWARAN,** M.Sc., M.Phil., Ph.D., Assistant Professor in Chemistry



P.G & Research Department of Chemistyr
RAJAH SERFOJI GOVERNMENT COLLEGE
(AUTONOMOUS, NAAC 'A' GRADE & DST- FIST COLLEGE
(AFFILIATED TO BHARATHIDASAN UNIVERSITY, TIRUCHIRAPALLI-24)
THANJAVUR - 613005.
TAMILNADU, INDIA

**JUNE - 2022** 

Dr. D. Ilangeswaran, M.Sc., M.Phil., Ph.D., RESEARCH SUPERVISOR & CONVENER

Department of Chemistry

Rajah Serfoji Govt. College (Autonomous)

Thanjavur – 613005



email: dhailangeswaran@gmail.com

Mobile: 8903853566

Date: 30.06.2022

### **CERTIFICATE**

This is to certify that the thesis entitled "INVESTIGATION FOR THE IDENTIFICATION OF EFFICIENT DEEP EUTECTIC SOLVENTS MEDIA FOR THE SYNTHESIS OF SOME METAL-BASED NANOPARTICLES" submitted by R. BALAJI (Ref. No: 10974 / Ph.D. K2 / Chemistry / Part-Time (3-5) / November - 2018) for the award of the Degree of Doctorate of Philosophy in Chemistry is a record of research work done under my supervision during the period from November 2018 - May 2021 and the thesis has not formed the basis of award of any Degree, Diploma, Associateship, and Fellowship or any other similar title of any University or Institution. Also, certify that the thesis represents an independent work on the part of the candidate.

Date: 30.06.2022

Place: Thanjavur - 05

Signature of the Research Supervisor

## Dr. D. Ilangeswaran, M.Sc., M.Phil., Ph.D., RESEARCH SUPERVISOR & CONVENER

Department of Chemistry

Rajah Serfoji Govt. College (Autonomous)

Thanjavur – 613005



email: dhailangeswaran@gmail.com

Mobile: 8903853566

Date: 30.06.2022

### **CERTIFICATE OF PLAGIARISM**

1	Name of the Research Scholar	Mr. R. BALAJI	
2	Course of Study	Ph. D. – Chemistry (Part-time)	
3	Ref. No.	(Ref. No: 10974 / Ph.D. K2 / Chemistry / Part-Time (3-5) / November - 2018	
4	Title of the Thesis/ Dissertation	Investigation for the Identification of Efficient Deep Eutectic Solvents Media for the Synthesis of some Metal-based Nanoparticles	
5	Name of the Research Supervisor	Dr. D. ILANGESWARAN	
6	Department / Institution / Research Centre	Department of chemistry  Rajah Serfoji Government College  (Autonomous)  Thanjavur-613005	
7	Acceptable Maximum Limit	20 %	
8	Percentage of Similarity of Content Identified	1 %	
9	Software Used	URKUND	
10	Date of Verification	27-06-2022	
11	Issued by	bdulib.bdu@analysis.urkund.com	

Report on plagiarism check, item with % of similarity is identified.

**Date**: 30.06.2022 **Place**: Thanjavur - 05

Signature of the Research Supervisor

### Curiginal

### **Document Information**

Analyzed document R. Balaji (Reg.No. 10974) Thesis[2149].pdf (D141297784)

Submitted 6/27/2022 7:58:00 AM
Submitted by Srinivasa ragavan S
Submitter email bdulib@gmail.com

Similarity 1%

Analysis address bdulib.bdu@analysis.urkund.com

### Sources included in the report

Sour	ces included in the report	
W	$URL: https://www.hindawi.com/journals/ijp/2014/453747/\#: \sim text = Cadmium \% 20 sulfide \% 20 nanoparticles \% 20 (CdS \% 2Dn, largely \% 20 on \% 20 the \% 20 synthesis \% 20 methodologies. Fetched: 6/27/20227:58:13~AM$	88
W	URL: https://www.intechopen.com/chapters/61218 Fetched: 8/9/2021 8:37:20 AM	88
W	URL: https://pubmed.ncbi.nlm.nih.gov/26726530/ Fetched: 1/11/2021 10:41:36 AM	88
W	URL: https://neuro.unboundmedicine.com/medline/citation/33677361/Interaction_of_Cun_Agn_and_Aunn_=_1_4nanoparticles_with_ChCl:Urea_deep_eutectic_solvent_Fetched: 6/27/2022 7:59:19 AM	
W	URL: https://en.wikipedia.org/wiki/Silver_nanoparticle Fetched: 9/25/2019 10:18:27 AM	88
W	URL: https://www.ncbi.nlm.nih.gov/pmc/articles/PMC7415816/ Fetched: 12/11/2020 5:59:04 PM	88
W	URL: https://www.hindawi.com/journals/bca/2018/9354708/ Fetched: 12/10/2020 8:37:23 PM	88
W	URL: https://docksci.com/quercetin-and-gallic-acid-mediated-synthesis-of-bimetallic-silver-and-selenium-n_5acd96d9d64ab2d469e47066.html Fetched: 6/8/2022 1:36:07 PM	88
w	URL: https://www.science.gov/topicpages/n/nanoparticle+formulation+exhibits Fetched: 4/25/2022 12:16:02 PM	88

### **Entire Document**

1. INTRODUCTION 1.1. GENERAL INTRODUCTION TO DEEP EUTECTIC SOLVENTS In this investigation, researchers mostly concentrated on the development of ionic liquids by blending met salts, chiefly Zinc, Aluminium, Tin, and Iron chlorides, with quaternary ammonium salts. Although both salts have very high melting points, their decent blending provided the production of a liq

R. BALAJI, M.Sc., M.Phil.,
Research scholar
Department of Chemistry
Rajah Serfoji Government College (Autonomous),
Thanjavur – 613 005.
TAMIL NADU, INDIA



### **DECLARATION**

I hereby declare that the thesis entitled "INVESTIGATION FOR THE IDENTIFICATION OF EFFICIENT DEEP EUTECTIC SOLVENTS MEDIA FOR THE SYNTHESIS OF SOME METAL-BASED NANOPARTICLES" has been originally carried out by me at Research Lab II, Department of Chemistry, Rajah Serfoji Government College (Autonomous), Thanjavur, India, under the guidance of Dr. D. Ilangeswaran, Assistant Professor, Department of Chemistry, Rajah Serfoji Government College (Autonomous), Thanjavur, India. This work has not formed the basis for the award of any Degree, Diploma, Associateship, Fellowship, or another similar title of Bharathidasan University or any other University.

**Date:** 30.06.2022

**Place:** Thanjavur - 05

### ACKNOWLEDGEMENT

First and foremost, I owe my debt to my Research Advisor **Dr. D. Ilangeswaran**, Assistant Professor, Department of Chemistry, Rajah Serfoji Govt. College (Autonomous), Thanjavur, for his friendly guidance, caring and creating curiosity in learning about all areas of research. I thank him from my bottom of heart for all his support including time, ideas and technical support about chemistry software, I really learned so many things from you sir. It would have been quite impossible to carry on the research work and make it into the final shape of a thesis without his constant support. His affection for me is fondly remembered.

I convey my sincere thanks to my Doctoral Committee members **Dr. S. Valarselvan**, Assistant Professor. H.H. The Rajahs College, Pudukkottai and **Dr. C. Kathiravan**, Assistant Professor, Department of Chemistry, Rajah Serfoji Govt.College (Autonomous), Thanjavur, for their insightful comments and encouragement in my research work.

I am very grateful to thank **Prof. S.P. Elangovan**, Head of the Department of Chemistry, Rajah Serfoji Govt College, (Autonomous), Thanjavur, for his personal care overwhelming support and constant encouragement.

I express my gratitude to **Dr. D. Rosi**, **Principal**, Rajah Serfoji Govt. College (Autonomous), Thanjavur, for permitting and providing facilities to carry out my work.

I express my Special Thanks to **Dr. A. Arulraj**, Assistant Professor, Department of Economics, Rajah Serfoji Govt College, (Autonomous), Thanjavur, for his continuous support starting from sending the application for registration and up to the end-stage of my work.

It is a great pleasure to express my special thanks to my Friend **Mrs .K. Sarjuna**, Research Scholar from our research group for her constant support in the research work.

I would like to thank **God (My Dear Amma Mrs. Jothy& Appa Mr. Rudrapathy)**, for letting me through all the difficulties. I have experienced your guidance day by day. You are the one who let me finish my research. I will keep on trusting you for my future.

On a personal front, a million words would be too short to say how grateful I am to my wife **Dr. A. Indumathi** and my son **B. Naveen Priyan** my adorable sister **Mrs. Jayabharathy**, Brother-in-Law **Er. A. Kanagaraj**, Executive Engineer and my lovable Kuty Mr.**A. K. Priyan**, Music Composer Chennai and my In-Law **Mr & Mrs. Bose-Viji** for their outpouring love and affection, for supporting me through my trials and tribulations, for bearing the pain of separation as I pursued my dreams.

Last but not least I would like to thank my Cousin **Dr. P. Sangeetha** and Teaching Staff Members of the Entire Department of Chemistry and Non-Teaching Members of Rajah Serfoji Govt College (Autonomous) Mr. A. Sivakumar and all my family friends for their timely help during my study.

Above all, I offer my thanks and praises to the Almighty God **Sri Santoshi Amman** for an immense shower of blessings.

R. BALAJI

### **CONTENTS**

Chapter	Title	Page No	
1	INTRODUCTION		
1.1	General introduction of deep eutectic solvents	1	
1.2	Deep eutectic solvents- Definition	4	
1.3	Physiochemical properties of deep eutectic solvents	6	
	1.3.1 Freezing point (T <sub>f</sub> )	6	
	1.3.2 Density	7	
	1.3.3 Viscosity	7	
	1.3.4 Ionic Conductivity	8	
	1.3.5 Acidity or Alkalinity	8	
1.4	Deep eutectic solvents (DES)		
	1.4.1 Types of deep eutectic solvents	9	
1.5	Choline chloride – urea based deep eutectic solvents	10	
1.6	Choline chloride - ethylene glycol based deep eutectic		
	Solvents	12	
1.7	Choline chloride - malonic acid based deep eutectic		
	Solvents	14	
1.8	Significance of deep eutectic solvents	14	
1.9	Comparison of Ionic liquids with deep eutectic solvents	15	
1.10	Applications of deep eutectic solvents	15	
	1.10.1 Applications of deep eutectic solvents in MNPs	16	
1.11	Metal Nanoparticles		

	1.11.1 Silver nanoparticles (AgNPs)	20
	1.11.2 Copper nanoparticles (CuNPs)	21
	1.11.3 Cadmium nanoparticles (CdNPs)	22
	1.11.4 Mercury nanoparticles (HgNPs)	23
	1.11.5 Zirconium nanoparticles (ZrNPs)	24
	1.11.6 Zinc nanoparticles (ZnNPs)	25
	1.11.7 Manganese nanoparticles (MnNPs)	25
	1.11.8 Vanadium nanoparticles (VNPs)	26
	1.11.9 Nickel nanoparticles (NiNPs)	27
1.12	Review of Literature	
	1.12.1 Deep eutectic solvents – synthesis and	
	Characterization	28
	1.12.2 Copper nanoparticles (CuNPs)	28
	1.12.3 Silver nanoparticles (AgNPs)	31
	1.12.4 Cadmium nanoparticles (CdNPs)	33
	1.12.5 Mercury nanoparticles (HgNPs)	34
	1.12.6 Zirconium nanoparticles (ZrNPs)	35
	1.12.7 Vanadium nanoparticles (VNPs)	36
	1.12.8 Zinc nanoparticles (ZnNPs)	36
	1.12.9 Manganese nanoparticles (MnNPs)	37
	1.12.10 Nickel nanoparticles (NiNPs)	38
1.13	Aim, Scope and Objectives of the present work	40
	References	42

2.1	Mater	ials	73
2.2	Experi	mental methods	74
	2.2.1	General preparation of Deep eutectic solvents (DES)	74
	2.2.2	Preparation of DES	75
	2.2.3	General procedure for the synthesis of nanoparticles	75
	2.2.4	Synthesis of CuNPs in ChCl- Urea/ Chcl-EG/	
		Ch.Cl- MA DES	75
	2.2.5	Synthesis of HgNPs in ChCl- Urea/ Chcl-EG/	
		Ch.Cl- MA DES	76
	2.2.6	Synthesis of MnNPs in ChCl- Urea/ Chcl-EG/	
		Ch.Cl- MA DES	76
	2.2.7	Synthesis of ZrNPs in ChCl- Urea/ Chcl-EG/	
		Ch.Cl- MA DES	76
	2.2.8	Synthesis of AgNPs in ChCl- Urea/ Chcl-EG/	
		Ch.Cl- MA DES	77
	2.2.9	Synthesis of ZnNPs in ChCl- Urea/ Chcl-EG/	
		Ch.Cl- MA DES	77
	2.2.10	Synthesis of CdNPs in ChCl- Urea/ Chcl-EG/	
		Ch.Cl- MA DES	78
	2.2.11	Synthesis of VNPs in ChCl- Urea/ Chcl-EG/	
		Ch.Cl- MA DES	78
	2.2.12	Synthesis of NiNPs in ChCl- Urea/ Chcl-EG/	
		Ch.Cl- MA DES	78
2.3	Fourie	r Transform Infrared Spectroscopy	79
2.4	Ultra	Violet- Visible Spectroscopy	79
2.5	Scanni	ing Electron Microscopy	79
2.6	X-Ray	Diffractometer	80
2.7	Energy	y Dispersive X-Ray Analysis	80
	Refere	ences	80

# 3 CHOLINE CHLORIDE – UREA DES MEDIA ASSISTED SYNTHESIS OF SOME METAL OXIDE NANOPARTICLES

3.1	Introd	action	83
3.2	Experi	mental	86
	3.2.1	Preparation of Choline chloride- urea deep eutectic solvent	86
	3.2.2	Synthesis of Copper nanoparticles in	
	3.2.3	Choline chloride- urea deep eutectic solvent Synthesis of Mercury nanoparticles in	86
		Choline chloride- urea deep eutectic solvent	87
	3.2.4	Synthesis of Manganese nanoparticles in Choline chloride- urea deep eutectic solvent	87
	3.2.5	Synthesis of Zirconium nanoparticles in	
		Choline chloride- urea deep eutectic solvent	88
	3.2.6	Synthesis of Silver nanoparticles in	
		Choline chloride- urea deep eutectic solvent	88
	3.2.7	Synthesis of Zinc nanoparticles in	
		Choline chloride- urea deep eutectic solvent	88
	3.2.8	Synthesis of Cadmium nanoparticles in	
		Choline chloride- urea deep eutectic solvent	89
	3.2.9	Synthesis of Vanadium nanoparticles in	
		Choline chloride- urea deep eutectic solvent	89
	3.2.10	Synthesis of Nickel nanoparticles in	
		Choline chloride- urea deep eutectic solvent	90
3.3	Result	s and Discussions	90
	3.3.1	UV- Visible Spectra of Metal Nanoparticles	
		prepared using Choline chloride – urea Deep	
		eutectic solvent	90
	3.3.2	FTIR Spectra of Metal Nanoparticles prepared	
		using Choline chloride – urea Deep eutectic solvent	92
	3.3.3	XRD patterns of Metal Nanoparticles prepared	
		using Choline chloride – urea Deep eutectic solvent	94

		3.3.4 S	EM analysis of Metal Nanoparticles prepared	
		u	sing Choline chloride – urea Deep eutectic solvent	96
		3.3.5 T	EM analysis of Metal Nanoparticles prepared	
		u	sing Choline chloride – urea Deep eutectic solvent	97
		3.3.6 E	EDAX analysis of Metal Nanoparticles prepared	
		u	sing Choline chloride – urea Deep eutectic solvent	98
	3.4	Conclus	ion	98
		Reference	ees	98
4	SYN	THESIS (	OF SOME METAL NANOPARTICLES USING	THE
	EFF]	ECTIVE	MEDIA OF CHOLINE CHLORIDE – ETHY	LENE
	GLY	COL DEE	CP EUTECTIC SOLVENT	
	4.1	Introduc	tion	137
	4.0	ъ.	. •	120
	4.2	Experim	ental	138
		4.2.1 P	reparation of Choline chloride- ethylene glycol	
		d	eep eutectic solvent	138
		4.2.2 S	ynthesis of Copper nanoparticles in Choline chloride-	
		e	thylene glycol deep eutectic solvent	139
		4.2.3 S	ynthesis of Mercury nanoparticles in Choline chloride-	
		e	thylene glycol deep eutectic solvent	139
		4.2.4 S	ynthesis of Manganese nanoparticles in Choline chloride	e-
		e	thylene glycol deep eutectic solvent	140
		4.2.5 S	ynthesis of Zirconium nanoparticles in Choline chloride	-
		e	thylene glycol deep eutectic solvent	140
		4.2.6 S	ynthesis of Silver nanoparticles in Choline chloride-	
		e	thylene glycol deep eutectic solvent	140
		4.2.7 S	ynthesis of Zinc nanoparticles in Choline chloride-	
		e	thylene glycol deep eutectic solvent	141
		4.2.8 S	ynthesis of Cadmium nanoparticles in Choline chloride-	
		e	thylene glycol deep eutectic solvent	141
		4.2.9 S	ynthesis of Vanadium nanoparticles in Choline chloride	-
		e	thylene glycol deep eutectic solvent	142
		4.2.10 S	ynthesis of Nickel nanoparticles in Choline chloride-	
		e	thylene glycol deep eutectic solvent	142

	4.3	Result	es and Discussions	142
		4.3.1	UV- Visible Spectra of Metal Nanoparticles prepared using	g
			Choline chloride – ethylene glycol deep eutectic solvent	143
		4.3.2	FTIR Spectra of Metal Nanoparticles prepared using	
			Choline chloride – ethylene glycol deep eutectic solvent	144
		4.3.3	XRD patterns of Metal Nanoparticles prepared using	
			Choline chloride – ethylene glycol deep eutectic solvent	145
		4.3.4	SEM analysis of Metal Nanoparticles prepared using	
			Choline chloride – ethylene glycol deep eutectic solvent	148
		4.3.5	EDAX analysis of Metal Nanoparticles prepared using	
			Choline chloride – ethylene glycol deep eutectic solvent	149
	4.4	Conc	lusion	150
		Refere	ences	151
5	CHOI	LINE	CHLORIDE - MALONIC ACID DEEP EUTEO	CTIC
	SOLV			XIDE
			TICLES	
	T 17 TT 1 /	/	. ICLED	
	5.1	Introd		183
		Introd		183 185
	5.1	Introd	uction	185
	5.1	Introd Exper	uction imental	185
	5.1	Introd Exper	uction imental Preparation of Choline chloride- Malonic acid deep eutecti	185
	5.1	Exper	uction imental Preparation of Choline chloride- Malonic acid deep eutecti solvent	185
	5.1	Exper	uction imental  Preparation of Choline chloride- Malonic acid deep eutecti solvent  Synthesis of Copper nanoparticles in Choline chloride-	185 ic 186
	5.1	Exper 5.2.1 5.2.2	uction imental  Preparation of Choline chloride- Malonic acid deep eutecti solvent  Synthesis of Copper nanoparticles in Choline chloride- Malonic acid deep eutectic solvent	185 ic 186
	5.1	Exper 5.2.1 5.2.2	reparation of Choline chloride- Malonic acid deep eutectic solvent  Synthesis of Copper nanoparticles in Choline chloride- Malonic acid deep eutectic solvent  Synthesis of Mercury nanoparticles in Choline chloride-	185 186 186
	5.1	Exper 5.2.1 5.2.2 5.2.3	preparation of Choline chloride- Malonic acid deep eutectic solvent  Synthesis of Copper nanoparticles in Choline chloride- Malonic acid deep eutectic solvent  Synthesis of Mercury nanoparticles in Choline chloride- Malonic acid deep eutectic solvent	185 186 186
	5.1	Exper 5.2.1 5.2.2 5.2.3	preparation of Choline chloride- Malonic acid deep eutectic solvent  Synthesis of Copper nanoparticles in Choline chloride- Malonic acid deep eutectic solvent  Synthesis of Mercury nanoparticles in Choline chloride- Malonic acid deep eutectic solvent  Synthesis of Manganese nanoparticles in Choline chloride-	185 cc 186 186
	5.1	Exper 5.2.1 5.2.2 5.2.3 5.2.4	preparation of Choline chloride- Malonic acid deep eutectic solvent  Synthesis of Copper nanoparticles in Choline chloride- Malonic acid deep eutectic solvent  Synthesis of Mercury nanoparticles in Choline chloride- Malonic acid deep eutectic solvent  Synthesis of Manganese nanoparticles in Choline chloride- Malonic acid deep eutectic solvent  Malonic acid deep eutectic solvent	185 cc 186 186
	5.1	Exper 5.2.1 5.2.2 5.2.3 5.2.4	Preparation of Choline chloride- Malonic acid deep eutectic solvent  Synthesis of Copper nanoparticles in Choline chloride- Malonic acid deep eutectic solvent  Synthesis of Mercury nanoparticles in Choline chloride- Malonic acid deep eutectic solvent  Synthesis of Manganese nanoparticles in Choline chloride- Malonic acid deep eutectic solvent  Synthesis of Zirconium nanoparticles in Choline chloride- Synthesis of Zirconium nanoparticles in Choline chloride-	185 cc 186 186 186
	5.1	Exper 5.2.1 5.2.2 5.2.3 5.2.4 5.2.5	Preparation of Choline chloride- Malonic acid deep eutectic solvent  Synthesis of Copper nanoparticles in Choline chloride- Malonic acid deep eutectic solvent  Synthesis of Mercury nanoparticles in Choline chloride- Malonic acid deep eutectic solvent  Synthesis of Manganese nanoparticles in Choline chloride- Malonic acid deep eutectic solvent  Synthesis of Zirconium nanoparticles in Choline chloride- Malonic acid deep eutectic solvent	185 cc 186 186 186
	5.1	Exper 5.2.1 5.2.2 5.2.3 5.2.4 5.2.5	Preparation of Choline chloride- Malonic acid deep eutectic solvent  Synthesis of Copper nanoparticles in Choline chloride- Malonic acid deep eutectic solvent  Synthesis of Mercury nanoparticles in Choline chloride- Malonic acid deep eutectic solvent  Synthesis of Manganese nanoparticles in Choline chloride- Malonic acid deep eutectic solvent  Synthesis of Zirconium nanoparticles in Choline chloride- Malonic acid deep eutectic solvent  Synthesis of Silver nanoparticles in Choline chloride- Malonic acid deep eutectic solvent	185 186 186 186 187

		5.2.8	Synthesis of Cadmium nanoparticles in Choline chloride-	
			Malonic acid deep eutectic solvent	188
		5.2.9	Synthesis of Vanadium nanoparticles in Choline chloride-	
			Malonic acid deep eutectic solvent	189
		5.2.10	Synthesis of Nickel nanoparticles in Choline chloride-	
			Malonic acid deep eutectic solvent	189
	5.3	Result	s and Discussions	190
		5.3.1	UV- Visible Spectra of Metal Nanoparticles prepared using	
			Choline chloride – Malonic acid deep eutectic solvent	190
		5.3.2	FTIR Spectra of Metal Nanoparticles prepared using	
			Choline chloride – Malonic acid deep eutectic solvent	191
		5.3.3	XRD patterns of Metal Nanoparticles prepared using	
			Choline chloride – Malonic acid deep eutectic solvent	193
		5.3.4	SEM analysis of Metal Nanoparticles prepared using	
			Choline chloride – Malonic acid deep eutectic solvent	196
		5.3.5	EDAX analysis of Metal Nanoparticles prepared using	
			Choline chloride – Malonic acid deep eutectic solvent	197
	5.4	Conclu	asion	197
		Refere	ences	198
6	SUMN	MARY	AND CONCLUSION	
	6.1	Summ	ary and Conclusion	230
	6.2	Future	perspective of the work	232
		List of	articles published in the UGC listed SCOPUS indexed Peer	-
		review	ved Journals	233
		List of	Papers Presented in the National and International Conferen	ices
				233

### **List of Tables**

Table No	Name of the Table Page	No
2.1	Chemicals used for the investigation	73
2.2.2	Prepared DES	75
3.1	UV-Visible absorption bands of metal oxide	
	nanoparticles obtained from ChCl- U DES	91
3.2	FTIR Absorption peaks of metal oxide nanoparticles obta	ined
	from ChCl- U DES	93
3.3	SEM morphology and size of metal oxide nanoparticles	
	obtained from ChCl- U DES	97
4.1	UV-Visible absorption bands of metal oxide nanoparticle	S
	obtained from ChCl- EG DES	143
4.2	FTIR Absorption peaks of metal oxide nanoparticles	
	obtained from ChCl- EG DES	145
4.3	SEM morphology and size of metal oxide nanoparticles	
	btained from ChCl- EG DES	149
5.1	UV-Visible absorption bands of metal oxide nanoparticle	s
	obtained from ChCl- MA DES	191
5.2	FTIR Absorption peaks of metal oxide nanoparticles obta	ined
	from ChCl- MA DES	192
5.3	SEM morphology and size of metal oxide nanoparticles	
	obtained from ChCl- MA DES	196
6.1	Size and morphology of the metal oxide nanoparticles	
	prepared from deep eutectic solvents	230
6.2	Weight and Atom % of metals present in the metal oxide	
	nanoparticles obtained in the DES media	231

### **List of Figures**

Figure No	Name of the Figure Page	No
3.1	UV- Visible spectrum of Copper oxide Nanoparticles	
3.1	obtained in ChCl-U DES	104
3.2		104
3.2	UV- Visible spectrum of Mercury oxide Nanoparticles obtained in ChCl-U DES	104
3.3	UV- Visible spectrum of Manganese oxide Nanoparticles	104
3.3	obtained in ChCl-U DES	105
3.4	UV- Visible spectrum of Zirconium oxide Nanoparticles	103
3.4	obtained in ChCl-U DES	105
3.5	UV- Visible spectrum of Silver oxide Nanoparticles	103
3.3	obtained in ChCl-U DES	106
3.6	UV- Visible spectrum of Zinc oxide Nanoparticles	100
3.0	obtained in ChCl-U DES	106
3.7	UV- Visible spectrum of Cadmium oxide Nanoparticles	100
3.1	obtained in ChCl-U DES	107
3.8	UV- Visible spectrum of Vanadium oxide Nanoparticles	107
3.0	obtained in ChCl-U DES	107
3.9	UV- Visible spectrum of Nickel oxide Nanoparticles	107
3.9	obtained in ChCl-U DES	108
3.10	FTIR spectrum of Copper oxide Nanoparticles	100
3.10	obtained in ChCl-U DES	108
3.11	FTIR spectrum of Mercury oxide Nanoparticles	100
5.11	obtained in ChCl-U DES	109
3.12	FTIR spectrum of Manganese oxide Nanoparticles	109
3.12	obtained in ChCl-U DES	109
3.13	FTIR spectrum of Zirconium oxide Nanoparticles	10)
5.15	obtained in ChCl-U DES	110
3.14	FTIR spectrum of Silver oxide Nanoparticles	110
J.1 <del>1</del>	ohtained in ChCl-II DES	110
	10000000000000000000000000000000000000	

3.15	FTIR spectrum of Zinc oxide Nanoparticles	
	obtained in ChCl-U DES	111
3.16	FTIR spectrum of Cadmium oxide Nanoparticles	
	obtained in ChCl-U DES	111
3.17	FTIR spectrum of Vanadium oxide Nanoparticles	
	obtained in ChCl-U DES	112
3.18	FTIR spectrum of Nickel oxide Nanoparticles	
	obtained in ChCl-U DES	112
3.19	XRD pattern of Copper oxide Nanoparticles	
	obtained in ChCl-U DES	113
3.20	XRD pattern of Mercury oxide Nanoparticles	
	obtained in ChCl-U DES	113
3.21	XRD pattern of Manganese oxide Nanoparticles	
	obtained in ChCl-U DES	114
3.22	XRD pattern of Zirconium oxide Nanoparticles	
	obtained in ChCl-U DES	114
3.23	XRD pattern of Silver oxide Nanoparticles	
	obtained in ChCl-U DES	115
3.24	XRD pattern of Zinc oxide Nanoparticles	
	obtained in ChCl-U DES	115
3.25	XRD pattern of Cadmium oxide Nanoparticles	
	obtained in ChCl-U DES	116
3.26	XRD pattern of Vanadium oxide Nanoparticles	
	obtained in ChCl-U DES	116
3.27	XRD pattern of Nickel oxide Nanoparticles	
	obtained in ChCl-U DES	117
3.28	SEM image of Copper oxide Nanoparticles	
	obtained in ChCl-U DES	117
3.29	SEM image of Mercury oxide Nanoparticles	
	obtained in ChCl-U DES	118
3.30	SEM image of Manganese oxide Nanoparticles	
	obtained in ChCl-U DES	118
3.31	SEM image of Zirconium oxide Nanoparticles	
	obtained in ChCl-U DES	119

3.32	SEM image of Silver oxide Nanoparticles	
	obtained in ChCl-U DES	119
3.33	SEM image of Zinc oxide Nanoparticles	
	obtained in ChCl-U DES	120
3.34	SEM image of Cadmium oxide Nanoparticles	
	obtained in ChCl-U DES	120
3.35	SEM image of Vanadium oxide Nanoparticles	
	obtained in ChCl-U DES	121
3.36	SEM image of Nickel oxide Nanoparticles	
	obtained in ChCl-U DES	121
3.37	SEM Histogram of Copper oxide Nanoparticles	
	obtained in ChCl-U DES	122
3.38	SEM Histogram of Mercury oxide Nanoparticles	
	obtained in ChCl-U DES	122
3.39	SEM Histogram of Manganese oxide Nanoparticles	
	obtained in ChCl-U DES	123
3.40	SEM Histogram of Zirconium oxide Nanoparticles	
	obtained in ChCl-U DES	123
3.41	SEM Histogram of Silver oxide Nanoparticles	
	obtained in ChCl-U DES	124
3.42	SEM Histogram of Zinc oxide Nanoparticles	
	obtained in ChCl-U DES	124
3.43	SEM Histogram of Cadmium oxide Nanoparticles	
	obtained in ChCl-U DES	125
3.44	SEM Histogram of Vanadium oxide Nanoparticles	
	obtained in ChCl-U DES	125
3.45	SEM Histogram of Nickel oxide Nanoparticles	
	obtained in ChCl-U DES	126
3.46	TEM image of Copper oxide Nanoparticles	
	obtained in ChCl-U DES	126
3.47	TEM image of Mercury oxide Nanoparticles	
	obtained in ChCl-U DES	127
3.48	TEM image of Manganese oxide Nanoparticles	
	obtained in ChCl-U DES	127

3.49	TEM image of Zirconium oxide Nanoparticles	
	obtained in ChCl-U DES	128
3.50	TEM image of Silver oxide Nanoparticles	
	obtained in ChCl-U DES	128
3.51	TEM image of Zinc oxide Nanoparticles	
	obtained in ChCl-U DES	129
3.52	TEM image of Cadmium oxide Nanoparticles	
	obtained in ChCl-U DES	129
3.53	TEM image of Vanadium oxide Nanoparticles	
	obtained in ChCl-U DES	130
3.54	TEM image of Nickel oxide Nanoparticles	
	obtained in ChCl-U DES	130
3.55	EDAX spectrum of Copper oxide Nanoparticles	
	obtained in ChCl-U DES	131
3.56	EDAX spectrum of Mercury oxide Nanoparticles	
	obtained in ChCl-U DES	131
3.57	EDAX spectrum of Manganese oxide Nanoparticles	
	obtained in ChCl-U DES	132
3.58	EDAX spectrum of Zirconium oxide Nanoparticles	
	obtained in ChCl-U DES	132
3.59	EDAX spectrum of Silver oxide Nanoparticles	
	obtained in ChCl-U DES	133
3.60	EDAX spectrum of Zinc oxide Nanoparticles	
	obtained in ChCl-U DES	133
3.61	EDAX spectrum of Cadmium oxide Nanoparticles	
	obtained in ChCl-U DES	134
3.62	EDAX spectrum of Vanadium oxide Nanoparticles	
	obtained in ChCl-U DES	134
3.63	EDAX spectrum of Nickel oxide Nanoparticles	
	obtained in ChCl-U DES	135
4.1	UV – Visible spectrum of Copper oxide Nanoparticles	
	obtained in ChCl- EG DES	155
4.2	UV – Visible spectrum of Mercury oxide Nanoparticles	
	obtained in ChCl- EG DES	155

4.3	UV – Visible spectrum of Manganese oxide Nanoparticles	
	obtained in ChCl- EG DES	156
4.4	UV – Visible spectrum of Zirconium oxide Nanoparticles	
	obtained in ChCl- EG DES	156
4.5	UV – Visible spectrum of Silver oxide Nanoparticles	
	obtained in ChCl- EG DES	157
4.6	UV – Visible spectrum of Zinc oxide Nanoparticles	
	obtained in ChCl- EG DES	157
4.7	UV – Visible spectrum of Cadmium oxide Nanoparticles	
	obtained in ChCl- EG DES	158
4.8	UV – Visible spectrum of Vanadium oxide Nanoparticles	
	obtained in ChCl- EG DES	158
4.9	UV – Visible spectrum of Nickel oxide Nanoparticles	
	obtained in ChCl- EG DES	159
4.10	FTIR spectrum of Copper oxide Nanoparticles	
	obtained in ChCl- EG DES	159
4.11	FTIR spectrum of Mercury oxide Nanoparticles	
	obtained in ChCl- EG DES	160
4.12	FTIR spectrum of Manganese oxide Nanoparticles	
	obtained in ChCl- EG DES	160
4.13	FTIR spectrum of Zirconium oxide Nanoparticles	
	obtained in ChCl- EG DES	161
4.14	FTIR spectrum of Silver oxide Nanoparticles	
	obtained in ChCl- EG DES	161
4.15	FTIR spectrum of Zinc oxide Nanoparticles	
	obtained in ChCl- EG DES	162
4.16	FTIR spectrum of Cadmium oxide Nanoparticles	
	obtained in ChCl- EG DES	162
4.17	FTIR spectrum of Vanadium oxide Nanoparticles	
	obtained in ChCl- EG DES	163
4.18	FTIR spectrum of Nickel oxide Nanoparticles	
	obtained in ChCl- EG DES	163
4.19	XRD pattern of Copper oxide Nanoparticles	
	obtained in ChCl- EG DES	164

4.20	XRD pattern of Mercury oxide Nanoparticles	
	obtained in ChCl- EG DES	164
4.21	XRD pattern of Manganese oxide Nanoparticles	
	obtained in ChCl- EG DES	165
4.22	XRD pattern of Zirconium oxide Nanoparticles	
	obtained in ChCl- EG DES	165
4.23	XRD pattern of Silver oxide Nanoparticles	
	obtained in ChCl- EG DES	166
4.24	XRD pattern of Zinc oxide Nanoparticles	
	obtained in ChCl- EG DES	166
4.25	XRD pattern of Cadmium oxide Nanoparticles	
	obtained in ChCl- EG DES	167
4.26	XRD pattern of Vanadium oxide Nanoparticles	
	obtained in ChCl- EG DES	167
4.27	XRD pattern of Nickel oxide Nanoparticles	
	obtained in ChCl- EG DES	168
4.28	SEM image of Copper oxide Nanoparticles	
	obtained in ChCl- EG DES	168
4.29	SEM image of Mercury oxide Nanoparticles	
	obtained in ChCl- EG DES	169
4.30	SEM image of Manganese oxide Nanoparticles	
	obtained in ChCl- EG DES	169
4.31	SEM image of Zirconium oxide Nanoparticles	
	obtained in ChCl- EG DES	170
4.32	SEM image of Silver oxide Nanoparticles	
	obtained in ChCl- EG DES	170
4.33	SEM image of Zinc oxide Nanoparticles	
	obtained in ChCl- EG DES	171
4.34	SEM image of Cadmium oxide Nanoparticles	
	obtained in ChCl- EG DES	171
4.35	SEM image of Vanadium oxide Nanoparticles	
	obtained in ChCl- EG DES	172
4.36	SEM image of Nickel oxide Nanoparticles	
	obtained in ChCl- EG DES	172

4.37	SEM Histogram of Copper oxide Nanoparticles	
	obtained in ChCl- EG DES	173
4.38	SEM Histogram of Mercury oxide Nanoparticles	
	obtained in ChCl- EG DES	173
4.39	SEM Histogram of Manganese oxide Nanoparticles	
	obtained in ChCl- EG DES	174
4.40	SEM Histogram of Zirconium oxide Nanoparticles	
	obtained in ChCl- EG DES	174
4.41	SEM Histogram of Silver oxide Nanoparticles	
	obtained in ChCl- EG DES	175
4.42	SEM Histogram of Zinc oxide Nanoparticles	
	obtained in ChCl- EG DES	175
4.43	SEM Histogram of Cadmium oxide Nanoparticles	
	obtained in ChCl- EG DES	176
4.44	SEM Histogram of Vanadium oxide Nanoparticles	
	obtained in ChCl- EG DES	176
4.45	SEM Histogram of Nickel oxide Nanoparticles	
	obtained in ChCl- EG DES	177
4.46	EDAX spectrum of Copper oxide Nanoparticles	
	obtained in ChCl- EG DES	177
4.47	EDAX spectrum of Mercury oxide Nanoparticles	
	obtained in ChCl- EG DES	178
4.48	EDAX spectrum of Manganese oxide Nanoparticles	
	obtained in ChCl- EG DES	178
4.49	EDAX spectrum of Zirconium oxide Nanoparticles	
	obtained in ChCl- EG DES	179
4.50	EDAX spectrum of Silver oxide Nanoparticles	
	obtained in ChCl- EG DES	179
4.51	EDAX spectrum of Zinc oxide Nanoparticles	
	obtained in ChCl- EG DES	180
4.52	EDAX spectrum of Cadmium oxide Nanoparticles	
	obtained in ChCl- EG DES	180
4.53	EDAX spectrum of Vanadium oxide Nanoparticles	
	obtained in ChCl- EG DES	181

4.54	EDAX spectrum of Nickel oxide Nanoparticles	
	obtained in ChCl- EG DES	181
5.1	UV-Visible spectrum of Copper oxide Nanoparticles	
	obtained in ChCl- MA DES	202
5.2	UV-Visible spectrum of Mercury oxide Nanoparticles	
	obtained in ChCl- MA DES	202
5.3	UV-Visible spectrum of Manganese oxide Nanoparticles	
	obtained in ChCl- MA DES	203
5.4	UV-Visible spectrum of Zirconium oxide Nanoparticles	
	obtained in ChCl- MA DES	203
5.5	UV-Visible spectrum of Silver oxide Nanoparticles	
	obtained in ChCl- MA DES	204
5.6	UV-Visible spectrum of Zinc oxide Nanoparticles	
	obtained in ChCl- MA DES	204
5.7	UV-Visible spectrum of Cadmium oxide Nanoparticles	
	obtained in ChCl- MA DES	205
5.8	UV-Visible spectrum of Vanadium oxide Nanoparticles	
	obtained in ChCl- MA DES	205
5.9	UV-Visible spectrum of Nickel oxide Nanoparticles	
	obtained in ChCl- MA DES	206
5.10	FTIR spectrum of Copper oxide Nanoparticles	
	obtained in ChCl- MA DES	206
5.11	FTIR spectrum of Mercury oxide Nanoparticles	
	obtained in ChCl- MA DES	207
5.12	FTIR spectrum of Manganese oxide Nanoparticles	
	obtained in ChCl- MA DES	207
5.13	FTIR spectrum of Zirconium oxide Nanoparticles	
	obtained in ChCl- MA DES	208
5.14	FTIR spectrum of Silver oxide Nanoparticles	
	obtained in ChCl- MA DES	208
5.15	FTIR spectrum of Zinc oxide Nanoparticles	
	obtained in ChCl- MA DES	209
5.16	FTIR spectrum of Cadmium oxide Nanoparticles	
	obtained in ChCl- MA DES	209

5.17	FTIR spectrum of Vanadium oxide Nanoparticles	
	obtained in ChCl- MA DES	210
5.18	FTIR spectrum of Nickel oxide Nanoparticles	
	obtained in ChCl- MA DES	210
5.19	XRD pattern of Copper oxide Nanoparticles	
	obtained in ChCl- MA DES	211
5.20	XRD pattern of Mercury oxide Nanoparticles	
	obtained in ChCl- MA DES	211
5.21	XRD pattern of Manganese oxide Nanoparticles	
	obtained in ChCl- MA DES	212
5.22	XRD pattern of Zirconium oxide Nanoparticles	
	obtained in ChCl- MA DES	212
5.23	XRD pattern of Silver oxide Nanoparticles	
	obtained in ChCl- MA DES	213
5.24	XRD pattern of Zinc oxide Nanoparticles	
	obtained in ChCl- MA DES	213
5.25	XRD pattern of Cadmium oxide Nanoparticles	
	obtained in ChCl- MA DES	214
5.26	XRD pattern of Vanadium oxide Nanoparticles	
	obtained in ChCl- MA DES	214
5.27	XRD pattern of Nickel oxide Nanoparticles	
	obtained in ChCl- MA DES	215
5.28	SEM image of Copper oxide Nanoparticles	
	obtained in ChCl- MA DES	215
5.29	SEM image of Mercury oxide Nanoparticles	
	obtained in ChCl- MA DES	216
5.30	SEM image of Manganese oxide Nanoparticles	
	obtained in ChCl- MA DES	216
5.31	SEM image of Zirconium oxide Nanoparticles	
	obtained in ChCl- MA DES	217
5.32	SEM image of Silver oxide Nanoparticles	
	obtained in ChCl- MA DES	217
5.33	SEM image of Zinc oxide Nanoparticles	
	obtained in ChCl- MA DES	218

5.34	SEM image of Cadmiuim oxide Nanoparticles	
	obtained in ChCl- MA DES	218
5.35	SEM image of Vanadium oxide Nanoparticles	
	obtained in ChCl- MA DES	219
5.36	SEM image of Nickel oxide Nanoparticles	
	obtained in ChCl- MA DES	219
5.37	SEM Histogram of Copper oxide Nanoparticles	
	obtained in ChCl- MA DES	220
5.38	SEM Histogram of Mercury oxide Nanoparticles	
	obtained in ChCl- MA DES	220
5.39	SEM Histogram of Manganese oxide Nanoparticles	
	obtained in ChCl- MA DES	221
5.40	SEM Histogram of Zirconium oxide Nanoparticles	
	obtained in ChCl- MA DES	221
5.41	SEM Histogram of Silver oxide Nanoparticles	
	obtained in ChCl- MA DES	222
5.42	SEM Histogram of Zinc oxide Nanoparticles	
	obtained in ChCl- MA DES	222
5.43	SEM Histogram of Cadmium oxide Nanoparticles	
	obtained in ChCl- MA DES	223
5.44	SEM Histogram of Vanadium oxide Nanoparticles	
	obtained in ChCl- MA DES	223
5.45	SEM Histogram of Nickel oxide Nanoparticles	
	obtained in ChCl- MA DES	224
5.46	EDAX spectrum of Copper oxide Nanoparticles	
	obtained in ChCl- MA DES	224
5.47	EDAX spectrum of Mercury oxide Nanoparticles	
	obtained in ChCl- MA DES	225
5.48	EDAX spectrum of Manganese oxide Nanoparticles	
	obtained in ChCl- MA DES	225
5.49	EDAX spectrum of Zirconium oxide Nanoparticles	
	obtained in ChCl- MA DES	226
5.50	EDAX spectrum of Silver oxide Nanoparticles	
	obtained in ChCl- MA DES	226

5.51	EDAX spectrum of Zinc oxide Nanoparticles	
	obtained in ChCl- MA DES	227
5.52	EDAX spectrum of Cadmium oxide Nanoparticles	
	obtained in ChCl- MA DES	227
5.53	EDAX spectrum of Vanadium oxide Nanoparticles	
	obtained in ChCl- MA DES	228
5.54	EDAX spectrum of Nickel oxide Nanoparticles	
	obtained in ChCl- MA DES	228

### LIST OF ABBREVIATIONS

DESs : Deep Eutectic Solvents

ILs : Ionic liquids

SDA : Structure Directing Agent

HBD : Hydrogen Bond Donor

HBA : Hydrogen Bond Acceptor

PMB : Poly (Methylene Blue)

ChCl : Choline Chloride

EG : Ethylene Glycol

MA : Malonic Acid

GCEs : Glassy Carbon Electrodes

MWCNTs : Multiwalled Carbon Nanotubes

NADES : Natural Deep Eutectic Solvents

DEILs : Deep Eutectic Ionic Liquids

MNPs : Metal Nanoparticles

LMMs : Low Melting Mixtures

AgNPs : Silver Nanoparticles

CuNPs : Copper Nanoparticles

HgNPs : Mercury Nanoparticles

CdNPs : Cadmium Nanoparticles

MnNPs : Manganese Nanoparticles

ZrNPs : Zirconium Nanoparticles

VNPs : Vanadium Nanoparticles

ZnNPs : Zinc Nanoparticles

NiNPs : Nickel Nanoparticles

UV : Ultraviolet-Visible Spectroscopy

FTIR : Fourier Transform Infrared Spectroscopy

SEM : Scanning Electron Microscopy

TEM : Transmission Electron Microscopy

XRD : X-Ray Diffractometer

EDAX : Energy Dispersive X-Ray Analysis

T<sub>f</sub> Freezing Temperature

### 1. INTRODUCTION

### 1.1. GENERAL INTRODUCTION TO DEEP EUTECTIC SOLVENTS

In this investigation, researchers mostly concentrated on the development of ionic liquids by blending metal salts, chiefly Zinc, Aluminium, Tin, and Iron chlorides, with quaternary ammonium salts. Although both salts have very high melting points, their decent blending provided the production of a liquid phase known as eutectic mixtures are usually characterized by a large depression of freezing point, probably higher than 150°C. After the introduction of the interpretation of green chemistry at the beginning of the 1990s, the inquiry for metal-free ionic liquids (ILs) has developed of spreading significance <sup>[1]</sup>. Since the prospective for new chemical technology was recognized two decades ago, research into ionic liquids (ILs) has exploded. During the previous two decennia, ionic liquids (ILs) have a noticeable effect, particularly in the fields of catalysis, electrochemistry, material chemistry, and new for the pre-treatment of biomes <sup>[2-4]</sup>

The ionic liquids (IL) play a noteworthy role recently in chemical applications because of their recognized physicochemical properties such as low toxicity, indistinct vapor pressure, high solubility, and their existence in the liquid state [5-7] over a wide range of temperatures. Due to these reasons ionic liquids are commonly used as solvents in chemical laboratories and for industrial processes such as CO<sub>2</sub> capture [8-10], extraction [9] and biomedical applications [9] battery development [11-12], electrochemical applications [13] and biocatalysts [14-15], organic synthesis [16], material synthesis [17].In this chapter, enormous works were carried to the improvement of Ionic Liquids by adding an organic cation (normally imidazolium-based cations) with a huge kind of anions, the most frequent ones being Cl<sub>2</sub>, BF<sub>4</sub>, PF<sub>6</sub>. From that point in time, ionic liquids have developed as innovative types of promising solvents. The chance to change chemically the cationic

moiety in a mixture with a large choice of anions offers researchers a wide range of ionic liquids showing various physical properties such as melting point, solubility, viscosity, density, conductivity, and refractivity. For example, Seddon and co-workers have reported that 1018 different ionic liquids can be theoretically produced in 2009. Among them, 250 ionic liquids were already commercialized [18]. Due to their low vapour pressure and high boiling point, they are eco-friendly and thus ionic liquids (ILs) were accepted as green solvents.

Many reports mentioned the harmful toxicity and the poor biodegradability of most ILs as reported by Romero et.al <sup>[19]</sup>. ILs with very high purity is mandatory since impurities even in little amounts change their physical properties. In addition, their synthesis is fair to be eco-friendly since it generally requires many salts and solvents to exchange the anions completely. Unfortunately, these drawbacks altogether with the high price of common ILs, slow down their industrial materialization. Thus, new concepts are now strongly desired to develop these systems in a more balanced way.

Qinghua Zhang et al. reported that to surmount the high price and toxicity of ILs, an invention of solvent, named Deep Eutectic Solvents (DES) [20], have emerged at the early stage of this century. Production of these DESs can be obtained by simple mixing of two safe components (cheap, renewable, and biodegradable), which has the capability of forming a eutectic mixture. One of the most common components used for the formation of these DESs is choline chloride (ChCl). Choline chloride is a very cheap, biodegradable, and non-toxic quaternary ammonium salt that can be either extracted from biomass or readily synthesized from fossil reserves (million metric tons) through a very high atom economy process. In combination with safe hydrogen bond donors such as urea, renewable carboxylic acids (e.g., oxalic, citric, succinic,oraminoacids) or renewable polyols (e.g., glycerol, carbohydrates), ChCl is capable of rapidly forming a

DES. Although most of DESs are made from ChCl as an ionic species, DESs cannot be considered as ILs due to two reasons. Firstly, DESs are not fully composed of ionic species and secondly, can also be obtained from non-ionic species.

When compared with the usual ionic liquids, deep eutectic solvents obtained from ChCl draw together many advantages as listed below.

- 1. Less Expensive
- 2. High inertness with water (i.e., safe, and easy storage)
- 3. Easy to synthesize since DESs are obtained by simply mixing two components, thus overcoming all problems of purification and waste disposal generally encountered with ILs.
- 4. Most of them are biodegradable <sup>[21]</sup>, biocompatible <sup>[22]</sup> and non-toxic <sup>[23]</sup>, reinforcing the greenness of these media <sup>[24]</sup> as reported by Y. Yu et al., K. D Weaver et al., F. Ilegan, et al., D. Reinhardt.

Cooper et al. <sup>[25]</sup> first announced another sort of solvothermal combination in which ILs were utilized as both the solvent and the structure-directing agent (SDA) in the blend of zeolites. This approach has been named ionothermal synthesis and, since this original work, has gotten perhaps the most broadly utilized synthetic strategies among the zeolite area. Curiously, it was likewise reached out to the preparation of not just other open-system structures metal—natural systems, covalent—natural structures or polymer—natural systems among others—yet in addition periodic mesoporous silica and organosilica. While perceiving the enormous concepts in this theme, the focal point of this audit won't be on the utilization of ILs helped synthetic measures for the readiness of open-system structures, on the grounds that there are now excellent reviews and books that cover most of the new advances here <sup>[26]</sup>.

Physico-chemical properties of DESs (density, viscosity, refractive index, conductivity, surface tension, chemical inertness, etc.) are very close to those of common ILs. For this reason, DESs derived from ChCl are named "biocompatible" or "renewable" ionic liquids in a few studies. Due to their low environmental path and attractive price, DESs have now become of rising interest both at intellectual and manufacturing levels. The number of publications dedicated to the use of DESs is now rapidly growing in the present literature and further indicating the magnetism of these media.

### 1.2. DEEP EUTECTIC SOLVENTS-DEFINITION

A Deep Eutectic Solvent is commonly a combination of two or three cheap and safe components which can blend with each other, through hydrogen bond interactions, to form a eutectic mixture. The prepared DES is characterized by a melting point lower than that of the individual component. Generally, DESs are characterized by a huge depression of freezing point and are liquid at temperatures lower than 150°C. Most of them are liquids between room temperature and 70°C. In most cases, mixing of a quaternary ammonium salt with a metal salts or a hydrogen bond donor (HBD) that can form a complex with the halide anion of the quaternary ammonium salts a DES is obtained. Large, nonsymmetric ions with low lattice energy and thus low melting points are found in DESs. A quaternary ammonium salt is normally complexed with a metal salt or a hydrogen bond donor (HBD) to prepare DES. The decrease in the melting point of the mixture compared to the melting points of the individual components is due to charge delocalization caused by hydrogen bonding between, for example, a halide ion and the hydrogen-donor moiety. Scheme 1 summarizes the different quaternary ammonium salts that are broadly used in combination with various HBDs in the formation of DESs.

# Halide Salts Hydrogen bond donors Halide Salts Hydrogen bond donors Hydrogen bond donors

Scheme 1: Typical structures of the halide salts and hydrogen bond donors used for DES syntheses

In 2007, Abbott and co-workers defined DESs using the general formula  $R_1$   $R_2$   $R_3$   $R_4$   $N^+$   $X^ Y^{-[27]}$ .

Type1: DES Y=MCl<sub>x</sub>, M=Zn, Sn, Fe, Al, Ga,

Type2: DES Y=MCl<sub>x</sub>. <sub>y</sub>H<sub>2</sub>O, M=Cr, Co, Cu, Ni, Fe

Type3: DES Y= RZ with Z=-CONH<sub>2</sub>, -COOH, -OH

The same group also defined a fourth type of DES which is composed of metal chlorides (e.g., ZnCl<sub>2</sub>mixed with different HBDs such as urea, ethylene glycol, acetamide or hexanediol (Type 4 DES).

Recently, deep eutectic solvents (DES) have emerged as the alternatives for ionic liquids at room temperature. Deep eutectic solvents commonly indicate a mixture of a halide salt and a hydrogen bond donor (HBD) to give a liquid below 100°C. The amazing qualities such as acceptance to humidity, non-combustible due to irrelevant vapour pressure, stability at high temperature, cheap, non-hazardous, reusable and recyclable [28] natures of DES make them replace ionic liquids.

### 1.3. PHYSICOCHEMICAL PROPERTIES OF DEEP EUTECTIC SOLVENTS

DESs are chemically modified solvents since they can be planned by properly combining various quaternary ammonium salts (e.g., ChCl) with different hydrogen bond donors (HBD). Hence, task-specific DESs with different physicochemical properties such as freezing point, viscosity, conductivity, and pH, among others, can be identified. Due to their potential applications, many works have been committed to the physicochemical characterization of DESs.

### **1.3.1** Freezing point (T<sub>f</sub>)

We know DESs are formed by mixing two solids capable of generating a new liquid phase by self-combination through hydrogen bonds. This new phase is generally characterized by a lower freezing point than that of individual components. For example, when ChCl and urea are mixed in a molar ratio of 1:2, the freezing point of the eutectic mixture is 12°C, which is considerably lower than that of ChCl and urea (melting point of ChCland urea are 302 and 133°C, respectively). The significant depression of the freezing point shows from an interaction between the halide anion and the hydrogen bond donor component, here urea. For all reported DESs, their freezing points are below 150°C. In general, DESs with a freezing point lower than 50°C are more attractive since they can be used as economical and eco-friendly solvents in many fields.

### **1.3.2. Density**

The density is one of the most vital physical properties of solvents. In general densities of DESs are calculated by means of a specific gravity meter. Most of DESs show higher densities than water. For instance, type IV ZnCl<sub>2</sub>-HBD eutectic mixtures have densities higher than 1.3 g cm<sup>-3</sup>. Among them, density of ZnCl<sub>2</sub>-urea (1:3.5) and ZnCl<sub>2</sub>-acetamide (1:4) are different (1.63 and 1.36 g cm<sup>-3</sup>, respectively. This significant difference in density might be attributed to a different molecular group or packing of the DES. Note that densities of both DESs are higher than those of pure HBDs (acetamide: 1.16 and urea: 1.32g cm<sup>-3</sup>). This phenomenon may be explained by the hole theory. Like imidazolium-based ILs, DESs are composed of holes or empty vacancies. When ZnCl<sub>2</sub> was mixed with urea, for instance, the average hole radius was decreased, resulting in a slight increase of the DES density as compared to that of urea [27].

### 1.3.3. Viscosity

Like most of the ILs, the viscosity of DESs is a significant topic that needs to be concerned. Except for the ChCl-ethylene glycol (EG) eutectic mixture, most of the DESs exhibit relatively high viscosities (>100cP) at room temperature. The high viscosity of DESs is often accepted to the presence of an extensive hydrogen bond system between each component, which results in lower mobility of free species within the DES. The large ion size and very small void volume of most DESs but also other forces such as electrostatic or Vander Waals interaction may contribute to the high viscosity of DES.Owing to their potential applications as green media, the development of DESs with low viscosities is highly enviable. In general, viscosities of eutectic mixtures are mainly exaggerated by the chemical nature of the DES components (type of the ammonium salts and HBDs, organic salt/HBD molar ratio, etc.), the temperature, and the water content. As discussed above, the viscosity of DES is also dependent on the

free volume. Hence, the hole theory can also be used to design DESs with low viscosities. For example, the use of small cations or fluorinated hydrogen-bond donors can lead to the formation of DES with low viscosity [29].

### 1.3.4. Ionic conductivity

Due to their comparatively high viscosities, most of DESs show poor ionic /conductivities (lower than 2 mS cm<sup>-1</sup> at room temperature). Conductivities of DESs generally increase noticeably as the temperature increases due to a decrease in the DES viscosity. Hence, the Arrhenius-like equation can also be used to calculate the conductivity behaviour of DESs. Taking into explanation the changes of the organic salt/HBD molar ratio greatly impact the viscosities of DES, this factor also radically influences the conductivities of DESs [30].

### 1.3.5 Acidity or Alkalinity

The Hammett function has been broadly used to calculate the acidity and basicity of non-aqueous solvents by determining the ionization ratio of indicators in a system. For a basic solution, the Hammett function shows the affinity of the solution to attracting protons. When weak acids are selected as indicators, the Hammett function His defined by the following equation.

$$H^{+}= pK (HI) + log([I^{-}] / [HI])$$

Where pK (HI) is the thermodynamic ionization constant of the indicator in water, [I<sup>-</sup>] and [HI] represent the molar concentrations of anionic and neutral forms of the indicator respectively. A medium with a largeH<sup>+</sup>valuehas strong basicity. Note that when the system contains 1-3wt% of water, the Hvalues decreases somewhat due to partial solvation of basic sites <sup>[31]</sup>.

### 1.4. DEEP EUTECTIC SOLVENTS (DES)

Deep eutectic solvents are eutectic mixtures of Lewis or Bronsted acids and bases that can contain a wide range of anionic and cationic species <sup>[32]</sup>. They are categorized as ionic solvents with unique properties. The combination of two compounds forms a eutectic with a melting point that is much lower than any of the individual components <sup>[33]</sup>.

A 1:2 mole ratio of choline chloride and urea created one of the most important deep eutectic phenomena ever observed. The resulting mixture has a melting point of 12 °C (much lower than choline chloride's melting point of 302 °C or urea's melting point of 133 °C), making it liquid at room temperature [34].

The first generation of eutectic solvents is composed of quaternary ammonium salts coupled with hydrogen bond donors including amines and carboxylic acids [35].

### **1.4.1 Types of Deep Eutectic Solvents:**

Eutectic solvents are divided into four categories:

Types of DES	Components
Type I	Quaternary ammonium salt + metal chloride
Type II	Quaternary ammonium salt + metal chloride hydrate
Type III	Quaternary ammonium salt + hydrogen bond donor
Type IV	Metal chloride hydrate + hydrogen bond donor

DES has a low density and can be liquid at a wide range of temperatures, up to -50 °C in some cases <sup>[36]</sup>. DESs are much less costly to manufacture and are often biodegradable. As a result, DES can be used as a solvent that is safe, efficient, simple, and inexpensive <sup>[37]</sup>. Deep eutectic solvent (DES) is a fluid made up of two inexpensive and harmless components that can self-associate, usually by hydrogen bond interactions, to

form a eutectic mixture with a melting point lower than the melting point of each component individually as reported by Zhang et al <sup>[20]</sup>.

For the first time, binary and ternary deep eutectic solvent (DES) mixtures based on choline chloride, ethylene glycol, oxalic acid, urea, and fructose were used as a medium for electro polymerized of poly(methylene blue) (PMB) on glassy carbon electrodes (GCEs) and GCEs changed with multiwalled carbon nanotubes (MWCNTs) as reported by Lucía Abad-Gil et al<sup>[38]</sup>.

The use of DESs and NADESs in biofuel <sup>[39, 40–42]</sup> and bio-oil extraction <sup>[43, 44]</sup>, as reaction media or extractive factors <sup>[45]</sup>, and as media to control intermolecular interactions <sup>[46]</sup> as one of broad lists of applications <sup>[20, 47, 48]</sup>.

## 1.5 CHOLINE CHLORIDE – UREA BASED DEEP EUTECTIC SOLVENTS

A broad spectrum of amides had been combined with choline chloride (ChCl) to produce DESs with a freezing point lower than 100°C. Among them, urea is capable of forming a liquid DES with ChCl at room temperature, apparently due to their stronger ability to form hydrogen bond interactions with ChCl. The freezing point (T<sub>f</sub>) of this 1:2 molar ratio, ChCl-Urea was reported as 12 °C <sup>[49]</sup>. A simple route for the shape-controlled synthesis of gold NPs utilizing ChCl/urea DES which replaced traditional surfactants <sup>[50]</sup>, and the synthesis of gold nanowire from direct reduction of HAuCl<sub>4</sub> by NaBH <sub>4</sub> in DES <sup>[52]</sup> explicitly showed the advantages of eliminating surfactants or seeds for the preparation of nonmaterial when DESs are used. In the latter synthesis, two different DESs, i.e. ChCl/ethylene glycol (1: 2) or ChCl/urea (1: 2), were employed in the absence of a surfactant. The formation of nanoparticles of various shapes and surfaces was controlled by adjusting the water content of the DES <sup>[51]</sup>. These DESs are treated as an effective medium for the preparation of nanoparticles. DES is advantageous over ILs in the range of recyclability, costs, biodegradability, and lower toxicity. Most DES is prepared from the

natural origin such as choline chloride - ethylene glycol, choline chloride - urea, choline chloride - phenyl acetic acid, choline chloride - glycerol, etc.

Thao Dao Vu Phuong et al., (2021) <sup>[53]</sup> focused on the early stages of copper electro deposition using a DES containing C <sup>5</sup> H <sup>14</sup> ClNO and urea (DES). Parsa et al., (2020) <sup>[54]</sup> studied the nickel nanostructures with wrinkles that were electrodeposited from a DES including C <sup>5</sup> H <sup>14</sup> ClNO and urea. Verma et al., (2019) <sup>[55]</sup> discussed the solvation and stability of the transitional metallic particles in several kinds of liquid ionic forms, as well as their characterization methodologies and catalysis applications. Tome et.al (2018) <sup>[56]</sup> reviewed current developments in novel nonmaterial, as well as the procedures that have been created to use DES as a solvent. The definition, preparation, and special features of DES are discussed first, followed by a more detailed discussion of their applicability in polymer, metal deposition, and nonmaterial research and sensing techniques. The Ni-Co alloy, that was created using the method, has high corrosion resistance. Li et al., (2021) <sup>[57]</sup> demonstrated the deposition method in choline chloride-urea to produce nano nickel-cobalt (Ni-Co) alloys with chosen orientation.

The Ni-Co alloy, which was created using the ChCl/U method, offers good corrosion resistance. Palomar EZ et al., (2019) [58] used the transitional quantity of potentiostat current to describe the electrical depositing of Fe NPs onto the HOPG electrode surface from Fe (III) ions blended in the C 5 H 14 ClNO-urea eutectic mixture. Delbecq et al., (2019) [59] studied the formation of supramolecular gels by adding long-chain alkyl amino amide to metal chloride solubilised in choline chloride – urea. Smaller noble metal nanoparticles (Co NP or Au NP) could be generated by employing these gels as a template without the addition of reducing agents. Ghenaatian et al., (2021) [60] investigated the noble metallic nanoparticle interaction with choline chloride –urea by the theory of density functional method. Kakaei et al., (2018) [61] focused on the synthesis of grapheme oxide

and its reduced form through the electrochemical method with the use of graphite rod using the supersaturated solution of choline chloride – urea and water.

#### 1.6 CHOLINE CHLORIDE- ETHYLENE GLYCOL-BASED DES

In a single step, P-doped nickel superstructure sheets (NiPx) were electrodeposited on Cu foil using a choline chloride-ethylene glycol-based deep eutectic solvent (DES). Using a potentiostatic deposition technique, these films were found to be very active for catalysing hydrogen evolution reaction (HER) in an alkaline environment. With an over potential as low as 105mV and an output current density as high as 10mA cm<sup>-2</sup>, the Ni/P ratio of 1:0.056 sample exhibited excellent catalytic stability for at least 60 hours. The slope of the Tafel was just 44.7 mV dec<sup>-1</sup> at the time. According to detailed experimental investigations and theoretical analyses, the high-performance catalytic activity of NiPx films is due to the enriched active sites and enhanced electronic conductivity induced by P-doping. In DES, a new electrochemical potentiodynamic technique was established for the manufacture of transition-metal-phosphide-based catalysts to increase HER catalysi [62]. Choline chloride and ethylene glycol can be combined to provide a novel deep eutectic solvent electrolyte for supercapacitors. It has a considerable influence on viscosity, electrical conductivity, and capacitance when the molar ratio of choline chloride and ethylene glycol is high (40–115 °C). Viscosity reduces as a result of temperature rise, yet electrical conductivity increases. Electrolyte with a molar ratio of 1:2, which has an apparent specific capacitance of 362 F g1 at 115°C, but only 102 F g1 at 40°C (with an energy density of 14.13W/kg1). The electrolyte's apparent specific capacitance drops to only 102 F g1 at 40°C (with an energy density of 14.13W/kg1). Adsorption energy of an electrolyte with a molar ratio of 1:2 is found to be greater than that for an electrolyte with a molar ratio of 1:2. A wide range of supercapacitors may be made using ethylene glycol and choline chloride as deep eutectic solvents [63]. As a result of the sol-gel synthesis, a silica decorated graphene (SDG) was synthesised and then dispersed in a deep eutectic solvent (DES) system in order to simultaneously address the poor thermal conductivity, stability, and temperature range restrictions. It is possible to sustain nanofluids for up to one week without precipitation or aggregation because graphene has a thin silica coating [64]. Cu and Ni were investigated using linear sweep voltammetry in the presence of 0.1 M CuCl + ChCl-EG DES. Due to the fact that Cu has a larger oxidation potential than Ni, it is possible to separate Cu and Ni via electrochemistry A rise in temperature aids in Ni decontamination from Cu-Ni alloys. According to the current density and reaction temperature, which vary from 2 to 10 milliamperes per square inch, electrorefining efficiency and specific energy consumption are also assessed. At 10 mA/cm2 and 363 K, a specific energy consumption of 281.492 kW•h•t1 is possible [65]. For the first time, potentiodynamic and potentiostatic electrochemical methods were used to study the kinetics and mechanism of electrochemical synthesis of palladium nanoparticles (PdNPs) from a deep eutectic solvent, DES, produced by choline chloride and ethylene glycol at 298 K. A 3D nucleation process with diffusion-controlled growth was used to create the cylinders. Those results were reported in Nano Letters, an international magazine of nanotechnology [66]. Choline chloride (ChCl) and ethylene glycol (EG) DES with nickel sulphate as the main precursor of Ni<sup>2+</sup> are used to deposit Ni/TiO<sub>2</sub>-composite coatings. Light green Ni (OH)<sub>2</sub> crystalline solids and trimethylamine have both been found in the coating's composition. As a result, Ni(OH)<sub>2</sub> cannot develop in the acidic environment of boric acid. Acidic environments such as those created by boric acid prevent solvent degradation. Thus, the nickel ion reduction rate will increase. When water is added to DES, the complex form of Ni2+ changes, and the average crystallite size of the coating decreases as a result. It was found that the green preparation of composites may be achieved both theoretically and experimentally.

#### 1.7 CHOLINE CHLORIDE – MALONIC ACID-BASED DES

A deep eutectic solvent (DES) made from choline chloride and malonic acid was made quickly and cheaply. In a one-pot, the four-component reaction of amines, aldehydes, 1,3-dicarbonyl compounds, and nitromethane, was used as a dual catalyst and reaction medium for the synthesis of functionalized pyrroles [67].

Some ChCl with Carboxylic-acid-based DESs has also been reported to undergo chemical reactions such as esterification between DES components. As a result, it was discovered that a number of DESs containing ChCl and carboxylic acids (lactic acid, glutaric acid, glycolic acid, malic acid, malonic acid, oxalic acid, and levulinic acid) undergo an esterification reaction between the hydroxyl group of choline chloride and the carboxylic acid [68].

The efficiency of two DESs - choline chloride-malonic acid of molar ratios 1:1 and 1:0.5 - in enhancing oil recovery was investigated for the first time by Iman Al-Wahaibi et.al <sup>[69]</sup>. Gunny et al investigated the use of the DES-cellulose mechanism to hydrolyze lignocellulose from rice husk. The DES is comprised of choline chloride and a hydrogen-bond donor molecule (glycerol, ethylene glycol, or malonic acid) <sup>[70]</sup>.

## 1.8. SIGNIFICANCE OF DEEP EUTECTIC SOLVENTS

Deep eutectic solvents (DESs) are a novel class of solvents that potentially overcome the major problems of traditional ILs, such as high toxicity, non-biodegradability, complex synthesis that necessitates purification, and expensive starting material costs [71]. DESs are made by blending two safe components (cheap, renewable, and biodegradable) into a eutectic mixture. Deep Eutectic Solvents (DESs), also known in the literature as Deep Eutectic Ionic Liquids (DEILs), Low Melting Mixtures (LMMs), Low Transition Temperature Mixtures (LTTMs), or Natural Deep Eutectic Solvents (NADES). According to the literature, at least two components are required to synthesize the desired

DES: I a hydrogen-bond donor (HBD), and ii) a hydrogen-bond acceptor (HBA) <sup>[72]</sup>. The hydrogen bond donor causes a weaker anion/cation coupling, allowing the DES to melt at low temperatures.

# 1.9. COMPARISON OF IONIC LIQUIDS WITH DEEP EUTECTIC SOLVENTS

As compared to ionic liquids, Deep Eutectic Solvents has many advantages [72],

- i) low cost,
- ii) chemical inertness with water,
- iii) simple to create (because DESs are made by just mixing two components, bypassing the purification and waste disposal issues that typical ILs have), and
- iv) biodegradable, biocompatible, and non-toxic, strengthening the greenness of these media.

Ionic Liquids	Deep Eutectic Solvents
Low melting point ionic compounds	Low melting eutectic mixture of
	compounds
Not always environmentally friendly,	Biodegradable and nontoxic starting
can be toxic	materials
Solution conductivity-moderate to	Highly conductive
high	
Expensive: recycling is critical	Cheaper than ILs

# 1.10. APPLICATIONS OF DEEP EUTECTIC SOLVENTS

Matthijs et al. investigated the environmental effects of DES in electroplating applications based on choline chloride and ethylene glycol <sup>[73]</sup>. Nanocellulose materials have developed as a fascinating new class of nanomaterials. This is owing to its

environmental benefits, which include renewable resource production, biodegradability, biocompatibility, and high potential availability reported by Angeles et al<sup>[74]</sup>.

Since DESs are less expensive than conventional ILs and are considerably easier to create in large batches, DES-based procedures in the metal polishing and metal extraction industries are being scaled up and commercialized <sup>[75]</sup>. Metal processing research has been classified into three broad categories: metal electrodeposition, metal electropolishing, metal extraction, and metal oxide processing <sup>[32]</sup>.

In suitable DES systems, the replacement of ecologically harmful metal coatings, the deposition of novel alloys and semiconductors, and new coating technologies for the deposition of corrosion-resistant metals such as Ti, Al, and W $^{[76-78]}$  are all possible.

Zn, [79, 80, 81] Sn, Cu, [82, 83] Ni, [84] Ag, [85] Cr, [86] Al, [87] Co, [88] are among the metal reduction processes investigated in DESs and reported. Addition reactions, cyclization reactions, replacement reactions, multicomponent reactions, condensation reactions, oxidation reactions, and reducing reactions are among the organic reactions studied in DES as reported by Peng Liu in a review [89].

When compared to a conventional solvent, a betaine-based DES with glycerol (molar ratio 1:2) was shown to be the most effective for extracting phenolic chemicals <sup>[90]</sup>. DES was used as a novel solvent and catalyst in a typical organic synthesis method, mainly including halogenation reaction, Diels-Alder reaction, Knoevenagel reaction, Henry reaction, Perkin reaction, Paal-Knorr reaction, Biginelli reaction <sup>[91]</sup>.

#### 1.10.1. APPLICATIONS OF DEEP EUTECTIC SOLVENTS IN MNPs

Ali Abo- Hamed et al., reported that due to the unique qualities as novel green solvents, effective dispersants, and large-scale media for chemical and electrochemical production of sophisticated functional nanomaterials, deep eutectic solvents (DESs) have recently piqued attention in a variety of sectors, including nanotechnology <sup>[92]</sup>.

DESs are used to synthesize and fabricate a variety of nanomaterials, including zeolite analogues <sup>[25]</sup>, carbon nanomaterials <sup>[93, 94]</sup>, micro-and nanostructured semiconductors <sup>[95-97]</sup>, and DNA nanostructures <sup>[98]</sup>.

As a result of their excellent chemical and physical features, DESs have shown to be adaptable media for nanoscale synthesis <sup>[99, 92]</sup>. Despite the ubiquitous influence of DESs, their involvement in the synthesis of noble metal nanoparticles, notably gold and silver nanoparticles, has received less attention <sup>[100]</sup>.

DES has been utilized as a reaction medium for nanomaterial production and electrodeposition, as well as a nanoparticle dispersion medium. The most popular nanomaterials include carbon, metal oxide, and gold nanoparticles, inorganic (bio) nanomaterials, and metal (bio)organic framework materials as reported by Abo-Hamed [92].

Muzamil Khatri et.al.used an electrospinning process to construct Zein nanofibers from DES and achieved extremely hydrophilic Zein nanofibers without any post-treatment. Choline chloride (HBA) and Furfuryl alcohol (HBD) in a 1:2 ratio was utilized to make the DES needed for electrospinning [101].

The use of DESs as a solvent for the shape-controlled production of metal nanoparticles is an intriguing and growing application that could have a significant impact on the science of electrocatalysts. Without the use of any surfactants or seeds, gold nanoparticles were produced to generate Au-based catalysts using a DES as the solvent [32,102]. DESs are a new type of reaction media for the synthesis of noble metal nanomaterials that holds a lot of promise. They have a lot of advantages that have been studied [103].

Due to the advantages of their small particle size, large specific surface area, reproducibility, environmentally friendly materials, and easy solid-liquid separation, literature has recently confirmed that the combination of DESs and magnetic nanoparticles

(MNPs), such as Fe<sub>3</sub>O<sub>4</sub>-DES <sup>[104]</sup> and SiO<sub>2</sub>@Fe<sub>3</sub>O<sub>4</sub>-DES, has a broad application prospect in the magnetic solid-phase extraction method <sup>[105]</sup>.

Ionic liquids (ILs) and Deep eutectic solvents (DESs) are being used in the development of nano-sorbents such as nanoparticles, nanogels, and nanofluids as good alternative solvents. In the extraction process, ILs and DESs are frequently utilised as carriers/modifiers/dispersers of nano-sorbents to improve adsorption capacity and selectivity [106].

Different metallic nanoparticles have been used by Ingrid Hagarová et.al.,<sup>[107]</sup> to separate and pre-concentrate organic and inorganic analytes in a variety of environmental, biological, pharmacological, and dietary samples. Iron oxide magnetic nanoparticles are useful in a variety of fields, including chemistry, physics, and materials science <sup>[108]</sup>. In ChCl/EG or urea DES, Anicai et al. described the electrochemical synthesis of high-grade TiO<sub>2</sub>nanopowders, a nanomaterial that is widely employed in industrial applications such as solar cells, photocatalysis, chemical sensors, microelectronics, and electrochemistry <sup>[109]</sup>. For the manufacture of Fe<sub>3</sub>O<sub>4</sub> magnetic nanoparticles, a novel oxidative precipitation-combined ionothermal approach is reported <sup>[110]</sup>. The nanoparticles created were stable and had a higher catalytic efficiency for degrading organic contaminants in water treatment.

The presence of stable and uniform ZnO nanoparticles, with increased dispersion stability and catalytic efficacy, was demonstrated using an ionothermal precipitation technique in ChCl/EG [111]. Laser ablation targeting a silver metal blank immersed in the DES produced silver nanoparticle colloidal suspensions in a ChCl/urea eutectic mixture. The silver nanoparticles' luminous characteristics were found to be superior to those obtained in aqueous solutions [112]. Karimi et al. [113] examined the ternary role of DES as a medium for the synthesis of monetite nanoparticles in ChCl-EG eutectic mixture.

A.J. Expositoet.al., [114] used a combination of ChCl and Urea as the reaction medium, as well as the high heat and mass transfer rate given by microreactors, to demonstrate for the first time fast continuous synthesis of Ceria nanoparticles under mild temperatures. For the development of more effective nanoparticle-based catalysts, deep eutectic solvents (DES) have been employed as sustainable media [115]. Bruna et al. investigated how the deposition of DES onto TiO<sub>2</sub> surfaces modifies the catalytic activity of TiO<sub>2</sub> in the photodecomposition of organic dyes. The DES consisting of choline chloride (ChCl) and maleic acid is used to make Spinel ferrites, phase-pure nanoparticles MFe<sub>2</sub>O<sub>4</sub> (M=Mg, Zn, Co, Ni) at temperatures significantly lower than the solid-phase reactions of the metal oxides. As a result, the approach lowers the total amount of energy required to make nanoparticles examined by Anika Soldner et.al [116].

Surface modifications of graphene oxide (GO) nanosheets with different functional groups have recently shown interest in using DESs <sup>[117]</sup>. Mehrabi et.al. Predicted that surfacefunctionalization of GO (and other carbon nanomaterials) using DESs based on choline chloride and urea will allow resynthesized Fe<sub>3</sub>O<sub>4</sub> nanoparticles to be conjugated onto GO nanosheets at various GO:Fe<sub>3</sub>O<sub>4</sub> ratios.Cojocaru et.al. described the experiments using a choline chloride – glycerol deep eutectic solvent with pulse reversed current to synthesize silver nanoparticles (Ag NPs) at 25°C<sup>[118]</sup>.

Jakubowska. et.al., extracted metal oxide NPs from plant material via NADES <sup>[119]</sup>. The root accumulated larger cerium(IV) oxide NPs, but the radish leaves accumulated smaller ones. The titanium (IV) oxide NPs were agglomerated and found in tiny amounts in radish leaves, with most of them aggregating in the root.

## 1.11. METAL NANOPARTICLES

Metallic nanoparticles have stimulated the interest of scientists for over a century, and they are now widely used in biological and engineering fields. Because of their

enormous potential in nanotechnology, they have attracted a lot of attention. Even though the phrase is new, it has become widely employed in the development of more efficient technologies. Due to its applications in the fields of electronic storage systems <sup>[120]</sup>, biotechnology, <sup>[121]</sup> magnetic separation and preconcentration of target analytes, targeted drug delivery, <sup>[122,123]</sup> and vehicles for gene and drug delivery, nanotechnology has recently been adopted by industrial sectors <sup>[120,122-124]</sup>. In general, nanoparticles utilised in biotechnology have particle sizes ranging from 10 to 500 nm, seldom reaching 700 nm.

## 1.11.1. Silver nanoparticles (Ag NPs)

Silver nanoparticles are ranging with the size of 1–100 nm. While many are classified as "silver," due to the enormous ratio of surface to bulk silver atoms, some have a high amount of silver oxide. There is now an endeavour to include silver nanoparticles into a variety of medical products, such as bone cement, surgical instruments, surgical masks, and so on. Furthermore, it has been demonstrated that ionic silver can be used to cure wounds in the correct amounts. [125–127]. They are usually made by reducing a silver salt in the presence of a colloidal stabiliser using a reducing agent like sodium borohydride. To develop silver nanoparticles, newer revolutionary ways include the use of d-glucose as reducing sugar and starch as a stabiliser, as well as ion implantation [128]. Furno et al. produced biomaterials by employing supercritical carbon dioxide to impregnate silicone covered with silver oxide nanoparticles [129]. These new biomaterials were created with the goal of reducing antimicrobial infection.

In general, three different approaches have been used to synthesize silver nanoparticles, including physical, chemical, and biological processes <sup>[130]</sup>. Several efforts have been made in the recent decade to develop green synthesis processes that prevent hazardous consequences <sup>[131]</sup>. The most common approach for developing Ag-NPs is chemical reduction <sup>[132,133,134]</sup> by using reducing agents like poly-ethylene glycol block

copolymers, sodium citrate, Tollen's reagent, Ascorbate, essential hydrogen, N,N-dimethyl formamide (DMF), and sodium borohydride (NaBH<sub>4</sub>) <sup>[134,135,136]</sup>. Silver nanoparticles (AgNPs) offer a lot of potential applications as antimicrobial agents, biomedical device coatings, drug delivery carriers, imaging probes, and diagnostic and optoelectronic platforms <sup>[137]</sup>.

Chemical synthesis of nanoparticles has the advantages of ease of manufacture, low cost, and high yield; nevertheless, chemical reducing agents are toxic to living organisms [138]. Abbasi et al. have published a full review of AgNPs synthesis methods, characteristics, and bio-application [139]. High electrical and thermal conductivity [140], surface-enhanced Raman scattering [141], catalytic activity [142], and non-linear optical properties [143] are just a few of the physicochemical properties of AgNPs that have led to many of the innovative products and related technologies [144]. Even if well-established methodologies for the manufacture of metallic nanoparticles exist, simple synthesis approaches with fast reaction times and inexpensive costs must be investigated in order to create nanoparticles with enhanced antibacterial activity [145]. To optimise the synthesis of AgNPs derived using the chemical reduction approach, a Face Centered Central Composite Design (FCCCD) was used by Quiroz et.al [146].

## 1.11.2. Copper nanoparticles (Cu NPs)

In recent years, the usage of copper (Cu) and Cu-based nanoparticles, which are based on abundant and inexpensive copper metal, has sparked a lot of attention, particularly in the field of catalysis.Cu NPs are particularly appealing due to copper's abundant natural resources and low cost, as well as the numerous practical and simple approaches to synthesize Cu-based nanomaterials<sup>[147]</sup>.Cu-based nanocatalysts offer a wide range of applications in nanotechnology, including catalytic organic transformations, electrocatalysis, and

photocatalysis, due to their unique qualities and properties. Copper nanoparticles have two functions: (i) they operate as an antibacterial agent, though not as well as other metal nanoparticles, and (ii) they increase the porosity of the beads, making the scattered AgNPs in the beads more accessible to bacteria<sup>[148]</sup>.Cu nanoparticles are frequently coated with a capping substance to prevent oxidation and control crystal formation by lowering the surface energy of crystals <sup>[149]</sup>.Laser ablation, thermal degradation, chemical reduction, and polyol synthesis are some of the currently developed nanoparticle synthesis methods. Chemical reduction is commonly favoured among these procedures because it is simple, cost-effective, and efficient, and it can provide better size and size dispersion control<sup>[150]</sup>. The size management of Cu NPs, as well as the presence of a surface coating to prevent oxidation, are essential to obtain Cu NPs with excellent antibacterial capabilities. For industrial applications, a simple route producing oxide-free Cu NPs by thermal disintegration of a copper precursor has recently been reported by Adner et.al <sup>[151]</sup>.

On the other hand, the production of copper oxides at the nanoscale has a wide range of applications <sup>[152]</sup>. Transition metal oxides, particularly cupric oxide (CuO), have unique catalytic and photocatalytic characteristics <sup>[153]</sup>.Cu-NPs synthesised in polymer media have various advantages over conventional agents, including simplicity of processing, solubility, low toxicity, and nanoparticle growth control <sup>[154]</sup>.

## 1.11.3. Cadmium nanoparticles (Cd NPs)

Cadmium sulphide nanoparticles were chosen as a compound of interest Because of its great stability, good physical, chemical, and structural qualities, and ease of synthesis and handling.CdS nanoparticles are commonly utilised for cancer detection and antibacterial treatment <sup>[155]</sup>.Gas phase reaction (with H<sub>2</sub>S or sulphur vapour), solvothermal technique, solution precipitation, microwave-assisted solution precipitation, and several other ways are used to synthesize CdS nanoparticles<sup>[156]</sup>.Cadmium sulphide (CdS) has

captivated researchers' interest not only because of its excellent semiconductor optical and electrical capabilities but also because of its wide spectrum absorption range [157,158].CdS has a bandgap of 2.4 eV and can absorb visible light when the semiconductor bandgap is small (i.e 3.0 eV) [159]. CdS nanoparticles have been employed in a variety of applications, including photocatalytic hydrogen production, solar batteries, and redox process [160-<sup>162]</sup>. CdSwas chosen to generate NADH by transferring electrons to the coenzyme NAD+. To speed up the biocatalytic reaction, an efficient coenzyme self-circulation reaction was created by Chang et.al [163].he ability of microbes to manufacture green Cd-containing nanocrystals has been attributed to their ability to oppose heavy metals via bio reduction and precipitation of soluble metallic ions, resulting in insoluble nanometriccomplexes [164]. Because of their smaller size, excellent optical fluorescence property, and ease of functionalization, the development of innovative cadmium-based quantum dots has significant potential in the treatment and identification of cancer as well as targeted drug delivery<sup>[165]</sup>.CdS is employed as a pigment in paints and engineered plastics because of its good thermal consistency and dirt repelling capabilities [166,167]. For its photochemical and catalytic characteristics CdS NPs can be utilised as an air-water cleaner as well as a source of hydrogen [168]. CdS nanoparticles can be employed for both visualisation and medication distribution to soft tissues such as the retina and cornea [169,170]. Durga et.al. Chose Annona muricata leaf extract to produce cadmium sulphide nanoparticles and attempted green synthesis, evaluation of structural and morphological properties, and analysis of microbial activity [171].

## 1.11.4. Mercury Nanoparticles (HgNPs)

Mercury is the only metal element in nature that exists as a liquid at room temperature, posing a challenge for material scientists to investigate Hg nanoparticles [172]. Nanoparticles have features that differ from bulk materials, and they frequently lead to

major technological applications <sup>[173-177]</sup>. For the synthesis of mercury metal nanoparticles, Harika et.al., used liquid mercury as the starting material, eliminating the need of reducing agents <sup>[178]</sup>. In aqueous solutions, mercury sulphide (HgS) nanoparticles (NPs) were generated by Kuno et.al., with water-soluble thiols as capping ligands <sup>[179]</sup>. Mazrui et.al studied the development and fate of -HgS(s)nano produced in combination with marine dissolved organic matter collected from the North Atlantic Ocean, as well as low molecular weight thiols <sup>[180]</sup>. Chemical deposition <sup>[181]</sup>, solvothermal <sup>[182]</sup>, microwave heating <sup>[183]</sup>, photochemical <sup>[184]</sup>, wet chemical <sup>[185]</sup>, and electrochemical <sup>[186]</sup> are all well-established processes for the synthesis of Hg nanoparticles. Because of its uses as acoustic optical materials <sup>[187]</sup> and infrared sensing <sup>[188]</sup>, HgS has gotten increased attention. By using pulsed laser ablation on a pellet of mercuric sulphide (-HgS) stilled in distilled water, J.Mohammed et.al, succeeded in a simple and straightforward technique for preparing the meta-cinnabar phase of mercuric sulphide (-HgS)<sup>[189]</sup>. For the preparation of  $\beta$  -HgS nanocrystals, Xin xu.et.al. employed a solvent-based method, followed by sonification and nitrogen purging at room temperature <sup>[190]</sup>.

## 1.11.5. Zirconium Nanoparticles (Zr NPs)

Datta et.al, identified the role of reline, an eutectic mixture of choline chloride and urea, one of the most popular DES, is elucidated during the synthesis of different families such as gold (noble metal), vanadium pentoxide (transition metal oxide), ceria and zirconia (ceramic oxides). The work focuses on gaining a holistic understanding on the interaction of reline with different precursors. It is found that reline can act as an 'all in one' platform such as template reagent, reducing agent, solvent platform and morphology directing agent in the synthesis of nanomaterials. It is important to highlight that there is no addition of any external additives in contrast to previously published work. It is demonstrated here that reline can actively form gold nanoparticles by reducing a salt precursor and simultaneously

stabilize the nuclei, delaying their growth, leading to highly monodispersed small gold particles. In the case of metal oxides, the templating role of reline is elucidated to produce different morphologies of vanadium pentoxide upon altering the water ratio in reline. Reline has been also shown to direct the growth of 1D ceria-zirconia nanorods. The effect of reline on the crystal phase of the zirconia nanomaterial is also investigated herein<sup>[191]</sup>..

## 1.11.6 Zinc Nanoparticles (ZnNPs)

Yao, H., et.al. To solve the problem of the low added value Zn-containing rotary hearth furnace (RHF) dust, two deep eutectic solvents (DESs) were employed, such as choline chloride-urea (ChCl-urea) and choline chloride-oxalic acid dihydrate (CC—OA) solvent and Zn-containing RHF dust (water-washed) as the research target. Then, we prepared ZnO nanoparticles using two DESs or their combination, namely, ChCl-urea (Method A), CC—OA (Method B), first CC—OA and then ChCl-urea (Method B-A) and first ChCl-urea and then CC-OA (Method A-B), respectively. The effects of these methods on the properties of as-obtained precursors and ZnO nanoparticles were investigated in detail. The results indicated that the precursor obtained by Method A was Zn<sub>4</sub>CO<sub>3</sub> (OH) 6⋅H<sub>2</sub>O, and those by Methods B, B-A, and A-B were all ZnC<sub>2</sub>O<sub>4</sub>⋅2H<sub>2</sub>O. Moreover, the decomposition steps of the last three methods were similar. The ZnO contents of 95.486%, 99.768%, 99.733%, and 99.76% were obtained by Methods A, B, B-A, and A-B, respectively. Methods A, B, and B-A led to the formation of spherical and agglomerated ZnO nanoparticles with normal size distributions, where Method B showed the best distribution with an average diameter 25 nm. The ZnO nanoparticles obtained by the Method A-B did not possess good properties [192].

## 1.11.7. Manganese Nanoparticles (Mn NPs)

Henam Sylvia Devi et,al. synthesied Mn<sub>2</sub>O<sub>3</sub> particles of nano scale were fabricated using deep eutectic solvent of choline chloride-ethylene glycol. Deep Eutectic Solvents

(DES) is a new family of ionic fluids.  $Mn_2O_3$  was fabricated by varying the amount of water in DES. With variation in amount of water, size and shape of particles also varied.  $Mn_2O_3$  prepared in absence of water is of orthorhombic crystal system and those prepared in presence of water are of tetrahedral crystal system. Photocatalytic property of these  $Mn_2O_3$  particles was also demonstrated using safranin-O dye<sup>[193]</sup>. Rate constant calculated by plotting log A vs Time follow:  $k_{0.5 \text{ ml water}} > k_{0.0 \text{ ml water}} > k_{1 \text{ ml water}}$ .

## 1.11.8 Vanadium Nanoparticles (VNPs)

Sukanya Datta, et,al. show a facile surfactant-free synthetic platform for the synthesis of nanostructured vanadium pentoxide (V<sub>2</sub>O<sub>5</sub>)<sup>[194]</sup>. using reline as a green and eco-friendly deep eutectic solvent. This new approach overcomes the dependence of the current synthetic methods on shape directing agents such as surfactants with potential detrimental effects on the final applications. Excellent morphological control is achieved by simply varying the water ratio in the reaction leading to the selective formation of V<sub>2</sub>O<sub>5</sub> 3D microbeads, 2D nanosheets and 1D randomly arranged nanofleece. Using electrospray ionization mass spectroscopy (ESI-MS), we demonstrate that alkyl amine based ionic species are formed during the reline/water solvothermal treatment and that these play a key role in the resulting material morphology with templating and exfoliating properties. This work enables fundamental understanding of the activity-morphology relationship of vanadium oxide materials in catalysis, sensing applications, energy conversion and energy storage as we prove on the effect of surfactant-free V<sub>2</sub>O<sub>5</sub> structuring on battery performance as cathode materials. Nanostructured V<sub>2</sub>O<sub>5</sub> cathodes showed a faster charge-discharge response than the counterpart bulk-V<sub>2</sub>O<sub>5</sub> electrode with V<sub>2</sub>O<sub>5</sub> 2D nanosheet presenting the highest improvement of the rate performance in galvanostatic charge-discharge tests.

## 1.11.9 Nickel Nanoparticles (Ni NPs)

Elsharkawya, S.,et.al. synthesied nanostructure Ni films were synthesized from two distinct baths and were assessed as electrocatalysts for hydrogen evolution reaction (HER) and oxygen evolution reaction (OER) in 1 M KOH. Herein, Ni was electrodeposited from two separate solvents, the aqueous acetate buffer and ethaline solvent as a kind of deep eutectic solvents (DESs) ) [195], and both the deposited films were investigated as electrocatalysts for HER and OER. The electrodeposition parameters such as pH and deposition potential were studied. The electrodeposition process was performed using chronoamperometry technique and Ni deposits were characterized by scanning electron microscopy (SEM), transmission electron microscopy (TEM), energy-dispersive X-ray spectroscopy (EDX), and X-ray diffraction (XRD). Fabricated Ni@PGE deposit from ethaline only requires an overpotential of – 154 mV and 350 mV to achieve a current density of 10 mA cm<sup>-2</sup> for HER and OER, respectively. While, Ni@PGE from acetate requires an overpotential of – 164 mV and 400 mV to produce the current density of 10 mA cm<sup>-2</sup> for HER and OER.

#### 1.12. REVIEW OF LITERATURE

# 1.12.1. Deep eutectic solvents -synthesis and characterization

Ionic liquids (ILs) are green solvents that can be used in a variety of applications. However, their production via chemical reactions with waste or by-products is incompatible with the concept of green chemistry, and the purity issue and cost feasibility restrict their use in several large-scale industrial applications. DES is produced, when halide salts and hydrogen bond donors (such as alcohol or acid) combine, resulting in a combination having a lower freezing/melting point than the individual components [196]. In green chemistry and processing, DES is becoming increasingly essential [197, 198]. Extensive research is being carried out to investigate the properties of newly synthesized DES [199– <sup>201]</sup>. The traditional DES is a binary deep eutectic solvent made up of two single components (DES). The addition of a third component to the ternary deep eutectic solvent (DES) improved the designable property much more than the standard DES. DES has been synthesized and used in a variety of applications so far [202-204]. DES were prepared by mixing the two components at a molar ratio of 1:1. By heating the binary mixture to 80°C with continuous stirring, clear liquids were obtained [205]. After cooling to room temperature, the binary mixture remains at a liquid state [206] and the evaporating method was employed in water as given by Dai et al. [207]. Their cost of production is less and used as safer solvents in several fields [208]. It is possible to create endeavor DESs with various physicochemical parameters, such as freezing point, viscosity, conductivity, and pH, among others.

## 1.12.2. Copper nanoparticles

Metallic nanoparticles have a lot of potential because of their chemical, physical, and catalytic capabilities <sup>[209]</sup>. Copper nanoparticles are a type of colloidal transition metal nanoparticle that receives a lot of interest since they are employed as an advanced material

with electrical, optical, and thermal properties<sup>[210]</sup>. A chemical reduction is a popular approach for making copper nanoparticles because it is low-cost, high-yielding, and requires little equipment. It is simple, and the control of particle size and shape obtained under-regulated parameters may be shown <sup>[211]</sup>. The copper nanoparticles were made using a wet chemical reduction method as reported by Jain et.al <sup>[212]</sup>. Mustafa G, et al. reported the synthesis of monoclinic CuO nanoparticles that were characterized by XRD analysis<sup>[213]</sup>.

CuO nanoparticles can be manufactured in a variety of methods, and synthesis parameters such as technique, solvents, surfactants, starting precursors, and temperature are employed to regulate the form and size of desired nanoparticles, according to Suleiman M, et al <sup>[214]</sup>. Wongpisutpaisana N, et al. suggested that well-defined CuO nanoparticles are generated by a sonochemical synthesis with ultrasound help, with a reaction duration of up to 30 minutes and pyrolysis at 600-700 °C <sup>[215]</sup>. CuO nanoparticles with a rectangular form and a monoclinic structure were generated by an aqueous precipitation technique, according to Lange AS, et al <sup>[216]</sup>.

H. Zhu et al. suggested a wet chemical approach for the large-scale production of stable CuO nanofluids <sup>[217]</sup>. Mousa MK suggested a rapid, economical, and simple method of precipitation with temperature control at 65, 75, and 85 ° C. The size of nanoparticles reduces as the temperature increases <sup>[218]</sup>. The latest research reports on the new production of Copper and Copper oxide nanoparticles utilizing the chemical reduction approach, as well as their physicochemical characterization according to Karthik AD et.al<sup>[219]</sup>.

Copper materials are synthesized first and then oxidized to copper oxide. UV-visible spectroscopy, Fourier transform infrared spectroscopy (FTIR), X-ray diffraction measurements (XRD), and scanning electron microscopy (SEM) were used to characterize the nanoparticles, according to the researchers S. Srivastava and co-workers reported the

chemical approach was used to synthesize cupric oxide (CuO) nanoparticles, which involved calcination at temperatures ranging from 300 to 400 ° C<sup>[220]</sup>.K. Phiwdanga et al. CuO nanoparticles were produced using a precipitation approach with different precursors such as copper nitrate (Cu (NO<sub>3</sub>)<sub>2)</sub> and copper chloride (CuCl<sub>2</sub>), and post-heating was used to compare the as-synthesized and after-calcination of CuO nanoparticles<sup>[221]</sup>. Thermal decomposition was used to generate spherical CuO nanoparticles with a mean diameter of 170 nm as reported by Darezereshki E, et al [222]. This process does not necessitate the use of organic solvents, costly raw materials, or sophisticated machinery. As a result, the given process to produce CuO nanoparticles from dilute CuSO<sub>4</sub> solution is better than the other methods. Cu nanoparticles (CuNPs) were made using a simple chemical reduction method at ambient temperature, with sodium borohydride and polyvinylpyrrolidone, the Cu<sup>2+</sup> ions were lowered and stabilized, respectively as reported by Aguilar et.al [223]. Chatterjee et al. proposed a straightforward approach for the manufacture of metallic copper nanoparticles with a size of 50-60 nm utilizing Cucl<sub>2</sub> as a reducing agent and gelatin as a stabilizer <sup>[224]</sup>. Copper nanoparticles were made by reducing aqueous copper chloride solution with NaBH<sub>4</sub> in non-ionic water-in-oil (w/o) microemulsions <sup>[225]</sup>. To generate copper nanoparticles, chemical methods such as chemical reduction, photochemical, electrochemical, and thermal decomposition are used, with the chemical reduction being the most used method for the creation of stable, colloidal dispersions in organic solvents<sup>[226]</sup>. Chemical reduction is the most practical way for fabricating nanoparticles out of all the methods. The chemical reduction process yielded a high yield of metallic nanoparticles. By manipulating the experimental conditions, this method is cost-effective, simple, and speedier, and it may produce a superior size distribution of nanoparticles [227]. Copper nanoparticles were generated by chemically reducing copper sulfate with sodium borohydride in water without the use of inert gas. During the synthesis process and during storage, ascorbic acid was used as a protective agent to prevent the nascent Cu nanoparticles from oxidation. The use of polyethylene glycol served as a size controller as well as a capping agent. Under inert argon-purged condition, copper nanoparticles were successfully produced by borohydride reduction of copper nitrate salt in a water/CH<sub>3</sub>CN mixed solvent. For the first time, Cu nanoparticles were generated in large-scale production by injecting CH<sub>3</sub>CN into the water and preventing oxidation throughout the nanoparticle preparation [228].

# 1.12.3. Silver nanoparticles

Metal nanoparticles can be synthesized in a variety of ways, including physical and chemical processes. Even though physical methods can make nanoparticles; the literature is full of data on chemical approaches. The reduction of metal ions in solution is the most common chemical technique (chemical reduction method) [229]. The polyol technique [230] and the liquid-liquid method <sup>[231]</sup> are two chemical methods for the manufacture of silver nanoparticles that have been developed in recent years. Chemical reduction, on the other hand, is the most widely used method due to its simplicity. Examples of bottom-up methods include metal reduction, electrochemical processes, and decomposition. Silver nanoparticles are fascinating because of their unique features, which can be used in antibacterial applications, biosensor materials, composite fibres, cryogenic superconducting materials, cosmetics, and electronic components. Silver NPs have been synthesized and stabilized using a variety of physical and chemical processes [232, 233]. Chemical reduction with organic and inorganic reducing chemicals is the most frequent method for producing silver NPs. For the reduction of silver ions (Ag<sup>+</sup>) in aqueous or nonaqueous solutions, several reducing agents such as sodium citrate, ascorbate, sodium borohydride (NaBH4), elemental hydrogen, polyol process, Tollen's reagent, N, Ndimethylformamide (DMF), and poly (ethylene glycol)-block copolymers are utilized [234].

In nanoparticle synthesis, it is necessary to observe nano silver content, size, shape, surface charge, crystal structure, surface chemistry, and surface change. Ojha et al. combined AgNO<sub>3</sub> and citrate in a solution and added NaOH to it. Then, while stirring, an ice-cold NaBH<sub>4</sub> solution was added <sup>[235]</sup>.T he aqueous solution containing AgNO<sub>3</sub> was made by Ajitha et al. with sodium citrate dihydrate as a stabilizer. Then, while vigorously stirring, a solution of sodium borohydride (a reducing agent) was added into the above solution all at once. The color of the solution was lightened <sup>[236]</sup>. Gebeyehu et al. used a simple polyol technique to make silver nanowire. Polyvinylpyrrolidone was utilized as a stabilizing and capping agent, along with sodium chloride and potassium bromide salts, ethylene glycol as a solvent and reducing agent, and silver nitrate as a silver precursor [237]. The reduction of silver nitrate with ethylene glycol in the presence of polyvinylpyrrolidone resulted in cubic silver nanoparticles (PVP). Ethylene glycol with hydroxyl groups serves as both a solvent and a reducing agent in the polyol process. The cubic form was developed using polyvinylpyrrolidone as a capping agent [238-240]. By adding a trace quantity of sodium sulfide (Na<sub>2</sub>S) or sodium hydro sulfide (NaHS) to the traditional polyol synthesis, Siekkien et al. achieved a quicker approach to produce cubic silver nanoparticles. For the synthesis of NPs with various chemical compositions, sizes, and morphologies, as well as regulated disparities, the reduction agent is critical <sup>[241]</sup>. Sun et al. investigated how reaction circumstances, such as the ratio of PVP to silver nitrate, reaction temperature, and seeding conditions, may change the shape of silver nanostructures, ranging from nanoparticles to nanorods to long nanowires. They discovered that silver nanowires with diameters ranging from 30 to 40 nm and lengths up to 50 m could be synthesized on a huge scale [242]. For the manufacture of silver nanoprisms, Métraux and Mirkin used the chemical reduction process. They used a reagent mixture of AgNO<sub>3</sub>/NaBH<sub>4</sub>/ polyvinylpyrrolidone/trisodium citrate/H<sub>2</sub>O<sub>2</sub> in an aqueous solution to make silver nanoprisms at room temperature <sup>[243]</sup>.

Silver nanoparticles have attracted a lot of attention in recent years due to their good conductivity, chemical stability, use as catalysts <sup>[244]</sup> and applications in a variety of industries (e.g., medical sciences to prevent the HIV virus, food industries as anti-bacterial agents in food packaging <sup>[245]</sup>, anti-bacterial properties) <sup>[246]</sup>, as well as their unique electrical and optical properties <sup>[247, 248]</sup>. The antibacterial action of silver ions and silver nanoparticles is related to morphological and structural changes in the bacterial cell, according to research <sup>[249, 250]</sup>.

# 1.12.4. Cadmium nanoparticles:

Cadmium Sulfide Nanoparticles (CdS. NPs) confirmed the bulk-sized material's distinct physical, chemical, and structural features. Cadmium Sulfide NPs are employed in everyday life because of their distinctive melting point, crystal arrangement, band gap energy, optoelectronic absorption spectra, high stability, availability, and ease of manufacture and handling. The atomic distribution over the nanoparticle shell, in addition to the surface/volume ratio, has a significant effect on semi conductivity [251].

Due to advantages in several areas, CdS NPs have been industrially developed. Chemical precipitation <sup>[252]</sup>, Chemical Vapour Deposition <sup>[253]</sup>, laser ablation <sup>[254]</sup>, physical evaporation <sup>[255]</sup>, template synthesis <sup>[256]</sup>, thermal evaporation <sup>[257]</sup>, hydrothermal synthesis <sup>[258]</sup>, pulsed laser deposition <sup>[259]</sup>, solvothermal <sup>[260]</sup>, and biosynthesis using bacteria, fungi, yeast, and plants <sup>[261]</sup> and Electrodeposition <sup>[262]</sup> have all been used to create nano-forms of CdS films or powder.

Chemical precipitation is commonly used since it requires ambient environmental conditions, simple lab equipment, and consistent findings, as opposed to other procedures that require extreme environmental conditions, sophisticated equipment, and are time-consuming. Limiting the reaction area with capping agents such as EDTA, long-chain alkyl xanthates, mercaptoacetic acid, phosphates, phosphine oxides, thioglycerol, thiols, and

thiourea  $^{[263]}$  controls the stability and size of CdSNPs. Chemical precipitation of cadmium sulfide (CdS) nanoparticles was carried out using cadmium chloride (CdCl<sub>2</sub>), sodium sulfide (Na<sub>2</sub>S), and water as a solvent at temperatures ranging from 20 to 80 degrees Celsius  $^{[264]}$ 

CdS NPs were formed by adding aqueous CdCl<sub>2</sub>, KOH, NH<sub>4</sub>NO<sub>3</sub>, and CS(NH<sub>2</sub>)<sub>2</sub> for 30 minutes at pH 10, temperature 80°C, and centrifugation at 6000 rpm for 1 hour <sup>[265]</sup>. Chemical precipitation of deionized aqueous CdCl<sub>2</sub> and thiourea solution with continuous stirring at 100 °C for 15 hours yielded CdS NPs. As a capping agent, ammonia was used by R.Gupta <sup>[266]</sup>. M. M. Kamble& co. developed Cadmium sulfide nanocrystals with oleylamine as the solvent, surfactant, and capping ligand by using the Hot Injection Method <sup>[267]</sup>

## 1.12.5. Mercury Nanoparticles

Mercury is one of the few metal elements that may exist as liquids in nature under normal conditions, posing a challenge to material scientists to learn more about Hg nanoparticles (NPs) [268]. Nanoparticles have properties that differ from bulk materials, and they frequently lead to significant technological applications [269-273]. Alireza et al. proposed an innovative processing method for manufacturing HgO nanoparticles by solid-state thermal decomposition of mercury (II) acetate nanostructures generated by sublimation at 150 °C for 2 hours [274]. Using ultrasonication under ambient conditions, V. K. Harika et al. proposed a simple synthetic technique for producing very stable crystalline mercury nanoparticles supported on solid carbon sources such as reduced graphene oxide, graphene, graphite oxide, graphite, and others [275]. Avik. J. G generated oxidized mercury nanoparticles using two methods i.e., vapor-phase condensation and aqueous nebulization using three basic chemicals like mercury (II) bromide, mercury (II) chloride, and mercury (II) oxide [276]. Synthesizing nano-sized β-HgS particles in a practical and simple manner

remains a difficulty. A lot of established methods such as chemical deposition <sup>[277]</sup>, photochemical <sup>[278]</sup>, wet chemical <sup>[279]</sup>, and electrochemical <sup>[280]</sup> have been used for the synthesis of Hg nanoparticles. At room temperature, nanocrystals are synthesized via sonication and nitrogen purging by Xin Xiu et.al. Surfactants and stabilizing ligands were not employed in the analyses of the NPs to avoid changing their chemical and toxicological behavior <sup>[281]</sup>. For the first time, Mercury Cadmium Telluride (MCT) nanoparticles are synthesized by R.R. Arnepelli using the Solvothermal technique. In the Teflon-Stainless-Steel autoclave, Mercury, Cadmium, and Tellurium in compound/elemental form were added to Ethylenediamine (solvent) together with a reducing agent <sup>[282]</sup>.

## 1.12.6. Zirconium Nanoparticles

Bumajdad, A., et.al. investigated, well-defined mesoporous zirconia nanoparticles (ZrO<sub>2</sub> NPs) <sup>[283]</sup> with cubic, tetragonal or monoclinic pure phase were synthesized via thermal recovery (in air) from chitosan (CS)- or polyvinyl alcohol (PVA)-ZrO<sub>x</sub> hybrid films, prepared using sol–gel processing. This facile preparative method was found to lead to an almost quantitative recovery of the ZrOx content of the film in the form of ZrO<sub>2</sub> NPs. Impacts of the thermal recovery temperature (450, 800 and 1100 °C) and polymer type (natural bio-waste CS or synthetic PVA) used in fabricating the organic/inorganic hybrid films on bulk and surface characteristics of the recovered NPs were probed by means of X-ray diffractometry and photoelectron spectroscopy, FT-IR and Laser Raman spectroscopy, transmission electron and atomic force microscopy, and N<sub>2</sub> absorptiometry. Results obtained showed that the method applied facilitates control over the size (6–30 nm) and shape (from loose cubes to agglomerates) of the recovered NPs and, hence, the bulk crystalline phase composition and the surface area (144–52 m²/g) and mesopore size (23–10 nm) and volume (0.31–0.11 cm³/g) of the resulting zirconias.

## 1.12.7. Vanadium Nanoparticles

Transition metal oxides have been a subject of research in recent years in view of their fundamental and technological aspects. Among these, vanadium creates many compounds with oxygen; these have different structural, optical and chemical properties. Meaningful differences between the properties of different phases of vanadium oxides like VO, VO<sub>2</sub>, V2O<sub>3</sub> and V<sub>2</sub>O<sub>5</sub> depend on their structure, which determines other properties [284] [285]. Different forms of vanadium oxides can be obtained by changing the deposition process parameters, or by post-process treatment, e.g., additional annealing [286]. From the application point of view, the most interesting vanadium oxides are VO<sub>2</sub> and V<sub>2</sub>O<sub>5</sub>. Vanadium dioxide is a very good candidate for thermochromic coatings due to the change of properties from semiconducting to semimetal at 68°C. Vanadium pentoxide (V<sub>2</sub>O<sub>5</sub>) is a thermodynamically stable form which exhibits electrochromic properties. V<sub>2</sub>O<sub>5</sub> thin films can also be used in optical filters, reflectance mirrors, smart windows and surfaces with tunable emittance for temperature control of space vehicles [287]. It can be received by selecting deposition parameters or by the annealing of VO<sub>2</sub> above 350°C <sup>[288]</sup>. In this article, vanadium oxide nanoparticles are fabricated by using sol-gel method. Structural and surface morphological properties have been studied.

## 1.12.8. Zinc Nanoparticles

Shelan M. Mustafa et.al. synthesized betaine and phenol with melting points ~300 °C and ~43 °C, respectively, combine with a molar ratio of 1:2 to form a liquid at room temperature with a eutectic melting point of ~20 °C. ZnO nanoparticles<sup>[289]</sup> (NPs) were synthesized by using an eco-friendly and green synthesis method utilizing betaine-based DES at low temperature ~80 °C for 2 h. X-ray diffraction analysis confirms the highly crystalline and single-phase formation of ZnO NPs with hexagonal-Wurtzite phase structure. The surface morphology of the ZnO NPs confirmed using scanning electron

microscopic images revealing the mostly spherical in shape and some n-pointed stars and transmission electron microscopy images confirms that NPs are sub-100 nm in range. Also, energy dispersive X-ray results confirm the elemental composition of Zn K ( $\sim$ 8.6 keV) and O K (0.52 keV) to be  $\sim$ 88.5  $\pm$  1.7% and 11.5  $\pm$  1.3%, respectively. Fourier transform infrared spectroscopy confirms the bands at 565 and 410 cm<sup>-1</sup> is assigned to asymmetric stretching and bending vibrations of the Zn–O tetrahedron. Thermogravimetric analysis verified the thermal stability with phase purity, resulting in the formation of the single-phase crystalline ZnO NPs. UV–Vis absorption study confirms the bandgap of  $\sim$ 3.1 eV. The high stability and dispersion of NPs in water confirms the interaction of DES molecules on the surface of the NPs with water. ZnO NPs incorporated in PVA thin films show strong UV–Vis absorption confirming use of these transparent thin films for UV-shielding applications. As far as we know, this study is unique, green, eco-friendly and cost-effective in that the authors were able to synthesize ZnO NPs from betaine-based DES.

## 1.12.9. Manganese Nanoparticles

Karimi, M. Et.al.Mn<sub>3</sub>O<sub>4</sub> nanoparticles have been synthesized using a facile and sustainable method using ethaline (ethylene glycol–choline chloride) deep eutectic solvent (DES). The as-synthesized nanoparticles have been characterized by X-ray diffraction (XRD), field emission scanning electron microscopy (FESEM), transmission electron microscopy (TEM), energy-dispersive X-ray spectroscopy (EDS), Fourier transform infrared (FTIR) spectroscopy, UV/vis absorption spectroscopy, and vibrating sample magnetometry (VSM). The XRD results point to crystallization of hausmannite Mn<sub>3</sub>O<sub>4</sub> in tetragonal crystal structure with an average crystallite size of 18 nm. The microscopy-elemental investigations suggest the synthesis of spherical nanoparticles with an average particle size of 25 nm and high elemental purity. The obtained band gap of 3.4 eV for the as–synthesized Mn<sub>3</sub>O<sub>4</sub> nanoparticles indicates the semiconductor nature of nanoparticles.

FTIR absorption bands further confirm the formation of pure  $Mn_3O_4$  nanoparticles. The magnetic characterization of as-synthesized  $Mn_3O_4$  nanoparticles clearly reveals their paramagnetic behavior at room temperature. Based on our proposed mechanism the ethaline plays a triple role (solvent, reactant, and template) during the synthesis thereby it provides a green all-in-one system for synthesis, stabilization and better control over growth of  $Mn_3O_4^{[290]}$  nanoparticles.

## 1.12.10. Nickel Nanoparticles

Jaji et.al. Over the last decade, nickel nanoparticles (Ni NPs) [291] have been investigated for various potential applications due to their superior ferromagnetic properties such as magneto-crystalline anisotropy, high coercive forces, and chemical stability. Therefore, there has been a tremendous enhancement in the synthesis techniques, proposed reaction mechanisms, and applications of Ni NPs. This paper presents a recent overview of the synthesis, reaction mechanisms, and applications of Ni NPs. Ni NPs in the size range of 1–100 nm are synthesized by various methods for research and commercial applications. The synthesis techniques are classified into three main types, namely, top-down, bottom-up, and hybrids of top-down and bottom-up protocols including solvothermal, physical, and chemical approaches. The detailed reaction mechanisms in the formation of Ni NPs, especially for biosynthesis techniques, are extensively described. Trends in Ni NPs applications in fields such as biomedical, catalysis, supercapacitors, and dye-sensitized solar cells are explored. The basic advantages and role of Ni NPs as a catalyst for various reactions are illustrated here

A new type of base fluid known as Deep Eutectic Solvents (DESs) is proposed in this work, which is generated by mixing solid substances that turn liquid under specified conditions, offering another option to utilizing traditional organic solvents. At room temperature, many of these combinations are liquids. Since their discovery, these deep

eutectic solvents have been the subject of significant research. Because of sharing many characteristics and properties with ionic liquids (e.g., similar conductivities, polarities, viscosities, densities, surface tensions, refractive indexes, chemical inertness, etc.,) deep eutectic solvents (DESs) are now commonly recognized as a new family of Ionic liquids (IL) substitutes. They are typically affordable due to the comparatively inexpensive components and their straightforward synthesis, which produces little waste and requires no additional purifying procedures. In addition, the components of DESs are frequently biodegradable and non-toxic.

Herein research focused on the synthesis of DESs using, ChCL-UREA, ChCl-EG, ChCL-MA followed by Preparation of Metal-based Nanoparticles using DESs and their Characterization. The preparation of metal nanoparticles Cu, Hg, Mn, Zr, Ag, Zn, Cd, V and Ni in the medium of ChCL-UREA, ChCl-EG, ChCL-MA DESs. Their characterization studies such as UV-Visible, FTIR, XRD, SEM, and EDAX analysis were discussed. The particle size of the nanoparticles formed was ascertained using histogram plots.

## 1.13. AIM, SCOPE, AND OBJECTIVES OF THE PRESENT WORK

The aim of the present study is to develop an eco-friendly a better alternative solvent. It should be cheap, harmless, bio-degradable and it should be highly stable even at high temperatures. The work proposes a new form of base liquid known as Deep Eutectic Solvents (DESs) as a viable replacement for conventional base fluid due to their unique solvent properties. Using the newly developed DESs, metal nanoparticles are synthesized and to study the antimicrobial activities.

The objectives of the present work are

- > To use an efficient method to develop DESs
- To find the cost-effective, cheaper, and low-cost method.
- To synthesize less toxic, most usable MNPs.
- To find any one application of the synthesized MNPs.

The implication of this study was the preparation of newer ChCl-UREA, ChCl-EG, ChCl-MA and physicochemical parameters such as viscosity, conductivity, pH, density were measured for the prepared DES. To find out whether they depict the nature, characteristics, and features of DES to substitute as the common solvents.

In this research work, we targeted the production of some metal nanoparticles using ChCl-UREA, ChCl-EG, ChCl-MA deep eutectic solvents. The research utilizes three DESs as greener media to produce various metal nanoparticles. The synthesized nanoparticles such as Ag, Hg, Mn, Cu, Zr, Ni, Cd, Zn, V have been analysed using Scanning Electron Microscopy (SEM), Ultraviolet Spectroscopy (UV), Fourier Transform Infrared absorptions (FTIR), X-Ray Diffraction patterns (XRD), and Energy Dispersive X-ray Analysis (EDAX) techniques.

**Chapter 1** deals with the introduction about the deep eutectic solvents and their applications, metal nanoparticles and their applications, also including literature review.

**Chapter 2** explains the materials and methodology used for the study.

Chapter 3 is Preparation of Metal-based Nanoparticles using Choline chloride – Urea DES and their Characterization. This chapter explains the preparation of metal nanoparticles of Cu, Hg, Mn, Zr, Ag, Zn, Cd, V and Ni in the medium of choline chloride – urea DES. Their characterization studies such as UV-Visible, FTIR, XRD, SEM, and EDAX analysis were discussed. The particle size of the nanoparticles formed was ascertained using histogram plots.

Chapter 4 is Preparation of Metal-based Nanoparticles using Chcl-EG DES and their Characterization. This chapter explains the preparation of metal nanoparticles of Cu, Hg, Mn, Zr, Ag, Zn, Cd, V and Ni in the medium of choline chloride –ethylene glycol DES. Their characterization studies such as UV-Visible, FTIR, XRD, SEM, and EDAX analysis were discussed. The particle size of the nanoparticles formed was ascertained using histogram plots.

Chapter 5 is Preparation of Metal-based Nanoparticles using Choline chloride – Malonic Acid DES and their Characterization. This chapter explains the preparation of metal nanoparticles of Cu, Hg, Mn, Zr, Ag, Zn, Cd, V and Ni in the medium of choline chloride –malonic acid DES. Their characterization studies such as UV-Visible, FTIR, XRD, SEM, and EDAX analysis were discussed. The particle size of the nanoparticles formed was ascertained using histogram plots.

**Chapter 6** is Summary and Conclusion. In this chapter, a précised summary of the research work and necessary conclusions are given. A detailed comparison of the size of the metal-based nanoparticles of Cu, Hg, Mn, Zr, Ag, Zn, Cd, V and Ni formed in the three DESs were reported

#### **REFERENCES**

- [1] R. Rogers, K. Seddon, and S. Volkov, Green Industrial Applications of Ionic Liquids, ed. Springer, 2003.
- [2] J.P. Hallett and T. Welton, Chem. Rev., 2011, 111, 3 08-3 76; P. Wasserscheid and W. Keim, Angew. Chem., Int, Ed., 2000, 39,3772-3789; (b) H. Wang, G. Gurau and R.D. Rogers, Chem. Soc.Rev., 2012, 41,1 19-1 37.
- [3] D. A. Walsh, K. R. J. Lovelock and P. Licence, Chem. Soc. Rev., 2010,39,418 -4194; Electrodeposition from Ionic Liquids, ed. F. Endres, D. MacFarlance and A. Abbott, Wiley-VCH,2008.
- [4] J. Dupont and J.D. Scholten, Chem. Soc. Rev., 2010, 39, 1780-1804; (b) J. L. Bideau,L. Viau and A. Vioux, Chem. Soc. Rev., 2011,40, 907-92.
- [5] P. Wasserschield, T. Welton, Ionic Liquids in Synthesis, Wiley-VCH, Weinheim, 2003 https://doi.org/10.1021/op0340210.
- [6] M. A. Kareem, F. S. Mjalli, M.A. Hashim, I. M. Alnashef, Phosphonium-based ionic liquidsanalogues and their physical properties, J. Chem. Eng. Data 55 (2010) 4632 4637. https://doi.org/10.1021/je100104v.
- [7] J. Sun, M. Forsyth, D. R. Mac Farlene, Room-temperature molten salts based on the quaternary ammonium ion, J. Phys. Chem. B 102 (1998) 8858 –8864. https://doi.org/10.1021/jp981159p.
- [8] S. J. Zhang, Y. H. Chen, R. X. F. Ren, et al., Solubility of CO2 in sulfonate ionic liquids at high pressure, J. Chem. Eng. Data 50 (2005) 230 233. https://doi.org/10.1021/je0497193.
- [9] A. Paiva, R. Craveiro, I. Aroso, et al., Natural deep eutectic solvents-solvents for the 21st century, ACS Sust. Chem. Eng. 2 (2014) 1063–1071. https://doi.org/10.1021/sc500096j.

- [10] C. M. Wang, X. Y. Luo, X. Zhu, et al., The strategies for improving carbon dioxide chemisorption by functionalized ionic liquids, RSC Adv. 3 (2013) 15518 15527. https://doi.org/10.1039/c3ra42366b.
- [11] M. A. Navarra, J. Manzi, L. Lombardo, S. Panero, B. Scrosati, Ionic liquid-based membranes as electrolytes for advanced lithium polymer batteries, Chem- Sus Chem 4 (2011) 125 130. https://doi.org/10.1002/cssc.201000254.
- [12] X. Ge, C.D. Gu, Y. Lu, X.L. Wang, J.P. Tu, A Versatile protocol for the ionothermal synthesis of nanostructured nickel compounds as energy storage materials from a choline chloride-based ionic liquid, J. Mater. Chem. A 1 (2013) 13454 13461. https://doi.org/10.1039/C3TA13303F.
- [13] M. Hayyan, F. S. Mjalli, M. A. Hashim, I. M. Alnashef, X. M. Tan, Electrochemical reduction of dioxygen in bis (trifluoromethylsulfonyl) imide based Ionic liquids, J. Electroanal. Chem. 657 (2011) 150 157. doi: 10.1016/j.jelechem.2011.04.008.
- [14] P. D. de Mara, Z. Maugeri, Ionic liquids in bio transformations: from proof-of concept to emerging deep-eutectic-solvents, Curr. Opin. Chem. Biol. 15 (2011) 220 225. doi: 10.1016/j.cbpa.2010.11.008.
- [15] N. V. Plechkova, K. R. Seddon, Applications of ionic liquids in the chemical industry, Chem. Soc. Rev. 37 (2008) 123 150. https://doi:10.1039/B006677J.
- [16] C. Rub, B. König, Low melting mixtures in organic synthesis-an alternative to ionic liquids, Green Chem. 14 (2012) 2969 2982. https://doi.org/10.1039/C2GC36005E.
- [17] X. Ge, C.D. Gu, X. L. Wang, J. P. Tu, Endowing manganese oxide with fast adsorption ability through controlling the manganese carbonate precursor assembled in ionic liquid, J. Colloid Interface Sci. 438 (2015) 149 158. https://doi.org/10.1016/j.jcis.2014.09.029.
- [18] (a) M. J. Earle, S. P. Kaydare and K.R. Seddon, Org. Lett., 2004,6,707-710; (b)Q.zhang, S. Zhang, S. Zhang and Y. Deng, Green Chem., 2011, 13, 2619-2637.

- [19] (a) A. Romero, A. Santos, J. Tojo and A. Rodriguez, J. Hazard. Mater., 2008, 268-273; (b) N. V. Plechkova and K. R. Seddo, Chem. Soc. Rev., 2008, 37, 123-1 0.
- [20] Qinghua Zhang, Karine De Oliveira Vigier, Sebastien Royer and Francois Jerome, Deep Eutectic solvents: synthesis, properties and applications, Chem. Soc. Rev. 2012, DOI:10.1039/c2cs3 178a.
- [21] Y. Yu, X. Lu, Q. Zhou, K. Dong, H. Yao and S. Zhang, Chem-Eur. J., 2008, 14, 11174-11182.
- [22] K. D. Weaver, H.J. Kim, J. Sun, D. R. MacFarlane and G. D. Elliott, Green Chem., 2010, 12, 07-13.
- [23] F. Ilegan, D. Ott, D. Kralish, C. Reil, A. Palmberger and B. konig, Green chem., 2009,11, 1948-19 4.
- [24] D. Reinhardt, F. Ilegan, D. Kralisch, B. konig and D. Kralish, Green chem., 2008, 10, 1170-1181.
- [25] E. R. Cooper, C. D. Andrews, P. S. Wheatley, P. B. Webb, P. Wormald and R. E. Morris, Ionic liquids and eutectic mixtures as solvent and template in synthesis of zeolite analogues, Nature, 2004, 430, 1012–1016.
- [26] Daniel Carriazo, Marı'a Concepcio' n Serrano, Marı'a Concepcio' n Gutie' rrez, Marı'a Luisa Ferrer and Francisco del Monte, Deep-eutectic solvents playing multiple roles in the synthesis of polymers and related materials, Chem. Soc. Rev., 2012, 41, 4996–5014 DOI: 10.1039/c2cs15353j.
- [27] A. P. Abbott, J. C. Barron, K. S. Ryder and D. Wilson, Chem-Eur. J., 2007, 13, 649 601.
- [28] M. Francisco, A. van den Bruinhorst, M. C. Kroon, Low-Temperature-Temperature Mixtures (LTTMs): a new generation of designer solvents, Angew. Chem. Int. Ed. 52 (2013) 3074 3085. https://doi.org/10.1002/anie.201207548.

- [29] A. P. Abbott, G. Capper and S. Gray, ChemPhysChem, 2006, 7, 803-806.
- [30] A. P. Abbott, D. Boopathy, G. Capper, D. L. Davies and R. K. Rasheed, J. Am. Chem. Soc., 2004, 126, 9142-9147.
- [31] W. Li, Z. Zhang, B. Han, S. Hu, J. Song, Y. Xie and X. Zhou, Green Chem., 2008, 10, 1142-114.
- [32] Emma L. Smith; Andrew P. Abbott; Karl S. Ryder (2014). "Deep Eutectic Solvents (DESs) and their applications". Chemical Reviews. 114 (21): 11060–11082. doi:10.1021/cr300162p. PMID 25300631.
- [33] "Deep Eutectic Solvents" (PDF). kuleuven.be. The University of Leicester. Retrieved 17 June 2014.
- [34] Andrew P. Abbott; Glen Capper; David L. Davies; Raymond K. Rasheed; Vasuki Tambyrajah (2003). "Novel solvent properties of choline chloride/urea mixtures". Chem. Commun. 0 (1): 70–71. doi:10.1039/B210714G.
- [35] Andrew Abbott; John Barron; Karl Ryder; David Wilson (2007). "Eutectic-Based Ionic Liquids with Metal-Containing Anions and Cations". Chem. Eur. J. 13 (22): 6495–6501. doi:10.1002/chem.200601738.
- [36] Mukhtar A. Kareem; Farouq S. Mjalli; Mohd Ali Hashim; Inas M. AlNashef (2010). "Phosphonium-Based Ionic Liquids Analogues and Their Physical Properties". Journal of Chemical & Engineering Data. 55 (11): 4632–4637. doi:10.1021/je100104v.
- [37] Clarke, Coby J.; Tu, Wei-Chien; Levers, Oliver; Bröhl, Andreas; Hallett, Jason P. (2018-01-24). "Green and Sustainable Solvents in Chemical Processes". Chemical Reviews. 118(2): 747–800. DOI: 10.1021/acs.chem rev.7b00571.
- [38] LucíaAbad-Gil; "Binary and ternary deep eutectic solvent mixtures: Influence on methylene blue electropolymerization"; Electrochemistry Communications Volume 124, March 2021,106967.

- [39] Xu, G.; Ding, J.; Han, R.; Dong, J.; Ni, Y. Enhancing cellulose accessibility of corn stover by deep eutectic solvent pretreatment for butanol fermentation. Bioresour. Technol. 2016, 203, 364–369.
- [40] Xia, S.; Baker, G.A.; Li, H.; Ravular, S.; Zhao, H. Aqueous ionic liquids and deep eutectic solvents for cellulosic biomass pretreatment and saccharification. RSC Adv. 2014, 4, 10586–10596.
- [41] Procentese, A.; Raganati, F.; Olivieri, G.; Elena, M.; Rehmann, L.; Marzocchella, A. Low-Energy biomass pretreatment with deep eutectic solvents for bio-butanol production. Bioresour. Technol. 2017, 243, 464–473.
- [42] Zhang, C.W.; Xia, S.Q.; Ma, P.S. Facile pretreatment of lignocellulosic biomass using deep eutectic solvents. Bioresour. Technol. 2016, 219, 1–5.
- [43] Alhassan, Y.; Pali, H.S.; Kumar, N.; Bugaje, I.M. Co-Liquefaction of whole Jatropha curcas seed and glycerol using deep eutectic solvents as catalysts. Energy 2017, 138, 48–59.
- [44] Alhassan, Y.; Kumar, N.; Bugaje, I.M. Hydrothermal liquefaction of de-oiled Jatropha curcas cake using deep eutectic solvents (DESs) as catalysts and co-solvents. Bioresour. Technol. 2016, 199, 375–381.
- [45] Cao, Q.; Li, J.; Xia, Y.; Li, W.; Luo, S.; Ma, C.; Liu, S. Green extraction of six phenolic compounds from rattan (calamoideaefaberii) with deep eutectic solvent by a homogenate-assisted vacuum-cavitation method. Molecules 2019, 24, 113.
- [46] Dwan, J.; Durant, D.; Ghandi, K.; Warsaw, V.; Heidelberg, S.B. Nuclear magnetic resonance spectroscopic studies of the trihexyl (tetradecyl) phosphonium chloride ionic liquid mixtures with water. Cent. Eur. J.Chem. 2008, 6, 347–358.
- [47] Lan, D.; Wang, X.; Zhou, P.; Hollmann, F.; Wang, Y. Deep eutectic solvents as performance additives in biphasic reactions. RSC Adv. 2017, 7, 40367–40370.

- [48] Tang, B.; Park, H.E.; Row, K.H. Simultaneous extraction of flavonoids from chamaecyparisobtusa using deep eutectic solvents as additives of conventional extractions solvents.
- [49] Qinghua Zhang, Karine De Oliveira Vigier, Sebastien Royer and Francois Jerome, Deep eutectic solvents: syntheses, properties and applications. Chem. Soc. Rev., 41 (2012), pp.7108–7146, DOI: 10.1039/c2cs35178a.
- [50] Emma L. Smith, Andrew P. Abbott, and Karl S. Ryder, Deep Eutectic Solvents (DESs) and Their Applications. pubs.acs.org/CR Chem. Rev. 114 (2014), pp. 11060-11082, dx.doi.org/10.1021/cr300162p.
- [51] Liao, H. G., Jiang, Y. X., Zhou, Z. Y., Chen, S. P. and Sun, S. G., Shape-Controlled Synthesis of Gold Nanoparticles in Deep Eutectic Solvents for Studies of Structure–Functionality Relationships in Electrocatalysis. Angew. Chem., Int. Ed., 47 (2008) pp. 9100–9103. https://doi.org/10.1002/anie.200803202
- [52] Chirea, M., Freitas, A., Vasile, B. S., Ghitulica, C., Pereira, C. M. and Silva, F., Gold Nanowire Networks: Synthesis, Characterization, and Catalytic Activity. Langmuir, 27 (2011) pp. 3906–3913. dx.doi.org/10.1021/la104092b |
- [53] Phuong, T.D.V., Phi, T.L., Phi, B.H., Van Hieu, N., Tang Nguyen, S. and Le Manh, T., Electrochemical Behavior and Electronucleation of Copper Nanoparticles from CuCl 2. H<sub>2</sub>O Using a Choline Chloride-Urea Eutectic Mixture. Journal of Nanomaterials, 7 (2021), pp. 1 14.
- [54] Parsa, A. and Heli, H., Electrodeposition of nickel wrinkled nanostructure from choline chloride: urea deep eutectic solvent (reline) and application for electroanalysis of simvastatin. Microchemical Journal, 152 (2020), p.104267.
- [55] Verma, C., Ebenso, E.E. and Quraishi, M.A., Transition metal nanoparticles in ionic liquids: Synthesis and stabilization. Journal of Molecular Liquids, 276 (2019),826-849.

- [56] Tome, L.I., Baiao, V., da Silva, W. and Brett, C.M., Deep eutectic solvents for the production and application of new materials. Applied Materials Today, 10 (2018),30-50. [57] Li, W., Hao, J., Liu, W. and Mu, S., Electrodeposition of nano Ni–Co alloy with (220) preferred orientation from choline chloride-urea: Electrochemical behavior and nucleation mechanism. Journal of Alloys and Compounds, 853 (2021), p.157158. [58] Palomar-Pardavé, M., Mostany, J., Muñoz-Rizo, R., Botello, L.E., Aldana-González, J., Arce-Estrada, E.M., de Oca-Yemha, M.G.M., Ramírez-Silva, M.T. and Romo, M.R., Electrochemical study and physicochemical characterization of iron nanoparticles electrodeposited onto HOPG from Fe (III) ions dissolved in the choline chloride-urea deep eutectic solvent. Journal of Electroanalytical Chemistry, 851 (2019), p.113453. [59] Delbecq, F., Delfosse, P., Laboureix, G., Paré, C. and Kawai, T., Study of a gelated Deep Eutectic solvent metal salt solution as template for the production of size-controlled small noble metal nanoparticles. Colloids and Surfaces A: Physicochemical and Engineering Aspects, 567 (2019), pp.55-62.
- [60] Ghenaatian, H.R., Shakourian-Fard, M. and Kamath, G., Interaction of Cun, Agn and Aun (n= 1–4) nanoparticles with ChCl: Urea deep eutectic solvent. Journal of Molecular Graphics and Modelling, 105 (2021), p.107866.
- [61] Kakaei, K., Alidoust, E. and Ghadimi, G., Synthesis of N-doped graphene nanosheets and its composite with urea choline chloride ionic liquid as a novel electrode for supercapacitor. Journal of Alloys and Compounds, 735 (2018), pp.1799-1806.
- [62] C. Sun, J. Zeng, H. Lei, W. Yang, and Q. Zhang, "Direct electrodeposition of phosphorus-doped nickel superstructures from choline chloride–ethylene glycol deep eutectic solvent for enhanced hydrogen evolution catalysts," *ACS Sustainable Chemistry & Engineering*, vol. 7, pp. 1529-1537, 2018.

- [63] M. Zhong, Q. F. Tang, Y. W. Zhu, X. Y. Chen, and Z. J. Zhang, "An alternative electrolyte of deep eutectic solvent by choline chloride and ethylene glycol for wide temperature range supercapacitors," *Journal of Power Sources*, vol. 452, p. 227847, 2020. [64] C. Liu, P. Jiang, Y. Huo, T. Zhang, and Z. Rao, "Experimental study on ethylene glycol/choline chloride deep eutectic solvent system based nanofluids," *Heat and Mass Transfer*, pp. 1-10, 2021.
- [65] Y. Xue, Y. Hua, J. Ru, C. Fu, Z. Wang, J. Bu, *et al.*, "High-efficiency separation of Ni from Cu-Ni alloy by electrorefining in choline chloride-ethylene glycol deep eutectic solvent," *Advanced Powder Technology*, 2021.
- [66] I. Espino-López, M. Romero-Romo, M. M. de Oca-Yamaha, P. Morales-Gil, M. Ramírez-Silva, J. Most any, *et al.*, "Palladium nanoparticles electrodeposition onto glassy carbon from a deep eutectic solvent at 298 K and their catalytic performance toward formic acid oxidation," *Journal of The Electrochemical Society*, vol. 166, p. D3205, 2018.
- [67] Hai-Chuan-Hu, Deep eutectic solvent based on choline chloride and malonic acid as an efficient and reusable catalytic system for one-pot synthesis of functionalized pyrroles, RSC Advances, Issue 10,2015.
- [68] Kroon, M.C.; Binnemans, K. Degradation of deep-eutectic solvents based on choline chloride and carboxylic acids. ACS Sustain. Chem. Eng. 2019, 7, 11521–11528.
- [69] Iman Al-Wahaibi et al., The novel use of malonic acid-based deep eutectic solvents forenhancing heavy oil recovery; International Journal of Oil, Gas and Coal Technology, 2019 Vol.20 No.1, pp.31 54; DOI: 10.1504/IJOGCT.2019.096493.
- [70] Gunny, A. A. N.; Arbain, D.; Nashef, E. M.; Jamal, P.; Bioresour. Technol. 2015, 181, 297.

- [71] Rajiv Kohli, Chapter 16 Applications of Ionic Liquids in Removal of Surface Contaminants; Developments in Surface Contamination and Cleaning: Applications of Cleaning Techniques; Vol 11 2019, pp 619-680.
- [72] Aydin K.Sunol, TizianaFornari, in handbook of solvents (3rd edition), Chapter 20-Substitution of solvents by safer products; ChemTec Publishing, Vol 2, Use, Health and Environment, 2019, pp 1455-1634.
- [73] Haerens, K.; Matthijs, E.; Chmielarz, A.; Van der Bruggen, B. J. Environ. Manage. 2009, 90, 3245
- [74] Angeles et al., Chapter 5 Nanocellulose for Industrial Use: Cellulose Nanofibers (CNF), Cellulose Nanocrystals (CNC), and Bacterial Cellulose (BC); Handbook of Nanomaterials for Industrial Applications; Micro and Nano Technologies; 2018, pp 74-126 [75] Smith, E. L.; Fullarton, C.; Harris, R. C.; Saleem, S.; Abbott, A. P.; Ryder, K. S. Trans. Inst. Met. Finish. 2010, 88, 285
- [76] Abbott, A. P.; Barron, J. C.; Elhadi, M.; Frisch, G.; Gurman, S. J.; Hillman, A. R.; Smith, E. L.; Mohamoud, M. A.; Ryder, K. S. ECS Trans. 2009, 16, 47
- [77] Abbott, A. P.; McKenzie, K. J. Phys. Chem. Chem. Phys. 2006, 8, 4265
- [78] Abbott, A. P.; Ryder, K. S.; Konig, U. Trans. Inst. Met. Finish. 2008, 86, 196
- [79] Abbott, A. P.; Barron, J. C.; Ryder, K. S. Trans. Inst. Met. Finish. 2009, 87, 201
- [80] Abbott, A. P.; Barron, J. C.; Frisch, G.; Ryder, K. S.; Silva, A. F. Electrochim. Acta 2011, 56, 5272
- [81] Abbott, A. P.; McKenzie, K. J. Phys. Chem. Chem. Phys. 2006, 8, 4265
- [82] Abbott, A. P.; El Taib, K.; Frisch, G.; McKenzie, K. J.; Ryder, K. S. Phys. Chem. Phys. 2009, 11, 4269.
- [83] Popescu, A. M.; Cojocaru, A.; Donath, C.; Constantin, V. Chem. Res. Chin. Univ. 2013, 29, 991

- [84] Abbott, A. P.; El Ttaib, K.; Ryder, K. S.; Smith, E. L. Trans. Inst. Met. Finish. 2008, 86, 234
- [85] Abbott, A. P.; El Ttaib, K.; Frisch, G.; Ryder, K. S.; Weston, D. Phys. Chem. Chem. Phys. 2012, 14, 2443
- [86] Abbott, A. P.; Capper, G.; Davies, D. L.; Rasheed, R. K. Chem.—Eur. J. 2004, 10, 3769
- [87] Abood, H. M. A.; Abbott, A. P.; Ballantyne, A. D.; Ryder, K. S. Chem. Commun. 2011, 47, 3523
- [88] Gomez, E.; Cojocaru, P.; Magagnin, L.; Valles, E. J. Electro anal. Chem. 2011, 658, 18
- [89] Peng Liu et.al., Recent advances in the application of deep eutectic solvents as sustainable media as well as catalysts in organic reactions; RSC Adv; Issue 60,2015,5, pp 48675-48704.
- [90] Chiara Fanali et al., Application of deep eutectic solvents for the extraction of phenolic compounds from extra-virgin olive oil; National Library of Medicine; Electrophoresis; 2020 Oct;41(20):1752-1759.
- [91] Wang Ailing et al., Deep Eutectic Solvents to Organic Synthesis; Progress in Chemistry, 2014, Vol. 26, Issue 5, pp 784-795.
- [92] Ali Abo-Hamed et.al., Potential applications of deep eutectic solvents in nanotechnology; Chem.Engg., Journal;2015;273;pp 551-567.
- [93] CarriazoD,et.al. Resorcinol-based deep eutectic solvents as both carbonaceous precursors and templating agents in the synthesis of hierarchically porous carbon monoliths. Chem. Mater. 2010, 22, 6146–6152.
- [94] Chakrabarti MH, et al., One-pot electrochemical gram-scale synthesis of graphene using deep eutectic solvents and acetonitrile. Chem. Eng. J. 2015, 274, 213–223.

- [95] Querejeta-Fernández A, et al., Unknown aspects of self-assembly of PbS microscale superstructures. ACS Nano. 2015, 6, 3800–3812.
- [96] Liu W,et.al.,. Synthesis of monoclinic structured BiVO4 spindly microtubes in deep eutectic solvent and their application for dye degradation. J. Hazard. Mater. 2010, 181, 1102–1108.
- [97] Dong J. et.al. Growth of ZnO nanostructures with controllable morphology using a facile green antisolvent method. J. Phys. Chem. C 2010, 114, 8867–8872.
- [98] Gallego I, et.al., Folding and imaging of DNA nanostructures in anhydrous and hydrated deep-eutectic solvents. Angew. Chem., Int. Ed. 2015, 54, 6765–6769.
- [99] Wagle DV, et.al., Deep eutectic solvents: sustainable media for nanoscale and functional materials. Acc. Chem. Res. 2014, 47, 2299–2308.
- [100] Ma Z, Yu JH, Dai S. Preparation of inorganic materials using ionic liquids. Adv. Mater. 2010, 22, 261–285.
- [101] Muzamil Khatri et al., Zein nanofibers via deep eutectic solvent electrospinning: tunable morphology with super hydrophilic properties; Scientific Reports 10, 15307,2020. [102] Liao, H.G.; Jiang, Y.-X.; Zhou, Z.-Y.; Chen, S.-P.; Sun, S.-G. Angew. Chem. 2008, 120, 9240
- [103] Jae-Seung Lee; Deep eutectic solvents as versatile media for the synthesis of noble metal nanomaterials; De Gruyter; Nanotechnology Rev;6,3, 2017.
- [104] Liu, Q., Huang, X., and Liang, P.; Preconcentration of copper and lead using deep eutectic solvent modified magnetic nanoparticles and determination by inductively coupled plasma optical emission spectrometry. Atomic Spectrosc. 41, 2020;pp 36–42. DOI: 10.46770/AS.2020.01.005
- [105] Majidi, S. M., and Hadjmohammadi, M. R.; Alcohol-based deep eutectic solvent as a carrier of SiO2@Fe3O4 for the development of magnetic dispersive micro-solid-phase

extraction method: application for the preconcentration and determination of morin in apple and grape juices, diluted and acidic extract of dried onion and green tea infusion samples.

J. Sep. Sci. 42, 2019; pp2842–2850. DOI: 10.1002/jssc.201900234

[106] LirongNie et al., Rethinking the Applications of Ionic Liquids and Deep Eutectic Solvents in Innovative Nano-Sorbents; Front.Chem.Apr.2021.

[107] Ingrid Hagarova et.al., Application of Metallic Nanoparticles and Their Hybrids as Innovative Sorbents for Separation and Pre-concentration of Trace Elements by Dispersive Micro-Solid Phase Extraction: A Minireview; Front.Chem.May 2021.

[108] N.Azizi et.al., Sci.Iranica C; Greener synthesis of magnetic nanoparticles in an aqueous deep eutectic solvent; 23(6), 2016, pp 2750-2755.

[109] L. Anicai, et.al, Electrochemical synthesis of nanosized TiO<sub>2</sub>nanopowder involving choline chloride-based ionic liquids, Mat. Sci. Eng. B 199,2015, pp 87-95.

[110] F. Chen, S. Xie, X. Huang, X. Qiu, Ionothermal synthesis of Fe3O4magnetic nanoparticles as efficient heterogeneous Fenton-like catalysts for degradation of organic pollutants with H2O2, J. Haz. Mater. 322 (2017) 152-162.

[111] T. Cun, C. Dong, Q. Huang, Ionothermal precipitation of highly dispersive ZnO nanoparticles with improved photocatalytic performance, Appl. Surface Sci. 384 (2016) 73-82.

[112] D.O. Oseguera-Galindo, R. Machorro-Mejia, Silver nanoparticles synthesized by laser ablation confined in urea choline chloride deep eutectic solvent, Colloids Interface Sci, Commun. 12 (2016) 1-4.

[113] M. Karimi, M.R. Ramsheh,et.al., One-step and low-temperature synthesis of monetite nanoparticles in an all-in-one system (reactant, solvent, and template) based on calcium chloride-choline chloride deep eutectic medium, Ceramics International 43 (2017) 2046-2050.

- [114] Antonio Jose et.al., Fast Synthesis of CeO2 Nanoparticles in a Continuous Microreactor Using Deep Eutectic Reline as Solvent; ACS Sustainable Chem.Engg.2020,8,49,pp18297-18302.
- [115] Bruna et.al., TiO<sub>2</sub> nanoparticles coated with deep eutectic solvents: characterization and effect on photodegradation of organic dyes; RSC, New J. Chem., 3,2019,43, pp 1415-1423.
- [116] Anika Soldner, Julia Zach et.al., Preparation of Magnesium, Cobalt and Nickel Ferrite Nanoparticles from Metal Oxides using Deep Eutectic Solvents; PUB MED NLM, 2016;22 (37):13108-13.
- [117] Mehrabi, Novin; Abdul Haq, Umar Faruq; Reza, M. Toufiq; Aich, Nirupam (2020): Using Deep Eutectic Solvent for Conjugation of Fe3O4 Nanoparticles onto Graphene Oxide for Water Pollutant Removal. ChemRxiv. Preprint. https://doi.org/10.26434/chemrxiv.12089658.v1
- [118] A. Cojocaru, O. Brincoveanu et.al., Electrochemical preparation of Ag nanoparticles involving choline chloride glycerol deep eutectic solvents; Bulgarian Chemical Communications, Volume 49 Special Issue C (pp. 194–204) 2017
- [119] Jakubowska M, Ruzik L et.al., Application of Natural Deep Eutectic Solvents for the metal nanoparticles extraction from plant tissue; Analytical Biochemistry, 2021, 617:114117
- [120] Kang YS, Risbud S, Rabolt JF, Stroeve P. Synthesis and characterization of nanometer-size Fe<sub>3</sub>O<sub>4</sub> and γ-Fe<sub>2</sub>O<sub>3</sub> Particles. Chem Mater. 1996;8:2209–11.
- [121] Pankhurst QA, J Connolly, Jones SK, Dobson J. Applications of magnetic nanoparticles in biomedicine. J Phys D Appl. Phys. 2003;36: R167.
- [122] Dobson J. Gene therapy progress and prospects: magnetic nanoparticle-based gene delivery. Gene Ther. 2006; 13:283–7. [PubMed]

- [123] Rudge S, Peterson C, Vesely C, Koda J, Stevens S, Catterall L. Adsorption, and desorption of chemotherapeutic drugs from a magnetically targeted carrier (MTC) J Control Release. 2001; 74:335–40. [PubMed]
- [124] Appenzeller T. The man who dared to think small. Science. 1991; 254:1300.
- [125] Qin Y. Silver-containing alginate fibers and dressings. Int Wound J. 2005; 2:172–6. [PMC free article]
- [126] Atiyeh BS, Costagliola M, Hayek SN, Dibo SA. Effect of silver on burn wound infection control and healing: a review of the literature. Burns. 2007; 33:139–48. [PubMed] [127] Lansdown AB. Silver in health care: antimicrobial effects and safety in use. CurrProbl Dermatol. 2006; 33:17–34. [PubMed]
- [128] Stepanov AL, Popok VN, Hole DE. Formation of Metallic Nanoparticles in Silicate Glass through Ion Implantation. Glass Phy Chem. 2002; 28:90–5.
- [129] Elechiguerra JL, Burt JL, Morones JR, Camacho-Bragado A, Gao X, Lara HH, et al. Interaction of silver nanoparticles with HIV-1. J Nanobiotechnology. 2005; 3:6.
- [130] Shabir Ahmad, Sidra Munir, Nadia Zeb; Green nanotechnology: a review on green synthesis of silver nanoparticles an ecofriendly approach; Int J Nanomedicine. 2019 Jul 10; 14:5087-5107. DOI: 10.2147/IJN.S200254.
- [131] Muhammad Rafique, Iqra Sadaf, M Shahid Rafique, M Bilal Tahir, A review on green synthesis of silver nanoparticles and their applications; Artif Cells NanomedBiotechnol. 2017 Nov; 45(7):1272-1291. DOI: 10.1080/21691401.2016.1241792.
- [132] Chitsazi MR, Korbekandi H, Asghari G, Bahri Najafi R, Badii A, Iravani S. 2016. Synthesis of silver nanoparticles using methanol and dichloromethane extracts of Pulicariagnaphalodes (Vent.) Boiss. aerial parts. Artifl cells, NanomedBiotechnol. 44:328–333.

- [133] Wang H, Qiao X, Chen J, Wang X, Ding S. 2005. Mechanisms of PVP in the preparation of silver nanoparticles. Mater Chem Phys. 94:449–453.
- [134] Guzmán MG, Dille J, Godet S. 2009. Synthesis of silver nanoparticles by chemical reduction method and their antibacterial activity. Int J Chem Biol Eng. 2:104–111.
- [135] Tran QH, Le AT. 2013. Silver nanoparticles: synthesis, properties, toxicology, applications, and perspectives. Adv Nat Sci NanosciNanotechnol. 4:033001.
- [136] Chou CW, Hsu SH, Wang PH. 2008. Biostability and biocompatibility of poly(ether)urethane containing gold or silver nanoparticles in a porcine model. J Biomed Mater Res A. 84:785–794. [PubMed]
- [137] Sang-Hun Lee 1, Bong-Hyun Jun; Silver Nanoparticles: Synthesis and Application for Nanomedicine; Int J Mol Sci. 2019 Feb 17;20(4):865. DOI: 10.3390/ijms20040865.
- [138] Gurunathan S., Han J.W., Kim E.S., Park J.H., Kim J.H. Reduction of graphene oxide by resveratrol: A novel and simple biological method for the synthesis of an effective anticancer nanotherapeutic molecule. Int. J. Nanomed. 2015;10:2951–2969. DOI: 10.2147/IJN.S79879.
- [139] Ganaie S.U., Abbasi T., Abbasi S.A. Green synthesis of silver nanoparticles using an otherwise worthless weed mimosa (Mimosa pudica): Feasibility and process development toward shape/size control. Part. Sci. Technol. 2015; 33:638–644. DOI: 10.1080/02726351.2015.1016644.
- [140] Alshehri, A. H., Jakubowska, M., Młozniak, A., Horaczek, M., Rudka, D., Free, C., et al. (2012). Enhanced electrical conductivity of silver nanoparticles for high-frequency electronic applications. ACS Appl. Mater. Interfaces 4, 7007–7010. DOI: 10.1021/am3022569.

- [141] Nie, S., and Emory, S. R. (1997). Probing single molecules and single nanoparticles by surface-enhanced Raman scattering. Science 275, 1102–1106. DOI: 10.1126/science.275.5303.1102.
- [142] Xu, R., Wang, D., Zhang, J., and Li, Y. (2006). The shape-dependent catalytic activity of silver nanoparticles for the oxidation of styrene. Chem. Asian J. 1, 888–893. DOI: 10.1002/asia.200600260.
- [143] Kelly, K. L., Coronado, E., Zhao, L. L., and Schatz, G. C. (2003). The optical properties of metal nanoparticles: the influence of size, shape, and dielectric environment. J. Phys. Chem. B. 107, 668–677. DOI: 10.1021/jp026731y.
- [144] Tran, Q. H., Nguyen, V. Q., and Le, A. T. (2013). Silver nanoparticles: synthesis, properties, toxicology, applications, and perspectives. Adv. Nat. Sci. 4, 20. DOI: 10.1088/2043-6262/4/3/033001.
- [145] Ajitha B, Reddy YA, Reddy P. Enhanced antimicrobial activity of silver nanoparticles with controlled particle size by pH variation. Powder Technol. 2015; 269(3):110–7. https://doi.org/10.1016/j.powtec.2014.08.049.
- [146] Catalina Quintero-Quiroz,et.al., Optimization of silver nanoparticle synthesis by chemical reduction and evaluation of its antimicrobial and toxic activity; Biomaterials Research volume 23, Article number: 27 (2019)
- [147] Manoj B. Gawande et.al., Cu and Cu-Based Nanoparticles: Synthesis and Applications in Catalysis; Chem. Rev. 2016, 116, 6, 3722–3811; https://doi.org/10.1021/acs.chemrev.5b00482
- [148] Prateek Khare; Synthesis of phenolic precursor-based porous carbon beads in situ dispersed with copper—silver bimetal nanoparticles for antibacterial applications; 2014; Journal of Colloid and Interface Science 418:216—224 DOI: 10.1016/j.jcis.2013.12.026

- [149] Cushing, B.L., Kolesnichenko, V.L., O'Connor, C.J.: Recent advances in the liquidphase syntheses of inorganic nanoparticles. Chem. Rev. 104, 3893–3946 (2004)
- [150] Dang, T.M.D., Le, T.T.T., Blanc, E.F., Dang, M.C.: Synthesis and optical properties of copper nanoparticles prepared by a chemical reduction method. Adv. Nat. Sci. Nanosci. Nanotechnol. 2, 15009–15012 (2011)
- [151] D. Adner, M. Korb, S. Schulze, M. Hietschold, and H. Lang, "A straightforward approach to oxide-free copper nanoparticles by thermal decomposition of a copper(I) precursor," Chemical Communications, vol. 49, pp. 6855–6857, 2013.
- [152] R. K. Bortoleto-Bugs, T. Mazon, M. TarozzoBiasoli, A. Pavani Filho, J. Willibrordus Swart, and M. Roque Bugs, "Understanding the formation of the self-assembly of colloidal copper nanoparticles by a surfactant: a molecular velcro," Journal of Nanomaterials, vol. 2013, Article ID 802174, 8 pages, 2013.
- [153] S. P. Meshram, P. V. Adhyapak, U. P. Mulik, and D. P. Amalnerkar, "Facile synthesis of CuO nanomorphs and their morphology dependent sunlight driven photocatalytic properties," Chemical Engineering Journal, vol. 204-205, pp. 158–168, 2012.
- [154] M. S. Usman, N. A. Ibrahim, K. Shameli, N. Zainuddin, and W. M. Z. W. Yunus, "Copper nanoparticles mediated by chitosan: synthesis and characterization via chemical methods," Molecules, vol. 17, no. 12, pp. 14928–14936, 2012.
- [155] Jiang W, Singhal A, Zheng J, Wang C, Chan CW, Optimizing the Synthesis of Redto Near-IR-Emitting CdS-Capped CdTexSe1-x Alloyed Quantum Dots for Biomedical Imaging. Chem Mate 2006; 18: 4845--4854.
- [156] Claudia Martínez-Alonso, Carlos A. Rodríguez-Castañeda, Paola Moreno-Romero, C. Selene Coria-Monroy, Hailin Hu, "Cadmium Sulfide Nanoparticles Synthesized by Microwave Heating for Hybrid Solar Cell Applications", International Journal of

- Photoenergy, vol. 2014, Article ID 453747, 11 pages, 2014. https://doi.org/10.1155/2014/453747
- [157] F. Chen, R. Zhou, L. Yang, M. Shi, G. Wu, M. Wang and H. Chen, J. Phys. Chem. C, 2008, 112, 13457–13462.
- [158] Y. Huang, F. Sun, T. Wu, Q. Wu, Z. Huang, H. Su, and Z. Zhang, J. Solid State Chem., 2011, 184, 644.
- [159] M. R. Gholipour, C. T. Dinh, F. Beland, and T. O. Do, Nanoscale, 2015, 7, 8187–8203 RSC.
- [160] W. Wei, P. Q. Sun and Z. Li, Sci. Adv., 2018, 4, 9253–9260.
- [161] M. Mollavali, C. Falamaki and S. Rohani, Int. J. Hydrogen Energy, 2018, 43(19), 9259–9278.
- [162] K. A. Brown, D. F. Harris, and M. B. Wilker, Science, 2016, 352, 447–451
- [163] Zhaoyu Chang; Cadmium sulfide net framework nanoparticles for photo-catalyzed cell redox; RSC Adv., 2020, 10, 37820-37825; DOI: 10.1039/D0RA08235J
- [164] K. B. Narayanan and N. Sakthivel, "Biological synthesis of metal nanoparticles by microbes," Advances in Colloid and Interface Science, vol. 156, no. 1–2, pp. 1–13, 2010.
- [165] B. A. Rzigalinski and J. S. Strobl, "Cadmium-containing nanoparticles: perspectives on pharmacology and toxicology of quantum dots," Toxicology and Applied Pharmacology, vol. 238, no. 3, pp. 280–288, 2009.
- [166] Acharya KP. Photocurrent spectroscopy of CdS/plastic, CdS/glass, and ZnTe/GaAs hetero-pairs formed with pulsed laser deposition. Doctoral dissertation, Bowling Green State University, USA; 2009.
- [167] Zhu H, Jiang R, Xiao L, Chang Y, Guan Y, Li X, et al. Photocatalytic decolorization and degradation of Congo Red on innovative cross-linked chitosan/nano-CdS composite catalyst under visible light irradiation. J Hazardous Mater 2009; 169:933-40.

- [168] Song X, Yao W, Zhang B, Wu Y. Application of Pt/CdS for the photocatalytic flue gas desulfurization. Int J Photoenergy 2012;1-5. http://dx.doi.org/10.1155/2012/684735 [169] El-Kemary M, El-Shamy H, Mosaad MM. The role of capping agent on the interaction of cadmium sulfide nanoparticles with flufenamic acid drug. Mater Chem Phys 2009; 118:81-5.
- [170] Kozhevnikova NS, Vorokh AS. Preparation of stable colloidal solution of cadmium sulfideCdS using ethylenediaminetetraacetic acid. Russian J Gen Chem 2010; 80:391-4. [171] Bokka Durga, Shaik Raziya,, Santoshi G Rajamahanti, BoddetiGovindh, Korimella Vijaya Raju, Nowduri Annapurna; Synthesis and Characterization of Cadmium Sulphide nanoparticles Using Annona Muricata Leaf Extract as Reducing/Capping Agent; DOI:10.7598/cst2016.1291 Chemical Science Transactions; 2016, 5(4), 1035-1041 [172] J. D. Blum Nat. Chem., 2013, 5, 1066.
- [173] J. Jeevanandam, A. Barhoum, Y. S. Chan, A. Dufresne and M. K. Danquah, Beilstein J. Nanotechnol., 2018, 9, 1050—1074.
- [174] W. Lin Chem. Rev., 2015, 115, 10407 —10409.
- [175] K. Watanabe, D. Menzel, N. Nilius and H. J. Freund, Chem. Rev., 2006, 106, 4301—4320.
- [176] F. J. Heiligtag and M. Niederberger, Mater. Today, 2013, 16, 262—271.
- [177] C. Wang and D. Astruc, Prog. Mater. Sci., 2018, 94, 306—383.
- [178] Villa Krishna Harika, Tirupathi Rao Penki, Sustainable existence of solid mercury (Hg) nanoparticles at room temperature and their applications; Chemical science; Issue 9,2021
- [179] Jumpei Kuno, Tsuyoshi Kawai, and Takuya Nakashima; The effect of surface ligands on the optical activity of mercury sulfide nanoparticles; J. Nanoscale; Issue 32, 2017

- [180] Nashaat M. Mazrui, Emily Seelen, Cecil K. King'ondu; The precipitation, growth and stability of mercury sulfide nanoparticles formed in the presence of marine dissolved organic matter; Environmental science: Peocesses and Impacts; Issue 4; 2018
- [181] Kale, S. S., Lokhande, C. D., "Preparation and Characterization of HgS Films by Chemical Deposition." Mater. Chem. Phys., 1999, 59, 242-246.
- [182] Qin, A., Fang, Y., Zhao, W., Liu, H., Su, C., "Directionally Dendritic Growth of Metal Chalcogenide Crystals via Mild Template-free Solvothermal Method." J. Cryst. Growth., 2005, 283, 230-241.
- [183] Ding, T., Zhu, J., "Microwave Heating Synthesis of HgS and PbS Nanocrystals in Ethanol Solvent." Mater. Sci. Eng., 2003, 100, 307-313.
- [184] Ren, T., Xu, S., Zhao, W., Zhu, J., "A Surfactant-Assisted Photochemical Route to Single-CrystallineHgS Nanotubes." J. Photochem. Photobiol., 2005, 173, 93-98.
- [185] Mahapatra, A., K., Dash, A., K., "alpha–HgS Nanocrystals: synthesis, structure and optical properties.," Physica, 2006, 35, 9-15.
- [186] Patel, B. K., Rath, S., Sarangi, S. N., Sahu, S. N., "HgS Nanoparticles: Structure and Optical Properties." Appl. Phys., 2007, 86, 447-450.
- [187] Sapriel, J., "Cinnabar (α HgS), a promising acoustic optical material." Appl. Phys. Lett., 1971, 19, 533-535.
- [188] Higginson, K. A., Kuno, M., Bonevich, J., Qadri, S. B., Yousuf, M., Mattoussi, H., "Synthesis and Characterization of Colloidal  $\beta$ -HgS Quantum Dots." J. Phys. Chem., 2002, 106, 9982-9985.
- [189] N. Jassim Mohammed and H. Fakher Dagher; Synthesis and Characterization of Mercuric Sulfide Nanoparticles Thin Films by Pulsed Laser Ablation (PLA) in Distilled Water (DW). IJMSE, 2020, Vol. 17, No. 3, DOI: 10.22068/ijmse.17.3.11

[190] Xin Xu, Elizabeth R. Carraway, Sonication-Assisted Synthesis of β-Mercuric Sulphide Nanoparticles, Nanomaterials and Nanotechnology, 2012, https://doi.org/10.5772/55823

[191] Datta, S. (2020). Synthesis of nanostructure materials in deep eutectic solvents (Doctoral thesis). https://doi.org/10.17863/CAM.54841

[192] Yao, H., Ma, H., Mao, R. et al. Preparation of ZnO Nanoparticles from Zn-containing Rotary Hearth Furnace Dust. J. Wuhan Univ. Technol.-Mat. Sci. Edit. **37**, 32–37 (2022).

[193] Henam Sylvia Devi & Thiyam David Singh (2017) Synthesis of Mn<sub>2</sub>O<sub>3</sub> nanoparticles using choline chloride-ethylene glycol deep eutectic solvent: A green solvent, Integrated Ferroelectrics, 185:1, 82-89, DOI: 10.

[194] Sukanya Datta, Changshin Jo, Michael De Volder, and Laura Torrente-Murciano Morphological Control of Nanostructured V<sub>2</sub>O<sub>5</sub> by Deep Eutectic Solvents

\*\*ACS Applied Materials & Interfaces **2020** 12 (16), 18803-18812

DOI:10.1021/acsami.9b17916

[195] Elsharkawya, S., Hammad, S. & El-hallaga, I. Electrodeposition of Ni nanoparticles from deep eutectic solvent and aqueous solution promoting high stability electrocatalyst for hydrogen and oxygen evolution reactions. J Solid State Electrochem **26**, 1501–1517 (2022).

[196] Jing Wang and Sheila N. Baker; Pyrrolidinium salt-based binary and ternary deep eutectic solvents: green preparations and physiochemical property characterizations; De Gruyter, Green Process Synth 2018; 7: 353–359

[197]. Kumar V, Nigam KDP. Green Process Synth. 2012, 1, 79–107.

[198] Durand E, Lecomte J, Villeneuve P. Biochimie 2016, 120, 119–123.

[199] Taysun MB, Sert E, Atalay FS. J. Mol. Liq. 2016, 223, 845–852.

- [200] Martins MA, Paveglio GC, Munchen TS, Meyer AR, Moreira DN,Rodrigues LV, Frizzo CP, Zanatta N, Bonacorso HG, Melo PA.J. Mol. Liq. 2016, 223, 934–938.
- [201] Craveiro R, Aroso I, Flammia V, Carvalho T, Viciosa M, Dionísio M, Barreiros S, Reis R, Duarte ARC, Paiva A. J. Mol. Liq. 2016, 215,534–540.
- [202] Sze LL, Pandey S, Ravula S, Pandey S, Zhao H, Baker GA, Baker SN. ACS Sust. Chem. Eng. 2014, 2, 2117–2123.
- [203] Chemat F, Anjum H, Shariff AM, Kumar P, Murugesan T. J. Mol.Liq. 2016, 218, 301–308.
- [204] Liu YT, Chen YA, Xing YJ. Chin. Chem. Lett. 2014, 25, 104–106.
- [205] Abbott, A. P., Boopathy, D., Capper, G., Davies, D. L., and Rasheed, R. K. (2004). Deep eutectic solvents formed between choline chloride and carboxylic acids: versatile alternatives to ionic liquids. J. Am. Chem. Soc. 126, 9142–9147. DOI: 10.1021/ja048266j. [206] Abbott AP, Harris RC, Ryder KS, D'Agostino C, Gladden LF, Mantle MD. Green Chem. 2011, 13, 82–90.
- [207] Y.T. Dai, J. van Spronsen, G.J. Witkamp, R. Verpoorte, Y.H. Choi, Anal. Chim.Acta 766 (2013) 61–68.
- [208] Q.H. Zhang, K. De Oliveira Vigier, S. Royer, F. Jer'ome, Chem. Soc. Rev. 41 (2012)7108–7146.
- [209] T.M.D. Dang, T.T.T. Le, M.C. Fribourg-Blanc Dang, Synthesis and optical properties of copper nanoparticles prepared by achemical reduction method, Adv. Nat. Sci. Nanosci.Nanotechnol. 2 (2011) 015009–015015.
- [210] V.L. Colvin, M.C. Schlamp, A.P. Alivisatos, Light-emittingdiodes made from cadmium selenide nanocrystals and a semiconducting polymer, Nature 370 (1994) 354–357.

- [211] Q. Liu, R.L. Yu, G.Z. Qiu, Z. Fang, A.L. Chen, Z.W. Zhao, Optimization of separation processing of copper and iron ofdump bioleaching solution by Lix 984 in indexing copper mine, Trans. Nonferrous Met. Soc. China 18 (2008) 1258–1261.
- [212] Shikha Jain, Ankita Jain, Vijay Devra; Copper nanoparticles catalyzed oxidation of threonine by peroxomonosulfate, Journal of Saudi Chemical Society (2017),21, 803-810.
- [213] Mustafa G, Tahir H, Sultan M, Akhtar N (2013) Synthesis and characterization of cupric oxide (CuO) nanoparticles and their application for the removal ofdyes12: 6650-6660.
- [214] Suleiman M, Mousa M, Hussein A, Hammouti B, Hadda TB, et al. (2013) Copper(II)-Oxide nanostructures: synthesis, characterizations, and their applications-review. J Mater Environ Sci 4: 792-797.
- [215] Wongpisutpaisan N, Charoonsuk P, Vittayakorn N, Pecharapa W (2011) Sonochemical synthesis and characterization of copper oxide nanoparticles. Energy Procedia 9: 404-409.
- [216] Lanje AS, Sharma SJ, Pode RB, Ningthoujam RS (2010) Synthesis and optical characterization of copper oxide nanoparticles. Adv Appl Sci Res 1:36-40.
- [217] Zhu H, Han D, Meng Z, Wu D, Zhang C (2011) Preparation and thermal conductivity of CuO nanofluid via a wet chemical method. Nanoscale Res Lett 6: 181.
- [218] Mousa MK (2015) Wastewater disinfection by synthesized copper oxide nanoparticles stabilized with surfactant. J Mater Environ Sci 6: 1924-1937.
- [219] Karthik AD, Kannappan G (2013) Synthesis of copper precursor, copper and its oxide nanoparticles by green chemical reduction method and its antimicrobial activity. J Appl. Pharm Sci 3: 016-021.
- [220] Srivastava S, Kumar M, Agrawal A, Dwivedi SK (2013) Synthesis and characterization of copper oxide nanoparticles. IOSR J Appl. Phys 5: 61-65.

- [221] Phiwdang K, Suphankij S, Mekprasart W, Pecharapa W (2013) Synthesis of CuO nanoparticles by precipitation method using different precursors. Energy Procedia 34: 740-745
- [222] Darezereshki E, Bakhtiari F (2011) A novel technique to synthesis of tenorite(CuO) nanoparticles from low concentration CuSO<sub>4</sub>solution. J Min Metall BMetall 47: 73-78.
- [223] M.S. Aguilar, R. Esparza, G. Rosas, Synthesis of Cu nanoparticles by chemical reduction method, Transactions of Nonferrous Metals Society of China, Volume 29, Issue 7, 2019, pp 1510-1515
- [224] Chatterjee, A.K., Sarkar, R.K., Chattopadhyay, A.P., Aich, P., Chakraborty, R. &Basu, T. (2012). A simple robust method for synthesis of metallic copper nanoparticles of high antibacterial potency against E. coli. Nanotechnology, 23(8), 85103-85113.
- [225] Qi, L., Ma, J., Shen, J. (1997). Synthesis of Copper Nanoparticles in Nonionic Water-in-Oil Microemulsions, Journal of Colloid and Interface Science, 186 (2), 498-500.
- [226] H.R.Ghorbani, Chemical synthesis of copper nanoparticles, 2014, Oriental Journal of Chemistry, Volume 30,2
- [227] Thi. M. D. D., Thi, T. T. L., Eric, F. B. and Mau, C. D., "Synthesis and optical properties of copper nanoparticles prepared by a chemical reduction method" Adv. Nat. Sci. Nanosci. Nanotechnol, 2, 6(2011).
- [228] Yoshizumi Kusumoto, Manickavachagam Muruganandham, Simple new synthesis of copper nanoparticles in water/acetonitrile mixed solvent and their characterization, Materials Letters 63(23), DOI: 10.1016/j.matlet.2009.06.037.
- [229] Chou K-S, Ren C-Y. Synthesis of nanosized silver particles by chemical reduction method. Materials Chemistry and Physics. 2000; 64:241-6.

- [230] Taguchi A, Fujii S, Ichimura T, Verma P, Inouye Y, Kawata S. Oxygen-assisted shape control in polyol synthesis of silver nanocrystals. Chemical Physics Letters. 2008; 462:92-5.
- [231] Cai M, Chen J, Zhou J. Reduction, and morphology of silver nanoparticles via a liquid-liquid method. Applied surface science. 2004;226:422-6.
- [232] Senapati S. Ph.D. Thesis. India: University of Pune; 2005. Biosynthesis and immobilization of nanoparticles and their applications; pp. 1–57.
- [233] Klaus-Joerger T, Joerger R, Olsson E, Granqvist CG. Bacteria as workers in the living factory: metal-accumulating bacteria and their potential for materials science. Trends Biotechnol. 2001; 19:15–20.
- [234] S. Iravani, H. Korbekandi, S.V. Mirmohammadi, B. Zolfaghari, Synthesis of silver nanoparticles: chemical, physical, and biological methods, Res Pharm Sci. 2014; 9(6): 385–406.
- [235] Ojha AK, Forster S, Kumar S, Vats S, Negi S, Fischer I. Synthesis of well-dispersed silver nanorods of different aspect ratios and their antimicrobial properties against grampositive and negative bacterial strains. Journal of Nanobiotechnology. 2013;11(42):1-7 [236] Ajitha B, Reddy YAK, Reddy PS. Influence of synthesis temperature on growth of silver nanorods. International Journal of Engineering Science. 2014;3(5):144-148 [237] Gebeyehu MB, Chala TF, Chang S-Y, Wu C-M, Lee J-Y. Synthesis, and highly effective purification of silver nanowires to enhance transmittance at low sheet resistance with simple polyol and scalable selective precipitation method. RSC Advances. 2017; 7:16139-16148
- [238] Im SH, Lee YT, Wiley B, Xia Y. Large-scale synthesis of silver nano cubes: The role of HCl in promoting cube perfection and mono dispersity. Angewandte Chemie International edition. 2005; 44:2154-2157

- [239] Sun Y, Xia Y. Shape-controlled synthesis of gold and silver nanoparticles. Science.2002a;298(5601):2176-2179
- [240] Tao A, Sinsermsuksakul P, Yang PD. Polyhedral silver nanocrystals with distinct scattering signatures. Angewandte Chemie International Edition. 2006;45(28):4597-4601
- [241] Siekkinen AR, McLellan JM, Chen J, Xia Y. Rapid synthesis of small silver nanocubes by mediating polyol reduction with a trace amount of sodium sulfide or sodium hydrosulfide. Chemical Physics Letters. 2006; 432:491-496
- [242] Sun Y, Yin Y, Mayers BT, Herricks T, Xia Y. Uniform silver nanowires synthesis by reducingAgNO<sub>3</sub> with ethylene glycol in the presence of seeds and poly (vinyl pyrrolidone). Chemistry of Materials. 2002;14(11):4736-4745
- [243] Me'traux GS, Mirkin CA. Rapid thermal synthesis of silver nanoprisms with chemically tailorable thickness. Advanced Materials. 2005;17(4):412-415.
- [244] S. Hussain, A.K. PalIncorporation of nanocrystalline silver on carbon nanotubes by electrodeposition technique Mater. Lett., 62 (2008), pp. 1874-1877
- [245] A. Ahmad, P. Mukherjee, S. Senapati, D. Mandal, M. Islam Khan, R. Kumar, M. Sastry Extracellular biosynthesis of silver nanoparticles using the fungus Fusarium oxysporum Colloids Surf., B, 28 (2003), pp. 313-318
- [246] W.R. Hill Pillsbury, DM: Argyria: The Pharmacology of Silver, Baltimore Md. Williams & Wilkins Co (1939), pp. 128-132
- [247] J.T. Lue A review characterization and physical property studies of metallic nanoparticles Phys. Chem. Solids, 62 (2001), pp. 1599-1612
- [248] M. Rai, A. Yadav, A. Gade Silver nanoparticles as a new generation of antimicrobials Biotechnol. Adv., 27 (2009), pp. 76-83
- [249] A. Henglein Small-particle research: physicochemical properties of extremely small colloidal metal and semiconductor particles Chem. Rev., 89 (1989), pp. 1861-1873

- [250] W.K. Jung, H.C. Koo, K.W. Kim, S. Shin, S.H. Kim, Y.H. Park Antibacterial activity and mechanism of action of the silver ion in Staphylococcus aureus and Escherichia coli Appl. Environ. Microbiol., 24 (2008), pp. 2171-2178, 10.1128/AEM.02001-07
- [251] Jamakala O, Rani AU. Mitigating role of zinc and iron against cadmium-induced toxicity in liver and kidney of the male albinorat: a study with reference to metallothionein quantification. Int J Pharm Pharm Sci 2014; 6:411-7.
- [252] Bandaranayake RJ, Wen GW, Lin JY, Jiang HX, Sorensen CM. Structural phase behavior in II-VI semiconductor nanoparticles. Appl Phys Lett 1995; 67:831-3.
- [253] Dneprovskii V, Zhukov E, Karavanskii V, Poborchii V, Salamatina I. Nonlinear optical properties of semiconductor quantum wires. Superlattices Microstruct 1998; 23:1217-21.
- [254] Anikin KV, Melnik NN, Simakin AV, Shafeev GA, Voronov VV, Vitukhnovsky AG. Formation of ZnSe and CdS quantum dots vialaser ablation in liquids. Chem Phys Lett 2002; 366:357-60.
- [255] Pan A, Yang H, Liu R, Yu R, Zou B, Wang Z. Color-tunable photoluminescence of alloyed CdSxSe1-x nanobelts. J Am ChemSoc 2005; 127:15692-3.
- [256] Chakravarti SK, Kumar V, Kumar S. Galvanic fabrication of CdS microstructures using nuclear track filter membranes. J Mater Sci 2005; 40:503-4.
- [257] Yu LM, Zhu CC, Fan XH, Qi LJ, Yan W. CdS/SiO2 nanowire arrays and CdS nanobelt synthesized by thermal evaporation. J Zhejiang Univ Sci A 2006; 7:1956-60.
- [258] Xiao J, Peng T, Dai K, Zan L, Peng Z. Hydrothermal synthesis, characterization and its photoactivity of CdS/Rectoritenanocomposites. J Solid State Chem 2007; 180:3188-95. [259] Mahdavi SM, Irajizad A, Azarian A, Tilaki RM. Optical and structural properties of copper doped CdS thin films prepared by pulsed laser deposition. Scientia Iranica 2008;

15:360-5.

- [260] Thongtem T, Phuruangrat A, Thongtem S. Solvothermal synthesis of CdS nanowires templated by polyethylene glycol Ceramics Int 2009;35:2817-22.
- [261] Pandian SR, Deepak V, Kalishwaralal K, Gurunathan S. Biologically synthesized fluorescent CdS NPs encapsulated by PHB. Enzyme Microb Technol 2011; 48:319-25.
- [262] Mammadov MN, Aliyev AS, Elrouby M. Electrodeposition of cadmium sulfide. Int J Thin Film Sci-Tech 2012; 1:43-53.
- [263] Girginer B, Galli G, Chiellini E, Bicak N. Preparation of stable CdS nanoparticles in aqueous medium and their hydrogengeneration efficiencies in the photolysis of water. Int J Hydrog. Energy 2009; 34:1176-84.
- [264] R Aruna Devi, M Latha, S Velumani, Goldie Oza, P Reyes-Figueroa, M Rohini, I G Becerril-Juarez, Jae-Hyeong Lee, Junsin Yi, Synthesis and Characterization of Cadmium Sulfide Nanoparticles by Chemical Precipitation Method, J Nanosci Nanotechnol. 2015 Nov;15(11):8434-9. DOI: 10.1166/jnn.2015.11472.
- [265] Rodriguez Fragoso P, Reyes Esparza J, Leon Buitimea A,Rodriguez Fragoso L. Synthesis, characterization, and toxicological evaluation of maltodextrin capped cadmiumsulfide nanoparticles in human cell lines and chicken embryos. J. Nanobiotech 2012; 10:47.
- [266] Rajnish Gupta, Cadmium nanoparticles and its toxicity Journal of Critical Reviews(6), Issue 5, 2019
- [267] Mahesh M Kamble, Sachin R Rondiya, Bharat R Bade, Kiran B Kore, et.al., Optical, structural, and morphological study of CdS nanoparticles: role of sulfur source, Nanomaterials, and Energy, (9),1, June 2020, pp. 72-81 https://doi.org/10.1680/jnaen.19.00041
- [268] J. D. Blum, Nat. Chem., 2013, 5, 1066.

- [269] J. Jeevanandam, A. Barhoum, Y. S. Chan, A. Dufresne and M. K. Danquah, Beilstein J. Nanotechnol., 2018, 9, 1050–1074
- [270] W. Lin, Chem. Rev., 2015, 115, 10407–10409.
- [271] K. Watanabe, D. Menzel, N. Nilius and H. J. Freund, Chem. Rev., 2006, 106, 4301–4320
- [272] F. J. Heiligtag and M. Niederberger, Mater. Today, 2013, 16, 262–271
- [273] C. Wang and D. Astruc, Prog. Mater. Sci., 2018, 94, 306–383
- [274] Alireza Mohadesia, Mehdi Ranjbarb, S.M. Hosseinpour-Mashkanic, Solvent-free synthesis of mercury oxide nanoparticles by a simple thermal decomposition method, Superlattices and Microstructures, 66, February 2014, Pages 48-53
- [275] Villa Krishna Harika, Tirupathi Rao Penki, Boddapati Loukya, Atanu Samanta, et.al., Sustainable existence of solid mercury (Hg) nanoparticles at room temperature and their applications, RSC, Chem. Sci., 2021, 12, 3226-3238, DOI: 10.1039/D0SC06139
- [276] Avik J. Ghoshdastidar, Janani Ramamurthy, Maxwell Morissette & Parisa A. Ariya, Development of methodology to generate, measure, and characterize the chemical composition of oxidized mercury nanoparticles, Analytical and Bioanalytical Chemistry, 412, pp 691–702 (2020)
- [277] Kale, SS, Lokhande, CD (1999) Preparation and Characterization of HgS Films by Chemical Deposition. Mater. Chem. Phys. 59: 242–246.
- [278] Ren, T, Xu, S, Zhao, W, Zhu, J (2005) A Surfactant-Assisted Photochemical Route to Single-Crystalline HgS Nanotubes. J. Photochem. Photobiol. A 173: 93–98.
- [279] Mahapatra, AK, Dash, AK (2006) α-HgS Nanocrystals: Synthesis, Structure and Optical Properties. Physica E. 35: 9–15.
- [280] Patel, BK, Rath, S, Sarangi, SN, Sahu, SN (2007) HgS Nanoparticles: Structure and Optical Properties. Appl. Phys. A 86, 447–450.

- [281] Xin Xu, Elizabeth R. Carraway, Sonication-Assisted Synthesis of β-Mercuric Sulphide Nanoparticles, Nanomaterials and Nanotechnology, 2012,https://doi.org/10.5772/55823
- [282] RangaRao Arnepalli, Viresh Dutta, Synthesis of Mercury Cadmium Telluride Nanoparticles by Solvothermal Method, Online proceedings, Cambridge University Press, February 2011
- [283] Bumajdad, A., Nazeer, A.A., Al Sagheer, F. *et al.* Controlled Synthesis of ZrO<sub>2</sub> Nanoparticles with Tailored Size, Morphology and Crystal Phases via Organic/Inorganic Hybrid Films. Sci Rep **8**, 3695 (2018). <a href="https://doi.org/10.1038/s41598-018-22088-0">https://doi.org/10.1038/s41598-018-22088-0</a>
- [284] K Sieradzka, D Wojcieszak, D Kaczmarek, J Domaradzki, G Kiriakidis, et al. (2011) Structural and optical properties of vanadium oxides prepared by microwave-assisted reactive magnetron sputtering. Optica Applicata 41(2): 463-469.
- [285] VS Reddy Channu, R Holze, B Rambabu (2011) Soft-Chemical Synthesis of Vanadium Oxide Nanostructures Using 3,3',3"-Nitrilotripropionic Acid (NTP) as a Carrier. Soft Nanoscience Letters 1(3): 66-70.
- [286] M Mousavi, A Kompany, N Shahtahmasebi, MM Bagheri Mohagheghi (2013) Study of structural, electrical and optical properties of vanadium oxide condensed films deposited by spray pyrolysis technique. Advanced Manufacture 1(4): 320-328.
- [287] B Vijaykumar, K Sangshetty, G Sharanappa (2012) Surface Morphology Studies and Thermal analysis of V<sub>2</sub>O<sub>5</sub> doped polyaniline composites. International Journal of Engineering Research and Applications 2: 611-616.
- [288] NN Dinh, TT Thao, VN Thuc, NT Thuy (2010) Thermochromic properties of VO<sub>2</sub> films made by RF-sputtering. Journal of Science, Mathematics-Physics 26: 201-206. [289] Shelan M. Mustafa, Azeez A. Barzinjy, Abubaker H. Hamad, Samir M. Hamad,

Betaine-based deep eutectic solvents mediated synthesis of zinc oxide nanoparticles at low temperature, Ceramics International, 2022, ISSN 0272-842,

https://doi.org/10.1016/j.ceramint.2022.04.131.

[290] Karimi, M. & Eshraghi, Mohamad. (2016). One-pot and green synthesis of Mn<sub>3</sub>O<sub>4</sub> nanoparticles using an all-in-one system (solvent, reactant and template) based on ethaline deep eutectic solvent. Journal of Alloys and Compounds. 696. 10.1016/j.jallcom.2016.11.259.

[291]. Jaji, Nuru-Deen & Lee, Hooi-Ling & Hussin, Mohd Hazwan & Md Akil, Hazizan & Zakaria, Muhammad Razlan & Othman, Muhammad Bisyrul Hafi. (2020). Advanced nickel nanoparticles technology: From synthesis to applications. Nanotechnology Reviews. 9. 1456-1480. 10.1515/ntrev-2020-0109.

# 2. MATERIALS AND METHODS

#### 2.1 Materials

The chemicals used for this investigation such as choline chloride, ethylene glycol, Urea, Malonic acid, hydrazine hydrate, sodium hydroxide, methanol, copper nitrate trihydrate, mercuric chloride, manganese chloride dihydrate, zirconium oxychloride, silver nitrate, zinc acetate dihydrate, cadmium chloride, vanadium pentoxide and nickel nitrate were purchased from Sigma–Aldrich, India and utilized as received. Barnstead nanopore water (>17.8 M-cm) was used to prepare all stock solutions.

Table: 2.1 Chemicals used for the investigation

S. No.	Chemical	Molecular	Molecular	
	components	formula	weight (g/mol)	
1.	Choline chloride	C <sub>5</sub> H <sub>14</sub> NO.Cl	139.62	
2.	Urea	CH <sub>4</sub> N <sub>2</sub> O	60.06	
3.	Ethylene glycol	$C_2H_6O_2$	62.07	
4.	Malonic acid	$C_3H_4O_4$	180.156	
5.	Manganese chloride	Cl <sub>2</sub> H <sub>4</sub> MnO <sub>2</sub>	125.844	
6.	zirconium oxychloride	Cl <sub>2</sub> H <sub>2</sub> OZr	180.14	
7.	zinc acetate dihydrate	$C_4H_{12}O_6Zn$	221.5	
8.	vanadium pentoxide	$V_2O_5$	181.88	
9.	nickel nitrate	Ni (NO <sub>3</sub> ) <sub>2</sub>	182.703	
10.	Zinc chloride	$ZnCl_2$	136.286	
11.	Manganese chloride	$MnCl_2$	125.844	
12.	Copper (II) nitrate	Cu (NO <sub>3</sub> ) <sub>2</sub> .3H <sub>2</sub> O	241.60	
	trihydrate			

S. No.	Chemical	Molecular	Molecular
	components	formula	weight (g/mol)
13.	Hydrazine hydrate	H <sub>6</sub> N <sub>2</sub> O	50.061
14.	Silver nitrate	$AgNO_3$	169.87
15.	Sodium hydroxide	NaOH	39.997
16.	Cadmium chloride	CdCl <sub>2</sub> .2H <sub>2</sub> O	147.01
	dihydrate		
17.	Mercuric chloride	$HgCl_2$	271.52
18.	Sodium borohydride	NaBH <sub>4</sub>	37.84
19.	Methanol	CH₃OH	32.04

#### 2. 2 Experimental methods

## 2.2.1 General Preparation of Deep Eutectic Solvents (DES)

Three types of DESs were prepared from a 1:1 mole ratio of the two components is given in table 2.2. The 1:1 mole ratio of respective substances for the preparation of these nine DESs was decided using the plot of a freezing point versus the percent composition of the above mixtures. The evaporating method was employed in water as reported by Dai et al. [1]. The 1:1 mole ratio of the components was taken, dissolved in double distilled water and excess water was removed by heating until the weight of the components remains constant. The mixtures were kept in a desiccator containing anhydrous CaCl<sub>2</sub>for about two weeks and as there was no turbidity appeared during this period. Then the DESs were subjected for the measurement of physical properties such as density, pH, conductivity, and viscosity. The H- bonded interactions between the components were characterized by FTIR.

**Table: 2.2.2 Prepared DESs** 

S.No.	Type of DES	Component-1	Component-2	Mole ratio
1.	Type-III	Choline chloride	Urea	1:1
2.	Type-III	Choline chloride	Ethylene glycol	1:1
3.	Type-III	Choline chloride	Malonic acid	1:1

#### 2.2.3. General procedure for the synthesis of nanoparticles

Nanoparticles were synthesized by various methods, including physical method, chemical reduction method, and biological method. We have followed the chemical reduction method for the synthesis of nanoparticles using various reducing agents such as hydrazine hydrate, sodium borohydride, yellow ammonium sulphide, and sodium hydroxide was used as a stabilizing agent. Then the nanoparticles were washed with deionized water followed by methanol.

## 2.2.4 Synthesis of CuNPs in ChCl-Urea/ ChCl-EG//Ch.Cl-MA DES.

Copper nanoparticles were synthesized in the DES of ChCl-Urea /ChCl-EG/ /Ch.Cl-MA as follows <sup>[2]</sup>. Nanoparticles were made by combining 10 ml of 0.01M copper nitrate trihydrate [Cu(NO<sub>3</sub>)<sub>2</sub>.3H<sub>2</sub>O] with 15 ml of choline chloride – ethylene glycol DES in beaker and magnetically stirring for 30 minutes at 1200 RPM with a magnetic stirrer. During vigorous stirring, about 8-10 ml of 0.01 M hydrazine hydrate as a reducing agent was added drop by drop, followed by 10 ml of 1 M sodium hydroxide as a stabilizing agent was injected slowly into the mixture. The obtained copper oxide nanoparticles in the beaker were centrifuged, rinsed several times with deionized water, then extracted using methanol, and dried at air-oven.

#### 2.2.5 Synthesis of HgNPs in ChCl-Urea /ChCl-EG//Ch.Cl-MA DES.

Nanoparticles of mercury were synthesized in the DES of ChCl-Urea /ChCl-EG//Ch.Cl-MA **as** follows <sup>[2]</sup>. Nanoparticles were made by combining 10 ml of 0.01M mercuric chloride [HgCl<sub>2</sub>] with 15 ml of choline chloride – ethylene glycol DES in a beaker and magnetically stirring for 30 minutes at 1200 RPM with a magnetic stirrer. During vigorous stirring, about 8-10 ml of 0.01 M hydrazine hydrate as a reducing agent was added drop by drop, followed by 10 ml of 1 M sodium hydroxide as a stabilizing agent was injected slowly into the mixture. The obtained mercury oxide nanoparticles in the beaker were centrifuged, rinsed several times with deionized water, then extracted using methanol, and dried at airoven.

## 2.2.6 Synthesis of MnNPs in ChCl-Urea/ ChCl-EG//Ch.Cl-MA DES.

Nanoparticles of manganese were synthesized in the DES of ChCl-Urea/ ChCl-EG//Ch.Cl-MA as follows <sup>[2]</sup>. Nanoparticles were made by combining 10 ml of 0.01M manganese chloride dihydrate [HgCl<sub>2</sub>.2H<sub>2</sub>O] with 15 ml of choline chloride – ethylene glycol DES in a beaker and magnetically stirring for 30 minutes at 1200 RPM with a magnetic stirrer. During vigorous stirring, about 8-10 ml of 0.01 M hydrazine hydrate as a reducing agent was added drop by drop, followed by 10 ml of 1 M sodium hydroxide as a stabilizing agent was injected slowly into the mixture. The obtained manganese oxide nanoparticles in the beaker were centrifuged, rinsed several times with deionized water, then extracted using methanol, and dried at air-oven.

#### 2.2.7 Synthesis of ZrNPs in ChCl-Urea /ChCl-EG//Ch.Cl-MA DES.

Zirconium nanoparticles were synthesized in the DES of ChCl-Urea/ ChCl-EG//Ch.Cl-MA as follows <sup>[2]</sup>. Nanoparticles were made by combining 10 ml of 0.01M zirconium oxychloride [ZrOCl<sub>2</sub>] with 15 ml of choline chloride – ethylene glycol DES in a beaker and magnetically stirring for 30 minutes at 1200 RPM with a magnetic stirrer.

During vigorous stirring, about 8-10 ml of 0.01 M hydrazine hydrate as a reducing agent was added drop by drop, followed by 10 ml of 1 M sodium hydroxide as a stabilizing agent was injected slowly into the mixture. The obtained zirconium oxide nanoparticles in the beaker were centrifuged, rinsed several times with deionized water, then extracted using methanol, and dried at air-oven.

## 2.2.8 Synthesis of AgNPs in ChCl-Urea/ ChCl-EG//Ch.Cl-MA DES.

Nanoparticles of silver were synthesized in the DES of ChCl-Urea/ ChCl-EG//Ch.Cl-MA as follows <sup>[2]</sup>. Nanoparticles were made by combining 10 ml of 0.01M silver nitrate [AgNO<sub>3</sub>] with 15 ml of choline chloride – ethylene glycol DES in a beaker and magnetically stirring for 30 minutes at 1200 RPM with a magnetic stirrer. During vigorous stirring, about 8-10 ml of 0.01 M hydrazine hydrate as a reducing agent was added drop by drop, followed by 10 ml of 1 M sodium hydroxide as a stabilizing agent was injected slowly into the mixture. The obtained silver oxide nanoparticles in the beaker were centrifuged, rinsed several times with deionized water, then extracted using methanol, and dried at airoven.

#### 2.2.9 Synthesis of ZnNPs in ChCl-Urea/ ChCl-EG//Ch.Cl-MA DES.

Zinc nanoparticles were synthesized in the DES of ChCl-Urea/ ChCl-EG/ /Ch.Cl-MA as follows <sup>[2]</sup>. Nanoparticles were made by combining 10 ml of 0.01M Zinc acetate dihydrate [Zn (COOCH<sub>3</sub>)<sub>2</sub>.2H<sub>2</sub>O] with 15 ml of choline chloride – ethylene glycol DES in a beaker and magnetically stirring for 30 minutes at 1200 RPM with a magnetic stirrer. During vigorous stirring, about 8-10 ml of 0.01 M hydrazine hydrate as a reducing agent was added drop by drop, followed by 10 ml of 1 M sodium hydroxide as a stabilizing agent was injected slowly into the mixture. The obtained zinc oxide nanoparticles in the beaker were centrifuged, rinsed several times with deionized water, then extracted using methanol, and dried at air-oven.

#### 2.2.10 Synthesis of CdNPs in ChCl-Urea/ ChCl-EG//Ch.Cl-MA DES.

Cadmium nanoparticles were synthesized in the DES of ChCl-Urea/ ChCl-EG//Ch.Cl-MA as follows <sup>[2]</sup>. Nanoparticles were made by combining 10 ml of 0.01M cadmium chloride [CdCl<sub>2</sub>] with 15 ml of choline chloride – ethylene glycol DES in a beaker and magnetically stirring for 30 minutes at 1200 RPM with a magnetic stirrer. During vigorous stirring, about 8-10 ml of 0.01 M hydrazine hydrate as a reducing agent was added drop by drop, followed by 10 ml of 1 M sodium hydroxide as a stabilizing agent was injected slowly into the mixture. The obtained cadmium oxide nanoparticles in the beaker were centrifuged, rinsed several times with deionized water, then extracted using methanol, and dried at air-oven.

## 2.2.11 Synthesis of VNPs in ChCl-Urea/ ChCl-EG//Ch.Cl-MA DES.

The vanadium nanoparticles were synthesized in the DES of ChCl-Urea/ ChCl-EG//Ch.Cl-MA as follows <sup>[2]</sup>. Nanoparticles were made by combining 10 ml of 0.01M vanadium pentoxide [V<sub>2</sub>O<sub>5</sub>] with 15 ml of choline chloride – ethylene glycol DES in a beaker and magnetically stirring for 30 minutes at 1200 RPM with a magnetic stirrer. During vigorous stirring, about 8-10 ml of 0.01 M hydrazine hydrate as a reducing agent was added drop by drop, followed by 10 ml of 1 M sodium hydroxide as a stabilizing agent was injected slowly into the mixture. The obtained vanadium oxide nanoparticles in the beaker were centrifuged, rinsed several times with deionized water, then extracted using methanol, and dried at air-oven.

#### 2.2.12 Synthesis of NiNPs in ChCl-Urea/ ChCl-EG//Ch.Cl-MA DES.

Nickel nanoparticles were synthesized in the DES of ChCl-Urea/ ChCl-EG//Ch.Cl-MA as follows <sup>[2]</sup>. Nanoparticles were made by combining 10 ml of 0.01M nickel nitrate [Ni (NO<sub>3</sub>)<sub>2</sub>] with 15 ml of choline chloride – ethylene glycol DES in a beaker and magnetically stirring for 30 minutes at 1200 RPM with a magnetic stirrer. During vigorous

stirring, about 8-10 ml of 0.01 M hydrazine hydrate as a reducing agent was added drop by drop, followed by 10 ml of 1 M sodium hydroxide as a stabilizing agent was injected slowly into the mixture. The obtained nickel oxide nanoparticles in the beaker were centrifuged, rinsed several times with deionized water, then extracted using methanol, and dried at airoven.

#### 2.3 Fourier Transform Infrared spectroscopy

Fourier-transform infrared spectroscopy (FTIR) is a technique for obtaining infrared frequencies of absorption or emission of solid, liquid, or gas. FTIR spectrum was recorded using a ShimadzuFTIR-8900 spectrometer between 4000 and 400 cm<sup>-1</sup>.FTIR is a very versatile tool for the functional group characterization of solvents and nanoparticles [3]. FTIR spectrum consists of absorption peaks that correspond to the frequencies of vibration between the bonds of atoms in the nanoparticles.

## 2.4 Ultraviolet-Visible spectroscopy

UV-Visible spectroscopy (UV-Vis) analyses the extinction (scatter + absorption) of light passing through a substance. UV-Vis is a great tool for discovering, characterizing, and investigating nanomaterials because nanoparticles have unique optical properties that are sensitive to size, shape, concentration, aggregation state, and refractive index near the nanoparticle surface. The preliminary investigation of nanoparticles was done by Perkin-Elmer make Lambda 35 UV-Visible Spectrophotometer range from 190 nm to 1100nm.

#### 2.5 Scanning Electron Microscopy

One of the most extensively used tools for the characterization of nanomaterials and nanostructures is the scanning electron microscope (SEM). The signals generated by electron-sample interactions disclose information about the surface morphology (texture) of the sample, as well as its particle size [4]. The morphology of nanoparticles was examined

in their natural state under a range of conditions including very high-water vapor pressure up to 3000 Pa using Carel Zeiss made model EVO18Scanning Electron Microscope.

#### 2.6 X-Ray Diffractometer

The analytical technique of X-ray diffraction (XRD) is based on the diffraction of X-rays by matter, particularly crystalline materials. As a more ordered material is studied, X-ray diffraction is elastic scattering (without loss of photon energy) that results in increasing interference <sup>[5]</sup>. The XRD pattern of nanoparticles was recorded on PANalytical made model X'pert3 powder X-ray diffractometer.

## 2.7 Energy Dispersive X-ray Analysis

EDAX works on the principle of generating X-rays from a specimen using an electron beam. The features and type of the elements contained in the sample are used to generate the X-rays <sup>[6]</sup>. The Energy Dispersive X-Ray Analysis of nanoparticles was recorded on EDAX Inc., USA made TEAM EDS model. From this, the elemental composition and the purity of the nanoparticles were known.

#### References

- [1] Y.T. Dai, J. van Spronsen, G.J. Witkamp, R. Verpoorte, Y.H. Choi, Anal. Chim.Acta 766 (2013) 61–68.
- [2] M. Abdulla-Al-Mamun, Y. Kusumoto, and M. Muruganandham, "Simple new synthesis of copper nanoparticles in water/acetonitrile mixed solvent and their characterization," Materials Letters, vol. 63, no. 23, pp. 2007–2009.
- [3] Biosynthesized Nanomaterials; Karina Torres-Rivero, Antonio Florido, in Comprehensive Analytical Chemistry, 2021
- [4] Sagadevan S, Koteeswari P (2015) Analysis of Structure, Surface Morphology, Optical and Electrical Properties of Copper Nanoparticles. J Nanomed Res 2(5): 00040.

- [5] Khadija El Bourakadi, Abou el Kacem Qaiss, Characterization techniques for hybrid nanocomposites based on cellulose nanocrystals/nanofibrils and nanoparticlesin Cellulose; Nanocrystal/Nanoparticles Hybrid Nanocomposites, 2021.
- [6] Nidhi Raval, Rakesh K. Tekade; Importance of Physicochemical Characterization of Nanoparticles in Pharmaceutical Product Development; Basic Fundamentals of Drug Delivery, 2019.

### 3. CHOLINE CHLORIDE – UREA DES MEDIA ASSISTED SYNTHESIS OF SOME METAL OXIDE NANOPARTICLES

#### 3.1 Introduction

Metal-based nanoparticles have different budding applications in biological, chemical, medical, and agricultural fields due to their interesting features. Metal nanoparticles are either cleaner forms of metals such as Au, Ag, Cu, Fe, etc., or their compounds such as sulfides, hydroxides, oxides, etc. Ionic liquids are commonly involved in the abstraction of nanoparticles but they are somewhat difficult due to their impoverished bio-degradability, bio-compatibility, and sustainability. Therefore, as a substitute for ionic liquids, Deep Eutectic Solvent (DES) is considered in the development of nanoparticles.

Nanoscience is learning that defines the particles of nanoscale having fewer than 100 nm, and examination of their varied physio-chemical characteristics and their opportunity in several fields. A lot of improvements have been made in nano-based technology due to the common properties such as the particle's surface area, size, shape, charge, and surface reactivity which are exclusive and better when related to the equivalent bulk particles [1]. The metal-based NPs, apart from their common properties, their structural and elemental compositions in nanoscales allow MNPs to be evolving contenders in pharmaceutical, environmental, agricultural, and chemical industries.

Copper oxide nanoparticle is essential and reasonably inexpensive when compared to precious metals such as Au and Ag <sup>[2]</sup>. Manganese oxide nanoparticle has budding applications in the medical field. Their application as MRI contrast agents in cancer multimodal therapy and modeling is a significant one <sup>[3]</sup>. Zirconium oxide nanoparticles claimed applications in fuel cells <sup>[4]</sup>.

A DES is typically self-possessed of two or three low-cost and harmless components that are capable of linking via hydrogen bond relations to generate a eutectic

mixture <sup>[5]</sup>. Regularly, DES can be signified by the common formula  $Cat^+ X^- zY$  where  $Cat^+$  is ammonium, phosphonium, or sulfonium cation, and X is a Lewis base, normally a halide anion and Y is either a Lewis or Bronsted acid. Here z refers to the number of Y molecules that interact with the anion  $X^-$ . In general, there are four types of DES and the choline chloride – urea DES used in this investigation belongs to type III DES <sup>[6]</sup>.

Urea is proficient in forming a liquid DES with Ch.Cl at room temperature, seemingly due to its sturdier nature to form hydrogen bond connections with Ch.Cl. The freezing point ( $T_f$ ) of this 1:2 molar ratio DES of Ch.Cl-Urea was stated as 12 °C <sup>[5]</sup>. An unpretentious road for the shape-controlled preparation of Au NPs involving Ch,Cl-urea DES which replaced traditional surfactants <sup>[7]</sup>. Further, the synthesis of Au nanowire from straight away reduction of HAuCl<sub>4</sub> by NaBH<sub>4</sub> in DES <sup>[8]</sup> obviously showed the rewards of removing surfactants or seeds for the formation of nanomaterials when DESs are used. In the latter synthesis, two different DESs, i.e. Ch-Cl - ethylene glycol (1:2-mole ratio) or Ch.Cl - urea (1:2-mole ratio) was deployed in the absence of a surfactant. The development of nanoparticles of several shapes and surfaces was controlled by adjusting the water content of the DES <sup>[6]</sup>.

Thus, DESs are considered an effective solvent media for the synthesis of nanoparticles. DES is beneficial over ILs in the range of recyclability, costs, biodegradability, and lower toxicity. Most DES is prepared from the natural origin such as are choline chloride - ethylene glycol, choline chloride - urea, choline chloride - phenylacetic acid, choline chloride - glycerol, etc. **Thao Dao Vu Phuong et al., (2021)** [9] focused on the early stages of copper electrodeposition using a DES containing C<sub>5</sub>H<sub>14</sub>ClNO and urea (DES). **Parsa et al., (2020)** [10] studied the nickel nanostructures with wrinkles that were electrodeposited from a DES including C<sub>5</sub>H<sub>14</sub>ClNO and urea. **Verma et al., (2019)** [11] discussed the solvation and stability of the transitional metallic particles in

several kinds of liquid ionic forms, as well as their characterization methodologies and catalysis applications. **Tome et.al (2018)** [12] reviewed current developments in novel nanomaterials, as well as the procedures that have been created to use DES as a solvent. The definition, preparation, and special features of DES are discussed first, followed by a more detailed discussion of their applicability in polymer, metal deposition, and nanomaterial research and sensing techniques. The Ni-Co alloy, that was created using the method, has high corrosion resistance. **Li et al., (2021)** [13] demonstrated the deposition method in choline chloride-urea to produce nano nickel-cobalt (Ni-Co) alloys with chosen orientation. The Ni-Co alloy, which was created using the ChCl/U method, offers good corrosion resistance.

Palomar EZ et al., (2019) [14] used the transitional quantity of potentiostat current to describe the electrical depositing of Fe NPs onto the HOPG electrode surface from Fe(III) ions blended in the C<sub>5</sub>H<sub>14</sub>ClNO-urea eutectic mixture. Delbecq et al.,(2019) [15] studied the formation of supramolecular gels by adding long-chain alkyl aminoamide to metal chloride solubilized in choline chloride – urea. Smaller noble metal nanoparticles (Co NP or Au NP) could be generated by employing these gels as a template without the addition of reducing agents. Ghenaatian et al., (2021) [16] investigated the noble metallic nanoparticle interaction with choline chloride –urea by the theory of density functional method. Kakaei et al., (2018) [17] focused on the synthesis of graphene oxide and its reduced form through the electrochemical method with the use of graphite rod using the supersaturated solution of choline chloride – urea and water.

This study involved an innovative Choline chloride – urea DES as a eco-friendly solvent to prepare copper, mercury, manganese, zirconium, silver, zinc, cadmium, vanadium and nickel oxide nanoparticles. The metal oxide nanoparticles prepared have been examined using UV-Visible, FTIR Spectroscopy, X-Ray Diffraction (XRD),

Scanning Electron Microscopy (SEM), Transmission Electron Microscopy (TEM), and Energy Dispersive X-Ray Analysis (EDAX). The creation of these metal oxide nanoparticles via Choline Chloride ( $C_5H_{14}CINO$ ) – Urea DES can be considered as a worthy route in chemical engineering.

#### 3.2 Experimental

The chemicals used for this investigation such as choline chloride, urea, hydrazine hydrate, sodium hydroxide, methanol, copper nitrate trihydrate, mercuric chloride, manganese chloride dihydrate, zirconium oxychloride, silver nitrate, zinc acetate dihydrate, cadmium chloride, vanadium pentoxide and nickel nitrate were purchased from Sigma–Aldrich, India and utilized as received. Barnstead nanopore water (>17.8 M-cm) was used to prepare all stock solutions.

#### 3.2.1 Preparation of choline chloride – urea deep eutectic solvent

The choline chloride (Ch.Cl) and urea (U) received were recrystallized, filtered, and vacuum dried before it was used. The 1:1 molar ratio of these two components were taken and heated to 100 °C and agitated until a homogeneous, colourless liquid was produced from the two components. A few hours' worth of heating choline chloride and urea at 100°C yielded a clear homogeneous liquid.

#### 3.2.2 Synthesis of copper nanoparticles in choline chloride – urea deep eutectic solvent

Copper nanoparticles were synthesized in the DES of ChCl-U as follows <sup>[18]</sup>. Nanoparticles were made by combining 10 ml of 0.01M copper nitrate trihydrate [Cu(NO<sub>3</sub>)<sub>2</sub>.3H<sub>2</sub>O] with 15 ml of choline chloride – urea DES in a beaker and magnetically stirring for 30 minutes at 1200 RPM with a magnetic stirrer. During vigorous stirring, about 8-10 ml of 0.01 M hydrazine hydrate as a reducing agent was added drop by drop, followed by 10 ml of 1 M sodium hydroxide as a stabilizing agent was injected slowly into the mixture. The obtained black colored copper oxide nanoparticles in the beaker were

centrifuged, rinsed several times with deionized water, then extracted using methanol, and dried at air-oven.

# 3.2.3 Synthesis of mercury nanoparticles in choline chloride – urea deep eutectic solvent

Nanoparticles of mercury were synthesized in the DES of ChCl-U as follows <sup>[18]</sup>. Nanoparticles were made by combining 10 ml of 0.01M mercuric chloride [HgCl<sub>2</sub>] with 15 ml of choline chloride – urea DES in a beaker and magnetically stirring for 30 minutes at 1200 RPM with a magnetic stirrer. During vigorous stirring, about 8-10 ml of 0.01 M hydrazine hydrate as a reducing agent was added drop by drop, followed by 10 ml of 1 M sodium hydroxide as a stabilizing agent was injected slowly into the mixture. The obtained ash colored mercury oxide nanoparticles in the beaker were centrifuged, rinsed several times with deionized water, then extracted using methanol, and dried at air-oven.

# 3.2.4 Synthesis of manganese nanoparticles in choline chloride – urea deep eutectic solvent

Nanoparticles of manganese were synthesized in the DES of ChCl-U as follows <sup>[18]</sup>. Nanoparticles were made by combining 10 ml of 0.01M manganese chloride dihydrate [MnCl<sub>2</sub>.2H<sub>2</sub>O] with 15 ml of choline chloride – urea DES in a beaker and magnetically stirring for 30 minutes at 1200 RPM with a magnetic stirrer. During vigorous stirring, about 8-10 ml of 0.01 M hydrazine hydrate as a reducing agent was added drop by drop, followed by 10 ml of 1 M sodium hydroxide as a stabilizing agent was injected slowly into the mixture. The obtained brown colored manganese oxide nanoparticles in the beaker were centrifuged, rinsed several times with deionized water, then extracted using methanol, and dried at air-oven.

# 3.2.5 Synthesis of zirconium nanoparticles in choline chloride – urea deep eutectic solvent

Zirconium nanoparticles were synthesized in the DES of ChCl-U as follows <sup>[18]</sup>. Nanoparticles were made by combining 10 ml of 0.01M zirconium oxychloride [ZrOCl<sub>2</sub>] with 15 ml of choline chloride – urea DES in a beaker and magnetically stirring for 30 minutes at 1200 RPM with a magnetic stirrer. During vigorous stirring, about 8-10 ml of 0.01 M hydrazine hydrate as a reducing agent was added drop by drop, followed by 10 ml of 1 M sodium hydroxide as a stabilizing agent was injected slowly into the mixture. The obtained white colored zirconium oxide nanoparticles in the beaker were centrifuged, rinsed several times with deionized water, then extracted using methanol, and dried at airoven.

#### 3.2.6 Synthesis of silver nanoparticles in choline chloride – urea deep eutectic solvent

Nanoparticles of silver were synthesized in the DES of ChCl-U as follows <sup>[12]</sup>. Nanoparticles were made by combining 10 ml of 0.01M silver nitrate [AgNO<sub>3</sub>] with 15 ml of choline chloride – urea DES in a beaker and magnetically stirring for 30 minutes at 1200 RPM with a magnetic stirrer. During vigorous stirring, about 8-10 ml of 0.01 M hydrazine hydrate as a reducing agent was added drop by drop, followed by 10 ml of 1 M sodium hydroxide as a stabilizing agent was injected slowly into the mixture. The obtained black colored silver oxide nanoparticles in the beaker were centrifuged, rinsed several times with deionized water, then extracted using methanol, and dried at air-oven.

#### 3.2.7 Synthesis of zinc nanoparticles in choline chloride – urea deep eutectic solvent

Zinc nanoparticles were synthesized in the DES of ChCl-U as follows <sup>[18]</sup>. Nanoparticles were made by combining 10 ml of 0.01M Zinc acetate dihydrate [Zn(COOCH<sub>3</sub>)<sub>2</sub>.2H<sub>2</sub>O] with 15 ml of choline chloride – urea DES in a beaker and magnetically stirring for 30 minutes at 1200 RPM with a magnetic stirrer. During vigorous

stirring, about 8-10 ml of 0.01 M hydrazine hydrate as a reducing agent was added drop by drop, followed by 10 ml of 1 M sodium hydroxide as a stabilizing agent was injected slowly into the mixture. The obtained dirty white colored zinc oxide nanoparticles in the beaker were centrifuged, rinsed several times with deionized water, then extracted using methanol, and dried at air-oven.

# 3.2.8 Synthesis of cadmium nanoparticles in choline chloride – urea deep eutectic solvent

Cadmium nanoparticles were synthesized in the DES of ChCl-U as follows <sup>[18]</sup>. Nanoparticles were made by combining 10 ml of 0.01M cadmium chloride [CdCl<sub>2</sub>] with 15 ml of choline chloride – urea DES in a beaker and magnetically stirring for 30 minutes at 1200 RPM with a magnetic stirrer. During vigorous stirring, about 8-10 ml of 0.01 M hydrazine hydrate as a reducing agent was added drop by drop, followed by 10 ml of 1 M sodium hydroxide as a stabilizing agent was injected slowly into the mixture. The obtained dark brown colored cadmium oxide nanoparticles in the beaker were centrifuged, rinsed several times with deionized water, then extracted using methanol, and dried at air-oven.

# 3.2.9 Synthesis of vanadium nanoparticles in choline chloride – urea deep eutectic solvent

The vanadium nanoparticles were synthesized in the DES of ChCl-U as follows <sup>[18]</sup>. Nanoparticles were made by combining 10 ml of 0.01M vanadium pentoxide [V<sub>2</sub>O<sub>5</sub>] with 15 ml of choline chloride – urea DES in a beaker and magnetically stirring for 30 minutes at 1200 RPM with a magnetic stirrer. During vigorous stirring, about 8-10 ml of 0.01 M hydrazine hydrate as a reducing agent was added drop by drop, followed by 10 ml of 1 M sodium hydroxide as a stabilizing agent was injected slowly into the mixture. The obtained blueish green colored vanadium oxide nanoparticles in the beaker were centrifuged, rinsed several times with deionized water, then extracted using methanol, and dried at air-oven.

#### 3.2.10 Synthesis of nickel nanoparticles in choline chloride – urea deep eutectic solvent

Nickel nanoparticles were synthesized in the DES of ChCl-U as follows <sup>[18]</sup>. Nanoparticles were made by combining 10 ml of 0.01M nickel nitrate [Ni(NO<sub>3</sub>)<sub>2</sub>] with 15 ml of choline chloride – urea DES in a beaker and magnetically stirring for 30 minutes at 1200 RPM with a magnetic stirrer. During vigorous stirring, about 8-10 ml of 0.01 M hydrazine hydrate as a reducing agent was added drop by drop, followed by 10 ml of 1 M sodium hydroxide as a stabilizing agent was injected slowly into the mixture. The obtained black colored nickel oxide nanoparticles in the beaker were centrifuged, rinsed several times with deionized water, then extracted using methanol, and dried at air-oven.

#### 3.3 Results and Discussions

The synthesized copper, mercury, manganese, zirconium, silver, zinc, cadmium, vanadium and nickel nanoparticles in the deep eutectic solvent of choline chloride – urea were characterized by the techniques such as UV-Visible spectroscopy, Fourier transform infrared spectroscopy, Scanning electron microscopy, Transmission Electron Microscopy (TEM), X-Ray diffraction and Energy dispersive X-ray analysis.

# 3.3.1 UV-Visible Spectra of Metal Nanoparticles Prepared Using Choline Chloride – Urea Deep Eutectic Solvent

The UV-Visible spectra of copper, mercury, manganese, zirconium, silver, zinc, cadmium, vanadium and nickel oxide nanoparticles obtained in their ethanolic solutions between the wavelengths 200 and 800nm are placed in figures 3.1 to 3.9. The surface plasmon absorption of metal nanoparticles are usually seen around 400 nm. Larger sizes shift the band to longer wavelength and broaden the band to some extent and however, very dumped plasmon and very broaden bands could be due to surface adsorptions [19, 20]. The bands due to either surface plasmon or surface adsorptions of these metal oxide nanoparticles are given in table 3.1 below.

Table 3.1: UV-Visible absorption bands of metal oxide nanoparticles obtained from Ch.Cl-U DES

S.No.	Metal Oxide NPs	λ <sub>max</sub> values (nm)	Nature of bands
1	Copper	357.1	Surface Adsorptions
2	Mercury	361.65, 689.6	Surface Adsorptions
3	Manganese	293.35, 680.9	Surface Adsorptions
4	Zirconium	272.15, 345.45	Surface Plasmon
5	Silver	342.3	Surface Plasmon
6	Zinc	272.1, 344.05, 432.8	Surface Plasmon
7	Cadmium	390.65	Surface Adsorptions
8	Vanadium	270.2	-
9	Nickel	270.45, 442.75	Surface Adsorptions

From the UV-Visible spectra of metal oxide nanoparticles displayed in figures 3.1 to 3.9, it was followed that the zirconium, silver and zinc showed surface plasmon absorption bands at the specific wavelengths as given in table 3.1. The copper, mercury, manganese, cadmium and nickel metal oxide nanoparticles obtained from the DES of Ch.Cl–U gave very broad and dumped absorption bands due to surface adsorptions while the vanadium oxides are transparent above 300 nm. Copper, zirconium, silver, cadmium and vanadium metal oxide nanoparticles prepared from the deep eutectic solvent of choline chloride – urea is almost transparent in the visible region. Thus, these metal oxide nanoparticles prepared from the deep eutectic solvent of choline chloride – urea are expected to have no photocatalytic activity.

# 3.3.2 FTIR Spectra of Metal Nanoparticles Prepared Using Choline Chloride – Urea Deep Eutectic Solvent

The FTIR spectra obtained in the range of 400 to 4000 cm<sup>-1</sup> for copper, mercury, manganese, zirconium, silver, zinc, cadmium, vanadium and nickel metal oxide nanoparticles prepared from the deep eutectic solvent of choline chloride-urea are reported in figures 3.10 to 3.18 of this section. The peaks of various metal oxide nanoparticles such as copper, mercury, manganese, zirconium, silver, zinc, cadmium, vanadium and nickel prepared from the DES of choline chloride – urea were presented in the following table 3.2.

The several peaks noticed in the range of 400 to 900 cm<sup>-1</sup> are correlated to respective M – O vibrations of MO nanoparticles <sup>[21, 22]</sup>. A few of the solvent molecules are capped on the surface of MO nanoparticles. These are indicated by the peaks around 1040 and 1120 cm<sup>-1</sup> corresponding to the C – O stretching vibrations. The peak due to C – H bending of alkane and CH<sub>2</sub> deformations of choline chloride is seen around 1470 cm<sup>-1</sup> and 1380 cm<sup>-1</sup> in all these spectra. The peak was noticed around 1600 cm<sup>-1</sup> denoted O – H bending vibrations of the choline chloride part of the deep eutectic solvent. The peaks observed around 2850 cm<sup>-1</sup> and 2920 cm<sup>-1</sup> are due to C – O asymmetric stretching <sup>[22]</sup>. Further, the broad peaks seen around 3420 cm<sup>-1</sup> in all the spectra due to different vibrations modes of water molecules adsorbed on the surface of metal oxide nanoparticles <sup>[21]</sup>.

Table 3.2: FTIR absorption peaks of metal oxide nanoparticles obtained from Ch.Cl-U DES

S.No.	Metal Oxide NPs	IR Vibrations							
		M-O Vibrations	C-O Stretch	CH <sub>2</sub> deform (methylene)	C-H bend (alkane)	O-H bend	C=O Stretch	C-O asym stretch	O-H stretch
1	Cu	466, 558,	1036,	1389	-	1611	-	2938	3406
		614, 735	1112						
2	Hg	477, 641,	1063	1374	1420	-	1730	2946	3459
		851							
3	Mn	536, 725,	1070	1376	1445	1583	1676	2915	3426
		972							
4	Zr	623, 861	1038,	1388	-	1619	-	2930	3441
			1106						
5	Ag	663	1039	1391	-	1639	-	2866,	3455
								2925	
6	Zn	583, 685,	1161	1363	1453	1589	-	2959	3416
		856							
7	Cd	514, 618	1092	1350	1432	1602	-	2912	3452
8	$\mathbf{V}$	466, 627	1054	1357	1428	1595	-	2933	3431
9	Ni	470, 611,	1087	1284	1479	-	1672	2941	3426
		951							

From these FTIR spectra data summarized in table 3.2 it is followed that one of the components of the DES used in the preparation of metal oxide nanoparticles, i.e. urea had been capped on the surface of mercury, manganese and nickel oxide nanoparticles. This fact is confirmed by the C= O stretching vibrations notice around 1700 cm<sup>-1</sup> in the respective FTIR spectra.

# 3.3.3 XRD Patterns of Metal Nanoparticles Prepared Using Choline Chloride – Urea Deep Eutectic Solvent

The XRD patterns obtained for copper, mercury, manganese, zirconium, silver, zinc, cadmium, vanadium and nickel metal oxide nanoparticles prepared from the deep eutectic solvent of choline chloride-urea are reported and discussed as follows. The powder x-ray diffraction patterns of copper oxide nanoparticles prepared from the deep eutectic solvents, Ch.Cl – U are given in figure 3.19. The XRD patterns give information about the grain size, structure, and phase cleanliness of the materials. In the case of CuO particles obtained in Ch.Cl – U DES, the diffraction peaks seen at 2θ values of 24.02°, 41.46° and 68.13° are indexed as (040), (420) and (300) respectively. The grain size of CuO nanoparticles is determined by using the Debye–Scherer formula,

$$D = k λ/β cos θ$$

where D denotes the grain size, K refers to a constant,  $\lambda$  refers to the wavelength of X-ray used,  $\beta$  denotes the fullwidth half-maximum of the diffraction peaks and  $\theta$  is the angle of the diffraction <sup>[21]</sup>. By using this formula, the average grain size of CuO nanoparticles prepared from the DES of Ch.Cl-U is found to be 45 nm.

All the diffraction points in the XRD can be assigned to the pure cubic lattice structure of mercury oxide nanoparticles as given in figure 3.20. The peaks correspond to (111), (200), (220), and (222) planes, which are in good pact with the JCPDS-pattern available in the literature. The average crystal width of the HgO nano particles obtained in the DES of Ch.Cl-EG was found to be 25 nm using the Scherrer formula of the XRD pattern. The crystalline behaviour of the prepared MnO nanoparticles was inspected by the XRD analysis and given in the figure 3.21. The XRD patterns revealed the diffraction peaks at 20 values for manganese oxide nanoparticles at 37.34, 55.21 and 66.37. These values are in accordance with the crystal planes (101), (110) and (200). The mean particle size for

MnO nanoparticles prepared from the DES of Ch.Cl-U is found to be 50 nm using the Scherrer formula.

The XRD pattern for zirconium oxide nanoparticle prepared using the solvent of choline chloride – urea is provided at the figure 3.22. The diffraction peaks noticed in this figure for ZrO nanoparticles are in agreement with the Joint Committee for Powder Diffraction Studies (JCPDS) [23]. The average grain size of the ZrO nanoparticles with respect to relative intensity peak at XRD pattern was found to be 20 nm when the Scherrer formula is applied. The AgO nanoparticles obtained in the case of Ch.Cl-EG DES reported in figure 3.23 showed intense peaks at 20 values of 45.68, 64.49 and 77.46 which are indexed corresponding to the planes of (110), (220) and (311) respectively. The structure of silver oxide nanoparticles is crystalline in nature, and it is face centred cubic this case. The average particle size of AgO NPs obtained in the case of Ch.Cl-U DES is calculated to be 130 nm by measuring the breadth of (111) Bragg's reflection.

Figure 3.24 noticed the XRD data of zinc oxide nanoparticles obtained from the DES of Ch.Cl-U. The XRD plots of the nanoparticles showed peaks of pure hexagonal structure of zinc oxide. Three reflection planes (100), (002) and (101) that have been seen are similar to the detected reflections in bulk materials of zinc oxide  $^{[24]}$ . The diffraction peaks obtained at 29.63°, 36.16°, 38.17°, 46.28°, 59.32°, 69.38 and 76.16° are intense and sharp representing that the nano-crystalline zinc oxide nanoparticles had good crystallinity. The highest intensity at figure 3.24 related to zinc oxide nanoparticles reflecting the nanorange size around 75 nm by using Debye – Scherrer formula. The particle size determined involving the comparative intensity peak (220) found at 2 $\theta$  value of 52.14° of CdO nanoparticles as given in figure 3.25 has been observed as 100 nm. This is calculated using the Scherrer formula from the figure 3.25 corresponding to the CdO nanoparticles obtained from the DES of Ch.Cl-U. The surge in sharpness of XRD peaks designates those particles

are in crystalline kind. The (111), (200), (220), (311) and (222) reflections which correspond to 42.13, 47.42, 50.32, 69.29 and 73.46 respectively, are obviously seen and meticulously bout the reference designs of CdO (JCPDS) File No. 05-0640). The piercing XRD peaks show that the particles were of polycrystalline assembly, further the nanostructure raised with a random orientation [25, 26].

The crystalline kind of DES media synthesized vanadium oxide nanoparticles was depicted in figure 3.26. The characteristic key diffraction peaks noticed at 2θ values of 14.18, 20.05, 22.3, 26.7, 30.21, 32.13, 34.23, 41.25, 42.6, 45.56, 48.4 and 52.23 that match with the hkl planes of (200), (001), (101), (110), (310), (011), (310), (002), (102), (411), (600) and (302) index planes were in decent arrangement with their standard JCPDS No. 41-1426 [27]. The size of vanadium oxide nanoparticles was found by using the Scherrer's formula to be roughly 95 nm. The XRD pattern obtained for NiO nanoparticles in Ch.Cl-U DES is shown in figure 3.27. Three peaks for NiO NPs at 2θ values of 44.52°, 51.72° and 76.32° corresponding to the (111), (200) and (222) lattice planes found established that the ensuing particles have been pure Nickel oxide nanoparticles [28]. The nanoparticles width was projected by using the Scherrer's equation to be around 65 nm.

# 3.3.4 SEM Analysis of Metal Nanoparticles Prepared Using Choline Chloride – Urea Deep Eutectic Solvent

The SEM images obtained for copper, mercury, manganese, zirconium, silver, zinc, cadmium, vanadium and nickel metal oxide nanoparticles prepared from the deep eutectic solvent of choline chloride-urea are reported and discussed herewith. To examine the morphological structure and particle size of metal oxide nanoparticles such as Cu, Hg, Mn, Zr, Ag, Zn, Cd, V and Ni, scanning electron microscopy was used [29, 30]. The assembly, geometry, and magnitude of the above metal oxide nanoparticles prepared using the DES of Ch.Cl-U were evaluated from the Scanning Electron Microscopy images which are

displayed in figures 3.28 to 3.36. The mean particle dimensions of these metal oxide nanoparticles were calculated from the histograms of the respective SEM images and they are shown in figures 3.37 to 3.45. Further, the shapes and mean size of the prepared metal oxide nanoparticles are given in table 3.3 below.

Table 3.3: SEM morphology and size of metal oxide nanoparticles obtained from Ch.Cl-U DES

S. No.	Metal Oxide NPs	Morphology	Size (nm)
1	Copper	Polygonal Rods	44.22
2	Mercury	Polymorphous Grains	23.51
3	Manganese	Spongy Buds	49.46
4	Zirconium	Spongy Like	19.16
5	Silver	Aggregated Spheres	130
6	Zinc	Spongy Rods	70
7	Cadmium	Scales Like	101
8	Vanadium	Spongy Scales	97
9	Nickel	Accumulated Scales	62

# 3.3.5 TEM Analysis of Metal Nanoparticles Prepared Using Choline Chloride – Urea Deep Eutectic Solvent

The transmission electron microscopy (TEM) dimensions were supported out at 100 nm scale on the nanomaterials prepared using Ch.Cl-Urea deep eutectic solvent and the images are shown in figures 3.46 to 3.54. Cluster formation takes place as a result of interactions among the nanoparticles formed. The size of individual particles can be distinguished and their sizes and shapes resemble well with the SEM images. A few of the particles noticed in figures 3.46 to 3.54 are different from each though some particles have sizes and shape identical to those measured from the SEM images within 100 nm

# 3.3.6 EDAX Analysis of Metal Nanoparticles Prepared Using Choline Chloride – Urea Deep Eutectic Solvent

The elemental composition and the purity of the DES media via prepared metal oxide nanoparticles are confirmed by Energy Dispersive X-ray Analysis. The elemental cleanliness of these metal oxide NPs was evaluated from the EDAX spectra and the peak values established the occurrence of target components in the synthesized NPs [31-34,35]. The EDAX spectra obtained for copper, mercury, manganese, zirconium, silver, zinc, cadmium, vanadium and nickel metal oxide nanoparticles prepared from the deep eutectic solvent of choline chloride-urea are reported in the figures 3.55 to 3.63. The elemental purity, weight percentage, atom percentage of metals, oxygen and the trace of elements of solvent were given in the tables as an insert of the respective EDAX spectra of metal oxide nanoparticles.

#### 3.4. Conclusion

Nine types of metal oxide nanoparticles were synthesized successfully using choline chloride – urea deep eutectic solvents. The copper, mercury, manganese, zirconium, silver, zinc, cadmium, vanadium and nickel metal oxide nanoparticles prepared were characterized by techniques such as UV spectroscopy, FTIR spectroscopy, X-Ray diffraction, Scanning Electron Microscopy, Transmission Electron Microscopy and Energy Dispersive X-ray Analysis. The nanoparticles were synthesized in a simple and convenient manner. There was no surfactant and seed were utilized for the formation of nanoparticles. The size of the particles formed was controlled by varying proportions of the water present in the DESs.

#### References

- [1] Bundschuh, M., Filser, J., Lüderwald, S., McKee, M.S., Metreveli, G., Schaumann, G.E., Schulz, R. and Wagner, S., Nanoparticles in the environment: where do we come from, where do we go to? Environmental Sciences Europe, 30(1) (2018), pp.1-17.
- [2] Khodashenas, B. and Ghorbani, H.R., Synthesis of copper nanoparticles: An overview of the various methods. Korean Journal of Chemical Engineering, 31 (7) (2014), 1105-1109.
- [3] Cai, X., Zhu, Q., Zeng, Y., Zeng, Q., Chen, X. and Zhan, Y., Manganese oxide nanoparticles as MRI contrast agents in tumor multimodal imaging and therapy. International journal of nanomedicine, 14 (2019), p.8321.
- [4] Sigwadi, R., Dhlamini, M., Mokrani, T. and Nemavhola, F., Preparation of a high surface area zirconium oxide for fuel cell application. International Journal of Mechanical and Materials Engineering, 14(1) (2019), pp.1-11.
- [5] Qinghua Zhang, Karine De Oliveira Vigier, Sebastien Royer and Francois Jerome, Deep eutectic solvents: syntheses, properties and applications. Chem. Soc. Rev., 41 (2012), pp.7108–7146, DOI: 10.1039/c2cs35178a.
- [6] Emma L. Smith, Andrew P. Abbott, and Karl S. Ryder, Deep Eutectic Solvents (DESs) and Their Applications. pubs.acs.org/CR Chem. Rev. 114 (2014), pp. 11060-11082, dx.doi.org/10.1021/cr300162p.
- [7] Liao, H. G., Jiang, Y. X., Zhou, Z. Y., Chen, S. P. and Sun, S. G., Shape-Controlled Synthesis of Gold Nanoparticles in Deep Eutectic Solvents for Studies of Structure–Functionality Relationships in Electrocatalysis. Angew. Chem., Int. Ed., 47 (2008) pp. 9100–9103. https://doi.org/10.1002/anie.200803202

- [8] Chirea, M., Freitas, A., Vasile, B. S., Ghitulica, C., Pereira, C. M. and Silva, F., Gold Nanowire Networks: Synthesis, Characterization, and Catalytic Activity. Langmuir, 27 (2011) pp. 3906–3913. dx.doi.org/10.1021/la104092b |
- [9] Phuong, T.D.V., Phi, T.L., Phi, B.H., Van Hieu, N., Tang Nguyen, S. and Le Manh, T., Electrochemical Behavior and Electronucleation of Copper Nanoparticles from CuCl<sub>2</sub>· H<sub>2</sub>O Using a Choline Chloride-Urea Eutectic Mixture. Journal of Nanomaterials, 7 (2021), pp1 14.
- [10] Parsa, A. and Heli, H., Electrodeposition of nickel wrinkled nanostructure from choline chloride: urea deep eutectic solvent (reline) and application for electroanalysis of simvastatin. Microchemical Journal, 152 (2020), p.104267.
- [11] Verma, C., Ebenso, E.E. and Quraishi, M.A., Transition metal nanoparticles in ionic liquids: Synthesis and stabilization. Journal of Molecular Liquids, 276 (2019), 826-849.
- [12] Tome, L.I., Baiao, V., da Silva, W. and Brett, C.M., Deep eutectic solvents for the production and application of new materials. Applied Materials Today, 10 (2018), 30-50. [13] Li, W., Hao, J., Liu, W. and Mu, S., Electrodeposition of nano Ni–Co alloy with (220)
- preferred orientation from choline chloride-urea: Electrochemical behavior and nucleation mechanism. Journal of Alloys and Compounds, 853 (2021), p.157158.
- [14] Palomar-Pardavé, M., Mostany, J., Muñoz-Rizo, R., Botello, L.E., Aldana-González, J., Arce-Estrada, E.M., de Oca-Yemha, M.G.M., Ramírez-Silva, M.T. and Romo, M.R., Electrochemical study and physicochemical characterization of iron nanoparticles electrodeposited onto HOPG from Fe (III) ions dissolved in the choline chloride-urea deep eutectic solvent. Journal of Electroanalytical Chemistry, 851 (2019), p.113453.
- [15] Delbecq, F., Delfosse, P., Laboureix, G., Paré, C. and Kawai, T., Study of a gelated Deep Eutectic solvent metal salt solution as template for the production of size-controlled

- small noble metal nanoparticles. Colloids and Surfaces A: Physicochemical and Engineering Aspects, 567 (2019), pp.55-62.
- [16] Ghenaatian, H.R., Shakourian-Fard, M. and Kamath, G., Interaction of Cun, Agn and Aun (n= 1–4) nanoparticles with ChCl: Urea deep eutectic solvent. Journal of Molecular Graphics and Modelling, 105 (2021), p.107866.
- [17] Kakaei, K., Alidoust, E. and Ghadimi, G., Synthesis of N-doped graphene nanosheets and its composite with urea choline chloride ionic liquid as a novel electrode for supercapacitor. Journal of Alloys and Compounds, 735 (2018), pp.1799-1806.
- [18] M. Abdulla-Al-Mamun, Y. Kusumoto, and M. Muruganandham, "Simple new synthesis of copper nanoparticles in water/acetonitrile mixed solvent and their characterization," Materials Letters, vol. 63, no. 23, pp. 2007–2009.
- [19] Shikha Jain, Ankita Jain, Vijay Devra, Copper nanoparticles catalyzed oxidation of threonine by peroxomonosulfate, Journal of Saudi chemical society 18 (2014), 149 153. [20] E.C. Njagi, H. Huang, L. Stafford, H. Genuino, et al., Langmuir 27 (2011) 264–271. [21] Tariq Jan, J. Iqbal, Umar Farooq, Asma Gul, Rashda Abbasi, Ishaq Ahmad, Maaza Malik, Structural, Raman and optical characteristics of Sn doped CuO nanostructures: A novel anticancer agent, Ceramics International, 41(10), Part A December 2015, 13074 79. http://dx.doi.org/10.1016/j.ceramint.2015.06.080.
- [22] A. Rita, A. Sivakumar, S. A. Martin Britto Dhas, Influence of shock waves on structural and morphological properties of copper oxide NPs for aerospace applications, Journal of Nanostructure in Chemistry, 9 (2019), 225 230. <a href="https://doi.org/10.1007/s40097-019-00313-0">https://doi.org/10.1007/s40097-019-00313-0</a>
- [23] Saeid and, Asadi Asadollah, Tamijani-Habibi Amir, and Negahdary M, Synthesis of Zirconia Nanoparticles and their Ameliorative Roles as Additives Concrete Structures,

- Journal of Chemistry, Volume 2013 | Article D 314862, 1-7. https://doi.org/10.1155/2013/314862
- [24] M.A. Ramadan, S.H. Nassar, A.S. Montaser, E.M. El-Khatib and M.S.Abdel-Aziz, Synthesis of Nano-sized Zinc Oxide and Its Application for Cellulosic Textiles, Egypt. J. Chem. 59, No.4, pp. 523 535 (2016).
- [25] A.S. Aldwayyan, F.M. Al-Jekhedab, M. Al-Noaimi, B. Hammouti, T. B. Hadda, M. Suleiman, I. Warad, Synthesis and Characterization of CdO Nanoparticles Starting from Organometalic Dmphen-CdI2 complex, Int. J. Electrochem. Sci., 8 (2013) 10506 10514. [26] H.P. Klug, and L.E. Alexander, X-ray Diffraction Procedures for Polycrystalline and Amorphous Materials, Wiley, New York (1954).
- [27] Mohammadhassan Gholami-Shabani, Fattah Sotoodehnejadnematalahi, Masoomeh Shams-Ghahfarokhi, Ali Eslamifar and Mehdi Razzaghi-Abyaneh, Mycosynthesis and Physicochemical Characterization of Vanadium Oxide Nanoparticles Using the Cell-Free Filtrate of Fusarium oxysporum and Evaluation of Their Cytotoxic and Antifungal Activities, Journal of Nanomaterials, Volume 2021, Article ID 7532660, 1-7. <a href="https://doi.org/10.1155/2021/7532660">https://doi.org/10.1155/2021/7532660</a>.
- [28] Szu-HanWu, Dong-HwangChen, Synthesis and characterization of nickel nanoparticles by hydrazine reduction in ethylene glycol, <u>Journal of Colloid and Interface Science</u>, <u>Volume 259</u>, (2), 15 March 2003, Pages 282-286, <a href="https://doi.org/10.1016/S0021-9797(02)00135-2">https://doi.org/10.1016/S0021-9797(02)00135-2</a>.
- [29] Sarjuna, K. and Ilangeswaran, D., Preparation and Physico-chemical studies of Ag2O nanoparticles using newly formed malonic acid and ZnCl2-based deep eutectic solvents. Mater. Today Proc. 49 (2022), pp. 2943–2948.
- [30] Thomas Nesakumar Jebakumar, Immanuel Edison, Raji Atchudan, Namachivayam Karthik Sundaram Chandrasekaran, Suguna Perumal, Pandian Bothi Raja,

Veeradasan Perumal, Yong Rok Lee, Deep eutectic solvent assisted electrosynthesis of ruthenium nanoparticles on stainless steel mesh for electrocatalytic hydrogen evolution reaction, Fuel 297 (1) (2021) 120786.

- [31] A. El-Trass, H. ElShamy, I. El-Mehasseb, M. El-Kemary, CuO nanoparticles: synthesis, characterization, optical properties and interaction with amino acids, Appl. Surf. Sci. 258 (2012) 2997–3001.
- [32] Sundararaju Sathyavathi, Arumugam Manjula, Jeyaprakash Rajendhran, Paramasamy Gunasekaran, Biosynthesis and characterization of mercury sulphide nanoparticles produced by Bacillus cereus MRS-1, Indian J. Exp. Biol. 51 (2013) 973–978.
- [33] S. Ganeshan, P. Ramasundari, A. Elangovan, G. Arivazhagan, R. Vijayalakshmi, Synthesis and characterization of MnO2 nanoparticles: study of structural and optical properties, Int. J. Scient. Res. Phys. Appl. Sci. 5 (6) (2017) 5–8.
- [34] Ahmed Mishaal Mohammed, Mahmood Mohammed Ali, Synthesis and characterisation of zirconium oxide nanoparticles via the hydrothermal method and evaluation of their antibacterial activity, Res. J. Pharm. Technol. 14 (2) (2021), 938–942.
- [35] A. Rita, A. Sivakumar, S.A. Martin Britto Dhas, Influence of shock waves on structural and morphological properties of copper oxide NPs for aerospace applications, J. Nanostruct. Chem. 9 (2019) 225–230.

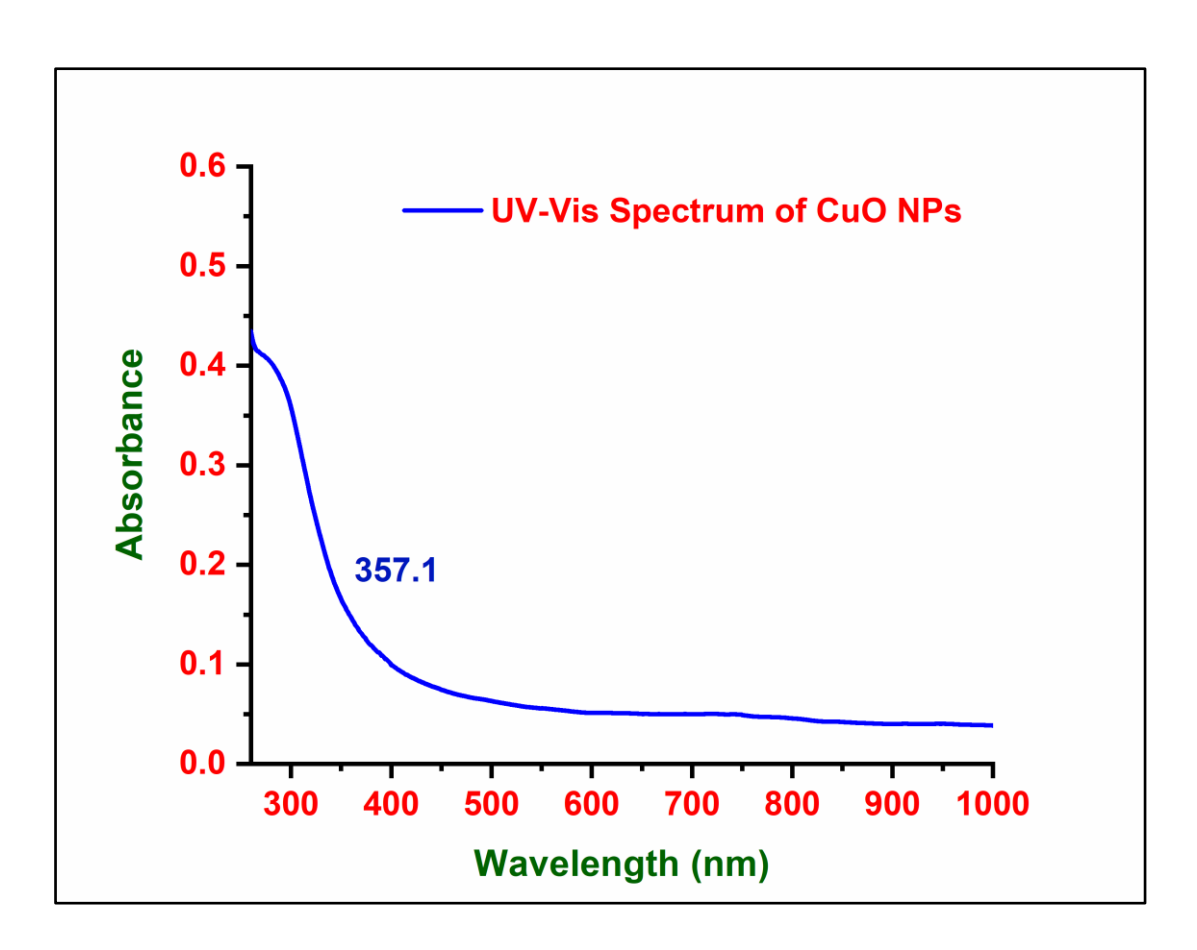


Figure 3.1: UV-Visible Spectrum of Copper Oxide Nanoparticle obtained in Ch. Cl-U DES

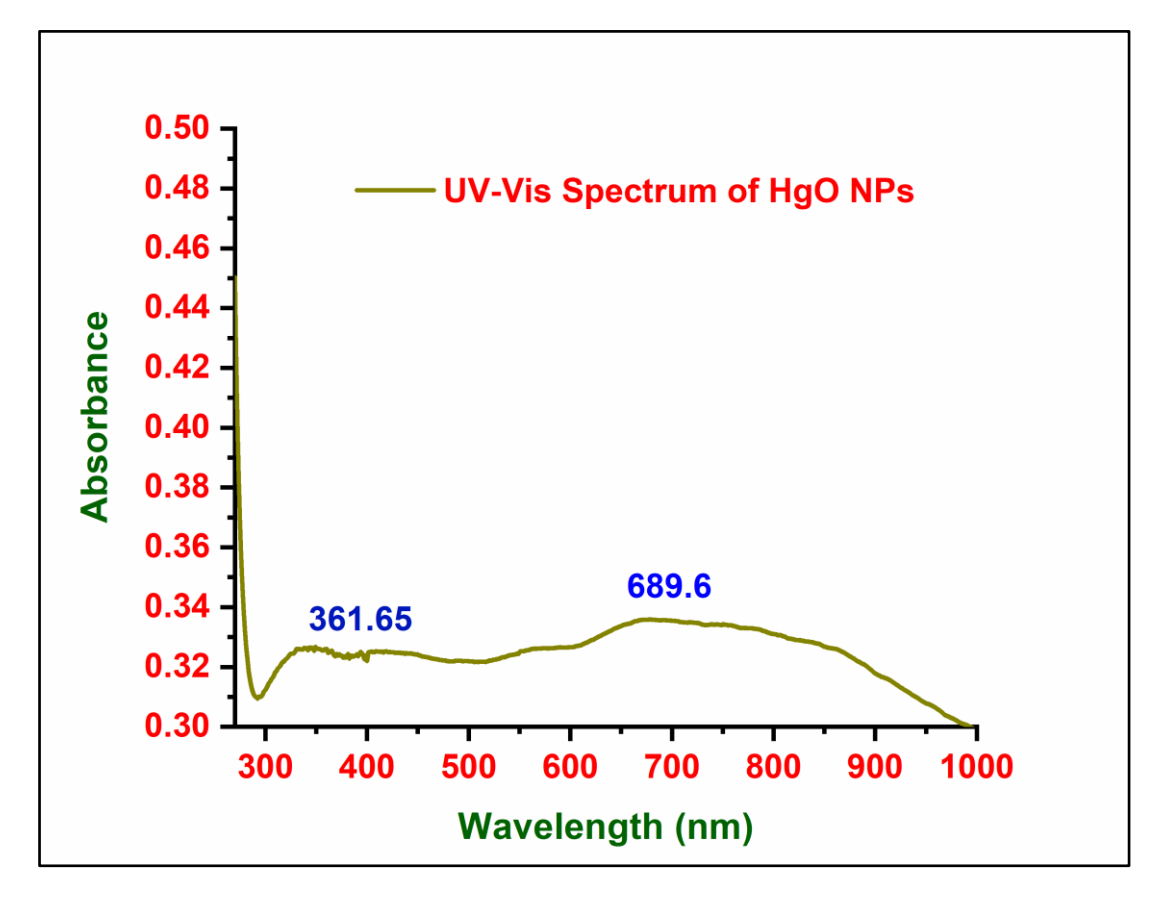


Figure 3.2: UV-Visible Spectrum of Mercury Oxide Nanoparticle obtained in Ch. Cl-U DES

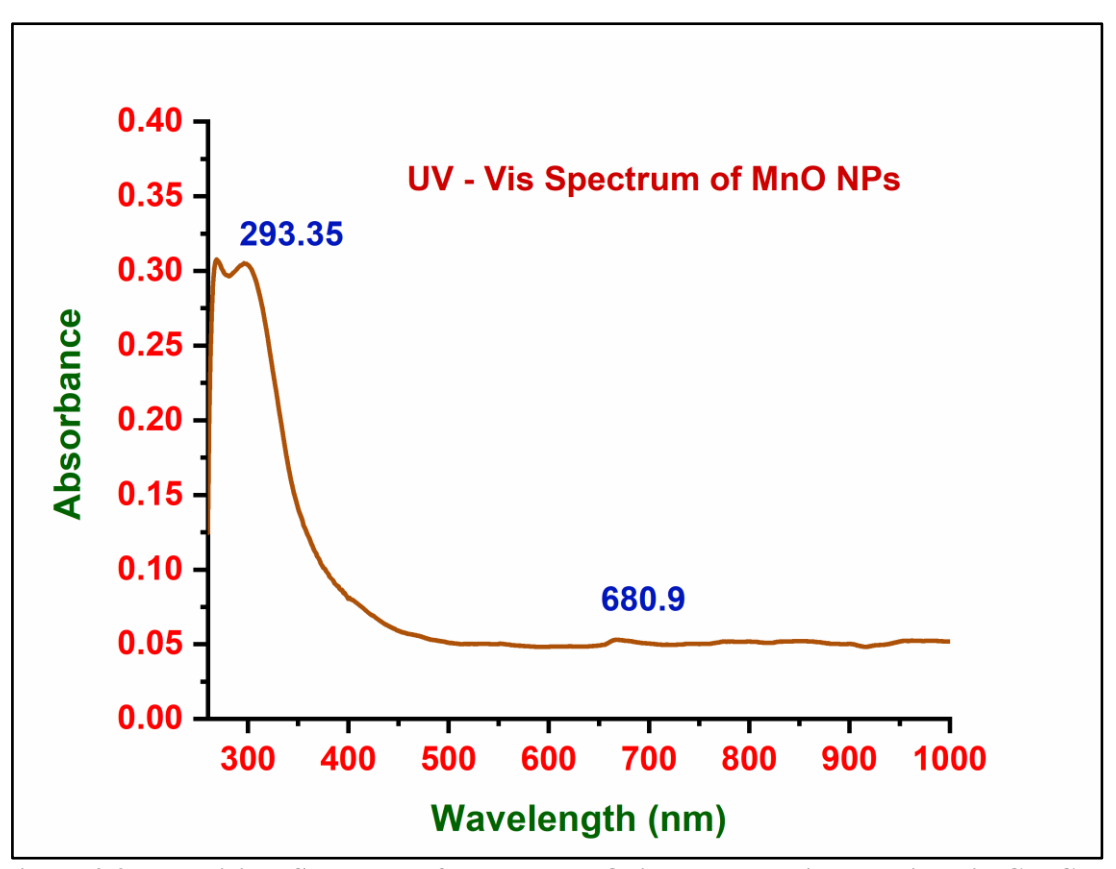


Figure 3.3: UV-Visible Spectrum of Manganese Oxide Nanoparticle obtained in Ch. Cl-U DES

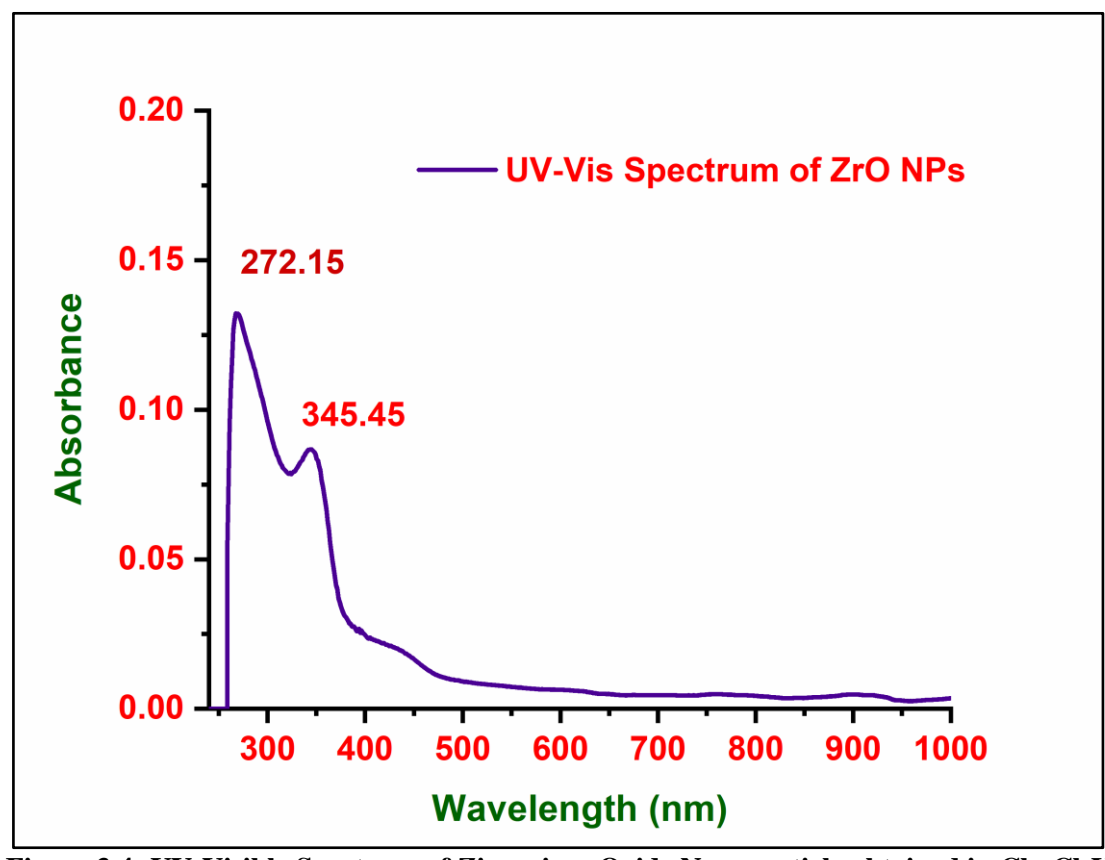


Figure 3.4: UV-Visible Spectrum of Zirconium Oxide Nanoparticle obtained in Ch. Cl-U DES

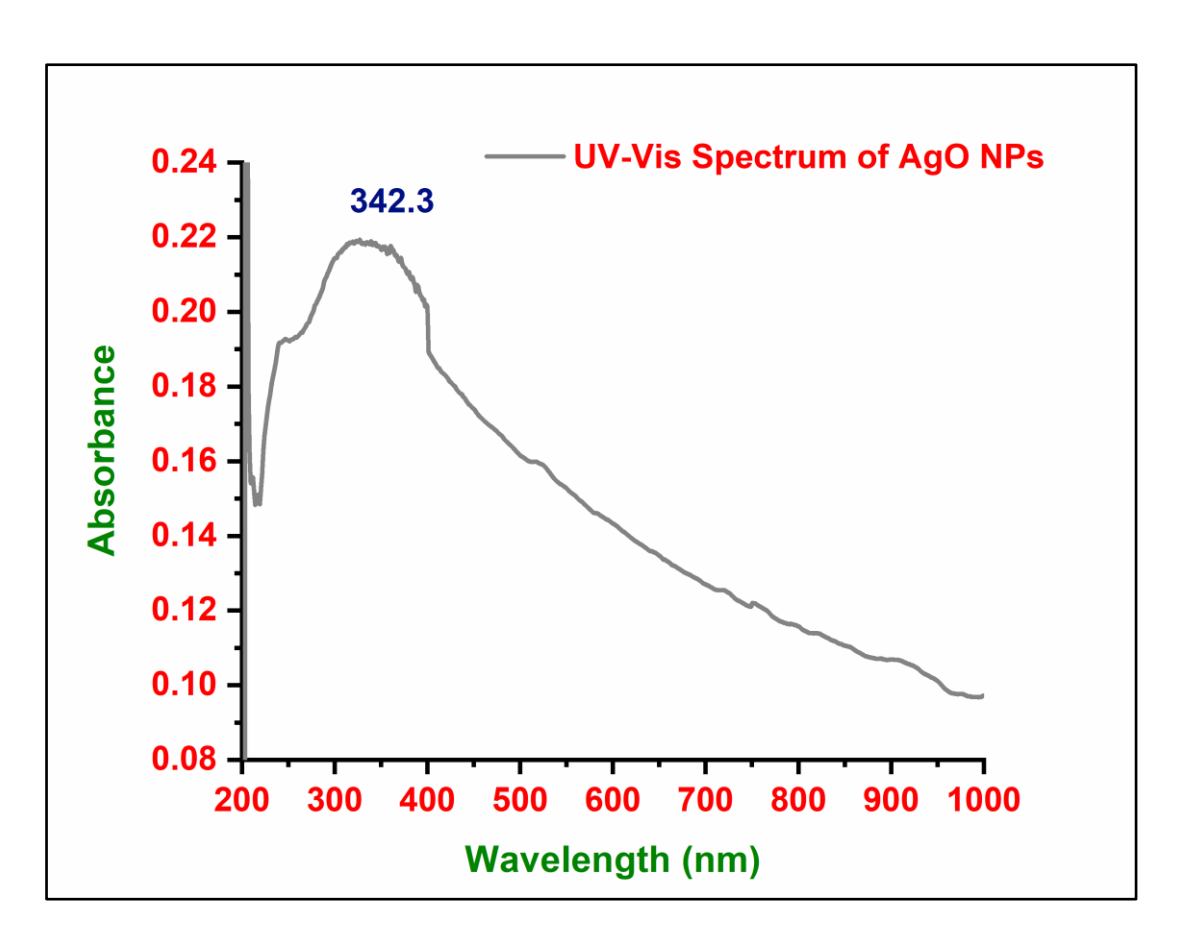


Figure 3.5: UV-Visible Spectrum of Silver Oxide Nanoparticle obtained in Ch. Cl-U DES

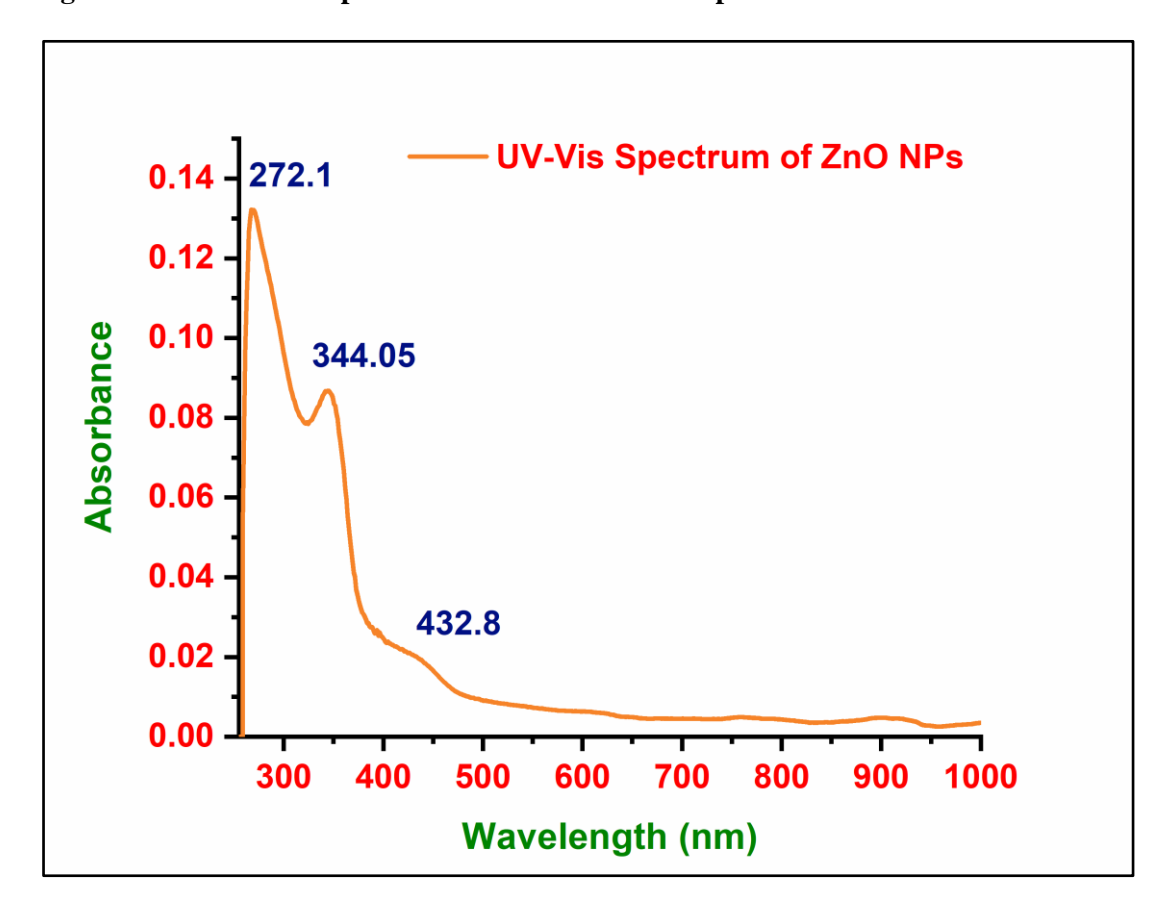


Figure 3.6: UV-Visible Spectrum of Zinc Oxide Nanoparticle obtained in Ch. Cl-U DES

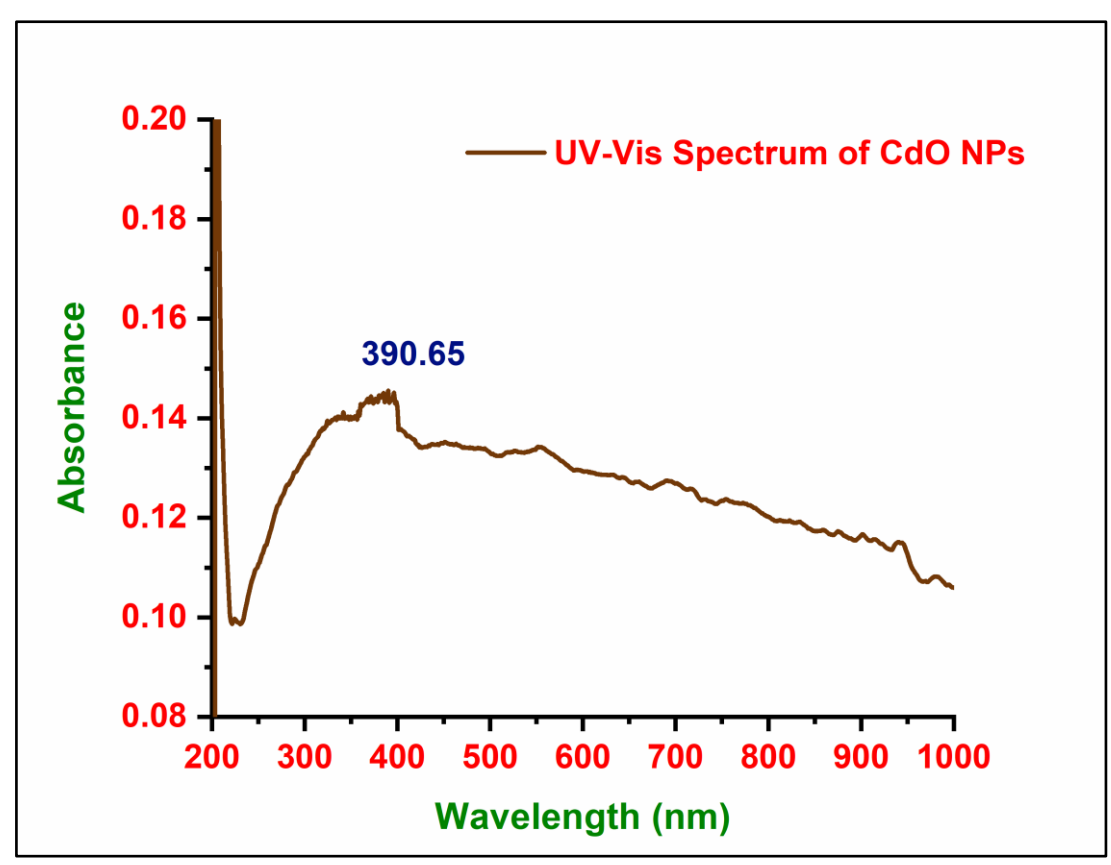


Figure 3.7: UV-Visible Spectrum of Cadmium Oxide Nanoparticle obtained in Ch. Cl-U DES

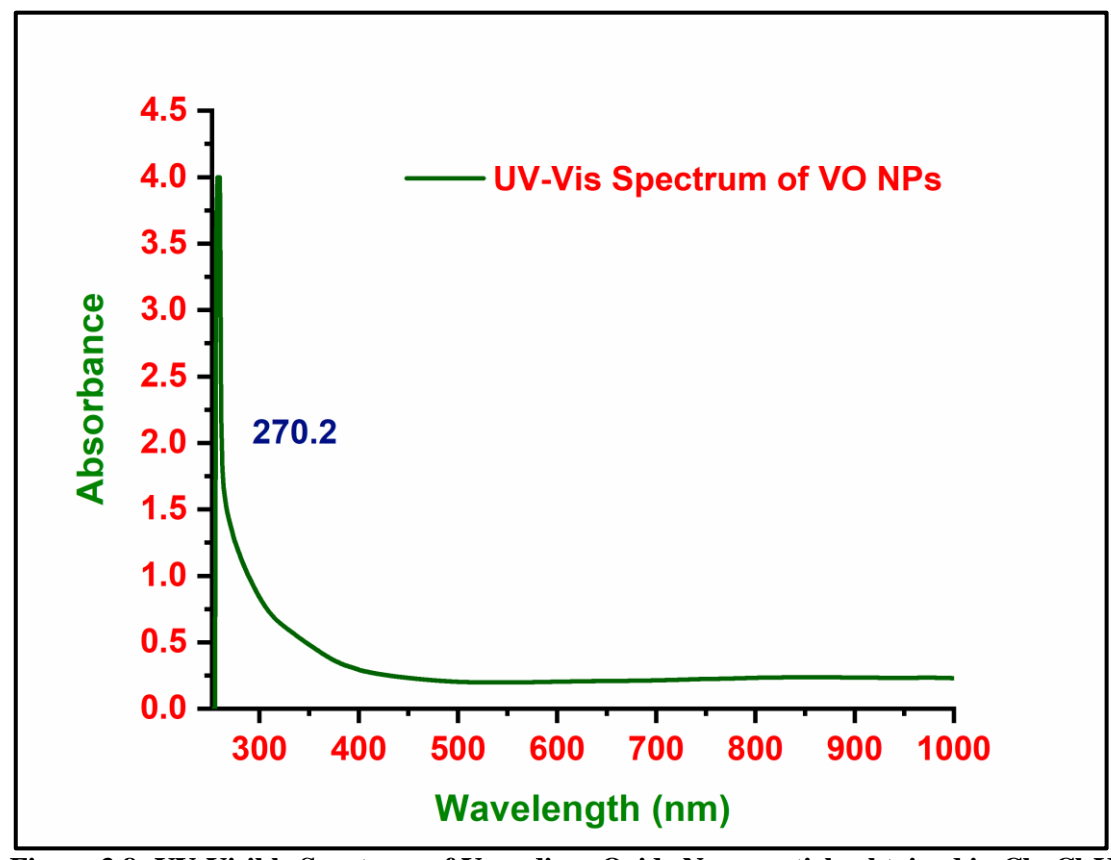


Figure 3.8: UV-Visible Spectrum of Vanadium Oxide Nanoparticle obtained in Ch. Cl-U DES

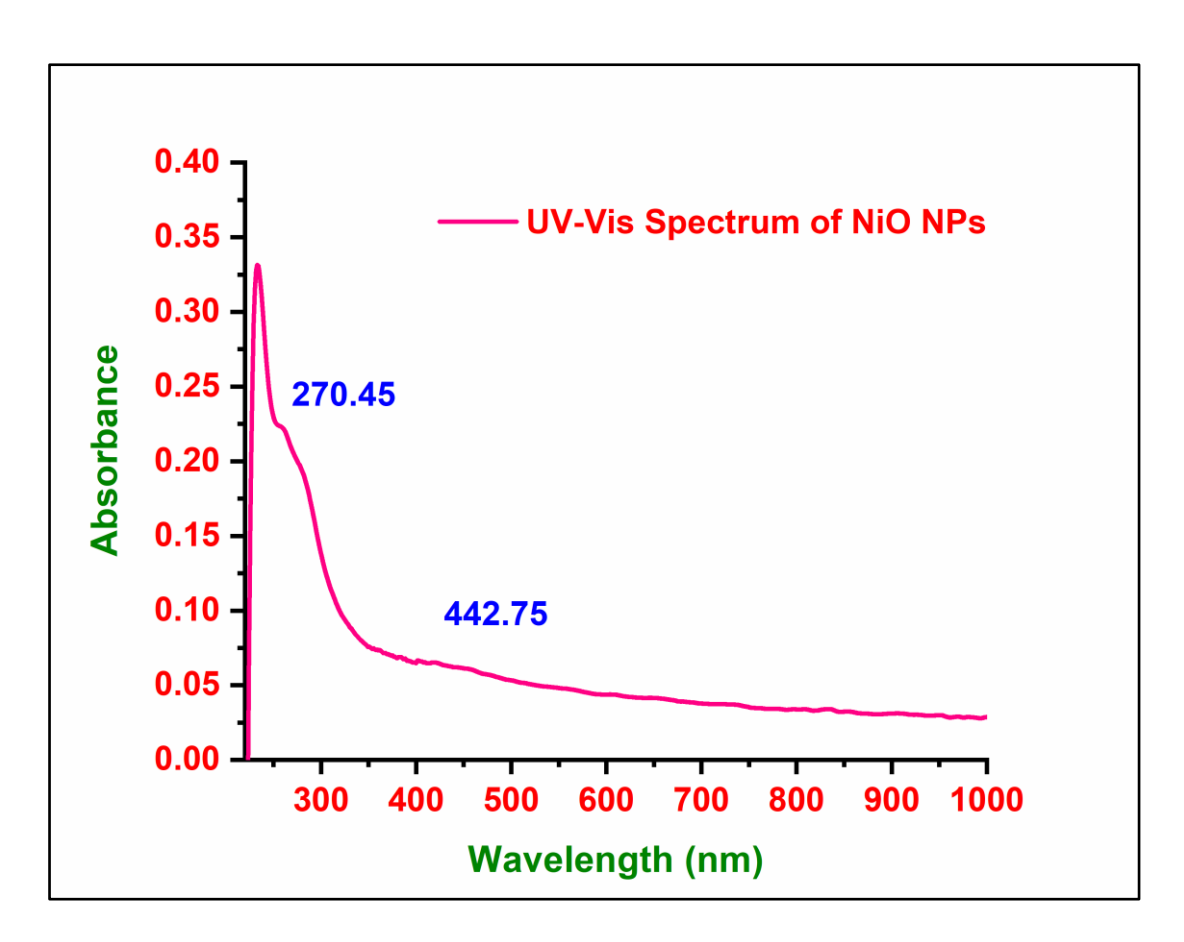


Figure 3.9: UV-Visible Spectrum of Nickel Oxide Nanoparticle obtained in Ch. Cl-U DES

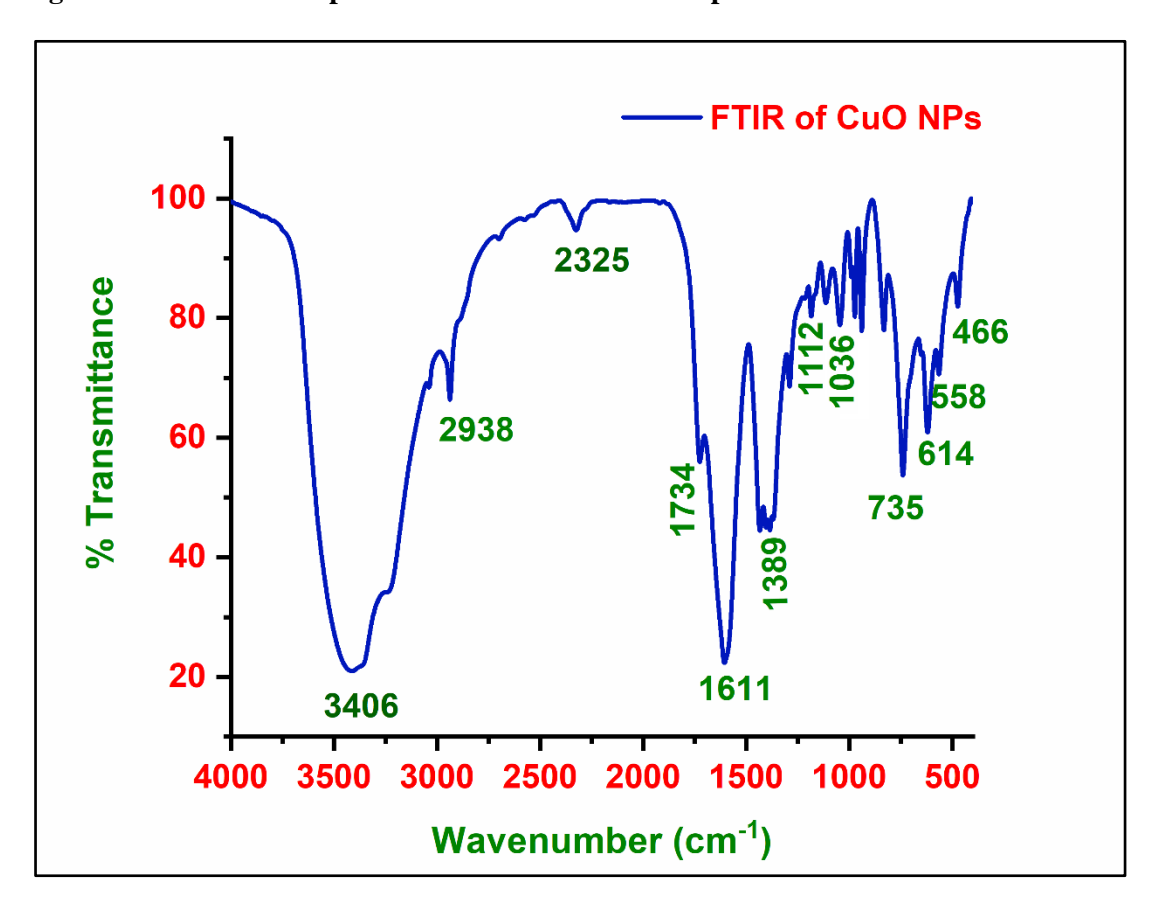


Figure 3.10: FTIR Spectrum of Copper Oxide Nanoparticle obtained in Ch. Cl-U DES

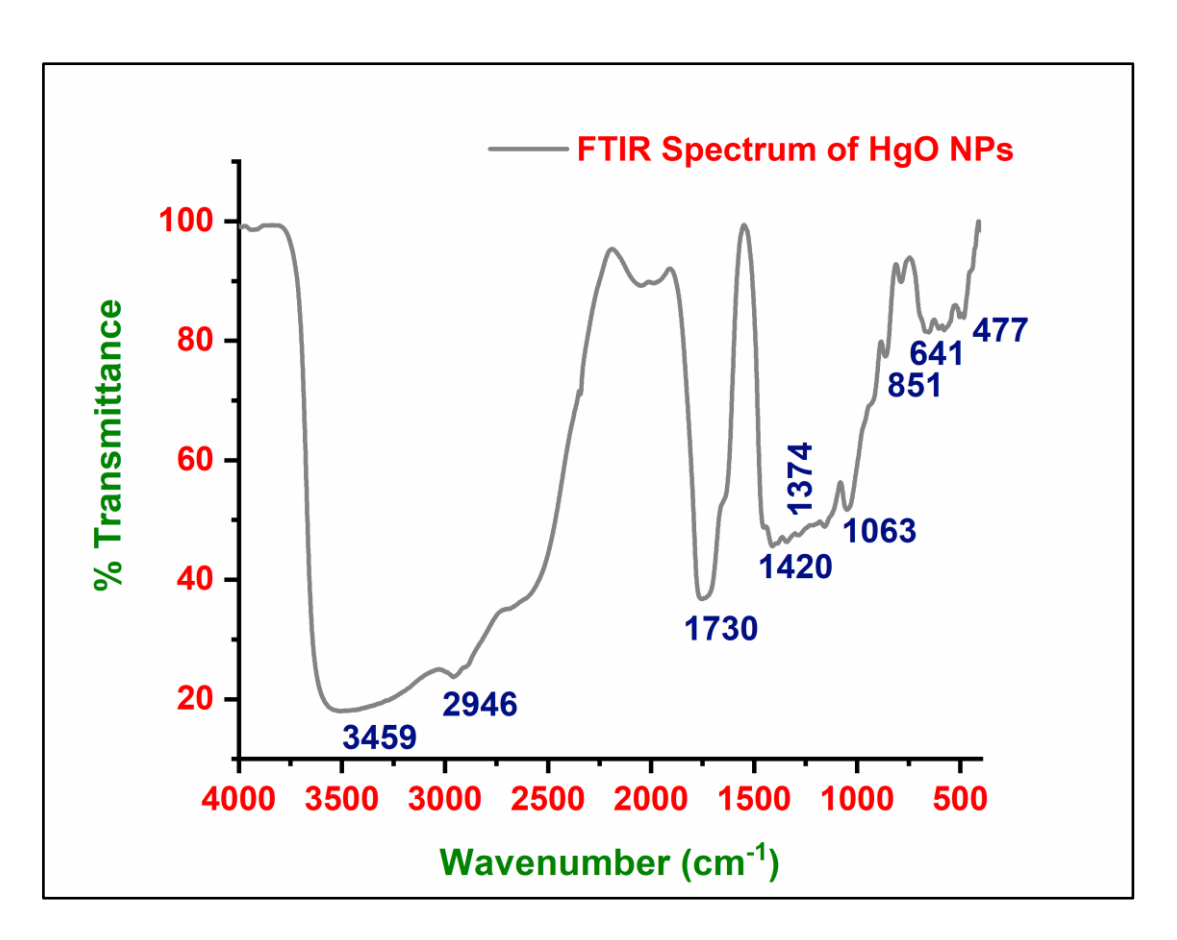


Figure 3.11: FTIR Spectrum of Mercury Oxide Nanoparticle obtained in Ch. Cl-U DES

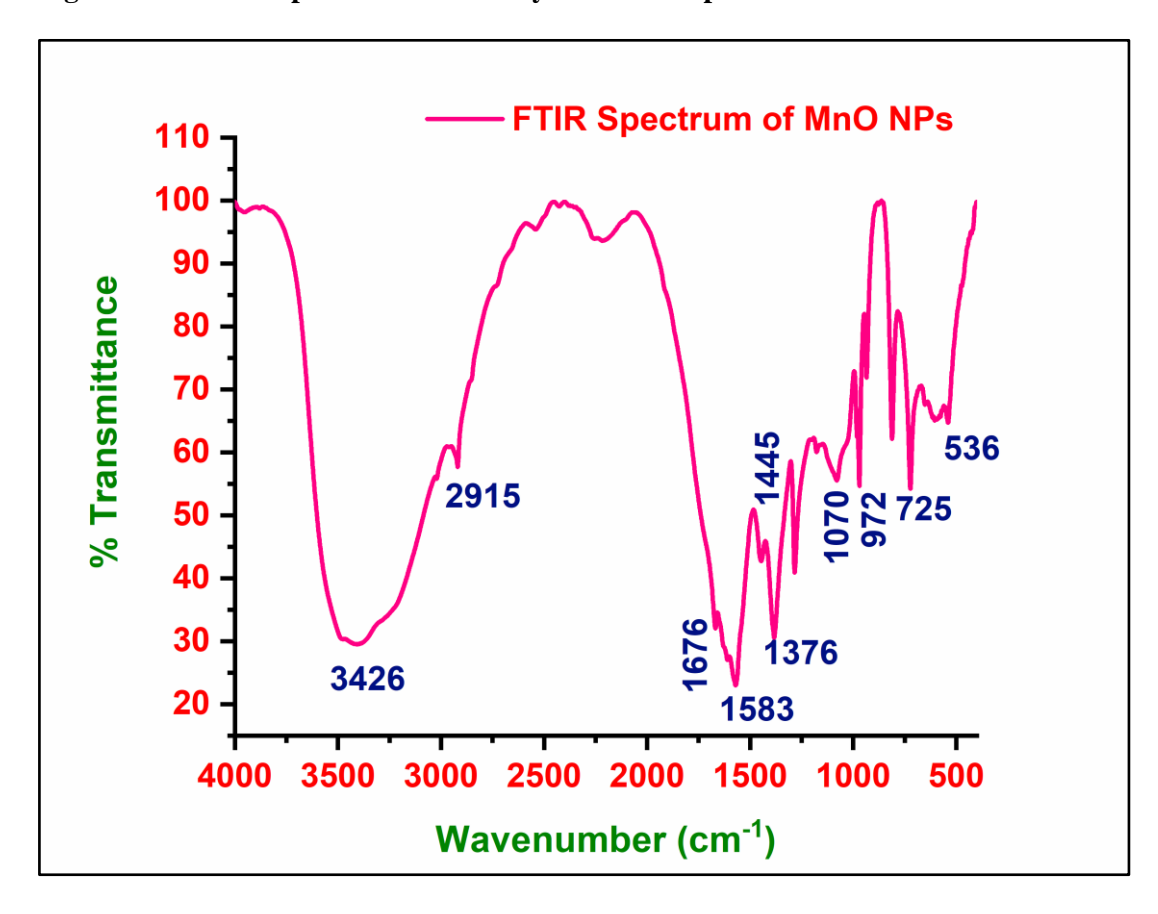


Figure 3.12: FTIR Spectrum of Manganese Oxide Nanoparticle obtained in Ch. Cl-U DES

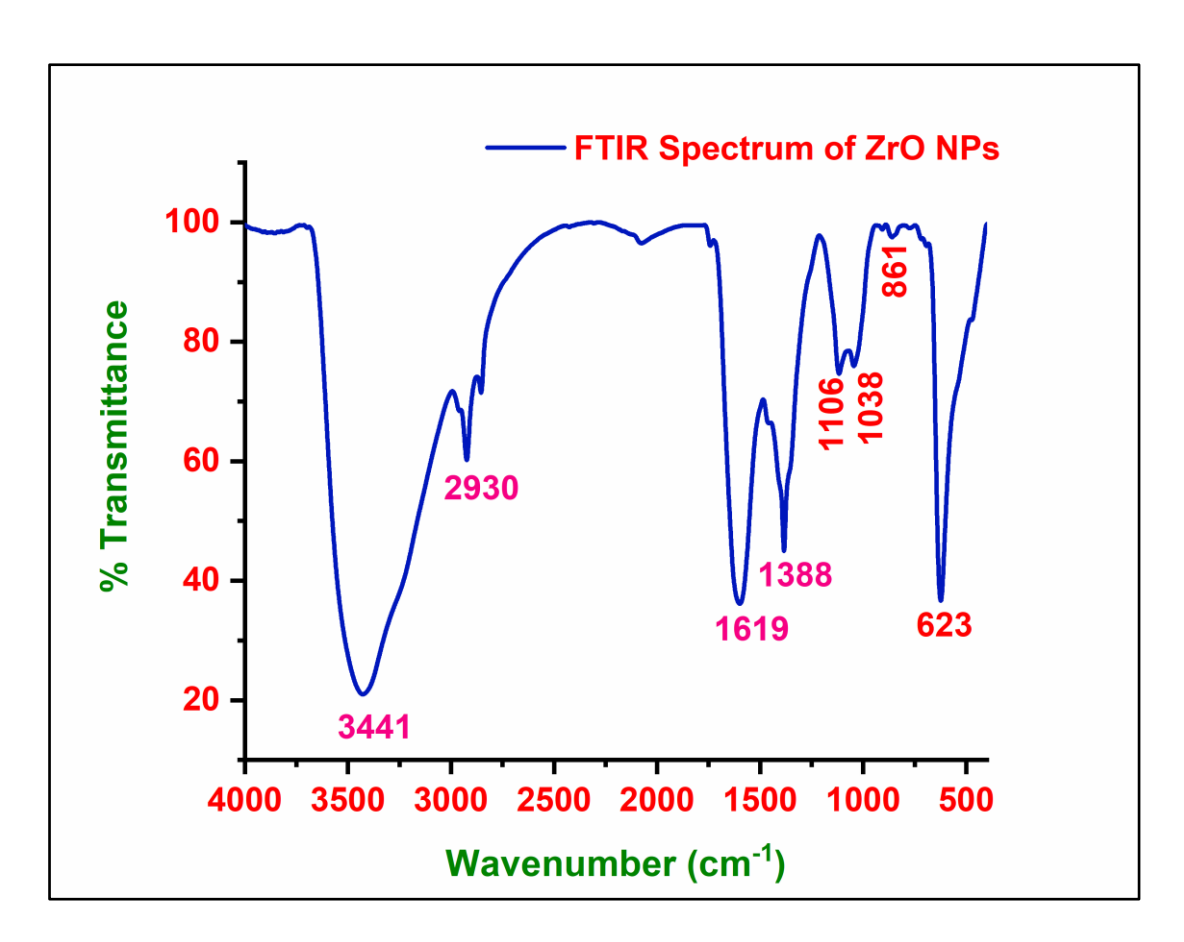


Figure 3.13: FTIR Spectrum of Zirconium Oxide Nanoparticle obtained in Ch. Cl-U DES

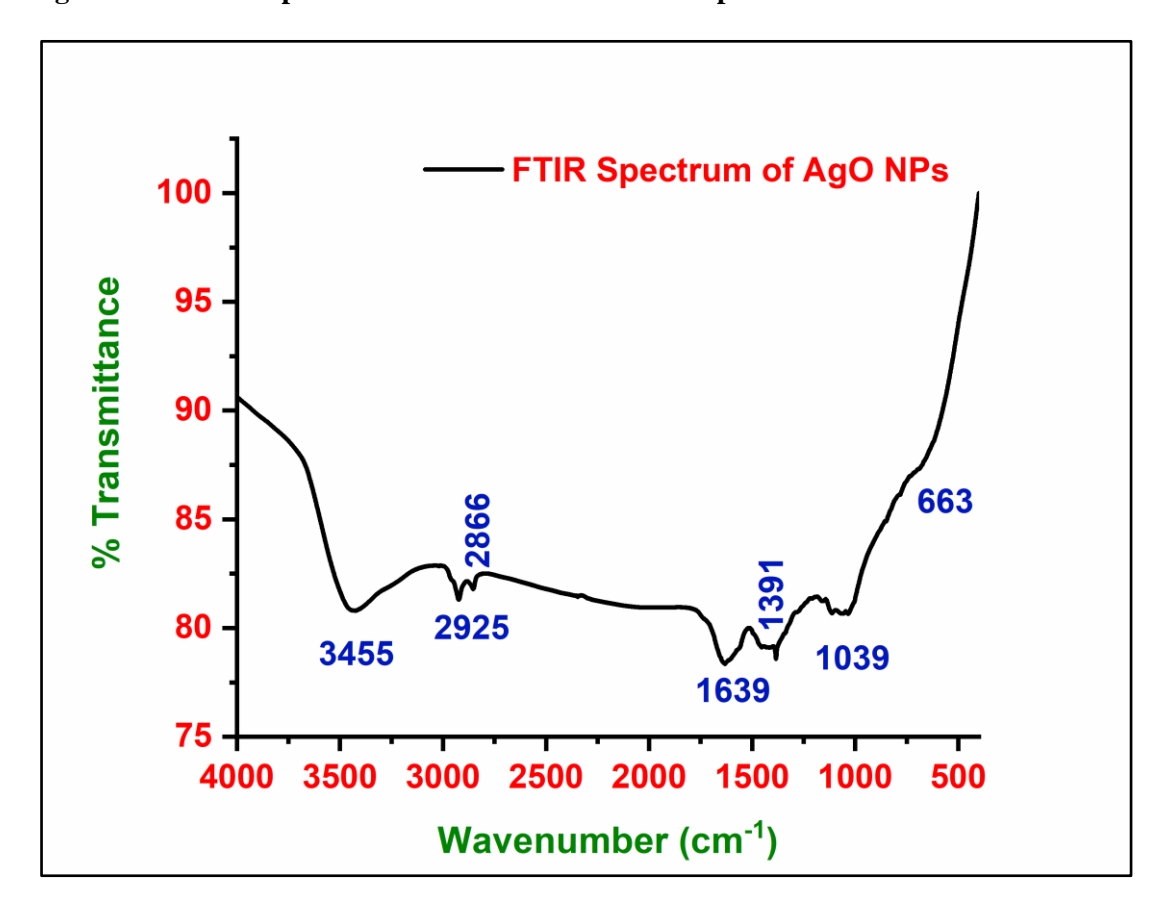


Figure 3.14: FTIR Spectrum of Silver Oxide Nanoparticle obtained in Ch. Cl-U DES

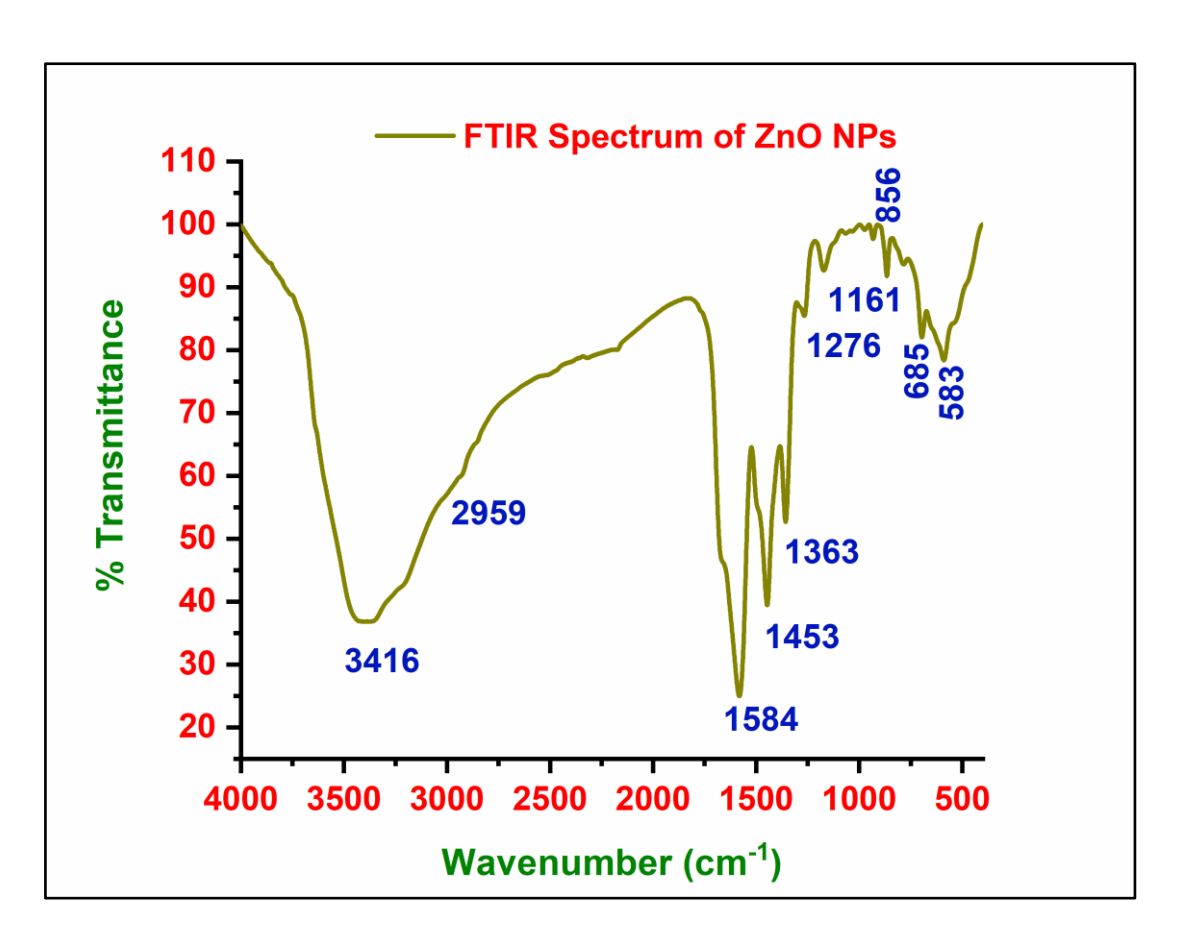


Figure 3.15: FTIR Spectrum of Zinc Oxide Nanoparticle obtained in Ch. Cl-U DES

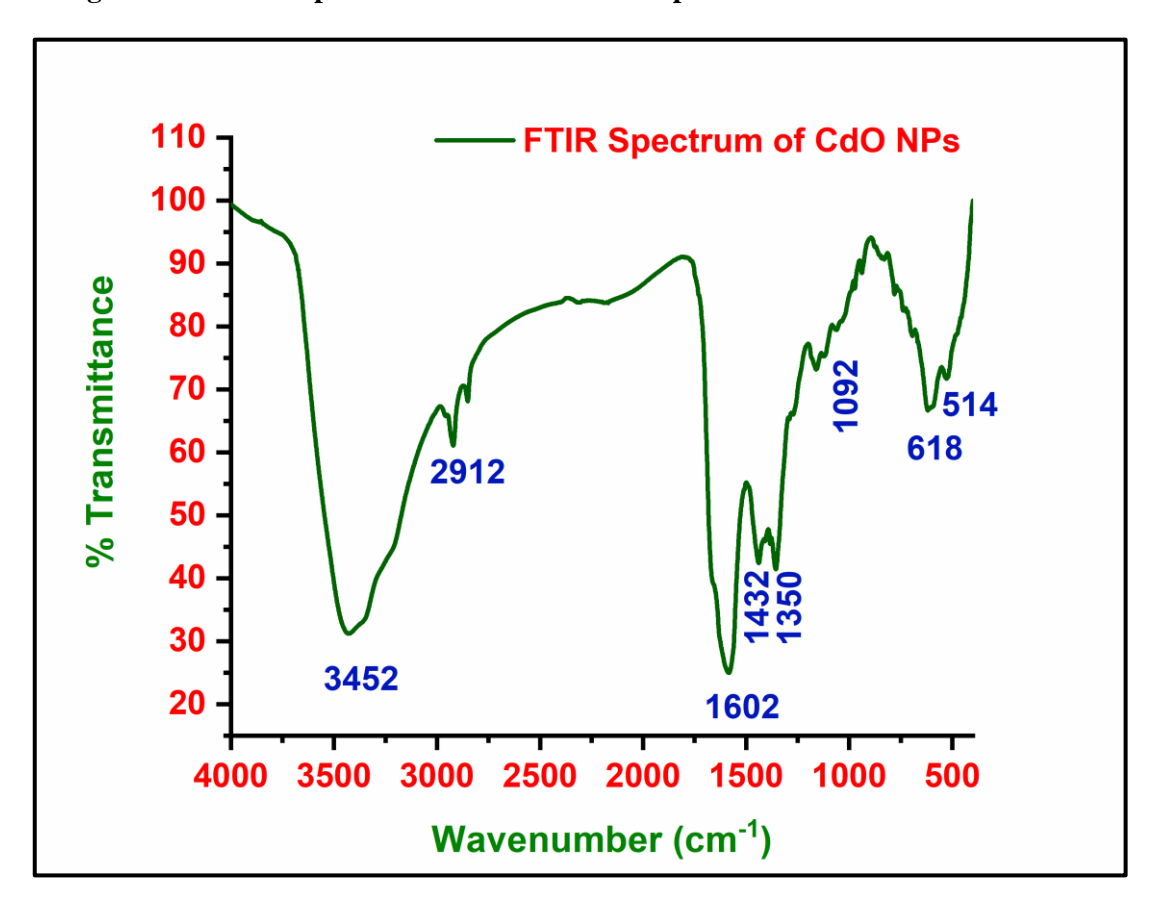


Figure 3.16: FTIR Spectrum of Cadmium Oxide Nanoparticle obtained in Ch. Cl-U DES

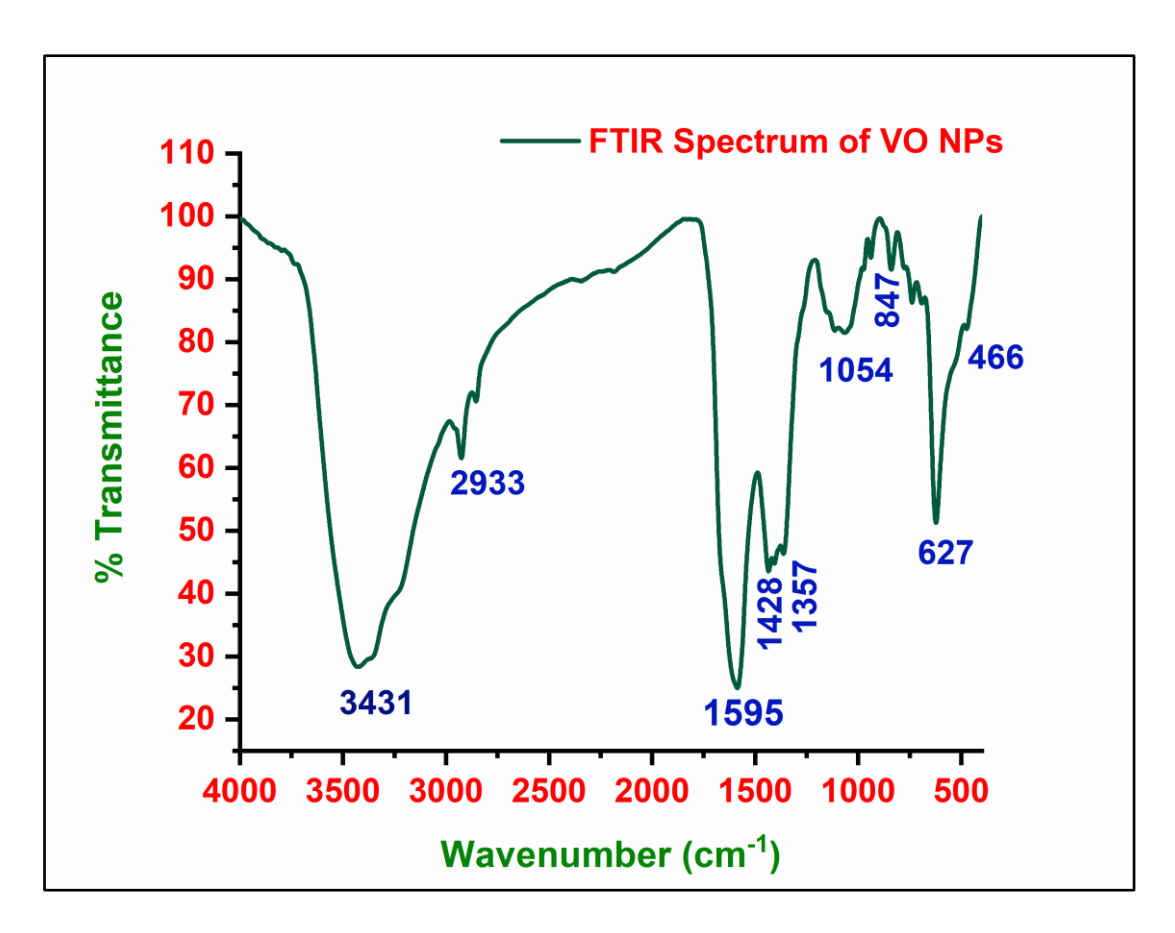


Figure 3.17: FTIR Spectrum of Vanadium Oxide Nanoparticle obtained in Ch. Cl-U DES

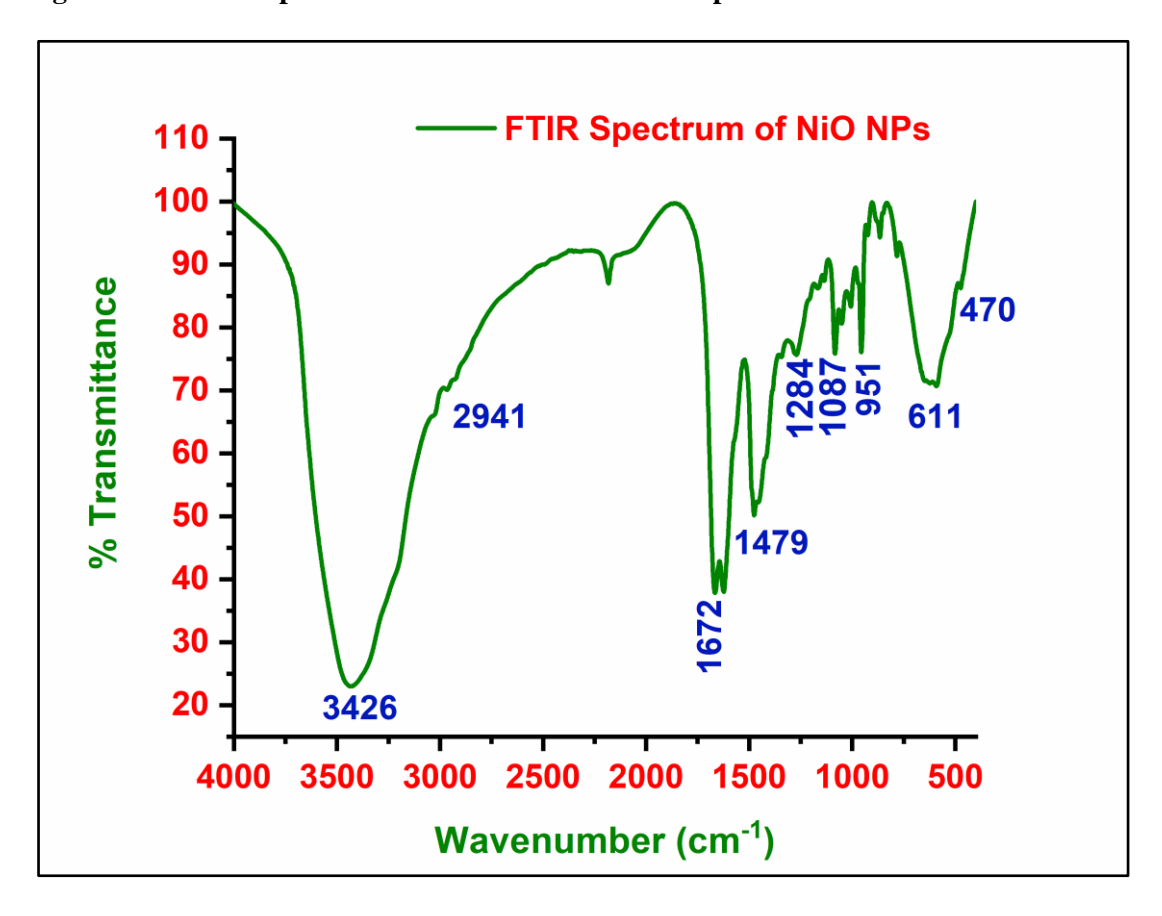


Figure 3.18: FTIR Spectrum of Nickel Oxide Nanoparticle obtained in Ch. Cl-U DES

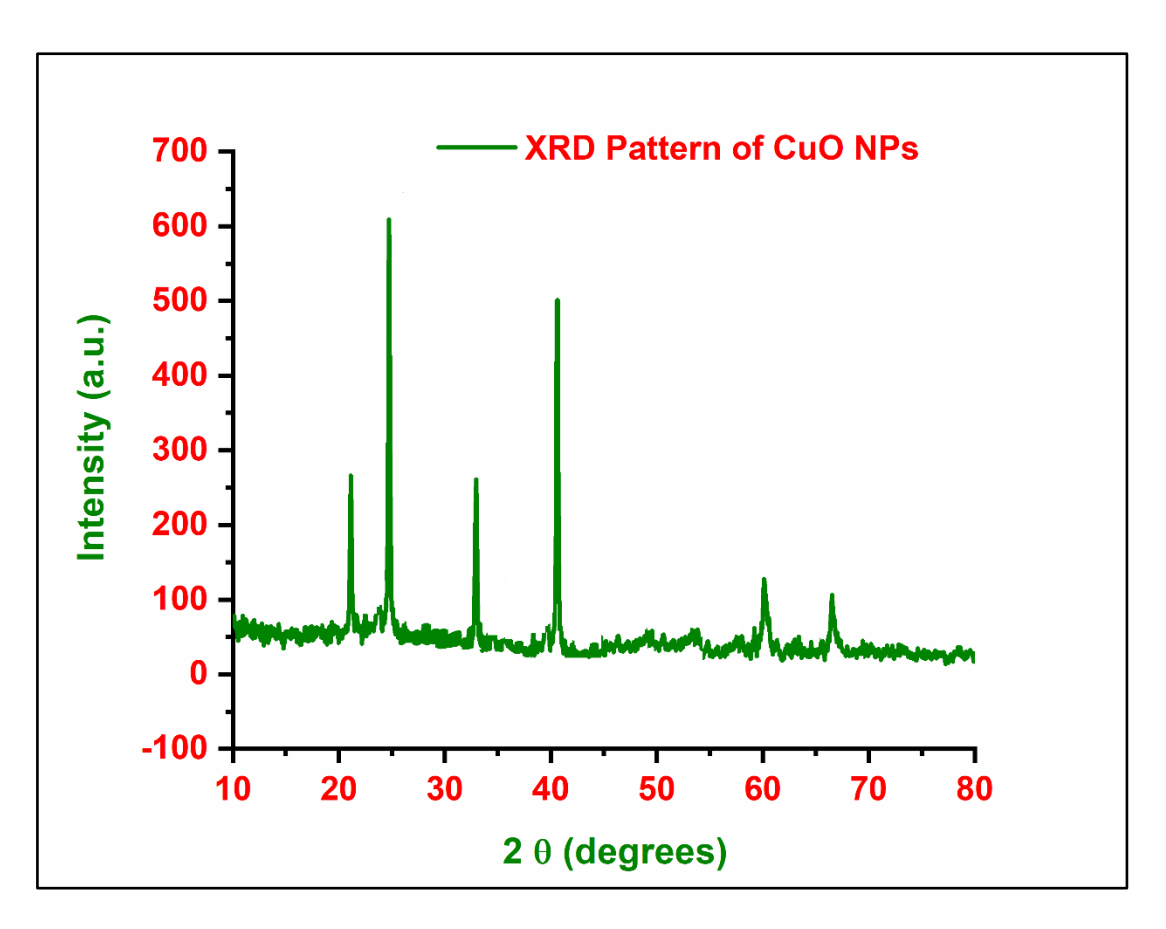


Figure 3.19: XRD Pattern of Copper Oxide Nanoparticle obtained in Ch. Cl-U DES

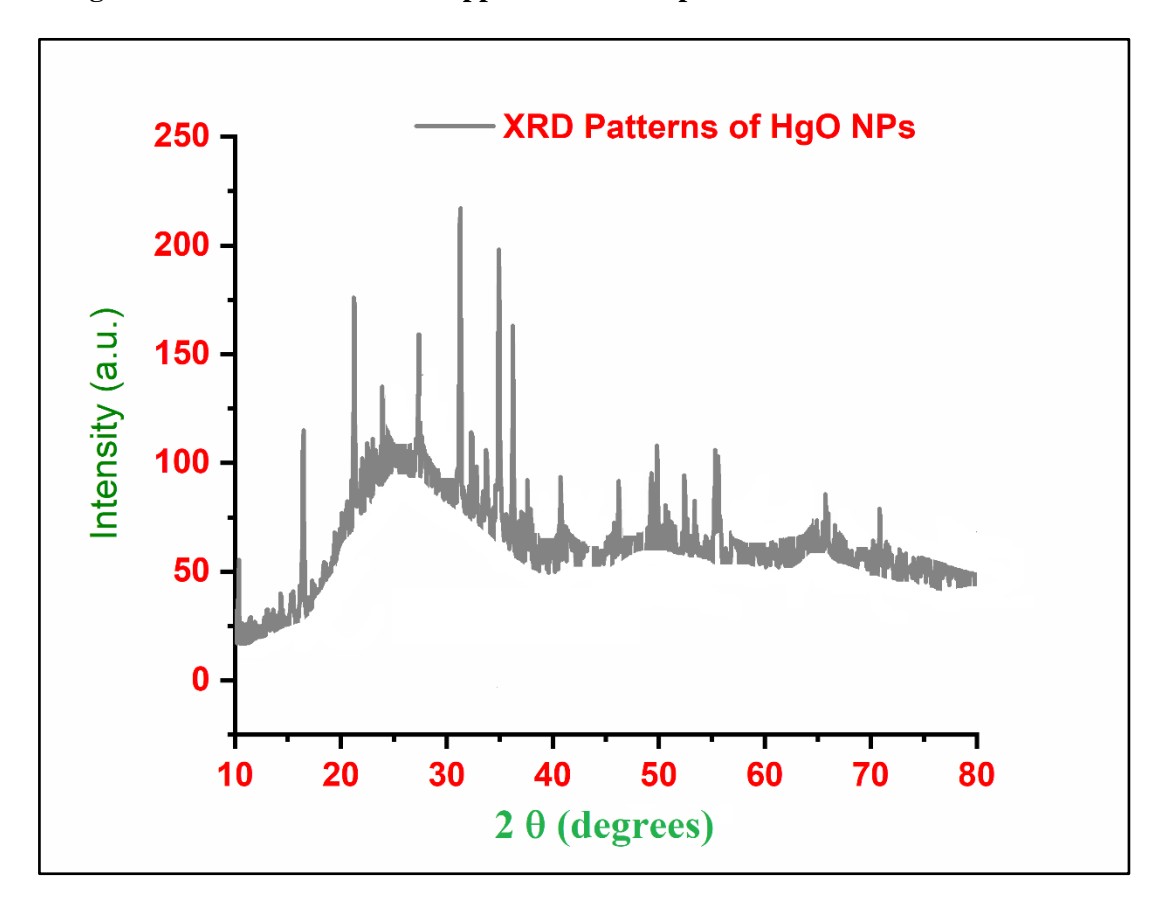


Figure 3.20: XRD Pattern of Mercury Oxide Nanoparticle obtained in Ch. Cl-U DES

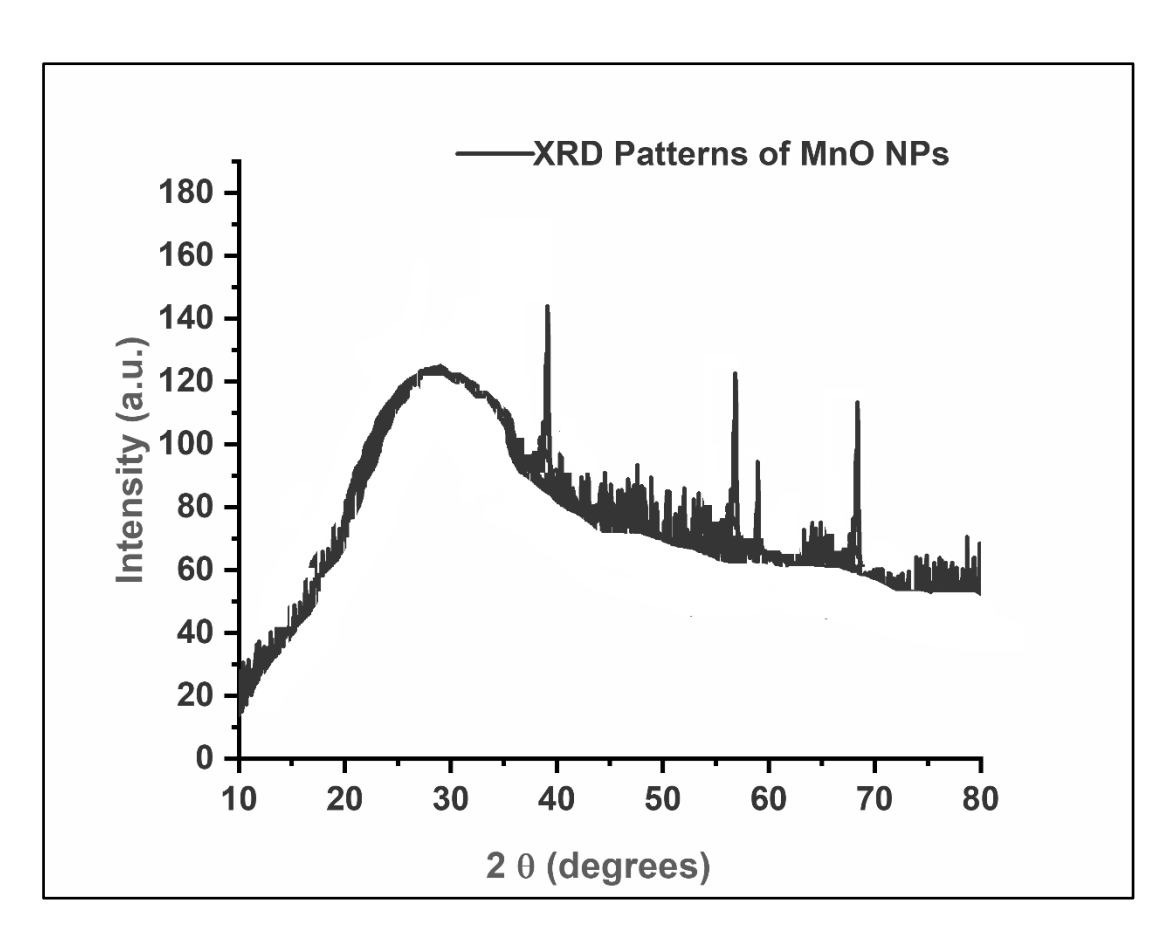


Figure 3.21: XRD Pattern of Manganese Oxide Nanoparticle obtained in Ch. Cl-U DES

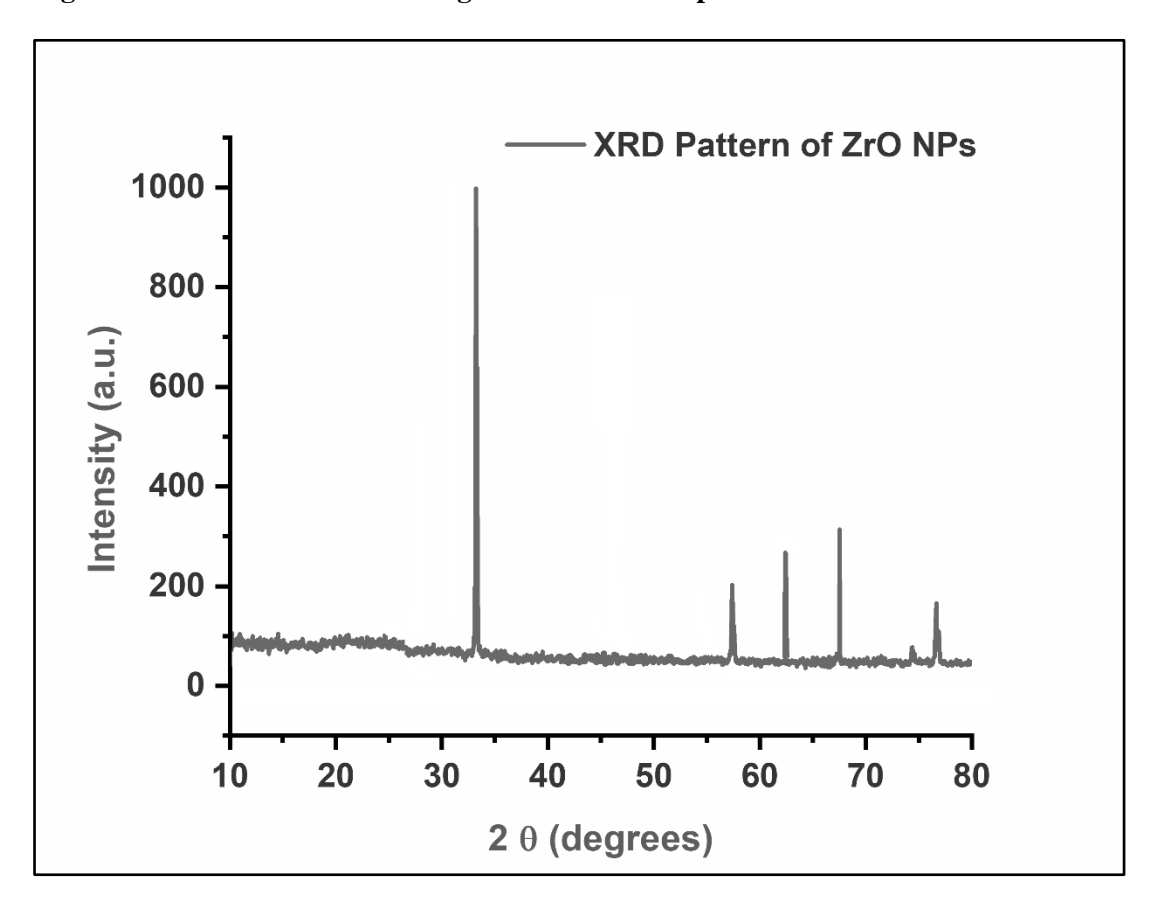


Figure 3.22: XRD Pattern of Zirconium Oxide Nanoparticle obtained in Ch. Cl-U DES

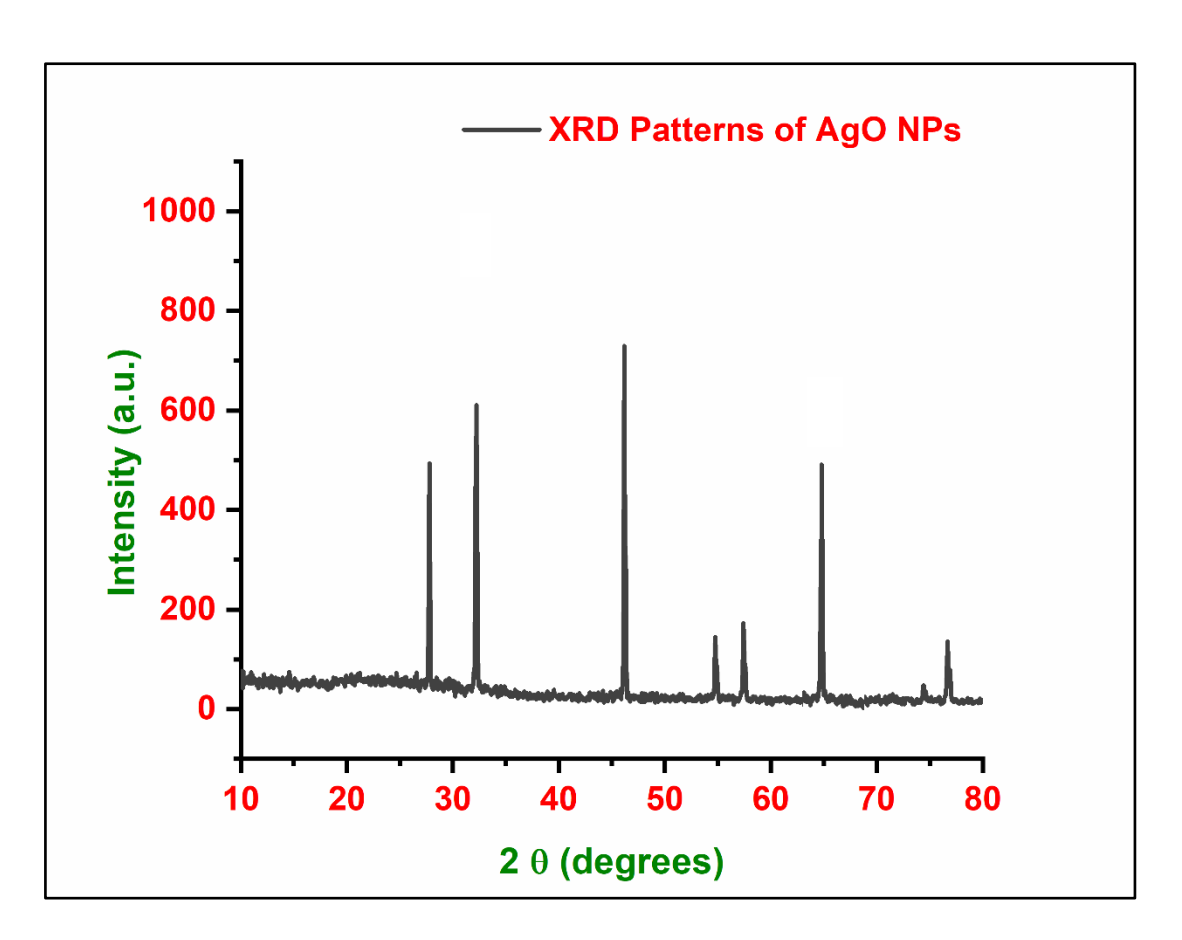


Figure 3.23: XRD Pattern of Silver Oxide Nanoparticle obtained in Ch. Cl-U DES

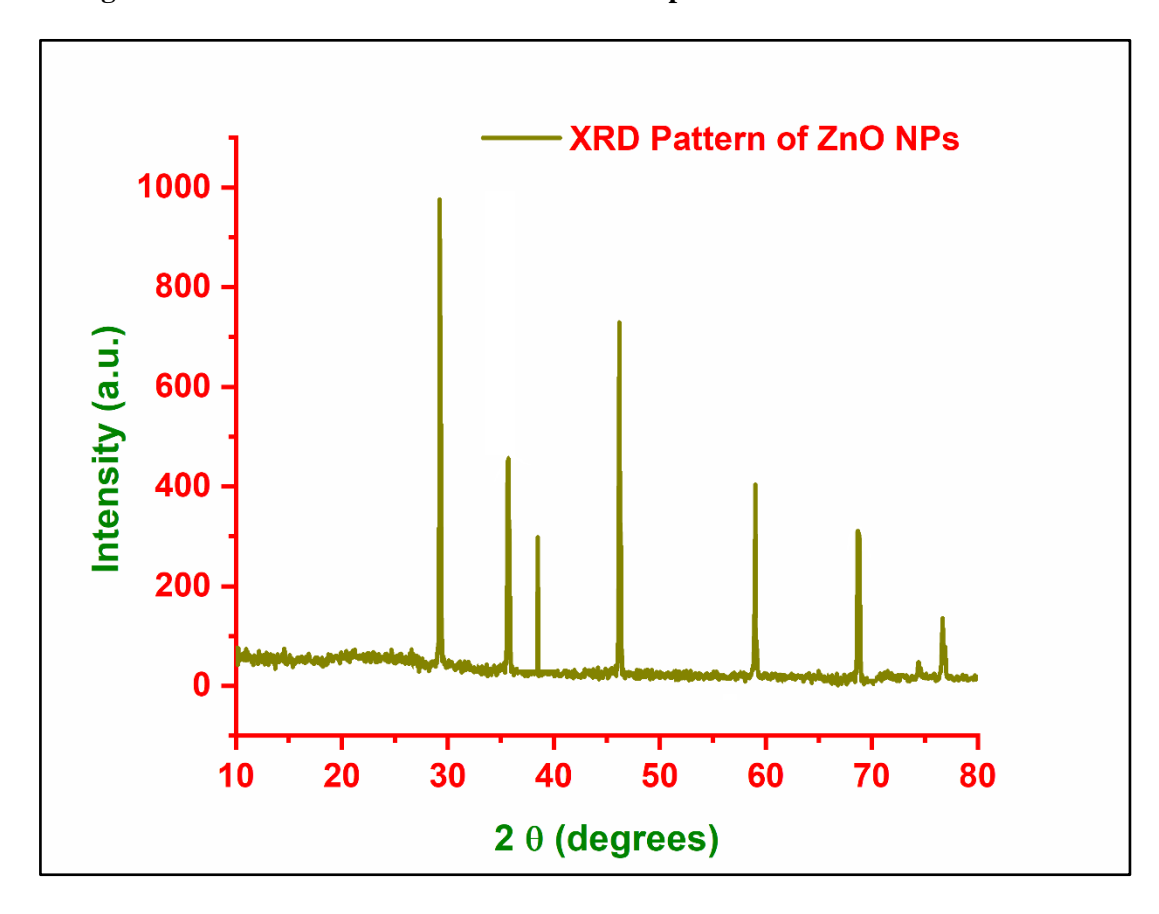


Figure 3.24: XRD Pattern of Zinc Oxide Nanoparticle obtained in Ch. Cl-U DES

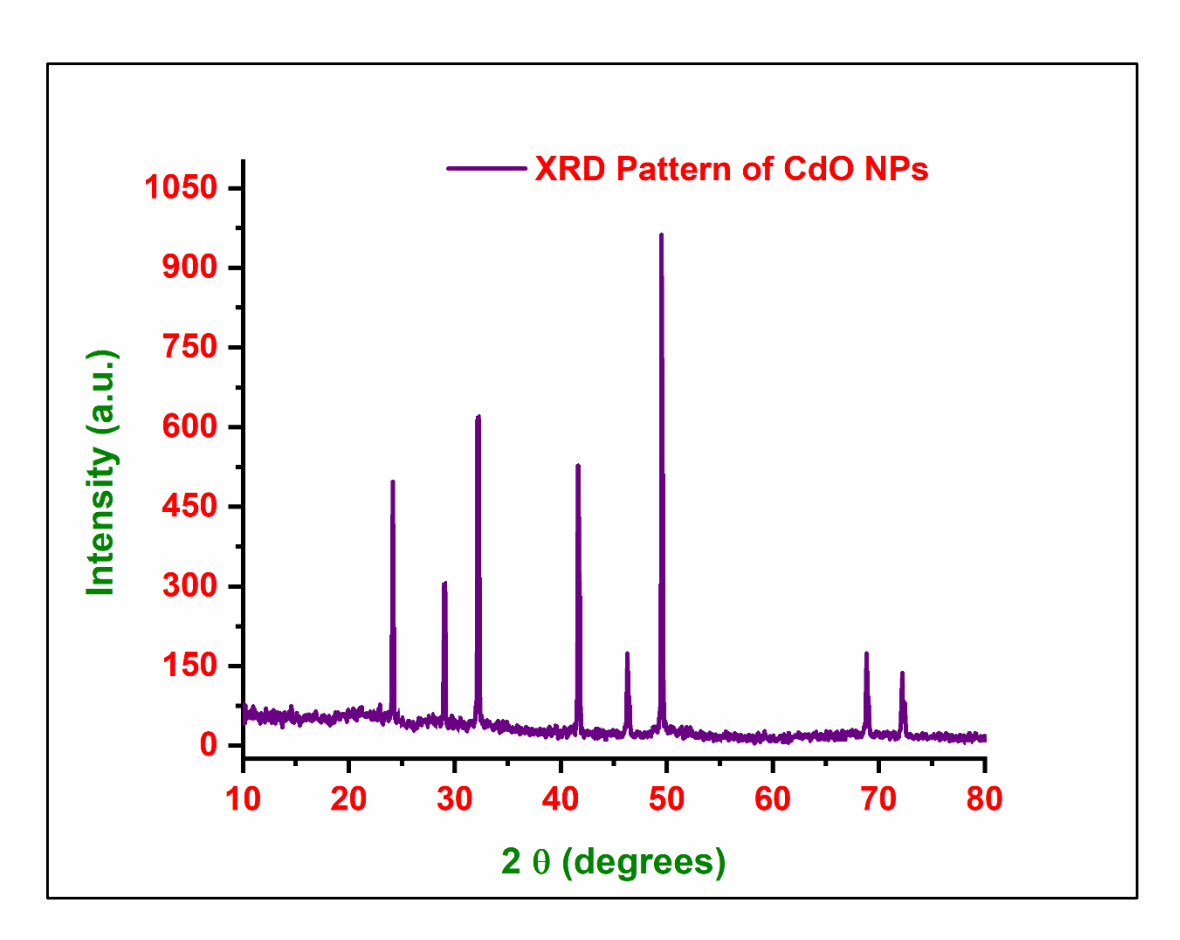


Figure 3.25: XRD Pattern of Cadmium Oxide Nanoparticle obtained in Ch. Cl-U DES

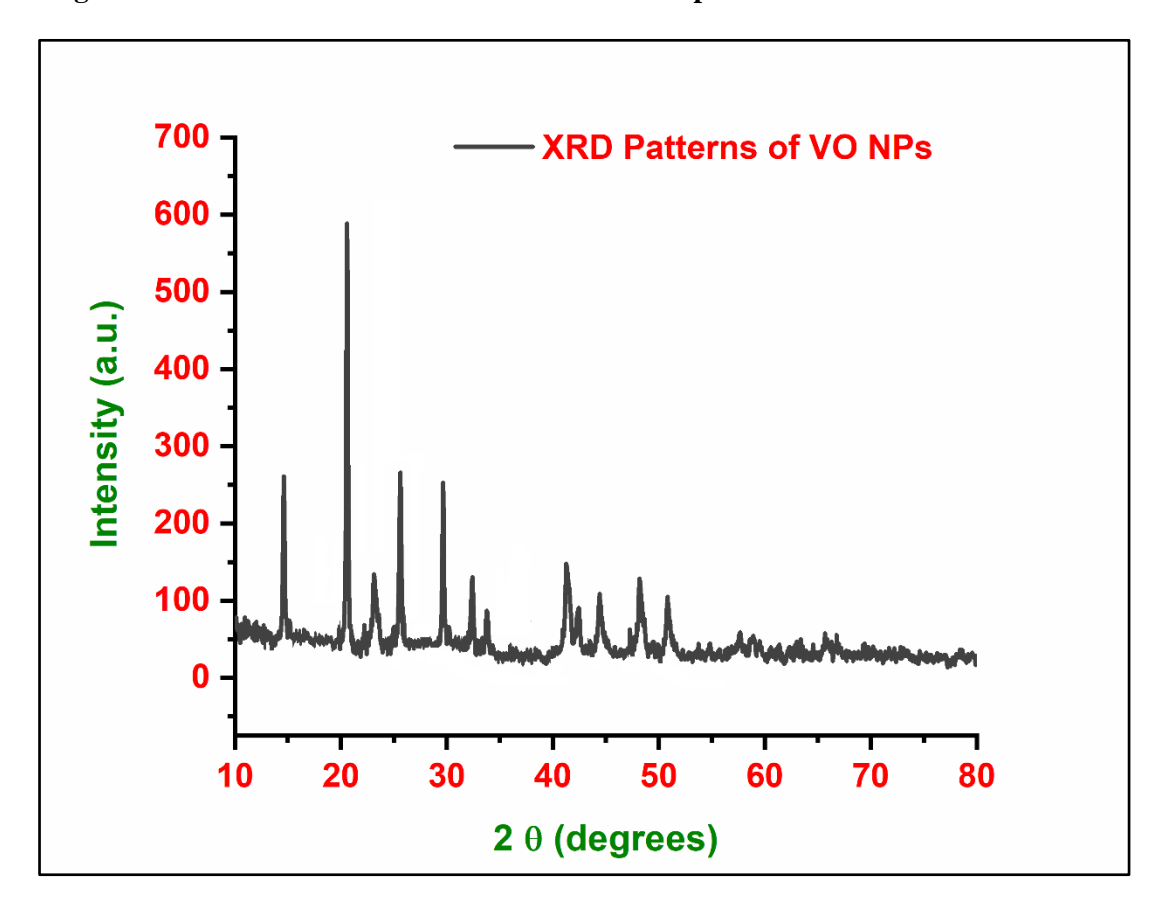


Figure 3.26: XRD Pattern of Vanadium Oxide Nanoparticle obtained in Ch. Cl-U DES

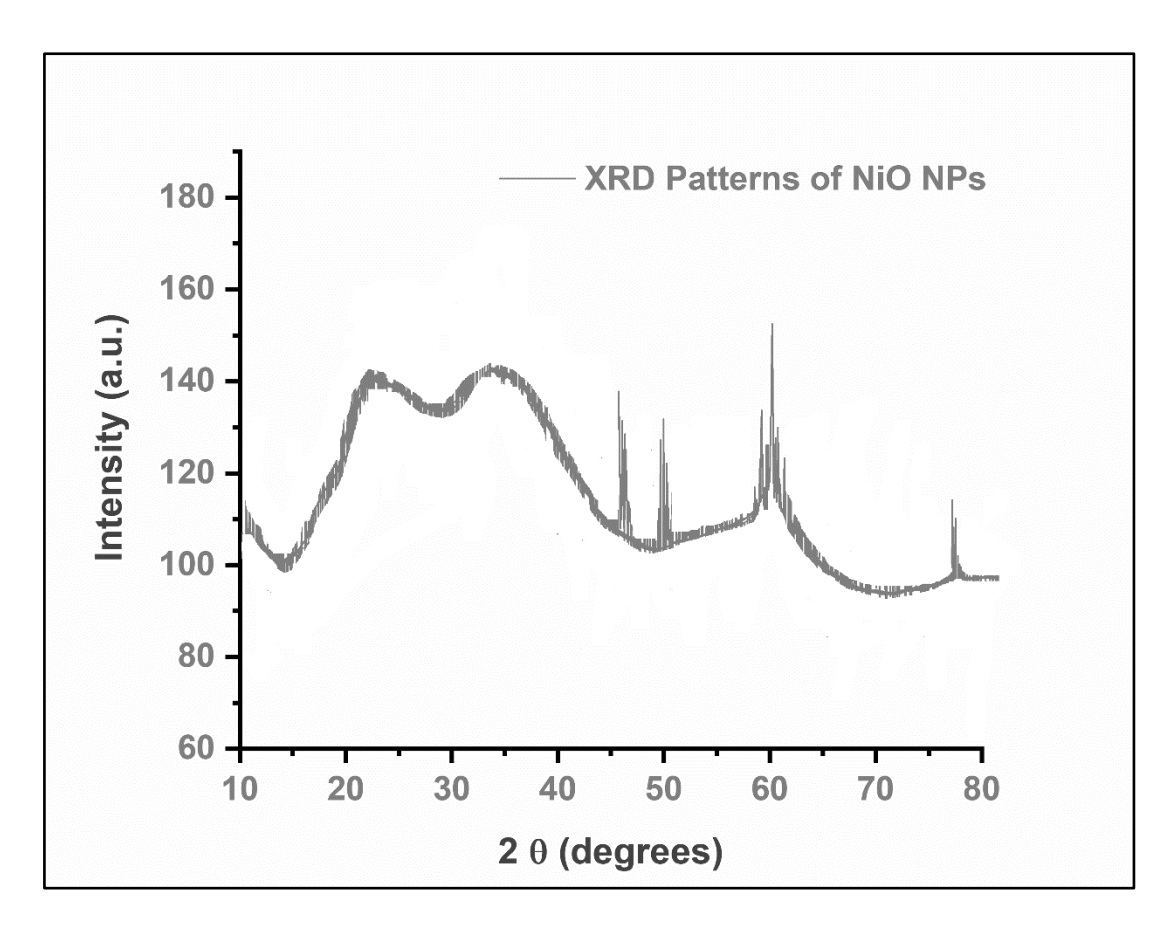


Figure 3.27: XRD Pattern of Nickel Oxide Nanoparticle obtained in Ch. Cl-U DES

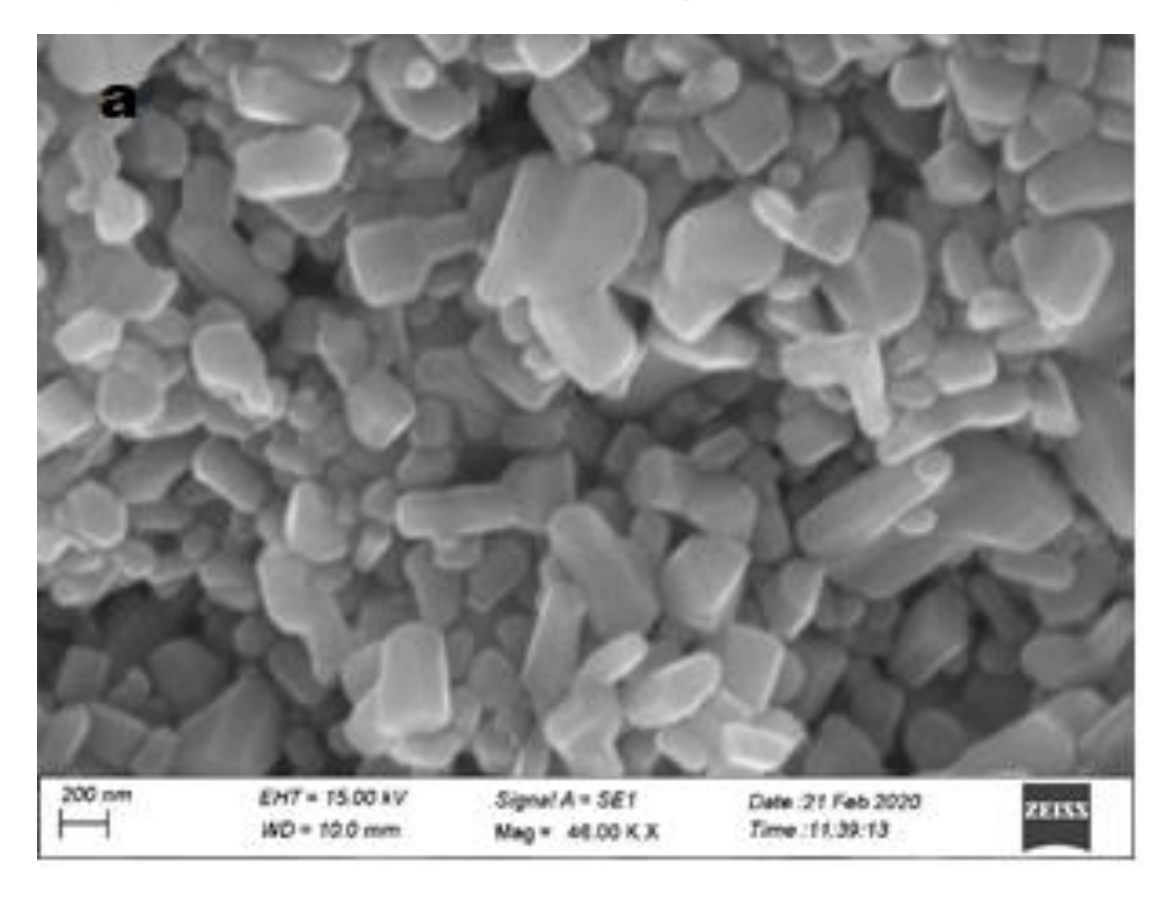


Figure 3.28: SEM Image of Copper Oxide Nanoparticle obtained in Ch. Cl-U DES

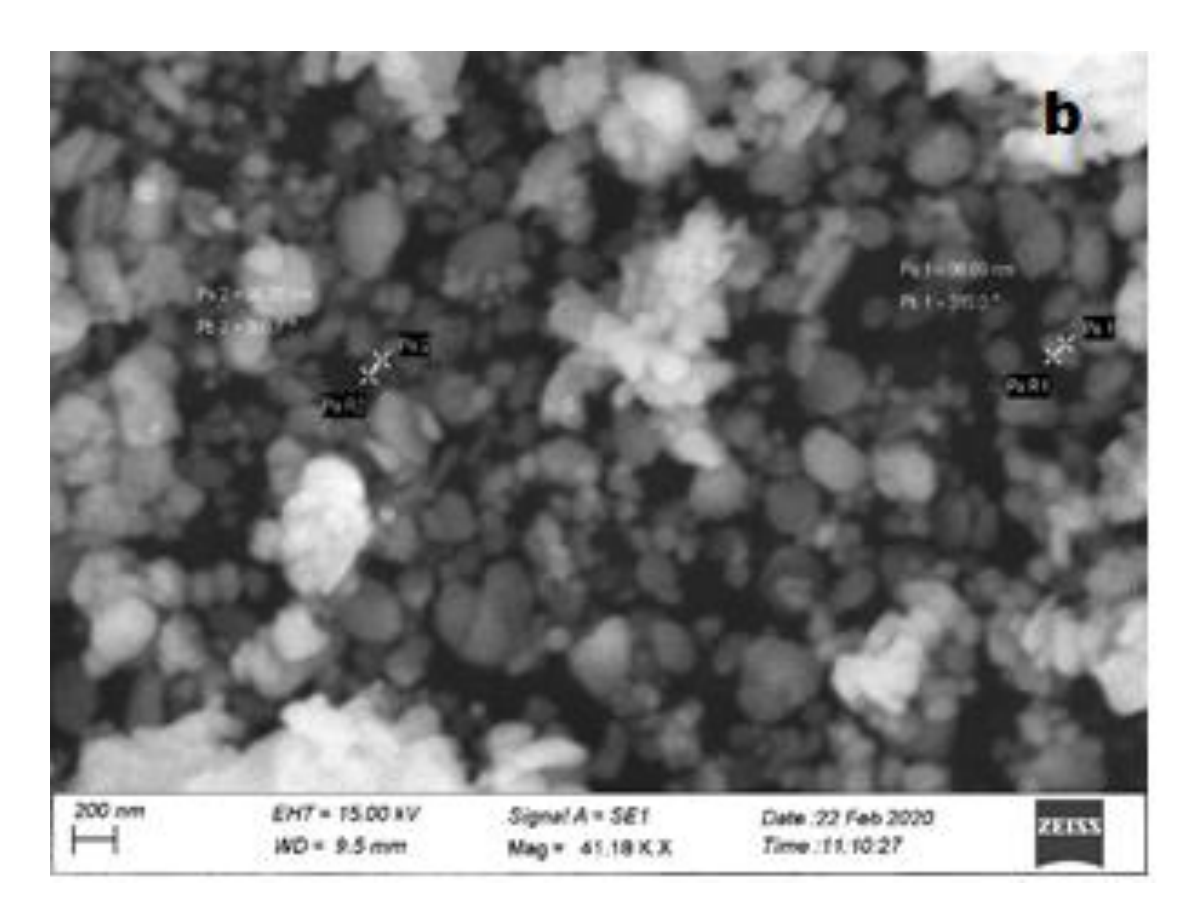


Figure 3.29: SEM Image of Mercury Oxide Nanoparticle obtained in Ch. Cl-U DES

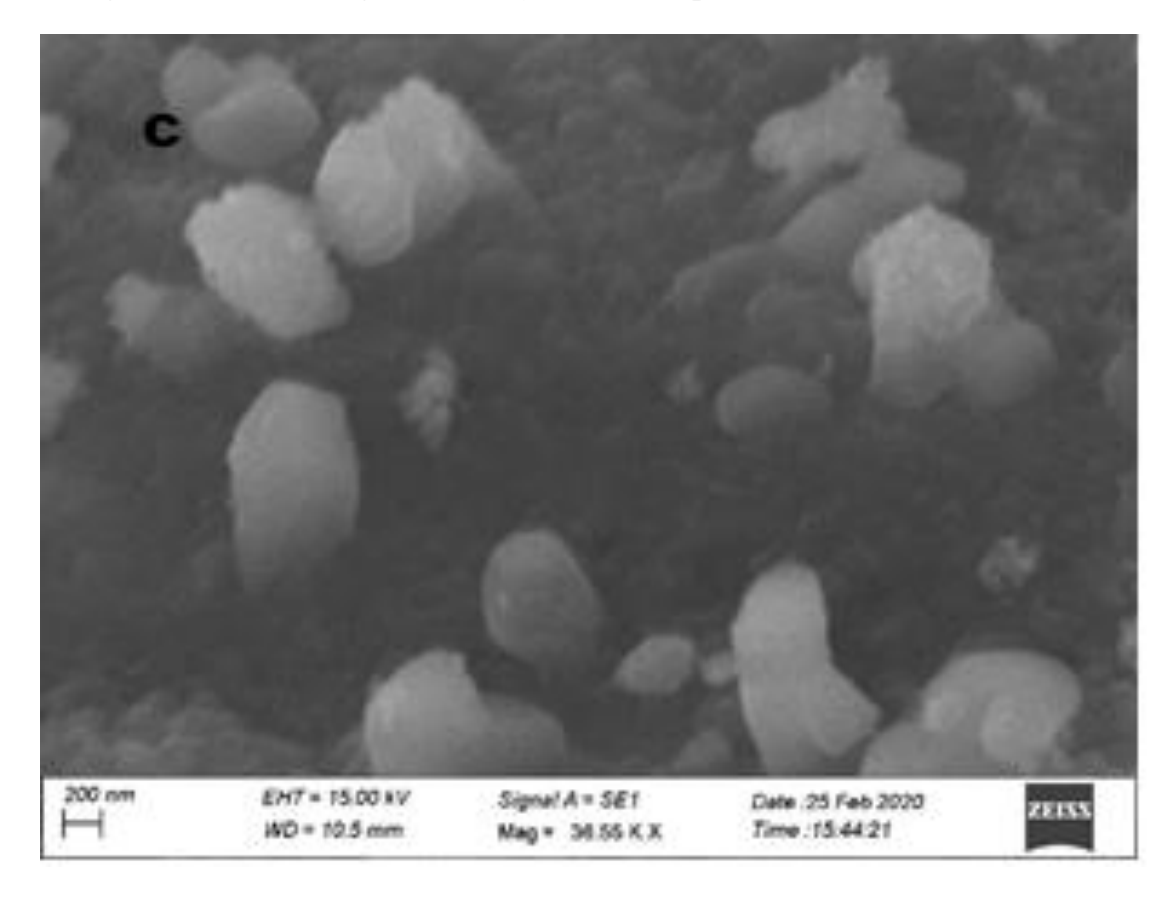


Figure 3.30: SEM Image of Manganese Oxide Nanoparticle obtained in Ch. Cl-U DES

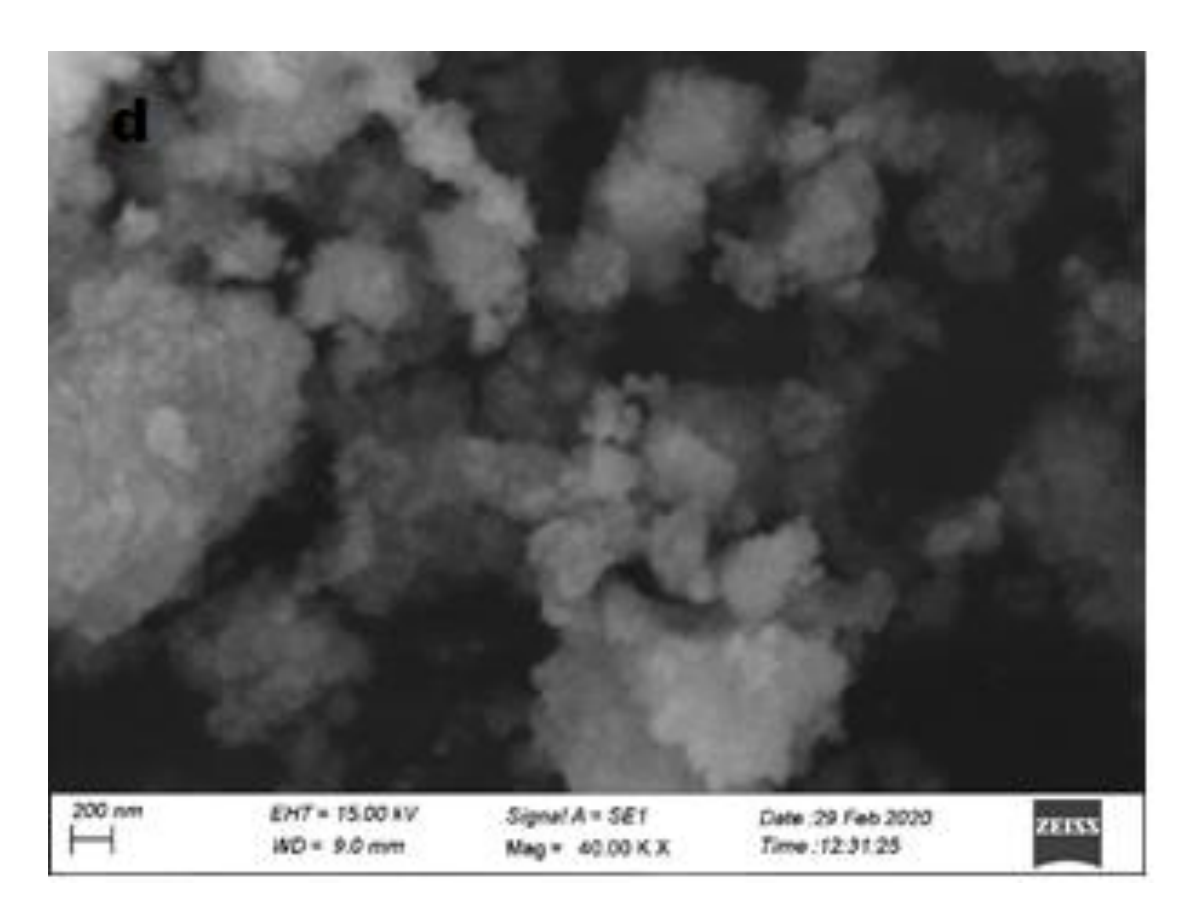


Figure 3.31: SEM Image of Zirconium Oxide Nanoparticle obtained in Ch. Cl-U DES

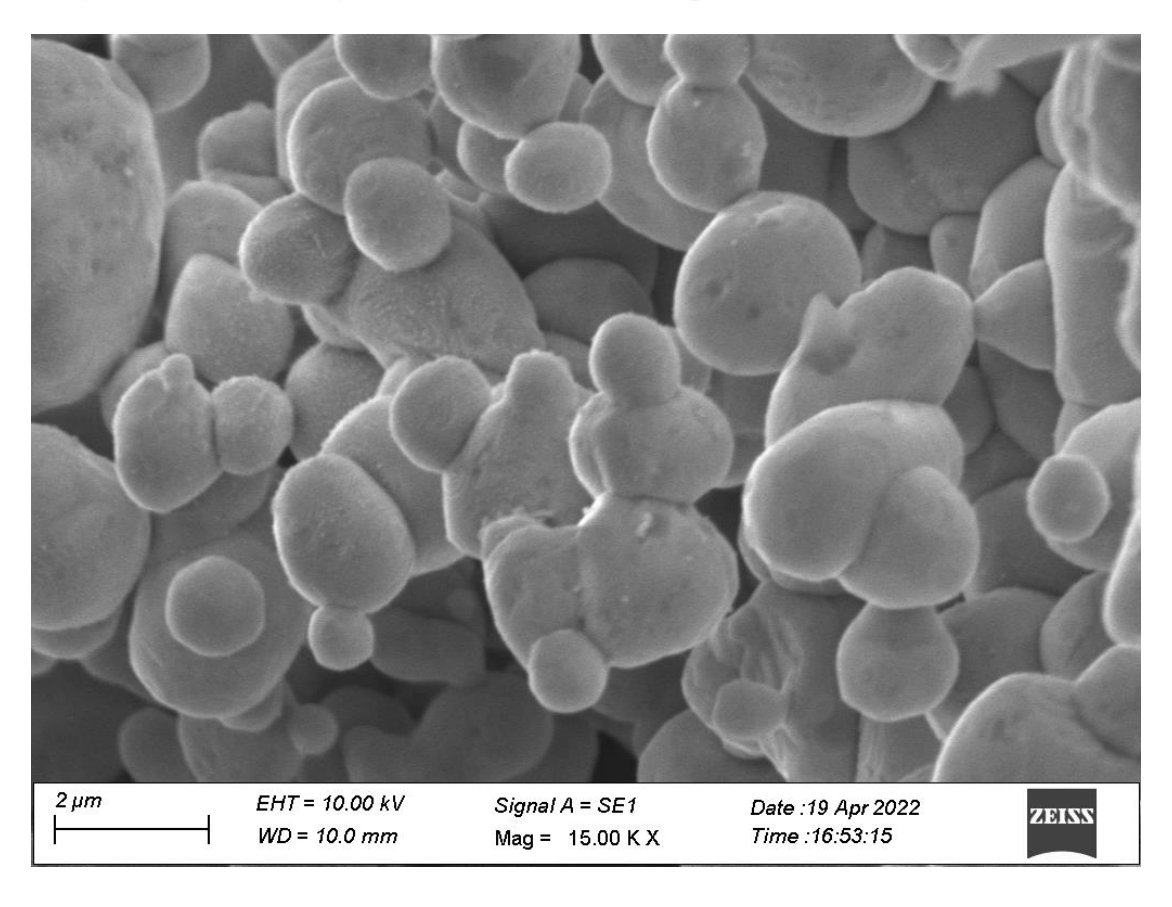


Figure 3.32: SEM Image of Silver Oxide Nanoparticle obtained in Ch. Cl-U DES

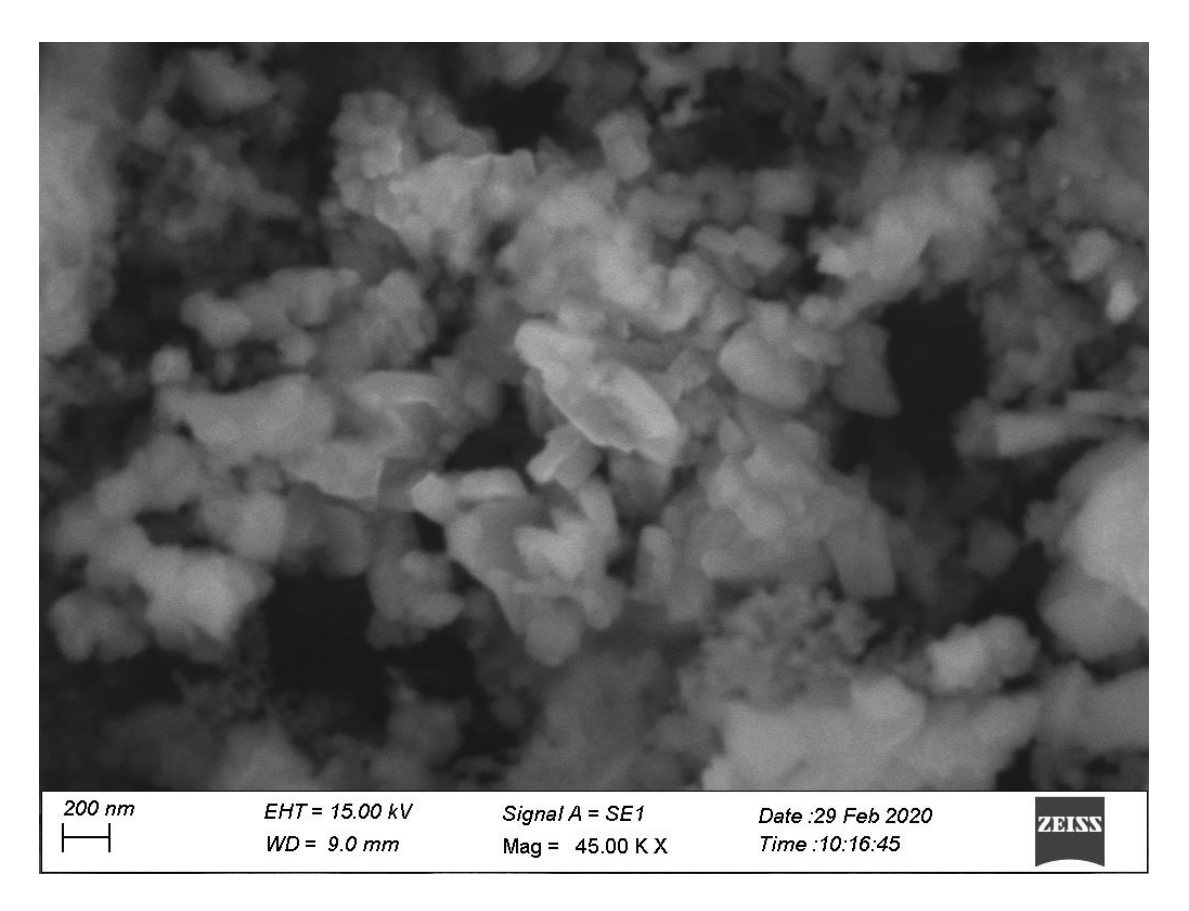


Figure 3.33: SEM Image of Zinc Oxide Nanoparticle obtained in Ch. Cl-U DES

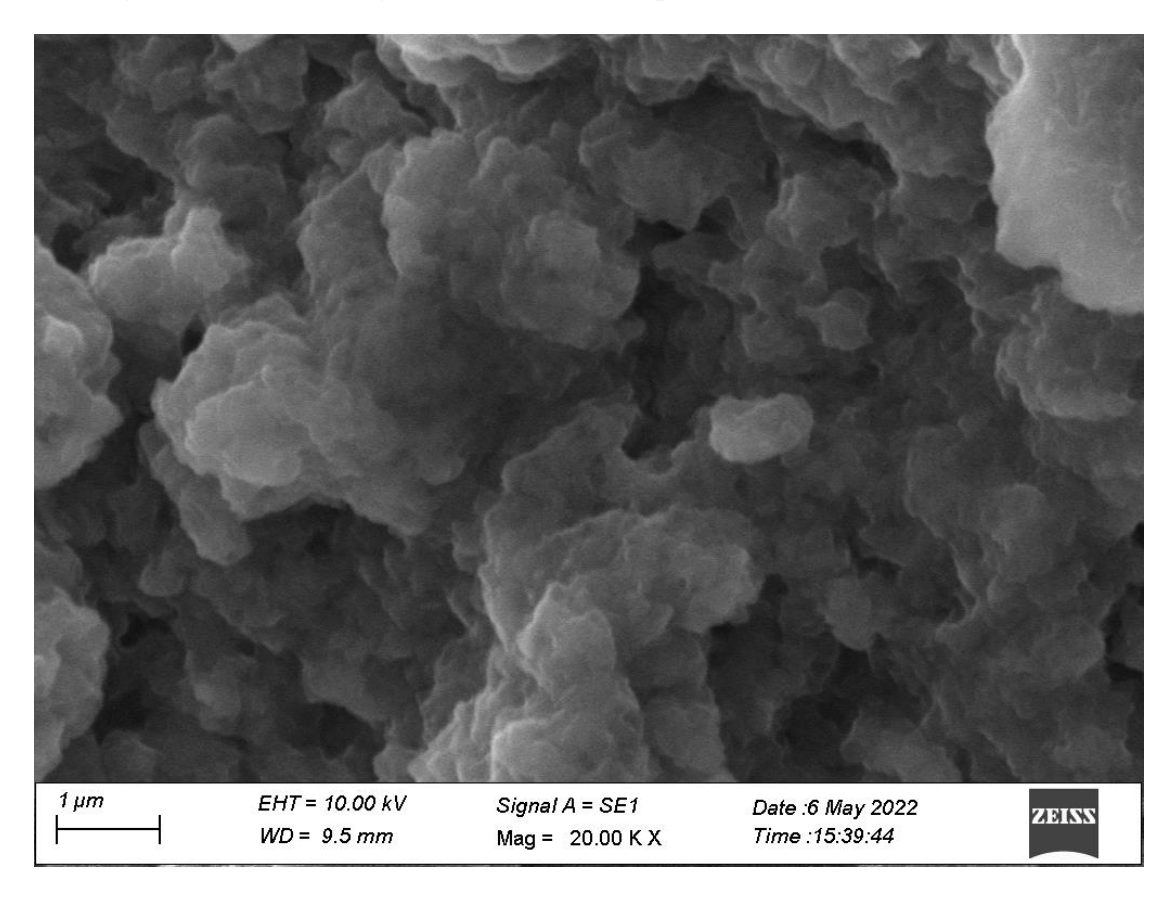


Figure 3.34: SEM Image of Cadmium Oxide Nanoparticle obtained in Ch. Cl-U DES

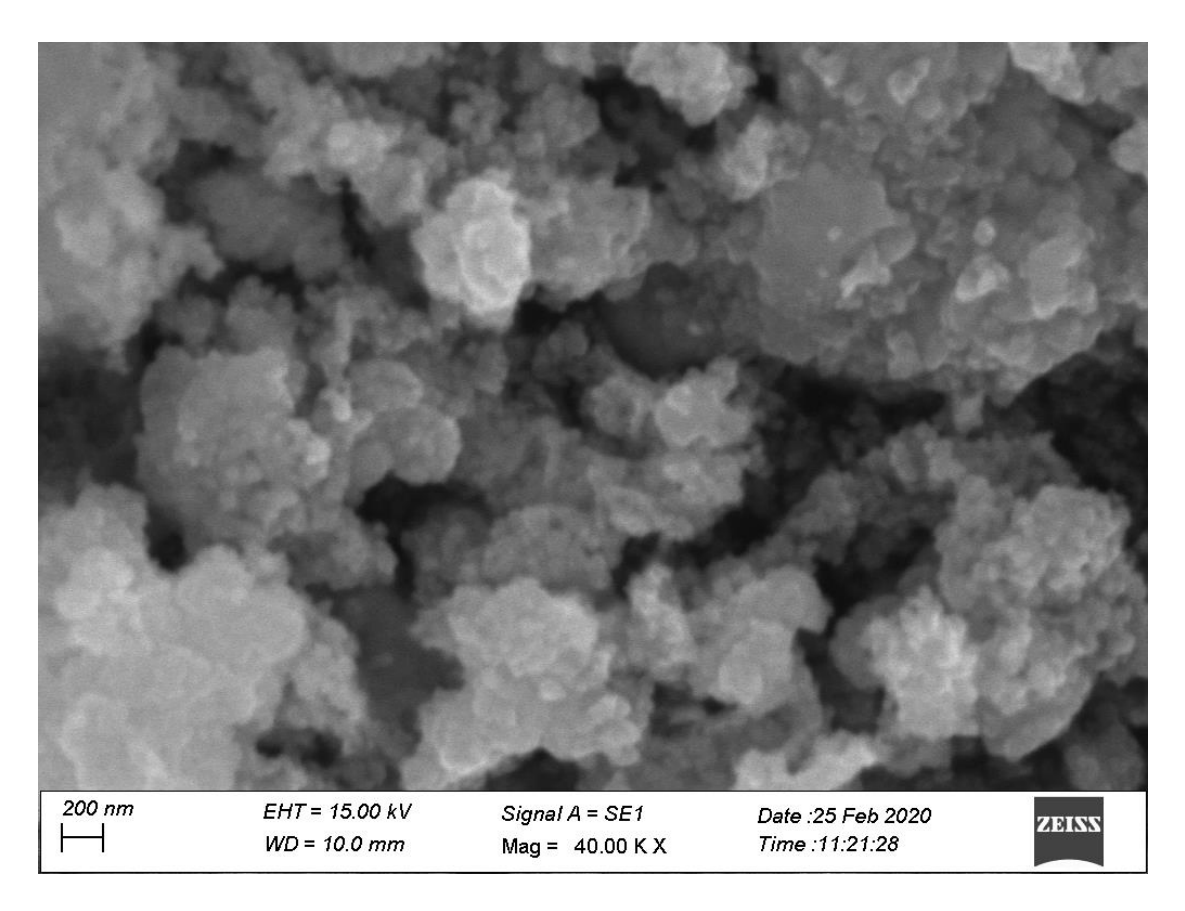


Figure 3.35: SEM Image of Vanadium Oxide Nanoparticle obtained in Ch. Cl-U DES

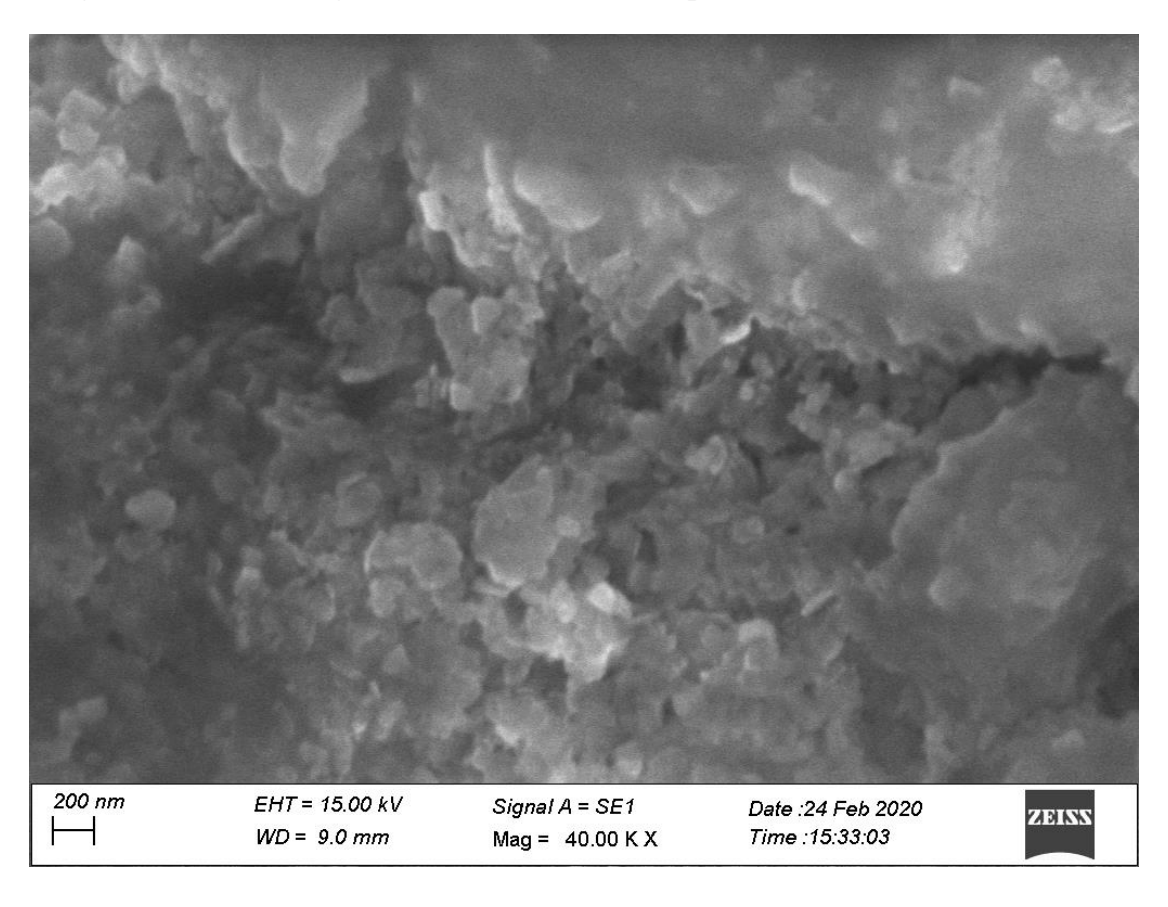


Figure 3.36: SEM Image of Nickel Oxide Nanoparticle obtained in Ch. Cl-U DES

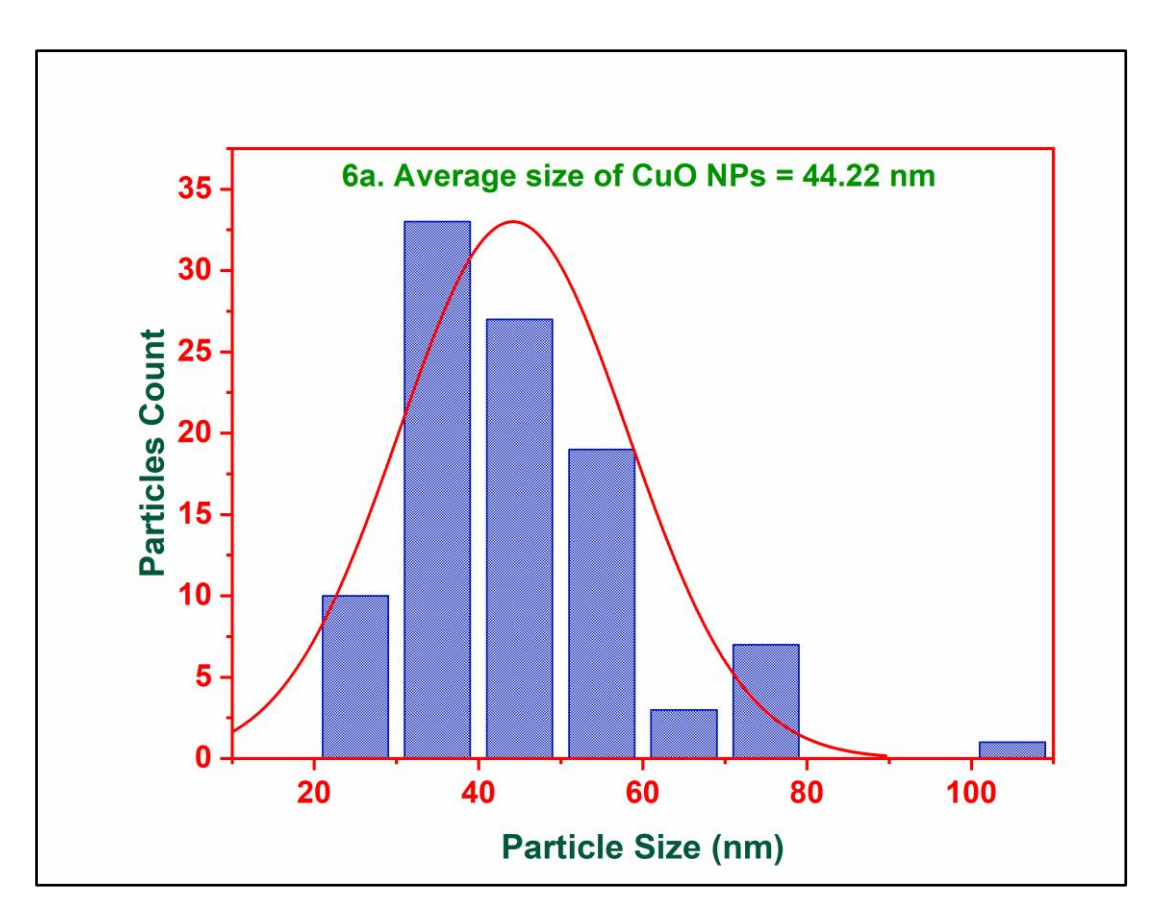


Figure 3.37: SEM Histogram of Copper Oxide Nanoparticle obtained in Ch. Cl-U DES

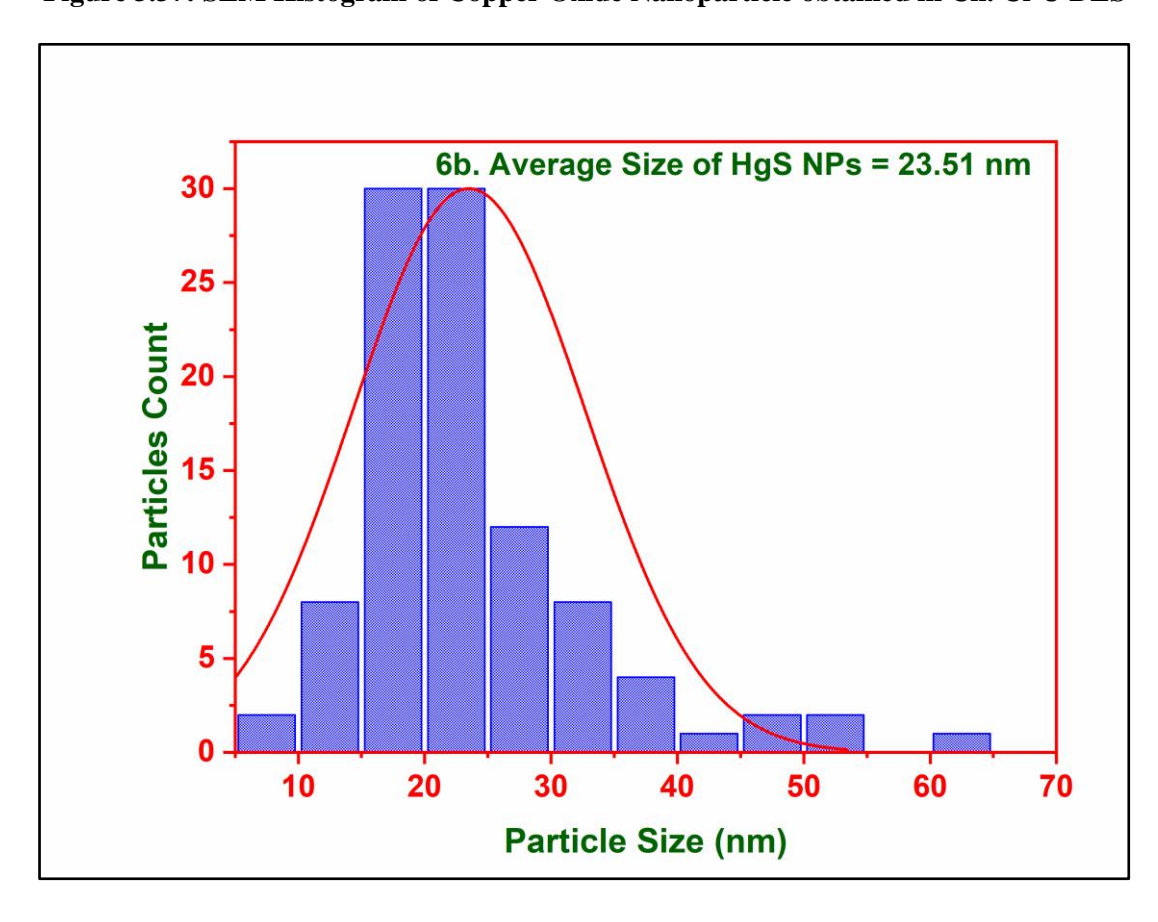


Figure 3.38: SEM Histogram of Mercury Oxide Nanoparticle obtained in Ch. Cl-U DES

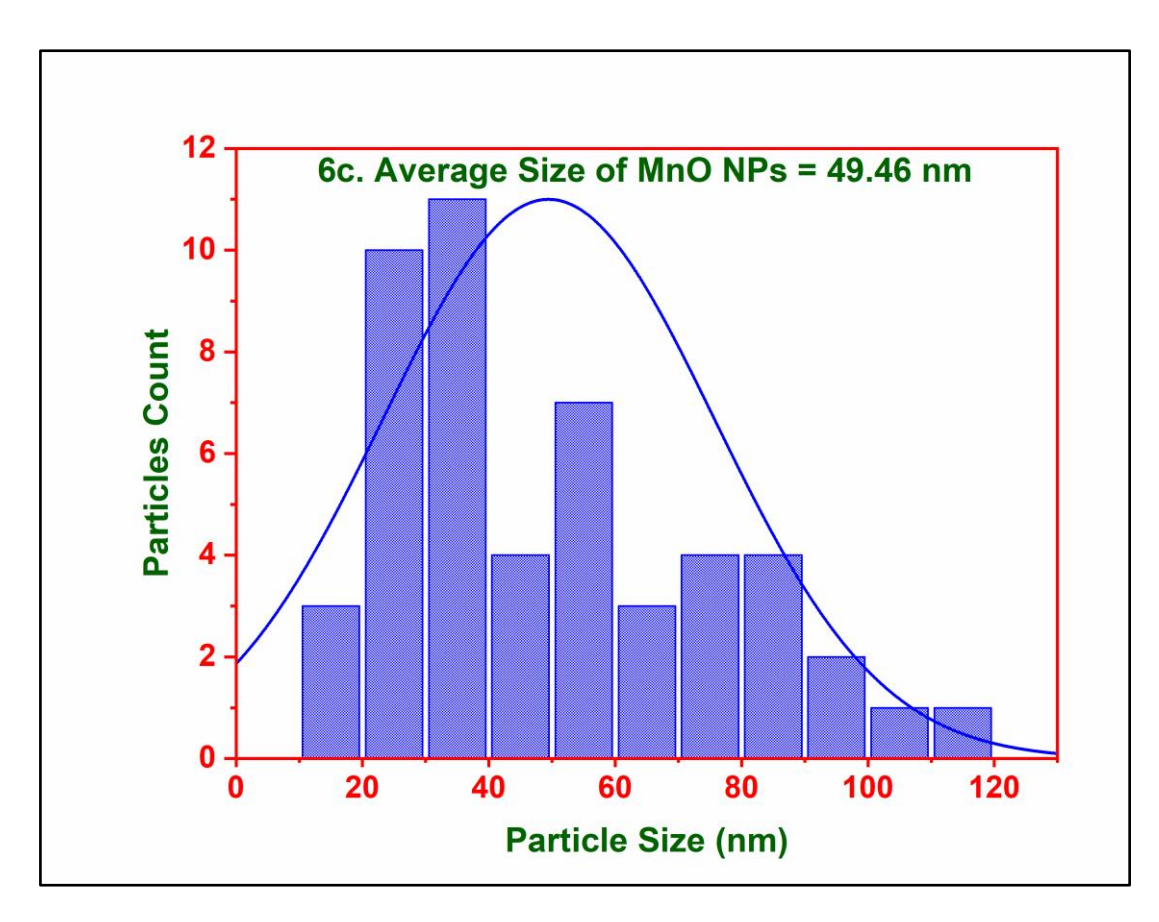


Figure 3.39: SEM Histogram of Manganese Oxide Nanoparticle obtained in Ch. Cl-U DES

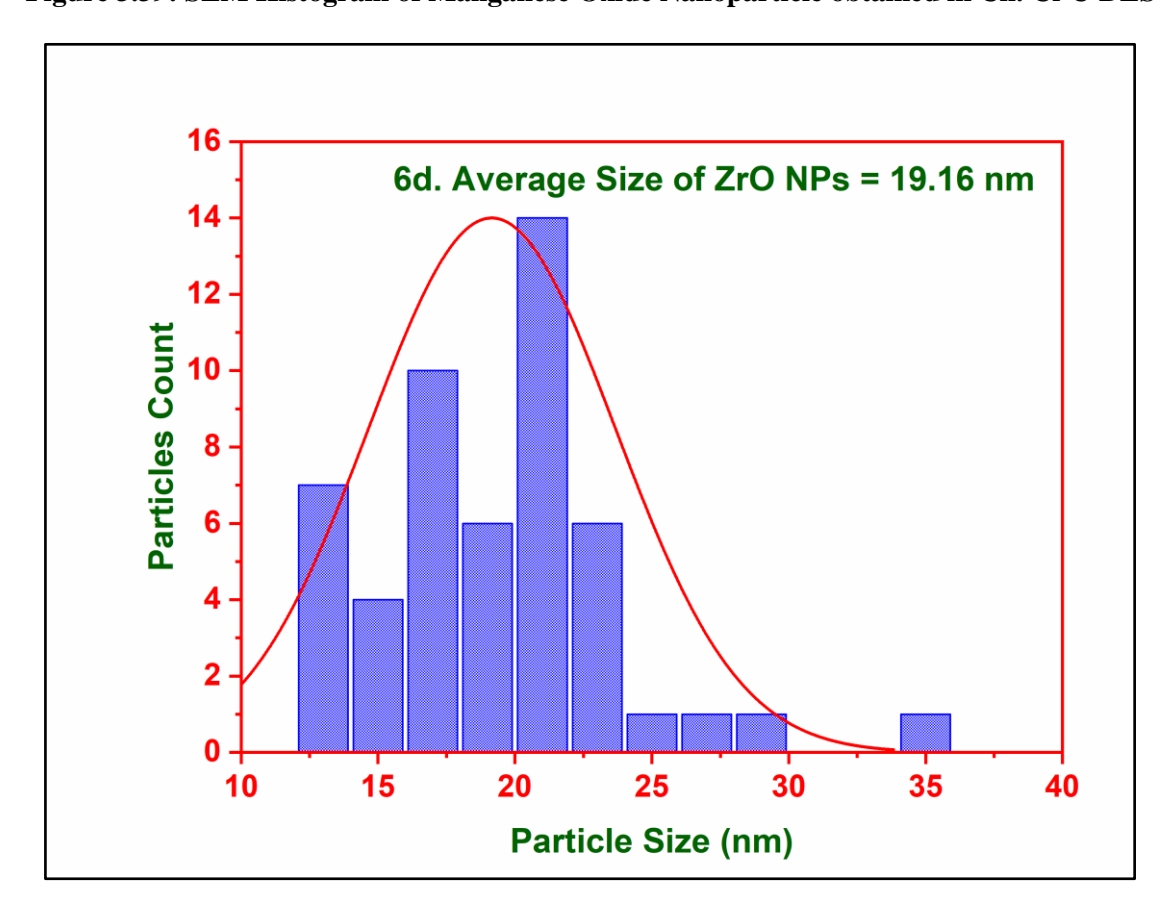


Figure 3.40: SEM Histogram of Zirconium Oxide Nanoparticle obtained in Ch. Cl-U DES

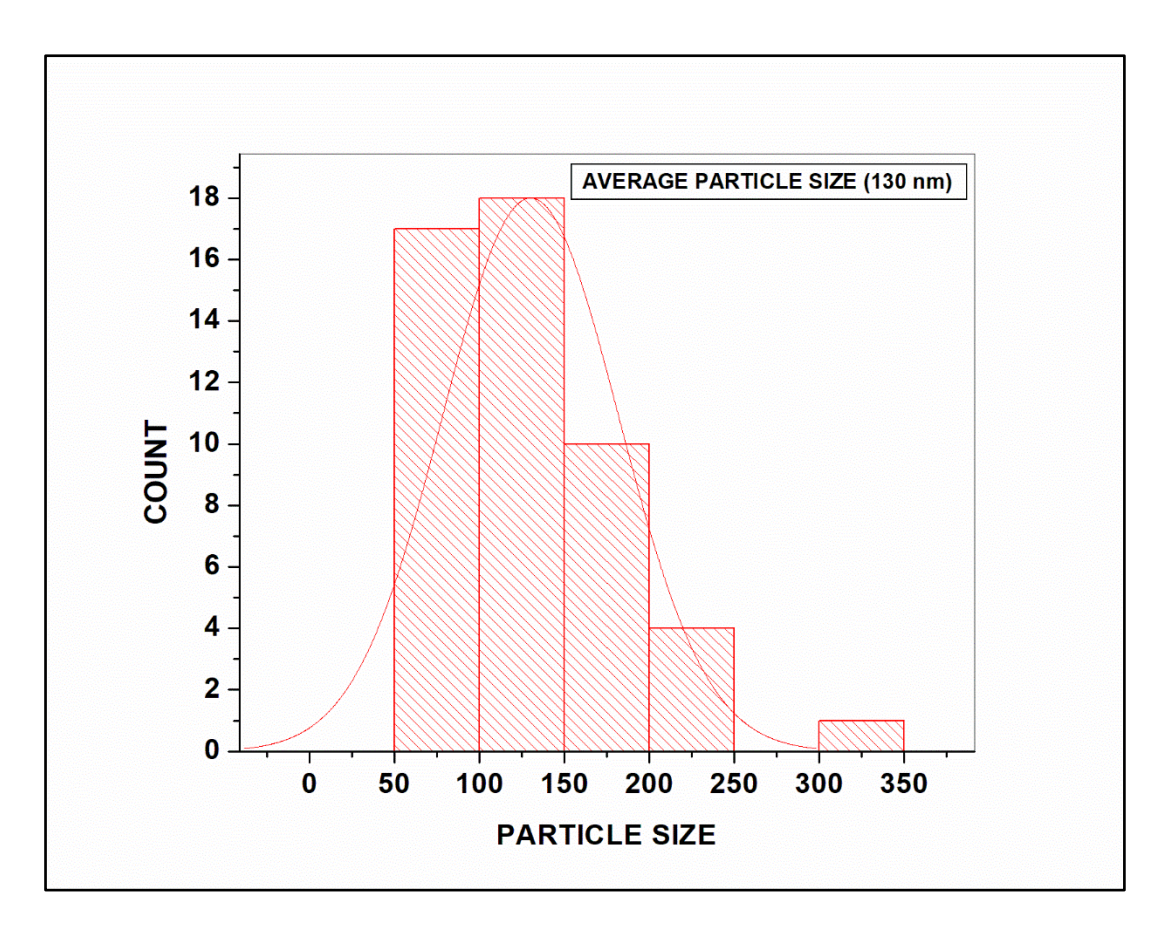


Figure 3.41: SEM Histogram of Silver Oxide Nanoparticle obtained in Ch. Cl-U DES

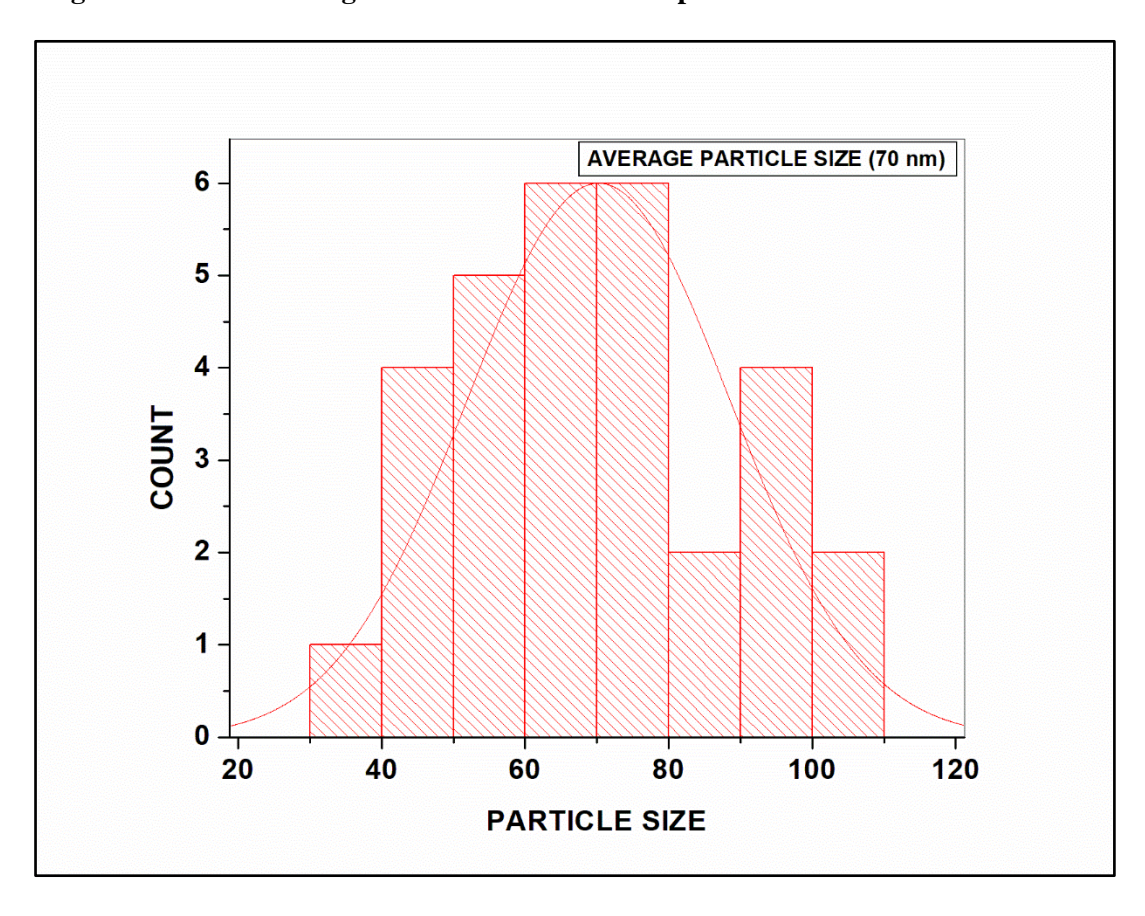


Figure 3.42: SEM Histogram of Zinc Oxide Nanoparticle obtained in Ch. Cl-U DES

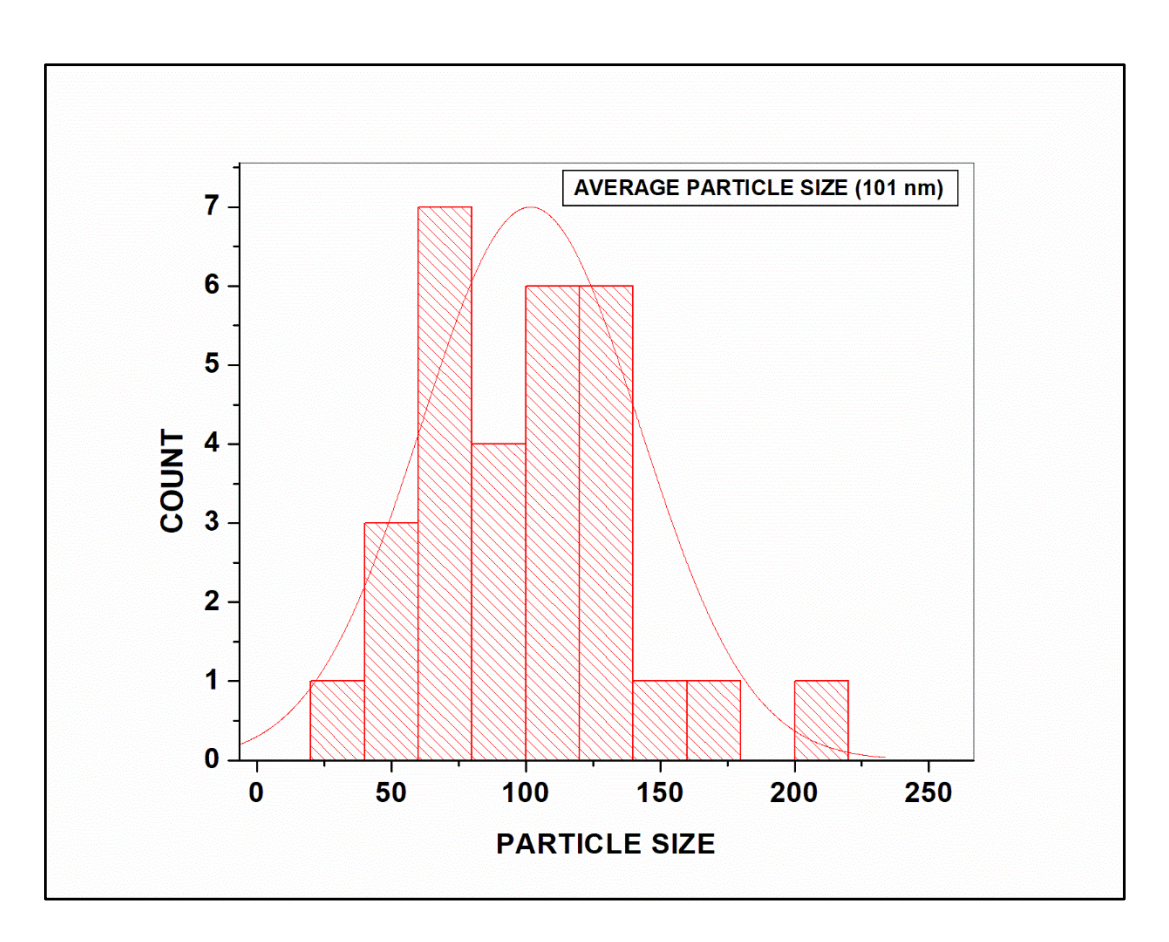


Figure 3.43: SEM Histogram of Cadmium Oxide Nanoparticle obtained in Ch. Cl-U DES

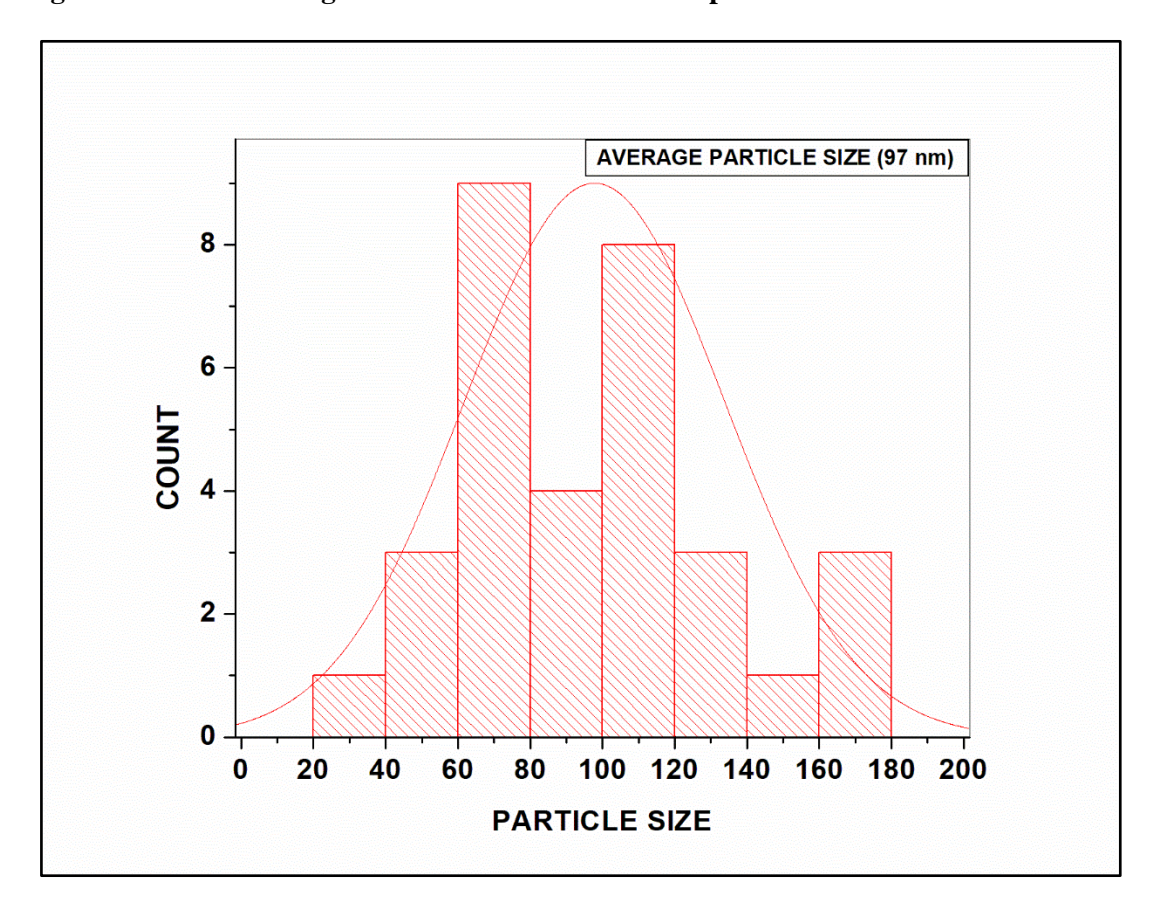


Figure 3.44: SEM Histogram of Vanadium Oxide Nanoparticle obtained in Ch. Cl-U DES

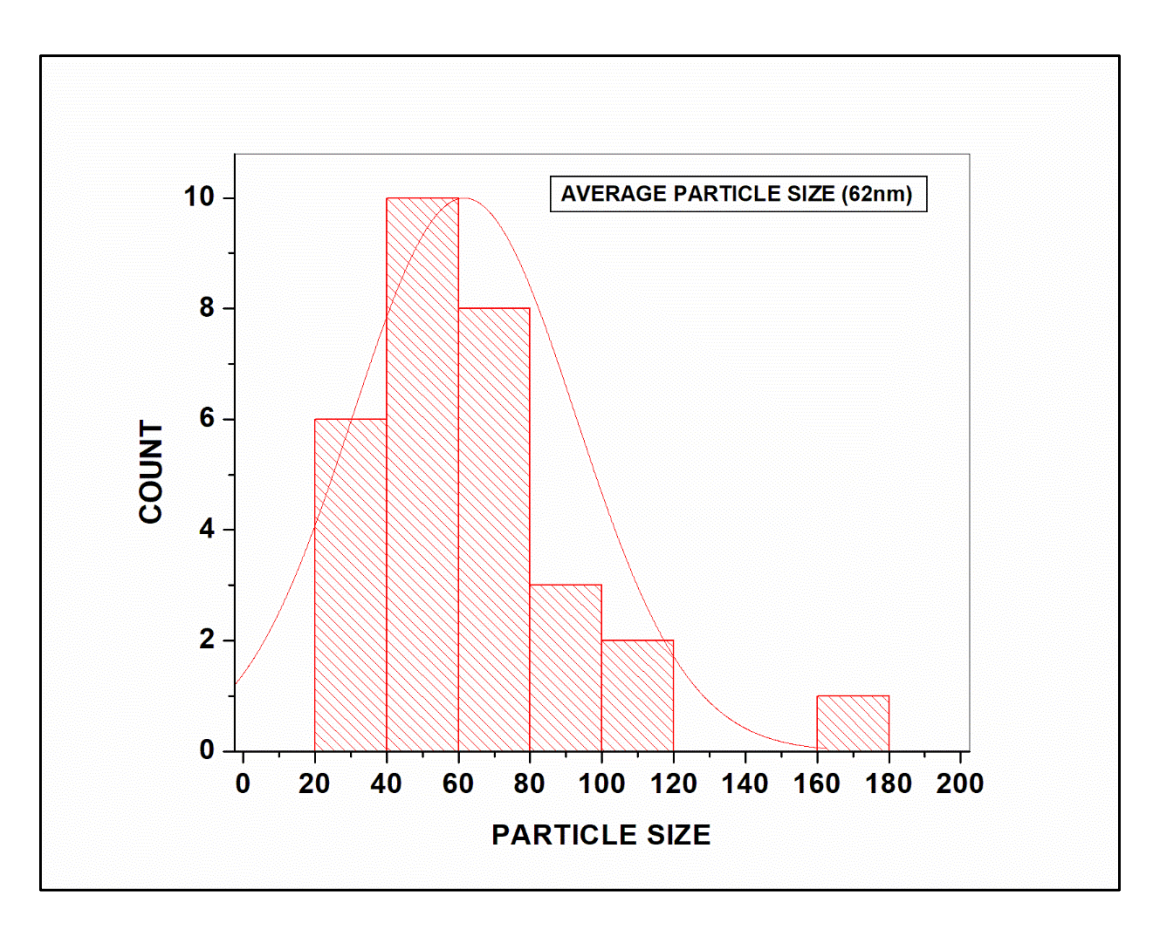


Figure 3.45: SEM Histogram of Nickel Oxide Nanoparticle obtained in Ch. Cl-U DES

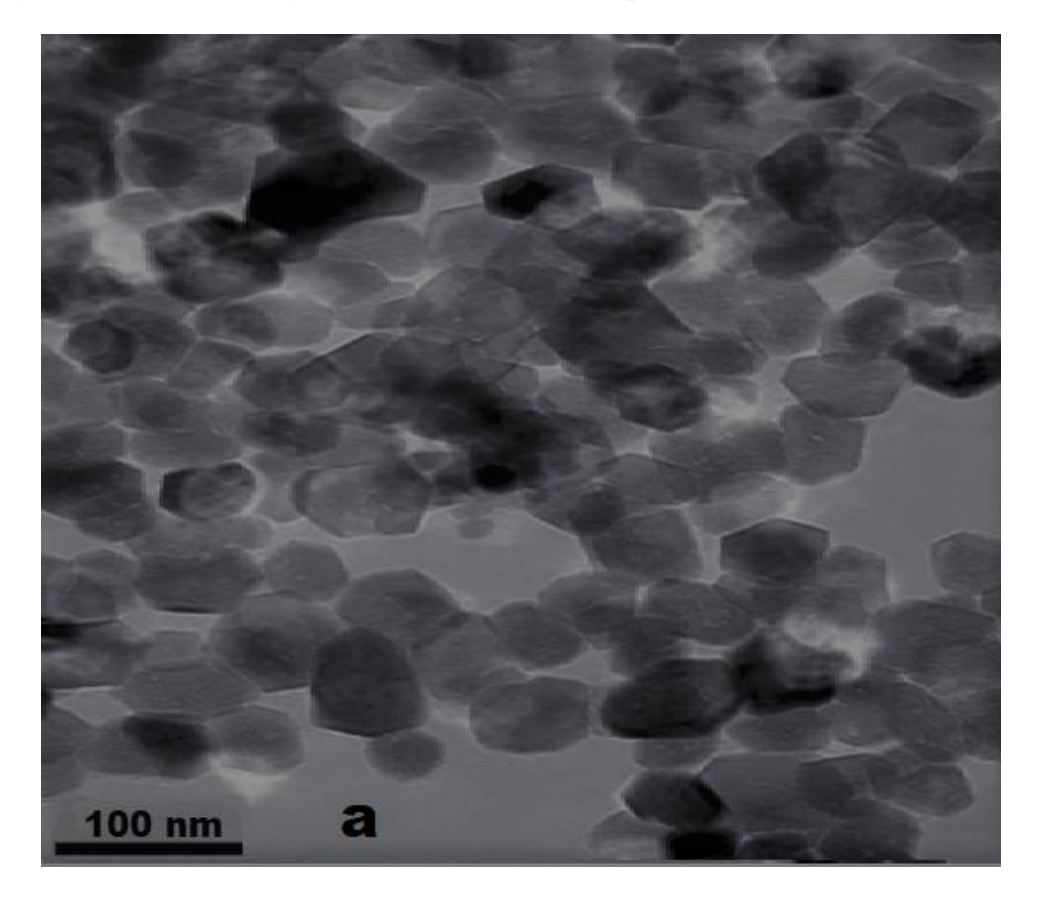


Figure 3.46: TEM Image of Copper Oxide Nanoparticle obtained in Ch. Cl-U DES

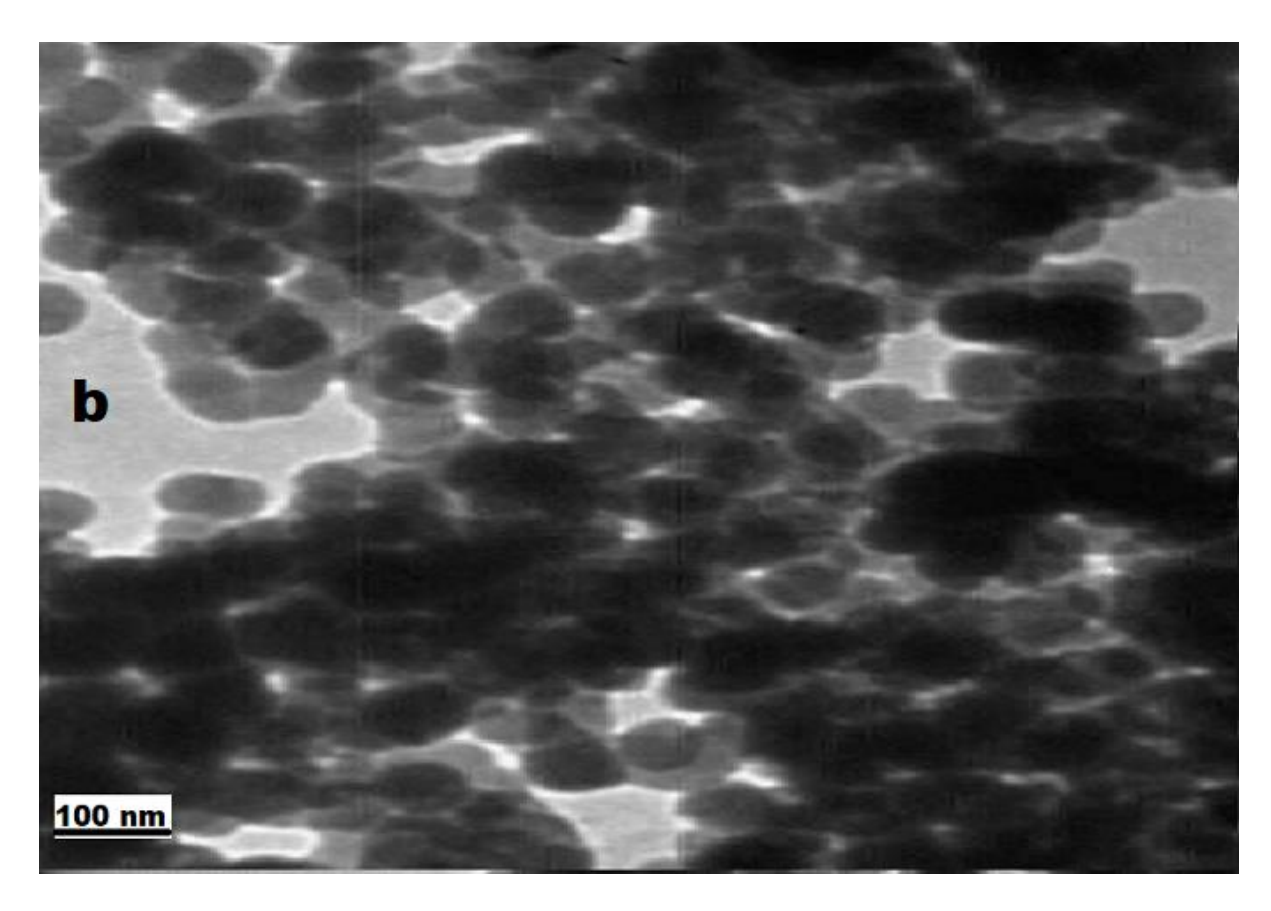


Figure 3.47: TEM Image of Mercury Oxide Nanoparticle obtained in Ch. Cl-U DES

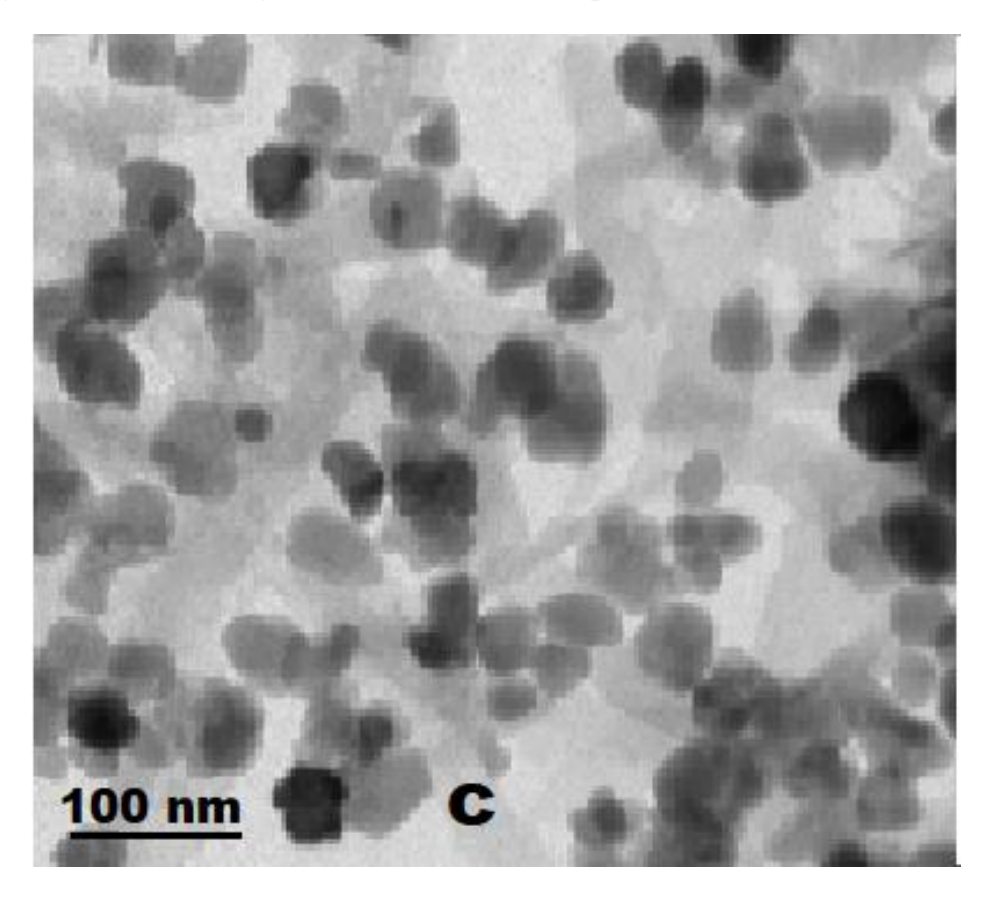


Figure 3.48: TEM Image of Manganese Oxide Nanoparticle obtained in Ch. Cl-U DES

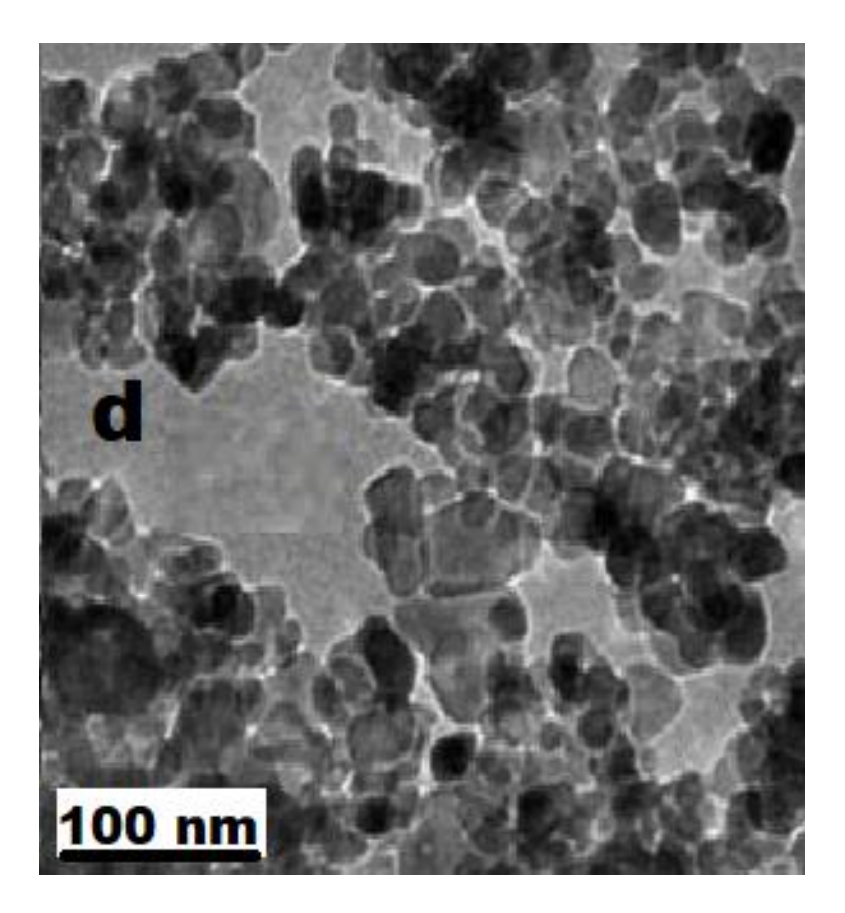


Figure 3.49: TEM Image of Zirconium Oxide Nanoparticle obtained in Ch. Cl-U DES

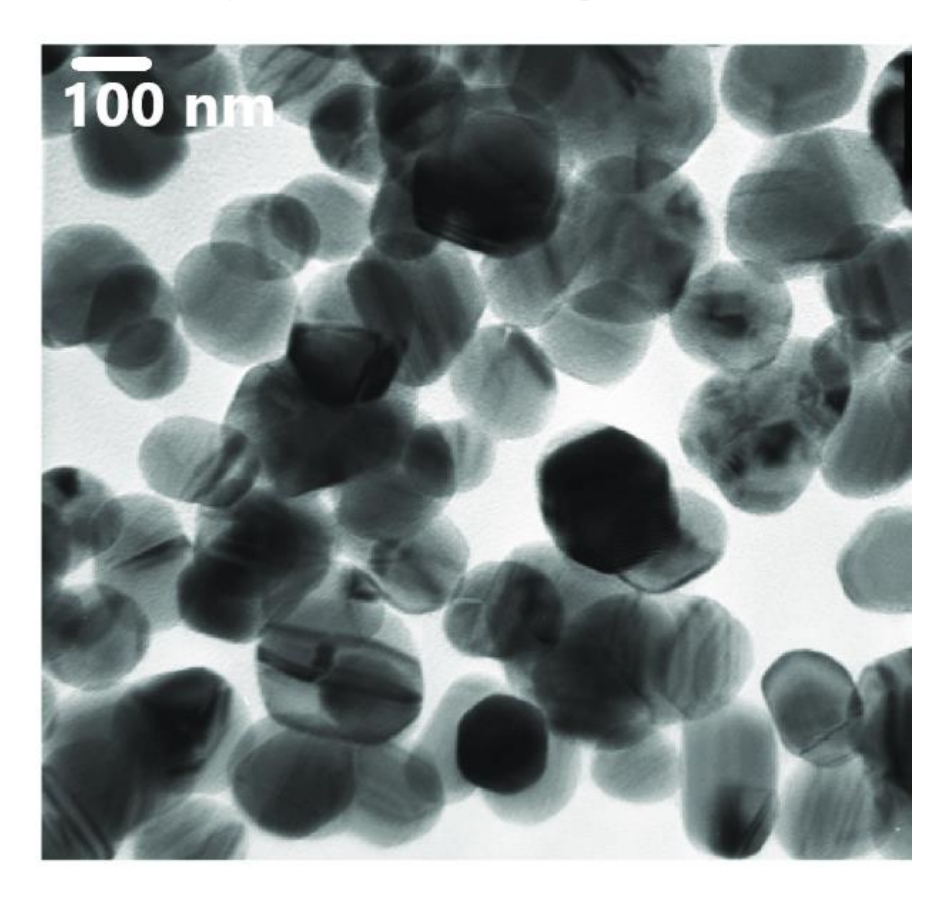


Figure 3.50: TEM Image of Silver Oxide Nanoparticle obtained in Ch. Cl-U DES

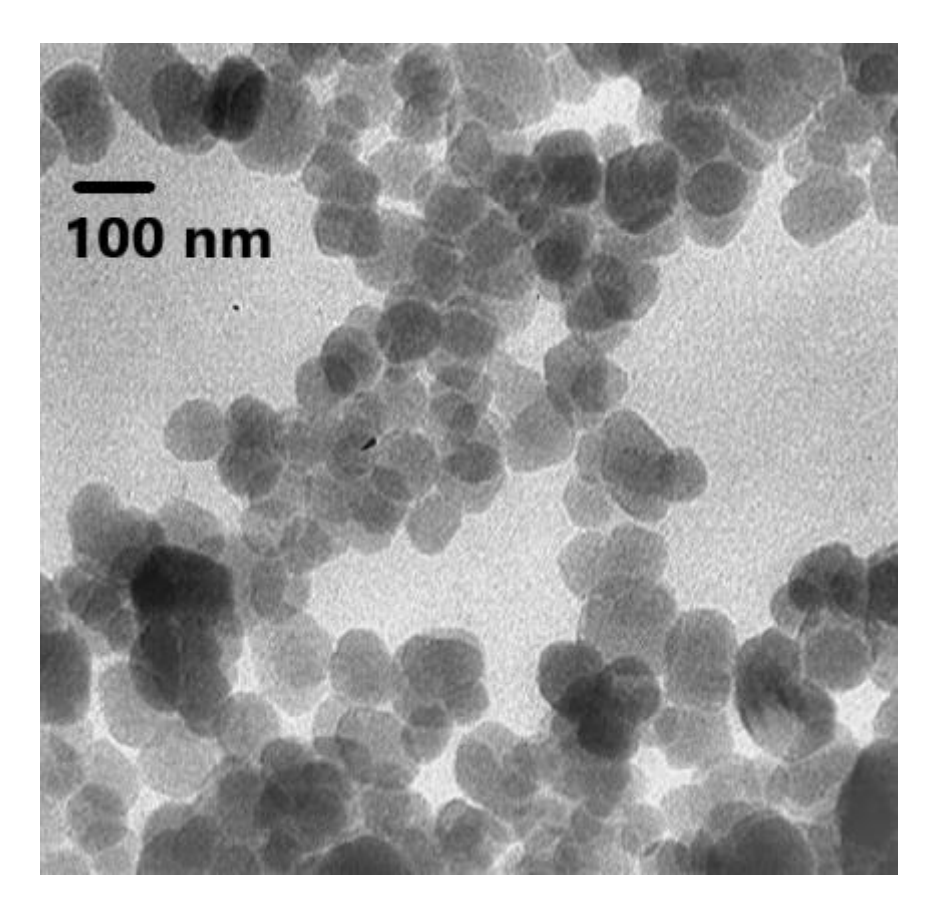


Figure 3.51: TEM Image of Zinc Oxide Nanoparticle obtained in Ch. Cl-U DES

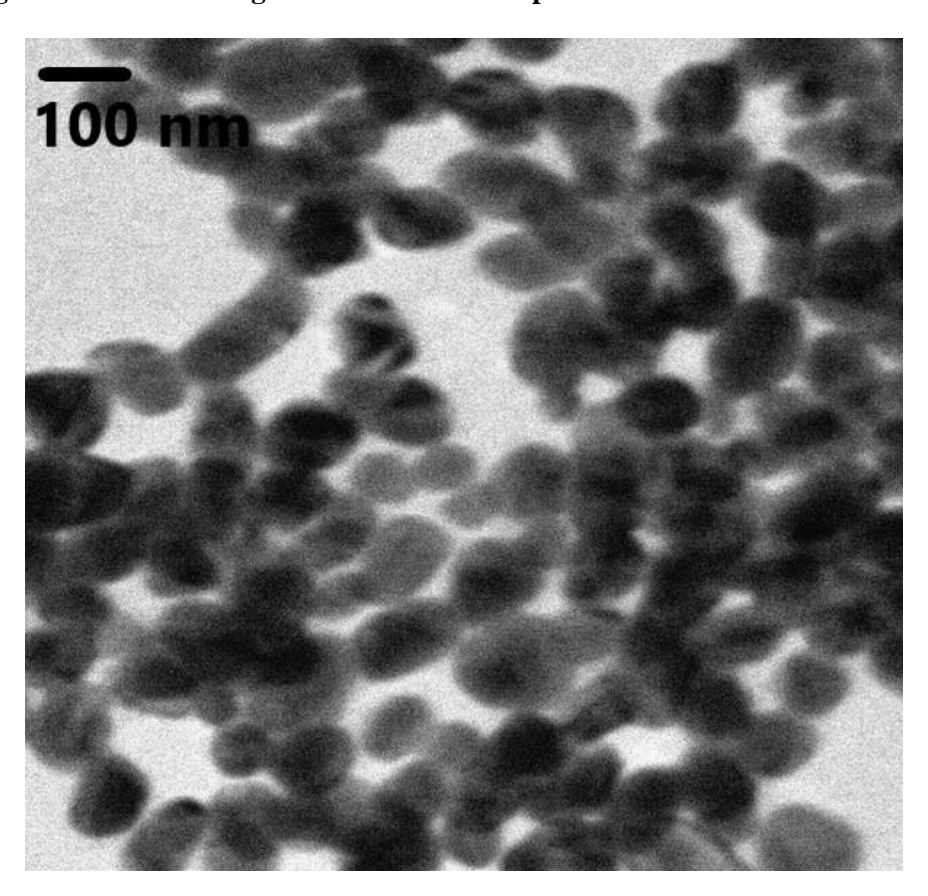


Figure 3.52: TEM Image of Cadmium Oxide Nanoparticle obtained in Ch. Cl-U DES

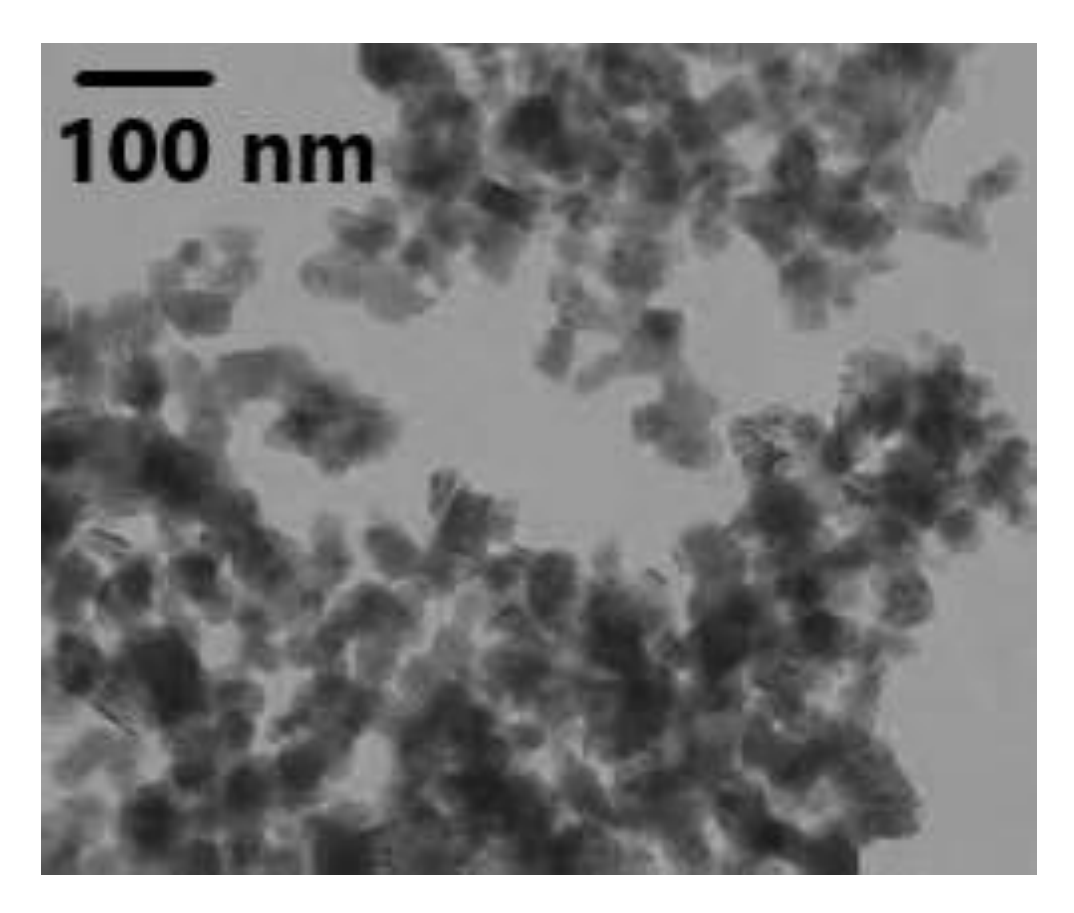


Figure 3.53: TEM Image of Vanadium Oxide Nanoparticle obtained in Ch. Cl-U DES

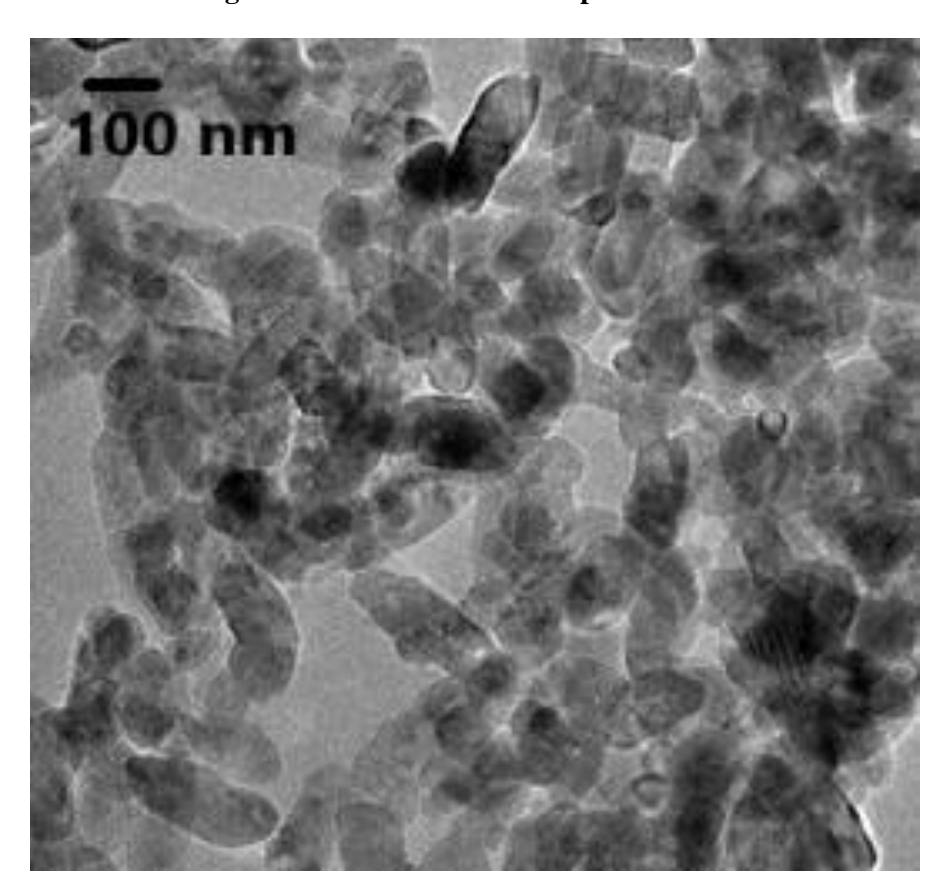


Figure 3.54: TEM Image of Nickel Oxide Nanoparticle obtained in Ch. Cl-U DES

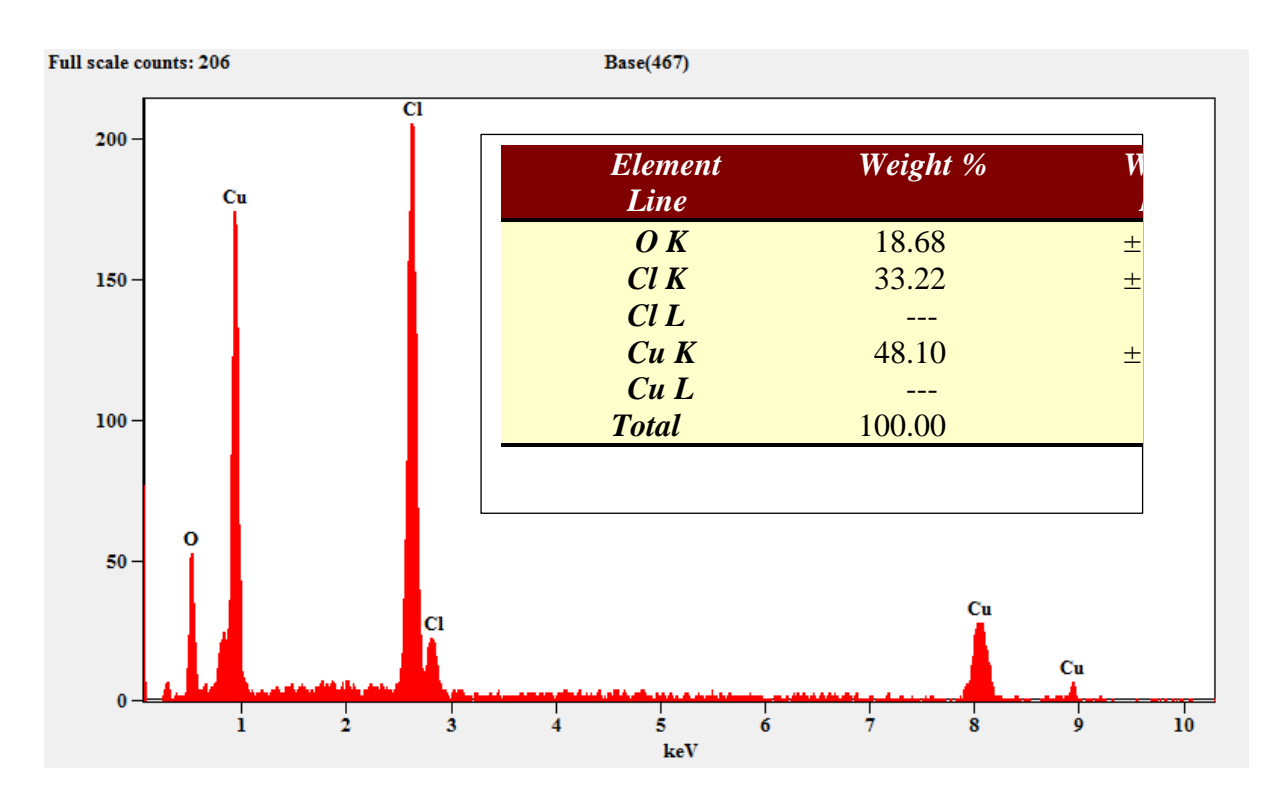


Figure 3.55: EDAX Spectrum of Copper Oxide Nanoparticle obtained in Ch. Cl-U DES

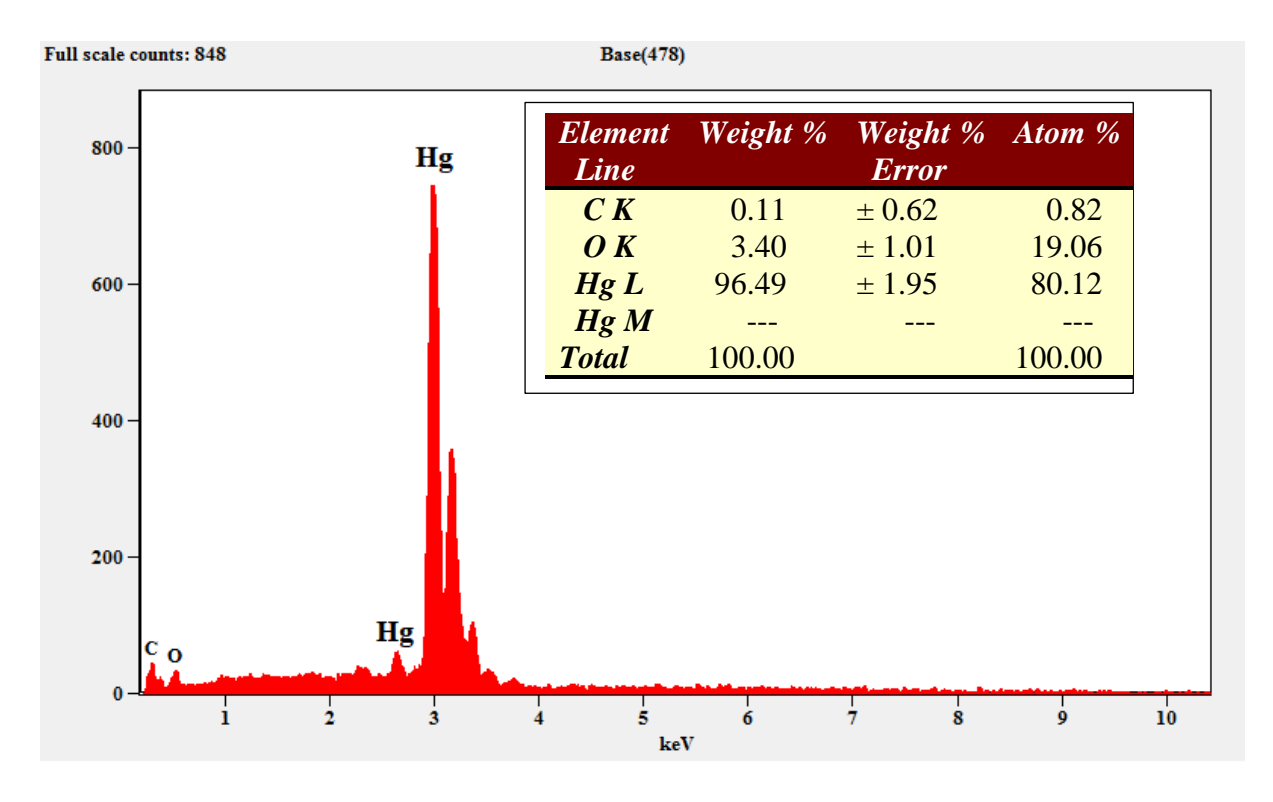


Figure 3.56: EDAX Spectrum of Mercury Oxide Nanoparticle obtained in Ch. Cl-U DES

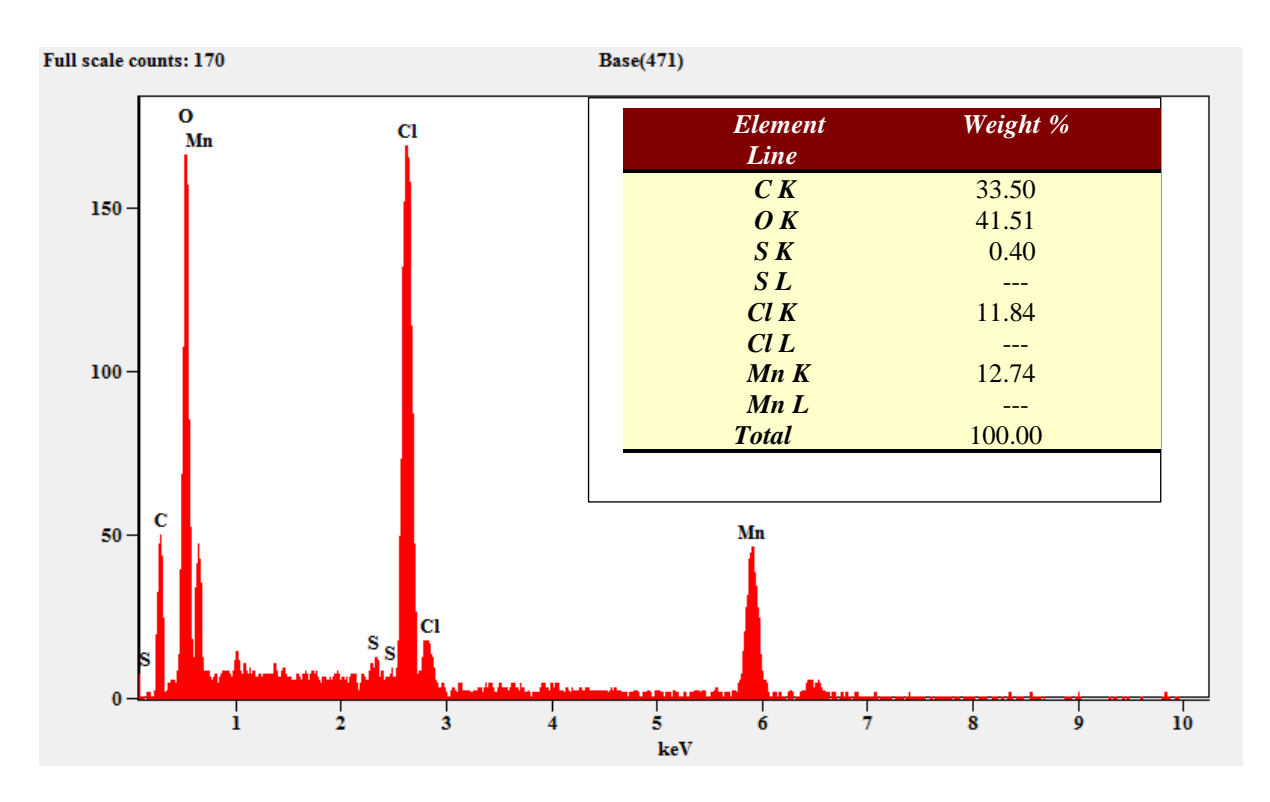


Figure 3.57: EDAX Spectrum of Manganese Oxide Nanoparticle obtained in Ch. Cl-U DES

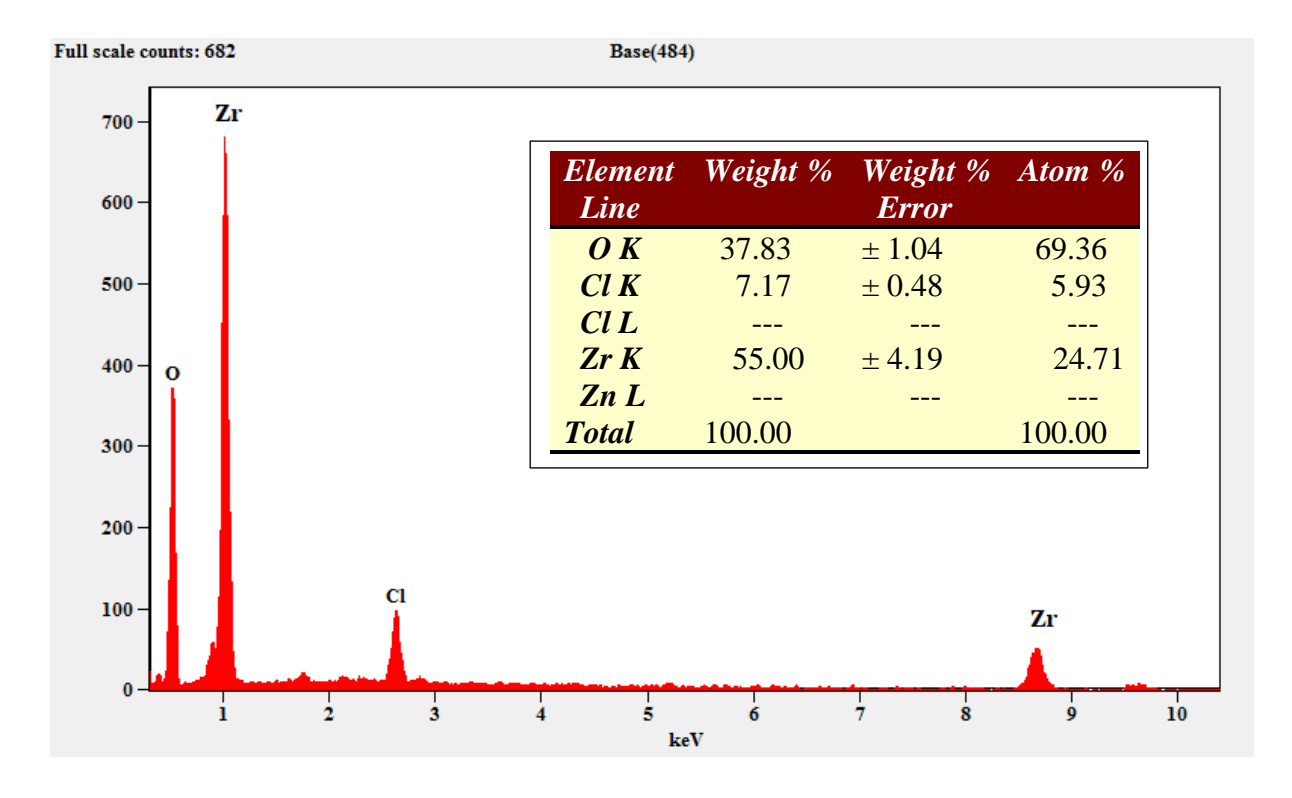


Figure 3.58: EDAX Spectrum of Zirconium Oxide Nanoparticle obtained in Ch. Cl-U DES

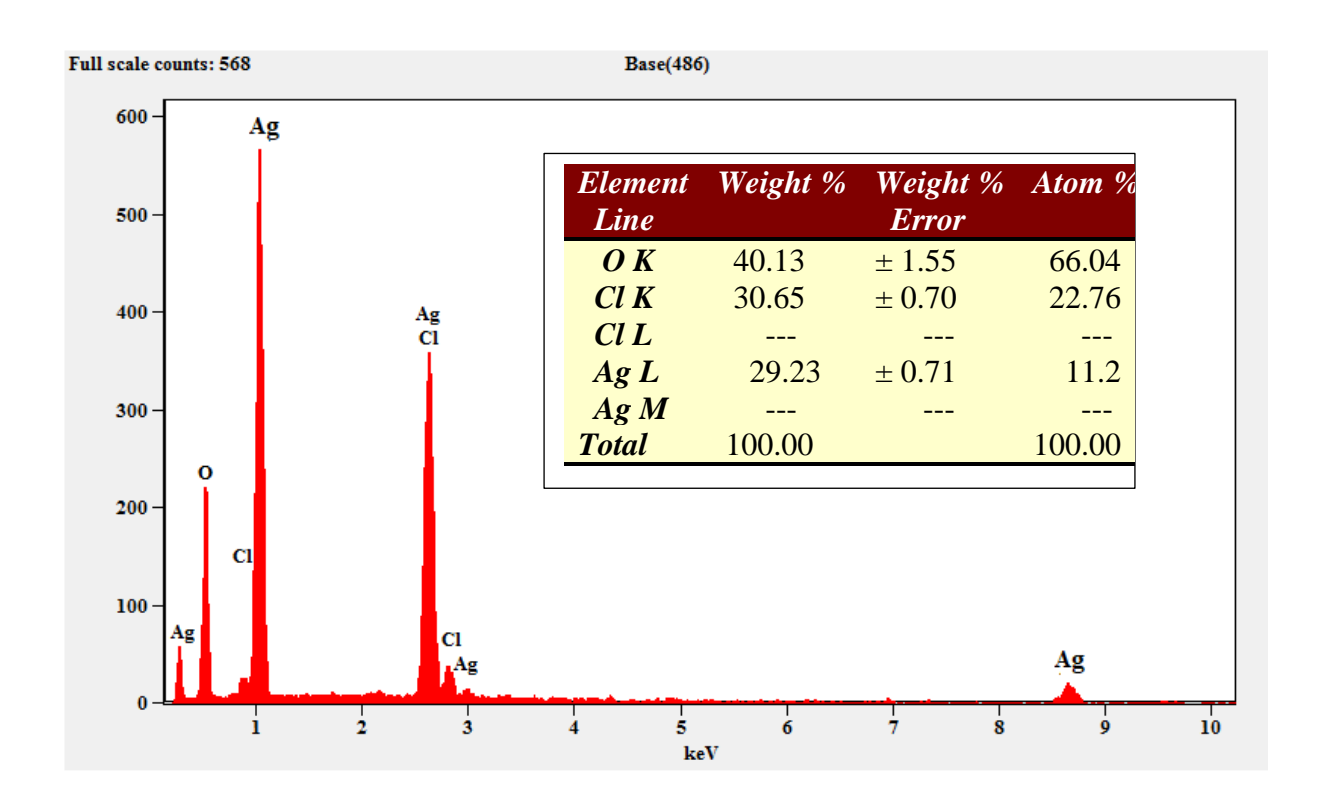


Figure 3.59: EDAX Spectrum of Silver Oxide Nanoparticle obtained in Ch. Cl-U DES

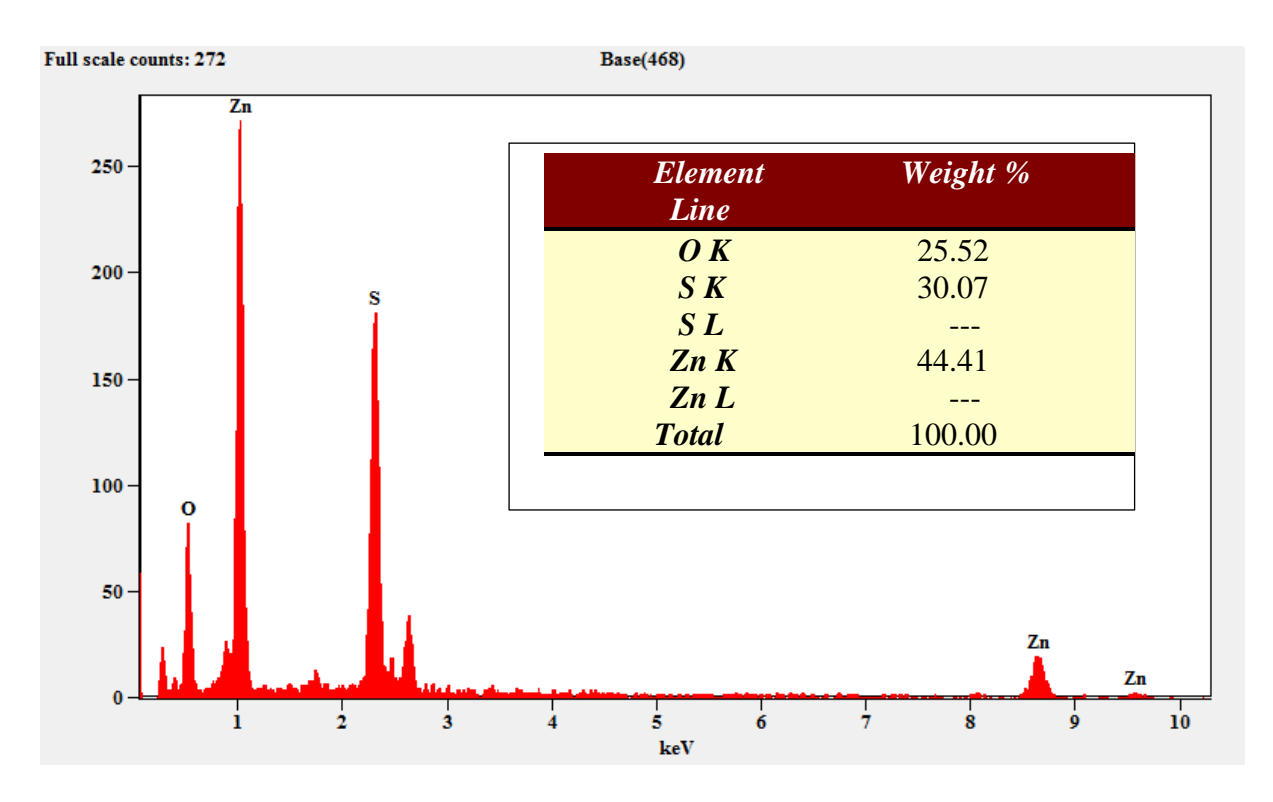


Figure 3.60: EDAX Spectrum of Zinc Oxide Nanoparticle obtained in Ch. Cl-U DES

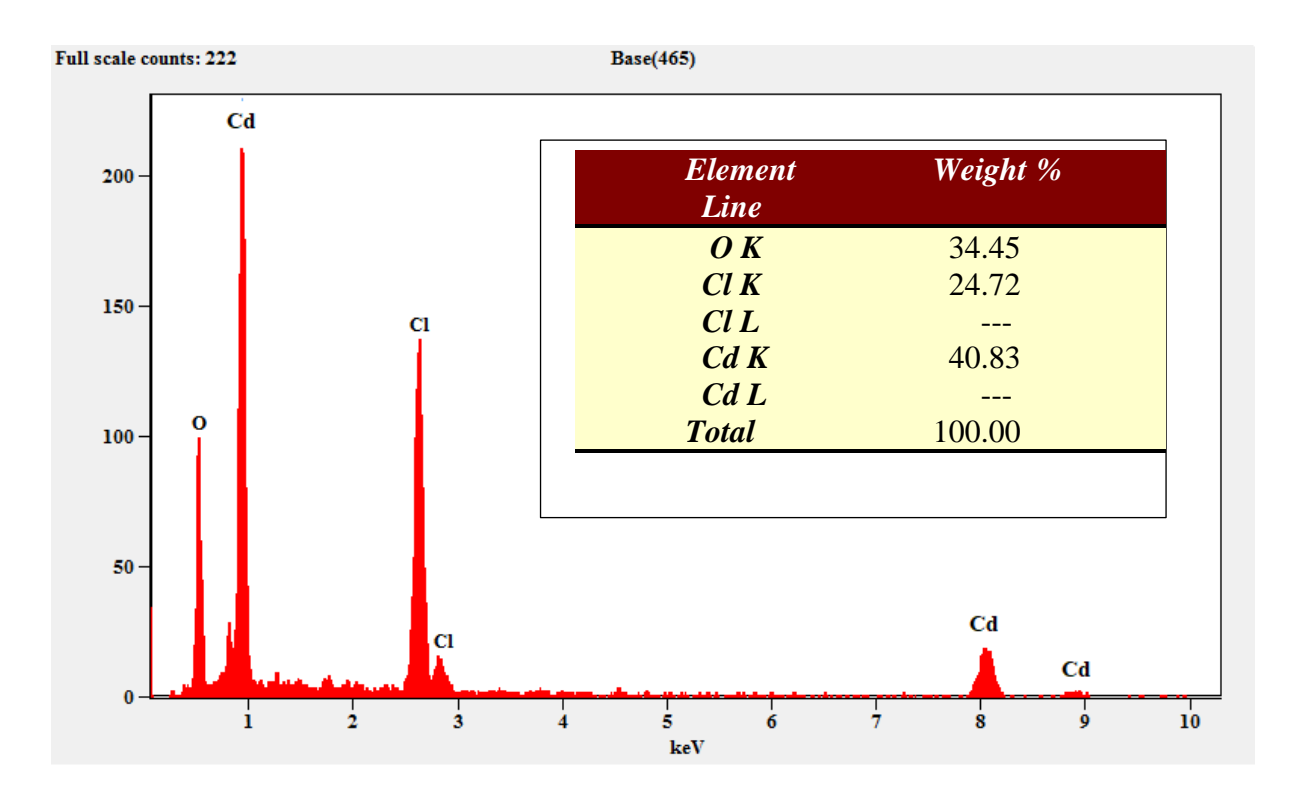


Figure 3.61: EDAX Spectrum of Cadmium Oxide Nanoparticle obtained in Ch. Cl-U DES

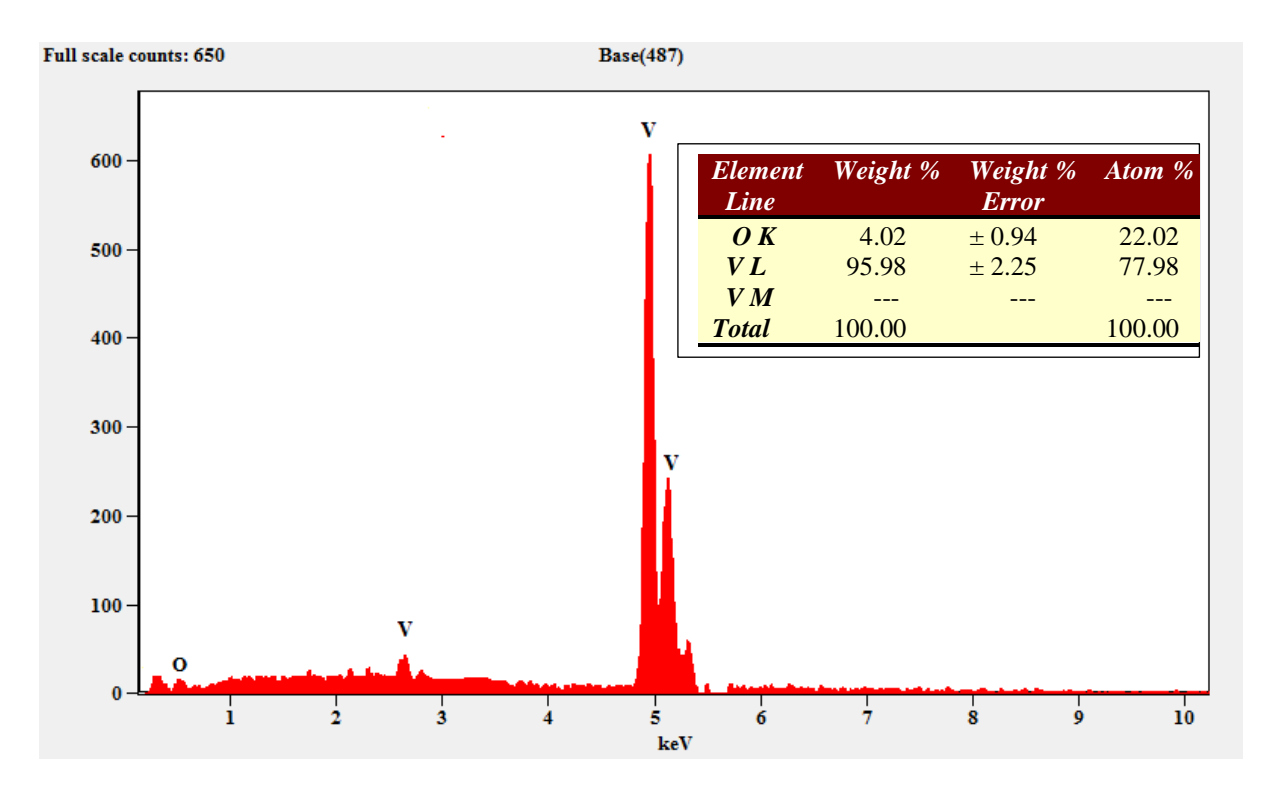


Figure 3.62: EDAX Spectrum of Vanadium Oxide Nanoparticle obtained in Ch. Cl-U DES

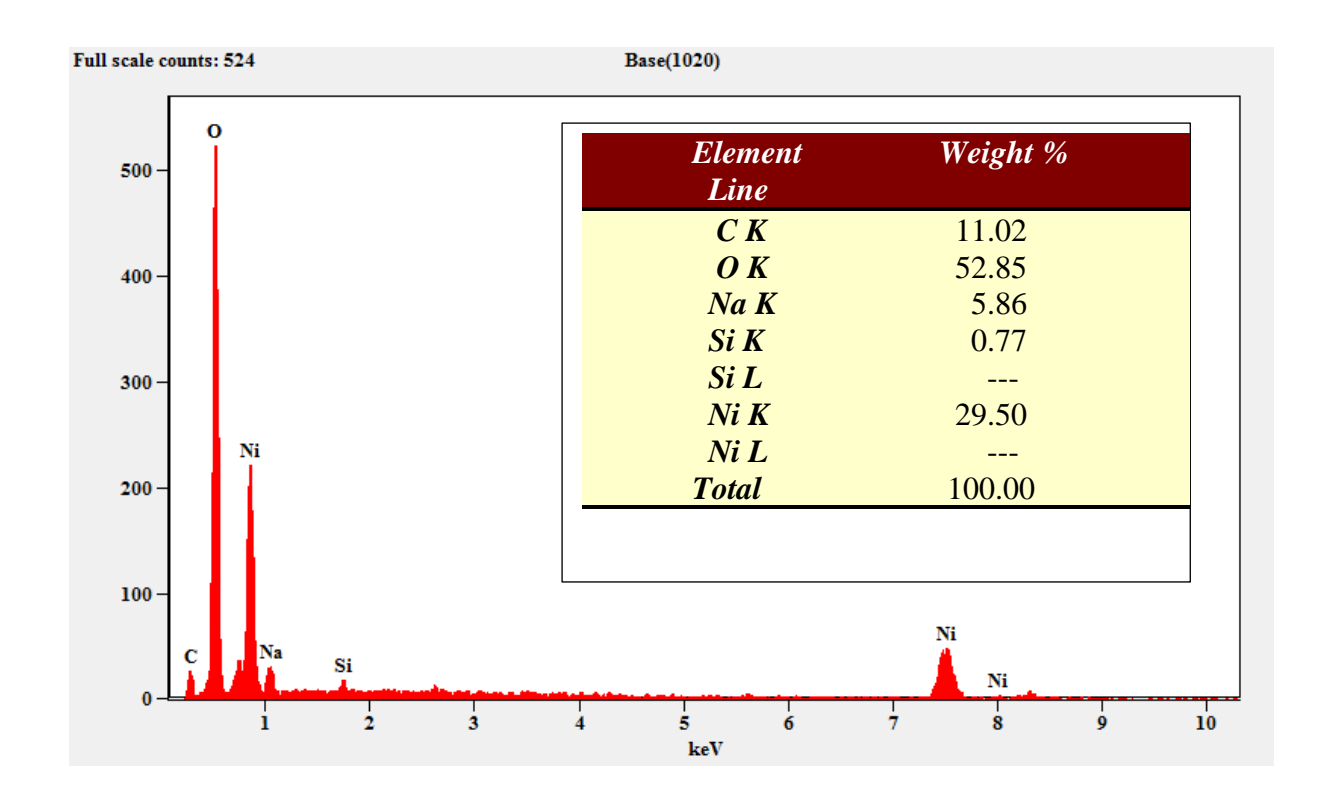


Figure 3.63: EDAX Spectrum of Nickel Oxide Nanoparticle obtained in Ch. Cl-U DES

# 4. SYNTHESIS OF SOME METAL NANOPARTICLES USING THE EFFECTIVE MEDIA OF CHOLINE CHLORIDE – ETHYLENE GLYCOL DEEP EUTECTIC SOLVENT

#### 4.1 Introduction

Nanoparticles are budding materials for have lots of biological as well as chemical usefulness due to their interesting characteristics [1-3]. The ions with low lattice energy are seen in deep eutectic solvents (DES). A quaternary ammonium salt is regularly complexed with a metal salt or hydrogen bond donor (HBD) to produce these solvents [4-6]. It was found that the green preparation of nano-composites may be achieved both theoretically and experimentally involving ionic liquids, [BF<sub>4</sub>] or [PF<sub>6</sub>] based liquids, and basic liquids [7]. The results of electrochemically polishing Ti-based alloys were presented [8] and electropolishing in a potentiostatic mode (E=3.0 V and E=4.0 V) at 25 °C took 30-40 minutes. Flaws were eliminated during electropolishing with Ethaline, which resulted in a surface smoothing and roughening impact on the surface. Relationships between surface roughness coefficients and wettability variables have been developed and explored in the course of electrochemically polishing a Ti-based alloy. Zirconium oxide nanoparticles were made using sodium hydroxide, zirconium oxychloride, and banana peel extract [9]. Biosynthesised zirconium oxide nanoparticles show fungicidal efficacy against P. Versicolor, a first in the field of fungicide research [10] groups were produced in green using Enterobacter sp. strain RNT10. Zinc oxide doping altered the surface of manganese oxide [11] XRD, EDS, and FTIR methods were used to assess the synthesized material. The catalyst was shown to prevent a photocatalytic degradation of textile dye (MB) and Zndoped MnO was shown to be a better photocatalyst than MnO against the dye. In addition to pH, hydroxyl-scavenger activity, reaction temperature and starting pigment concentration, photocatalysts were tested to determine if Methylene blue dye could be degraded in an ecologically acceptable way using photocatalysts.

The green synthesis of nanoparticles involving DESs is a continuously eco-friendly and attractive route. The present investigation in this chapter focuses on the synthesis of copper, mercury, manganese, zirconium, silver, zinc, cadmium, vanadium and nickel nanoparticles in their oxide forms, utilizing the Choline Chloride - Ethylene Glycol DES as the solvent in presence of a reducing agent, hydrazine hydrate. The UV-Visible spectra, Fourier Transformation Infra-Red (FTIR) spectra, X-Ray diffraction (XRD), Scanning Electron Microscopy (SEM), and Energy Dispersive X-Ray (EDAX) analysis were carried out on these metal nanoparticles. The average sizes of these metal nanoparticles were found to be 50 to 200nm. Hence the synthesis of metal nanoparticles using Ch. Cl – EG can be considered as a substitute greener route in the chemical synthesis of metal nanoparticles.

#### 4.2 Experimental

The chemicals used for this investigation such as choline chloride, ethylene glycol, hydrazine hydrate, sodium hydroxide, methanol, copper nitrate trihydrate, mercuric chloride, manganese chloride dihydrate, zirconium oxychloride, silver nitrate, zinc acetate dihydrate, cadmium chloride, vanadium pentoxide and nickel nitrate were purchased from Sigma–Aldrich, India and utilized as received. Barnstead nanopore water (>17.8 M-cm) was used to prepare all stock solutions.

#### 4.2.1 Preparation of choline chloride – ethylene glycol deep eutectic solvent

The choline chloride (Ch.Cl) received was recrystallized, filtered, and vacuum dried before it was used. The original version of ethylene glycol (EG) was used. The 1:1 molar ratio of these two components were taken and heated to 100 °C and agitated until a homogeneous, colourless liquid was produced from the two components. An hour's worth

of heating choline chloride and ethylene glycol at 100°C yielded a clear homogenous liquid.

#### 4.2.2 Synthesis of copper nanoparticles in choline chloride – ethylene glycol deep eutectic solvent

Copper nanoparticles were synthesized in the DES of ChCl-EG as follows <sup>[12]</sup>. Nanoparticles were made by combining 10 ml of 0.01M copper nitrate trihydrate [Cu(NO<sub>3</sub>)<sub>2</sub>.3H<sub>2</sub>O] with 15 ml of choline chloride – ethylene glycol DES in a beaker and magnetically stirring for 30 minutes at 1200 RPM with a magnetic stirrer. During vigorous stirring, about 8-10 ml of 0.01 M hydrazine hydrate as a reducing agent was added drop by drop, followed by 10 ml of 1 M sodium hydroxide as a stabilizing agent was injected slowly into the mixture. The obtained copper oxide nanoparticles in the beaker were centrifuged, rinsed several times with deionized water, then extracted using methanol, and dried at airoven.

### 4.2.3 Synthesis of mercury nanoparticles in choline chloride – ethylene glycol deep eutectic solvent

Nanoparticles of mercury were synthesized in the DES of ChCl-EG as follows <sup>[12]</sup>. Nanoparticles were made by combining 10 ml of 0.01M mercuric chloride [HgCl<sub>2</sub>] with 15 ml of choline chloride – ethylene glycol DES in a beaker and magnetically stirring for 30 minutes at 1200 RPM with a magnetic stirrer. During vigorous stirring, about 8-10 ml of 0.01 M hydrazine hydrate as a reducing agent was added drop by drop, followed by 10 ml of 1 M sodium hydroxide as a stabilizing agent was injected slowly into the mixture. The obtained mercury oxide nanoparticles in the beaker were centrifuged, rinsed several times with deionized water, then extracted using methanol, and dried at air-oven.

#### 4.2.4 Synthesis of manganese nanoparticles in choline chloride – ethylene glycol deep eutectic solvent

Nanoparticles of manganese were synthesized in the DES of ChCl-EG as follows <sup>[12]</sup>. Nanoparticles were made by combining 10 ml of 0.01M manganese chloride dihydrate [MnCl<sub>2</sub>.2H<sub>2</sub>O] with 15 ml of choline chloride – ethylene glycol DES in a beaker and magnetically stirring for 30 minutes at 1200 RPM with a magnetic stirrer. During vigorous stirring, about 8-10 ml of 0.01 M hydrazine hydrate as a reducing agent was added drop by drop, followed by 10 ml of 1 M sodium hydroxide as a stabilizing agent was injected slowly into the mixture. The obtained manganese oxide nanoparticles in the beaker were centrifuged, rinsed several times with deionized water, then extracted using methanol, and dried at air-oven.

### 4.2.5 Synthesis of zirconium nanoparticles in choline chloride – ethylene glycol deep eutectic solvent

Zirconium nanoparticles were synthesized in the DES of ChCl-EG as follows <sup>[12]</sup>. Nanoparticles were made by combining 10 ml of 0.01M zirconium oxychloride [ZrOCl<sub>2</sub>] with 15 ml of choline chloride – ethylene glycol DES in a beaker and magnetically stirring for 30 minutes at 1200 RPM with a magnetic stirrer. During vigorous stirring, about 8-10 ml of 0.01 M hydrazine hydrate as a reducing agent was added drop by drop, followed by 10 ml of 1 M sodium hydroxide as a stabilizing agent was injected slowly into the mixture. The obtained zirconium oxide nanoparticles in the beaker were centrifuged, rinsed several times with deionized water, then extracted using methanol, and dried at air-oven.

#### 4.2.6 Synthesis of silver nanoparticles in choline chloride – ethylene glycol deep eutectic solvent

Nanoparticles of silver were synthesized in the DES of ChCl-EG as follows <sup>[12]</sup>. Nanoparticles were made by combining 10 ml of 0.01M silver nitrate [AgNO<sub>3</sub>] with 15 ml

of choline chloride – ethylene glycol DES in a beaker and magnetically stirring for 30 minutes at 1200 RPM with a magnetic stirrer. During vigorous stirring, about 8-10 ml of 0.01 M hydrazine hydrate as a reducing agent was added drop by drop, followed by 10 ml of 1 M sodium hydroxide as a stabilizing agent was injected slowly into the mixture. The obtained silver oxide nanoparticles in the beaker were centrifuged, rinsed several times with deionized water, then extracted using methanol, and dried at air-oven.

#### 4.2.7 Synthesis of zinc nanoparticles in choline chloride – ethylene glycol deep eutectic solvent

Zinc nanoparticles were synthesized in the DES of ChCl-EG as follows <sup>[12]</sup>. Nanoparticles were made by combining 10 ml of 0.01M Zinc acetate dihydrate [Zn(COOCH<sub>3</sub>)<sub>2</sub>.2H<sub>2</sub>O] with 15 ml of choline chloride – ethylene glycol DES in a beaker and magnetically stirring for 30 minutes at 1200 RPM with a magnetic stirrer. During vigorous stirring, about 8-10 ml of 0.01 M hydrazine hydrate as a reducing agent was added drop by drop, followed by 10 ml of 1 M sodium hydroxide as a stabilizing agent was injected slowly into the mixture. The obtained zinc oxide nanoparticles in the beaker were centrifuged, rinsed several times with deionized water, then extracted using methanol, and dried at air-oven.

#### 4.2.8 Synthesis of cadmium nanoparticles in choline chloride – ethylene glycol deep eutectic solvent

Cadmium nanoparticles were synthesized in the DES of ChCl-EG as follows <sup>[12]</sup>. Nanoparticles were made by combining 10 ml of 0.01M cadmium chloride [CdCl<sub>2</sub>] with 15 ml of choline chloride – ethylene glycol DES in a beaker and magnetically stirring for 30 minutes at 1200 RPM with a magnetic stirrer. During vigorous stirring, about 8-10 ml of 0.01 M hydrazine hydrate as a reducing agent was added drop by drop, followed by 10 ml of 1 M sodium hydroxide as a stabilizing agent was injected slowly into the mixture.

The obtained cadmium oxide nanoparticles in the beaker were centrifuged, rinsed several times with deionized water, then extracted using methanol, and dried at air-oven.

### 4.2.9 Synthesis of vanadium nanoparticles in choline chloride – ethylene glycol deep eutectic solvent

The vanadium nanoparticles were synthesized in the DES of ChCl-EG as follows <sup>[12]</sup>. Nanoparticles were made by combining 10 ml of 0.01M vanadium pentoxide [V<sub>2</sub>O<sub>5</sub>] with 15 ml of choline chloride – ethylene glycol DES in a beaker and magnetically stirring for 30 minutes at 1200 RPM with a magnetic stirrer. During vigorous stirring, about 8-10 ml of 0.01 M hydrazine hydrate as a reducing agent was added drop by drop, followed by 10 ml of 1 M sodium hydroxide as a stabilizing agent was injected slowly into the mixture. The obtained vanadium oxide nanoparticles in the beaker were centrifuged, rinsed several times with deionized water, then extracted using methanol, and dried at air-oven.

#### 4.2.10 Synthesis of nickel nanoparticles in choline chloride – ethylene glycol deep eutectic solvent

Nickel nanoparticles were synthesized in the DES of ChCl-EG as follows <sup>[12]</sup>. Nanoparticles were made by combining 10 ml of 0.01M nickel nitrate [Ni(NO<sub>3</sub>)<sub>2</sub>] with 15 ml of choline chloride – ethylene glycol DES in a beaker and magnetically stirring for 30 minutes at 1200 RPM with a magnetic stirrer. During vigorous stirring, about 8-10 ml of 0.01 M hydrazine hydrate as a reducing agent was added drop by drop, followed by 10 ml of 1 M sodium hydroxide as a stabilizing agent was injected slowly into the mixture. The obtained nickel oxide nanoparticles in the beaker were centrifuged, rinsed several times with deionized water, then extracted using methanol, and dried at air-oven.

#### **4.3 Results and Discussions**

The synthesized copper, mercury, manganese, zirconium, silver, zinc, cadmium, vanadium and nickel nanoparticles in the deep eutectic solvent of choline chloride –

ethylene glycol were characterized by the techniques such as UV-Visible spectroscopy, Fourier transform infrared spectroscopy, Scanning electron microscopy, X-Ray diffraction and Energy dispersive X-ray analysis.

### 4.3.1 UV-Visible Spectra of Metal Nanoparticles Prepared Using Choline Chloride – Ethylene Glycol Deep Eutectic Solvent

The UV-Visible spectra of copper, mercury, manganese, zirconium, silver, zinc, cadmium, vanadium and nickel oxide nanoparticles obtained in their ethanolic solutions between the wavelengths 200 and 800nm are placed in figures 4.1 to 4.9. The surface plasmon absorption of metal nanoparticles are usually seen around 400 nm. Larger sizes shift the band to longer wavelength and broaden the band to some extent and however, very dumped plasmon and very broaden bands could be due to surface adsorptions [13, 14]. The bands due to either surface plasmon or surface adsorptions of these metal oxide nanoparticles are given in table 4.1 below.

Table 4.1: UV-Visible absorption bands of metal oxide nanoparticles

S. No.	Metal Oxide NPs	λ <sub>max</sub> values (nm)	Nature of bands
1	Copper	412.4	Surface Plasmon
2	Mercury	350.85	Surface Plasmon
3	Manganese	385.24	Surface Adsorptions
4	Zirconium	352.70	Surface Adsorptions
5	Silver	326.9	Surface Plasmon
6	Zinc	343.95	Surface Plasmon
7	Cadmium	388.6	Surface Plasmon
8	Vanadium	270.05	-
9	Nickel	275.25	-

From the UV-Visible spectra of metal oxide nanoparticles displayed in figures 4.1 to 4.9, it was followed that the copper, mercury, silver, zinc and cadmium showed surface plasmon absorption bands at the specific wavelengths as given in table 4.1. The manganese and zirconium metal oxide nanoparticles gave very broad and dumped absorption bands due to surface adsorptions while the vanadium and nickel-metal oxides are transparent above 300 nm. Except copper all other metal oxide nanoparticles prepared from the deep eutectic solvent of choline chloride – ethylene glycol is almost transparent in the visible region. Thus, the copper oxide nanoparticles prepared from the deep eutectic solvent of choline chloride – ethylene glycol are expected to have photocatalytic activity.

### 4.3.2 FTIR Spectra of Metal Nanoparticles Prepared Using Choline Chloride – Ethylene Glycol Deep Eutectic Solvent

The FTIR spectra obtained in the range of 400 to 4000 cm<sup>-1</sup> for copper, mercury, manganese, zirconium, silver, zinc, cadmium, vanadium and nickel metal oxide nanoparticles prepared from the deep eutectic solvent of choline chloride-ethylene glycol are reported in figures 4.10 to 4.18 of this section. The peaks of various metal oxide nanoparticles such as copper, mercury, manganese, zirconium, silver, zinc, cadmium, vanadium and nickel prepared from the DES of choline chloride – ethylene glycol were presented in the following table 4.2.

The several peaks noticed in the range of 400 to 900 cm<sup>-1</sup> are correlated to respective M – O vibrations of MO nanoparticles <sup>[15, 16]</sup>. A few of the solvent molecules are capped on the surface of MO nanoparticles. These are indicated by the peaks around 1040 and 1120 cm<sup>-1</sup> corresponding to the C – O stretching vibrations. The peak due to C – H bending of alkane and CH<sub>2</sub> deformations of choline chloride and ethylene glycol is seen around 1470 cm<sup>-1</sup> and 1380 cm<sup>-1</sup> respectively in all these spectra. The peak was noticed around 1600 cm<sup>-1</sup> denoted O – H bending vibrations of both the components of the deep eutectic

solvent. The peaks observed around 2850 cm<sup>-1</sup> and 2920 cm<sup>-1</sup> are due to C – O asymmetric stretching <sup>[16]</sup>. Further, the broad peaks seen around 3420 cm<sup>-1</sup> in all the spectra due to different vibrations modes of water molecules adsorbed on the surface of metal oxide nanoparticles <sup>[15]</sup>.

Table 4.2: FTIR absorption peaks of metal oxide nanoparticles

S.No.	Metal Oxide	IR Vibrations						
	NPs	M-O Vibrations	C-O Stretch	CH <sub>2</sub> deform (methylene)	C-H bend (alkane)	O-H bend	C-O asym stretch	O-H stretch
1	Cu	421, 620	1023,	1384	-	1630	2851,	3436
			1113				2924	
2	Hg	586, 875	1125	1385	1474	1626	2928	3425
3	Mn	515, 627	1084	1385	1474	1621	-	3384
4	Zr	618, 687	1085	1384	-	1631	2931	3404
5	Ag	620	1027	1384	-	1638	2850,	3434
							2925	
6	Zn	466, 636	1020	1399	-	1594	2925	3404
7	Cd	522, 590,	1086	-	1445	1617	2958	3435
		858						
8	$\mathbf{V}$	526, 599	1038	1385	1471	1634	2921	3420
9	Ni	451, 617	1018	1384	1478	1630	2923	3421

## 4.3.3 XRD Patterns of Metal Nanoparticles Prepared Using Choline Chloride – Ethylene Glycol Deep Eutectic Solvent

The XRD patterns obtained for copper, mercury, manganese, zirconium, silver, zinc, cadmium, vanadium and nickel metal oxide nanoparticles prepared from the deep eutectic solvent of choline chloride-ethylene glycol are reported and discussed as follows.

The powder x-ray diffraction patterns of copper oxide nanoparticles prepared from the deep eutectic solvents, Ch.Cl – EG are given in figure 4.19. The XRD patterns give information about the grain size, structure, and phase cleanliness of the materials. In the case of CuO particles obtained in Ch.Cl – EG DES, the diffraction peaks seen at 2θ values of 23.45°, 27.85°, 41.35° and 66.24° are indexed as (040), (021), (420), (300) respectively. The grain size of CuO nanoparticles is determined by using the Debye–Scherer formula,

$$D = k λ/β cosθ$$

where D denotes the grain size, K refers to a constant,  $\lambda$  refers to the wavelength of X-ray used,  $\beta$  denotes the fullwidth half-maximum of the diffraction peaks and  $\theta$  is the angle of the diffraction [15]. By using this formula, the average grain size of CuO nanoparticles prepared from the DES of Ch.Cl-EG is found to be 80 nm.

All the diffraction points in the XRD can be assigned to the pure cubic lattice structure of mercury oxide nanoparticles as given in figure 4.20. The peaks correspond to (111), (200), (220), and (222) planes, which are in good pact with the JCPDS-pattern available in the literature. The average crystal width of the HgO nano particles obtained in the DES of Ch.Cl-EG was found to be 45 nm using the Scherrer formula of the XRD pattern. The crystalline behaviour of the prepared MnO nanoparticles was inspected by the XRD analysis and given in the figure 4.21. The XRD patterns revealed the diffraction peaks at 20 values for manganese oxide nanoparticles at 37.82, 55.19 and 66.26. These values are in accordance with the crystal planes (101), (110) and (200). The mean particle size for MnO nanoparticles prepared from the DES of Ch.Cl-EG is found to be 60 nm using the Scherrer formula.

The XRD pattern for zirconium oxide nanoparticle prepared using the solvent of choline chloride – ethylene glycol is provided at the figure 4.22. The diffraction peaks noticed in this figure for ZrO nanoparticles are in agreement with the Joint Committee for

Powder Diffraction Studies (JCPDS) <sup>[17]</sup>. The average grain size of the ZrO nanoparticles with respect to relative intensity peak at XRD pattern was found to be 70 nm when the Scherrer formula is applied. The AgO nanoparticles obtained in the case of Ch.Cl-EG DES reported in figure 4.23 showed intense peaks at 2θ values of 45.34, 64.37 and 77.23 which are indexed corresponding to the planes of (110), (220) and (311) respectively. The structure of silver oxide nanoparticles is crystalline in nature, and it is face centred cubic this case. The average particle size of AgO NPs obtained in the case of Ch.Cl-EG DES is calculated to be 170 nm by measuring the breadth of (111) Bragg's reflection.

Figure 4.24 noticed the XRD data of zinc oxide nanoparticles obtained from the DES of Ch.Cl-EG. The XRD plots of the nanoparticles showed peaks of pure hexagonal structure of zinc oxide. Three reflection planes (100), (002) and (101) that have been seen are similar to the detected reflections in bulk materials of zinc oxide [18]. The diffraction peaks obtained at 31.63°, 34.16°, 36.17°, 47.30°, 56.43°, 62.66°, 67.80°, and 69.27° are intense and sharp representing that the nano-crystalline zinc oxide nanoparticles had good crystallinity. The highest intensity at figure 4.24 related to zinc oxide nanoparticles reflecting the nano-range size around 100 nm by using Debye – Scherrer formula. The particle size determined involving the comparative intensity peak (220) found at  $2\theta$  value of 52.23° of CdO nanoparticles as given in figure 4.25 has been observed as 48 nm. This is calculated using the Scherrer formula from the figure 4.25 corresponding to the CdO nanoparticles obtained from the DES of Ch.Cl-EG. The surge in sharpness of XRD peaks designates those particles are in crystalline kind. The (111), (200), (220), (311) and (222) reflections which correspond to 42.31, 47.14, 52.23, 70.92 and 73.64 respectively, are obviously seen and meticulously bout the reference designs of CdO (JCPDS) File No. 05-0640). The piercing XRD peaks show that the particles were of polycrystalline assembly, further the nanostructure raised with a random orientation [19, 20].

The crystalline kind of DES media synthesized vanadium oxide nanoparticles was depicted in figure 4.26. The characteristic key diffraction peaks noticed at 2θ values of 14.91, 20.1, 21.4, 25.9, 31.1, 32.3, 33.6, 34.4, 41.2, 41.3, 45.9, 47.6 and 48.4 that match with the hkl planes of (200), (001), (101), (110), (310), (011), (111), (310), (002), (102), (411), (600) and (302) index planes were in decent arrangement with their standard JCPDS No. 41-1426 <sup>[21]</sup>. The XRD pattern obtained for NiO nanoparticles in Ch.Cl-EG DES is shown in figure 4.27. Three peaks for NiO NPs at 2θ values of 44.25°, 51.38° and 76.14° corresponding to the (111), (200) and (222) lattice planes found established that the ensuing particles have been pure Nickel oxide nanoparticles <sup>[22]</sup>. The nanoparticles width was projected by using the Scherrer's equation to be around 50 nm.

### 4.3.4 SEM Analysis of Metal Nanoparticles Prepared Using Choline Chloride – Ethylene Glycol Deep Eutectic Solvent

The SEM images obtained for copper, mercury, manganese, zirconium, silver, zinc, cadmium, vanadium and nickel metal oxide nanoparticles prepared from the deep eutectic solvent of choline chloride-ethylene glycol are reported and discussed herewith. To examine the morphological structure and particle size of metal oxide nanoparticles such as Cu, Hg, Mn, Zr, Ag, Zn, Cd, V and Ni, scanning electron microscopy was used [23, 24]. The assembly, geometry, and magnitude of the above metal oxide nanoparticles prepared using the DES of Ch.Cl-EG were evaluated from the Scanning Electron Microscopy images which are displayed in figures 4.28 to 4.36. The mean particle dimensions of these metal oxide nanoparticles were calculated from the histograms of the respective SEM images and they are shown in figures 4.37 to 4.45. Further, the shapes and mean size of the prepared metal oxide nanoparticles are given in table 4.3 below.

Table 4.3: SEM morphology and size of metal oxide nanoparticles

S. No.	Metal Oxide NPs	Morphology	Size (nm)
1	Copper	Spongy like	77
2	Mercury	Irregular beads	43
3	Manganese	Irregular Scales	55
4	Zirconium	Spongy like	66
5	Silver	Spongy spheres	168
6	Zinc	Broken rods	92
7	Cadmium	Buds like	45
8	Vanadium	Scales like	65
9	Nickel	Scales like	50

# 4.3.5 EDAX Analysis of Metal Nanoparticles Prepared Using Choline Chloride – Ethylene Glycol Deep Eutectic Solvent

The elemental composition and the purity of the DES media via prepared metal oxide nanoparticles are confirmed by Energy Dispersive X-ray Analysis. The elemental cleanliness of these metal oxide NPs was evaluated from the EDAX spectra and the peak values established the occurrence of target components in the synthesized NPs <sup>[25-28, 29]</sup>. The EDAX spectra obtained for copper, mercury, manganese, zirconium, silver, zinc, cadmium, vanadium and nickel metal oxide nanoparticles prepared from the deep eutectic solvent of choline chloride-ethylene glycol are reported in the figures 4.46 to 4.54. The elemental purity, weight percentage, atom percentage of metals, oxygen and the trace of elements of solvent were given in the tables as an insert of the respective EDAX spectra of metal oxide nanoparticles.

#### 4.4. Conclusion

Nine types of metal oxide nanoparticles were synthesized successfully using choline chloride – ethylene glycol deep eutectic solvents. The copper, mercury, manganese, zirconium, silver, zinc, cadmium, vanadium and nickel metal oxide nanoparticles prepared were characterized by techniques such as UV spectroscopy, FTIR spectroscopy, X-Ray diffraction, Scanning Electron Microscopy, and Energy Dispersive X-ray Analysis. The nanoparticles were synthesised in a simple and convenient manner. There was no surfactant and seed were utilized for the formation of nanoparticles. The size of the particles formed was controlled by varying proportions of the water present in the DESs.

#### References

- [1] C. Sun, J. Zeng, H. Lei, W. Yang, and Q. Zhang, "Direct electrodeposition of phosphorus-doped nickel superstructures from choline chloride—ethylene glycol deep eutectic solvent for enhanced hydrogen evolution catalysts," *ACS Sustainable Chemistry & Engineering*, vol. 7, pp. 1529-1537, 2018.
- [2] M. Zhong, Q. F. Tang, Y. W. Zhu, X. Y. Chen, and Z. J. Zhang, "An alternative electrolyte of deep eutectic solvent by choline chloride and ethylene glycol for wide temperature range supercapacitors," *Journal of Power Sources*, vol. 452, p. 227847, 2020.
  [3] C. Liu, P. Jiang, Y. Huo, T. Zhang, and Z. Rao, "Experimental study on ethylene glycol/choline chloride deep eutectic solvent system based nanofluids," *Heat and Mass Transfer*, pp. 1-10, 2021.
- [4] Y. Xue, Y. Hua, J. Ru, C. Fu, Z. Wang, J. Bu, *et al.*, "High-efficiency separation of Ni from Cu-Ni alloy by electrorefining in choline chloride-ethylene glycol deep eutectic solvent," *Advanced Powder Technology*, 2021.
- [5] I. Espino-López, M. Romero-Romo, M. M. de Oca-Yamaha, P. Morales-Gil, M. Ramírez-Silva, J. Most any, *et al.*, "Palladium nanoparticles electrodeposition onto glassy carbon from a deep eutectic solvent at 298 K and their catalytic performance toward formic acid oxidation," *Journal of The Electrochemical Society*, vol. 166, p. D3205, 2018.
- [6] S. Liu, R. Ji, Y. Liu, F. Zhang, H. Jin, X. Li, *et al.*, "Effects of boric acid and water on the deposition of Ni/TiO2 composite coatings from deep eutectic solvent," *Surface and Coatings Technology*, vol. 409, p. 126834, 2021.
- [7] T. Zhang, T. Doert, H. Wang, S. Zhang, and M. Ruck, "Inorganic Synthesis Using Reactions of Ionic Liquids and Deep Eutectic Solvents," *Angewandte Chemie International Edition*, 2021.

- [8] A. Kityk, V. Protsenko, F. Danilov, V. Pavlik, M. Hnatko, and J. Šoltýs, "Enhancement of the surface characteristics of Ti-based biomedical alloy by electropolishing in environmentally friendly deep eutectic solvent (Ethaline)," *Colloids and Surfaces A: Physicochemical and Engineering Aspects*, vol. 613, p. 126125, 2021.
- [9] L. Dillion, H. Shanley, and B. L. C. Han, "Facile and One-Step Synthesis of Zirconium Oxide Nanoparticles for Removal of Phosphate and Lead (II) Ions," in *IRC-SET 2020*, ed: Springer, 2021, pp. 675-688.
- [10] T. Ahmed, H. Ren, M. Noman, M. Shahid, M. Liu, M. A. Ali, *et al.*, "Green synthesis and characterization of zirconium oxide nanoparticles by using a native Enterobacter sp. and its antifungal activity against bayberry twig blight disease pathogen Pestalotiopsis Versicolor," *NanoImpact*, vol. 21, p. 100281, 2021.
- [11] M. Siddique, N. Fayaz, and M. Saeed, "Synthesis, characterization, photocatalytic activity and gas sensing properties of zinc doped manganese oxide nanoparticles," *Physica B: Condensed Matter*, vol. 602, p. 412504, 2021.
- [12] M. Abdulla-Al-Mamun, Y. Kusumoto, and M. Muruganandham, "Simple new synthesis of copper nanoparticles in water/acetonitrile mixed solvent and their characterization," Materials Letters, vol. 63, no. 23, pp. 2007–2009.
- [13] Shikha Jain, Ankita Jain, Vijay Devra, Copper nanoparticles catalyzed oxidation of threonine by peroxomonosulfate, Journal of Saudi chemical society 18 (2014), 149 153.
- [14] E.C. Njagi, H. Huang, L. Stafford, H. Genuino, et al., Langmuir 27 (2011) 264–271.
- [15] Tariq Jan, J. Iqbal, Umar Farooq, Asma Gul, Rashda Abbasi, Ishaq Ahmad, Maaza Malik, Structural, Raman and optical characteristics of Sn doped CuO nanostructures: A novel anticancer agent, Ceramics International, 41(10), Part A December 2015, 13074 79. http://dx.doi.org/10.1016/j.ceramint.2015.06.080.

- [16] A. Rita, A. Sivakumar, S. A. Martin Britto Dhas, Influence of shock waves on structural and morphological properties of copper oxide NPs for aerospace applications, Journal of Nanostructure in Chemistry, 9 (2019), 225–230. <a href="https://doi.org/10.1007/s40097-019-00313-0">https://doi.org/10.1007/s40097-019-00313-0</a>
- [17] Saeid and, Asadi Asadollah, Tamijani-Habibi Amir, and Negahdary M, Synthesis of Zirconia Nanoparticles and their Ameliorative Roles as Additives Concrete Structures, Journal of Chemistry, 2013 |Article D 314862, 1-7, <a href="https://doi.org/10.1155/2013/314862">https://doi.org/10.1155/2013/314862</a> [18] M.A. Ramadan, S.H. Nassar, A.S. Montaser, E.M. El-Khatib and M.S.Abdel-Aziz, Synthesis of Nano-sized Zinc Oxide and Its Application for Cellulosic Textiles, Egypt. J. Chem. 59, No.4, pp. 523 535 (2016).
- [19] A.S. Aldwayyan, F.M. Al-Jekhedab, M. Al-Noaimi, B. Hammouti, T. B. Hadda, M. Suleiman, I. Warad, Synthesis and Characterization of CdO Nanoparticles Starting from Organometalic Dmphen-CdI2 complex, Int. J. Electrochem. Sci., 8 (2013) 10506 10514. [20] H.P. Klug, and L.E. Alexander, X-ray Diffraction Procedures for Polycrystalline and Amorphous Materials, Wiley, New York (1954).
- [21] Mohammadhassan Gholami-Shabani, Fattah Sotoodehnejadnematalahi, Masoomeh Shams-Ghahfarokhi, Ali Eslamifar and Mehdi Razzaghi-Abyaneh, Mycosynthesis and Physicochemical Characterization of Vanadium Oxide Nanoparticles Using the Cell-Free Filtrate of Fusarium oxysporum and Evaluation of Their Cytotoxic and Antifungal Activities, Journal of Nanomaterials, Volume 2021, Article ID 7532660, 1-7. <a href="https://doi.org/10.1155/2021/7532660">https://doi.org/10.1155/2021/7532660</a>.
- [22] Szu-HanWu, Dong-HwangChen, Synthesis and characterization of nickel nanoparticles by hydrazine reduction in ethylene glycol, <u>Journal of Colloid and Interface</u>

  <u>Science, Volume 259, (2), 15, 2003, pp 282-286, https://doi.org/10.1016/S0021-9797(02)00135-2.</u>

- [23] Sarjuna, K. and Ilangeswaran, D., Preparation and Physico-chemical studies of Ag<sub>2</sub>O nanoparticles using newly formed malonic acid and ZnCl<sub>2</sub>-based deep eutectic solvents. Mater. Today Proc. 49 (2022), pp. 2943–2948.
- [24] Thomas Nesakumar Jebakumar, Immanuel Edison, Raji Atchudan, Namachivayam Karthik Sundaram Chandrasekaran, Suguna Perumal, Pandian Bothi Raja, Veeradasan Perumal, Yong Rok Lee, Deep eutectic solvent assisted electrosynthesis of ruthenium nanoparticles on stainless steel mesh for electrocatalytic hydrogen evolution reaction, Fuel 297 (1) (2021) 120786.
- [25] A. El-Trass, H. ElShamy, I. El-Mehasseb, M. El-Kemary, CuO nanoparticles: synthesis, characterization, optical properties and interaction with amino acids, Appl. Surf. Sci. 258 (2012) 2997–3001.
- [26] Sundararaju Sathyavathi, Arumugam Manjula, Jeyaprakash Rajendhran, Paramasamy Gunasekaran, Biosynthesis and characterization of mercury sulphide nanoparticles produced by Bacillus cereus MRS-1, Indian J. Exp. Biol. 51 (2013) 973–978.
- [27] S. Ganeshan, P. Ramasundari, A. Elangovan, G. Arivazhagan, R. Vijayalakshmi, Synthesis and characterization of MnO2 nanoparticles: study of structural and optical properties, Int. J. Scient. Res. Phys. Appl. Sci. 5 (6) (2017) 5–8.
- [28] Ahmed Mishaal Mohammed, Mahmood Mohammed Ali, Synthesis and characterisation of zirconium oxide nanoparticles via the hydrothermal method and evaluation of their antibacterial activity, Res. J. Pharm. Technol. 14 (2) (2021), 938–942. [29] A. Rita, A. Sivakumar, S.A. Martin Britto Dhas, Influence of shock waves on structural and morphological properties of copper oxide NPs for aerospace applications, J. Nanostruct. Chem. 9 (2019) 225–230.

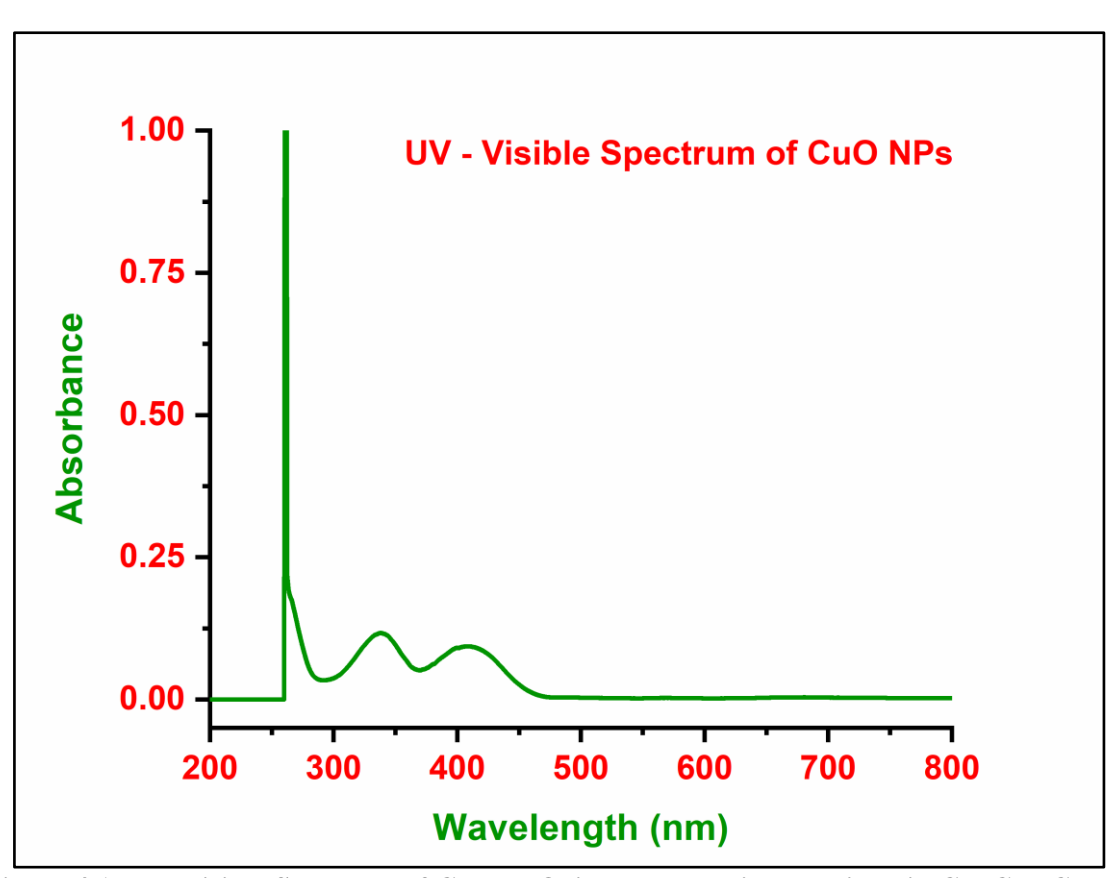


Figure 4.1: UV-Visible Spectrum of Copper Oxide Nanoparticle obtained in Ch. Cl-EG DES

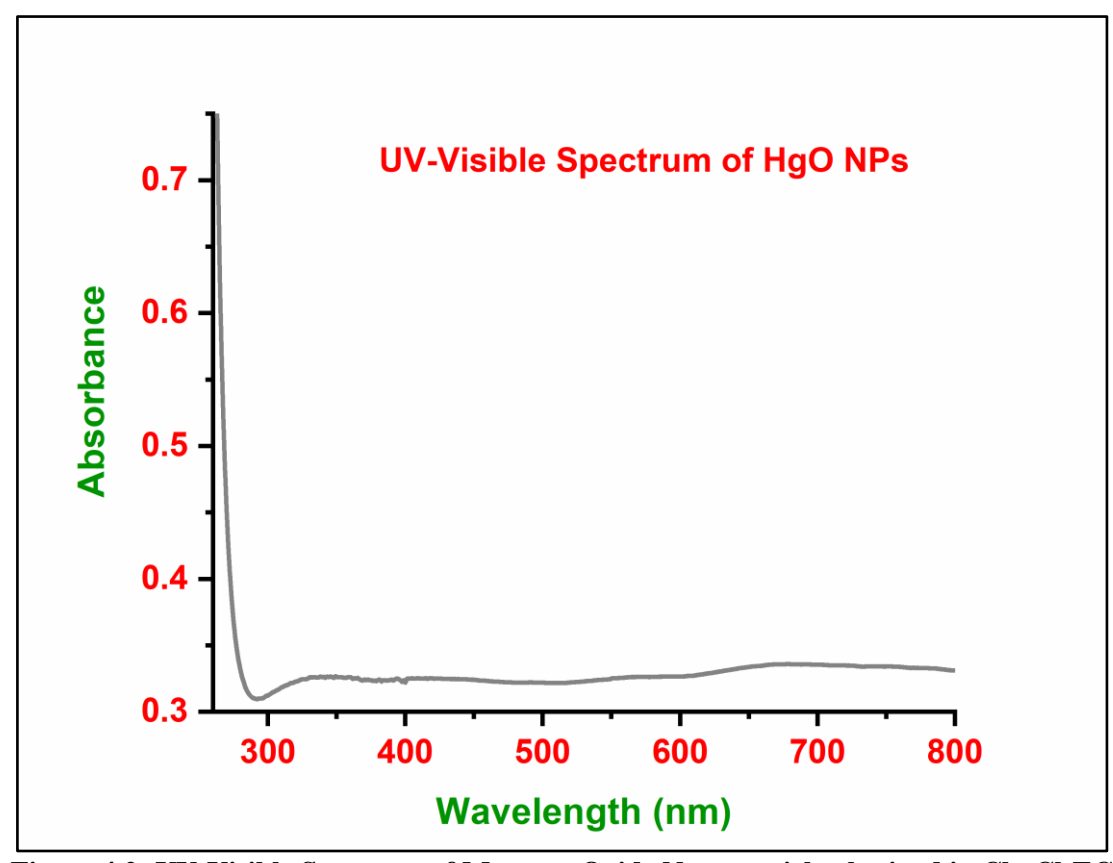


Figure 4.2: UV-Visible Spectrum of Mercury Oxide Nanoparticle obtained in Ch. Cl-EG DES

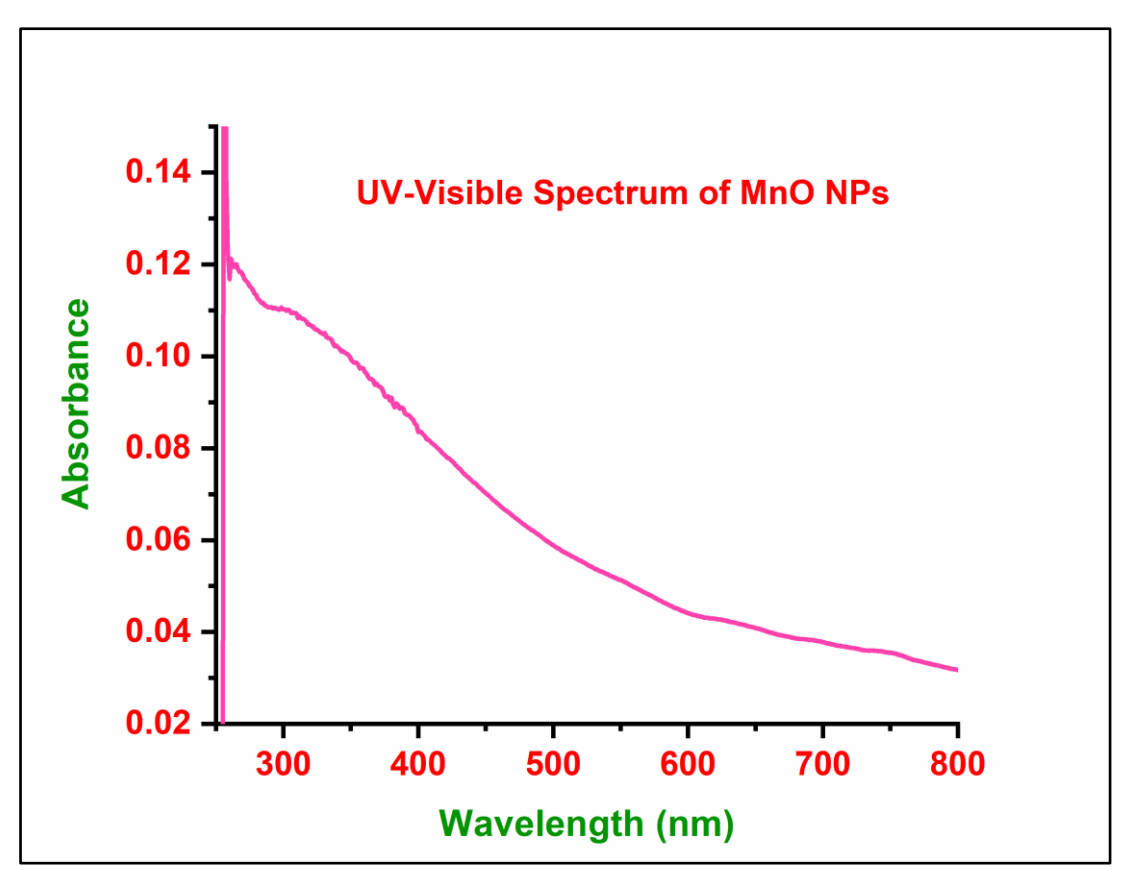


Figure 4.3: UV-Visible Spectrum of Manganese Oxide Nanoparticle obtained in Ch. Cl-EG DES

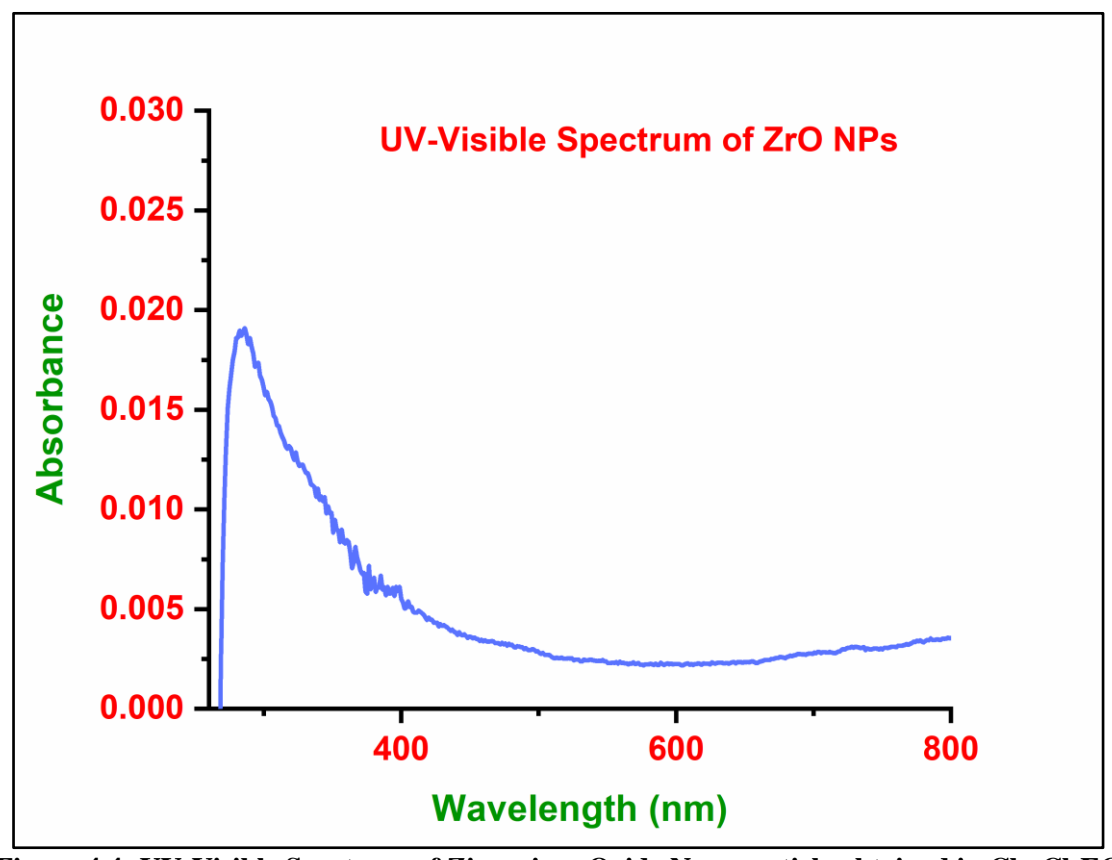


Figure 4.4: UV-Visible Spectrum of Zirconium Oxide Nanoparticle obtained in Ch. Cl-EG DES

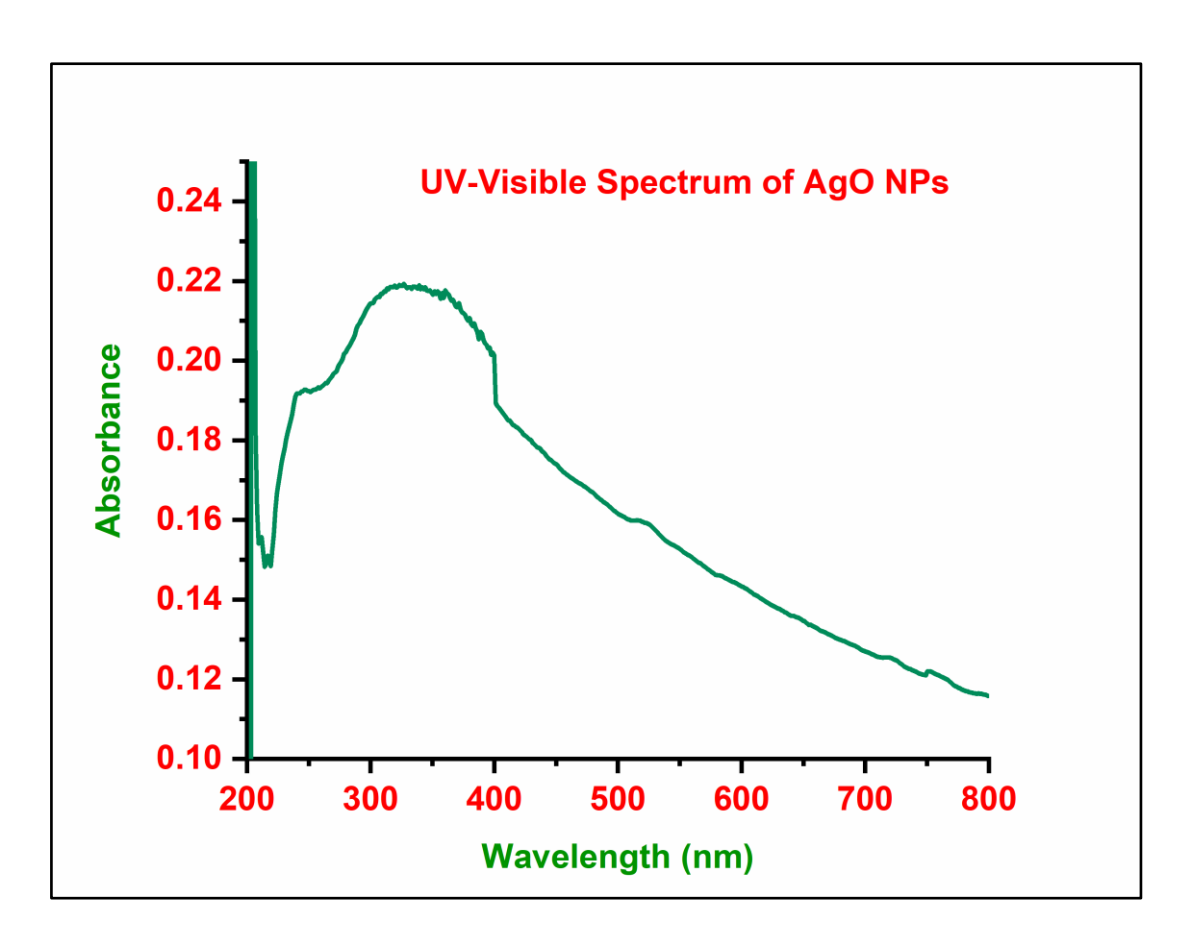


Figure 4.5: UV-Visible Spectrum of Silver Oxide Nanoparticle obtained in Ch. Cl-EG DES

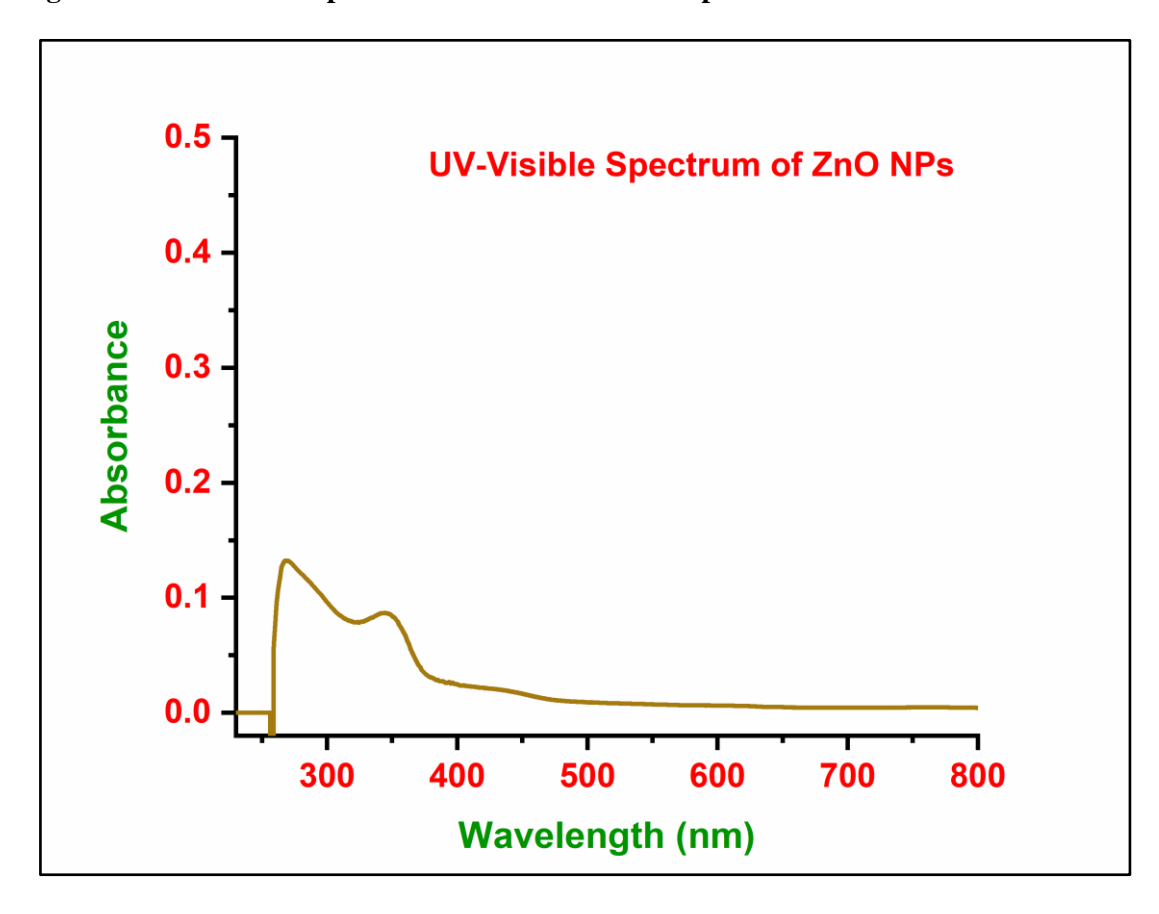


Figure 4.6: UV-Visible Spectrum of Zinc Oxide Nanoparticle obtained in Ch. Cl-EG DES

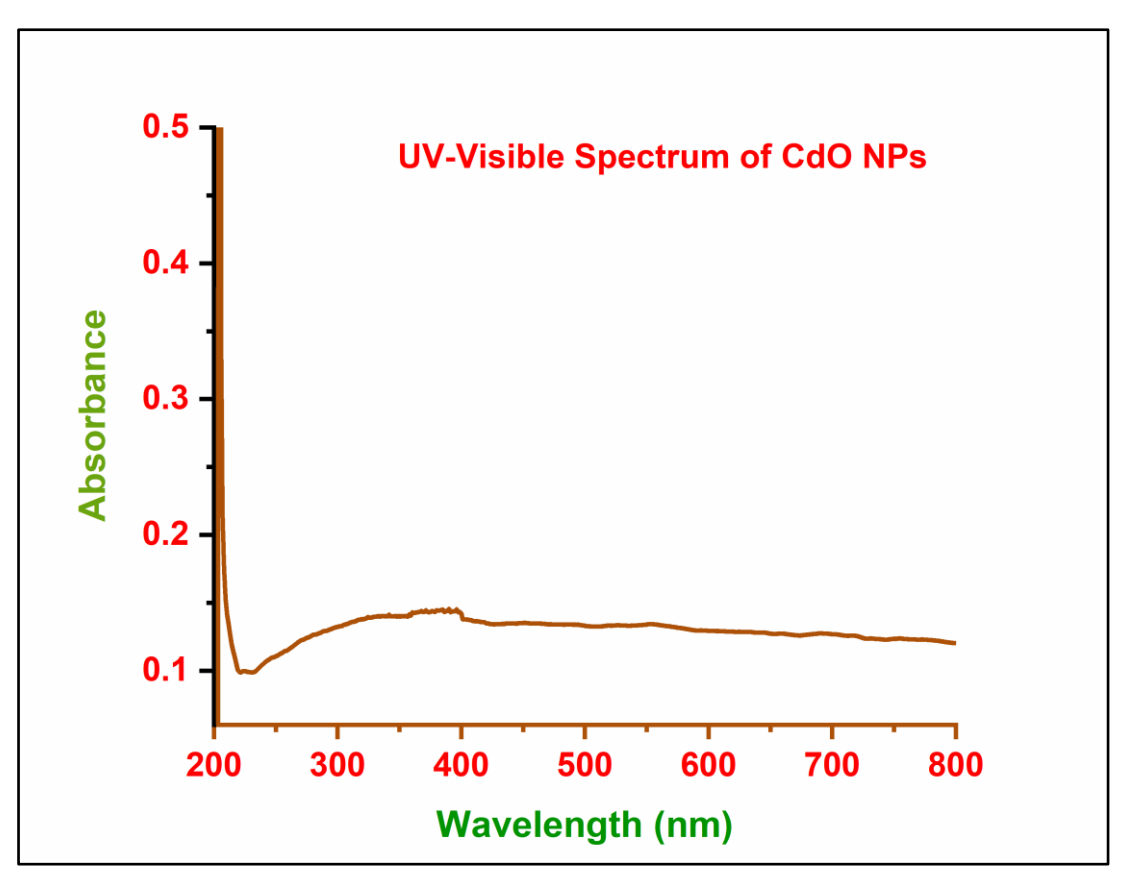


Figure 4.7: UV-Visible Spectrum of Cadmium Oxide Nanoparticle obtained in Ch. Cl-EG DES

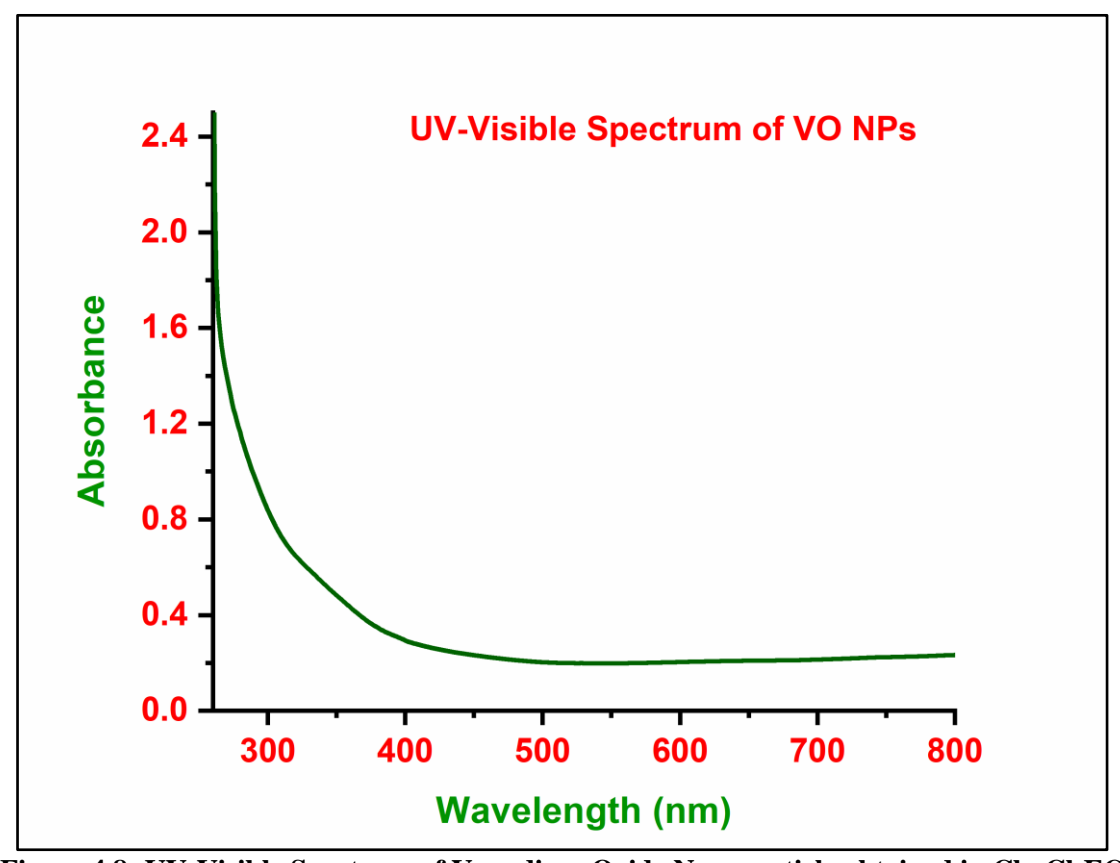


Figure 4.8: UV-Visible Spectrum of Vanadium Oxide Nanoparticle obtained in Ch. Cl-EG DES

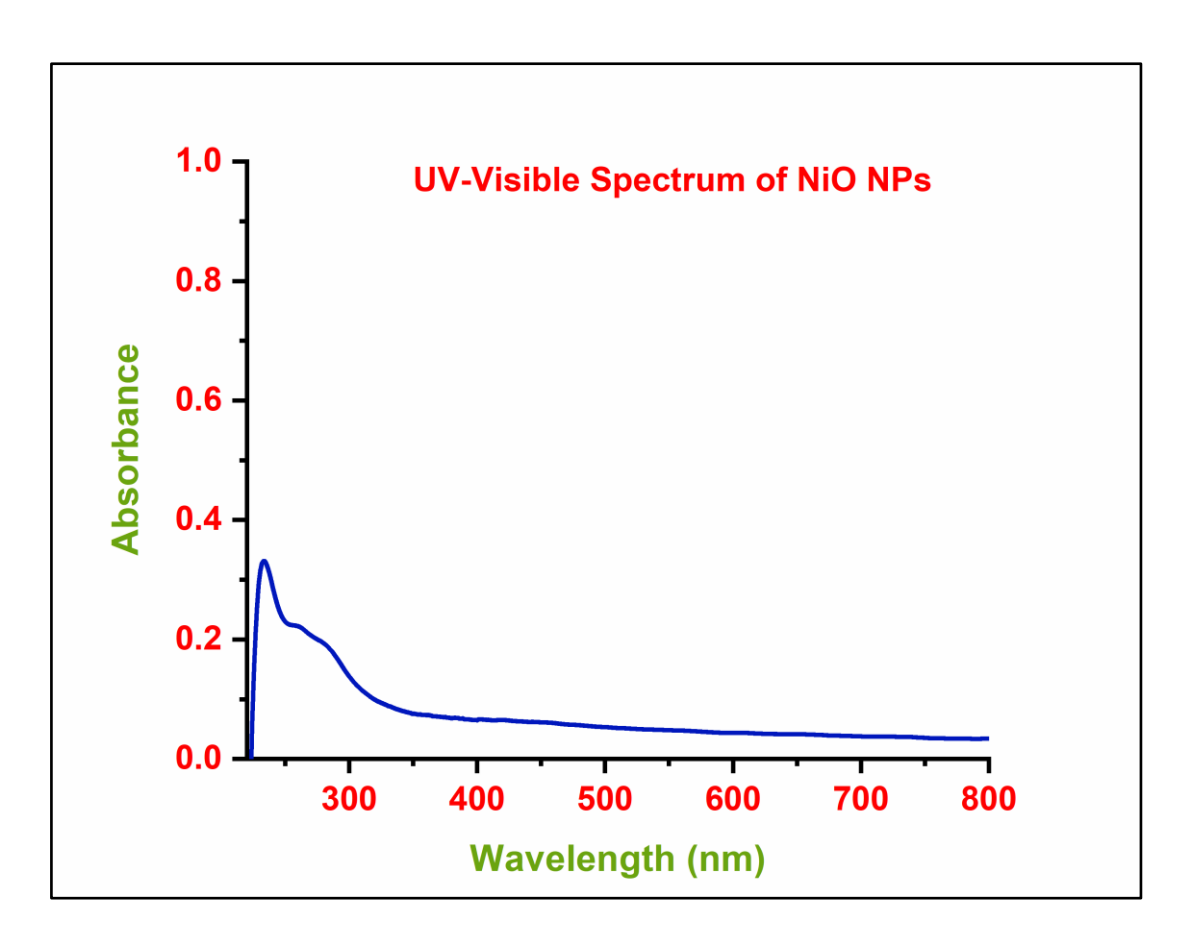


Figure 4.9: UV-Visible Spectrum of Nickel Oxide Nanoparticle obtained in Ch. Cl-EG DES

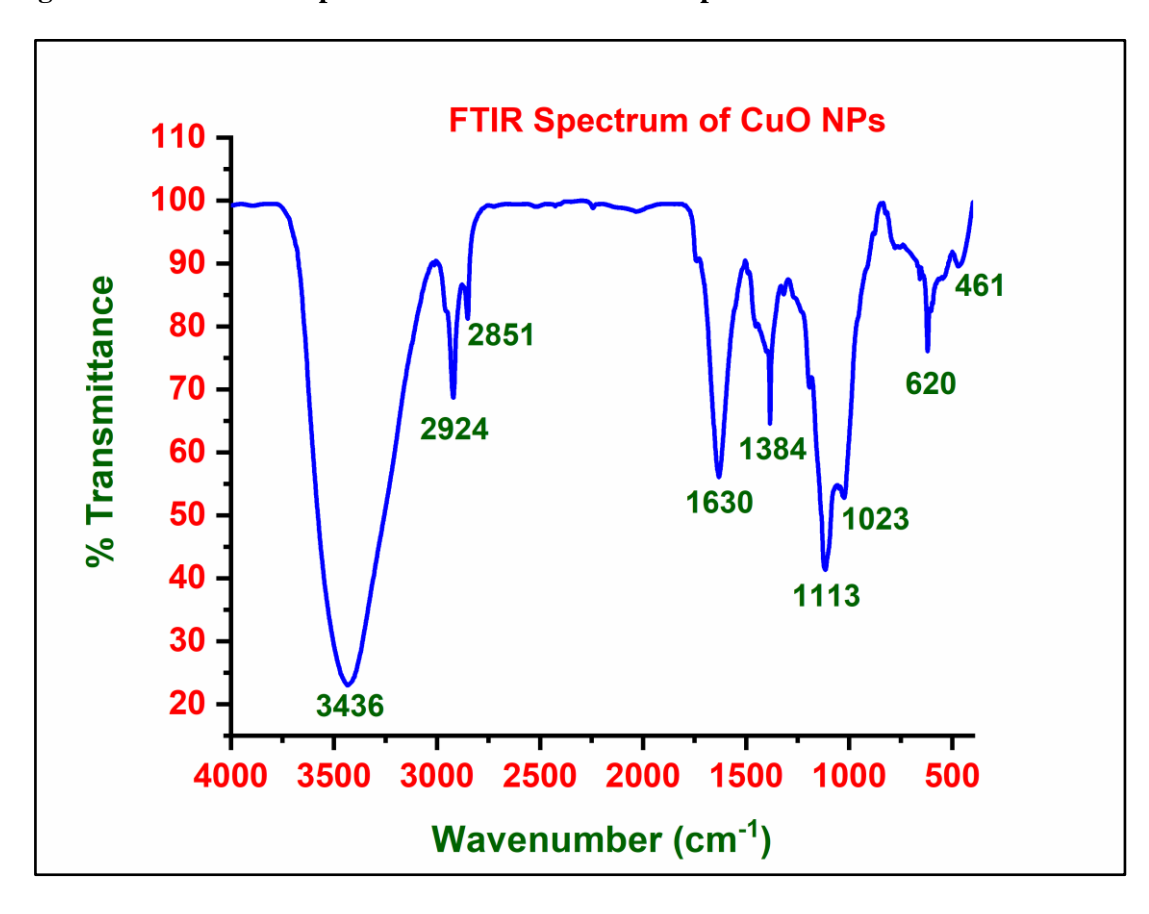


Figure 4.10: FTIR Spectrum of Copper Oxide Nanoparticle obtained in Ch. Cl-EG DES

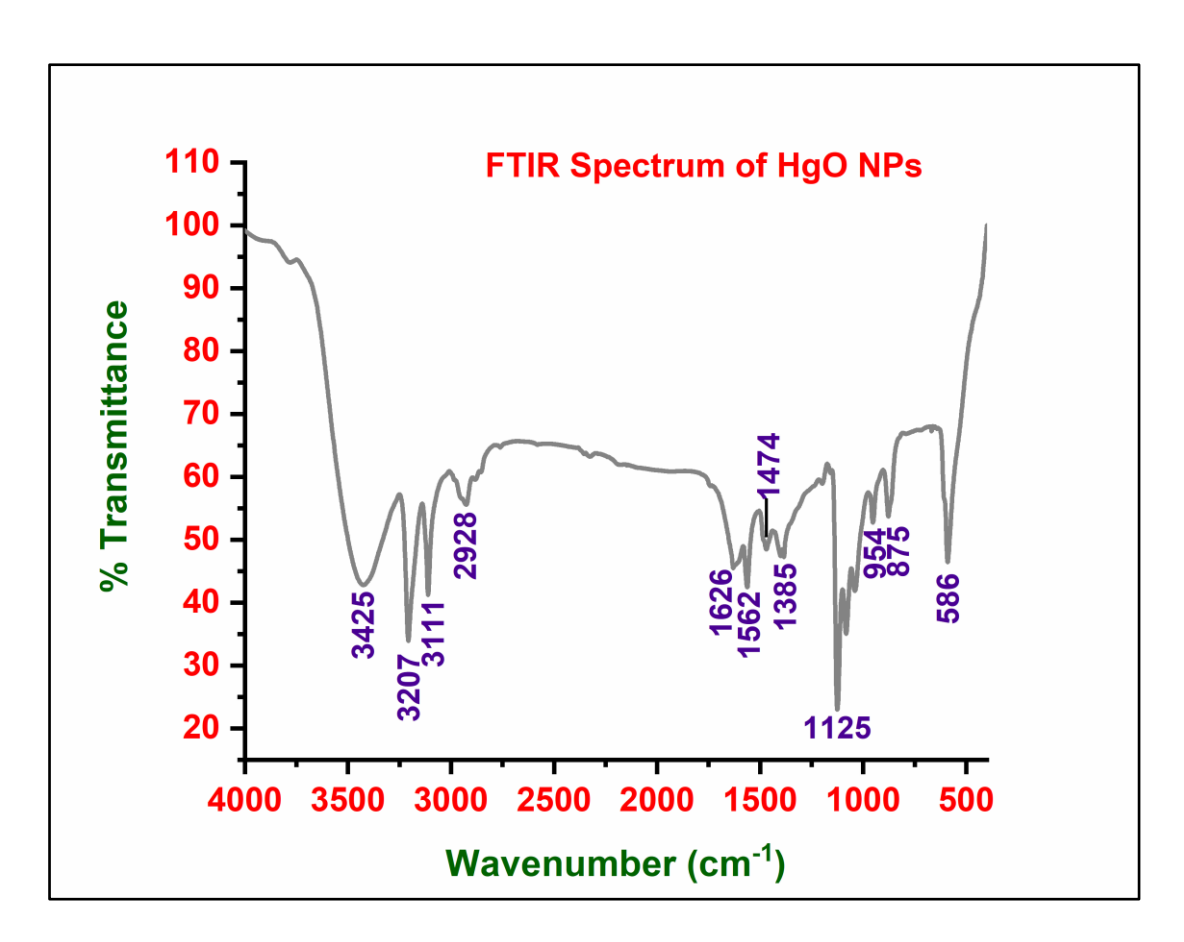


Figure 4.11: FTIR Spectrum of Mercury Oxide Nanoparticle obtained in Ch. Cl-EG DES

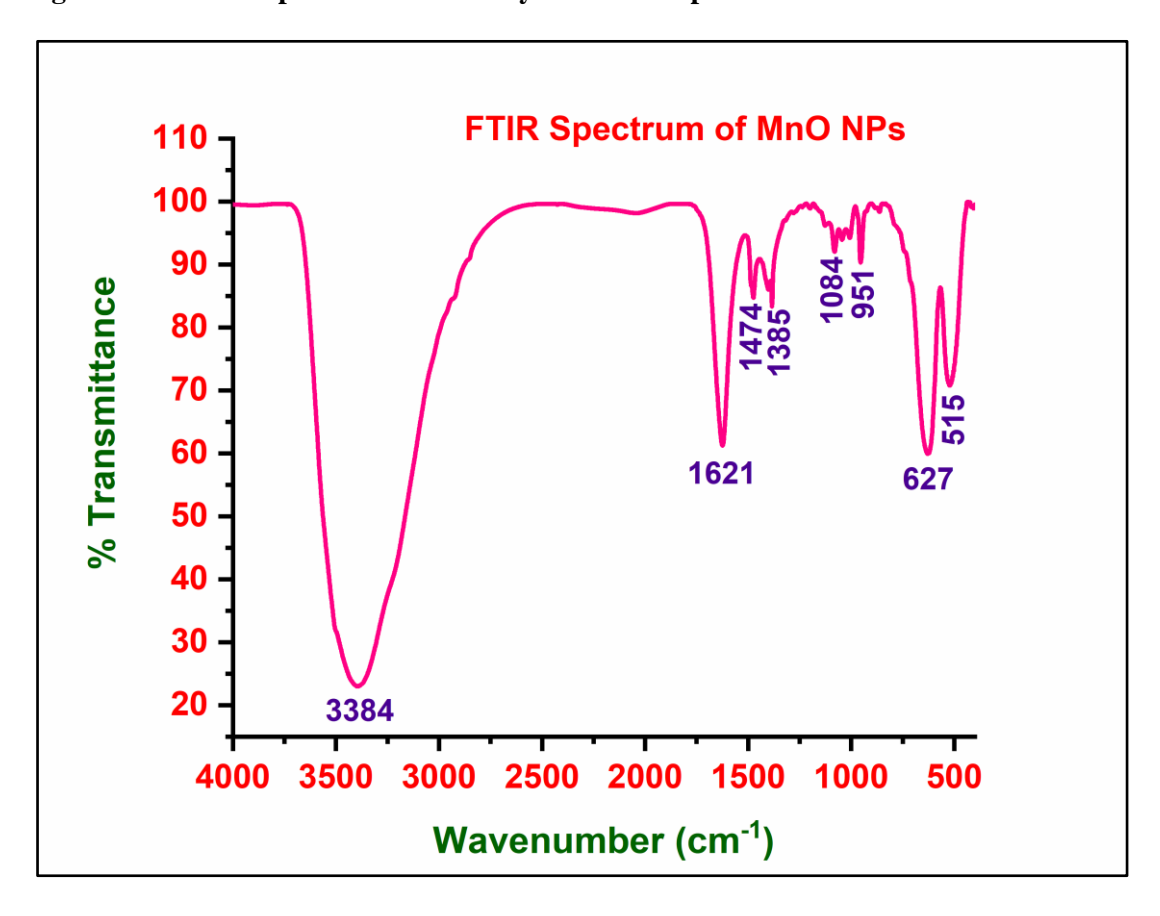


Figure 4.12: FTIR Spectrum of Manganese Oxide Nanoparticle obtained in Ch. Cl-EG DES

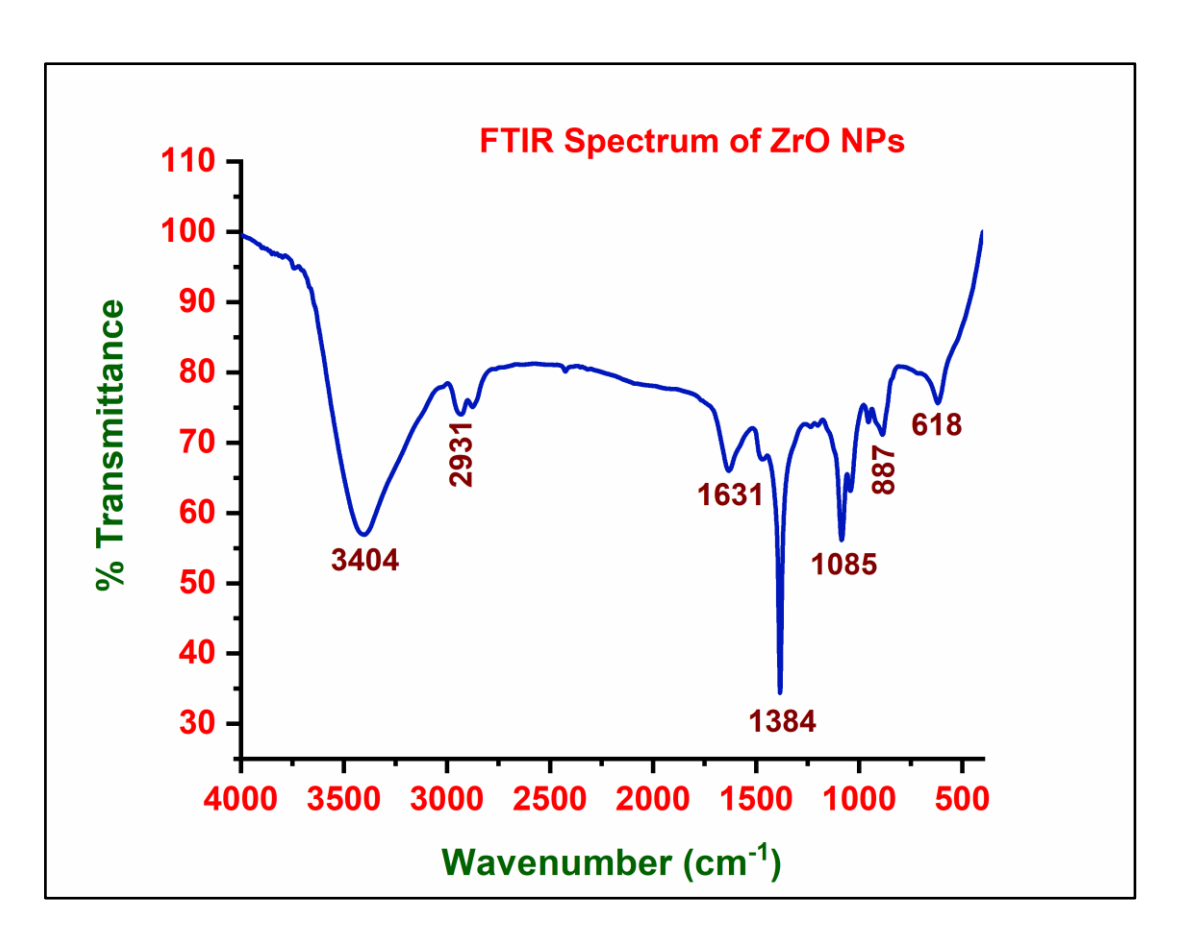


Figure 4.13: FTIR Spectrum of Zirconium Oxide Nanoparticle obtained in Ch. Cl-EG DES

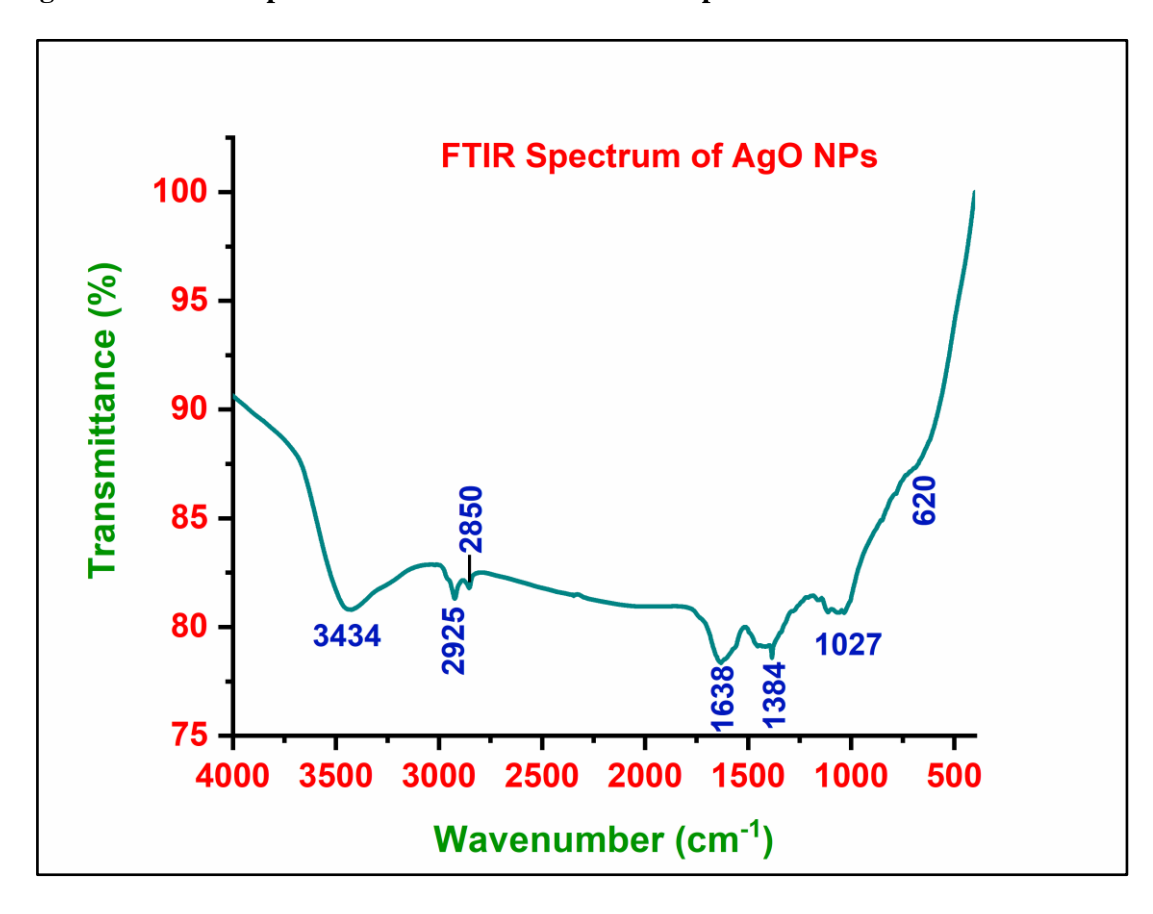


Figure 4.14: FTIR Spectrum of Silver Oxide Nanoparticle obtained in Ch. Cl-EG DES

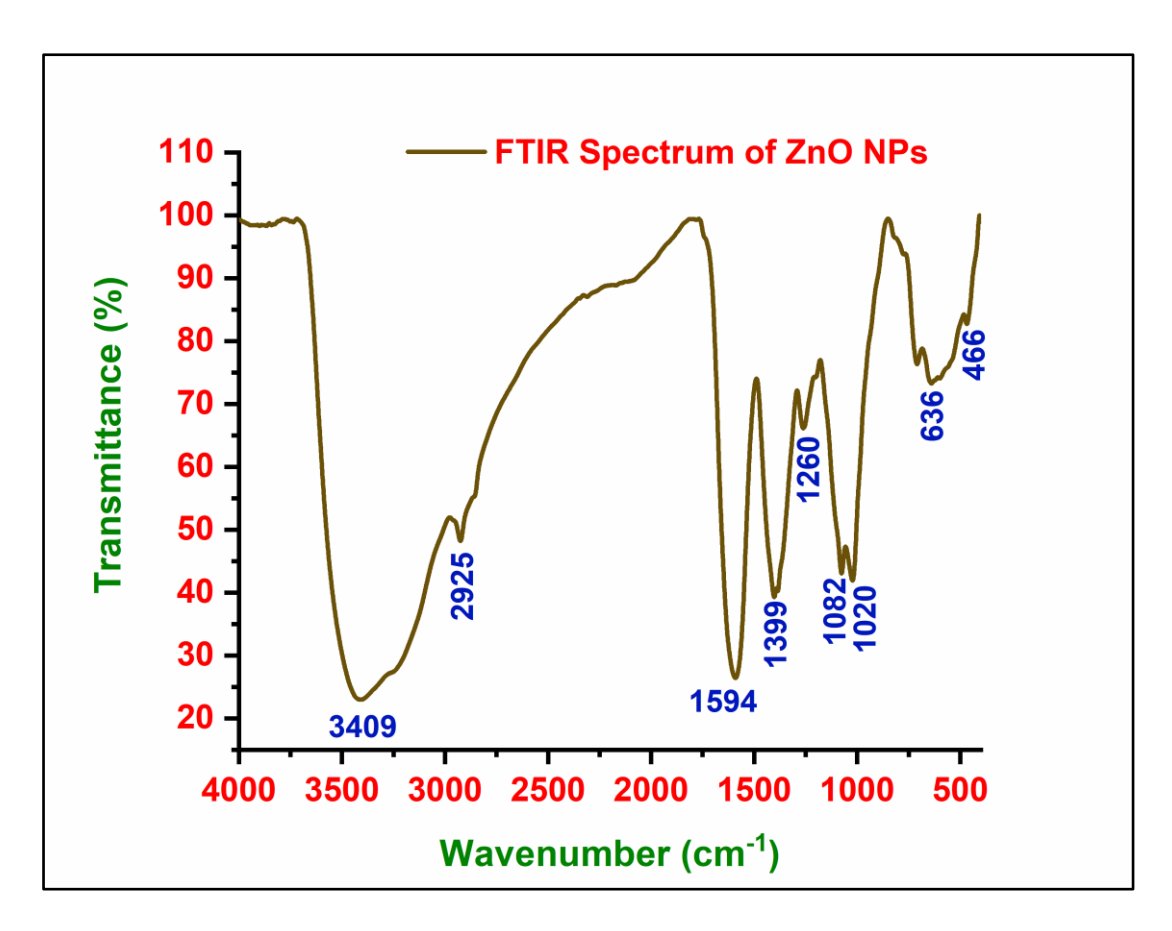


Figure 4.15: FTIR Spectrum of Zinc Oxide Nanoparticle obtained in Ch. Cl-EG DES

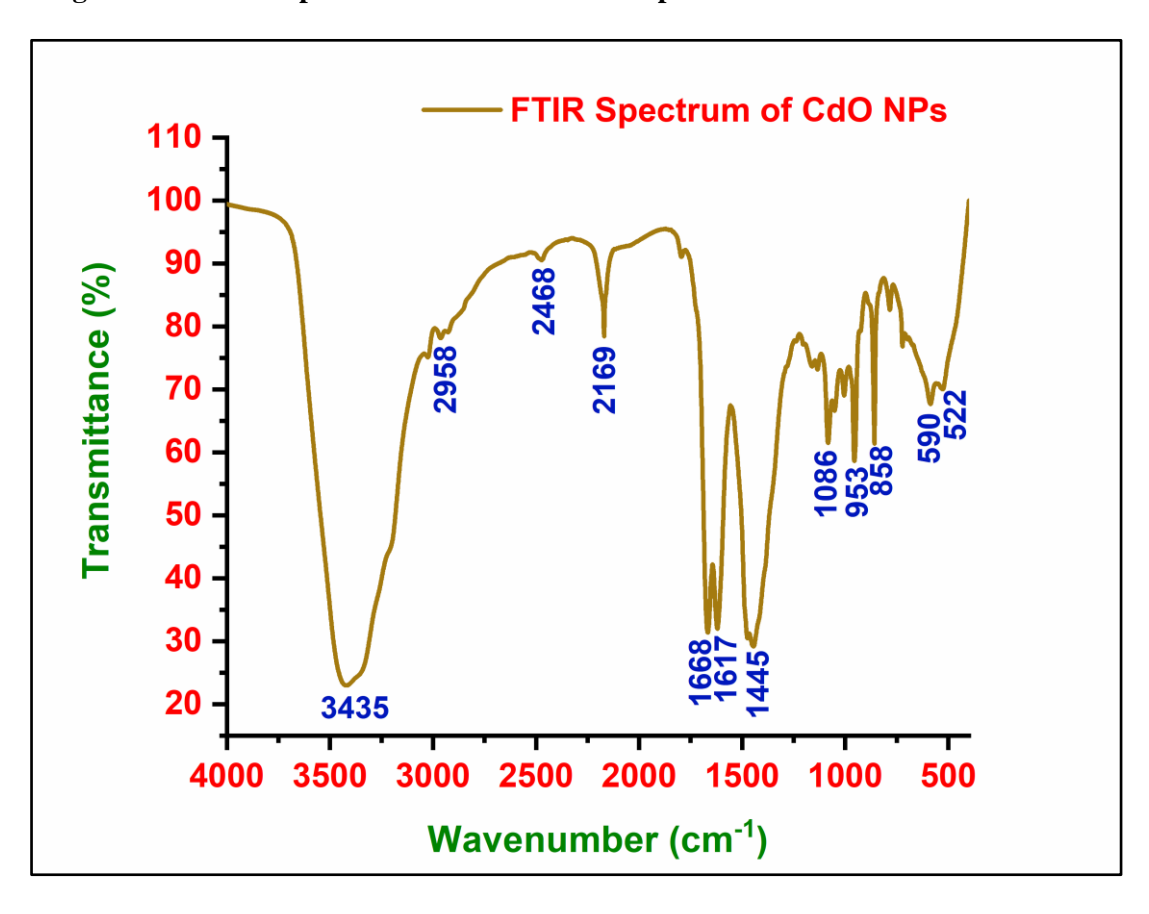


Figure 4.16: FTIR Spectrum of Cadmium Oxide Nanoparticle obtained in Ch. Cl-EG DES

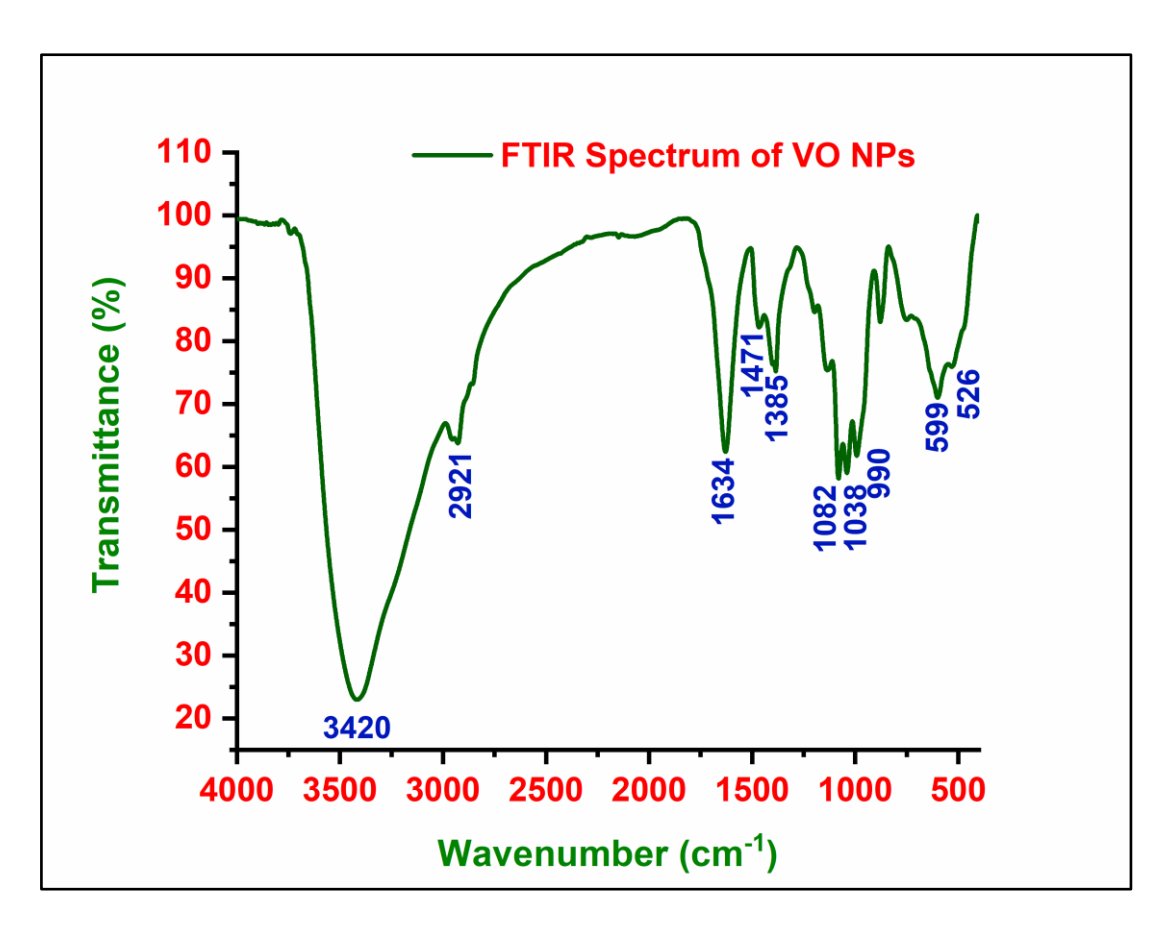


Figure 4.17: FTIR Spectrum of Vanadium Oxide Nanoparticle obtained in Ch. Cl-EG DES

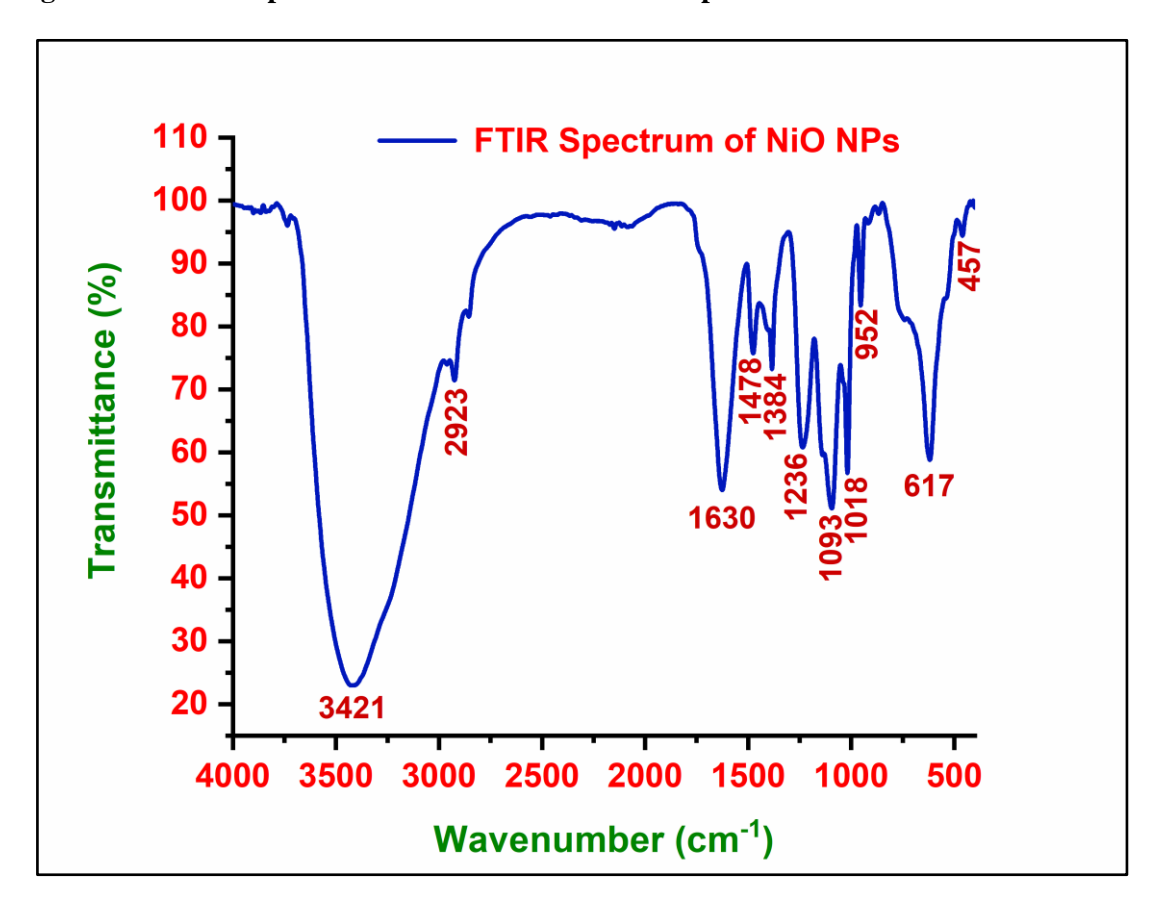


Figure 4.18: FTIR Spectrum of Nickel Oxide Nanoparticle obtained in Ch. Cl-EG DES

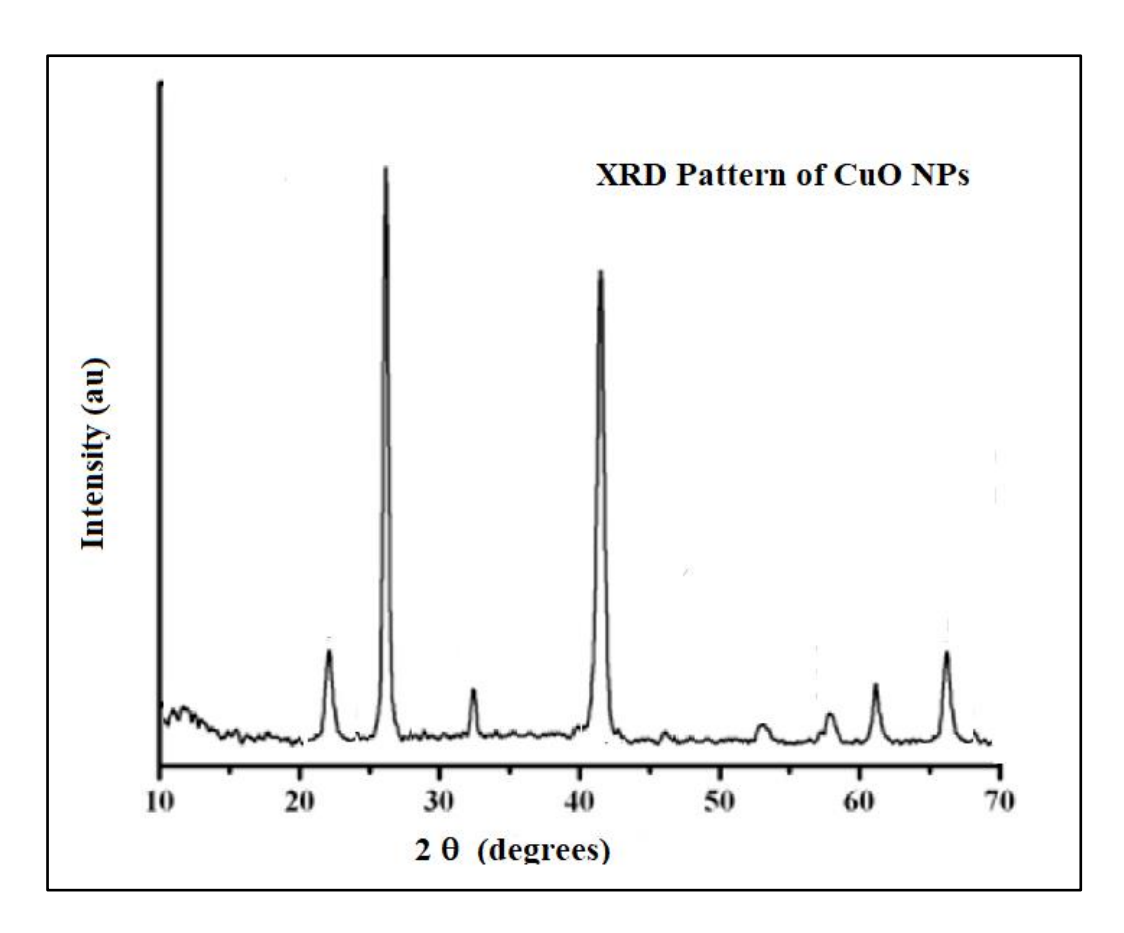


Figure 4.19: XRD Pattern of Copper Oxide Nanoparticle obtained in Ch. Cl-EG DES

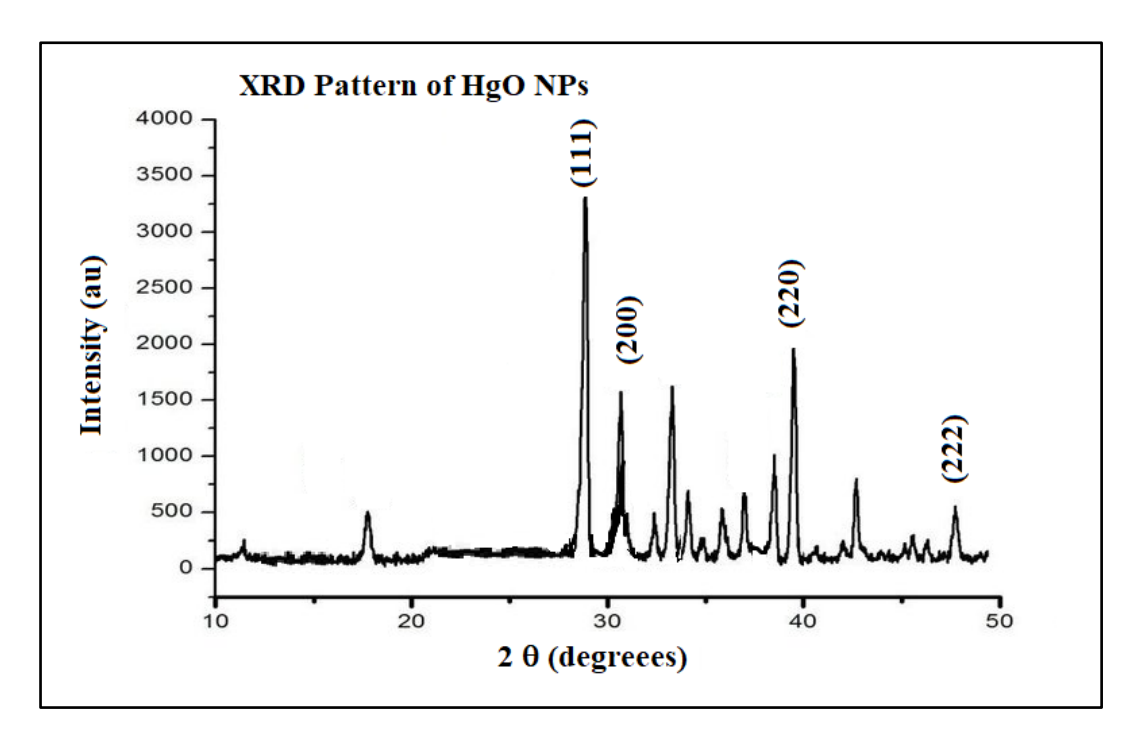


Figure 4.20: XRD Pattern of Mercury Oxide Nanoparticle obtained in Ch. Cl-EG DES

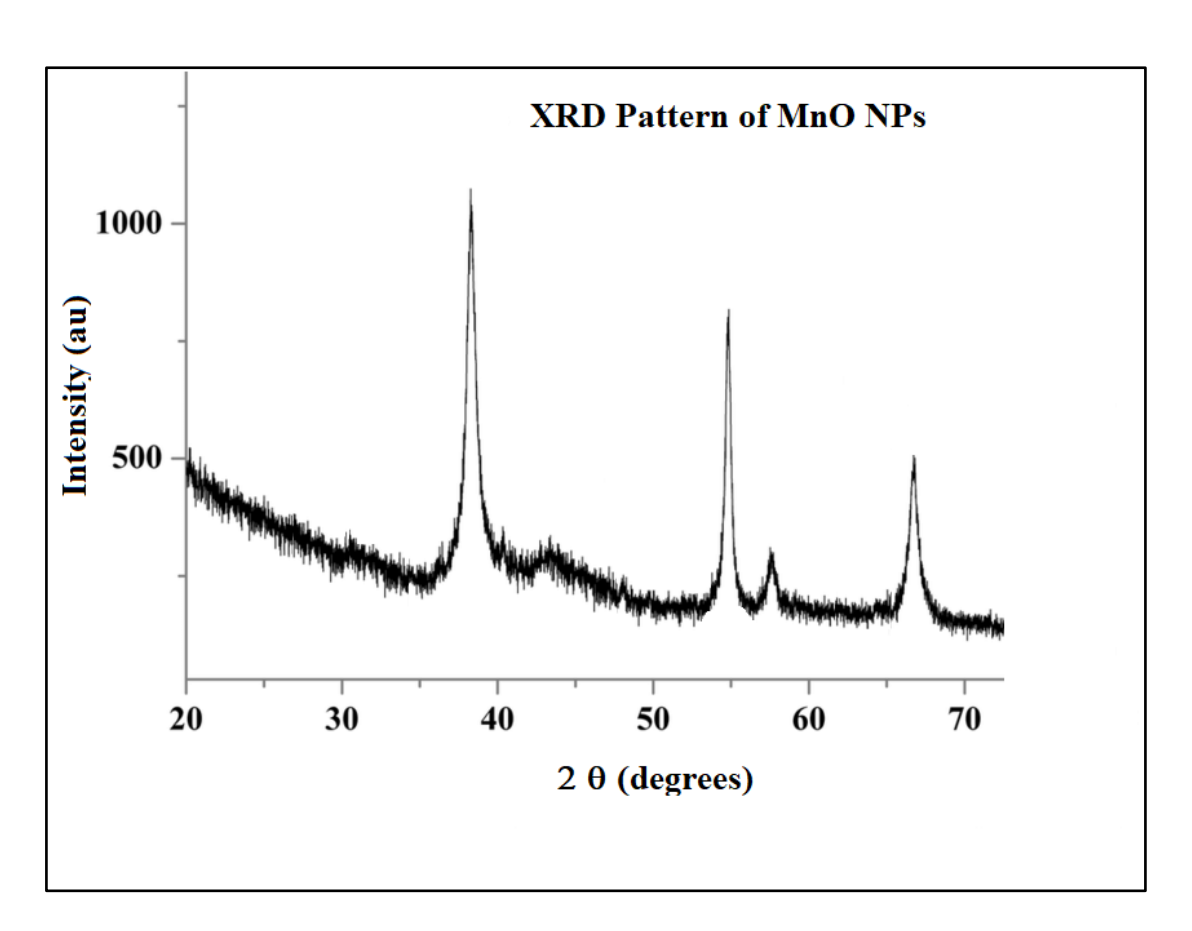


Figure 4.21: XRD Pattern of Manganese Oxide Nanoparticle obtained in Ch. Cl-EG DES

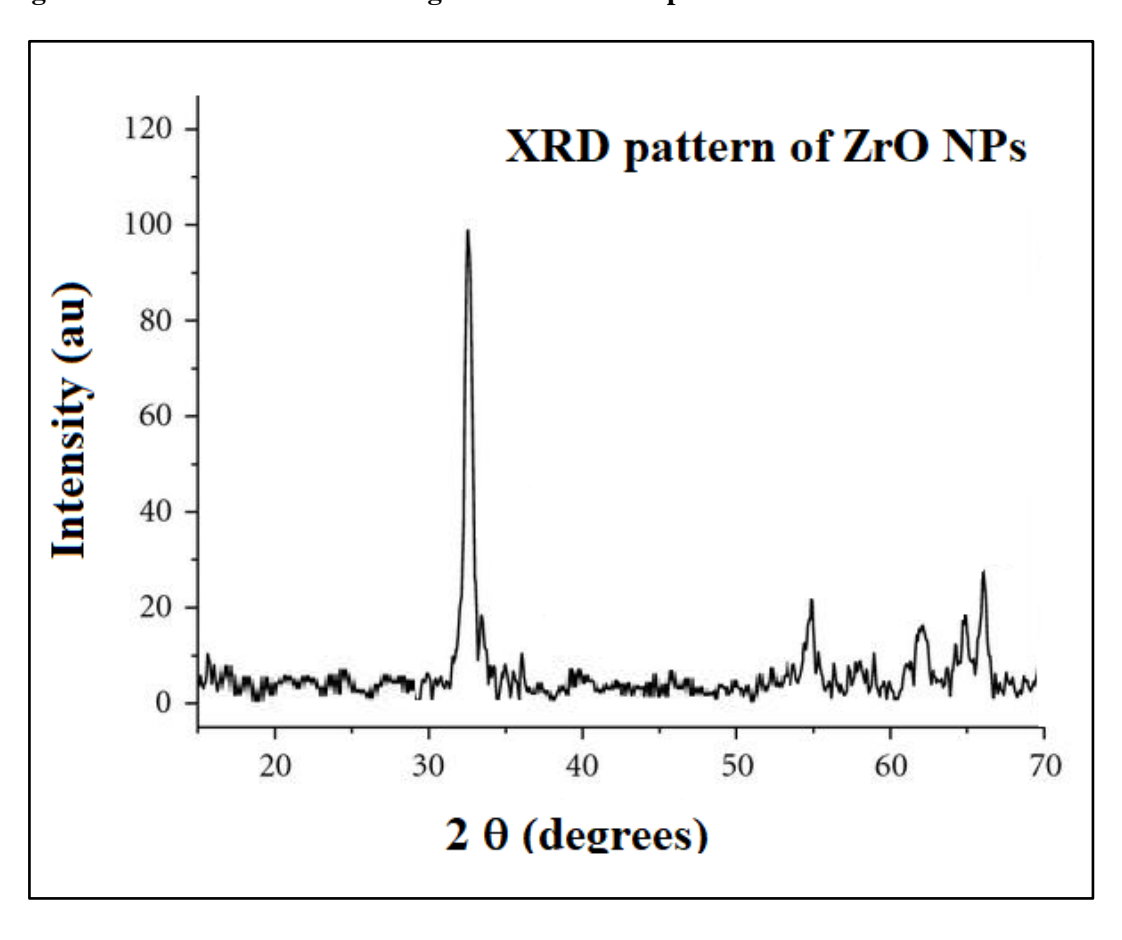


Figure 4.22: XRD Pattern of Zirconium Oxide Nanoparticle obtained in Ch. Cl-EG DES

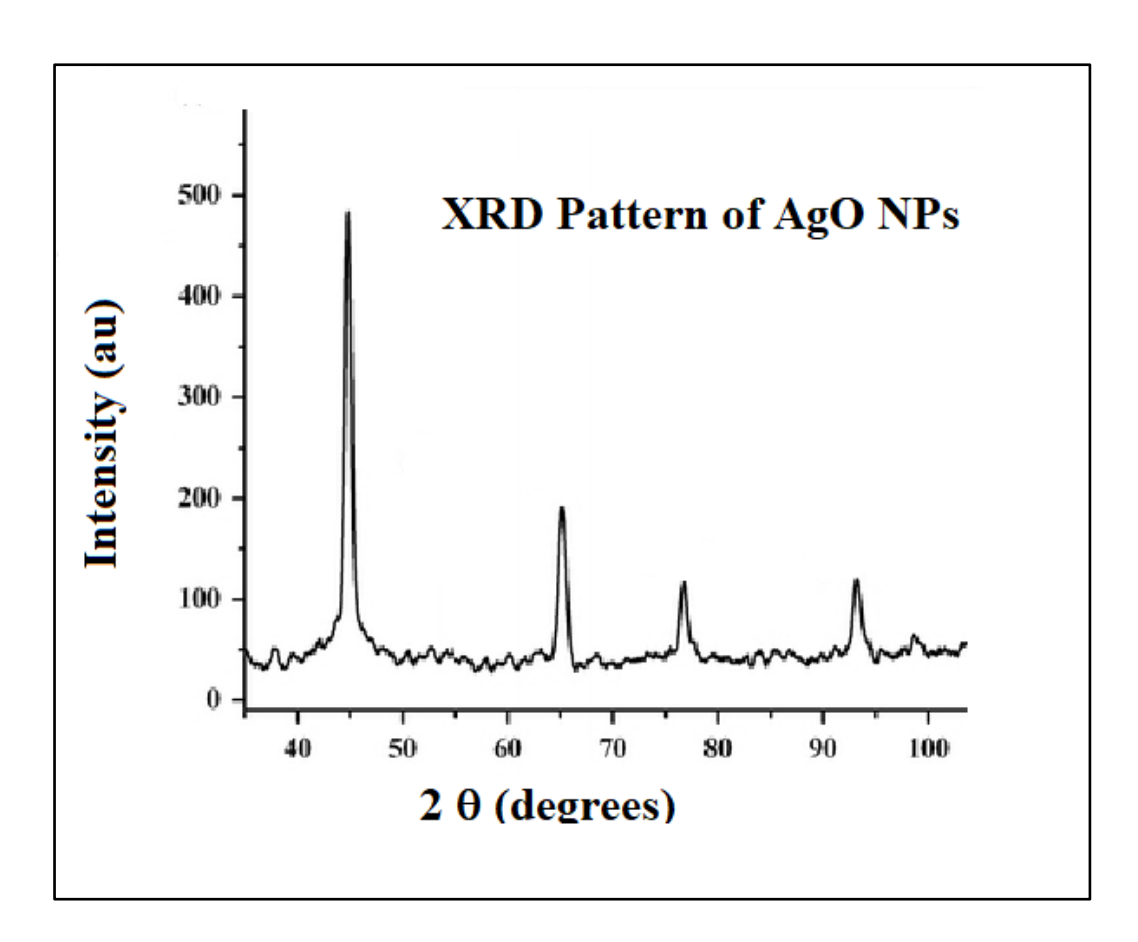


Figure 4.23: XRD Pattern of Silver Oxide Nanoparticle obtained in Ch. Cl-EG DES

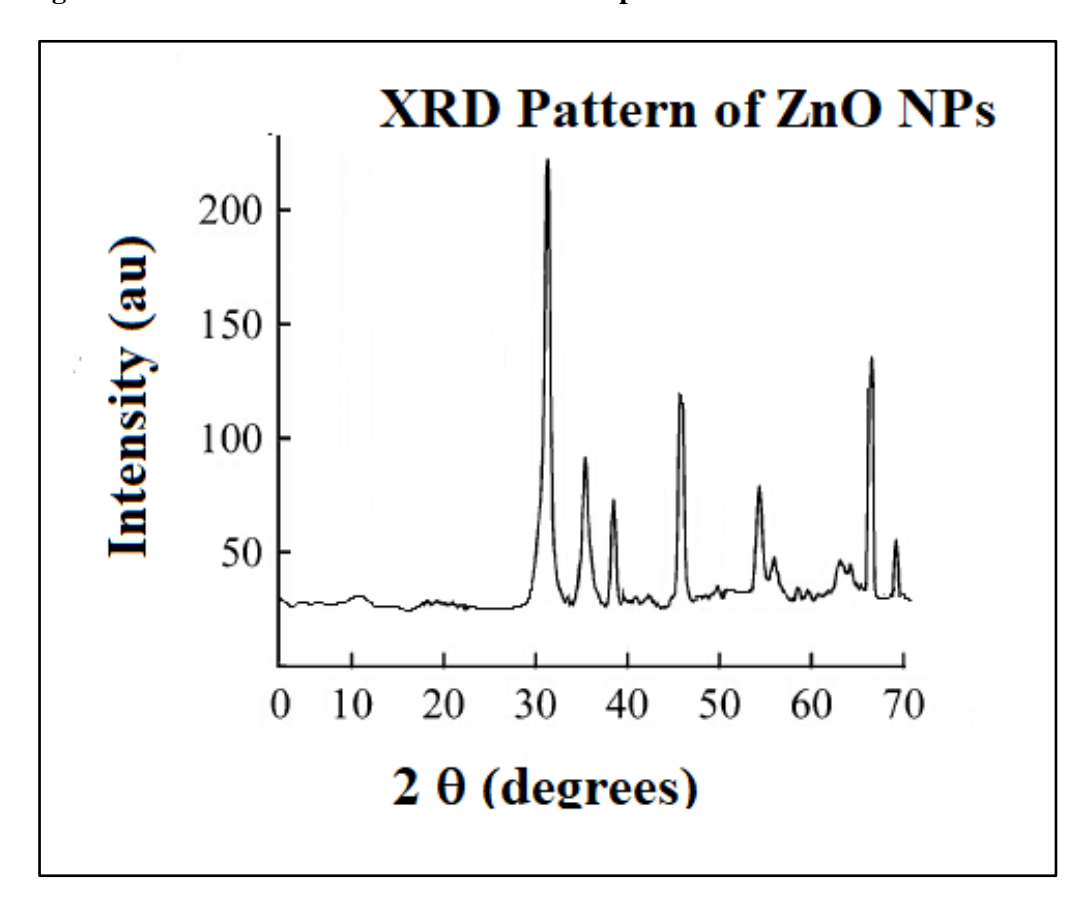


Figure 4.24: XRD Pattern of Zinc Oxide Nanoparticle obtained in Ch. Cl-EG DES

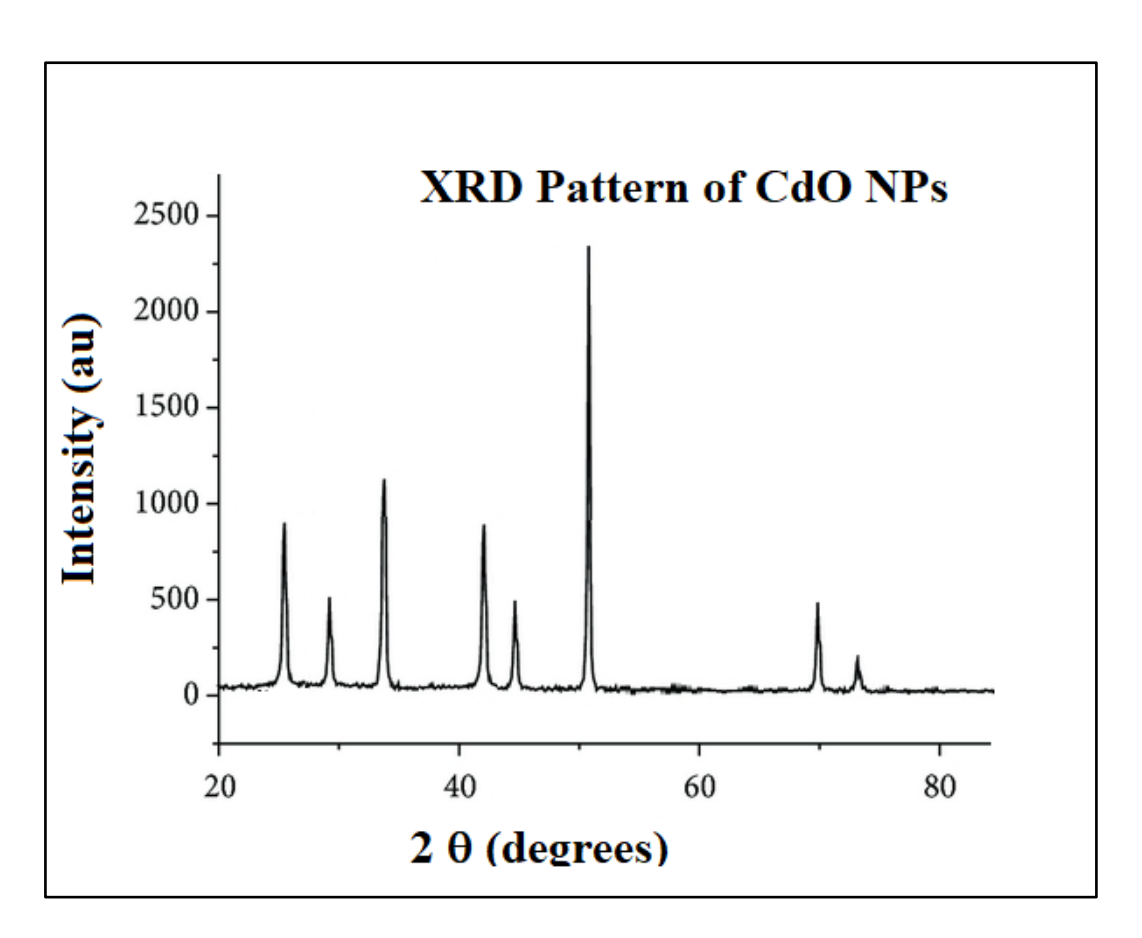


Figure 4.25: XRD Pattern of Cadmium Oxide Nanoparticle obtained in Ch. Cl-EG DES

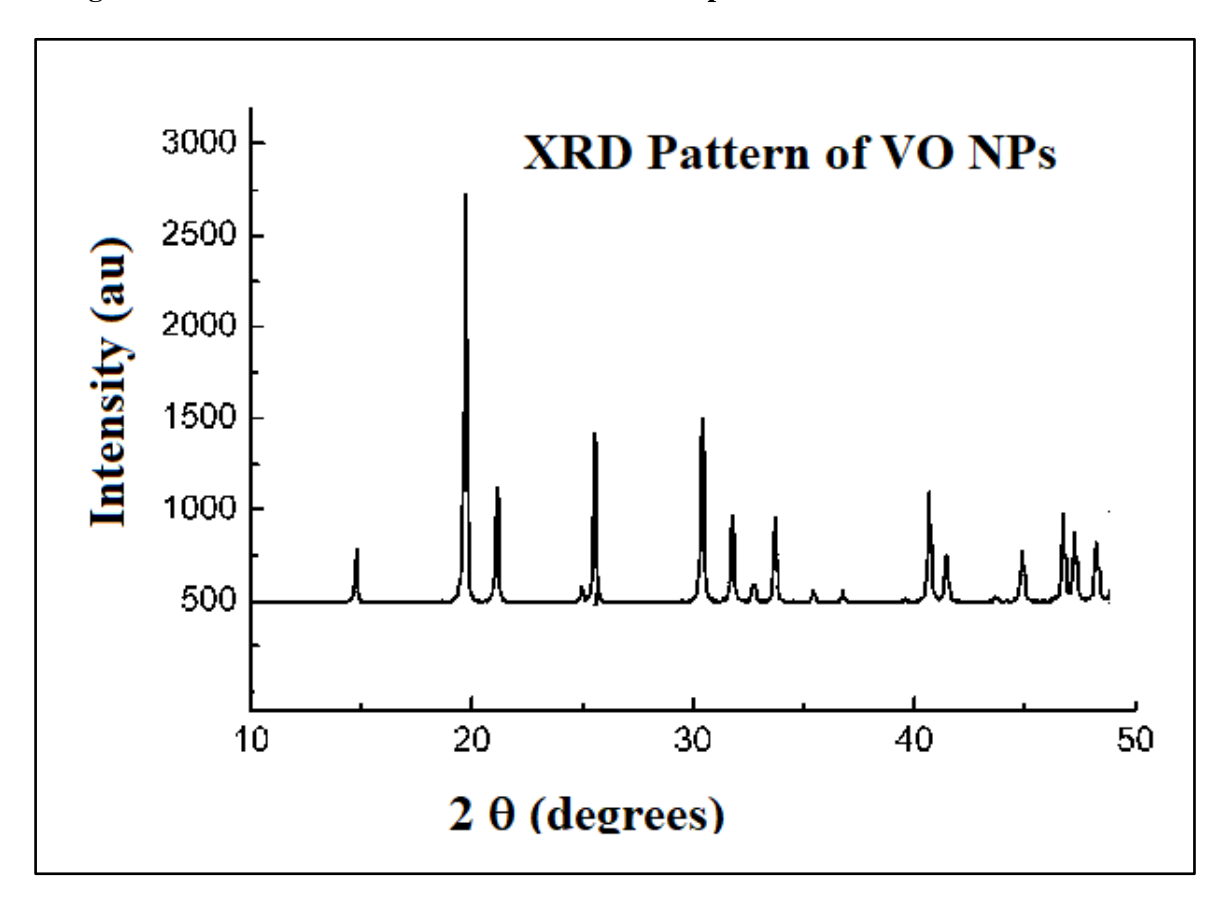


Figure 4.26: XRD Pattern of Vanadium Oxide Nanoparticle obtained in Ch. Cl-EG DES

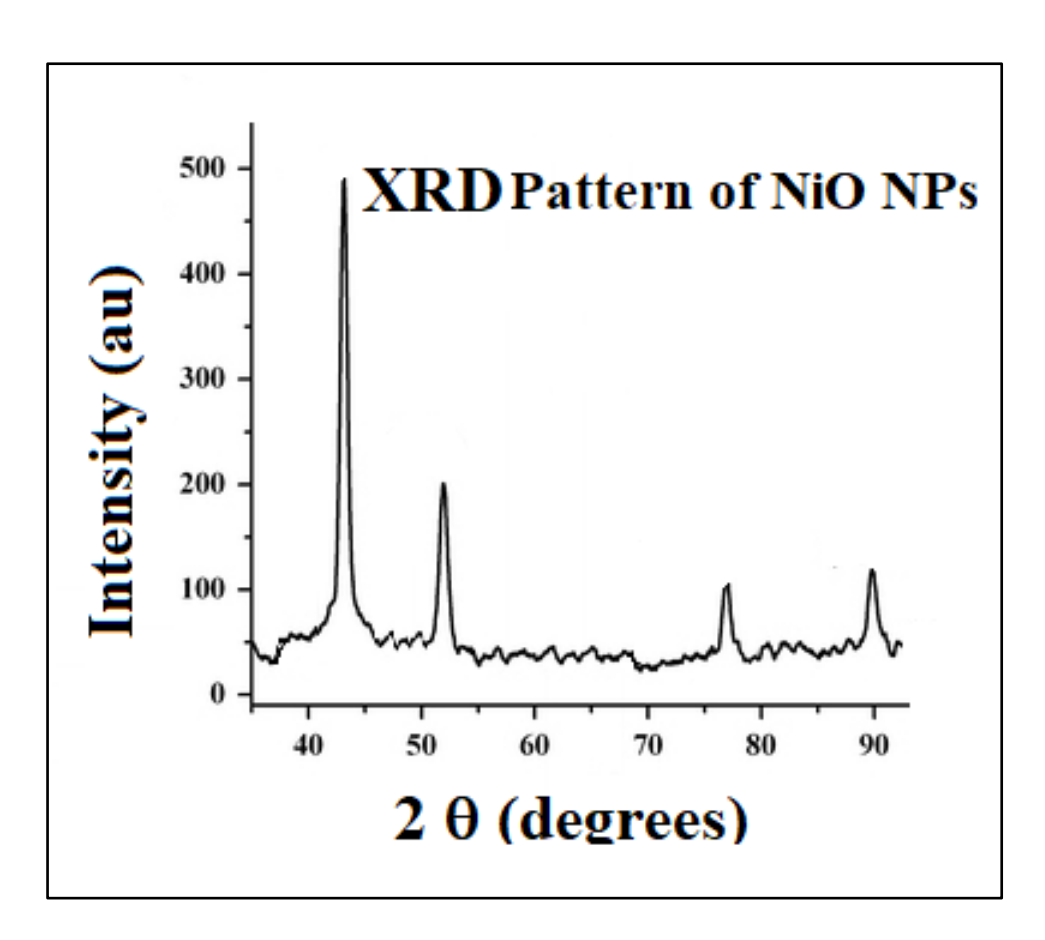


Figure 4.27: XRD Pattern of Nickel Oxide Nanoparticle obtained in Ch. Cl-EG DES

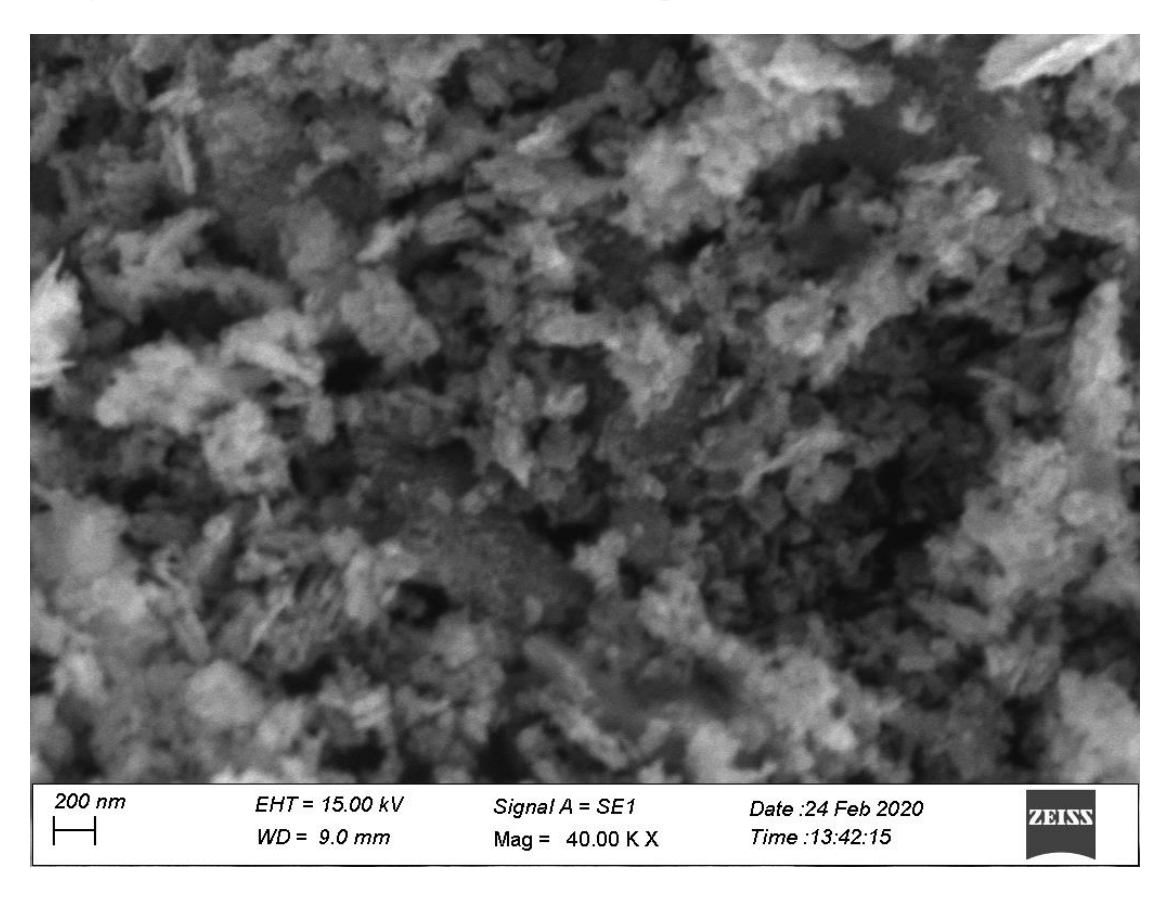


Figure 4.28: SEM Image of Copper Oxide Nanoparticle obtained in Ch. Cl-EG DES

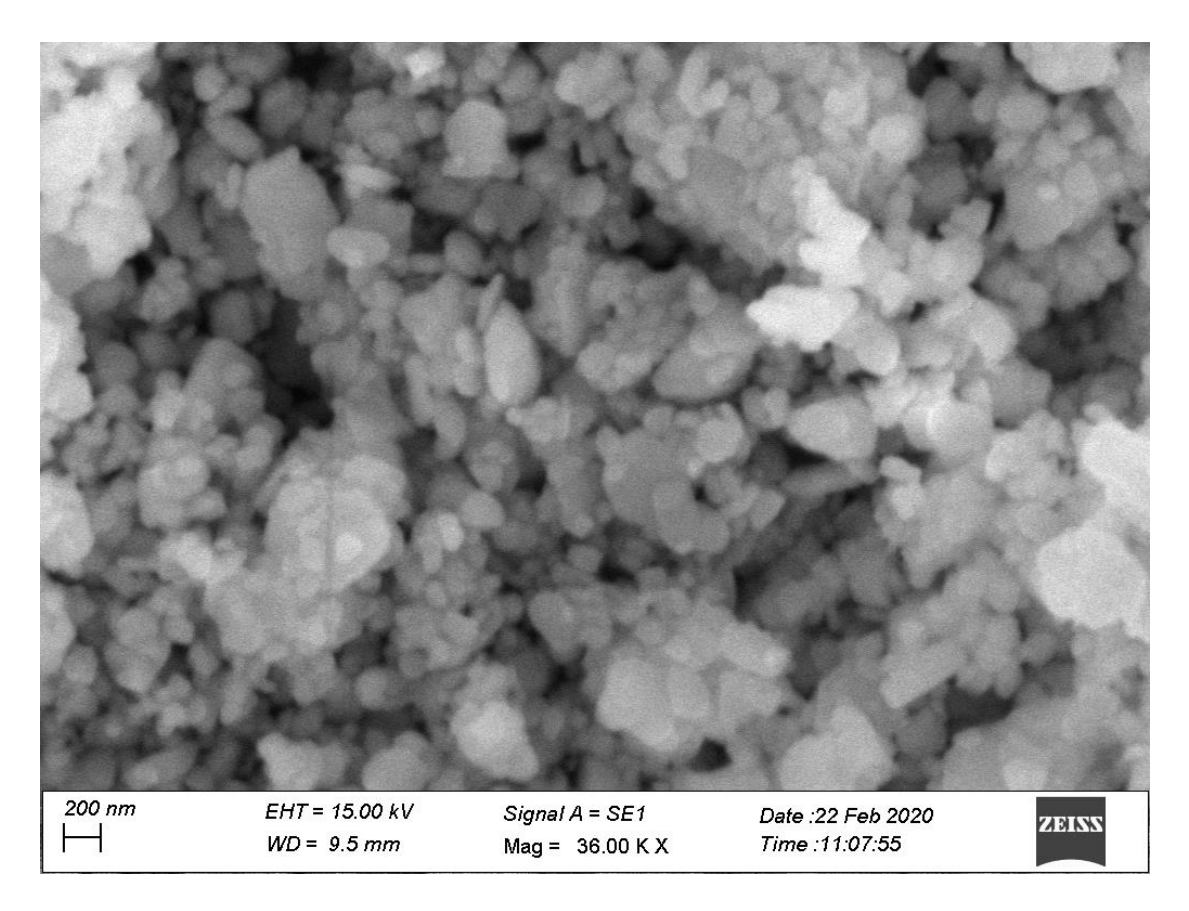


Figure 4.29: SEM Image of Mercury Oxide Nanoparticle obtained in Ch. Cl-EG DES

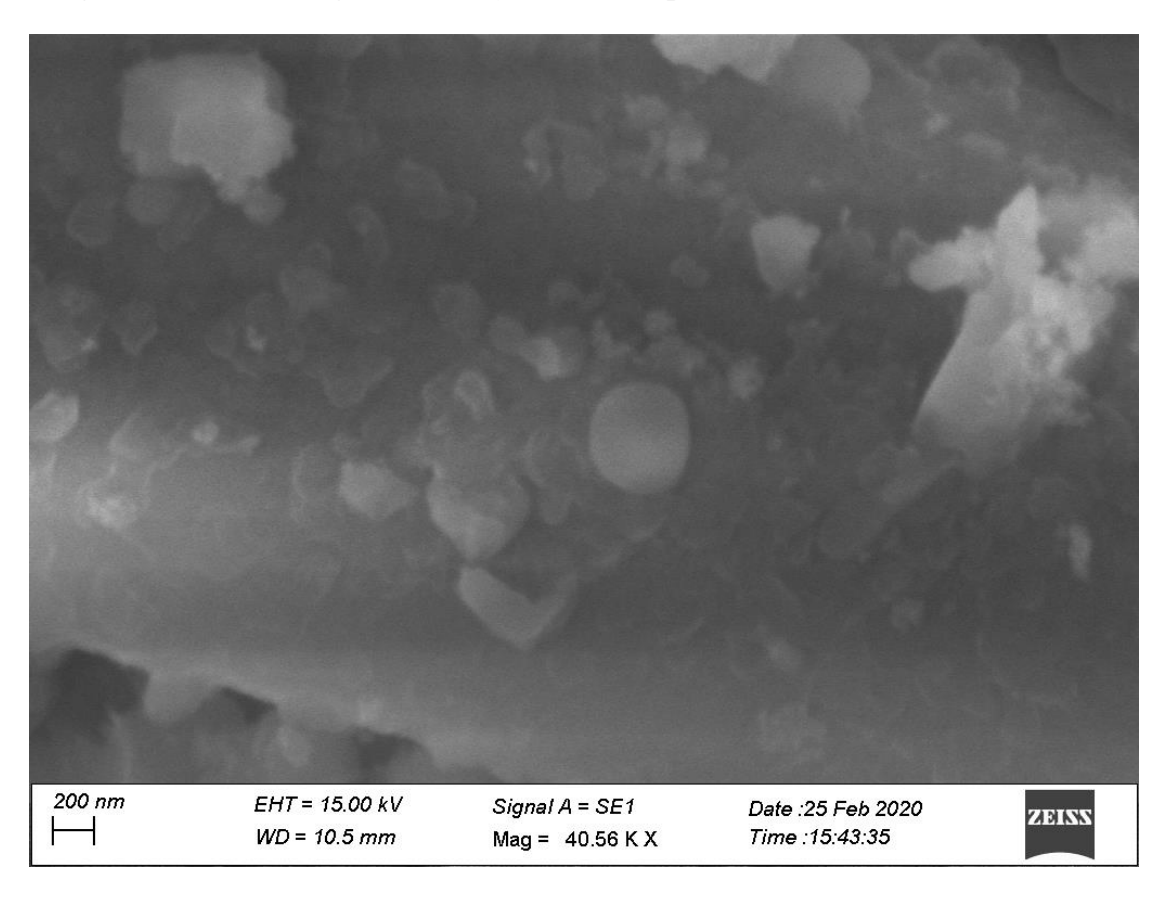


Figure 4.30: SEM Image of Manganese Oxide Nanoparticle obtained in Ch. Cl-EG DES

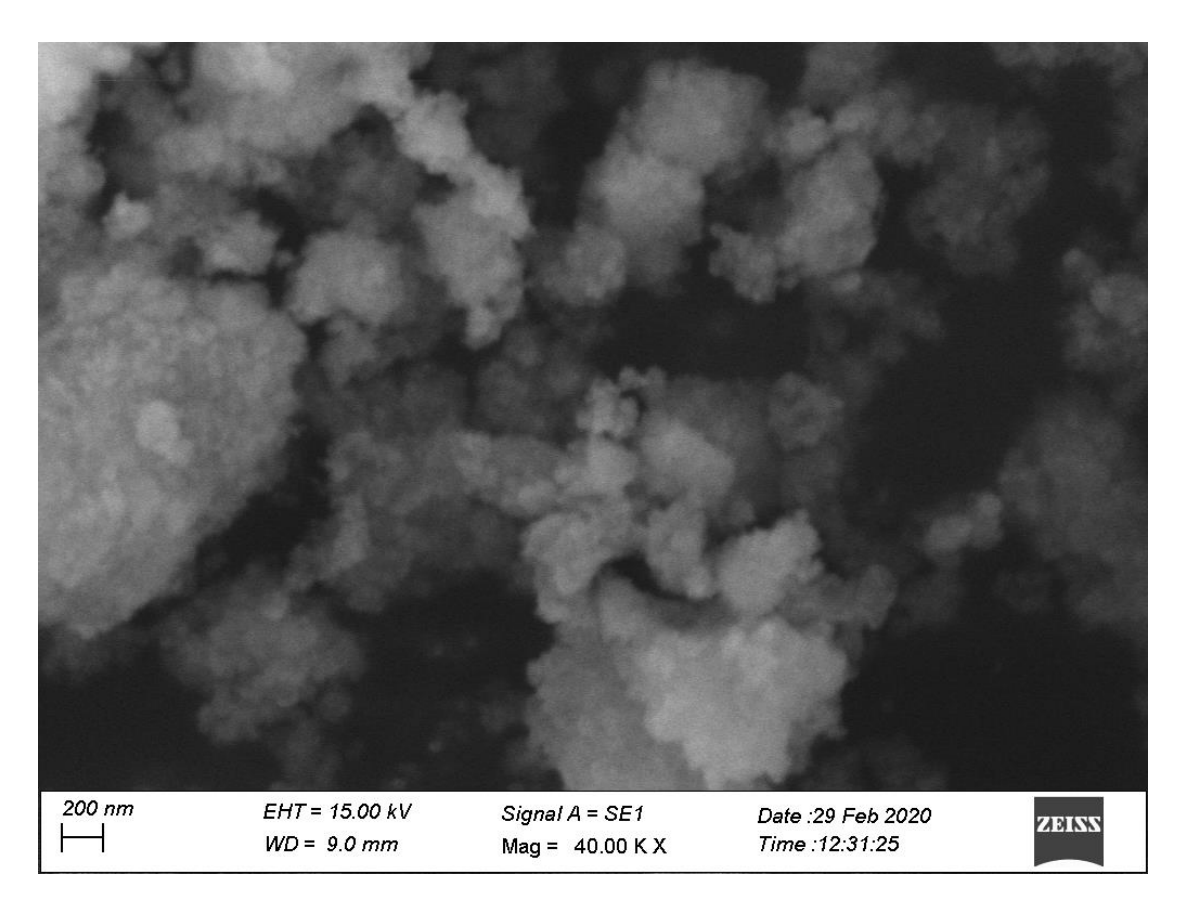


Figure 4.31: SEM Image of Zirconium Oxide Nanoparticle obtained in Ch. Cl-EG DES

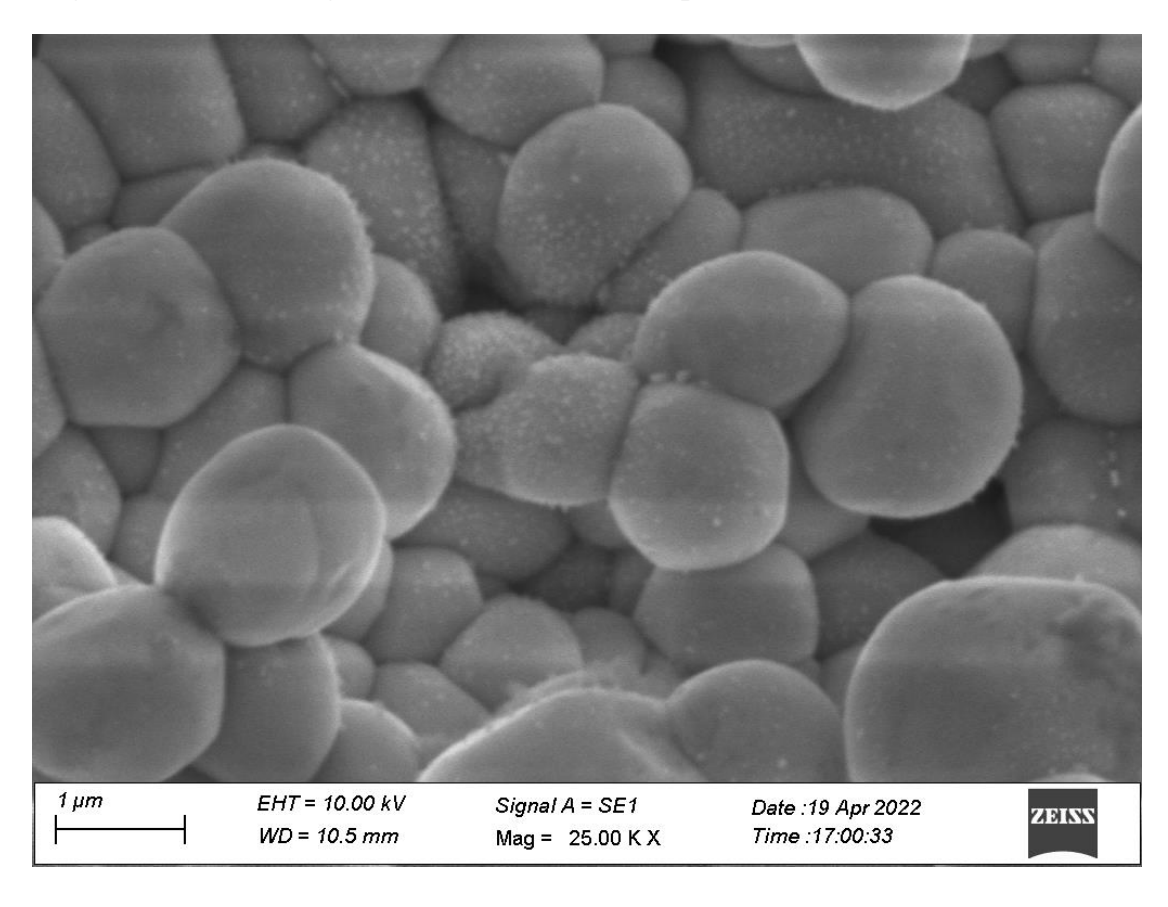


Figure 4.32: SEM Image of Silver Oxide Nanoparticle obtained in Ch. Cl-EG DES

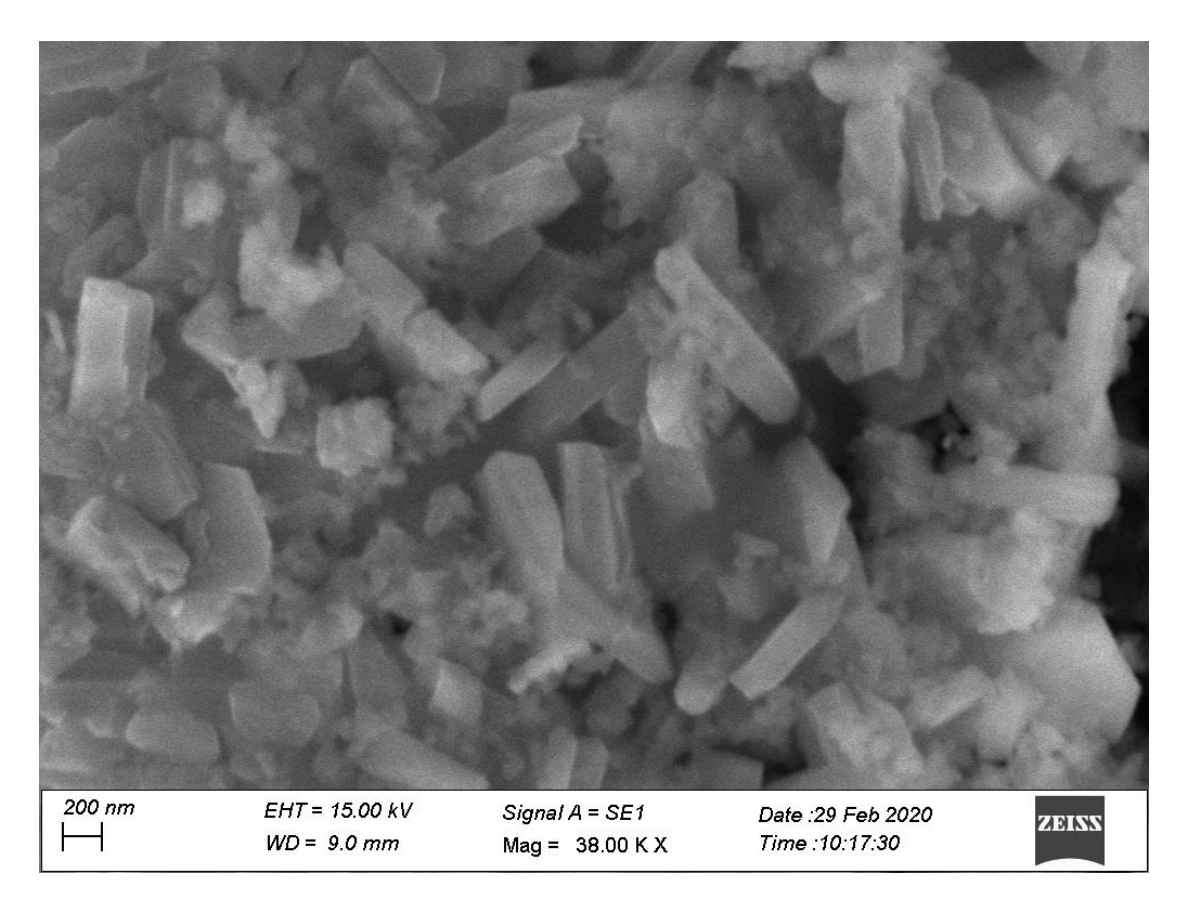


Figure 4.33: SEM Image of Zinc Oxide Nanoparticle obtained in Ch. Cl-EG DES

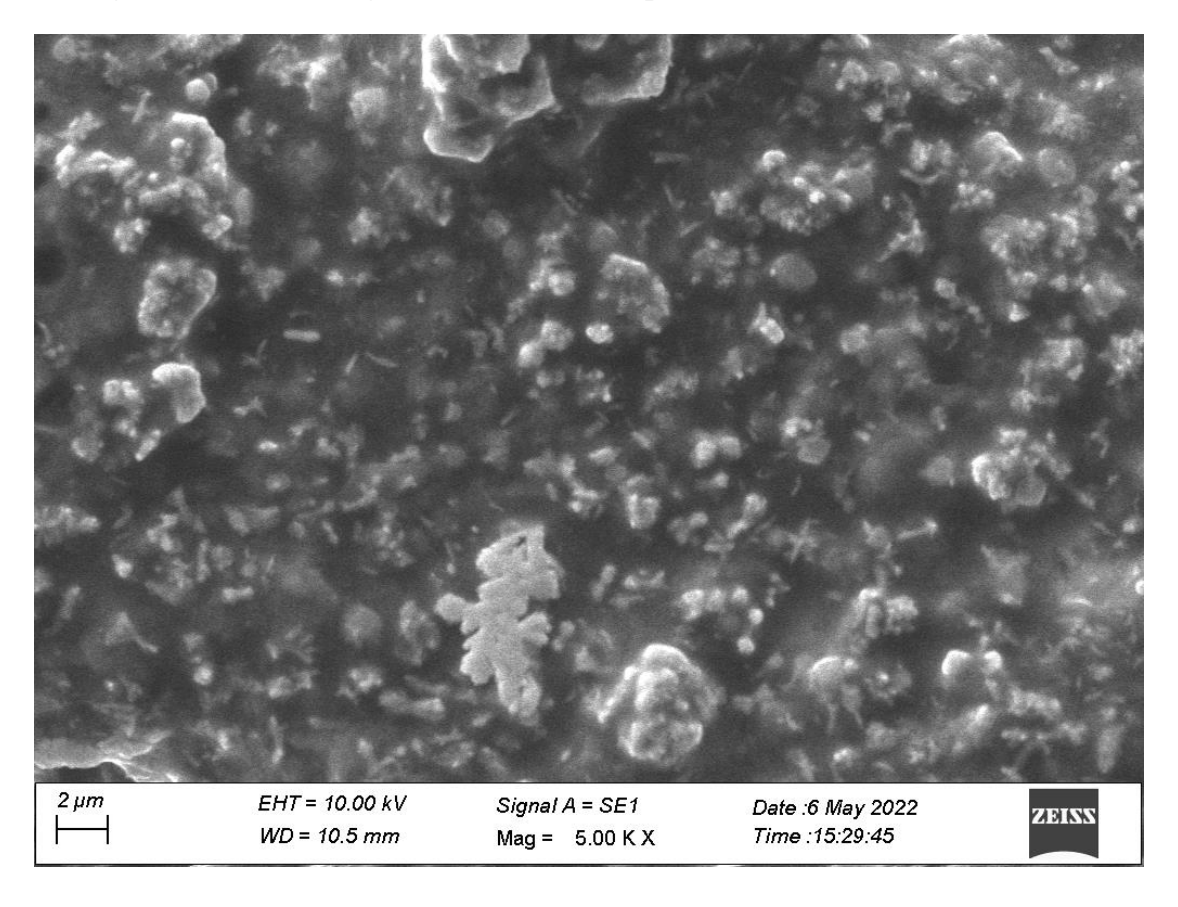


Figure 4.34: SEM Image of Cadmium Oxide Nanoparticle obtained in Ch. Cl-EG DES

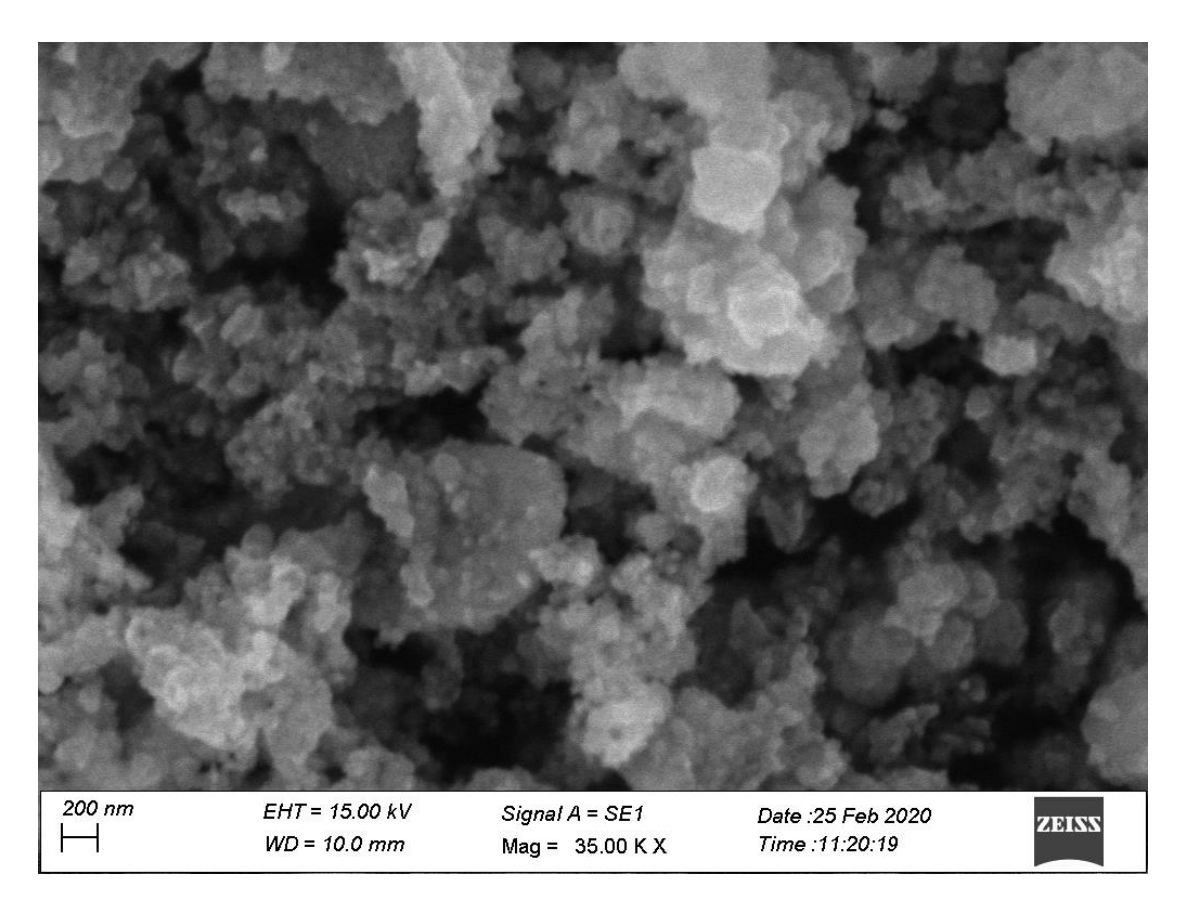


Figure 4.35: SEM Image of Vanadium Oxide Nanoparticle obtained in Ch. Cl-EG DES

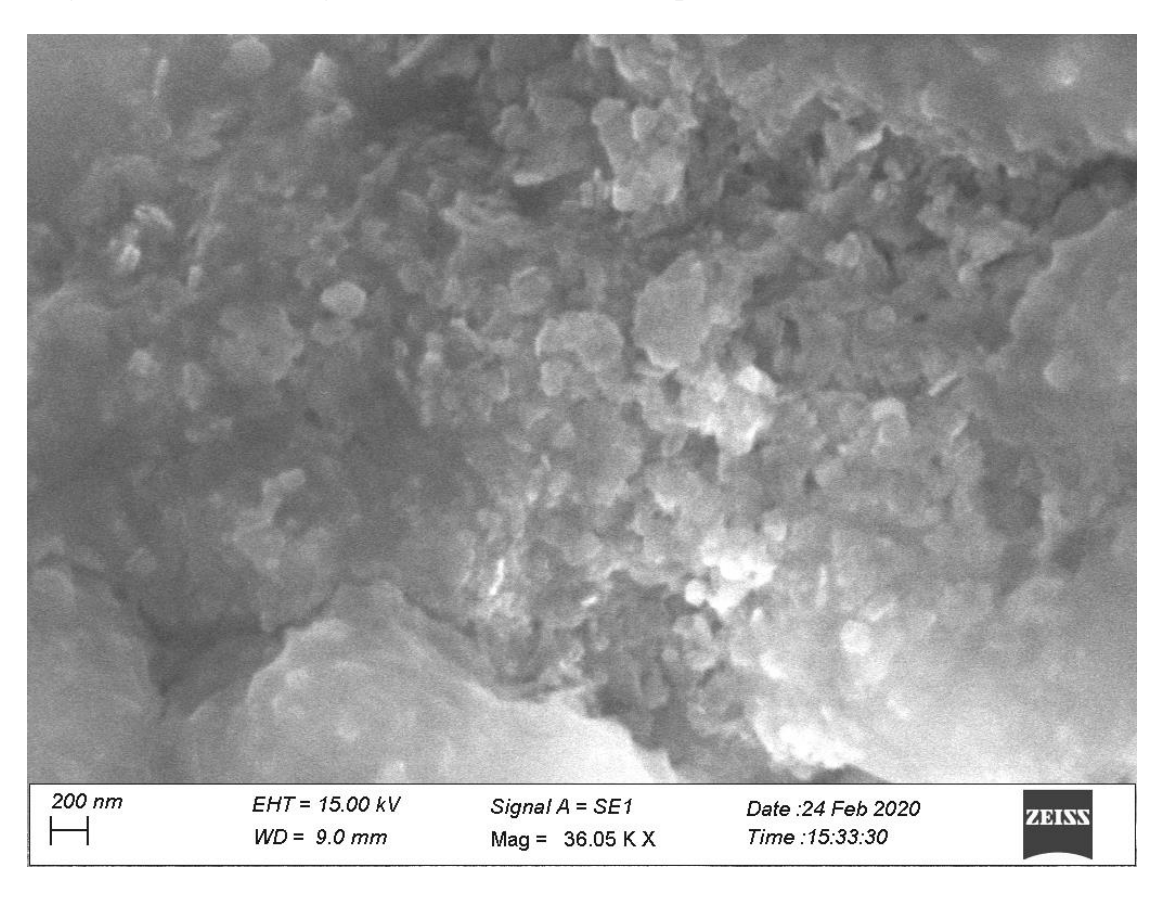


Figure 4.36: SEM Image of Nickel Oxide Nanoparticle obtained in Ch. Cl-EG DES

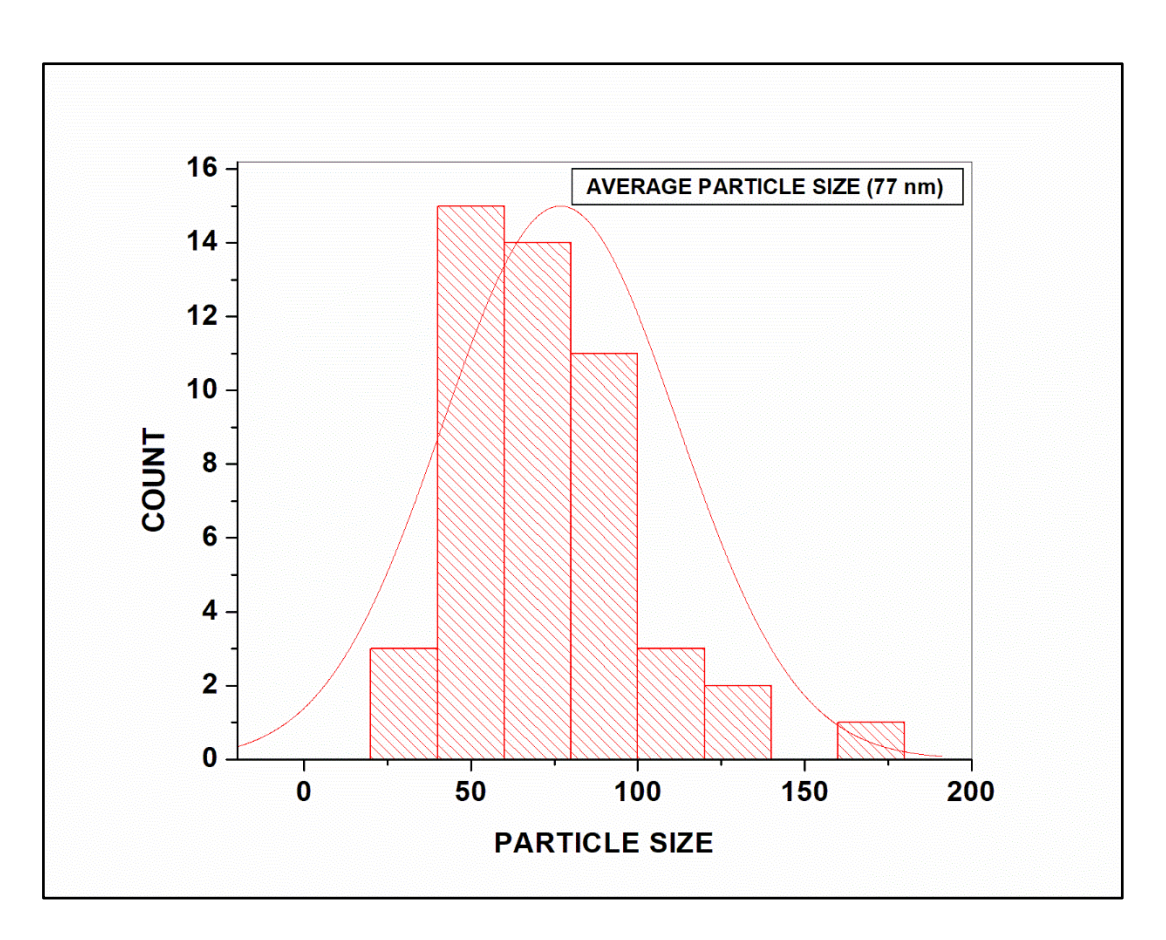


Figure 4.37: SEM Histogram of Copper Oxide Nanoparticle obtained in Ch. Cl-EG DES

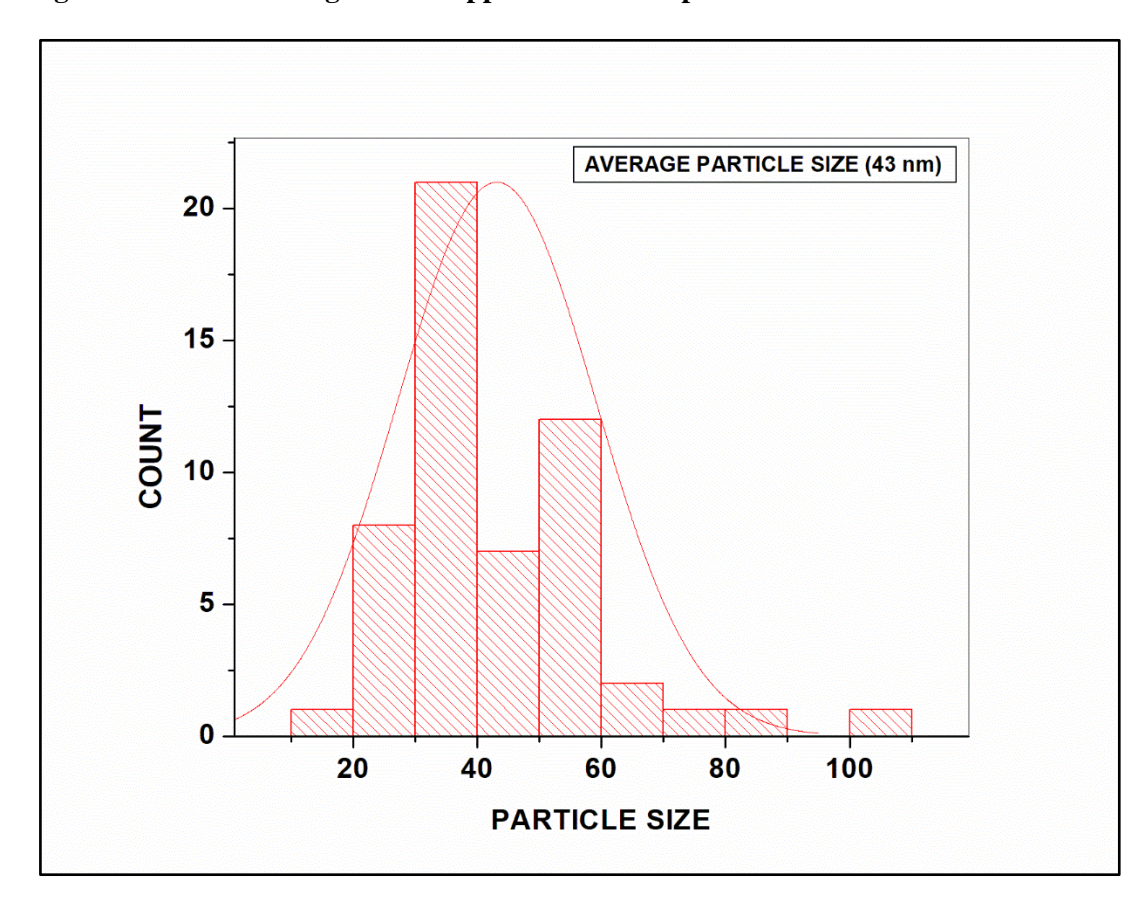


Figure 4.38: SEM Histogram of Mercury Oxide Nanoparticle obtained in Ch. Cl-EG DES

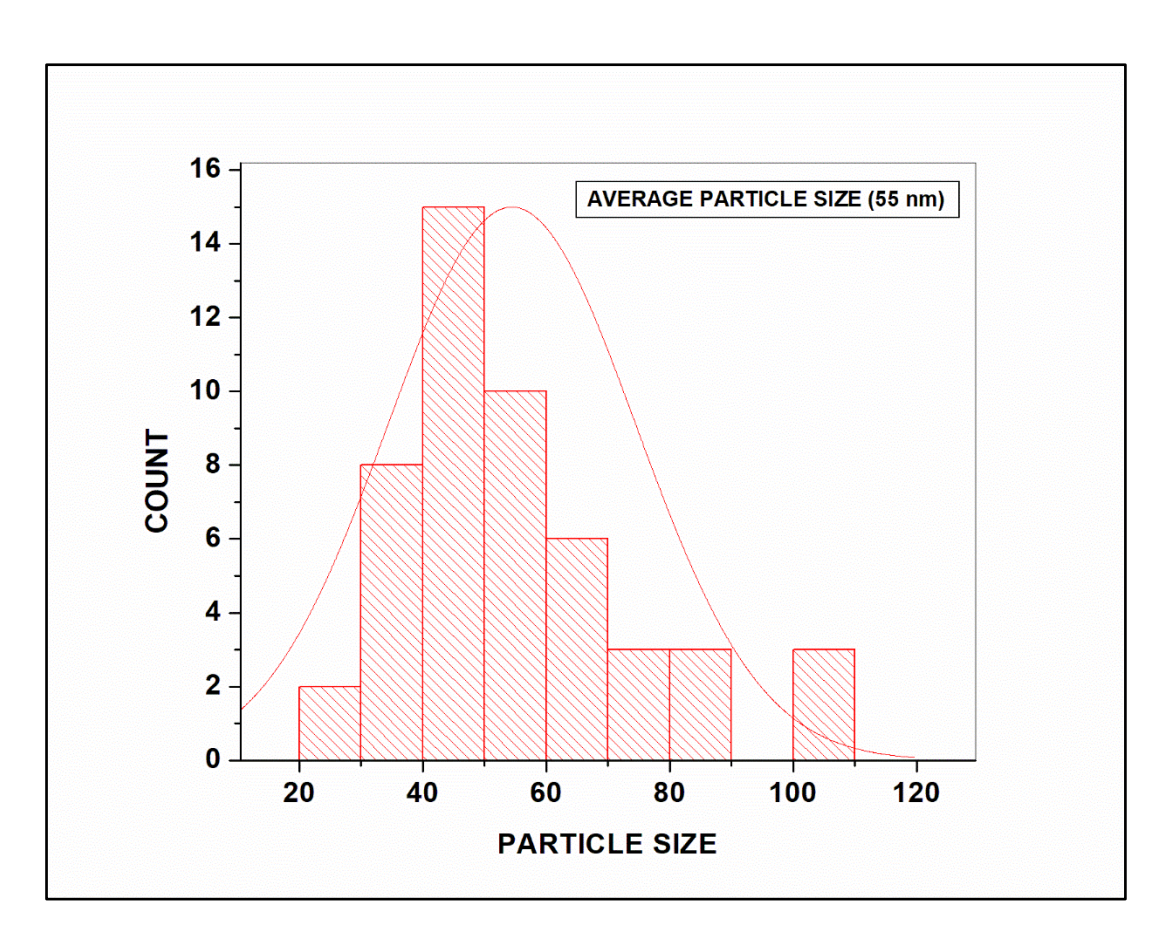


Figure 4.39: SEM Histogram of Manganese Oxide Nanoparticle obtained in Ch. Cl-EG DES

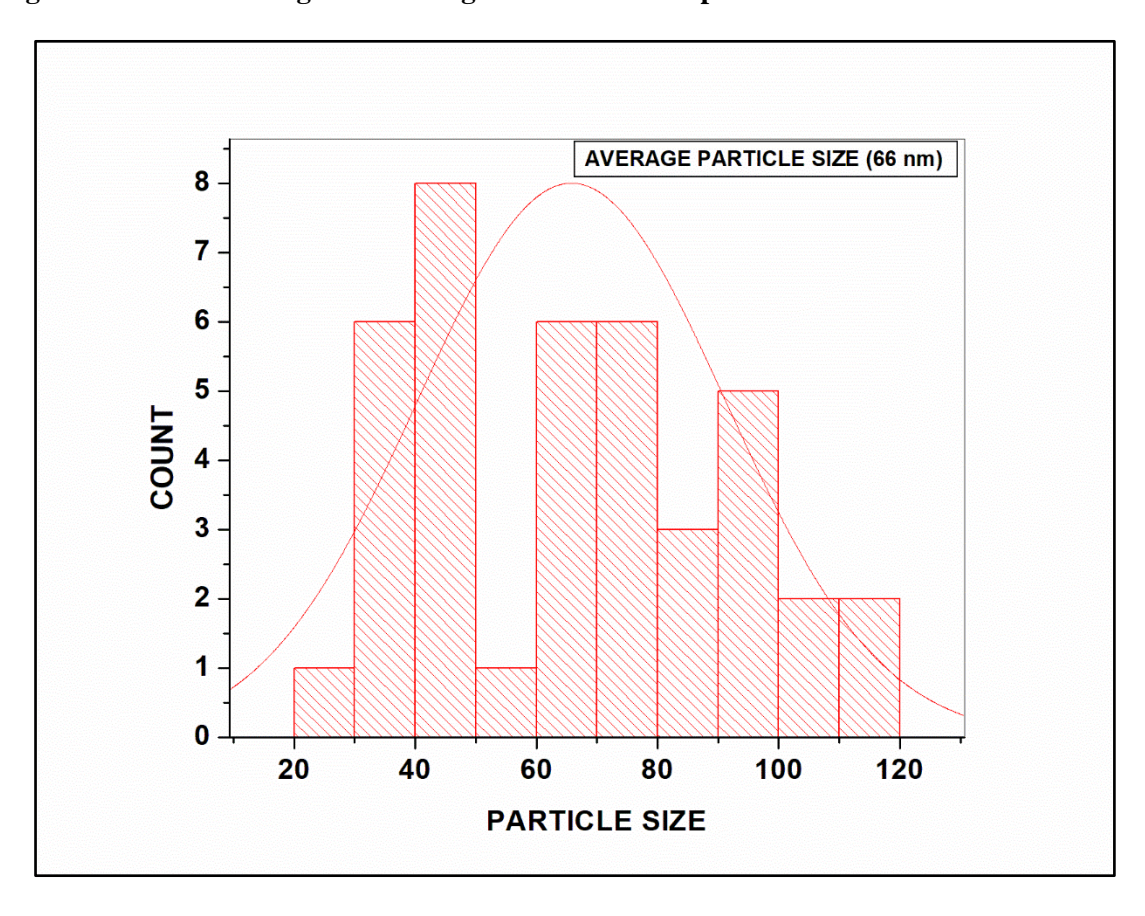


Figure 4.40: SEM Histogram of Zirconium Oxide Nanoparticle obtained in Ch. Cl-EG DES

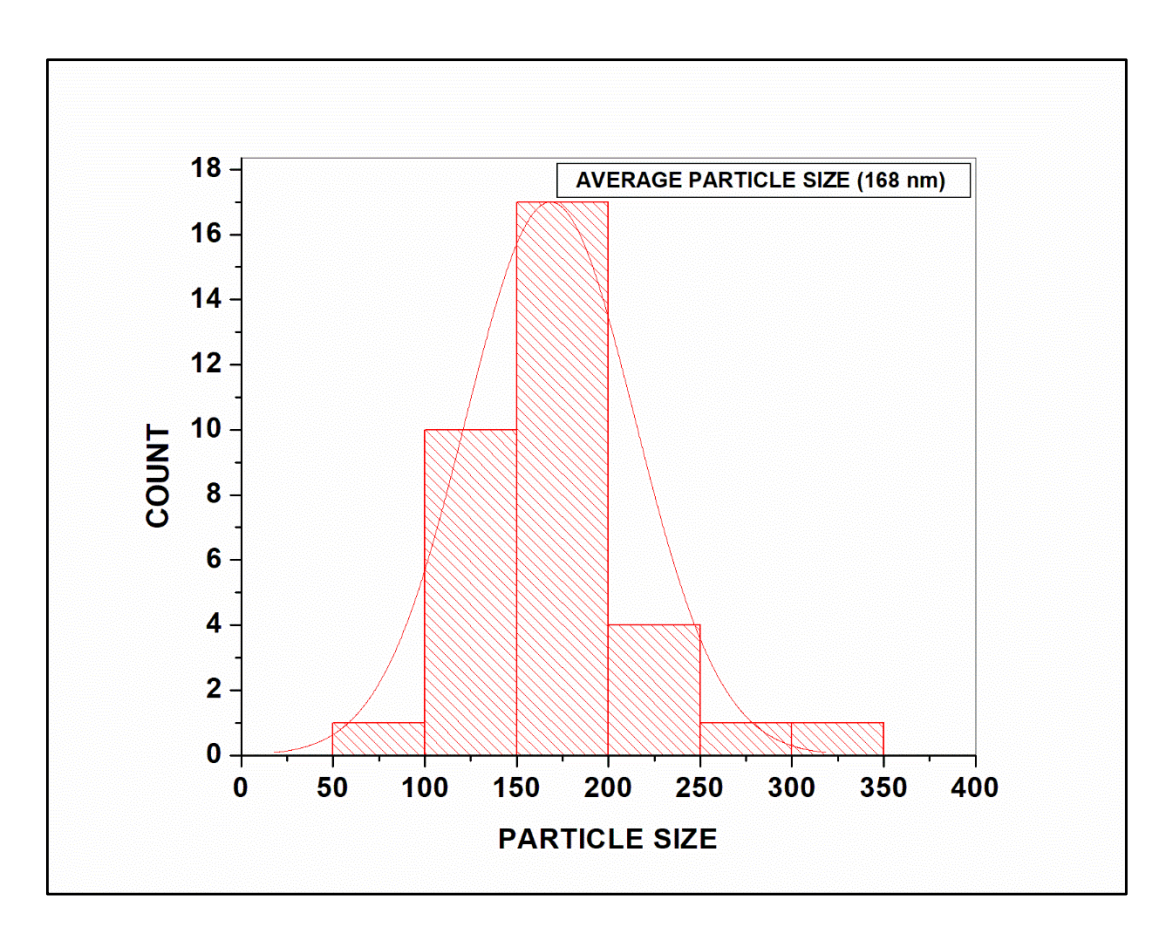


Figure 4.41: SEM Histogram of Silver Oxide Nanoparticle obtained in Ch. Cl-EG DES

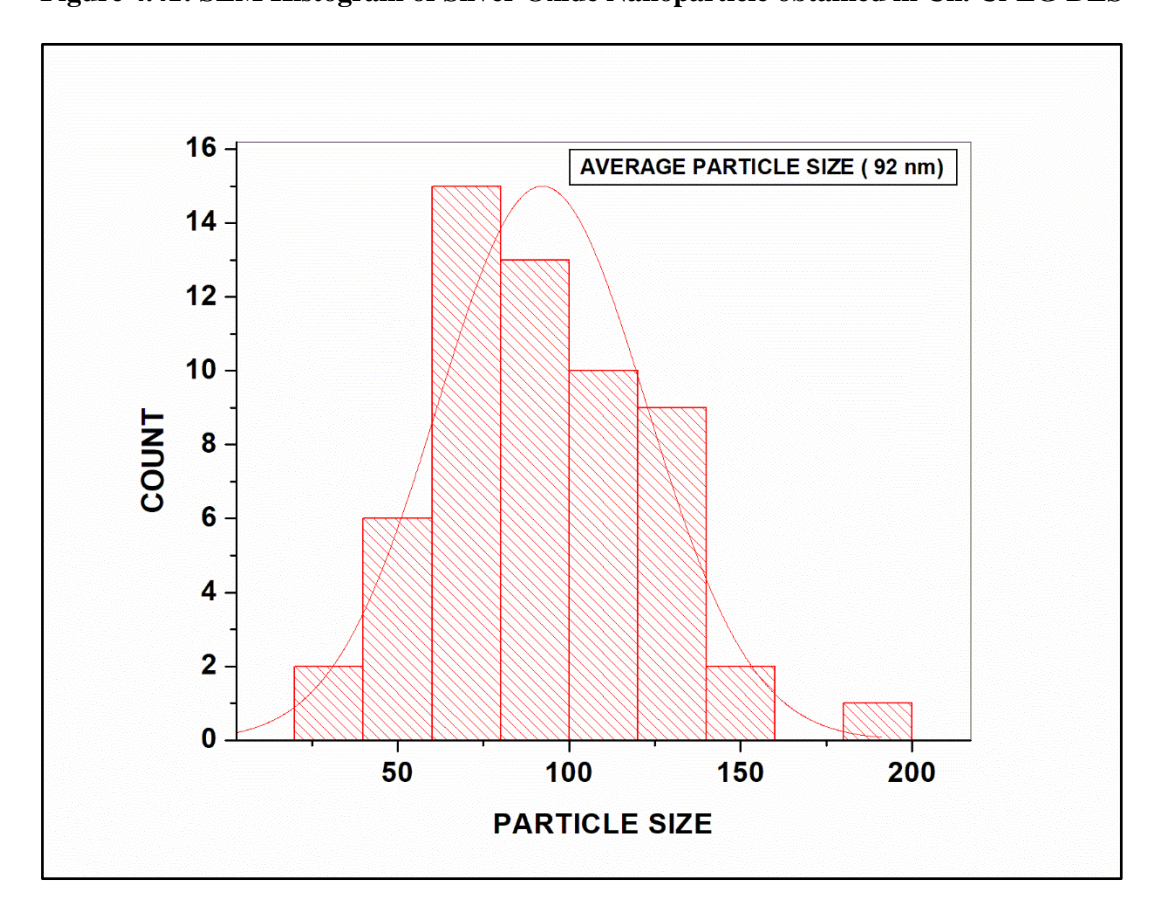


Figure 4.42: SEM Histogram of Zinc Oxide Nanoparticle obtained in Ch. Cl-EG DES

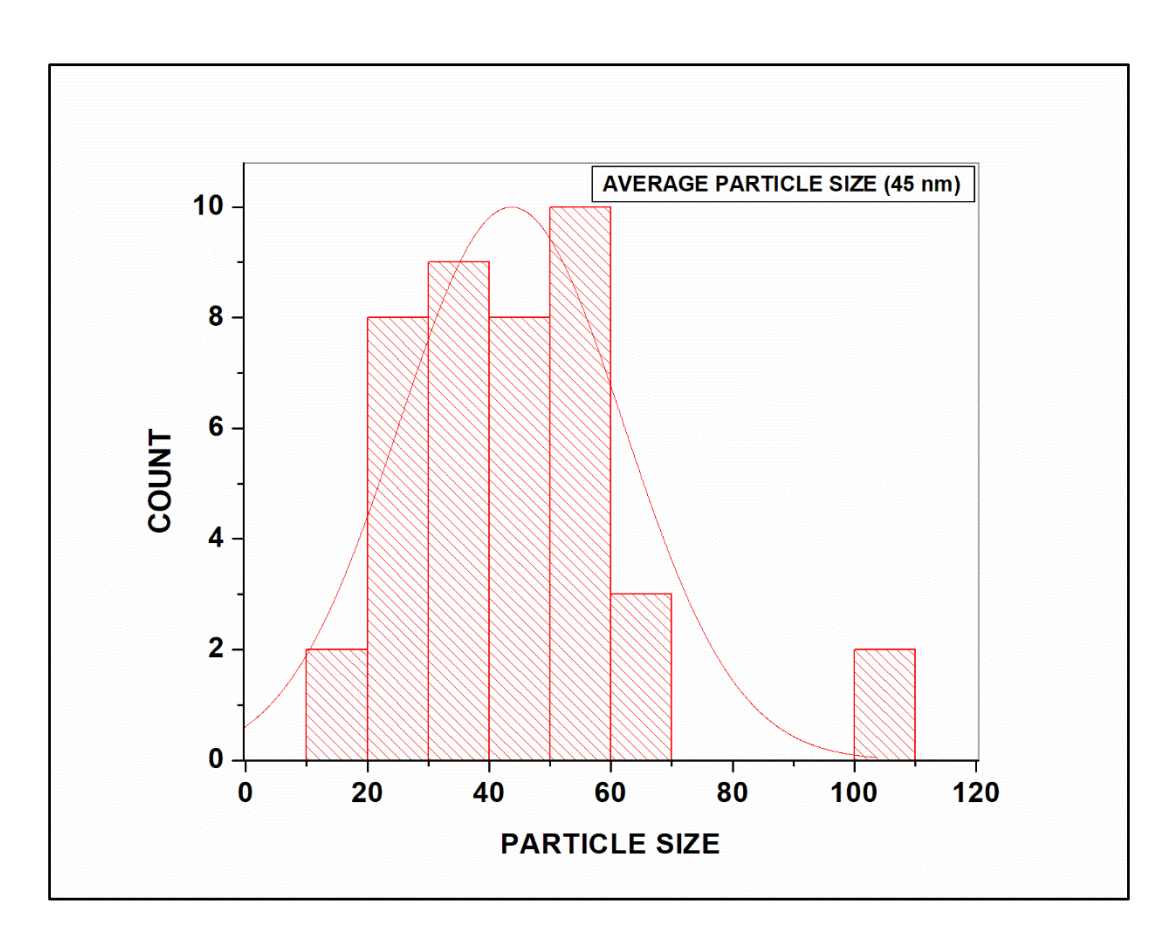


Figure 4.43: SEM Histogram of Cadmium Oxide Nanoparticle obtained in Ch. Cl-EG DES

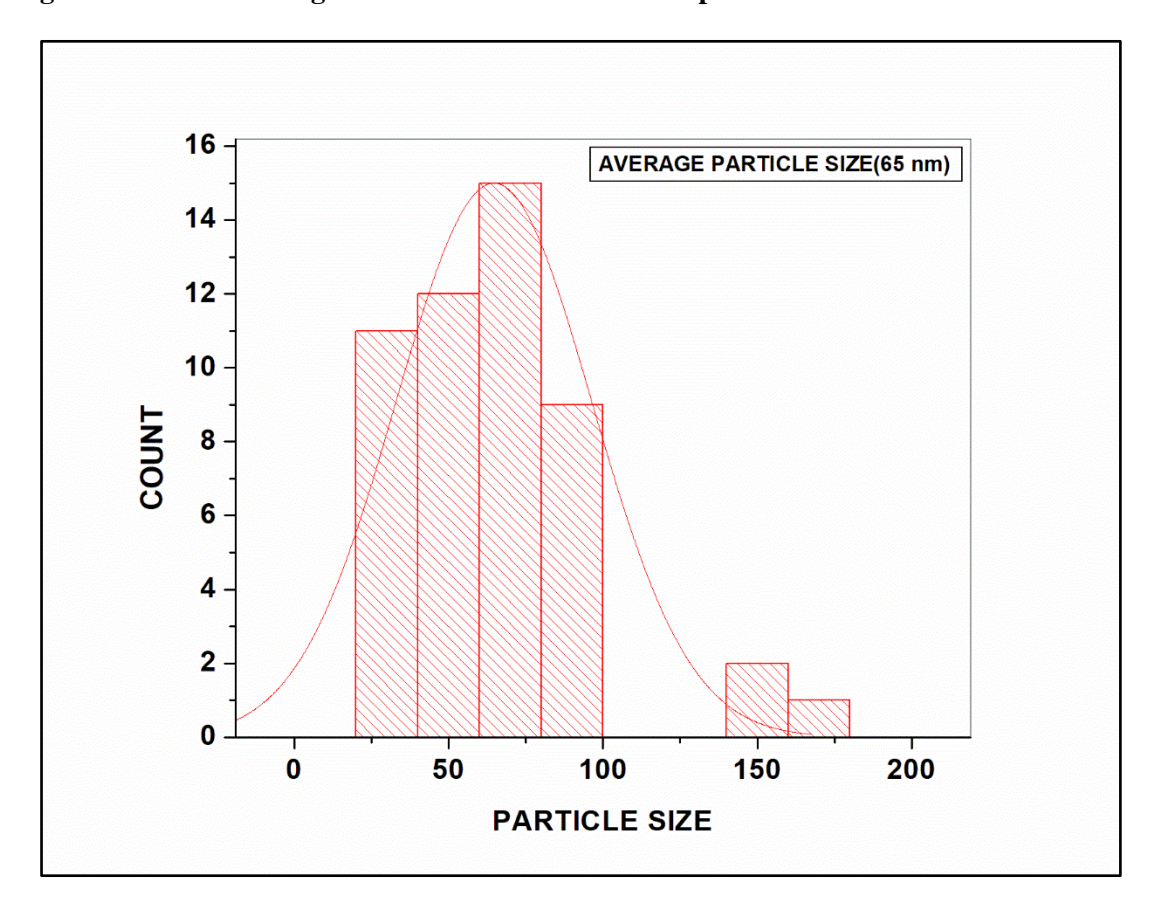


Figure 4.44: SEM Histogram of Vanadium Oxide Nanoparticle obtained in Ch. Cl-EG DES

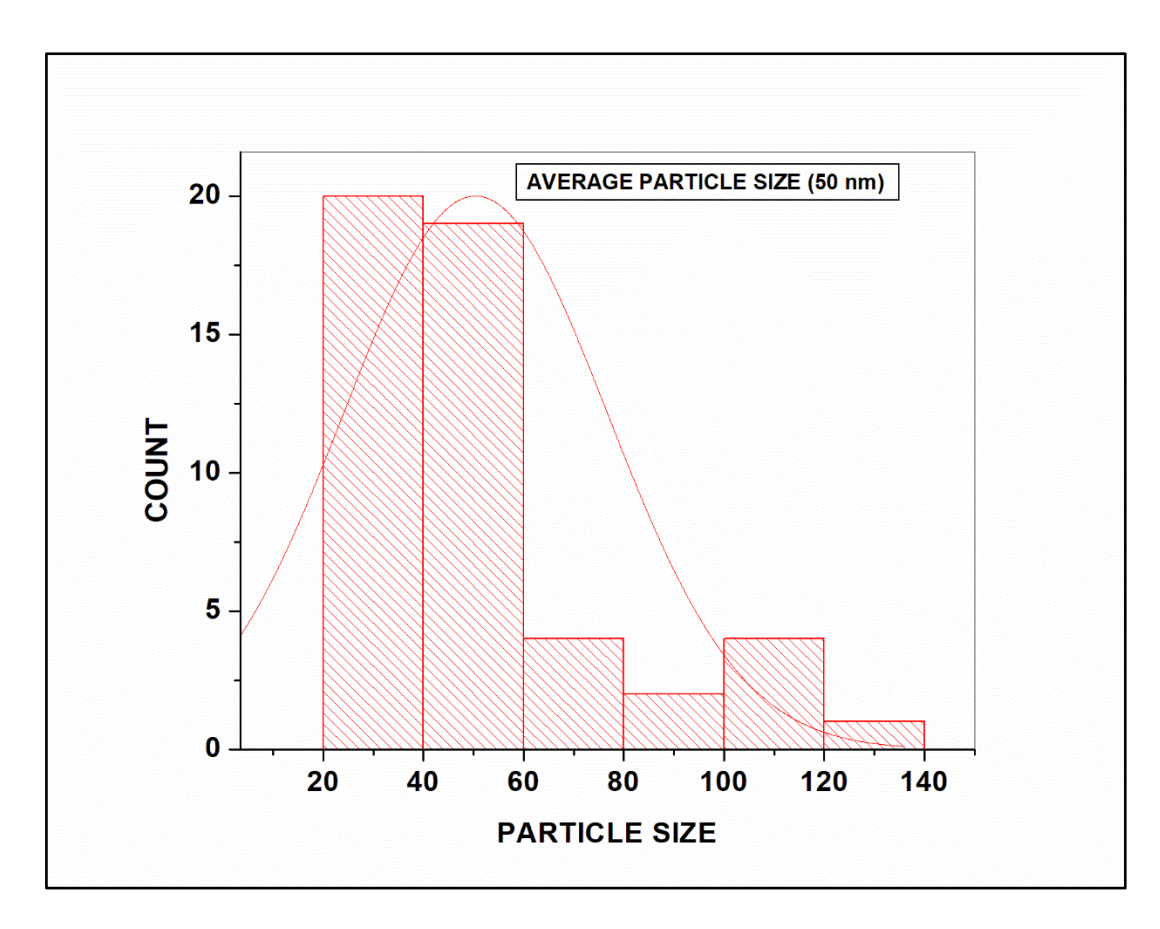


Figure 4.45: SEM Histogram of Nickel Oxide Nanoparticle obtained in Ch. Cl-EG DES

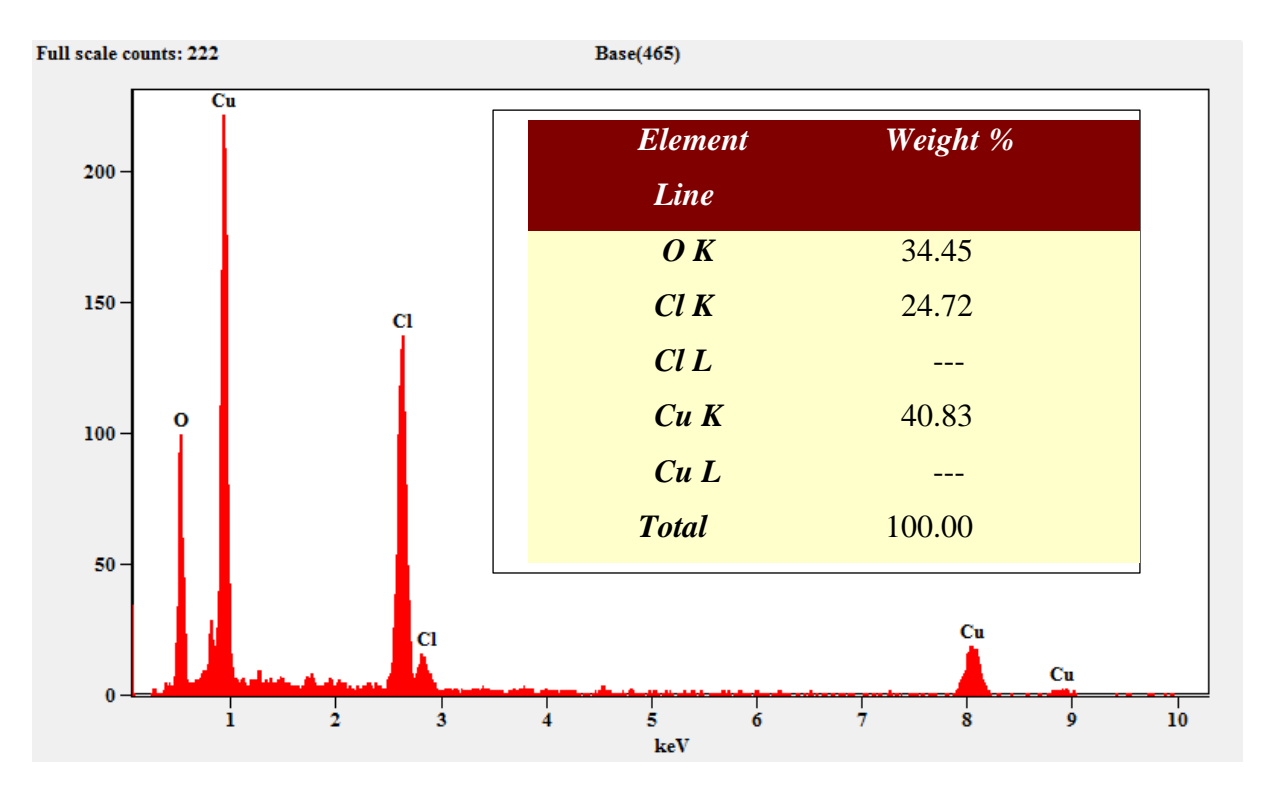


Figure 4.46: EDAX Spectrum of Copper Oxide Nanoparticle obtained in Ch. Cl-EG DES

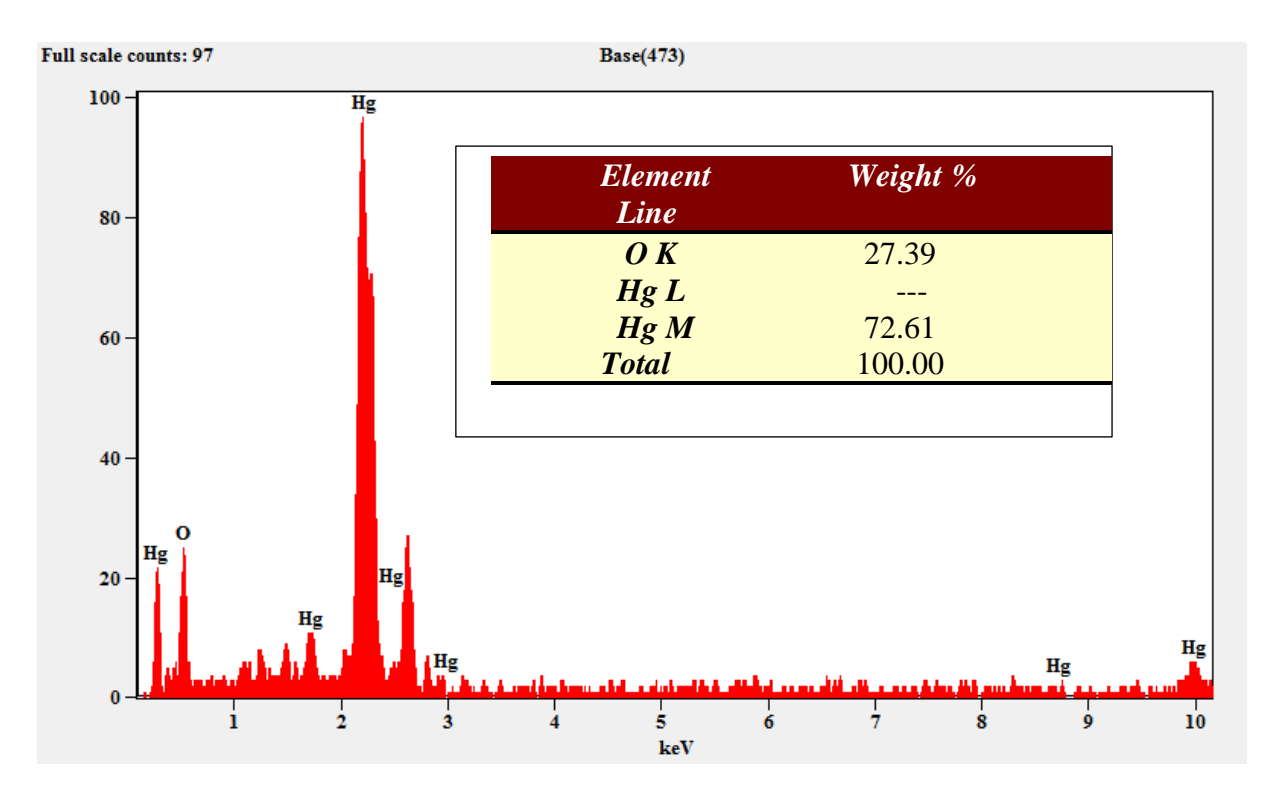


Figure 4.47: EDAX Spectrum of Mercury Oxide Nanoparticle obtained in Ch. Cl-EG DES

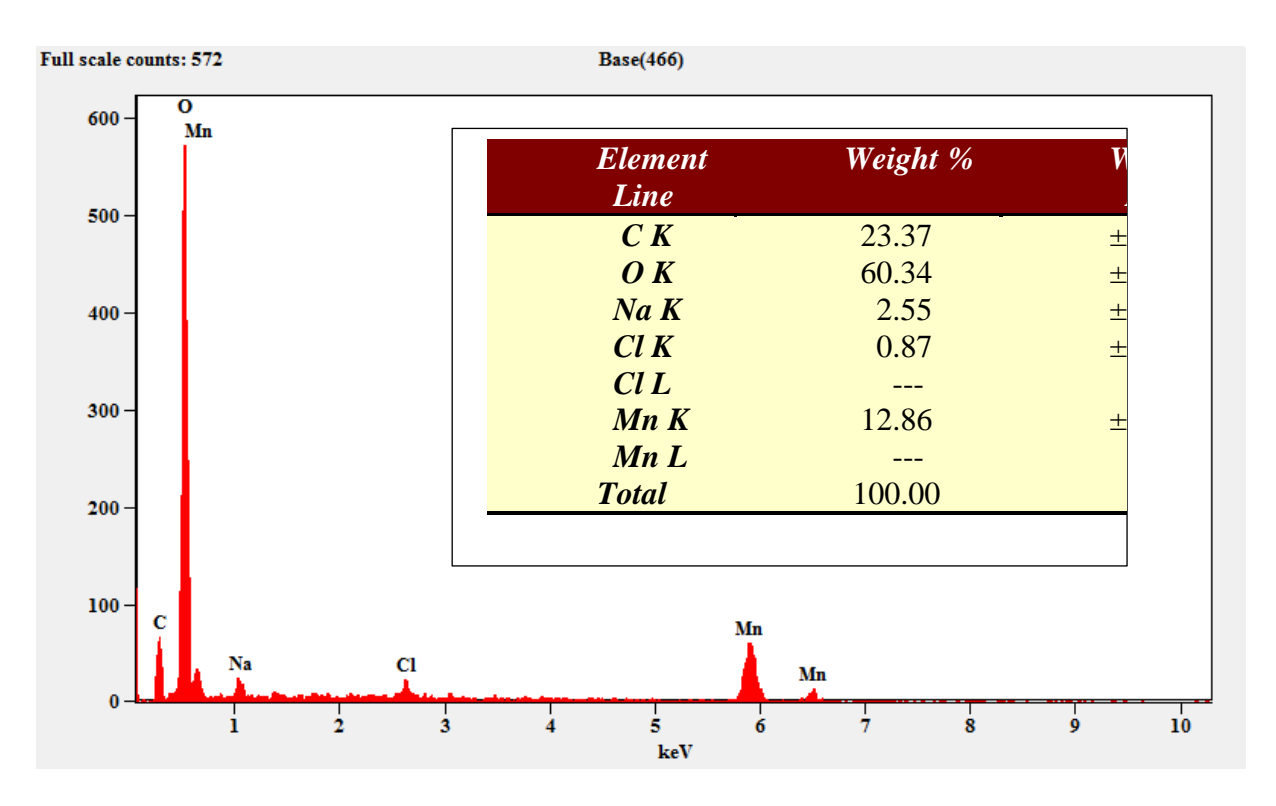


Figure 4.48: EDAX Spectrum of Manganese Oxide Nanoparticle obtained in Ch. Cl-EG DES

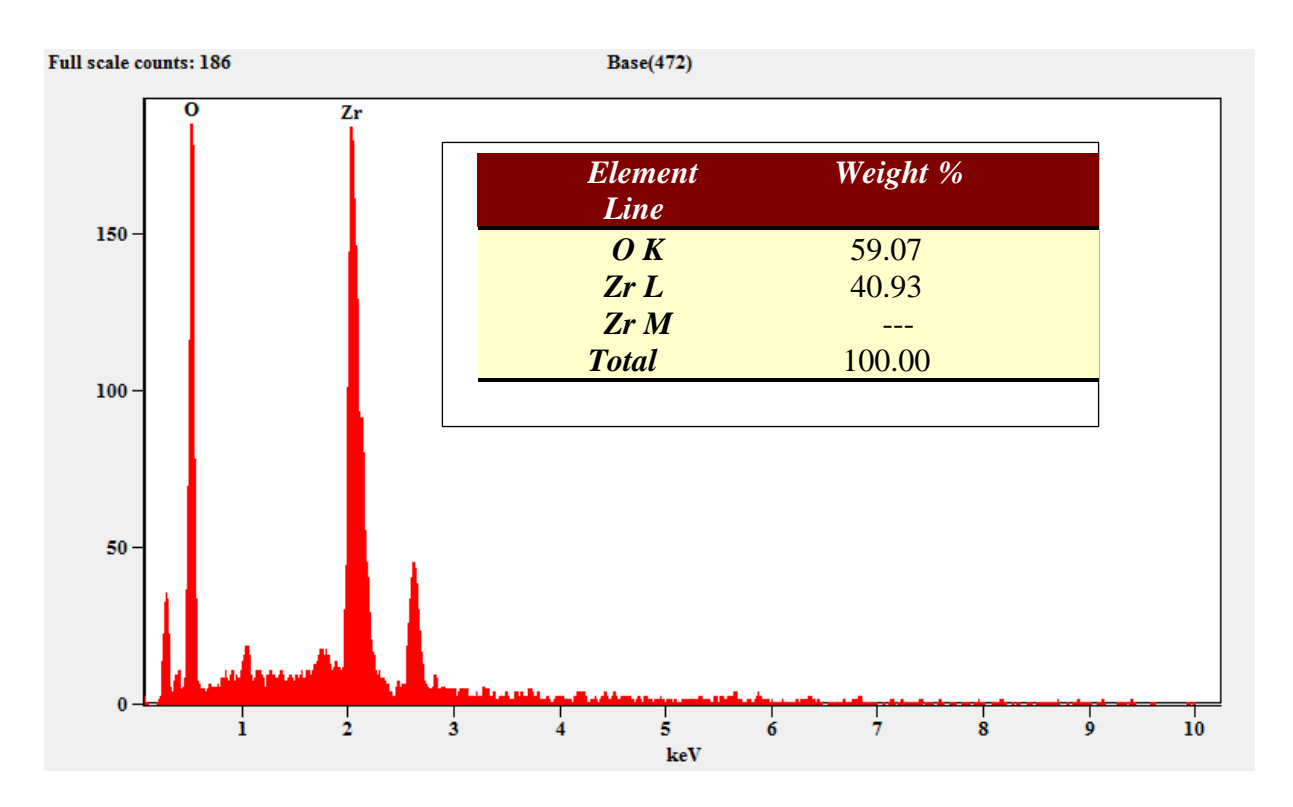


Figure 4.49: EDAX Spectrum of Zirconium Oxide Nanoparticle obtained in Ch. Cl-EG DES

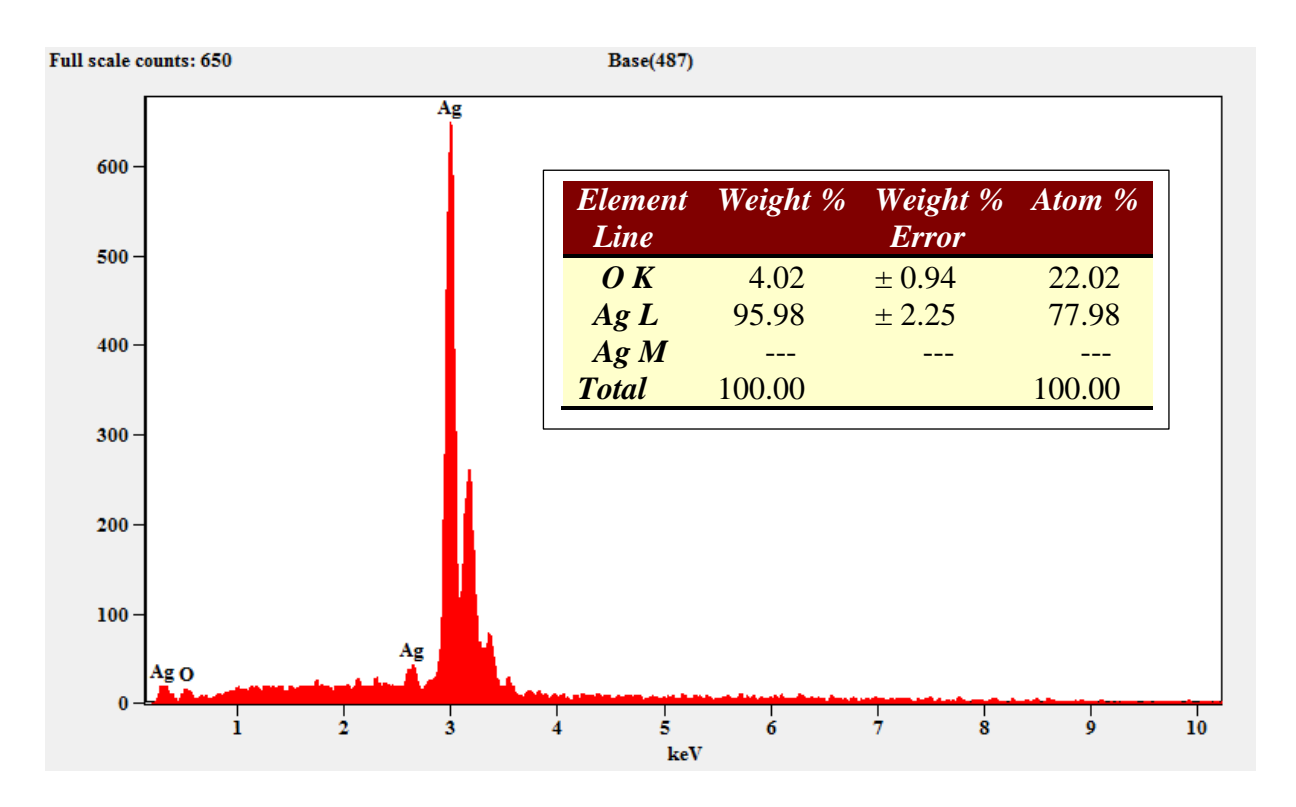


Figure 4.50: EDAX Spectrum of Silver Oxide Nanoparticle obtained in Ch. Cl-EG DES

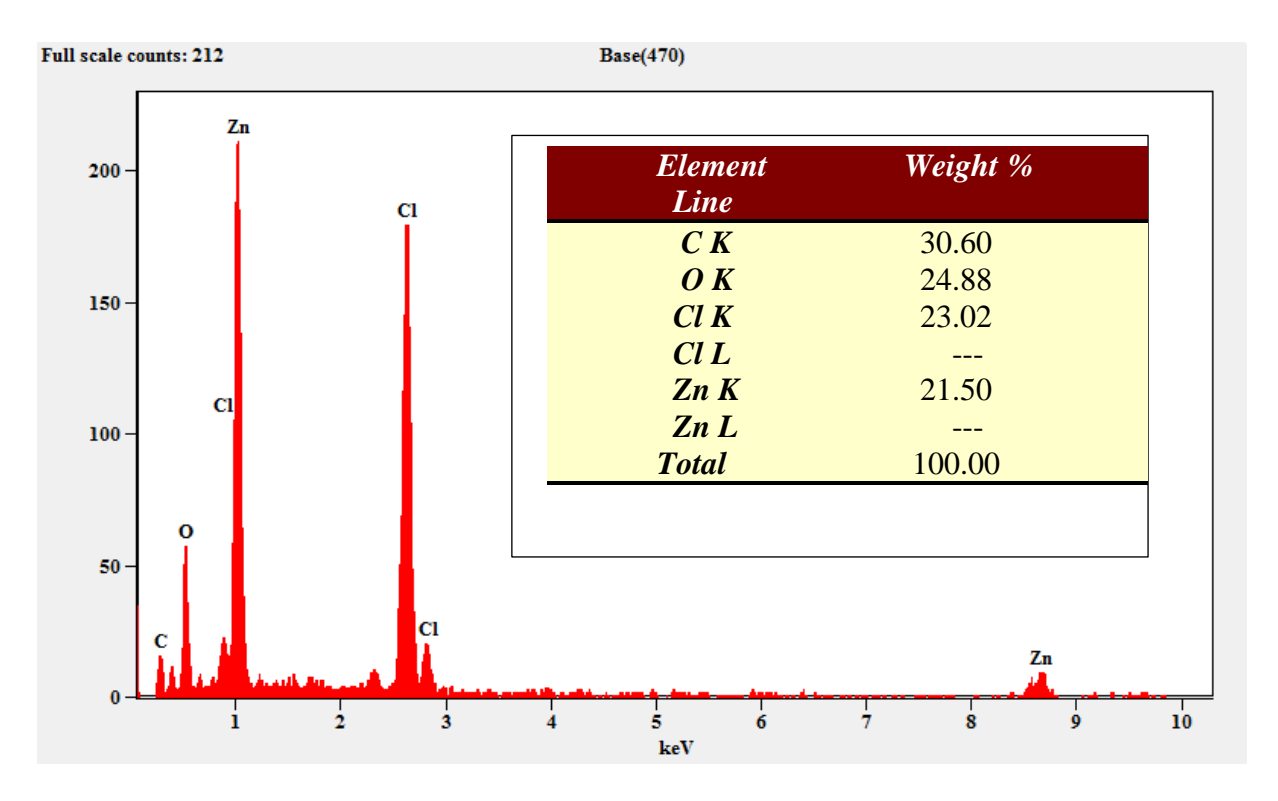


Figure 4.51: EDAX Spectrum of Zinc Oxide Nanoparticle obtained in Ch. Cl-EG DES

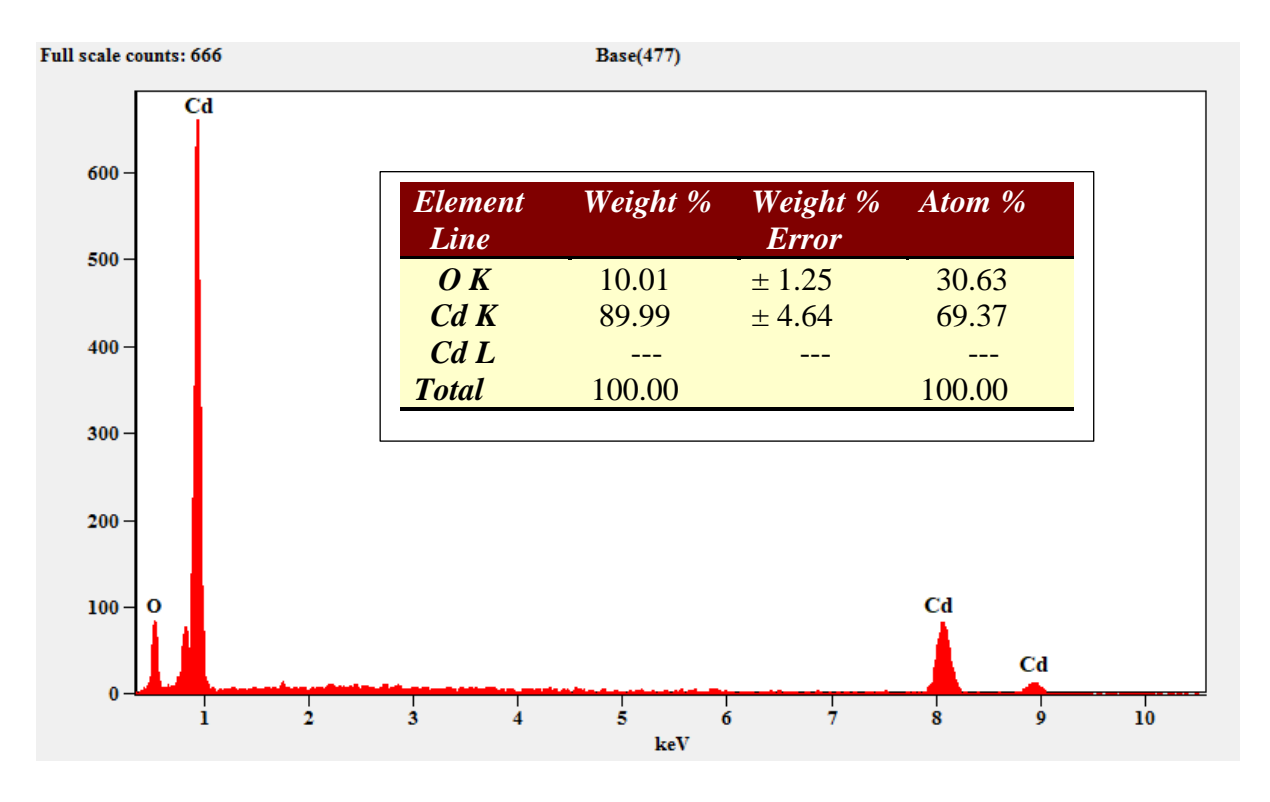


Figure 4.52: EDAX Spectrum of Cadmium Oxide Nanoparticle obtained in Ch. Cl-EG DES

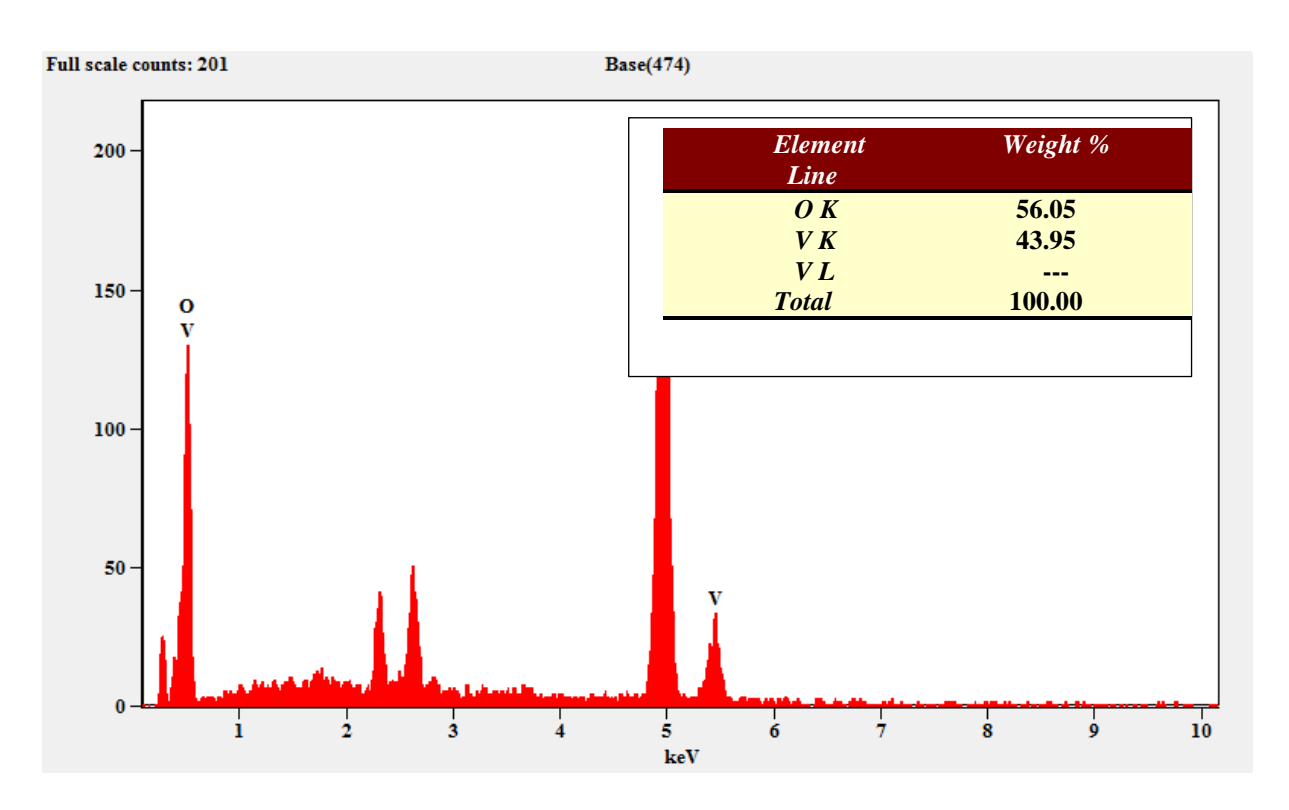


Figure 4.53: EDAX Spectrum of Vanadium Oxide Nanoparticle obtained in Ch. Cl-EG DES

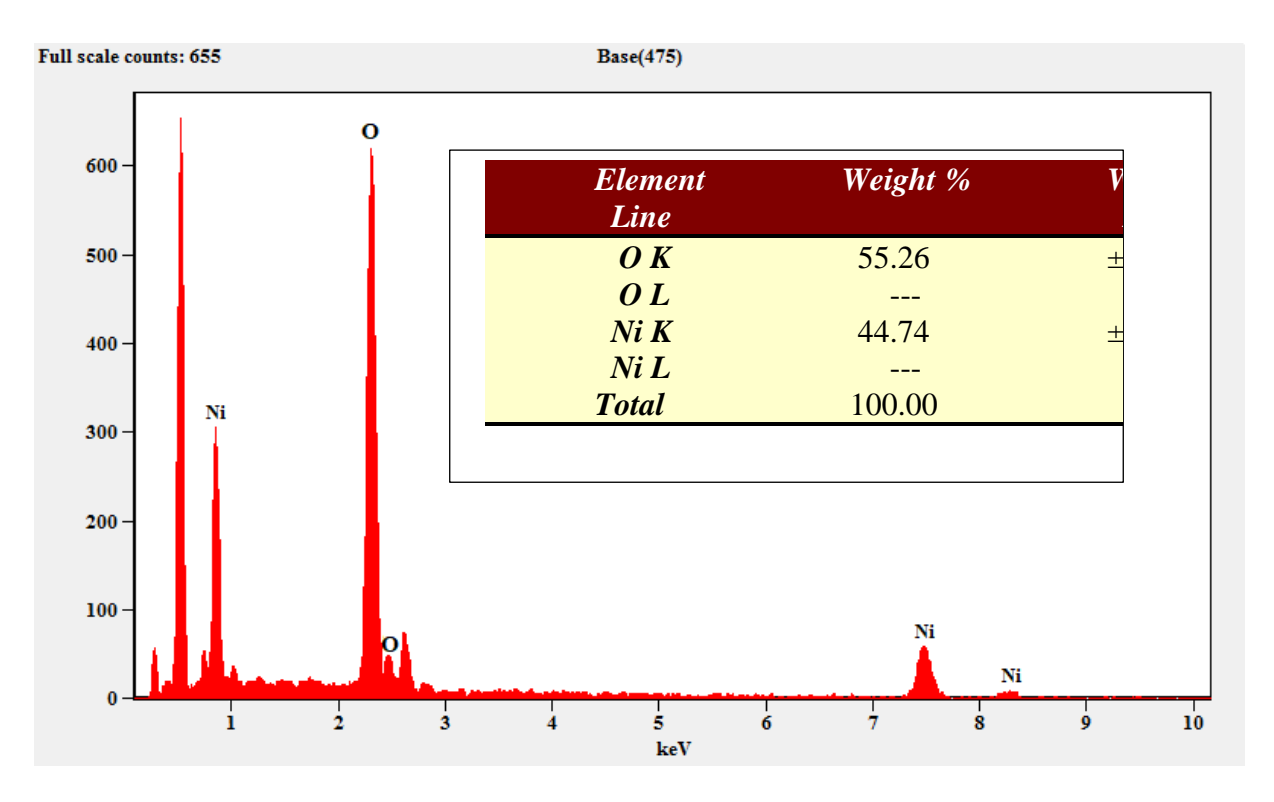


Figure 4.54: EDAX Spectrum of Nickel Oxide Nanoparticle obtained in Ch. Cl-EG DES

#### 5. CHOLINE CHLORIDE – MALONIC ACID DEEP EUTECTIC SOLVENT AIDED SYNTHESIS OF SOME METAL OXIDE NANOPARTICLES

#### 5.1 Introduction

Metal-based nanoparticles have different budding applications in biological, chemical, medical, and agricultural fields due to their interesting features. Metal nanoparticles are either cleaner forms of metals such as Au, Ag, Cu, Fe, etc., or their compounds such as sulfides, hydroxides, oxides, etc. Ionic liquids are commonly involved in the abstraction of nanoparticles but they are somewhat difficult due to their impoverished bio-degradability, bio-compatibility, and sustainability. Therefore, as a substitute for ionic liquids, Deep Eutectic Solvent (DES) is considered in the development of nanoparticles.

Nanoscience is learning that defines the particles of nanoscale having fewer than 100 nm, and examination of their varied physio-chemical characteristics and their opportunity in several fields. A lot of improvements have been made in nano-based technology due to the common properties such as the particle's surface area, size, shape, charge, and surface reactivity which are exclusive and better when related to the equivalent bulk particles [1]. The metal-based NPs, apart from their common properties, their structural and elemental compositions in nanoscales allow MNPs to be evolving contenders in pharmaceutical, environmental, agricultural, and chemical industries.

Copper oxide nanoparticle is essential and reasonably inexpensive when compared to precious metals such as Au and Ag <sup>[2]</sup>. Manganese oxide nanoparticle has budding applications in the medical field. Their application as MRI contrast agents in cancer multimodal therapy and modelling is a significant one <sup>[3]</sup>. Zirconium oxide nanoparticles claimed applications in fuel cells <sup>[4]</sup>.

A DES is typically self-possessed of two or three low-cost and harmless components that are capable of linking via hydrogen bond relations to generate a eutectic mixture <sup>[5]</sup>. Regularly, DES can be signified by the common formula  $Cat^+X^-zY$  where  $Cat^+$  is ammonium, phosphonium, or sulfonium cation, and X is a Lewis base, normally a halide anion and Y is either a Lewis or Bronsted acid. Here z refers to the number of Y molecules that interact with the anion  $X^-$ . In general, there are four types of DES and the choline chloride – urea DES used in this investigation belongs to type III DES <sup>[6]</sup>.

Urea is proficient in forming a liquid DES with Ch.Cl at room temperature, seemingly due to its sturdier nature to form hydrogen bond connections with Ch.Cl. The freezing point ( $T_f$ ) of this 1:2 molar ratio DES of Ch.Cl-Urea was stated as 12 °C <sup>[5]</sup>. An unpretentious road for the shape-controlled preparation of Au NPs involving Ch,Cl-urea DES which replaced traditional surfactants <sup>[7]</sup>. Further, the synthesis of Au nanowire from straight away reduction of HAuCl<sub>4</sub> by NaBH<sub>4</sub> in DES <sup>[8]</sup> obviously showed the rewards of removing surfactants or seeds for the formation of nanomaterials when DESs are used. In the latter synthesis, two different DESs, i.e. Ch-Cl - ethylene glycol (1:2-mole ratio) or Ch.Cl - urea (1:2-mole ratio) was deployed in the absence of a surfactant. The development of nanoparticles of several shapes and surfaces was controlled by adjusting the water content of the DES <sup>[6]</sup>.

A deep eutectic solvent (DES) of choline chloride and malonic acid was formed rapidly and inexpensively. In a one-pot four-component reaction of amines, aldehydes, 1,3-dicarbonyl compounds, and nitromethane this DES was deployed not only as a catalyst but also a medium for the formation of functionalized pyrroles <sup>[7]</sup>.

Choline chloride with some carboxylic acid-based DESs has also been described to undergo chemical reactions such as esterification. As a result, it was discovered that a number of DESs containing Ch. Cl and carboxylic acids such as lactic acid, glutaric acid,

glycolic acid, malic acid, malonic acid, oxalic acid, and levulinic acid undergo an esterification reaction between the hydroxyl group of choline chloride and the carboxylic acid [8].

The efficiency of two DESs obtained from choline chloride-malonic acid of molar ratios 1:1 and 1:0.5 - in enhancing oil recovery was investigated for the first time by Iman Al-Wahaibi et.al <sup>[9]</sup>. Gunny et al investigated the use of the DES-cellulose mechanism to hydrolyze lignocellulose from rice husk. The DES is comprised of choline chloride and a hydrogen-bond donor molecule (glycerol, ethylene glycol, or malonic acid) <sup>[10]</sup>.

The present investigation described in this chapter involved an advanced Choline chloride – malonic acid DES as an eco-friendly solvent to prepare copper, mercury, manganese, zirconium, silver, zinc, cadmium, vanadium and nickel oxide nanoparticles. The metal oxide nanoparticles prepared have been examined using UV-Visible, FTIR Spectroscopy, X-Ray Diffraction (XRD), Scanning Electron Microscopy (SEM), and Energy Dispersive X-Ray Analysis (EDAX). The creation of these metal oxide nanoparticles via Choline Chloride (C<sub>5</sub>H<sub>14</sub>ClNO) – Malonic acid DES can be considered a well-intentioned way in chemical engineering.

#### **5.2** Experimental

The chemicals used for this investigation such as choline chloride, malonic acid, hydrazine hydrate, sodium hydroxide, methanol, copper nitrate trihydrate, mercuric chloride, manganese chloride dihydrate, zirconium oxychloride, silver nitrate, zinc acetate dihydrate, cadmium chloride, vanadium pentoxide and nickel nitrate were purchased from Sigma–Aldrich, India and utilized as received. Barnstead nanopore water (>17.8 M-cm) was used to prepare all stock solutions.

#### 5.2.1 Preparation of choline chloride – malonic acid deep eutectic solvent

The choline chloride (Ch.Cl) and malonic acid (MA) received were recrystallized, filtered, and vacuum dried before it was used. The 1:1 molar ratio of these two components were taken and heated to 100 °C and agitated until a homogeneous, colourless liquid was produced from the two components. A couple of hours' heating of choline chloride and malonic acid at 100 °C yielded a clear homogeneous liquid.

### 5.2.2 Synthesis of copper nanoparticles in choline chloride – malonic acid deep eutectic solvent

Copper nanoparticles were synthesized in the DES of Ch.Cl-MA as follows <sup>[11]</sup>. Nanoparticles were made by combining 10 ml of 0.01M copper nitrate trihydrate [Cu(NO<sub>3</sub>)<sub>2</sub>.3H<sub>2</sub>O] with 15 ml of choline chloride – malonic acid DES in a beaker and magnetically stirring for 30 minutes at 1200 RPM with a magnetic stirrer. During vigorous stirring, about 8-10 ml of 0.01 M hydrazine hydrate as a reducing agent was added drop by drop, followed by 10 ml of 1 M sodium hydroxide as a stabilizing agent was injected slowly into the mixture. The copper oxide nanoparticles formed in the beaker were centrifuged, rinsed several times with deionized water, then extracted using methanol, and dried in an air oven.

# 5.2.3 Synthesis of mercury nanoparticles in choline chloride – malonic acid deep eutectic solvent

Nanoparticles of mercury were synthesized in the DES of Ch.Cl-MA as follows [11].

Nanoparticles were made by combining 10 ml of 0.01M mercuric chloride [HgCl<sub>2</sub>] with 15 ml of choline chloride – malonic acid DES in a beaker and magnetically stirring for 30 minutes at 1200 RPM with a magnetic stirrer. During vigorous stirring, about 8-10 ml of 0.01 M hydrazine hydrate as a reducing agent was added drop by drop, followed by 10 ml of 1 M sodium hydroxide as a stabilizing agent was injected slowly into the mixture. The

mercury oxide nanoparticles produced in the beaker were centrifuged, rinsed several times with deionized water, then extracted using methanol, and dried in an air oven.

### 5.2.4 Synthesis of manganese nanoparticles in choline chloride – malonic acid deep eutectic solvent

Nanoparticles of manganese were synthesized in the DES of Ch.Cl-MA as follows <sup>[11]</sup>. Nanoparticles were made by combining 10 ml of 0.01M manganese chloride dihydrate [MnCl<sub>2</sub>.2H<sub>2</sub>O] with 15 ml of choline chloride – malonic acid DES in a beaker and magnetically stirring for 30 minutes at 1200 RPM with a magnetic stirrer. During vigorous stirring, about 8-10 ml of 0.01 M hydrazine hydrate as a reducing agent was added drop by drop, followed by 10 ml of 1 M sodium hydroxide as a stabilizing agent was injected slowly into the mixture. The manganese oxide nanoparticles formed in the beaker were centrifuged, rinsed several times with deionized water, then extracted using methanol, and dried in an air oven.

# 5.2.5 Synthesis of zirconium nanoparticles in choline chloride – malonic acid deep eutectic solvent

Zirconium nanoparticles were synthesized in the DES of Ch.Cl-MA as follows <sup>[11]</sup>. Nanoparticles were made by combining 10 ml of 0.01M zirconium oxychloride [ZrOCl<sub>2</sub>] with 15 ml of choline chloride – malonic acid DES in a beaker and magnetically stirring for 30 minutes at 1200 RPM with a magnetic stirrer. During vigorous stirring, about 8-10 ml of 0.01 M hydrazine hydrate as a reducing agent was added drop by drop, followed by 10 ml of 1 M sodium hydroxide as a stabilizing agent was injected slowly into the mixture. The zirconium oxide nanoparticles produced in the beaker were centrifuged, rinsed several times with deionized water, then extracted using methanol, and dried in an air-oven.

# 5.2.6 Synthesis of silver nanoparticles in choline chloride – malonic acid deep eutectic solvent

Nanoparticles of silver were synthesized in the DES of Ch.Cl-MA as follows <sup>[11]</sup>. Nanoparticles were made by combining 10 ml of 0.01M silver nitrate [AgNO<sub>3</sub>] with 15 ml of choline chloride – malonic acid DES in a beaker and magnetically stirring for 30 minutes at 1200 RPM with a magnetic stirrer. During vigorous stirring, about 8-10 ml of 0.01 M hydrazine hydrate as a reducing agent was added drop by drop, followed by 10 ml of 1 M sodium hydroxide as a stabilizing agent was injected slowly into the mixture. The silver oxide nanoparticles attained in the beaker were centrifuged, rinsed several times with deionized water, then extracted using methanol, and dried in an air oven.

# 5.2.7 Synthesis of zinc nanoparticles in choline chloride – malonic acid deep eutectic solvent

Zinc nanoparticles were synthesized in the DES of Ch.Cl-MA as follows [11]. Nanoparticles were made by combining 10 ml of 0.01M Zinc acetate dihydrate [Zn(COOCH<sub>3</sub>)<sub>2</sub>.2H<sub>2</sub>O] with 15 ml of choline chloride – malonic acid DES in a beaker and magnetically stirring for 30 minutes at 1200 RPM with a magnetic stirrer. During vigorous stirring, about 8-10 ml of 0.01 M hydrazine hydrate as a reducing agent was added drop by drop, followed by 10 ml of 1 M sodium hydroxide as a stabilizing agent was injected slowly into the mixture. The zinc oxide nanoparticles gained in the beaker were centrifuged, rinsed several times with deionized water, then extracted using methanol, and dried in an air oven. **5.2.8 Synthesis of cadmium nanoparticles in choline chloride – malonic acid deep eutectic solvent** 

Cadmium nanoparticles were synthesized in the DES of Ch.Cl-MA as follows <sup>[11]</sup>. Nanoparticles were made by combining 10 ml of 0.01M cadmium chloride [CdCl<sub>2</sub>] with 15 ml of choline chloride – malonic acid DES in a beaker and magnetically stirring for 30

minutes at 1200 RPM with a magnetic stirrer. During vigorous stirring, about 8-10 ml of 0.01 M hydrazine hydrate as a reducing agent was added drop by drop, followed by 10 ml of 1 M sodium hydroxide as a stabilizing agent was injected slowly into the mixture. The cadmium oxide nanoparticles yielded in the beaker were centrifuged, rinsed several times with deionized water, then extracted using methanol, and dried in an air oven.

# 5.2.9 Synthesis of vanadium nanoparticles in choline chloride – malonic acid deep eutectic solvent

The vanadium nanoparticles were synthesized in the DES of Ch.Cl-MA as follows [11]. Nanoparticles were made by combining 10 ml of 0.01M vanadium pentoxide [V<sub>2</sub>O<sub>5</sub>] with 15 ml of choline chloride – malonic acid DES in a beaker and magnetically stirring for 30 minutes at 1200 RPM with a magnetic stirrer. During vigorous stirring, about 8-10 ml of 0.01 M hydrazine hydrate as a reducing agent was added drop by drop, followed by 10 ml of 1 M sodium hydroxide as a stabilizing agent was injected slowly into the mixture. The vanadium oxide nanoparticles formed in the beaker were centrifuged, rinsed several times with deionized water, then extracted using methanol, and dried in an air oven.

# 5.2.10 Synthesis of nickel nanoparticles in choline chloride – malonic acid deep eutectic solvent

Nickel nanoparticles were synthesized in the DES of Ch.Cl-MA as follows <sup>[11]</sup>. Nanoparticles were made by combining 10 ml of 0.01M nickel nitrate [Ni(NO<sub>3</sub>)<sub>2</sub>] with 15 ml of choline chloride – malonic acid DES in a beaker and magnetically stirring for 30 minutes at 1200 RPM with a magnetic stirrer. During vigorous stirring, about 8-10 ml of 0.01 M hydrazine hydrate as a reducing agent was added drop by drop, followed by 10 ml of 1 M sodium hydroxide as a stabilizing agent was injected slowly into the mixture. The nickel oxide nanoparticles formed in the beaker were centrifuged, rinsed several times with deionized water, then extracted using methanol, and dried in an air oven.

#### **5.3 Results and Discussions**

The synthesized copper, mercury, manganese, zirconium, silver, zinc, cadmium, vanadium and nickel nanoparticles in the deep eutectic solvent of choline chloride – malonic acid were characterized by the techniques such as UV-Visible spectroscopy, Fourier transform infrared spectroscopy, Scanning electron microscopy, X-Ray diffraction and Energy dispersive X-ray analysis.

### 5.3.1 UV-Visible Spectra of Metal Nanoparticles Prepared Using Choline Chloride – Malonic Acid Deep Eutectic Solvent

The UV-Visible spectra of copper, mercury, manganese, zirconium, silver, zinc, cadmium, vanadium and nickel oxide nanoparticles obtained in their ethanolic solutions between the wavelengths 200 and 800nm are placed in figures 5.1 to 5.9. The surface plasmon absorption of metal nanoparticles are usually seen around 400 nm. Larger sizes shift the band to a longer wavelength and broaden the band to some extent and however, very dumped plasmon and very broad bands could be due to surface adsorptions [12, 13]. The bands due to either surface plasmon or surface adsorptions of these metal oxide nanoparticles are given in table 5.1 below.

From the UV-Visible spectra of metal oxide nanoparticles displayed in figures 5.1 to 5.9, it was followed that the copper, manganese and zirconium showed surface plasmon absorption bands at the specific wavelengths as given in table 5.1. The mercury, silver, zinc, cadmium, vanadium and nickel oxide nanoparticles obtained from the DES of Ch.Cl – MA gave very broad and dumped absorption bands due to surface adsorptions. All metal-oxide nanoparticles except mercury which were prepared from the deep eutectic solvent of choline chloride – malonic acid are showing the absorptions in the visible region. Therefore, these metal oxide nanoparticles prepared from the deep eutectic solvent of

choline chloride – malonic acid except mercury are anticipated to have photocatalytic activity.

Table 5.1: UV-Visible absorption bands of metal oxide nanoparticles obtained from Ch.Cl-MA DES

S. No.	Metal Oxide NPs	λ <sub>max</sub> values (nm)	Nature of bands	
1	Copper	340.65, 406.75	Surface Plasmon	
2	Mercury	380	Surface Adsorption	
3	Manganese	340.45, 427.10	Surface Plasmon	
4	Zirconium	352.42, 548.65, 679.35	Surface Plasmon	
5	Silver	253.9, 305.9, 434.85	Surface Adsorption	
6	Zinc	226.9, 278.55, 372.65,	Surface Adsorption	
U	ZIIIC	547.15	Surface Adsorption	
7	Cadmium	378.85, 756.85	Surface Adsorption	
8	Vanadium	389.15, 568.45	Surface Adsorption	
9	Nickel	224.25, 286.55, 372.1,	Surface Adsorption	
J	IVICKCI	692.95	Surface Ausorption	

# 5.3.2 FTIR Spectra of Metal Nanoparticles Prepared Using Choline Chloride – Malonic acid Deep Eutectic Solvent

The FTIR spectra obtained in the range of 400 to 4000 cm<sup>-1</sup> for copper, mercury, manganese, zirconium, silver, zinc, cadmium, vanadium and nickel metal oxide nanoparticles prepared from the deep eutectic solvent of choline chloride-malonic acid are reported in figures 5.10 to 5.18 of this section. The infra-red peaks of various metal oxide nanoparticles such as copper, mercury, manganese, zirconium, silver, zinc, cadmium, vanadium and nickel prepared from the DES of choline chloride – urea were presented in the following table 5.2.

Table 5.2: FTIR absorption peaks of metal oxide nanoparticles obtained from Ch.Cl-MA DES

S.No.	Metal Oxide	IR Vibrations						
	NPs	M-O Vibrations	C-O Stretch	CH2 deform (methylene)	C-H bend (alkane)	O-H bend	C-O asym stretch	O-H stretch
1	Cu	437, 514,	1026	1383	-	1623	2921	3431
		601, 846						
2	Hg	580, 716,	1066	1360	1440	1619	2940	3462
		829						
3	Mn	537, 720,	1082	1377	1467	1675	2916	3411
		814						
4	Zr	626, 854	1109,	1382	-	1621	2929	3466
			1036					
5	Ag	430. 637	-	-	1401	1617	2914	3421
6	Zn	466, 725	1086	1399	1481	1624	2955	3441
7	Cd	513, 614	1087	1357	1436	1609	2921	3448
8	V	465, 632,	1068	1369	1430	1601	2928	3429
		839						
9	Ni	456, 681	1102	1368	1437	1611	2919	3421

The several peaks noticed in the range of  $400 \text{ to } 900 \text{ cm}^{-1}$  are correlated to respective M – O vibrations of MO nanoparticles <sup>[14, 15]</sup>. A few of the solvent molecules are capped on the surface of MO nanoparticles. These are indicated by the peaks around 1040 and 1120 cm<sup>-1</sup> corresponding to the C – O stretching vibrations. The peak due to C – H bending of alkane and CH<sub>2</sub> deformations of both the components of the DES choline chloride and malonic acid is seen around 1470 cm<sup>-1</sup> and 1380 cm<sup>-1</sup> in all these spectra. The peak was

noticed around 1600 cm<sup>-1</sup> denoted O – H bending vibrations of the choline chloride part of the deep eutectic solvent. The peaks observed around 2850 cm<sup>-1</sup> and 2920 cm<sup>-1</sup> are due to C – O asymmetric stretching <sup>[15]</sup>. Further, the broad peaks seen around 3420 cm<sup>-1</sup> in all the spectra due to different vibrations modes of water molecules adsorbed on the surface of metal oxide nanoparticles <sup>[14]</sup>.

From these FTIR spectra data summarized in table 5.2, it is followed that either of the component's choline chloride or malonic acid, or both of the DES used in the preparation of metal oxide nanoparticles had been capped on the surface of these metal oxide nanoparticles.

# 5.3.3 XRD Patterns of Metal Nanoparticles Prepared Using Choline Chloride – Malonic Acid Deep Eutectic Solvent

The XRD patterns obtained for copper, mercury, manganese, zirconium, silver, zinc, cadmium, vanadium and nickel oxide nanoparticles prepared from the deep eutectic solvent of choline chloride-malonic acid are reported and discussed as follows. The powder x-ray diffraction patterns of copper oxide nanoparticles prepared from the deep eutectic solvents, Ch.Cl – MA are given in figure 5.19. The XRD patterns give information about the grain size, structure, and phase cleanliness of the materials. In the case of CuO particles obtained in Ch.Cl – MA DES, the diffraction peaks seen at 2θ values of 24.56°, 41.89° and 68.73° are indexed as (040), (420) and (300) respectively. The grain size of CuO nanoparticles is determined by using the Debye–Scherer formula,

$$\mathbf{D} = k \lambda / \beta \cos \theta$$

where D denotes the grain size, K refers to a constant,  $\lambda$  refers to the wavelength of X-ray used,  $\beta$  denotes the fullwidth half-maximum of the diffraction peaks and  $\theta$  is the angle of the diffraction [14]. By using this formula, the average grain size of CuO nanoparticles prepared from the DES of Ch. Cl-MA is found to be 75 nm.

All the diffraction points in the XRD can be assigned to the pure cubic lattice structure of mercury oxide nanoparticles as given in figure 5.20. The peaks correspond to (111), (200), (220), and (222) planes, which are in good pact with the JCPDS pattern available in the literature. The average crystal width of the HgO nanoparticles obtained in the DES of Ch.Cl-MA was found to be 55 nm using the Scherrer formula of the XRD pattern. The crystalline behaviour of the prepared MnO nanoparticles was inspected by the XRD analysis and given in figure 5.21. The XRD patterns revealed the diffraction peaks at 20 values for manganese oxide nanoparticles at 37.23, 55.10 and 66.26. These values are in accordance with the crystal planes (101), (110) and (200). The mean particle size for MnO nanoparticles prepared from the DES of Ch. Cl-MA is found to be 79 nm using the Scherrer formula.

The XRD pattern for zirconium oxide nanoparticles prepared using the solvent of choline chloride – malonic acid is provided at figure 5.22. The diffraction peaks noticed in this figure for ZrO nanoparticles are in agreement with the Joint Committee for Powder Diffraction Studies (JCPDS) [16]. The average grain size of the ZrO nanoparticles with respect to relative intensity peak at XRD pattern was found to be 102 nm when the Scherrer formula is applied. The AgO nanoparticles obtained in the case of Ch. Cl-MA DES reported in figure 5.23 showed intense peaks at 20 values of 45.57, 63.28 and 77.35 which are indexed corresponding to the planes of (110), (220) and (311) respectively. The structure of silver oxide nanoparticles is crystalline in nature, and it is face-centered cubic in this case. The average particle size of AgO NPs obtained in the case of Ch. Cl-MA DES is calculated to be 59 nm by measuring the breadth of (111) Bragg's reflection.

Figure 5.24 noticed the XRD data of zinc oxide nanoparticles obtained from the DES of Ch. Cl-MA. The XRD plots of the nanoparticles showed peaks of pure hexagonal structure of zinc oxide. Three reflection planes (100), (002) and (101) that have been seen

are similar to the detected reflections in bulk materials of zinc oxide <sup>[17]</sup>. The diffraction peaks obtained at 29.36°, 36.61°, 38.62°, 46.71°, 59.14°, 69.72 and 76.52° are intense and sharp representing that the nano-crystalline zinc oxide nanoparticles had good crystallinity. The highest intensity at figure 5.24 related to zinc oxide nanoparticles reflecting the nanorange size around 131 nm by using Debye – Scherrer formula. The particle size determined involving the comparative intensity peak (220) found at 20 value of 52.32° of CdO nanoparticles as given in figure 5.25 has been observed as 60 nm. This is calculated using the Scherrer formula from figure 5.25 corresponding to the CdO nanoparticles obtained from the DES of Ch. Cl-MA. The surge in sharpness of XRD peaks designates those particles are in crystalline kind. The (111), (200), (220), (311) and (222) reflections which correspond to 42.22, 47.32, 50.12, 69.81 and 73.53 respectively, are obviously seen and meticulously bout the reference designs of CdO (JCPDS) File No. 05-0640). The piercing XRD peaks show that the particles were of polycrystalline assembly, further the nanostructure was raised with a random orientation <sup>[18, 19]</sup>.

The crystalline kind of DES media synthesized vanadium oxide nanoparticles was depicted in figure 5.26. The characteristic key diffraction peaks noticed at  $2\theta$  values of 14.70, 20.41, 22.20, 26.61, 30.09, 32.20, 34.21, 41.41, 42.50, 45.54, 48.31 and 52.21 that match with the hkl planes of (200), (001), (101), (110), (310), (011), (310), (002), (102), (411), (600) and (302) index planes were in decent arrangement with their standard JCPDS No. 41-1426 [20]. The size of vanadium oxide nanoparticles was found by using Scherrer's formula to be roughly 57 nm. The XRD pattern obtained for NiO nanoparticles in Ch. Cl-MA DES is shown in figure 5.27. Three peaks for NiO NPs at  $2\theta$  values of 43.06°, 51.23° and 74.92° corresponding to the (111), (200) and (222) lattice planes found established that the ensuing particles have been pure Nickel oxide nanoparticles [21]. The nanoparticle width was projected by using Scherrer's equation to be around 82 nm.

## 5.3.4 SEM Analysis of Metal Nanoparticles Prepared Using Choline Chloride – Malonic Acid Deep Eutectic Solvent

The SEM images were obtained for copper, mercury, manganese, zirconium, silver, zinc, cadmium, vanadium and nickel oxide nanoparticles prepared from the deep eutectic solvent of choline chloride-malonic acid are reported and discussed herewith. To examine the morphological structure and particle size of metal oxide nanoparticles such as Cu, Hg, Mn, Zr, Ag, Zn, Cd, V and Ni, scanning electron microscopy was used [22, 23]. The assembly, geometry, and magnitude of the above metal oxide nanoparticles prepared from the DES of Ch. Cl-MA were evaluated from the Scanning Electron Microscopy images which are displayed in figures 5.28 to 5.36. The mean particle dimensions of these metal oxide nanoparticles were calculated from the histograms of the respective SEM images and they are shown in figures 5.37 to 5.45. Further, the shapes and mean size of the prepared metal oxide nanoparticles are given in table 5.3 below.

Table 5.3: SEM morphology and size of metal oxide nanoparticles obtained from Ch. Cl-MA DES

S. No.	Metal Oxide NPs	Morphology	Size (nm)
1	Copper	Irregular Tiles	75
2	Mercury	Spongy Beads	55
3	Manganese	Manganese Polygonal Scales	
4	Zirconium	Scales Like	102
5	Silver	Irregular Spheres	59
6	Zinc	Flower Like	131
7	Cadmium	Broken Tiles	60
8	Vanadium	Clogged Buds	57
9	Nickel	Spongy Scales	82

## 5.3.5 EDAX Analysis of Metal Nanoparticles Prepared Using Choline Chloride – Malonic Acid Deep Eutectic Solvent

The elemental composition and the purity of the DES media via prepared metal oxide nanoparticles are confirmed by Energy Dispersive X-ray Analysis. The elemental cleanliness of these metal oxide NPs was evaluated from the EDAX spectra and the peak values established the occurrence of target components in the synthesized NPs [24-28]. The EDAX spectra obtained for copper, mercury, manganese, zirconium, silver, zinc, cadmium, vanadium and nickel oxide nanoparticles prepared from the deep eutectic solvent of choline chloride-malonic acid are reported in the figures 5.46 to 5.54. The elemental purity, weight percentage, atom percentage of metals, oxygen and the trace of elements of solvent were given in the tables as an insert of the respective EDAX spectra of metal oxide nanoparticles.

#### **5.4.** Conclusion

Nine types of metal oxide nanoparticles were synthesized successfully using choline chloride – malonic acid deep eutectic solvents. The copper, mercury, manganese, zirconium, silver, zinc, cadmium, vanadium and nickel oxide nanoparticles prepared were characterized by techniques such as UV spectroscopy, FTIR spectroscopy, X-Ray diffraction, Scanning Electron Microscopy and Energy Dispersive X-ray Analysis. The nanoparticles were synthesized in a simple and convenient manner. There was no surfactant and seeds were utilized for the formation of nanoparticles. The size of the particles formed was controlled by varying proportions of the water present in the DESs.

#### References

- [1] Bundschuh, M., Filser, J., Lüderwald, S., McKee, M.S., Metreveli, G., Schaumann, G.E., Schulz, R. and Wagner, S., Nanoparticles in the environment: where do we come from, where do we go to? Environmental Sciences Europe, 30(1) (2018), pp.1-17.
- [2] Khodashenas, B. and Ghorbani, H.R., Synthesis of copper nanoparticles: An overview of the various methods. Korean Journal of Chemical Engineering, 31(7) (2014), pp.1105-1109.
- [3] Cai, X., Zhu, Q., Zeng, Y., Zeng, Q., Chen, X. and Zhan, Y., Manganese oxide nanoparticles as MRI contrast agents in tumor multimodal imaging and therapy. International journal of nanomedicine, 14 (2019), p.8321.
- [4] Sigwadi, R., Dhlamini, M., Mokrani, T. and Nemavhola, F., Preparation of a high surface area zirconium oxide for fuel cell application. International Journal of Mechanical and Materials Engineering, 14(1) (2019), pp.1-11.
- [5] Qinghua Zhang, Karine De Oliveira Vigier, Sebastien Royer and Francois Jerome, Deep eutectic solvents: syntheses, properties and applications. Chem. Soc. Rev., 41 (2012), pp.7108–7146, DOI: 10.1039/c2cs35178a.
- [6] Emma L. Smith, Andrew P. Abbott, and Karl S. Ryder, Deep Eutectic Solvents (DESs) and Their Applications. pubs.acs.org/CR Chem. Rev. 114 (2014), pp. 11060-11082, dx.doi.org/10.1021/cr300162p.
- [7] Hai-Chuan-Hu, Deep eutectic solvent based on choline chloride and malonic acid as an efficient and reusable catalytic system for one-pot synthesis of functionalized pyrroles, RSC Advances, Issue 10,2015.
- [8] Kroon, M.C.; Binnemans, K. Degradation of deep-eutectic solvents based on choline chloride and carboxylic acids. ACS Sustain. Chem. Eng. 2019, 7, 11521–11528.

- [9] Iman Al-Wahaibi et al., The novel use of malonic acid-based deep eutectic solvents forenhancing heavy oil recovery; International Journal of Oil, Gas and Coal Technology, 2019 Vol.20 No.1, pp.31 54; DOI: 10.1504/IJOGCT.2019.096493.
- [10] Gunny, A. A. N.; Arbain, D.; Nashef, E. M.; Jamal, P.; Bioresour. Technol. 2015, 181, 297.
- [11] M. Abdulla-Al-Mamun, Y. Kusumoto, and M. Muruganandham, "Simple new synthesis of copper nanoparticles in water/acetonitrile mixed solvent and their characterization," Materials Letters, vol. 63, no. 23, pp. 2007–2009.
- [12] Shikha Jain, Ankita Jain, Vijay Devra, Copper nanoparticles catalyzed oxidation of threonine by peroxomonosulfate, Journal of Saudi chemical society 18 (2014), 149 153.
- [13] E.C. Njagi, H. Huang, L. Stafford, H. Genuino, et al., Langmuir 27 (2011) 264–271.
- [14] Tariq Jan, J. Iqbal, Umar Farooq, Asma Gul, Rashda Abbasi, Ishaq Ahmad, Maaza Malik, Structural, Raman and optical characteristics of Sn doped CuO nanostructures: A novel anticancer agent, Ceramics International, 41(10), Part A December 2015, 13074 79. http://dx.doi.org/10.1016/j.ceramint.2015.06.080.
- [15] A. Rita, A. Sivakumar, S. A. Martin Britto Dhas, Influence of shock waves on structural and morphological properties of copper oxide NPs for aerospace applications, Journal of Nanostructure in Chemistry, 9 (2019), 225 230. https://doi.org/10.1007/s40097-019-00313-0
- [16] Saeid and, Asadi Asadollah, Tamijani-Habibi Amir, and Negahdary M, Synthesis of Zirconia Nanoparticles and their Ameliorative Roles as Additives Concrete Structures, Journal of Chemistry, Volume 2013 | Article D 314862, 1-7. https://doi.org/10.1155/2013/314862

- [17] M.A. Ramadan, S.H. Nassar, A.S. Montaser, E.M. El-Khatib and M.S.Abdel-Aziz, Synthesis of Nano-sized Zinc Oxide and Its Application for Cellulosic Textiles, Egypt. J. Chem. 59, No.4, pp. 523 535 (2016).
- [18] A.S. Aldwayyan, F.M. Al-Jekhedab, M. Al-Noaimi, B. Hammouti, T. B. Hadda, M. Suleiman, I. Warad, Synthesis and Characterization of CdO Nanoparticles Starting from Organometalic Dmphen-CdI2 complex, Int. J. Electrochem. Sci., 8 (2013) 10506 10514. [19] H.P. Klug, and L.E. Alexander, X-ray Diffraction Procedures for Polycrystalline and Amorphous Materials, Wiley, New York (1954).
- [20] Mohammad hassan Gholami-Shabani, Fattah Sotoodehnejadnematalahi, Masoomeh Shams-Ghahfarokhi, Ali Eslamifar and Mehdi Razzaghi-Abyaneh, Mycosynthesis and Physicochemical Characterization of Vanadium Oxide Nanoparticles Using the Cell-Free Filtrate of Fusarium oxysporum and Evaluation of Their Cytotoxic and Antifungal Activities, Journal of Nanomaterials, Volume 2021, Article ID 7532660, 1-7. <a href="https://doi.org/10.1155/2021/7532660">https://doi.org/10.1155/2021/7532660</a>.
- [21] Szu-HanWu, Dong-HwangChen, Synthesis and characterization of nickel nanoparticles by hydrazine reduction in ethylene glycol, <u>Journal of Colloid and Interface</u> <u>Science, Volume 259, (2)</u>, 15 March 2003, Pages 282-286, <a href="https://doi.org/10.1016/S0021-9797(02)00135-2">https://doi.org/10.1016/S0021-9797(02)00135-2</a>.
- [22] Szu-HanWu, Dong-HwangChen, Synthesis and characterization of nickel nanoparticles by hydrazine reduction in ethylene glycol, <u>Journal of Colloid and Interface Science</u>, <u>Volume 259</u>, (2), 15 March 2003, Pages 282-286, <a href="https://doi.org/10.1016/S0021-9797(02)00135-2">https://doi.org/10.1016/S0021-9797(02)00135-2</a>.
- [23] Sarjuna, K. and Ilangeswaran, D., Preparation and Physico-chemical studies of Ag<sub>2</sub>O nanoparticles using newly formed malonic acid and ZnCl2-based deep eutectic solvents. Mater. Today Proc. 49 (2022), pp. 2943–2948.

- [24] A. El-Trass, H. ElShamy, I. El-Mehasseb, M. El-Kemary, CuO nanoparticles: synthesis, characterization, optical properties and interaction with amino acids, Appl. Surf. Sci. 258 (2012) 2997–3001.
- [25] Sundararaju Sathyavathi, Arumugam Manjula, Jeyaprakash Rajendhran, Paramasamy Gunasekaran, Biosynthesis and characterization of mercury sulphide nanoparticles produced by Bacillus cereus MRS-1, Indian J. Exp. Biol. 51 (2013) 973–978.
- [26] S. Ganeshan, P. Ramasundari, A. Elangovan, G. Arivazhagan, R. Vijayalakshmi, Synthesis and characterization of MnO2 nanoparticles: study of structural and optical properties, Int. J. Scient. Res. Phys. Appl. Sci. 5 (6) (2017) 5–8.
- [27] Ahmed Mishaal Mohammed, Mahmood Mohammed Ali, Synthesis and characterisation of zirconium oxide nanoparticles via the hydrothermal method and evaluation of their antibacterial activity, Res. J. Pharm. Technol. 14 (2) (2021), 938–942. [28] A. Rita, A. Sivakumar, S.A. Martin Britto Dhas, Influence of shock waves on structural and morphological properties of copper oxide NPs for aerospace applications, J. Nanostruct. Chem. 9 (2019) 225–230.

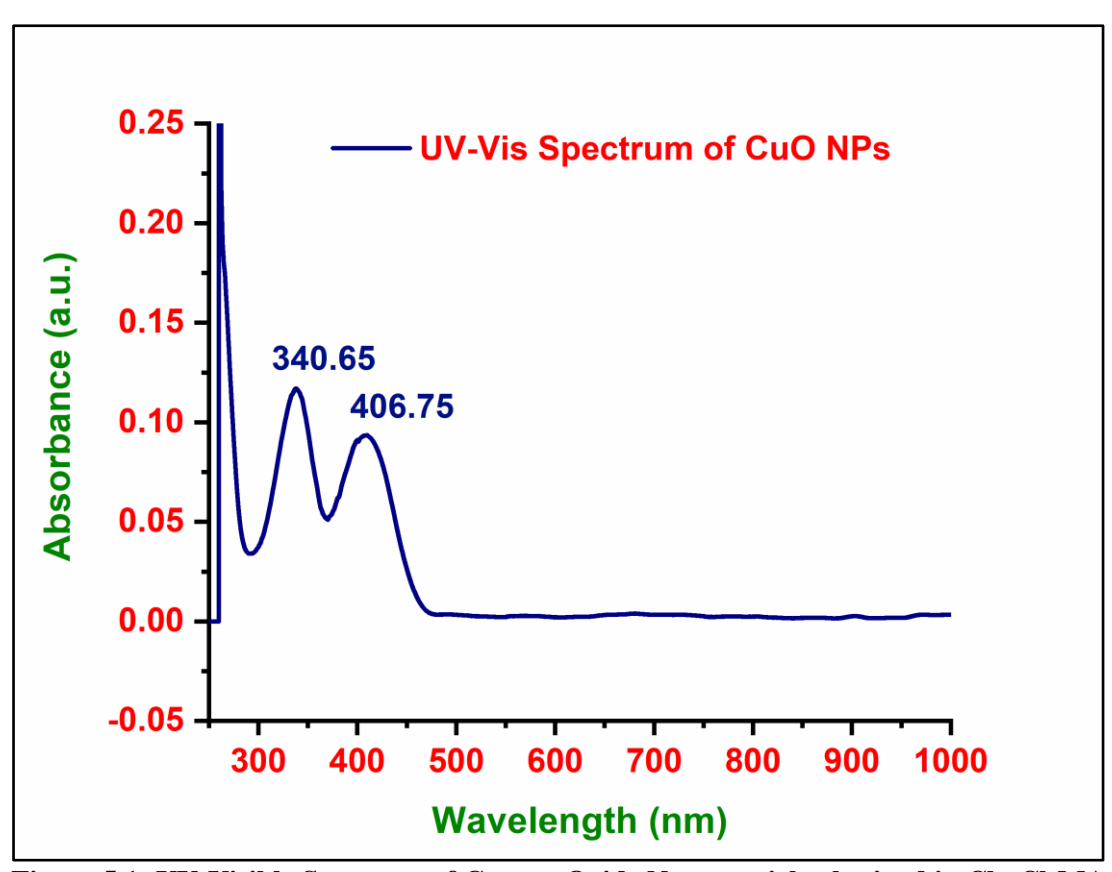


Figure 5.1: UV-Visible Spectrum of Copper Oxide Nanoparticle obtained in Ch. Cl-MA DES

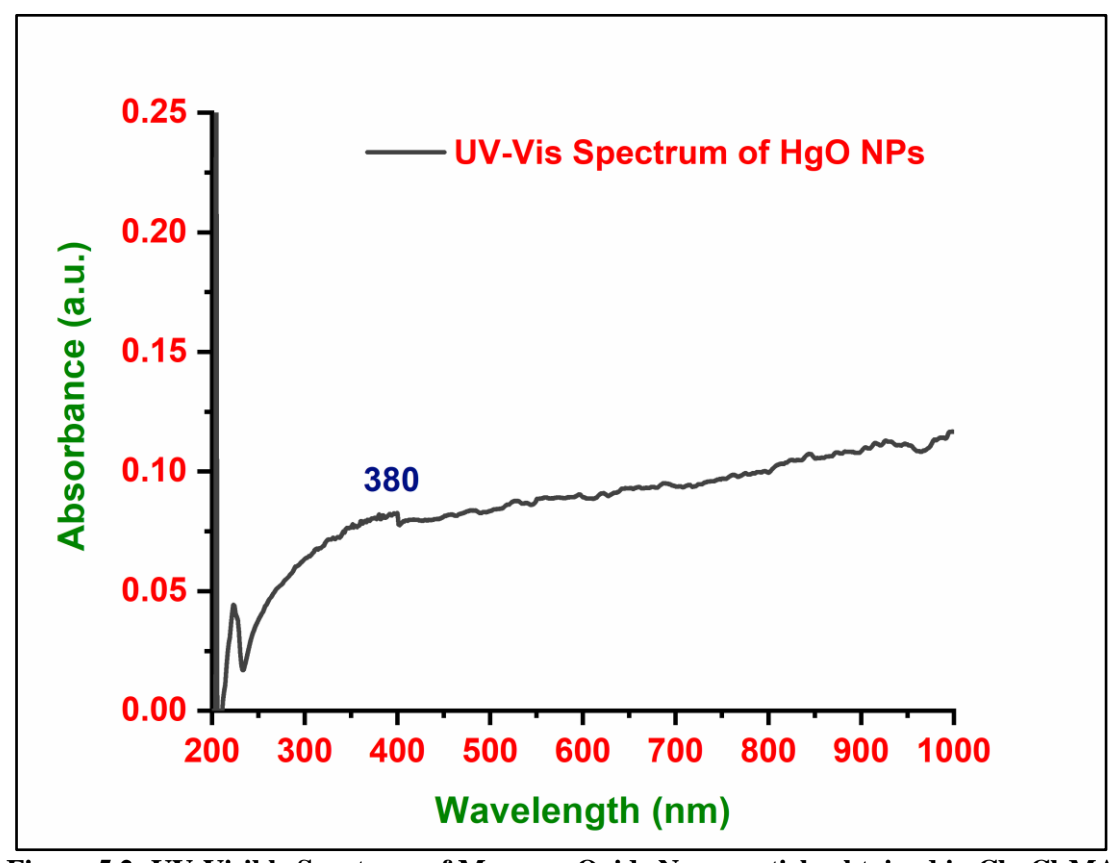


Figure 5.2: UV-Visible Spectrum of Mercury Oxide Nanoparticle obtained in Ch. Cl-MA DES

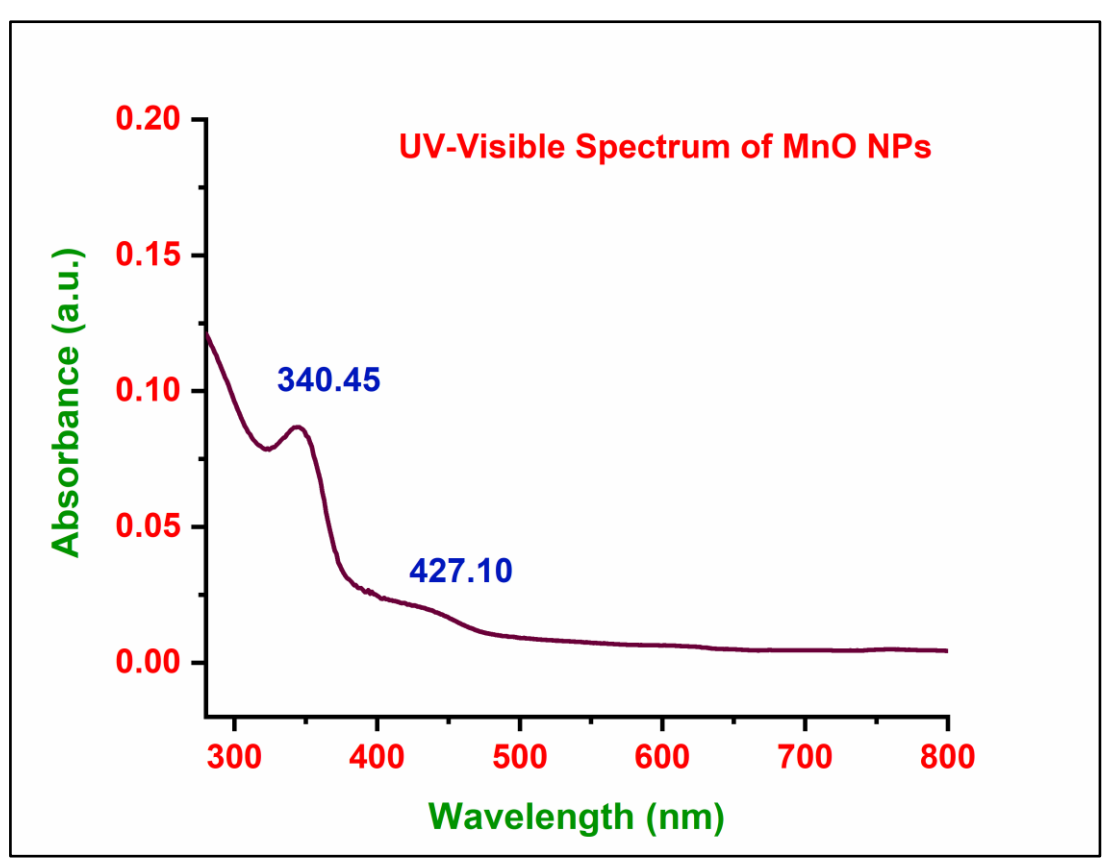


Figure 5.3: UV-Visible Spectrum of Manganese Oxide Nanoparticle obtained in Ch. Cl-MA DES

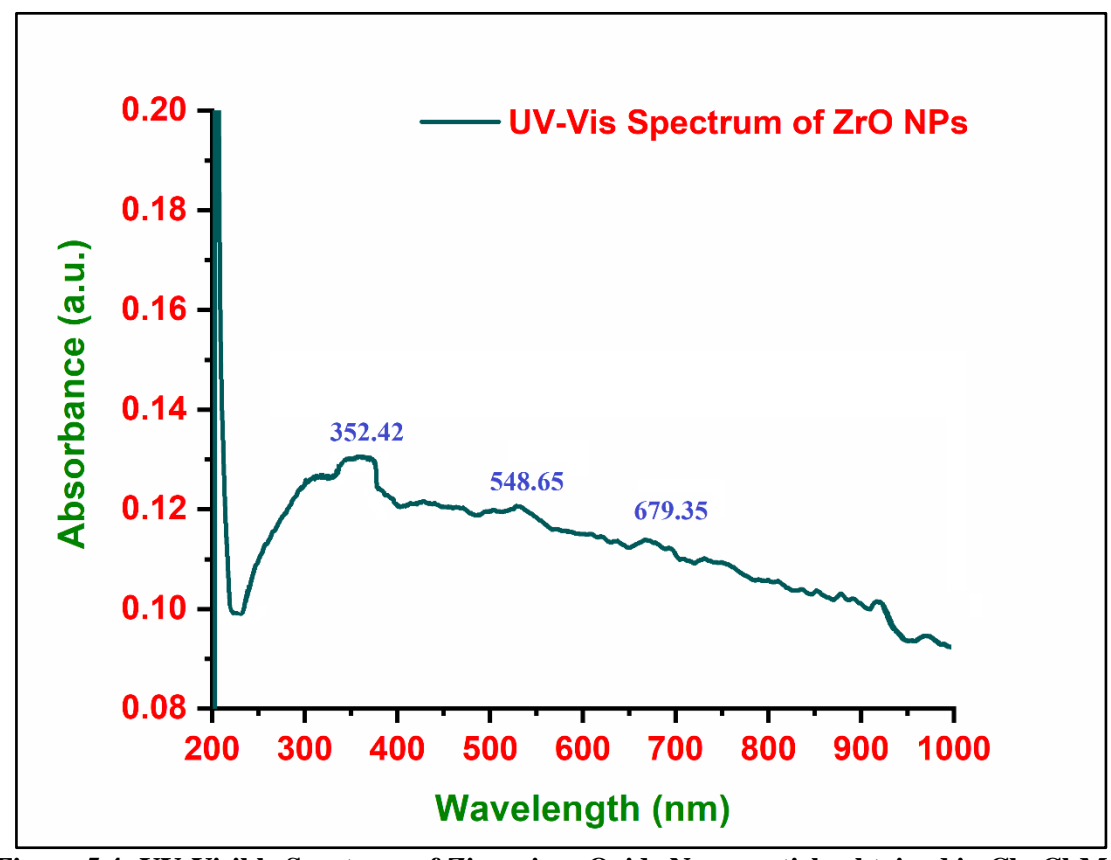


Figure 5.4: UV-Visible Spectrum of Zirconium Oxide Nanoparticle obtained in Ch. Cl-MA DES

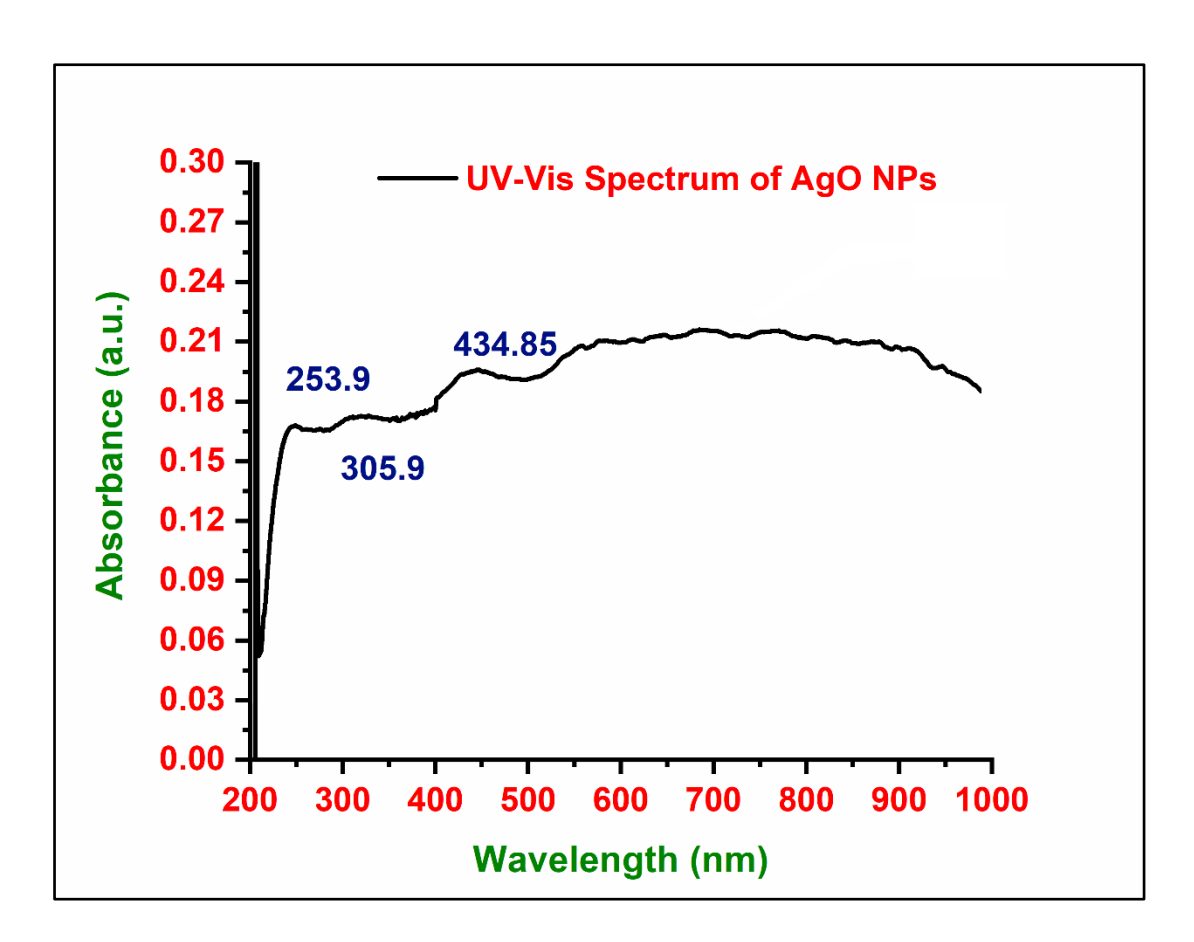


Figure 5.5: UV-Visible Spectrum of Silver Oxide Nanoparticle obtained in Ch. Cl-MA DES

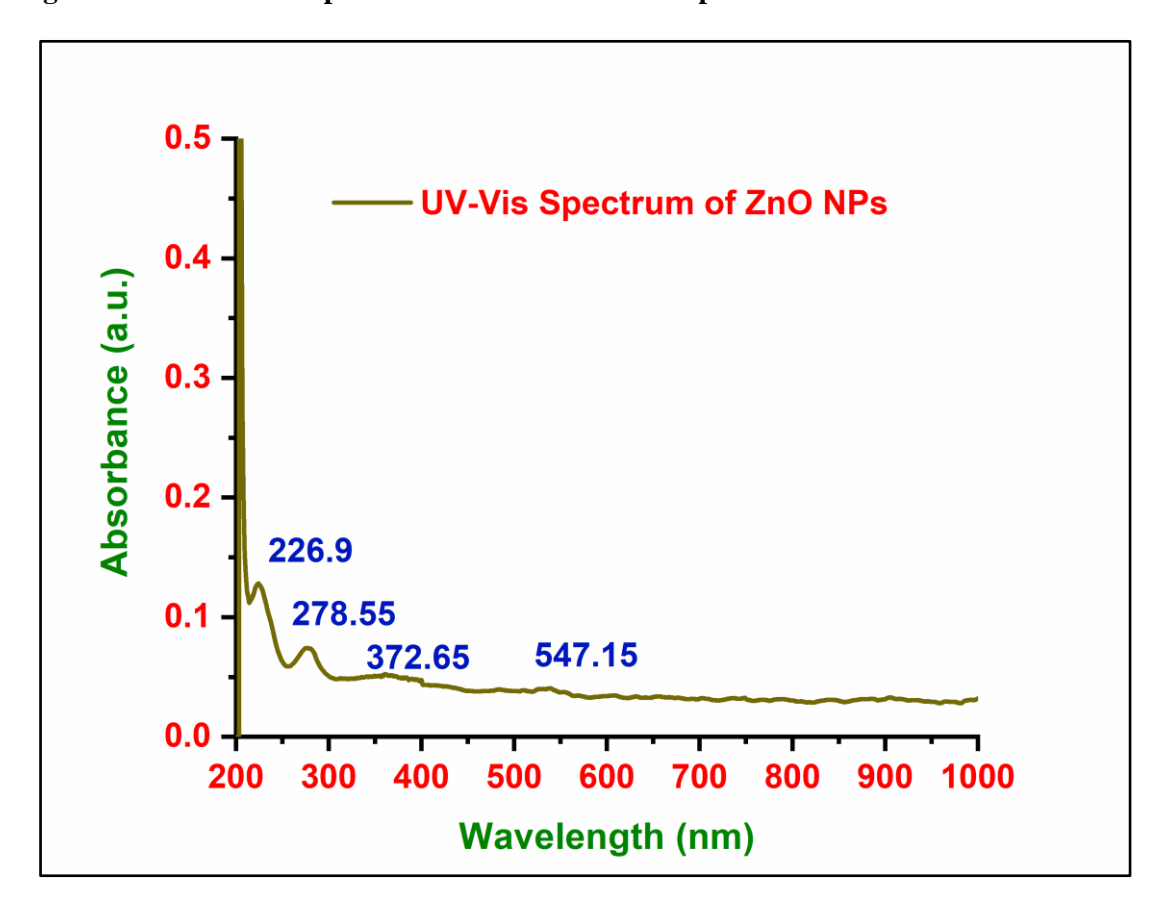


Figure 5.6: UV-Visible Spectrum of Zinc Oxide Nanoparticle obtained in Ch. Cl-MA DES

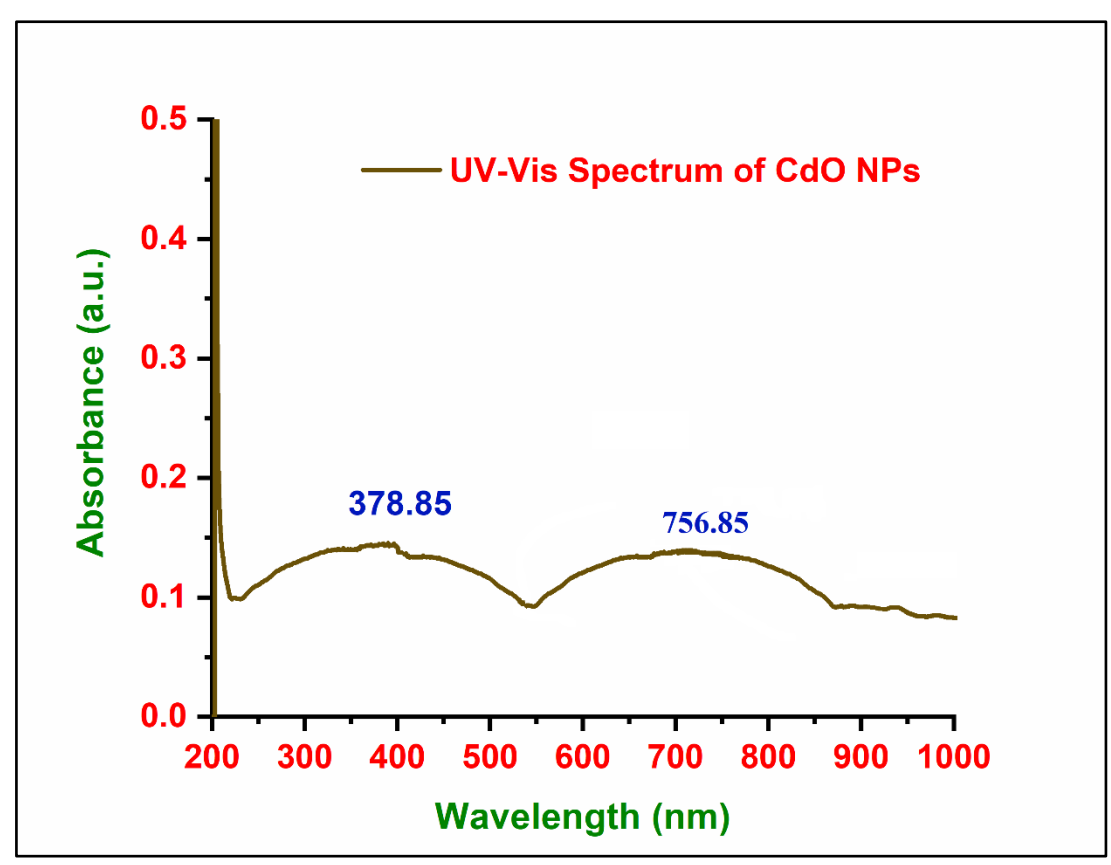


Figure 5.7: UV-Visible Spectrum of Cadmium Oxide Nanoparticle obtained in Ch. Cl-MA DES

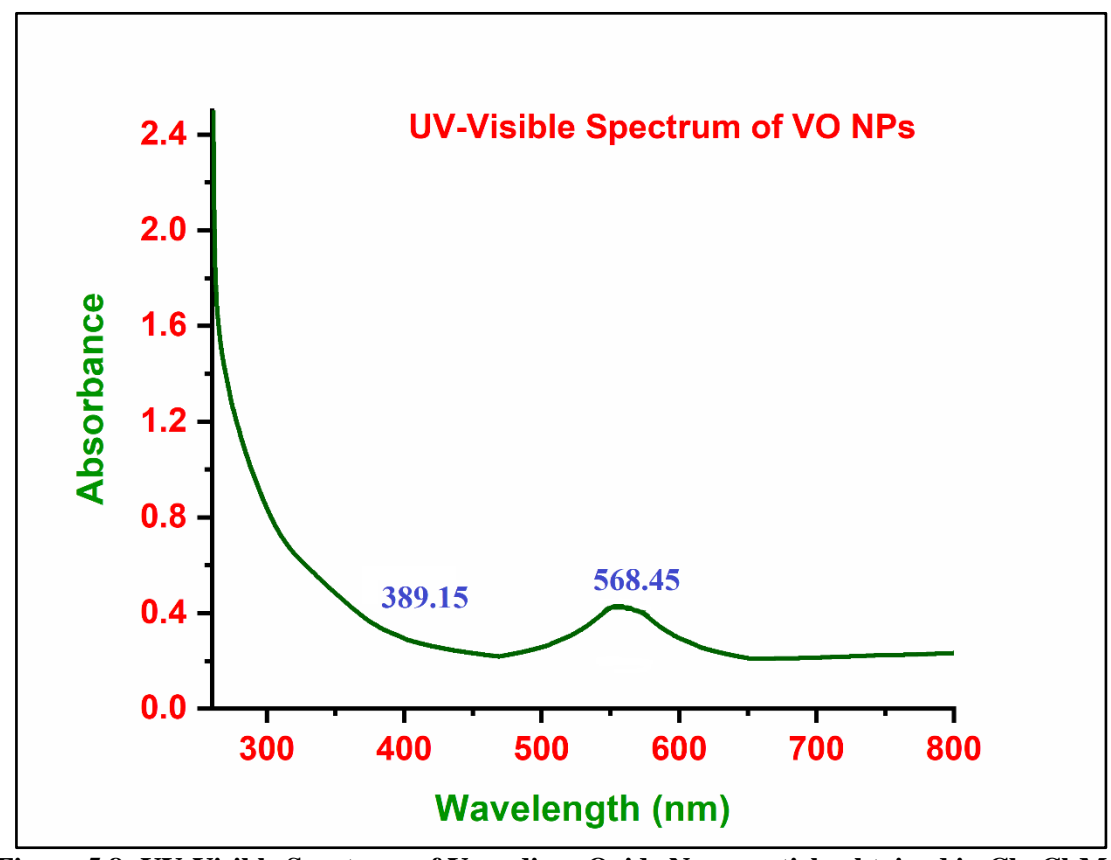


Figure 5.8: UV-Visible Spectrum of Vanadium Oxide Nanoparticle obtained in Ch. Cl-MA DES

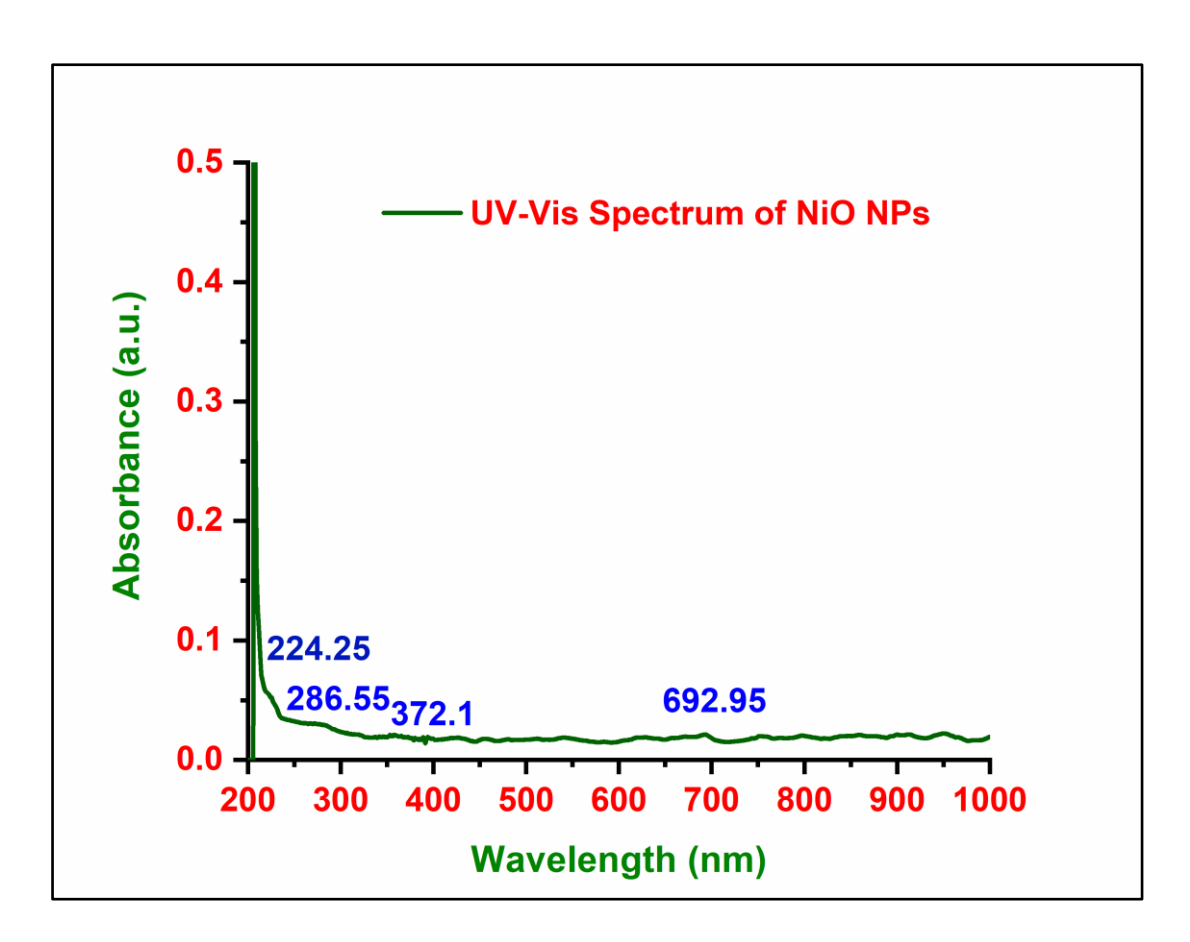


Figure 5.9: UV-Visible Spectrum of Nickel Oxide Nanoparticle obtained in Ch. Cl-MA DES

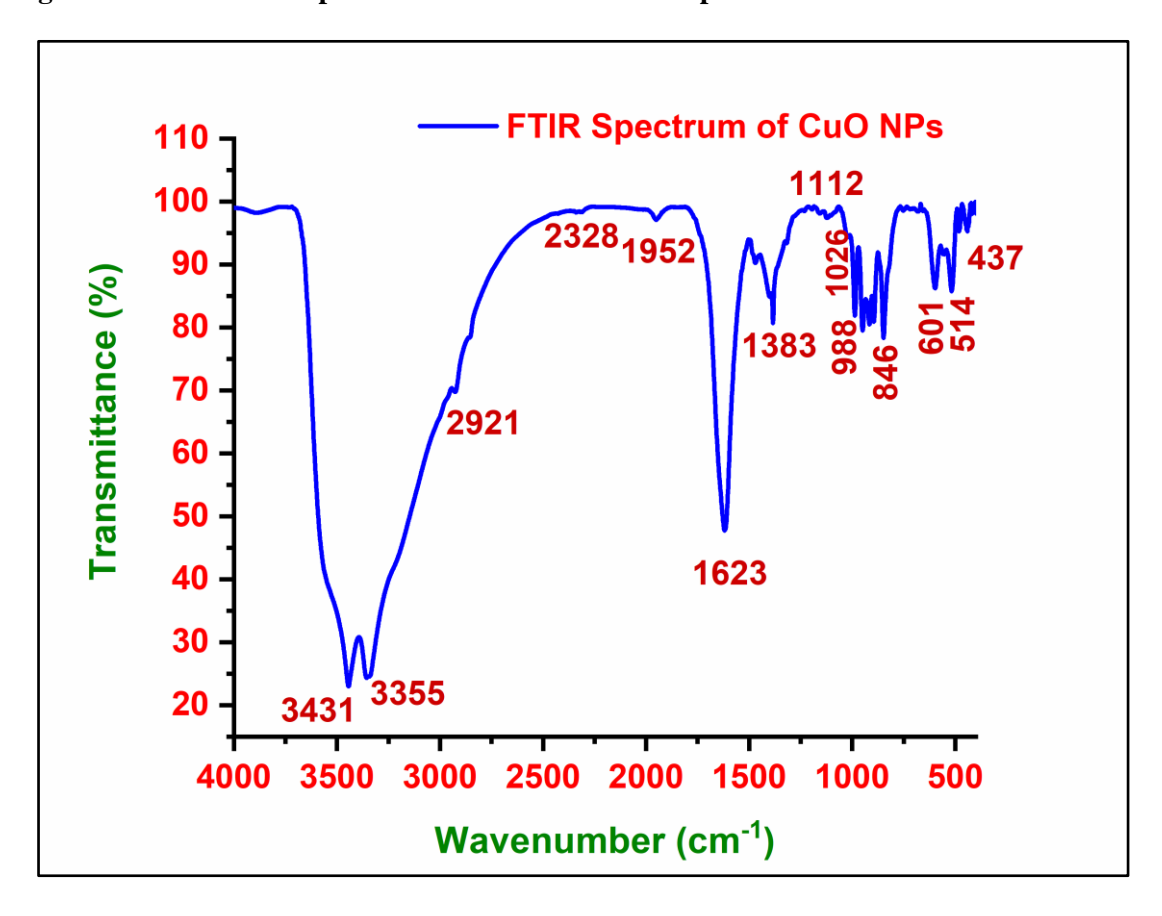


Figure 5.10: FTIR Spectrum of Copper Oxide Nanoparticle obtained in Ch. Cl-MA DES

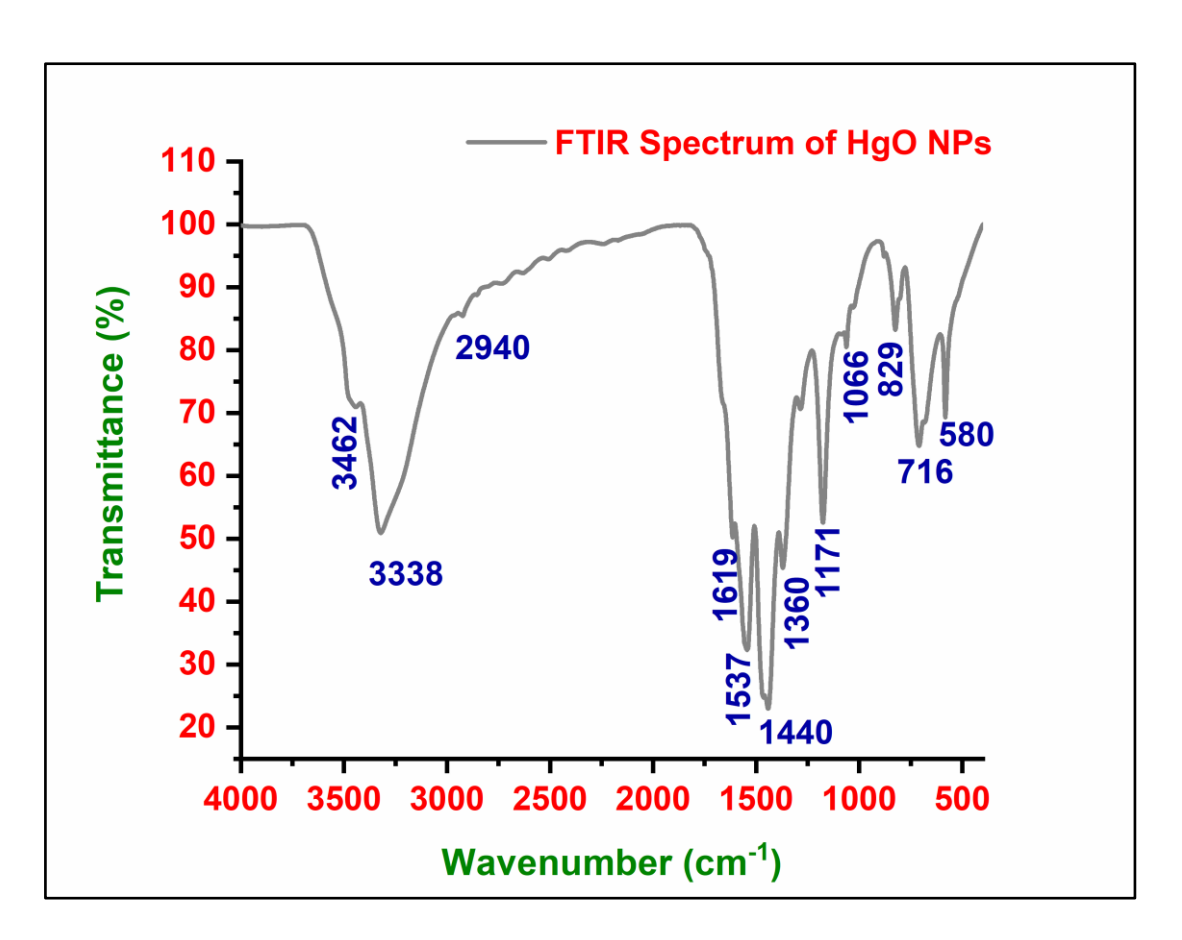


Figure 5.11: FTIR Spectrum of Mercury Oxide Nanoparticle obtained in Ch. Cl-MA DES

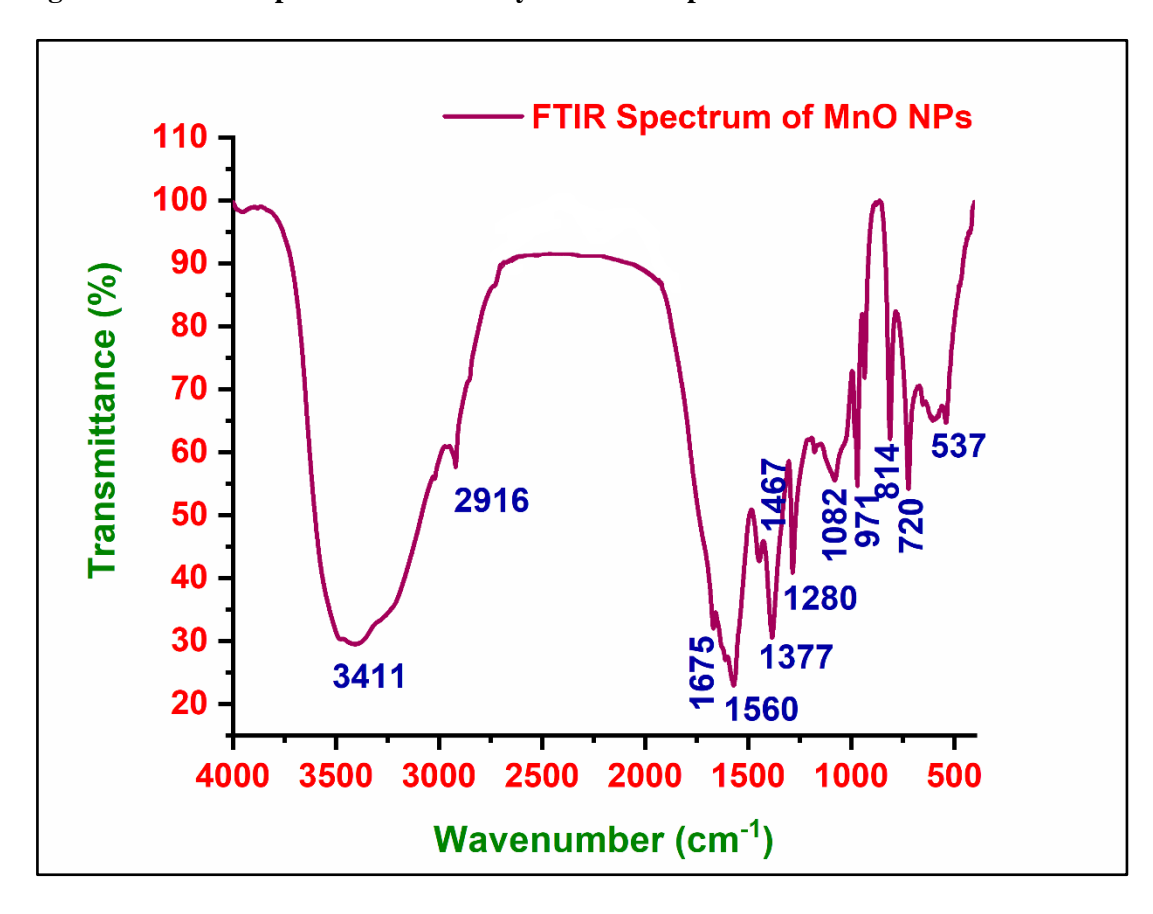


Figure 5.12: FTIR Spectrum of Manganese Oxide Nanoparticle obtained in Ch. Cl-MA DES

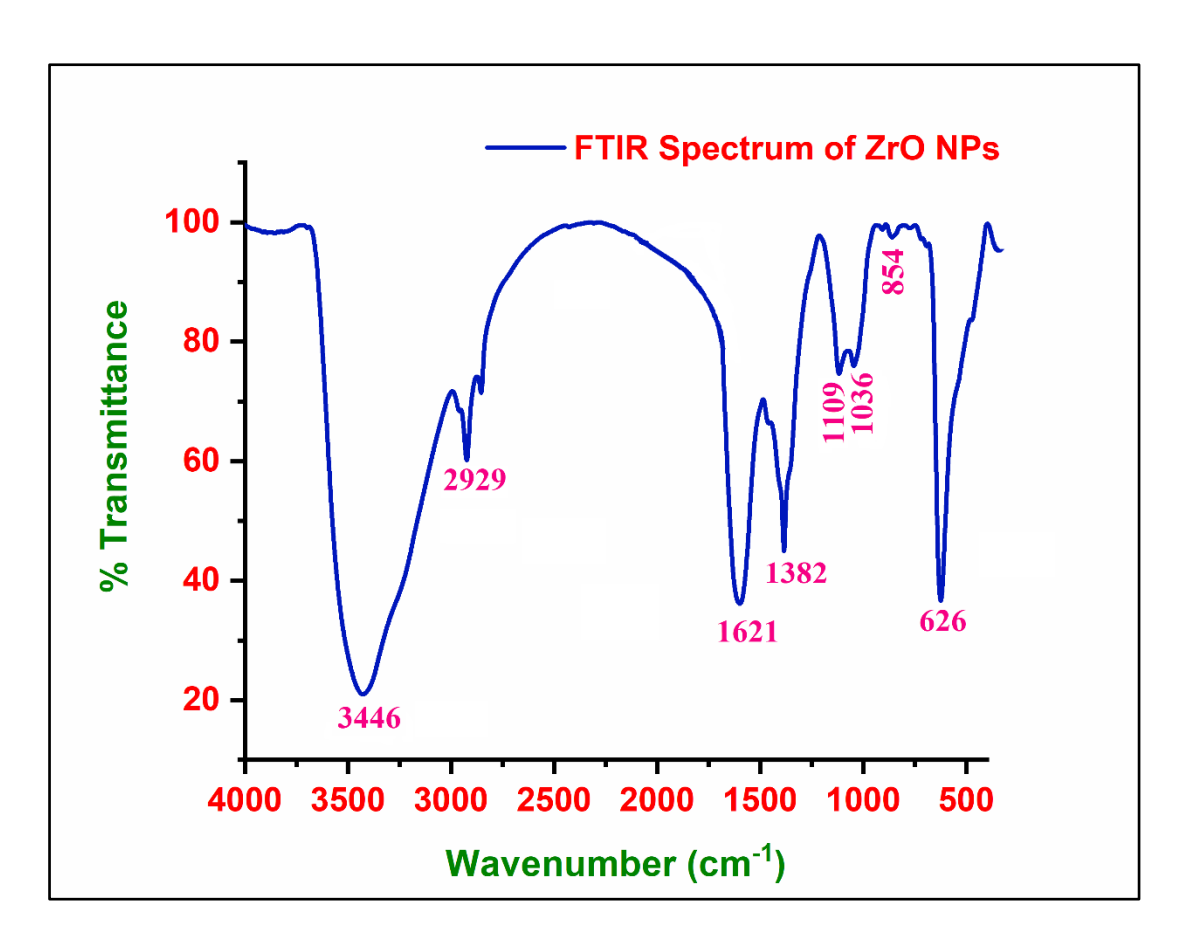


Figure 5.13: FTIR Spectrum of Zirconium Oxide Nanoparticle obtained in Ch. Cl-MA DES

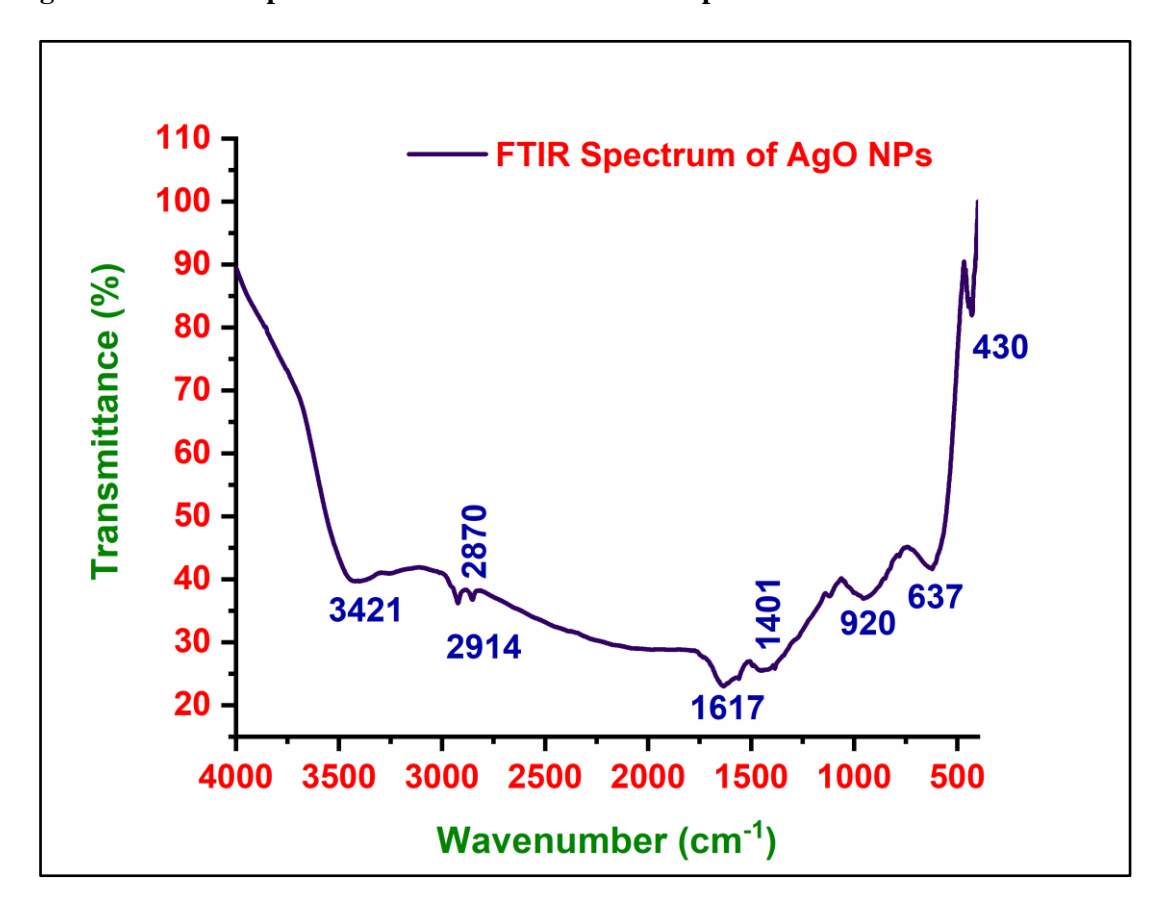


Figure 5.14: FTIR Spectrum of Silver Oxide Nanoparticle obtained in Ch. Cl-MA DES

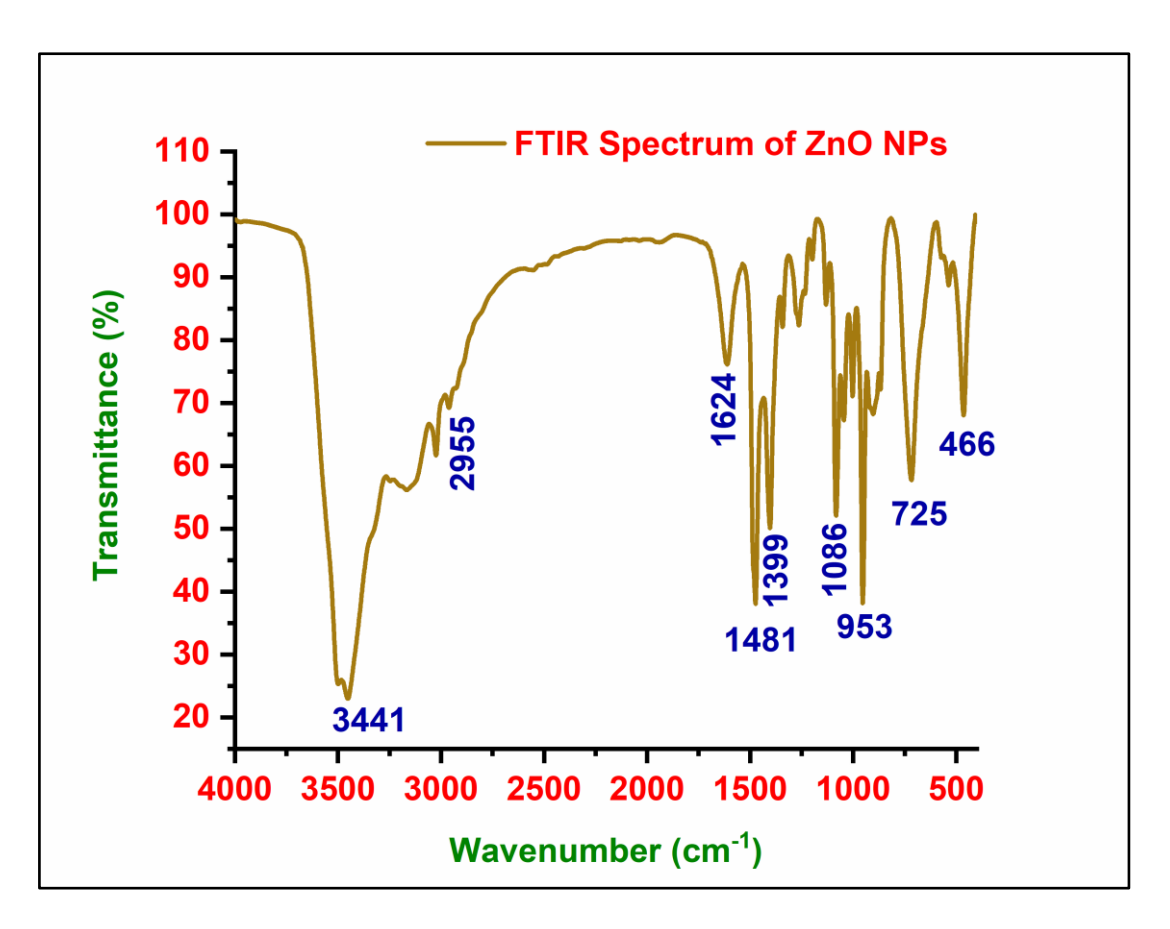


Figure 5.15: FTIR Spectrum of Zinc Oxide Nanoparticle obtained in Ch. Cl-MA DES

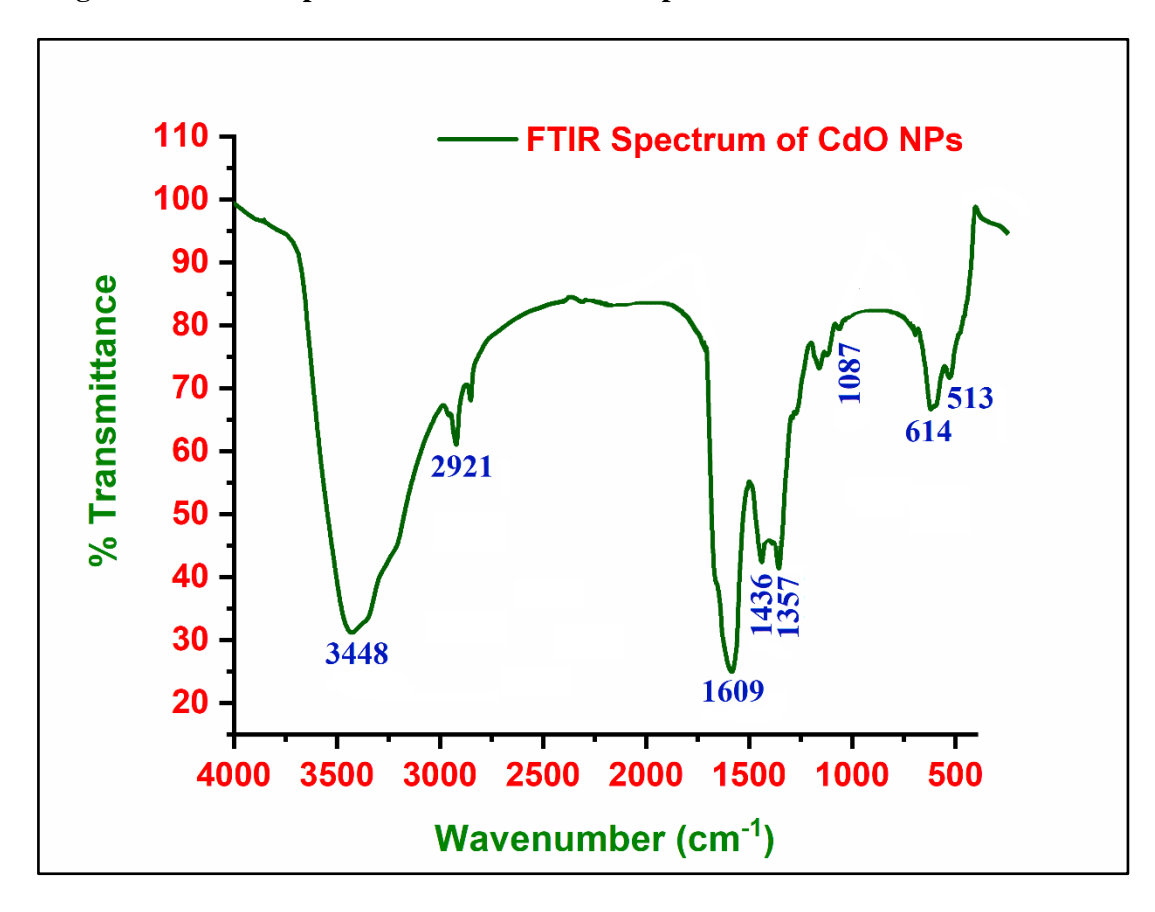


Figure 5.16: FTIR Spectrum of Cadmium Oxide Nanoparticle obtained in Ch. Cl-MA DES

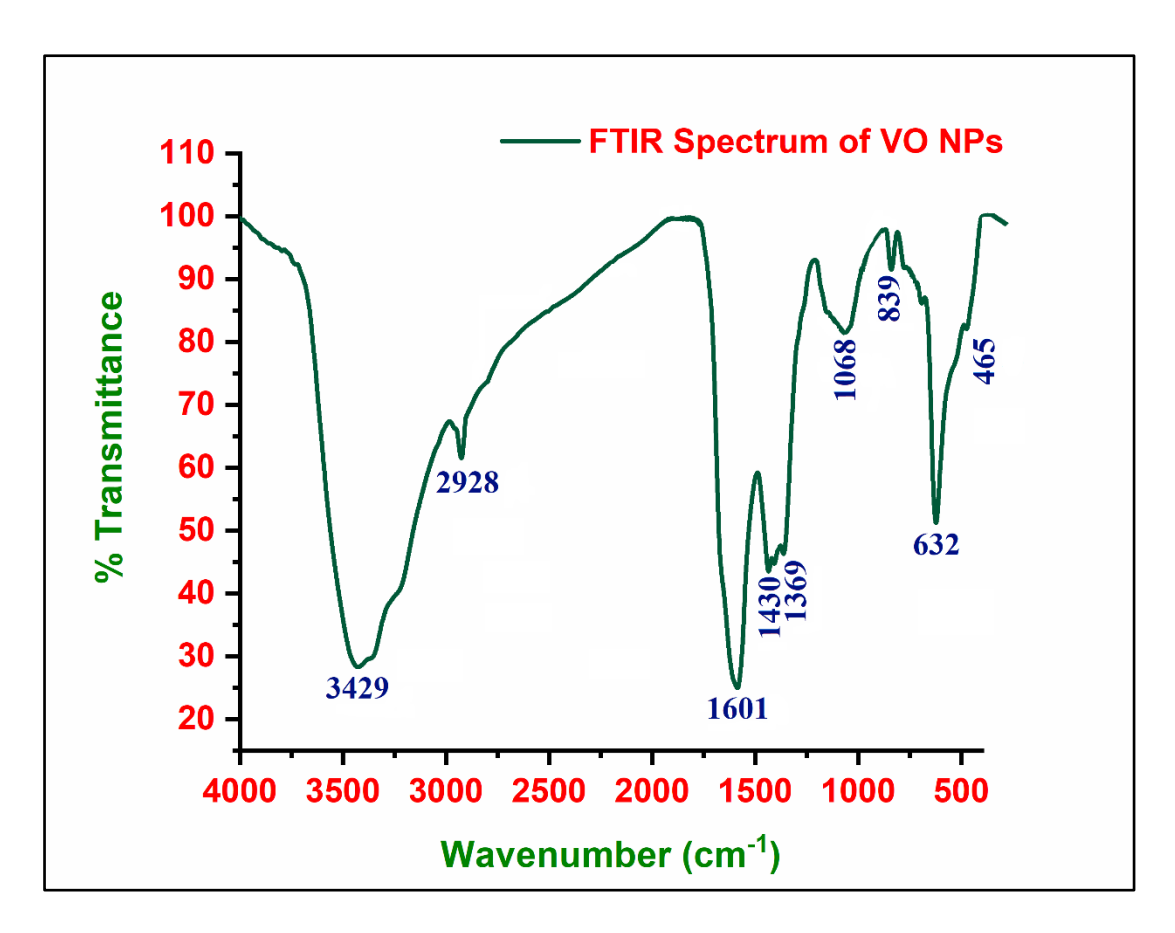


Figure 5.17: FTIR Spectrum of Vanadium Oxide Nanoparticle obtained in Ch. Cl-MA DES

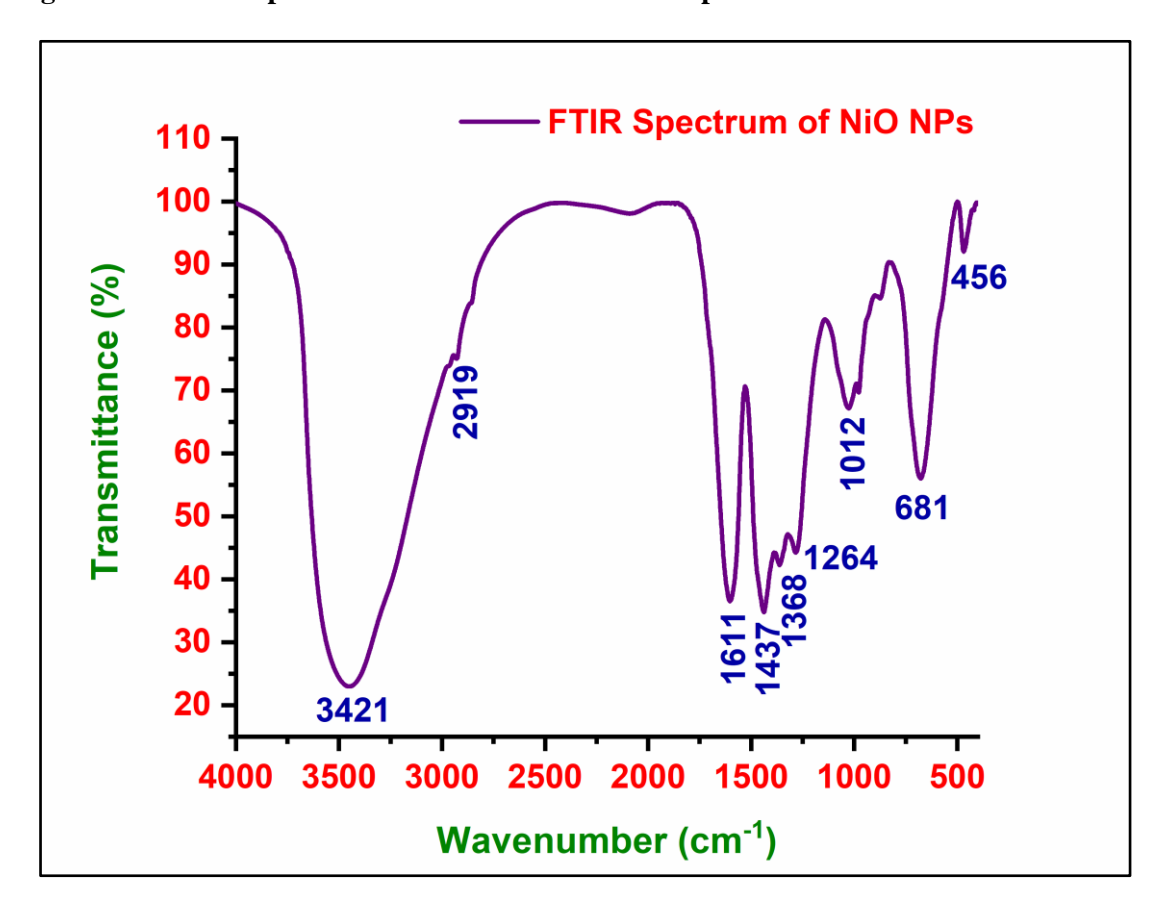


Figure 5.18: FTIR Spectrum of Nickel Oxide Nanoparticle obtained in Ch. Cl-MA DES

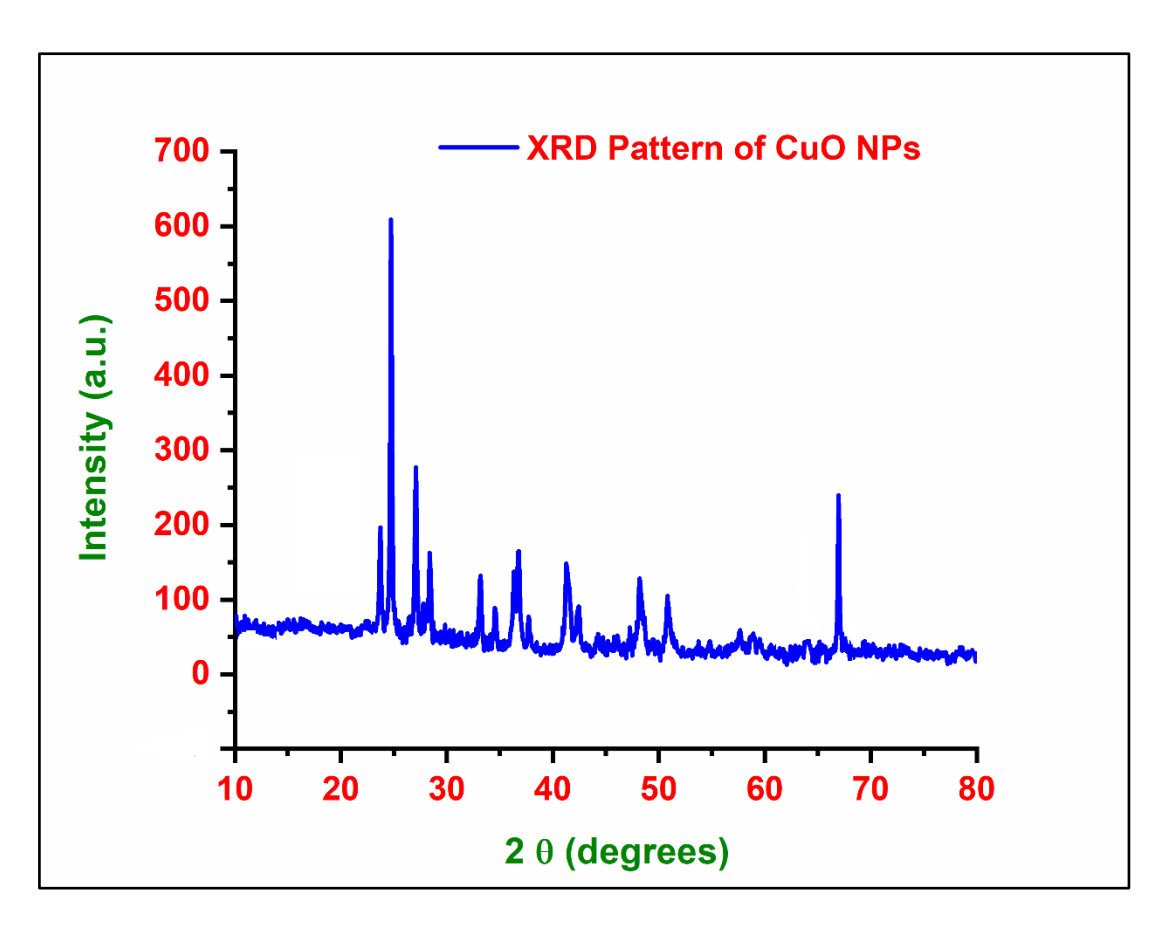


Figure 5.19: XRD Pattern of Copper Oxide Nanoparticle obtained in Ch. Cl-MA DES

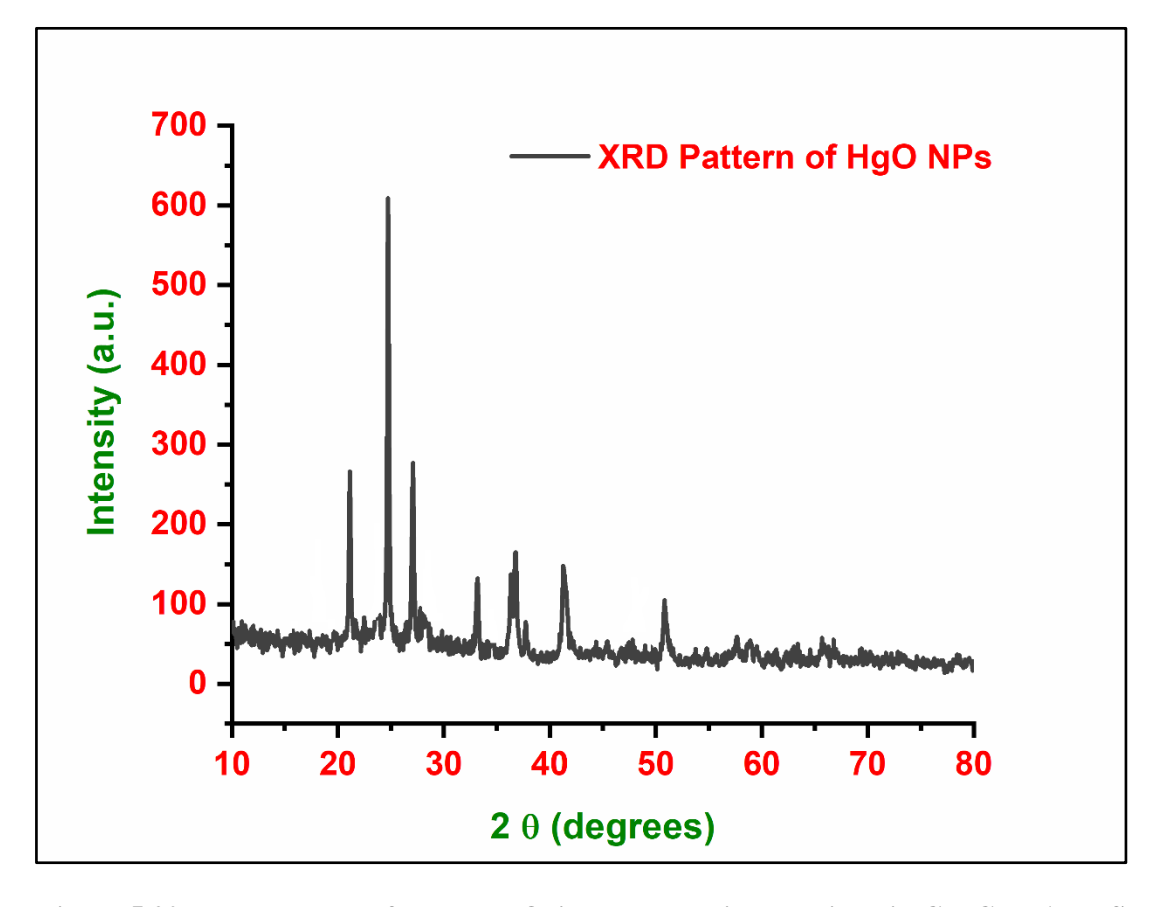


Figure 5.20: XRD Pattern of Mercury Oxide Nanoparticle obtained in Ch. Cl-MA DES

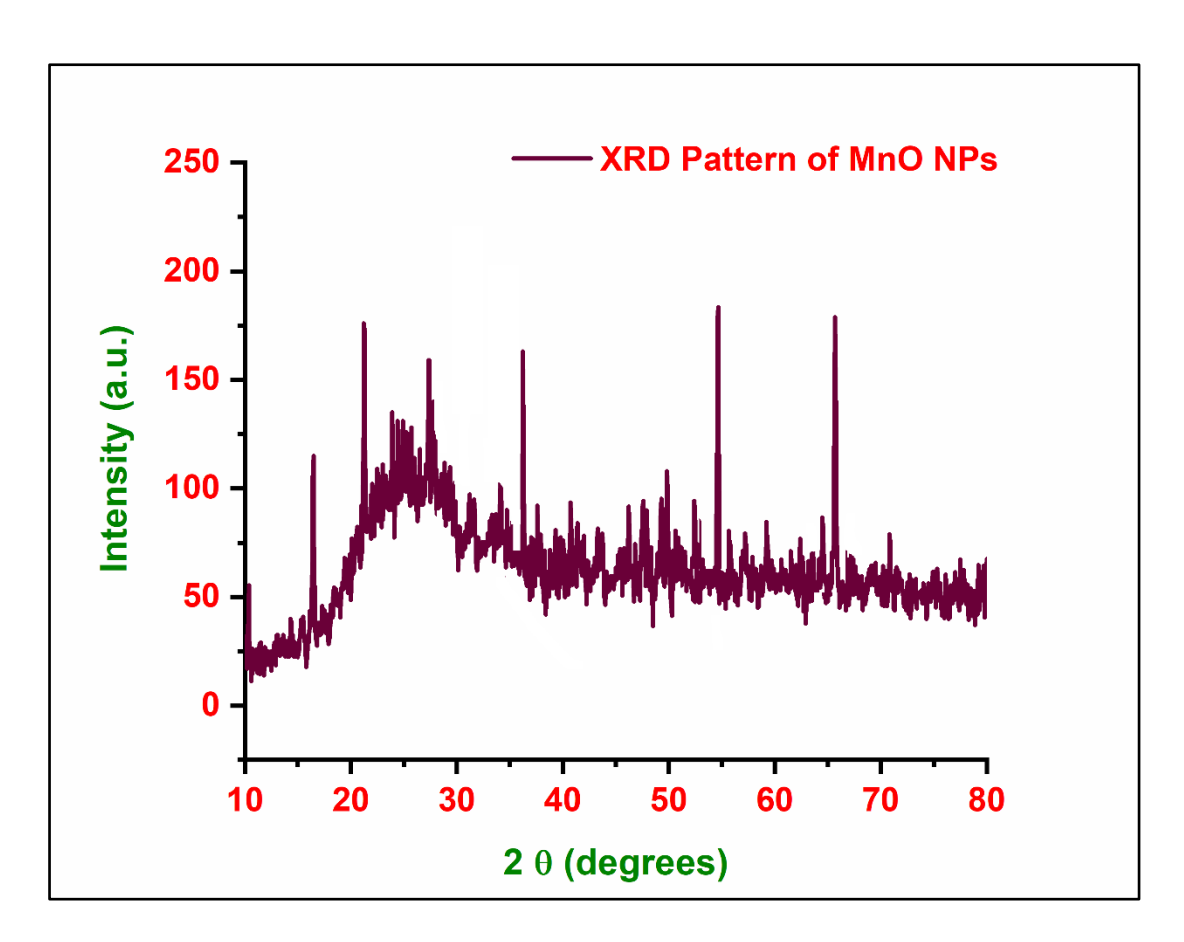


Figure 5.21: XRD Pattern of Manganese Oxide Nanoparticle obtained in Ch. Cl-MA DES

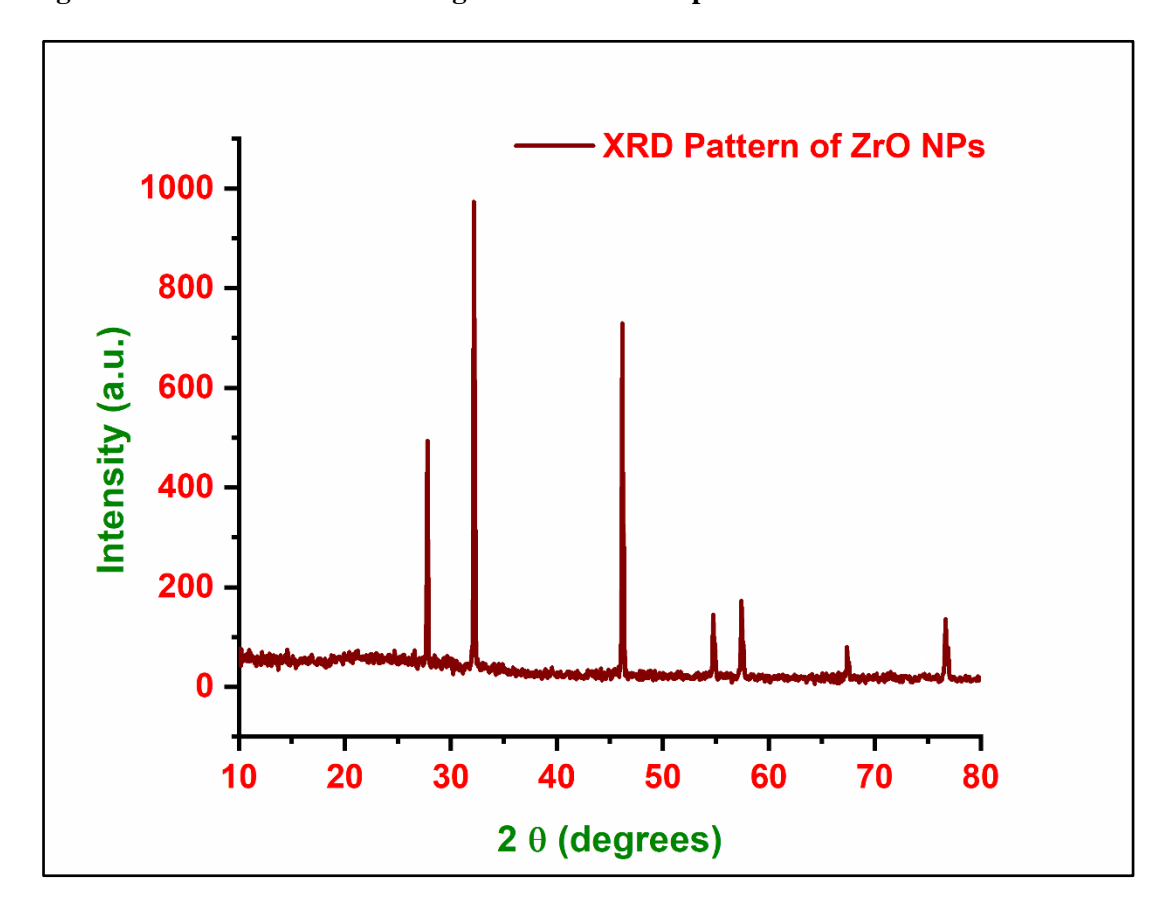


Figure 5.22: XRD Pattern of Zirconium Oxide Nanoparticle obtained in Ch. Cl-MA DES

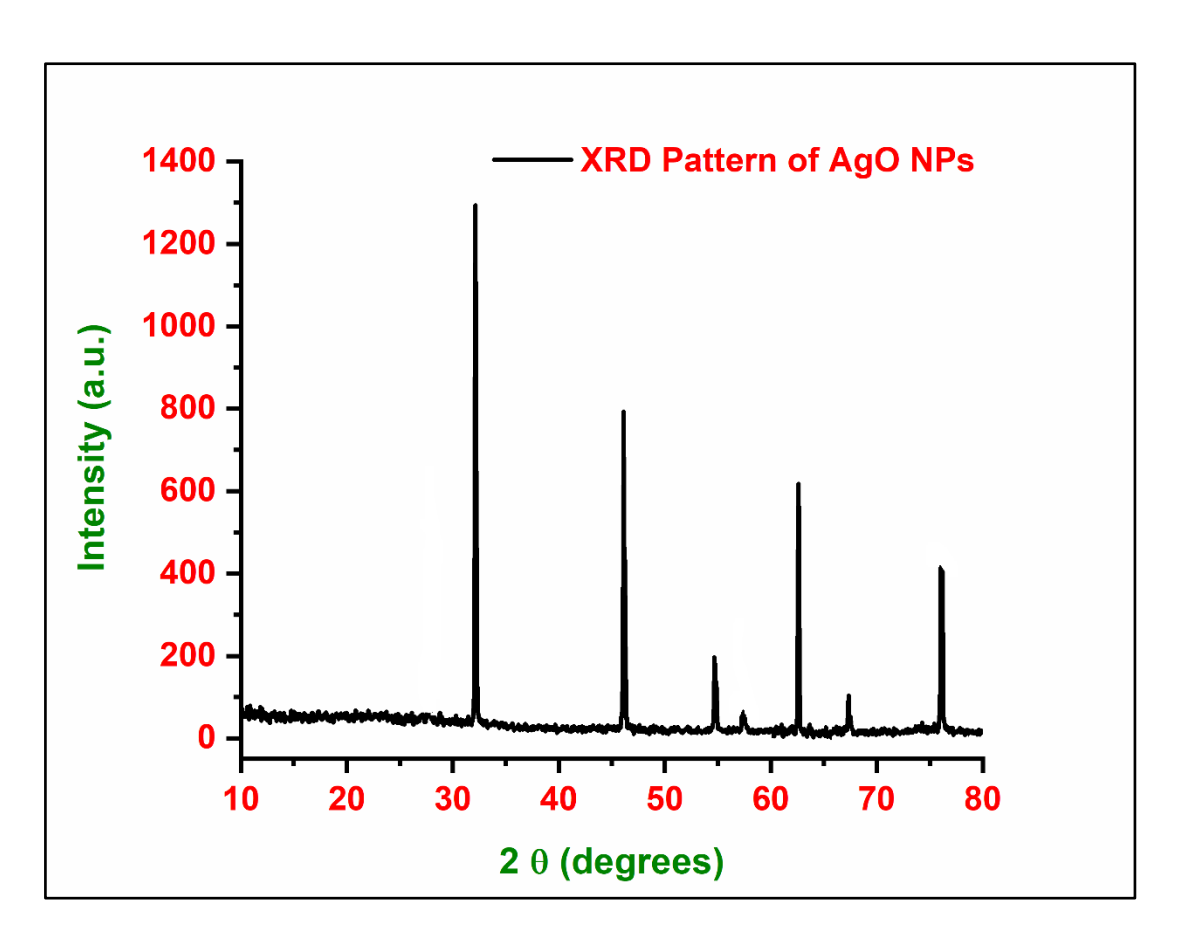


Figure 5.23: XRD Pattern of Silver Oxide Nanoparticle obtained in Ch. Cl-MA DES

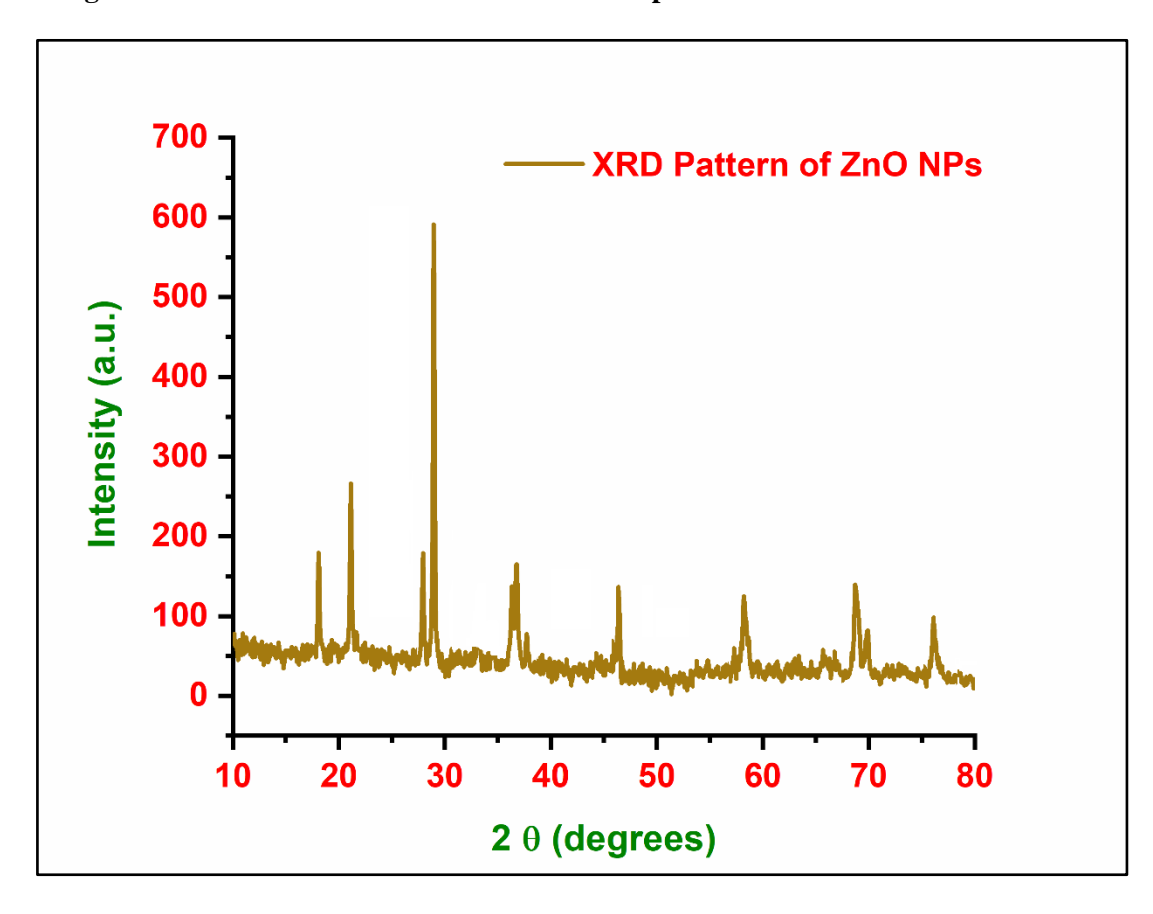


Figure 5.24: XRD Pattern of Zinc Oxide Nanoparticle obtained in Ch. Cl-MA DES

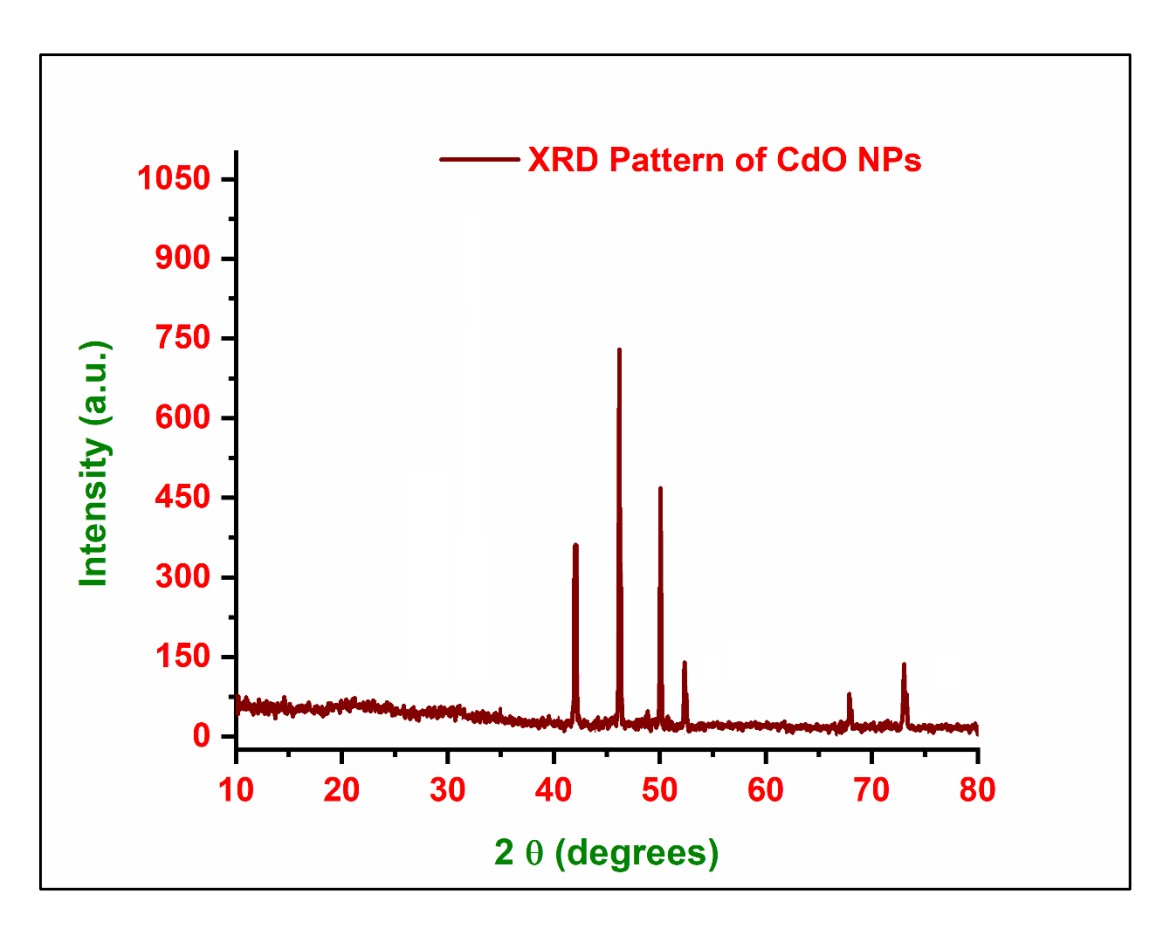


Figure 5.25: XRD Pattern of Cadmium Oxide Nanoparticle obtained in Ch. Cl-MA DES

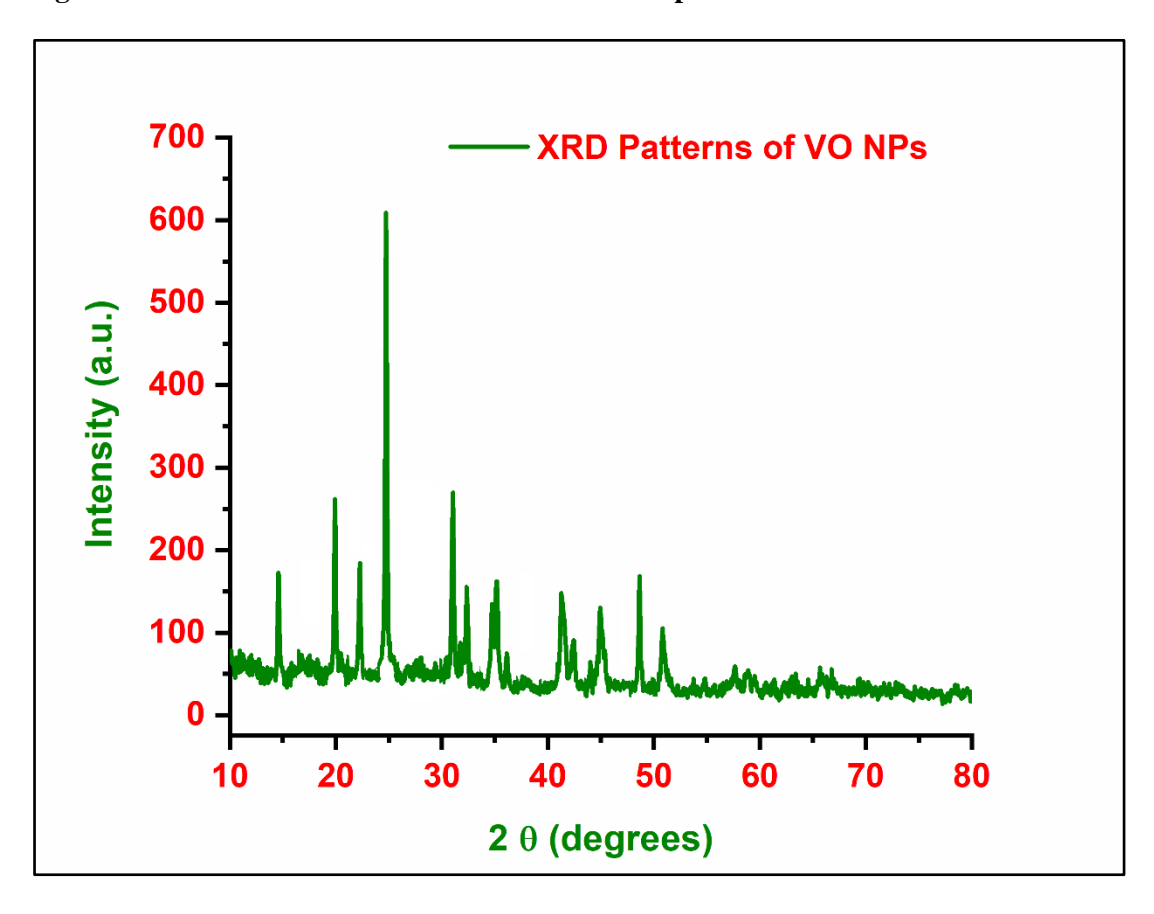


Figure 5.26: XRD Pattern of Vanadium Oxide Nanoparticle obtained in Ch. Cl-MA DES

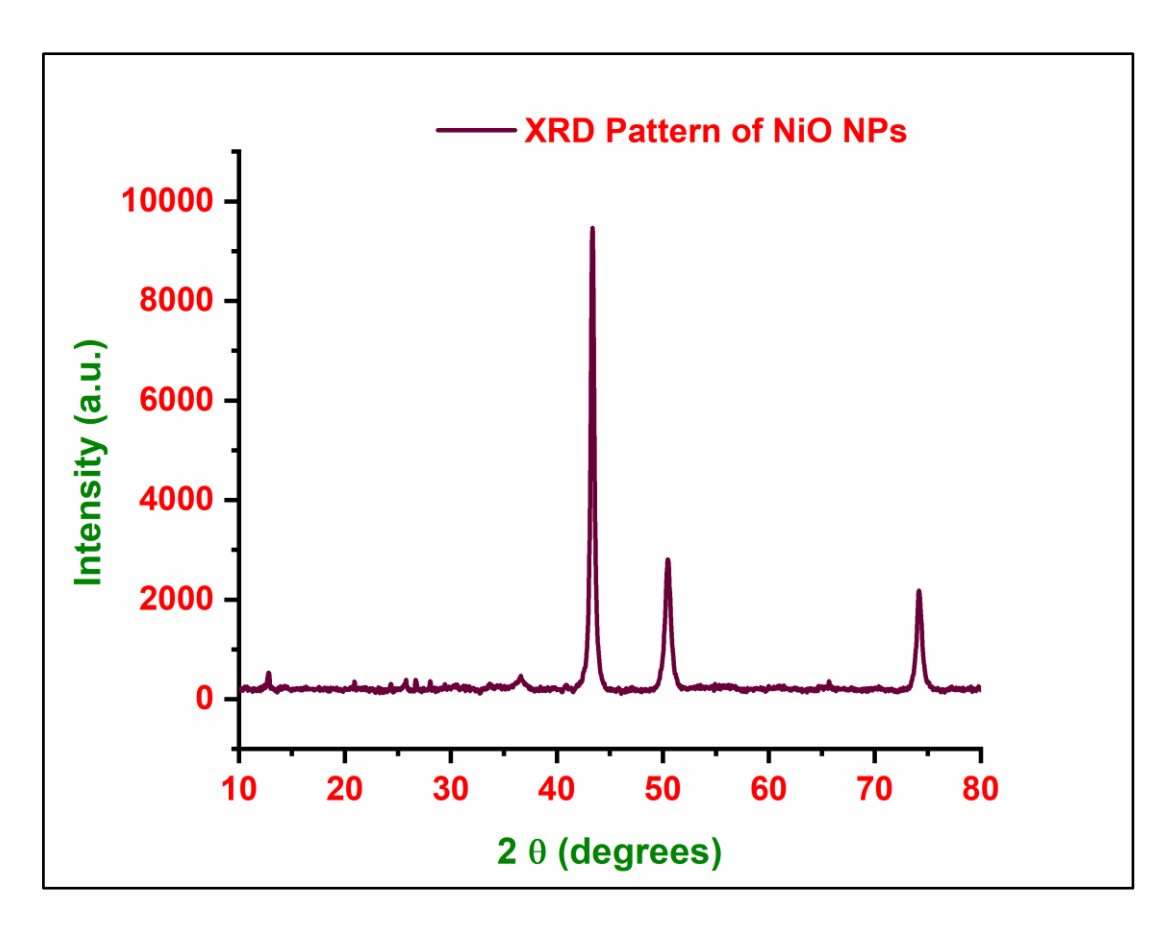


Figure 5.27: XRD Pattern of Nickel Oxide Nanoparticle obtained in Ch. Cl-MA DES

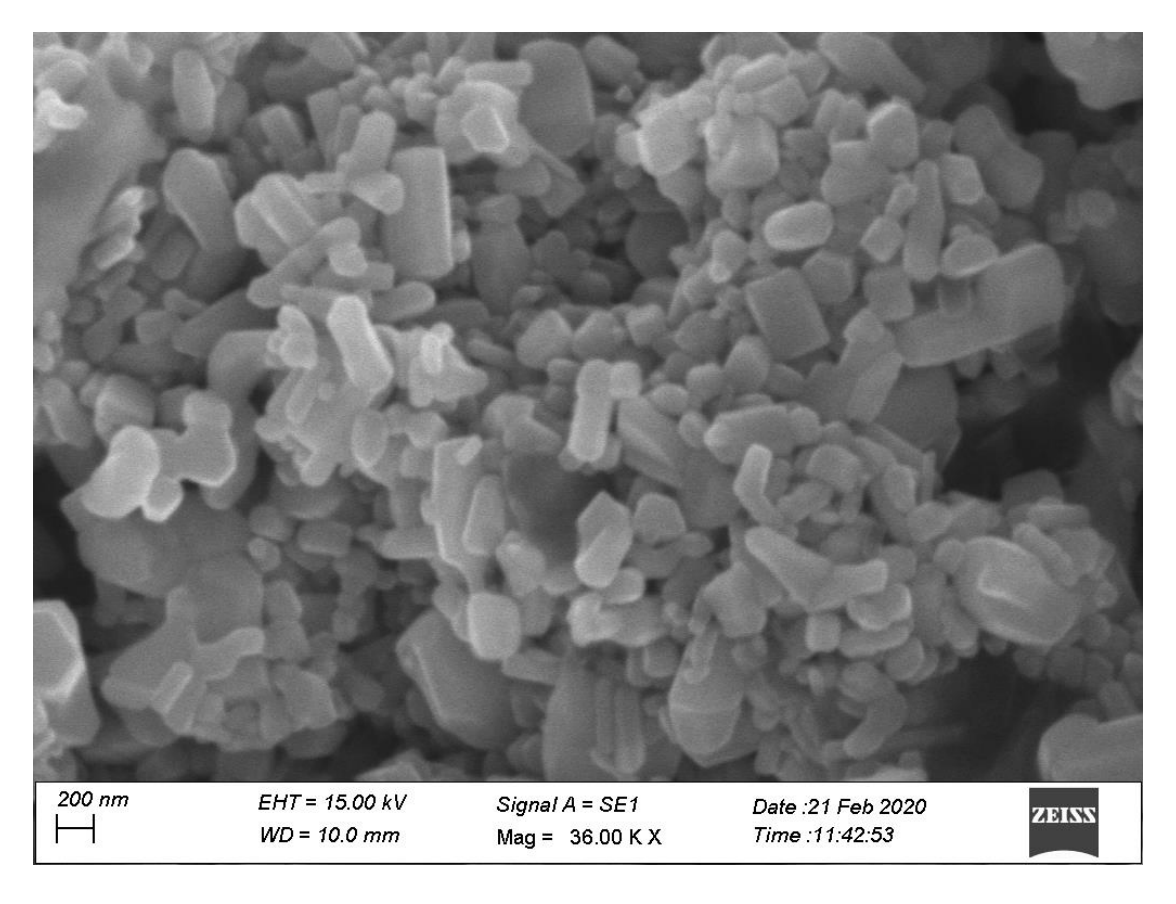


Figure 5.28: SEM Image of Copper Oxide Nanoparticle obtained in Ch. Cl-MA DES

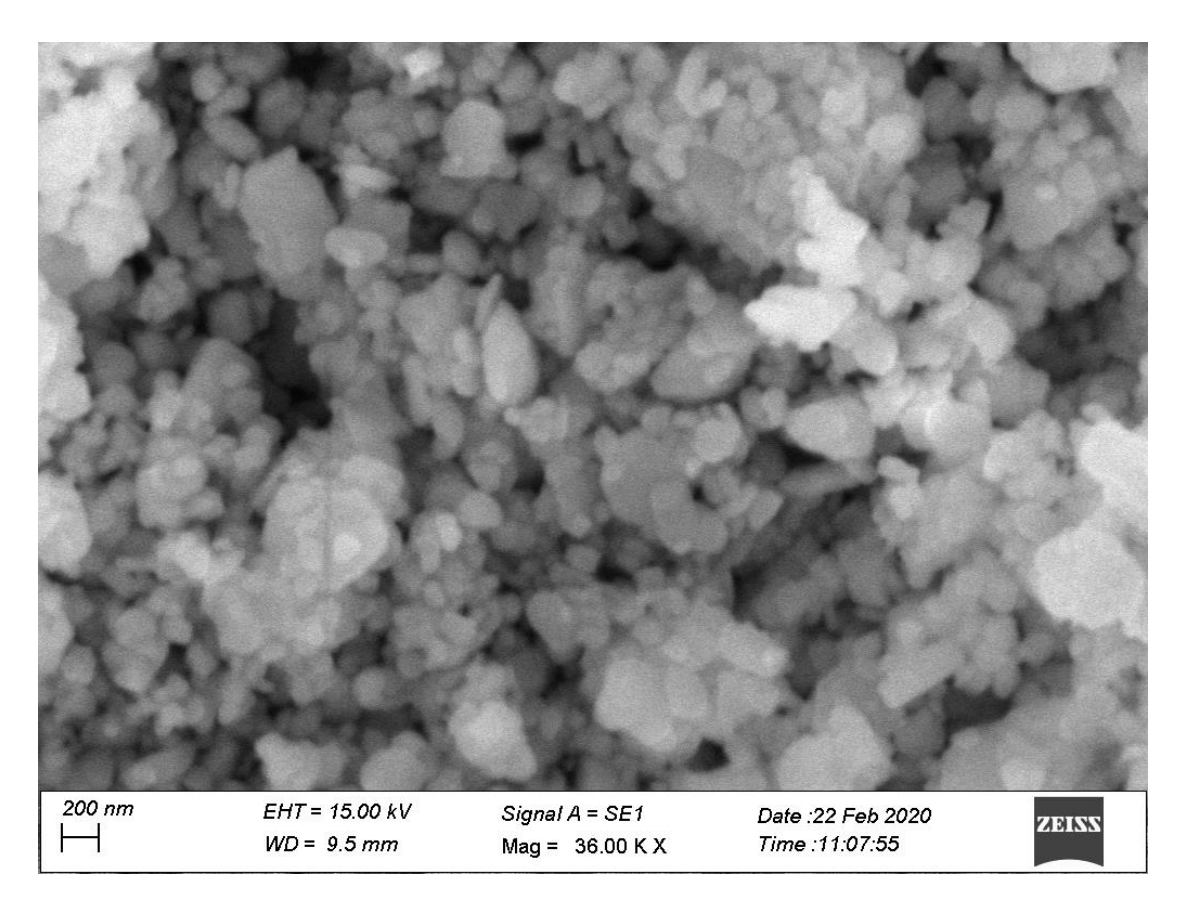


Figure 5.29: SEM Image of Mercury Oxide Nanoparticle obtained in Ch. Cl-MA DES

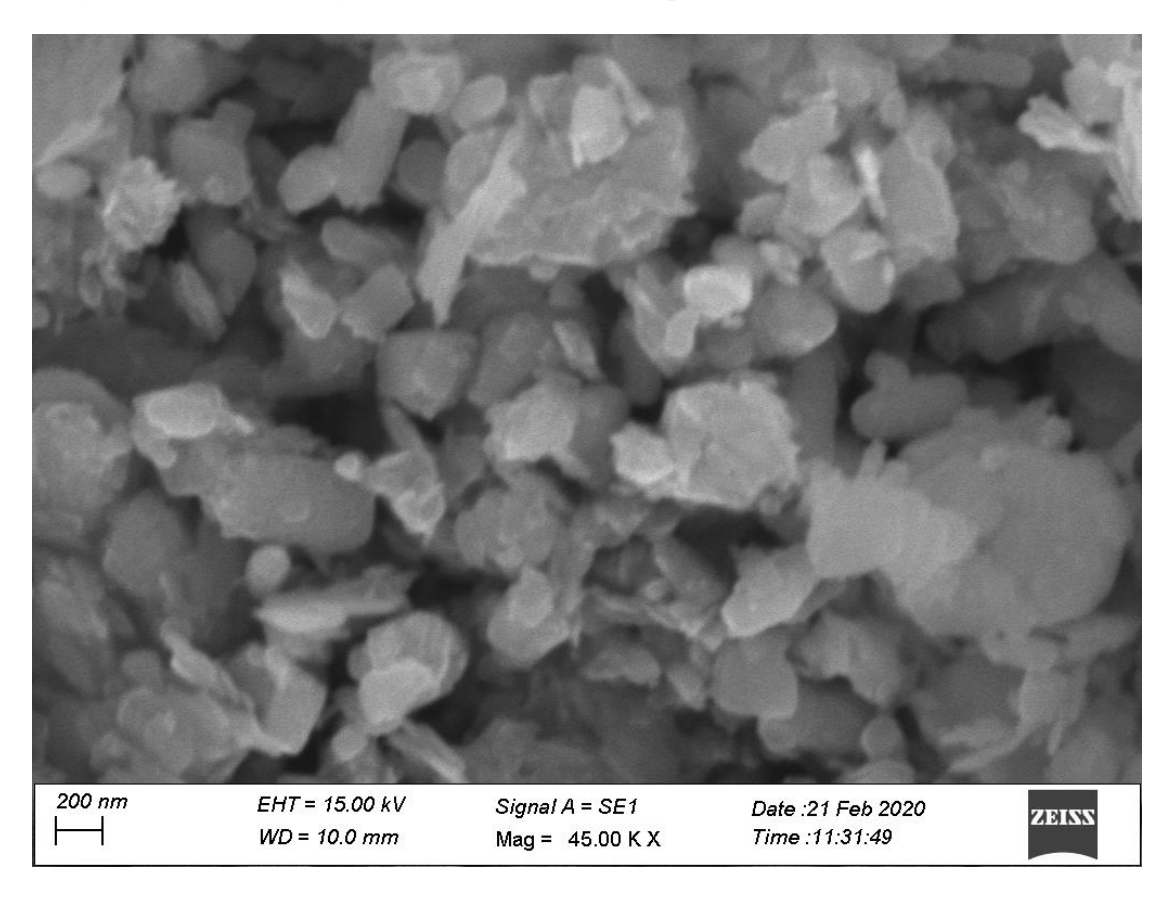


Figure 5.30: SEM Image of Manganese Oxide Nanoparticle obtained in Ch. Cl-MA DES

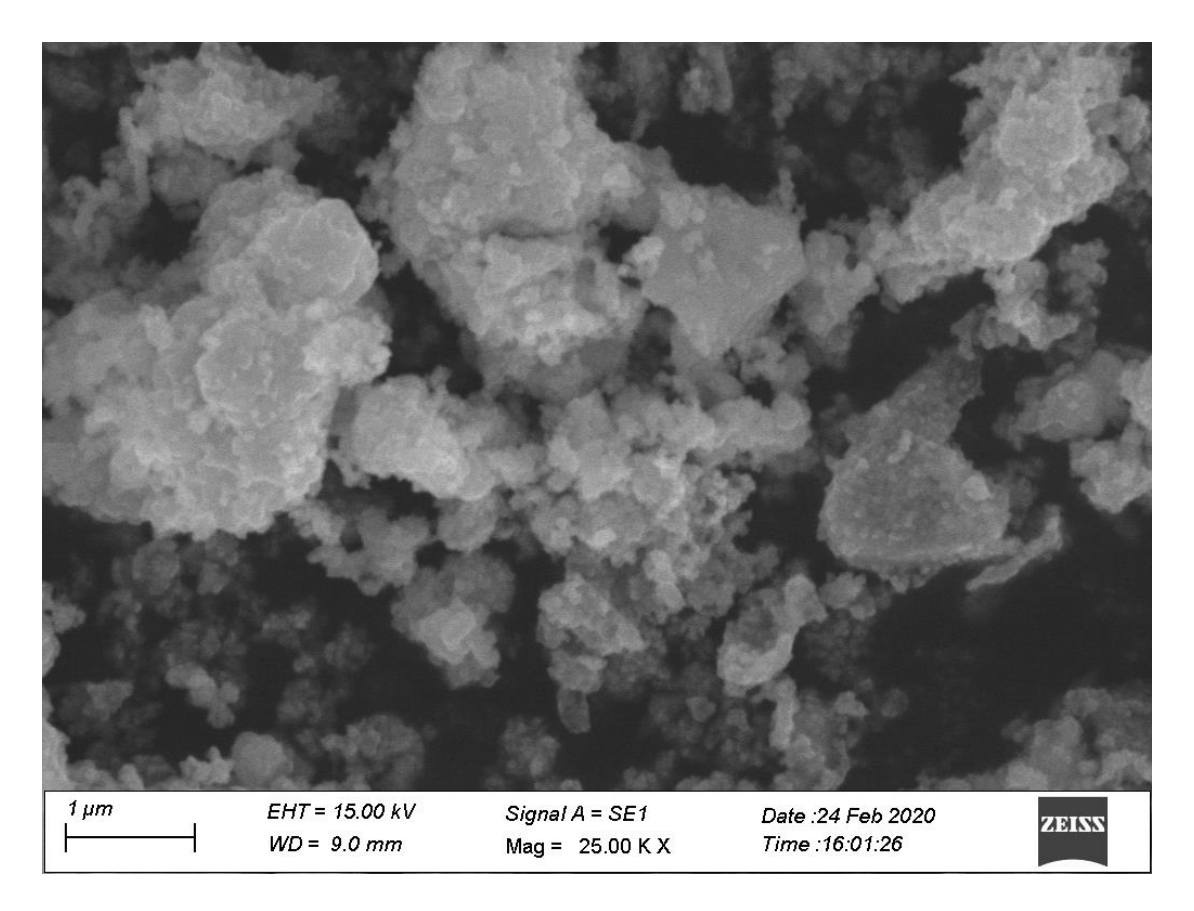


Figure 5.31: SEM Image of Zirconium Oxide Nanoparticle obtained in Ch. Cl-MA DES

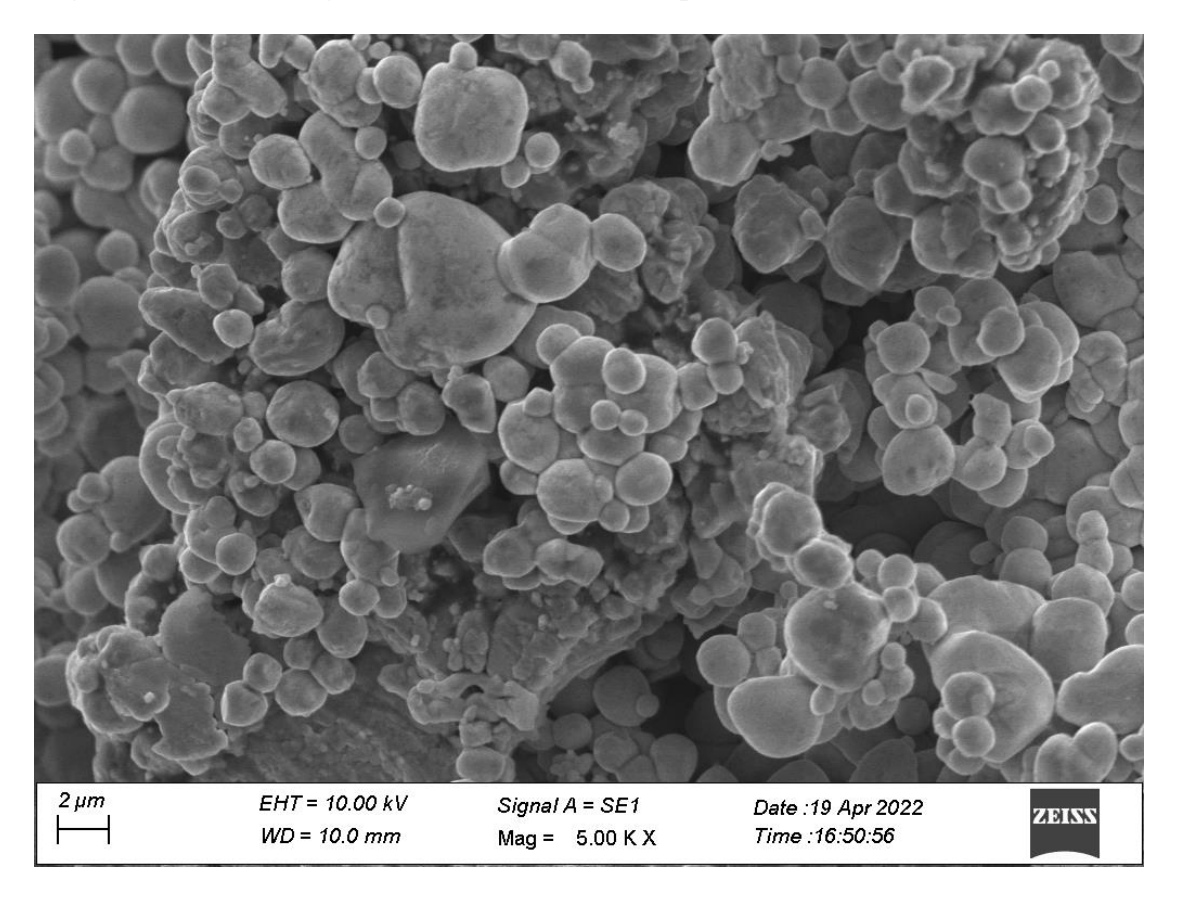


Figure 5.32: SEM Image of Silver Oxide Nanoparticle obtained in Ch. Cl-MA DES

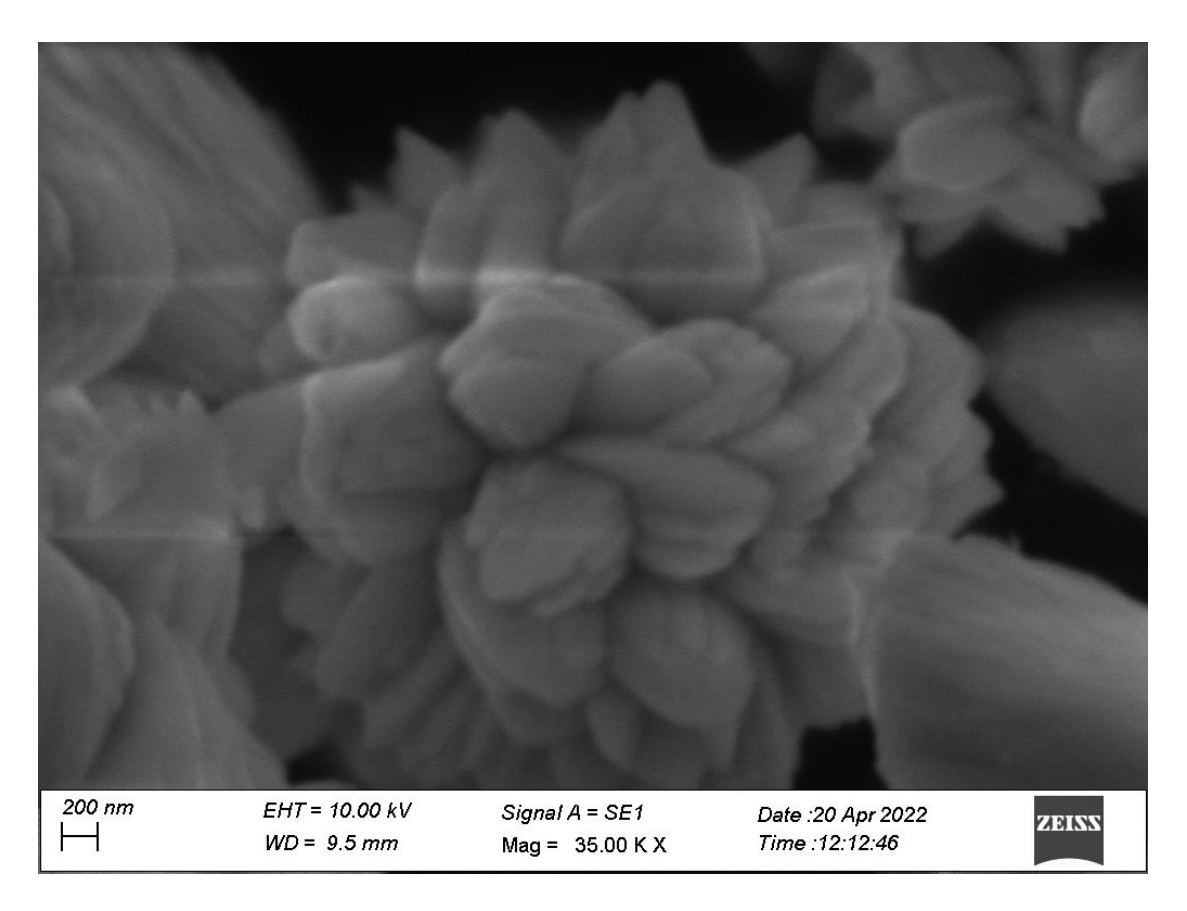


Figure 5.33: SEM Image of Zinc Oxide Nanoparticle obtained in Ch. Cl-MA DES

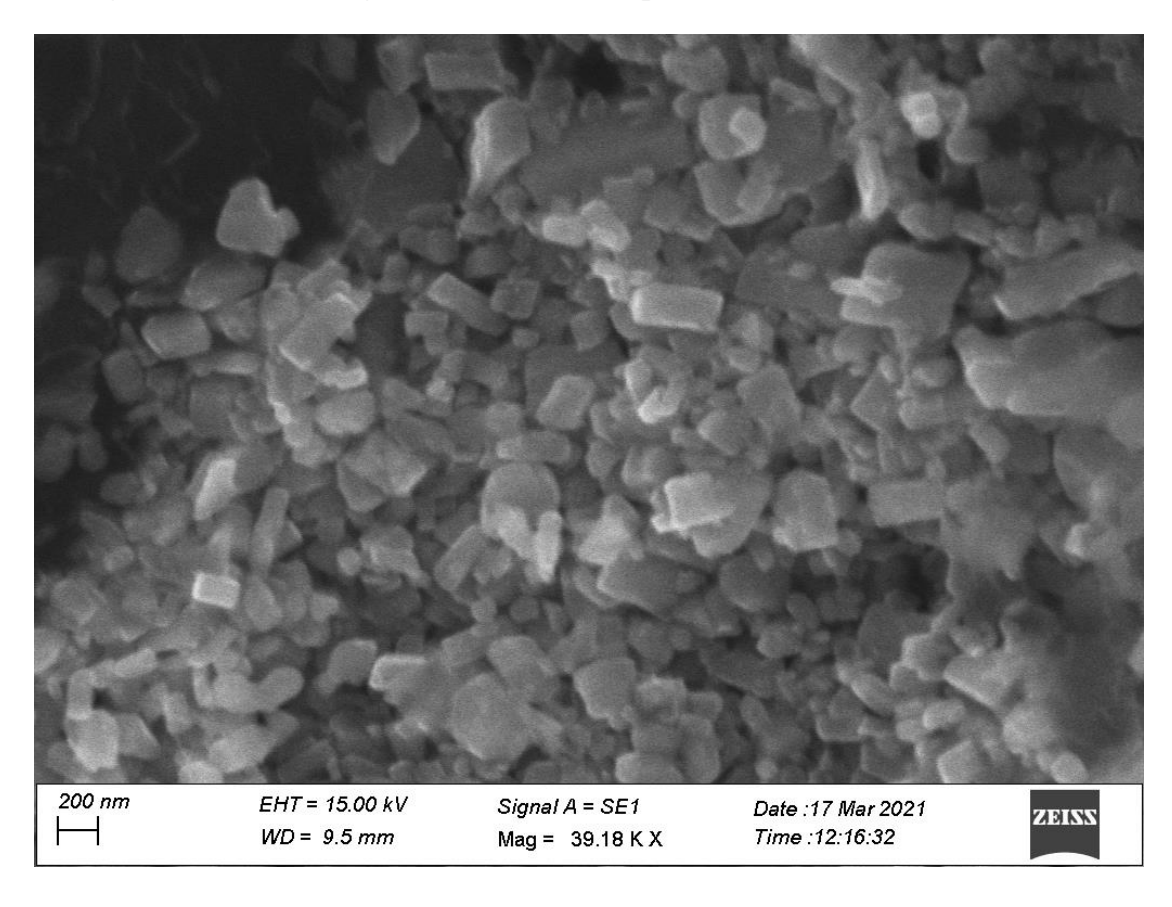


Figure 5.34: SEM Image of Cadmium Oxide Nanoparticle obtained in Ch. Cl-MA DES

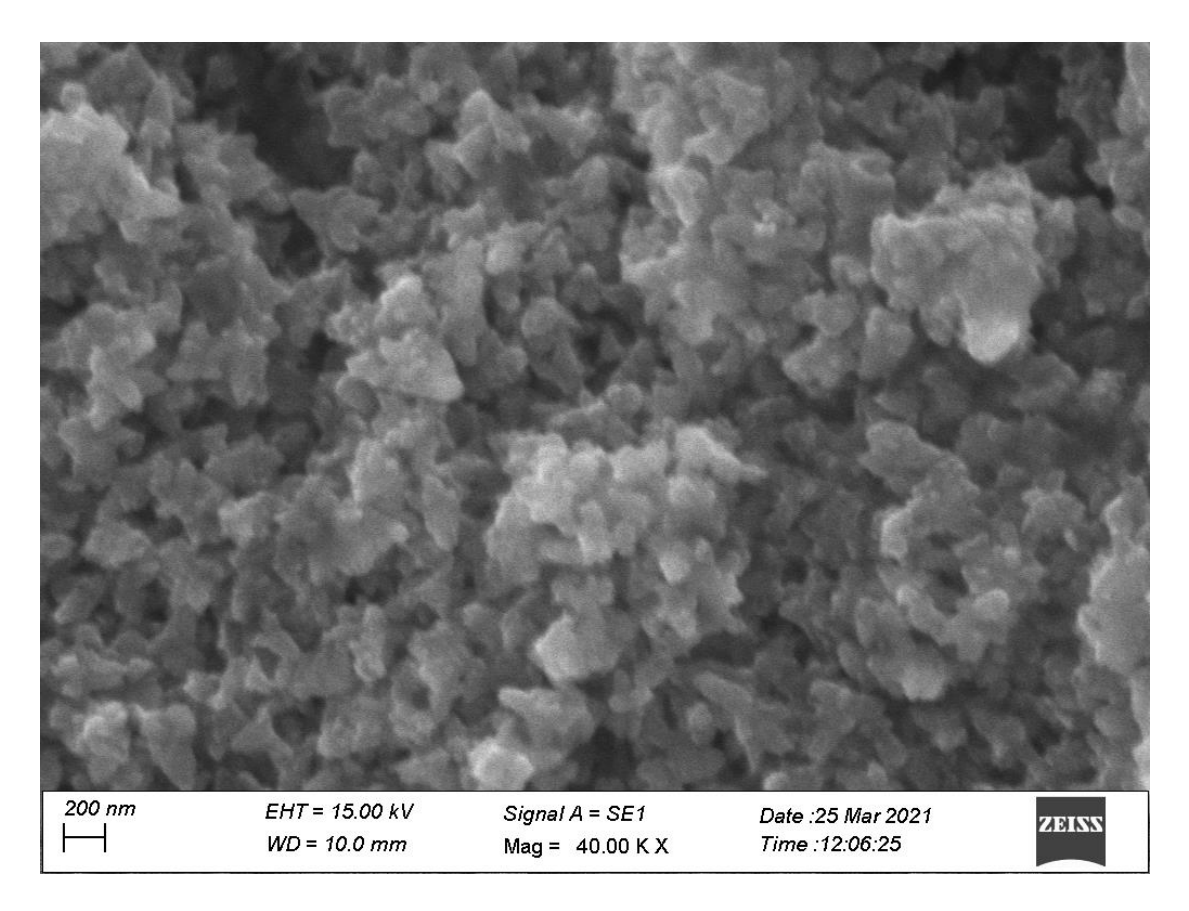


Figure 5.35: SEM Image of Vanadium Oxide Nanoparticle obtained in Ch. Cl-MA DES

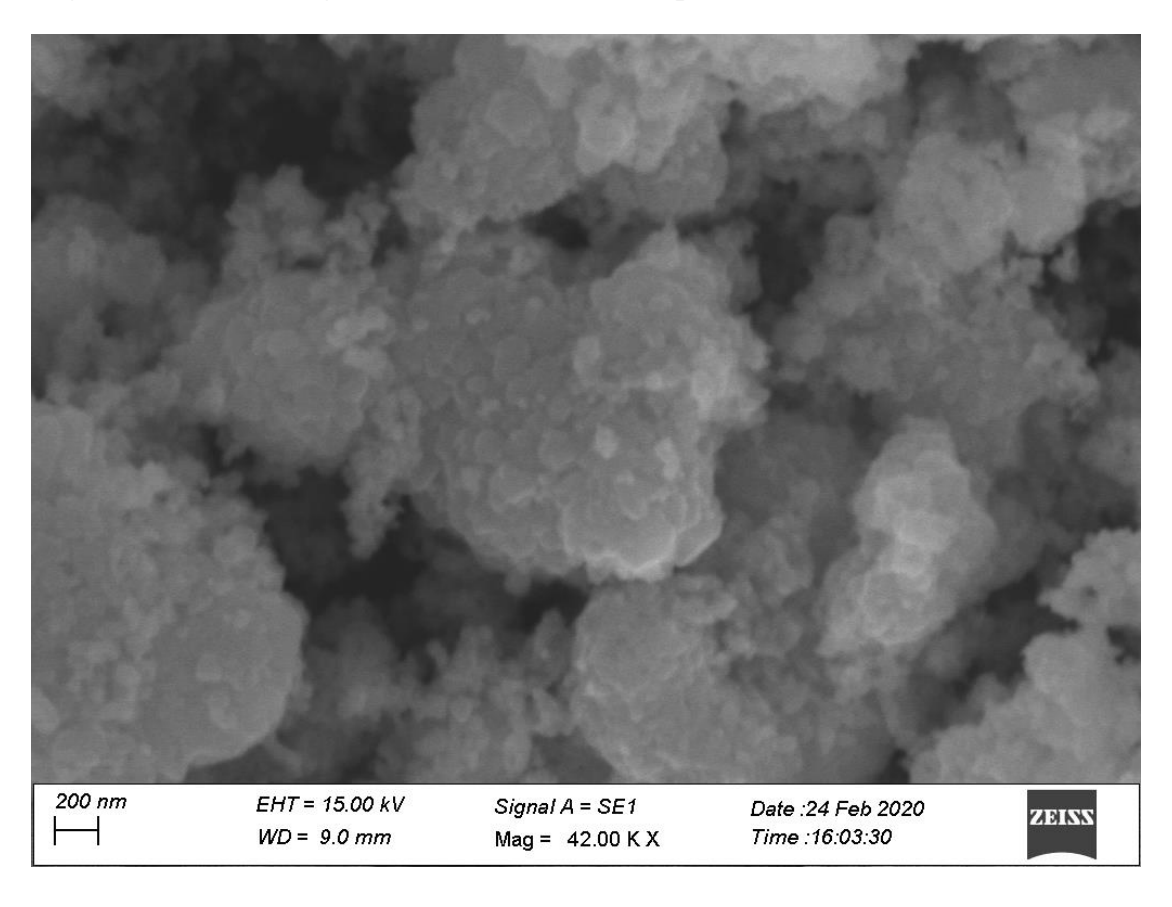


Figure 5.36: SEM Image of Nickel Oxide Nanoparticle obtained in Ch. Cl-MA DES

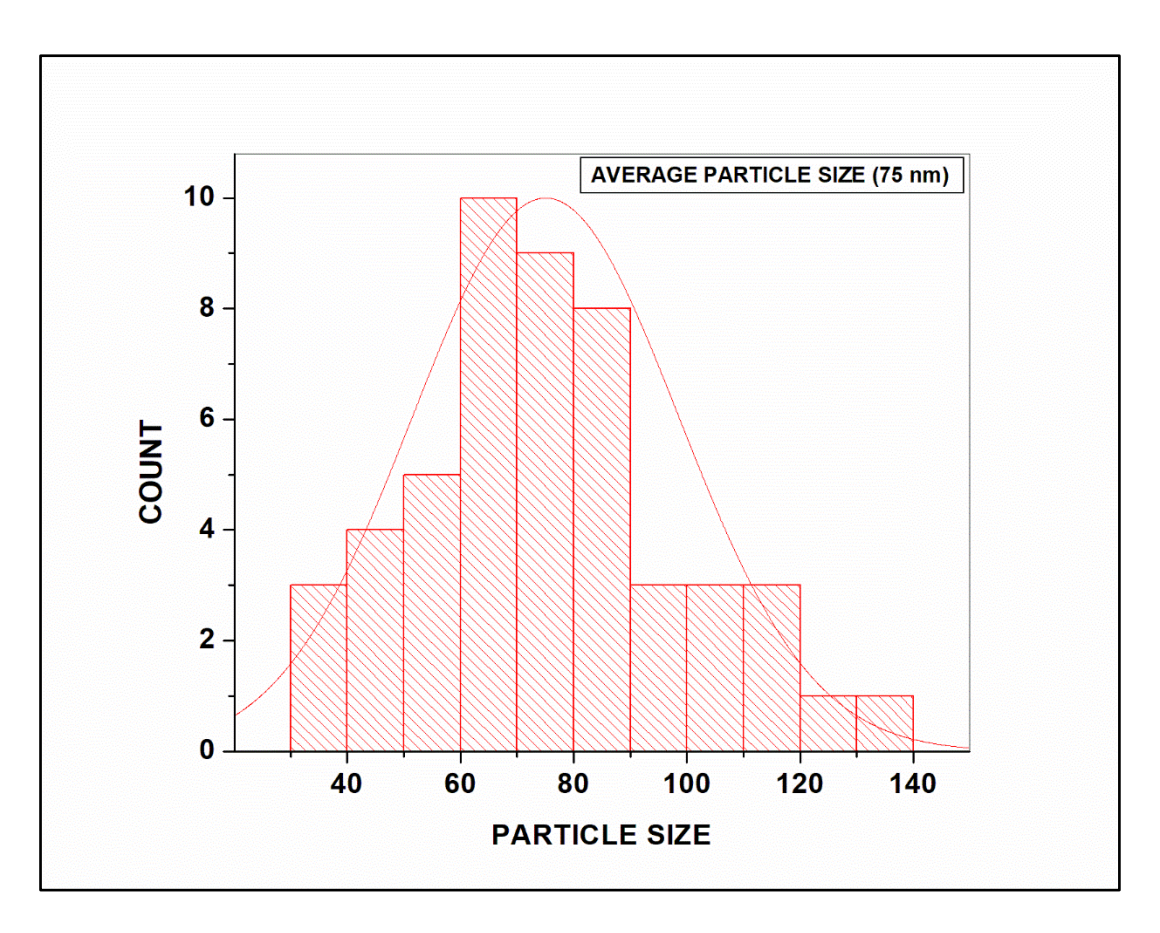


Figure 5.37: SEM Histogram of Copper Oxide Nanoparticle obtained in Ch. Cl-MA DES

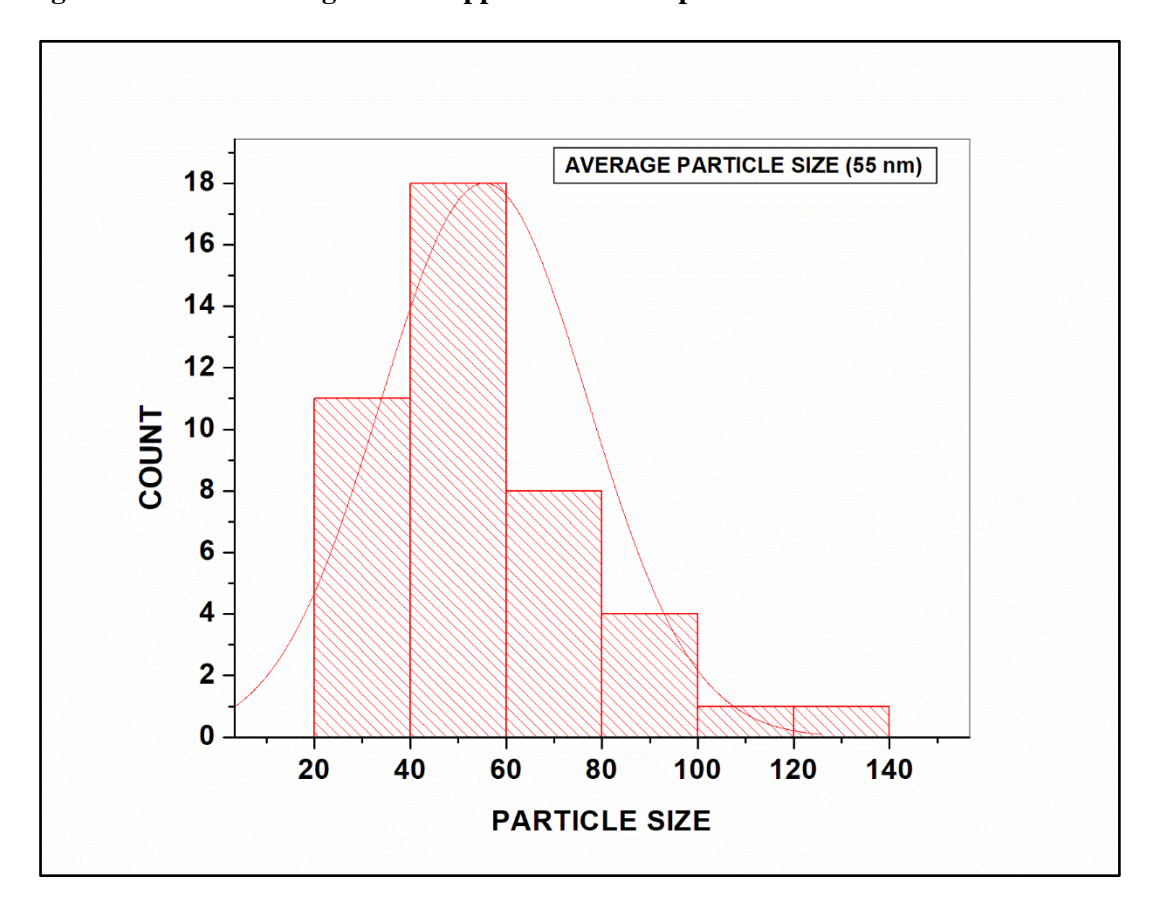


Figure 5.38: SEM Histogram of Mercury Oxide Nanoparticle obtained in Ch. Cl-MA DES

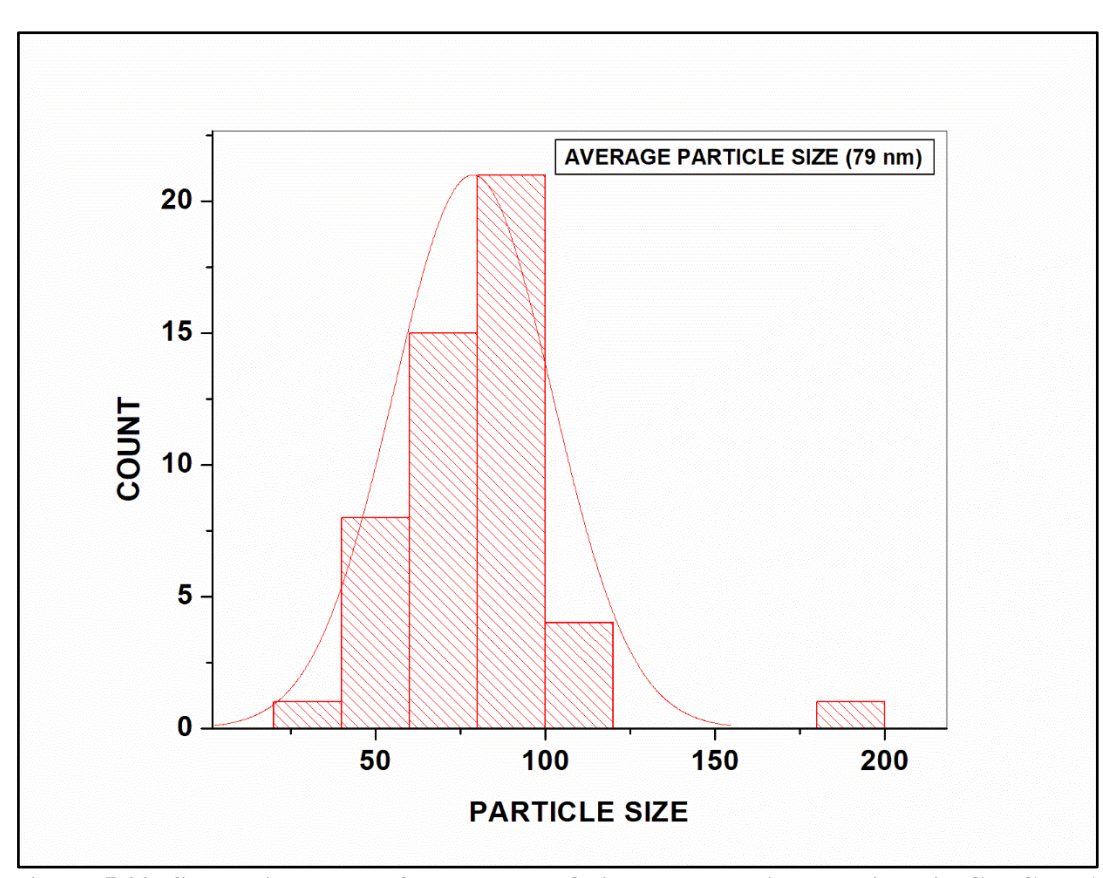


Figure 5.39: SEM Histogram of Manganese Oxide Nanoparticle obtained in Ch. Cl-MA DES

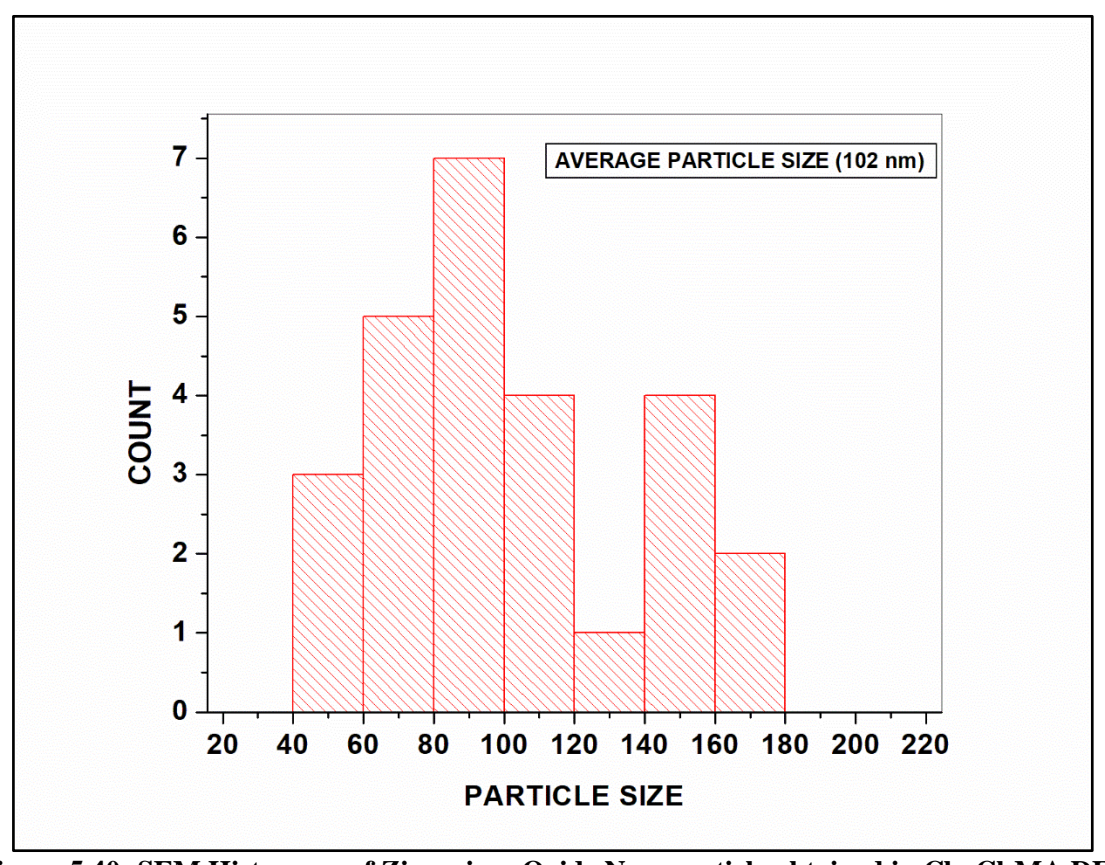


Figure 5.40: SEM Histogram of Zirconium Oxide Nanoparticle obtained in Ch. Cl-MA DES

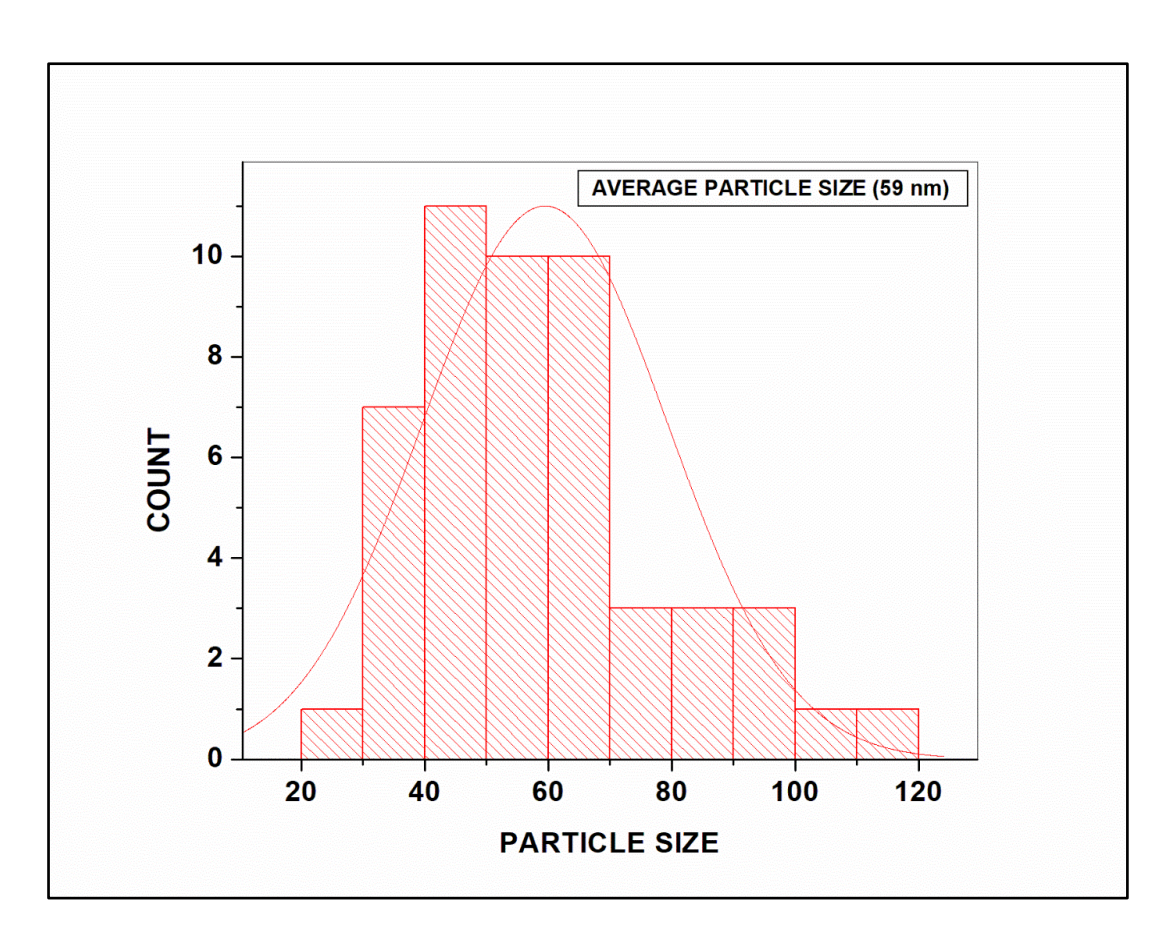


Figure 5.41: SEM Histogram of Silver Oxide Nanoparticle obtained in Ch. Cl-MA DES

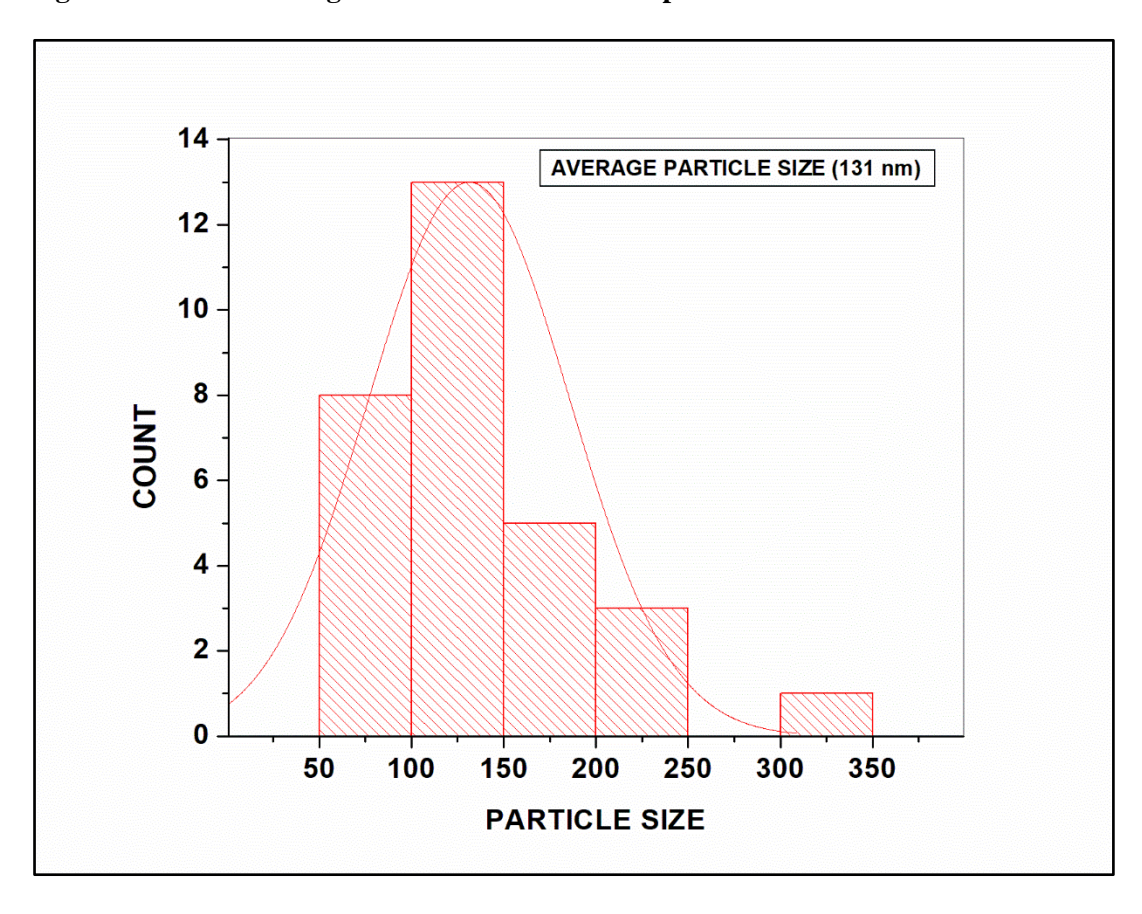


Figure 5.42: SEM Histogram of Zinc Oxide Nanoparticle obtained in Ch. Cl-MA DES

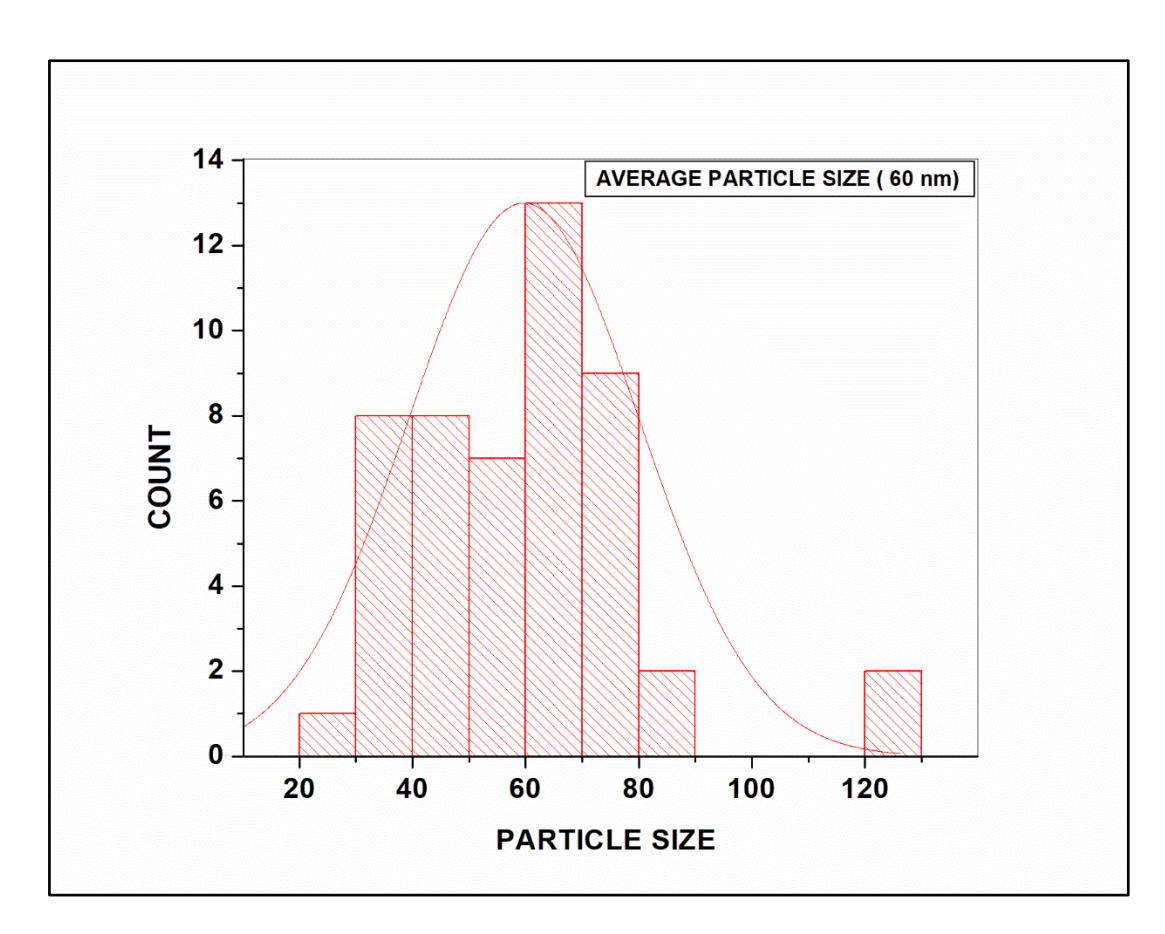


Figure 5.43: SEM Histogram of Cadmium Oxide Nanoparticle obtained in Ch. Cl-MA DES

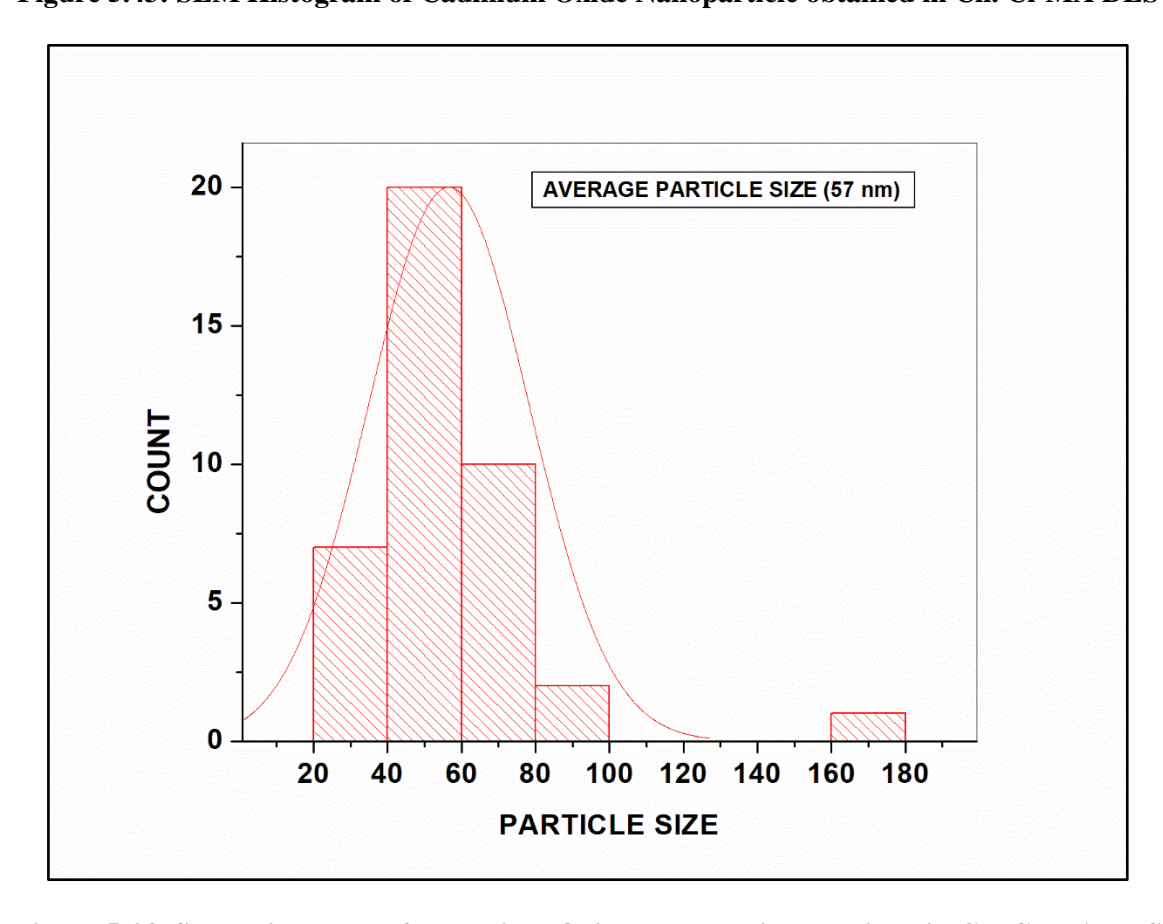


Figure 5.44: SEM Histogram of Vanadium Oxide Nanoparticle obtained in Ch. Cl-MA DES

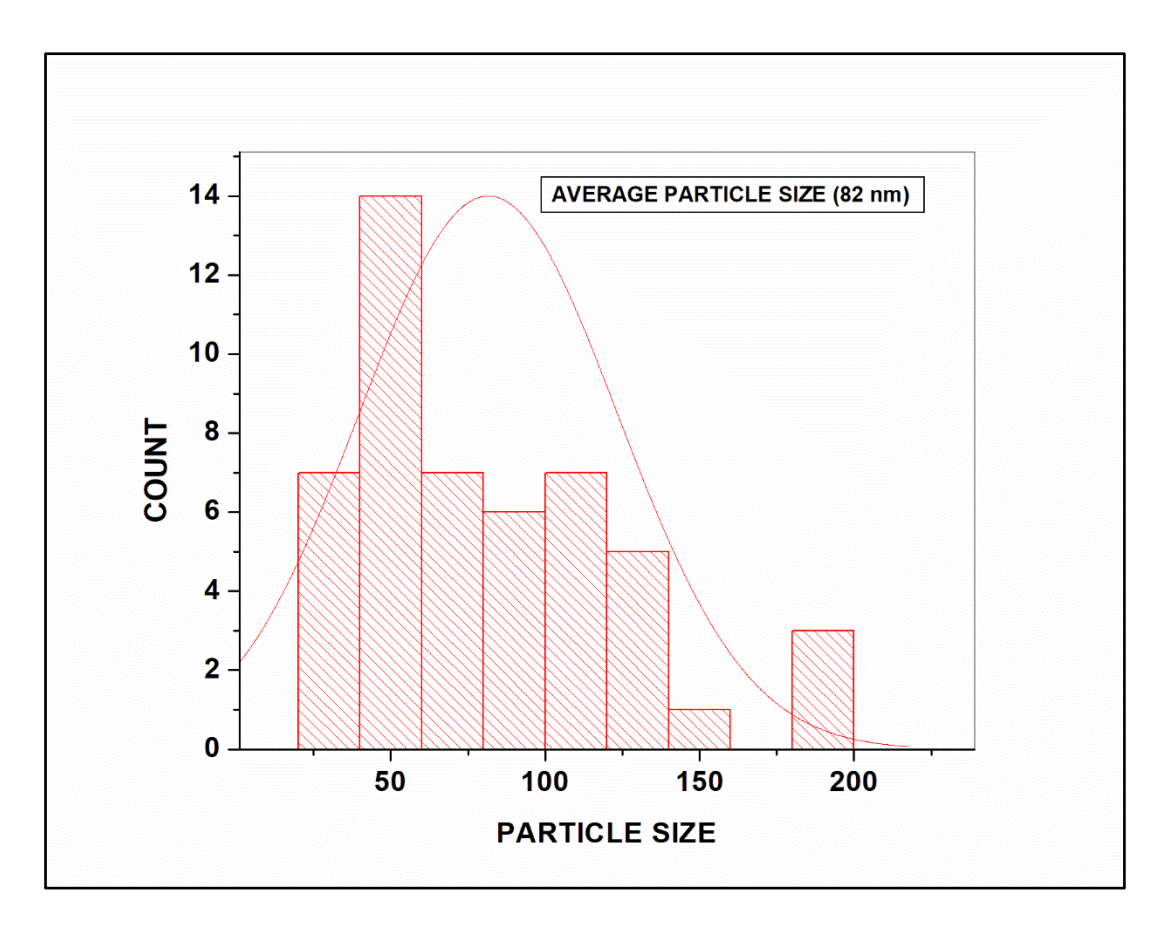


Figure 5.45: SEM Histogram of Nickel Oxide Nanoparticle obtained in Ch. Cl-MA DES

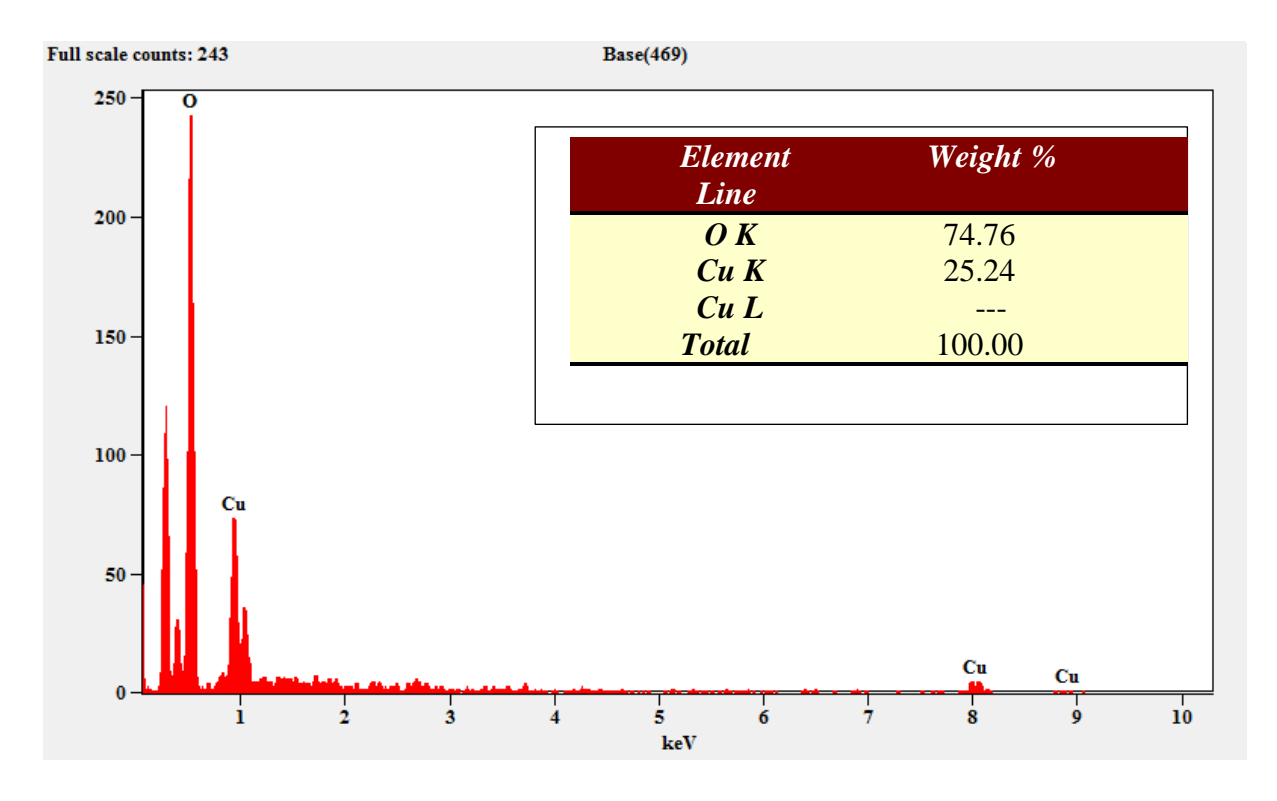


Figure 5.46: EDAX Spectrum of Copper Oxide Nanoparticle obtained in Ch. Cl-MA DES

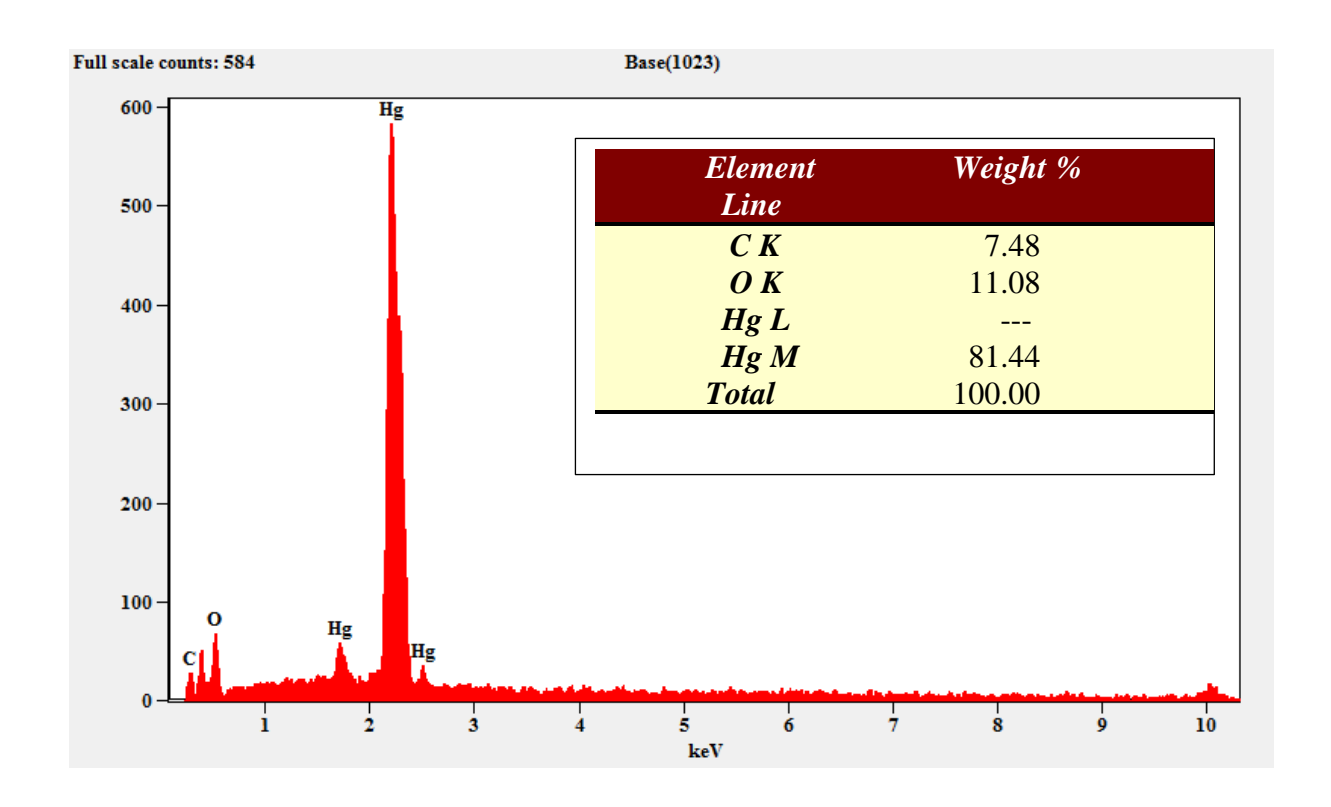


Figure 5.47: EDAX Spectrum of Mercury Oxide Nanoparticle obtained in Ch. Cl-MA DES

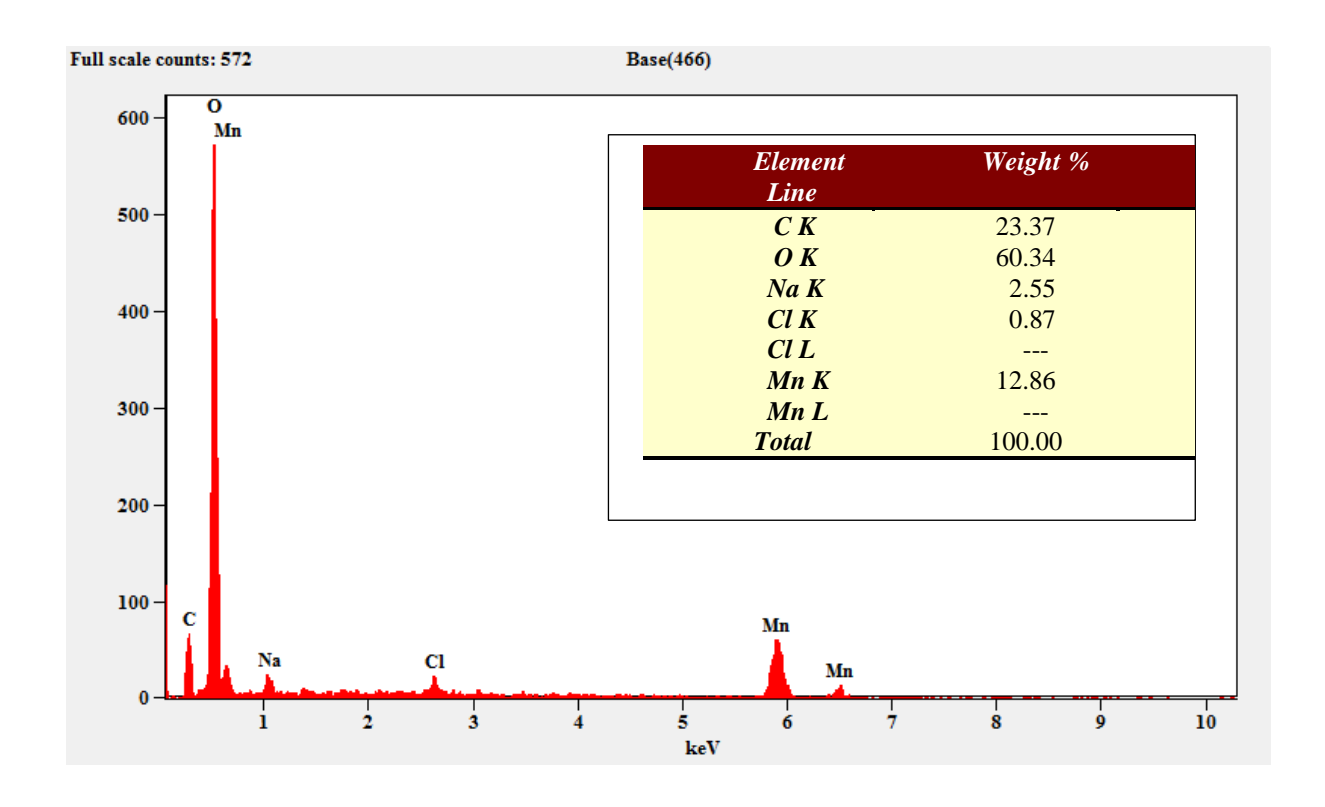


Figure 5.48: EDAX Spectrum of Manganese Oxide Nanoparticle obtained in Ch. Cl-MA DES

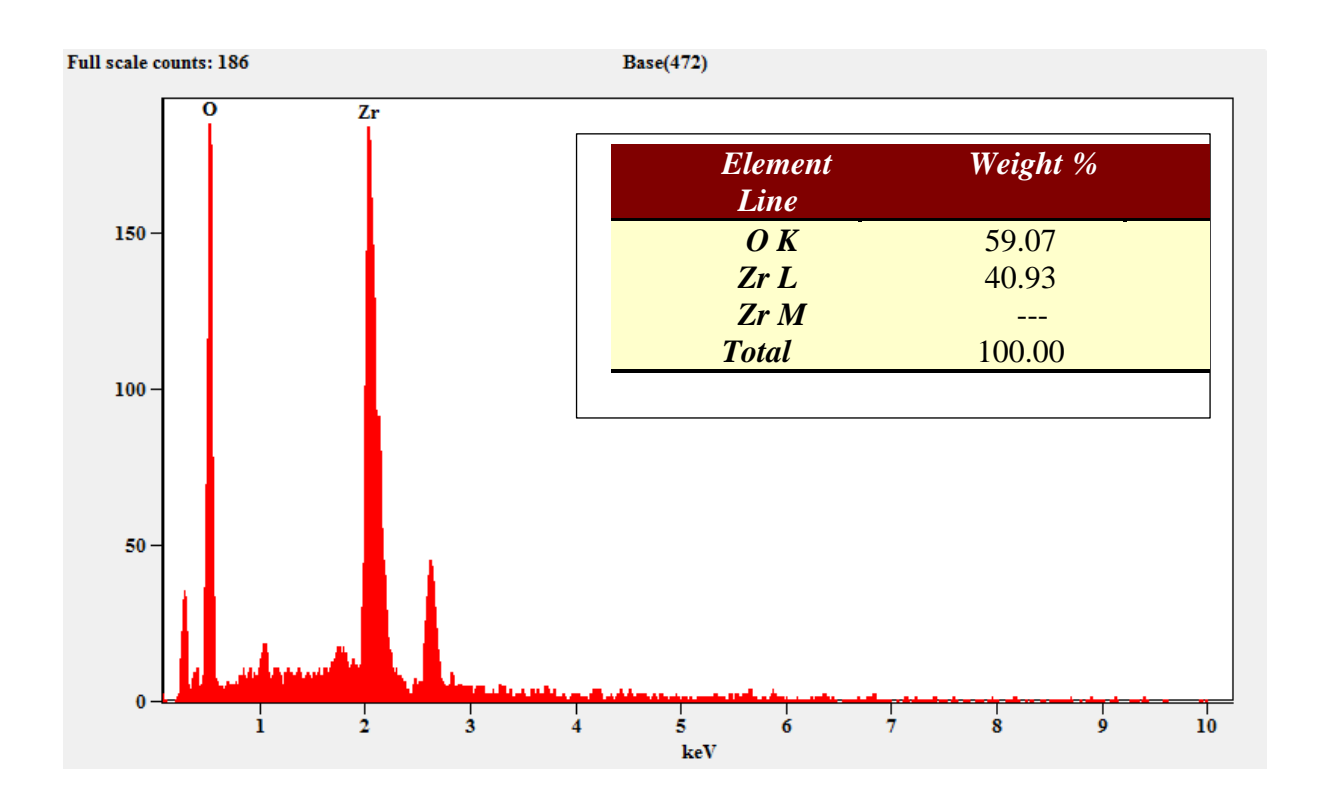


Figure 5.49: EDAX Spectrum of Zirconium Oxide Nanoparticle obtained in Ch. Cl-MA DES

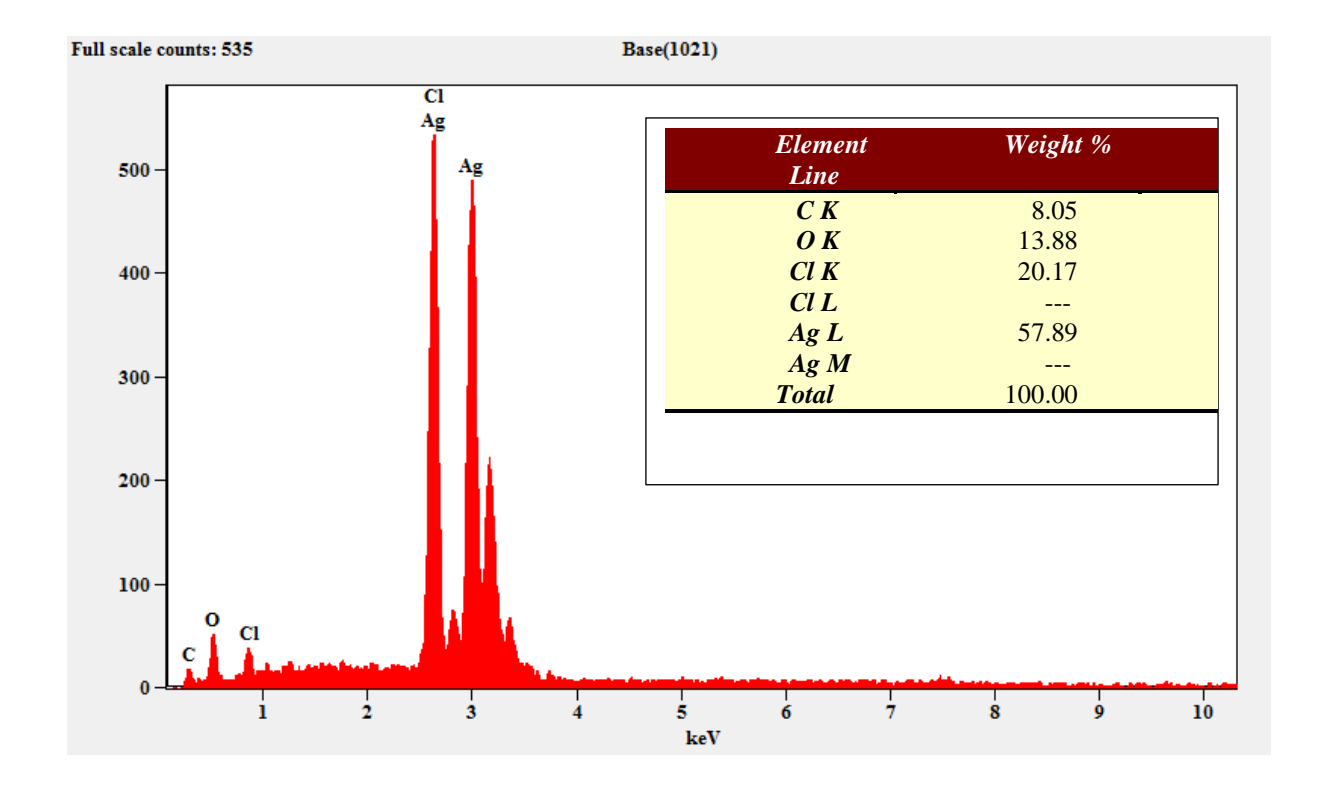


Figure 5.50: EDAX Spectrum of Silver Oxide Nanoparticle obtained in Ch. Cl-MA DES

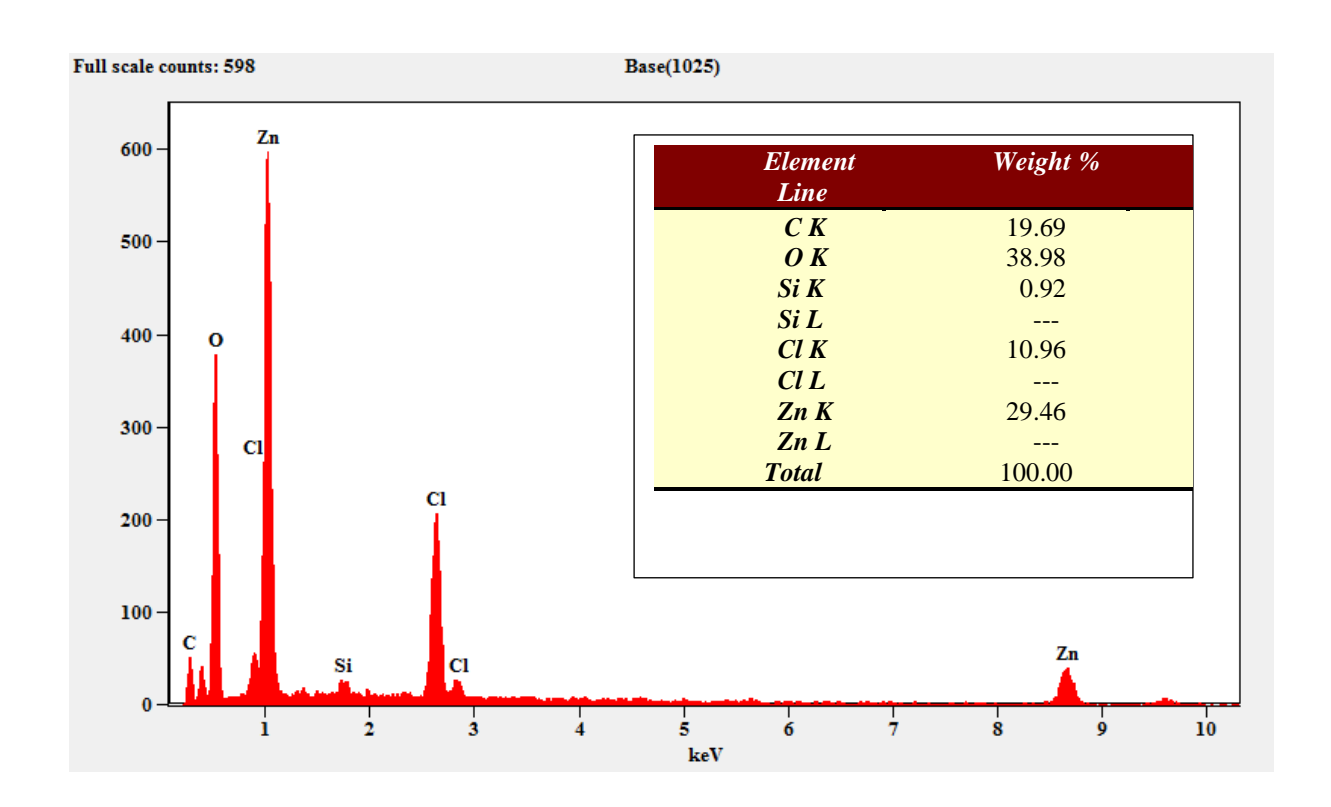


Figure 5.51: EDAX Spectrum of Zinc Oxide Nanoparticle obtained in Ch. Cl-MA DES

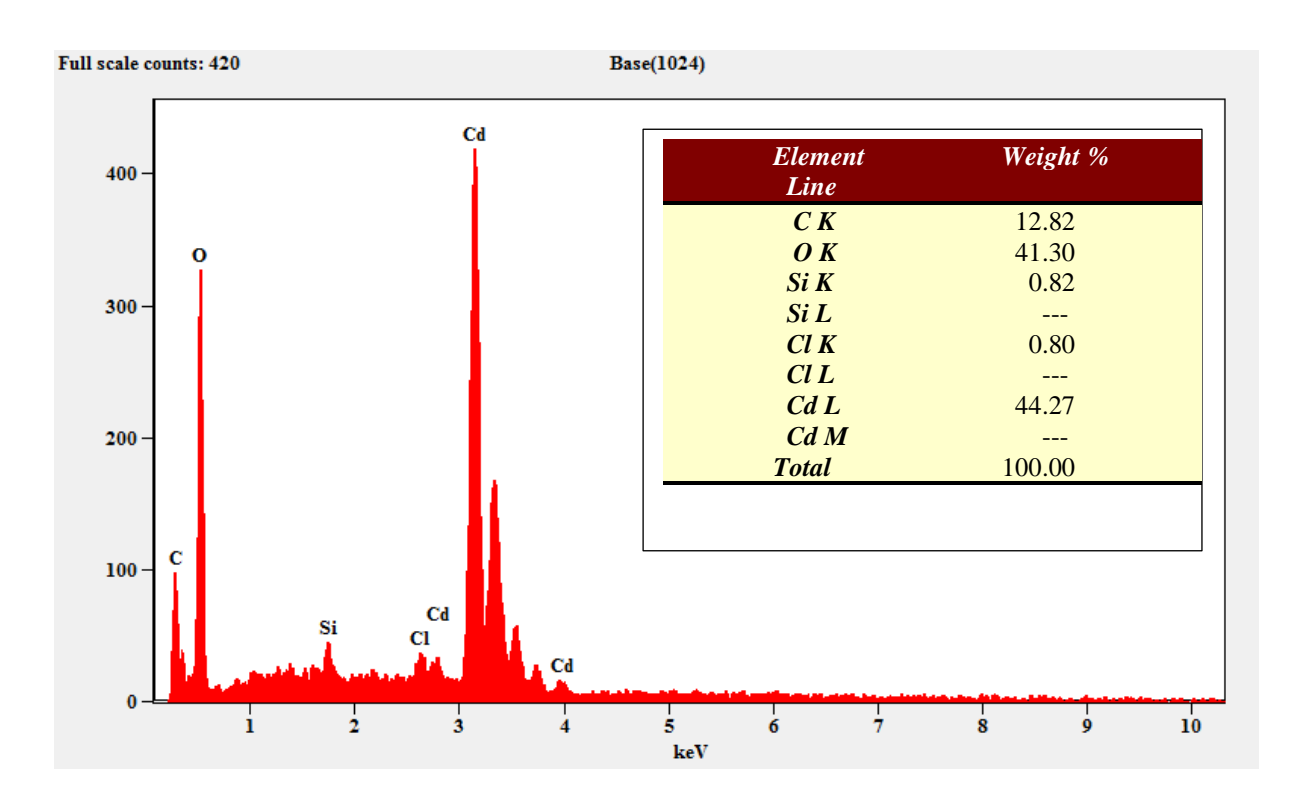


Figure 5.52: EDAX Spectrum of Cadmium Oxide Nanoparticle obtained in Ch. Cl-MA DES

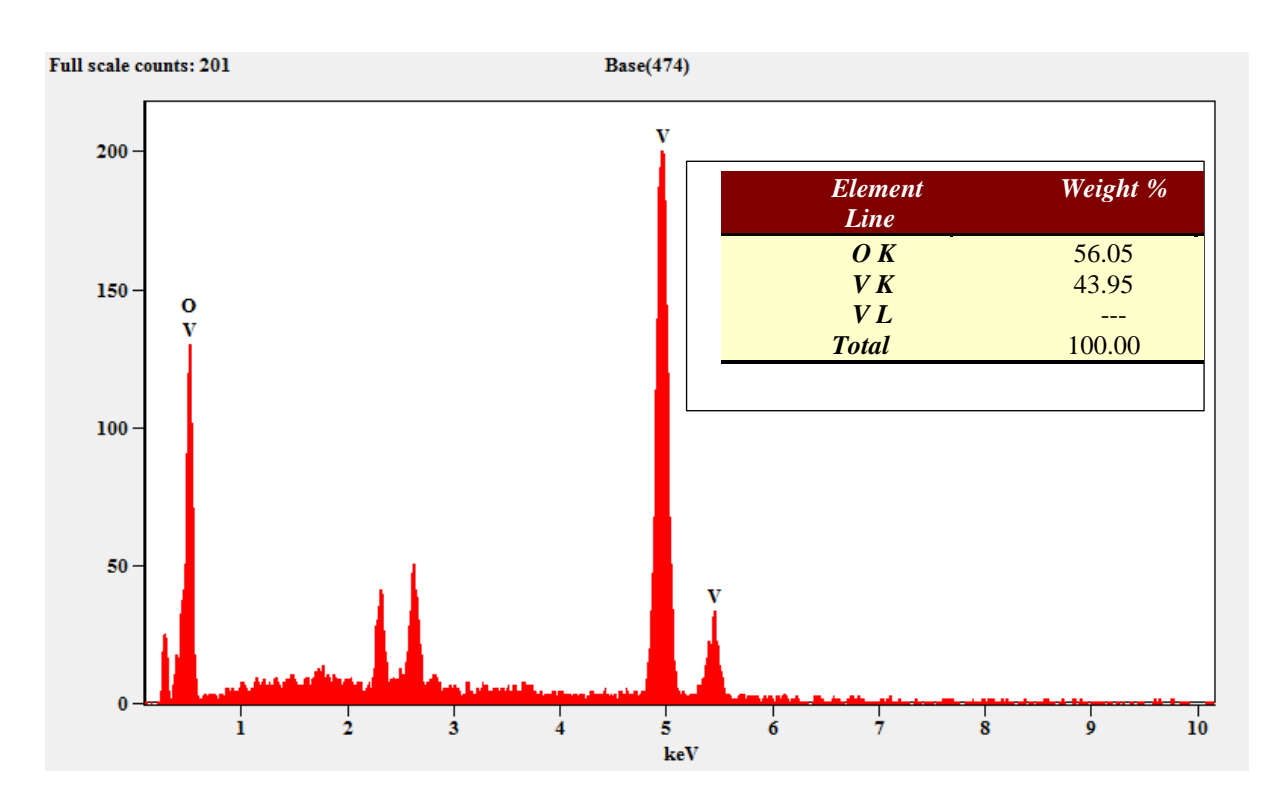


Figure 5.53: EDAX Spectrum of Vanadium Oxide Nanoparticle obtained in Ch. Cl-MA DES

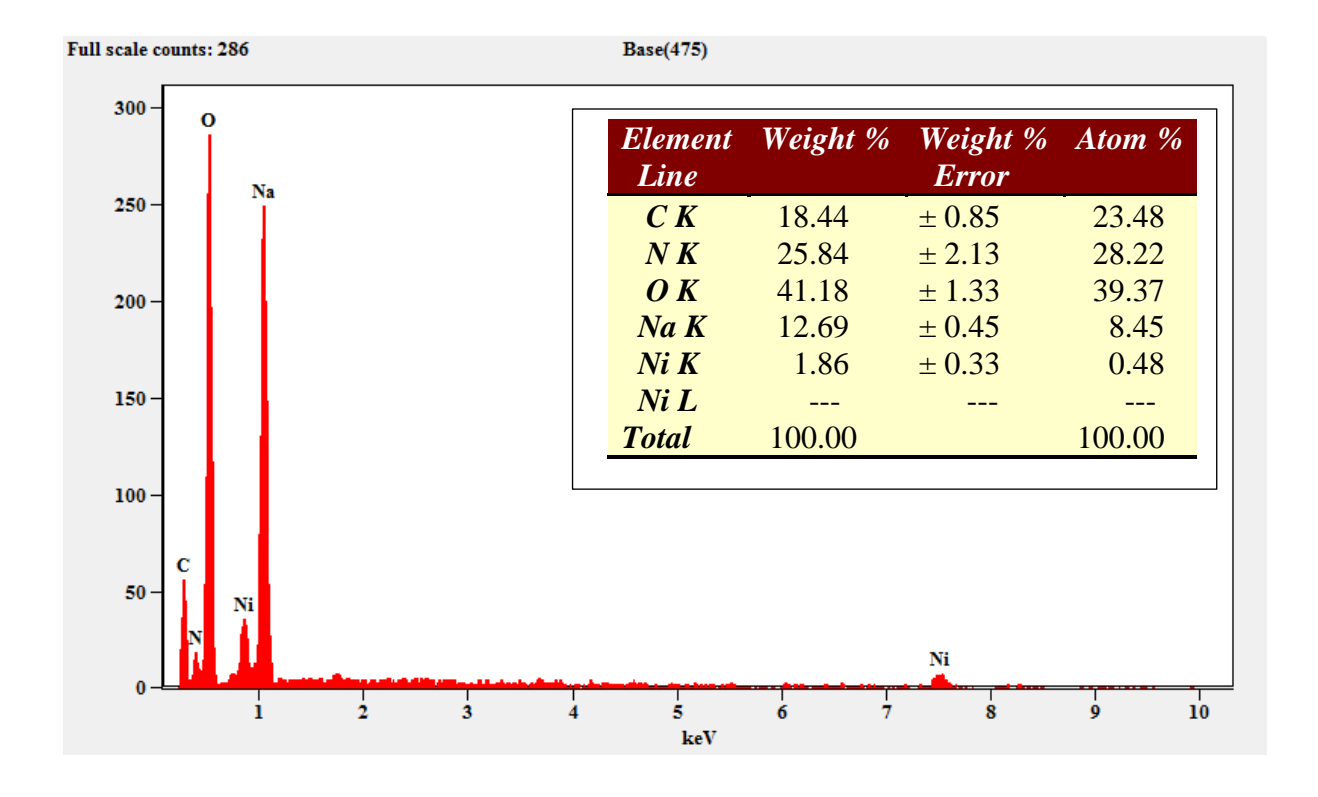


Figure 5.54: EDAX Spectrum of Nickel Oxide Nanoparticle obtained in Ch. Cl-MA DES

### 6. SUMMARY AND CONCLUSIONS

In this investigation, we prepared about nine metal oxide nanoparticles utilizing three different choline chloride-based deep eutectic solvents by the chemical reduction method. The DESs used for the synthesis of metal oxide nanoparticles are

- 1. Choline Chloride Urea
- 2. Choline Chloride Ethylene Glycol
- 3. Choline Chloride Malonic Acid.

The metal oxide nanoparticles prepared in this study are copper, mercury, manganese, zirconium, silver, zinc, cadmium, vanadium and nickel. The reducing agent used for the preparation of these metal oxide nanoparticles is hydrazine hydrate. These methods are simple and very convenient as no surfactant or seeds are needed for the formation of nanoparticles.

The size of the nanoparticles formed in these DES depends upon the amount of water content present in it. Viscosity is an important property to be used as solvents. The liquids with a moderate viscosity are well suitable for the synthesis of nanoparticles due to the availability of fewer voids. If the solvents are too viscous, it is difficult to dissolve the materials in them and there is less possibility for the formation of nanoparticles.

Nanoparticles are emerging technological materials due to their smaller size in the nano range, novel physical and chemical properties. Their nano size is the base of their novel and peculiar characters like particle size distribution and optoelectronic properties. They are of great interest in diverse fields such as clinical pharmacy, agriculture, environmental, chemical, waste treatment, and electronic industries. Several methods such as hydrothermal synthesis, sputtering, sol-gel technique, laser ablation, biological and chemical synthesis are in existence for the synthesis of NPs. Ionic liquids are a newer class of compounds that are used as a solubilizing medium for the synthesis of NPs. But they

have some drawbacks in the view of degradability and toxicity. So eco-friendly synthesis of nanoparticles using DES which is an eco-friendly efficient technique is an emerging technology in the field of nanotechnology.

Table 6.1: Size and morphology of the metal oxide nanoparticles prepared from the deep eutectic solvents

S.No	MO NPs	Ch. Cl-U DES		Ch. Cl-EG DES		Ch. Cl-MA DES		
		Morphology	Size (nm)	Morphology	Size (nm)	Morphology	Size (nm)	
1	Cu	Polygonal Rods	44.22	Spongy like	77	Irregular Tiles	75	
2	Hg	Polymorphous	23.51	Irregular	43	Spongy Beads	55	
		Grains		beads		1 05		
3	Mn	Spongy Buds	49.46	Irregular	55	Polygonal	79	
		spengy Batas	15.10	Scales		Scales		
4	Zr	Spongy Like	19.16	Spongy like	66	Scales Like	102	
5	Ag	Aggregated	130	Spongy	168	Irregular	59	
		Spheres	150	spheres	100	Spheres		
6	Zn	Spongy Rods	70	Broken rods	92	92 Flower Like		
7	Cd	Scales Like	101	Buds like	45	Broken Tiles	60	
8	V	Spongy Scales	97	Scales like	65	Clogged Buds	57	
9	Ni	Accumulated	62	Scales like	50	Spongy	82	
		Scales	02	Scales like	50	Scales		

The formation of nanoparticles was confirmed by UV, FTIR, XRD, SEM, and EDAX techniques. The method used for the synthesis of nanoparticles is a very simple and eco-friendly one. All these metals mentioned above yielded their nanoparticles in all three deep eutectic solvents with varying sizes and morphology.

The size and morphology of these metal oxide nanoparticles prepared from these deep eutectic solvents are summarized in table 6.1 given above. From this table, it was observed that the choline chloride – urea DES is efficient in producing comparatively smaller nanoparticles in the case of Cu, Hg, Mn, Zr and Zn metal oxides with respect to the other two DESs. The choline chloride – ethylene glycol is more efficient in producing Cd and Ni oxide nanoparticles while the choline chloride – malonic acid is efficient in producing Ag and V oxide nanoparticles.

The elemental composition and the purity of the DES media via prepared metal oxide nanoparticles are confirmed by Energy Dispersive X-ray Analysis. The elemental cleanliness of metals in these metal oxide NPs was evaluated from the EDAX spectra and the values are reported in Table 6.2.

Table 6.2: The weight and atom % of metals present in the metal oxide nanoparticles obtained in the DES media

		Ch. Cl-U D	LO	Ch. Cl-EG DES		Ch. Cl-MA DES		
	-	Weight %	Atom %	Weight %	Atom %	Weight %	Atom %	
1 (	Cu	48.1	26.45	40.83	18.4	25.24	7.86	
2 H	Нg	96.49	80.12	72.61	17.46	85.44	23.58	
3 N	Мn	12.74	3.89	12.86	3.84	12.86	3.84	
4 Z	Zr	55	24.71	40.93	10.84	4.93	10.84	
5 A	Ag	29.23	11.2	95.98	77.98	53.89	20.3	
6 Z	Zn	44.41	21.14	21.5	6.47	29.46	9.26	
7 0	Cd	40.83	18.4	89.99	69.37	44.27	9.62	
8 V	V	95.98	77.98	43.95	19.76	43.95	19.76	
9 N	Ni	29.5	10.04	44.74	30.66	1.86	0.48	

From table 6.2, it is noticed that the DES, Ch. Cl-U had produced Cu, Hg, Zr, Zn and V oxide nanoparticles in purer form when compared to the other two DES. The DES,

Ch. Cl-EG had formed Ag, Cd and Ni oxide nanoparticles in purer form when compared to the other DES. But the Mn oxide nanoparticles obtained in all the three DES is comparatively less pure which is due to the varying oxidation states of Manganese.

Thus, the choline chloride-based DES is gaining importance nowadays in NPs formation as there is no need for the use of any surfactants or seeds during the formation of nanoparticles when DESs is used as a solvent. Hence choline chloride – urea/ethylene glycol/malonic acid, DES-based synthesis approach could be a promising technique in the synthesis of nanoparticles.

### **Future perceptive of the work**

- Investigation of some other deep eutectic solvents for the formation of metallic nanoparticles
- ❖ For synthesizing different metal-based nanoparticles using varying types of DES
- ❖ To check the different applications of metal nanoparticles.
- ❖ To check the reusability and recyclability of deep eutectic solvents during the synthesis of metal nanoparticles.

#### List of articles published as in the UGC listed Scopus indexed peer-reviewed journals

- 1. R. Balaji, D. Ilangeswaran; Synthesis of some metal nanoparticles using the effective media of choline chloride based deep eutectic solvents, Materials Today: Proceedings 56 (2022) 3366 –3375. https://doi.org/10.1016/j.matpr.2021.10.324
- 2. R. Balaji, D. Ilangeswaran; Choline chloride Urea deep eutectic solvent an efficient media for the preparation of metal nanoparticles. Journal of the Indian Chemical Society; 99 (2022) 1 9. <a href="https://doi.org/10.1016/j.jics.2022.100446">https://doi.org/10.1016/j.jics.2022.100446</a>

#### List of papers presented in the National/International conferences

- 1. R. Balaji, D. Ilangeswaran, Synthesis of silver nanoparticles at UGC/SAP, ACT, RSC&BRNS Sponsored National Seminar on Recent Advances in Chemical and environmental Research (RACE-2017), Organized by Annamalai University on 20&21 January 2017.
- 2. R. Balaji, D. Ilangeswaran, Synthesis and applications of nanomaterials at International Conference on Recent Trends in Synthetic methods and Material Chemistry (RTSMC-2018) Organized by the Dept of Chemistry, Annamalai University, Annamalai Nagar, Tamilnadu on 2 & 3 <sup>rd</sup> February 2018.
- 3. R. Balaji, D. Ilangeswaran, Green synthesis of Cu/CuO / Mn/MnO/ Zr/ZrO Nanoparticles using EG-Ch, Cl DES at International Conference on Frontiers in Chemical and Material Sciences (ICFCMS-2020) organized by Dept of chemistry, The Gandhigram Rural Institute, on 24& 25 th February 2020.
- 4. R. Balaji, D. Ilangeswaran, Deep Eutectic solvent of Choline chloride-Ethylene glycol an effective media for the synthesis of HgS Nanoparticles., National conference on frontiers in chemical Sciences (NCFC-2020) held during March 29-30 2021 at Central University of Tamilnadu, Thiruvarur.